

# Unmasking metabolic dependencies for anti-cancer treatment in cancer

**Edited by**

Johannes Fahrmann and Satyendra Chandra Tripathi

**Published in**

Frontiers in Oncology



## FRONTIERS EBOOK COPYRIGHT STATEMENT

The copyright in the text of individual articles in this ebook is the property of their respective authors or their respective institutions or funders. The copyright in graphics and images within each article may be subject to copyright of other parties. In both cases this is subject to a license granted to Frontiers.

The compilation of articles constituting this ebook is the property of Frontiers.

Each article within this ebook, and the ebook itself, are published under the most recent version of the Creative Commons CC-BY licence. The version current at the date of publication of this ebook is CC-BY 4.0. If the CC-BY licence is updated, the licence granted by Frontiers is automatically updated to the new version.

When exercising any right under the CC-BY licence, Frontiers must be attributed as the original publisher of the article or ebook, as applicable.

Authors have the responsibility of ensuring that any graphics or other materials which are the property of others may be included in the CC-BY licence, but this should be checked before relying on the CC-BY licence to reproduce those materials. Any copyright notices relating to those materials must be complied with.

Copyright and source acknowledgement notices may not be removed and must be displayed in any copy, derivative work or partial copy which includes the elements in question.

All copyright, and all rights therein, are protected by national and international copyright laws. The above represents a summary only. For further information please read Frontiers' Conditions for Website Use and Copyright Statement, and the applicable CC-BY licence.

ISSN 1664-8714  
ISBN 978-2-8325-4954-4  
DOI 10.3389/978-2-8325-4954-4

## About Frontiers

Frontiers is more than just an open access publisher of scholarly articles: it is a pioneering approach to the world of academia, radically improving the way scholarly research is managed. The grand vision of Frontiers is a world where all people have an equal opportunity to seek, share and generate knowledge. Frontiers provides immediate and permanent online open access to all its publications, but this alone is not enough to realize our grand goals.

## Frontiers journal series

The Frontiers journal series is a multi-tier and interdisciplinary set of open-access, online journals, promising a paradigm shift from the current review, selection and dissemination processes in academic publishing. All Frontiers journals are driven by researchers for researchers; therefore, they constitute a service to the scholarly community. At the same time, the *Frontiers journal series* operates on a revolutionary invention, the tiered publishing system, initially addressing specific communities of scholars, and gradually climbing up to broader public understanding, thus serving the interests of the lay society, too.

## Dedication to quality

Each Frontiers article is a landmark of the highest quality, thanks to genuinely collaborative interactions between authors and review editors, who include some of the world's best academicians. Research must be certified by peers before entering a stream of knowledge that may eventually reach the public - and shape society; therefore, Frontiers only applies the most rigorous and unbiased reviews. Frontiers revolutionizes research publishing by freely delivering the most outstanding research, evaluated with no bias from both the academic and social point of view. By applying the most advanced information technologies, Frontiers is catapulting scholarly publishing into a new generation.

## What are Frontiers Research Topics?

Frontiers Research Topics are very popular trademarks of the *Frontiers journals series*: they are collections of at least ten articles, all centered on a particular subject. With their unique mix of varied contributions from Original Research to Review Articles, Frontiers Research Topics unify the most influential researchers, the latest key findings and historical advances in a hot research area.

Find out more on how to host your own Frontiers Research Topic or contribute to one as an author by contacting the Frontiers editorial office: [frontiersin.org/about/contact](https://frontiersin.org/about/contact)



# Unmasking metabolic dependencies for anti-cancer treatment in cancer

## Topic editors

Johannes Fahrmann — University of Texas MD Anderson Cancer Center, United States

Satyendra Chandra Tripathi — All India Institute of Medical Sciences Nagpur, India

## Citation

Fahrmann, J., Tripathi, S. C., eds. (2024). *Unmasking metabolic dependencies for anti-cancer treatment in cancer*. Lausanne: Frontiers Media SA.  
doi: 10.3389/978-2-8325-4954-4

# Table of contents

|     |  |
|-----|--|
| 04  | <b>Fatty acid metabolism: A new therapeutic target for cervical cancer</b><br>Pengbin Ping, Juan Li, Hongbin Lei and Xiaoying Xu   |
| 17  | <b>Abnormal lipid metabolism in cancer-associated cachexia and potential therapy strategy</b><br>Ruoxin Fang, Ling Yan and Zhengkai Liao   |
| 30  | <b>Ability of metformin to deplete NAD<sup>+</sup> contributes to cancer cell susceptibility to metformin cytotoxicity and is dependent on NAMPT expression</b><br>Yongxian Zhuang, Allison B. Haugrud, Meg A. Schaefer, Shanta M. Messerli and W. Keith Miskimins |
| 40  | <b>Branched-chain amino acids catabolism and cancer progression: focus on therapeutic interventions</b><br>Er Xu, Bangju Ji, Ketao Jin and Yefeng Chen   |
| 49  | <b>Metabolic barriers in non-small cell lung cancer with <i>LKB1</i> and/or <i>KEAP1</i> mutations for immunotherapeutic strategies</b><br>Ichidai Tanaka, Junji Koyama, Hideyuki Itoigawa, Shunsaku Hayai and Masahiro Morise                                     |
| 63  | <b>Integrative analysis of mitochondrial metabolic reprogramming in early-stage colon and liver cancer</b><br>Yeongmin Kim, So-Yeon Shin, Jihun Jeung, Yumin Kim, Yun-Won Kang, Sunjae Lee and Chang-Myung Oh  |
| 76  | <b>The potential and challenges of targeting <i>MTAP</i>-negative cancers beyond synthetic lethality</b><br>Chandler Bray, Cristina Balcells, Iain A. McNeish and Hector C. Keun   |
| 90  | <b>Cellular specificity of lactate metabolism and a novel lactate-related gene pair index for frontline treatment in clear cell renal cell carcinoma</b><br>Xiangsheng Li, Guangsheng Du, Liqi Li and Ke Peng  |
| 106 | <b>The kynurenine pathway presents multi-faceted metabolic vulnerabilities in cancer</b><br>Ricardo A. León-Letelier, Rongzhang Dou, Jody Vykoukal, Ali Hussein Abdel Sater, Edwin Ostrin, Samir Hanash and Johannes F. Fahrman                                    |
| 127 | <b>Prognosis stratification and response to treatment in breast cancer based on one-carbon metabolism-related signature</b><br>Tongxin Zhang, Jingyu Liu, Meihuan Wang, Xiao Liu, Jia Qu and Huawei Zhang  |
| 142 | <b>Metabolomics analysis reveals novel serum metabolite alterations in cancer cachexia</b><br>Tushar H. More, Karsten Hiller, Martin Seifert, Thomas Illig, Rudi Schmidt, Raphael Gronauer, Thomas von Hahn, Hauke Weilert and Axel Stang                          |



## OPEN ACCESS

## EDITED BY

Juan Carlos Gallardo-Pérez,  
National Institute of Cardiology Ignacio  
Chavez, Mexico

## REVIEWED BY

Yinu Wang,  
Northwestern University, United States  
Hui Wang,  
Huazhong University of Science and  
Technology, China

## \*CORRESPONDENCE

Xiaoying Xu  
✉ xiaoyingxu73@aliyun.com

<sup>†</sup>These authors share first authorship

## SPECIALTY SECTION

This article was submitted to  
Cancer Metabolism,  
a section of the journal  
Frontiers in Oncology

RECEIVED 30 November 2022

ACCEPTED 13 March 2023

PUBLISHED 28 March 2023

## CITATION

Ping P, Li J, Lei H and Xu X (2023) Fatty  
acid metabolism: A new therapeutic  
target for cervical cancer.  
*Front. Oncol.* 13:1111778.  
doi: 10.3389/fonc.2023.1111778

## COPYRIGHT

© 2023 Ping, Li, Lei and Xu. This is an open-  
access article distributed under the terms of  
the [Creative Commons Attribution License](#)  
(CC BY). The use, distribution or  
reproduction in other forums is permitted,  
provided the original author(s) and the  
copyright owner(s) are credited and that  
the original publication in this journal is  
cited, in accordance with accepted  
academic practice. No use, distribution or  
reproduction is permitted which does not  
comply with these terms.

# Fatty acid metabolism: A new therapeutic target for cervical cancer

Pengbin Ping<sup>†</sup>, Juan Li<sup>†</sup>, Hongbin Lei and Xiaoying Xu\*

Department of Radiotherapy Oncology, The Second Affiliated Hospital of Dalian Medical University,  
Dalian, China

Cervical cancer (CC) is one of the most common malignancies in women. Cancer cells can use metabolic reprogramming to produce macromolecules and ATP needed to sustain cell growth, division and survival. Recent evidence suggests that fatty acid metabolism and its related lipid metabolic pathways are closely related to the malignant progression of CC. In particular, it involves the synthesis, uptake, activation, oxidation, and transport of fatty acids. Similarly, more and more attention has been paid to the effects of intracellular lipolysis, transcriptional regulatory factors, other lipid metabolic pathways and diet on CC. This study reviews the latest evidence of the link between fatty acid metabolism and CC; it not only reveals its core mechanism but also discusses promising targeted drugs for fatty acid metabolism. This study on the complex relationship between carcinogenic signals and fatty acid metabolism suggests that fatty acid metabolism will become a new therapeutic target in CC.

## KEYWORDS

cervical cancer, fatty acids, fatty acid metabolism, metabolic reprogramming, therapeutic target

## 1 Introduction

Cervical cancer (CC) seriously affects women's life and health. Globally, approximately 530,000 new cases and 266,000 new deaths are reported annually (1). Early HPV detection and vaccination have greatly reduced the incidence of CC and grade 3 cervical intraepithelial neoplasia (CIN3) in young women (2). Even though CC can be actively prevented, it still remains the second leading cause of cancer-related death among young and middle-aged women (3). The most common histological subtype of CC is cervical squamous cell carcinoma (CSCC) (4), which accounts for approximately 70% of all CC cases in the United States (5) and approximately 90% of CC cases in China (6, 7). SCC Ag is considered to be the most clinically valuable serum tumor marker of SCC, and its levels are usually associated with larger primary tumors, later stage, and lymph node involvement (8–10). Of note, nearly a quarter of CC patients do not have elevated SCC Ag levels (11). Furthermore, almost all CCs are related to high-risk human papillomavirus (HPV) infections, of which nearly 50% are HPV16 infections (12, 13). However, HPV infection is not a requirement. Approximately 3–8% of cases are HPV-negative CC (14–16). The

American Joint Committee on Cancer (AJCC) 9th edition TNM CC staging, based on histopathological observations, was updated to reflect HPV-associated and HPV-unrelated carcinomas. Moreover, HPV-independent cervical cancer is usually linked to early lymph node metastasis and is more often diagnosed with nonsquamous histology (17, 18). Interestingly, HPV infection does not always develop into cancer; there must be additional changes. At present, most patients diagnosed with advanced CC miss the opportunity for radical surgery. The standard therapy for locally advanced cervical cancer (LACC) is concurrent chemoradiotherapy (CCRT) (19). However, the prognosis of stage III and IV patients remains poor, with 5-year progression-free survival (PFS) and overall survival (OS) rates of 51% and 55%, respectively (20). Pelvic lymph node metastasis remains an important independent prognostic factor for CC. In addition, it is associated with a lower 5-year survival rate and a higher recurrence rate (21–23). However, there is no effective method to control and prevent lymph node metastasis. Although the use of targeted and immunological agents has improved survival to some extent (24, 25), there is still an unmet need for additional treatment for patients with node-positive and recurrent CC. Therefore, it is necessary to explore novel and promising therapeutic targets for CC.

As early as 1956, Otto Warburg found that glucose metabolism differed substantially between normal cells and cancer cells. Even when oxygen is abundant, cancer cells preferentially convert pyruvate to lactate rather than utilizing glucose to produce maximum energy; thus, glucose consumption increases (26). Recently, increasing studies have revealed the metabolic kinetics of cancer and subsequently introduced the concept of metabolic plasticity or metabolic recombination of cancer cells. In addition to

the use of glucose, cancer cells undergo a variety of carcinogenic mutations or adaptations to allow the use of more diverse nutrients, including fatty acids, to promote tumor survival, metastasis and disease progression (27). These research achievements have led to renewed interest in defining the various roles of lipid metabolism in cancer. Moreover, the dysregulation of fatty acids and related lipid metabolism pathways can affect the occurrence of a variety of malignant tumors and lead to poor prognosis (28, 29). Interestingly, in previous studies, CC was considered to be related to lipid metabolism, which can promote the occurrence and development of cervical cancer to a certain extent (30, 31).

This review aimed to better understand the roles of fatty acid metabolism and related lipid metabolism pathways in CC. We reviewed a large number of studies, examined the effects of various fatty acid metabolic pathways in CC, and focused on their mechanisms of action and future perspectives (Figure 1 and Table 1).

## 2 Targeting *de novo* fatty acid synthesis

A well-studied aspect of cancer metabolism is the upregulation of *de novo* fatty acid synthesis (60). Unlike normal cells, tumor cells shift lipid acquisition from fatty acid uptake to enhanced *de novo* fatty acid synthesis to acquire characteristics of unlimited proliferation, thus providing survival advantages for tumor cells and inducing tolerance to radiotherapy and chemotherapy (61, 62). The production of nascent fatty acids is mediated by a variety of enzymes, including fatty acid synthase (FASN), stearoyl-CoA

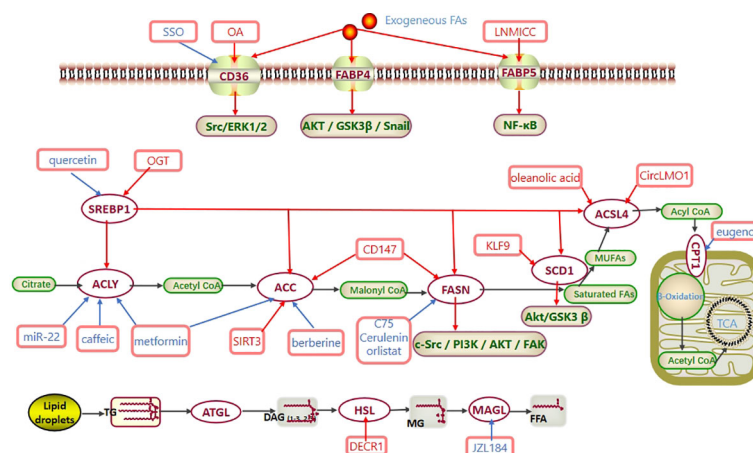


FIGURE 1

Fatty acid metabolism in CC. Exogenous fatty acids are ingested through CD36 and FABP. SREBP1 regulates the expression of ACYL, ACC, FASN, SCD1 and ACSL4 at the transcriptional level. Activated acyl-CoA enters mitochondria via CPT to participate in  $\beta$ -oxidation and generate acetyl-CoA. Eventually, acetyl-CoA enters the TCA cycle to produce ATP. In CC, CD36 promotes the Src/ERK1/2 pathway, FABP4 promotes the AKT/GSK3 $\beta$ /Snail pathway, FABP5 promotes the NF- $\kappa$ B pathway, FASN promotes the c-Src/PI3K/AKT/FAK pathway, and SCD1 promotes the Akt/GSK3 $\beta$  pathway to regulate the progression of cervical cancer. Abbreviations: TCA cycle, tricarboxylic acid cycle; CD36, cluster of differentiation 36; FABP, FA-binding protein; SREBP1, sterol regulatory element-binding protein 1; ACYL, ATP-citrate lyase; ACC, acetyl-CoA carboxylase; FASN, fatty acid synthase; SCD1, stearoyl-CoA desaturase-1; MUFAs, monounsaturated fatty acids; ACSL4, long-chain acyl-CoA synthetases 4; CPT1, carnitine palmitoyltransferase 1; ATGL, adipose triglyceride lipase; HSL, hormone-sensitive lipase; MAGL, monoglyceride lipase; SSO, an inhibitor of CD36; OA, oleic acid; OGT, O-linked N-acetylglucosamine transferase; C75, cerulenin, orlistat, the inhibitors of FASN; eugenol, an inhibitor of CPT1; JZL184, an inhibitor of MAGL.

TABLE 1 Role of fatty acid metabolism and related lipid metabolism pathways in cervical cancer (CC).

| FA Metabolism                             | Target | Effects and Features   | References   |
|---|--------|--|--------------|
| FA Synthesis                              | FASN   | FASN promoted CC cell migration, invasion, and lymphangiogenesis   | (28, 32, 33) |
|   | ACLY   | Mir22 downregulated ACLY and attenuated CC cell proliferation and invasion   | (34)         |
|   | ACC    | Silencing of ACC $\alpha$ significantly promoted the apoptosis of CC cells   | (35–37)      |
|   | SCD1   | SCD1 level was associated with the CC stage, the overall survival rate, and the disease-free survival rate         | (38)         |
| FA Uptake                                 | CD36   | Overexpression of CD36 promoted the invasion and metastasis of CC cells <i>in vitro</i> and <i>in vivo</i>         | (39–42)      |
| FA Transport                              | FABP   | FABP promoted epithelial-mesenchymal transition, lymphangiogenesis, and LNM by reprogramming fatty acid metabolism | (43–47)      |
| FA Activation                             | ACSL4  | Upregulated ACSL4 expression promoted CC cells ferroptosis   | (48–50)      |
| FA Oxidation                              | CPT1A  | High expression of CPT1A promoted lipid metabolism modification and CC progress                                    | (51)         |
| Intracellular Lipolysis                   | ATGL   |  | (52)         |
|   | HSL    | Enhanced lipid catabolism contributes to the malignant progression of CC   | (53)         |
|   | MAGL   |  | (54)         |
| Transcription Factors<br>Lipid Metabolism | SREBP  | High expression of SREBP-1 promoted the proliferation of CC cells  | (55, 56)     |
|   | LPA    | LPA inhibited apoptosis of CC cells induced by chemotherapy  | (57, 58)     |
|   | CHOL   | Intersection of different metabolic pathways in CC   | (28, 59)     |

desaturase 1 (SCD1), ATP-citrate lyase (ACLY), and acetyl-CoA carboxylase (ACC). Here, we study their respective mechanisms of action in CC.

## 2.1 Fatty acid synthase (FASN)

Enhanced expression of fatty acid synthesis enzymes is one of the important metabolic adaptations in some malignant tumors (60, 63). For example, free fatty acids promote the proliferation and invasiveness of estrogen receptor alpha-positive breast cancer cells by activating the mTOR pathway (64). In addition, studies have shown that elevated fatty acid synthesis levels may be an early metabolic deregulation in Myc-driven prostate cancer (63). Xu et al. demonstrated that plasma fatty acid composition levels are highly likely to be potential biomarkers for ovarian cancer and other gynecological tumors (65, 66). Carcinogenic transformation is closely related to fatty acid metabolism (67). Because it provides a large amount of energy for the proliferation of malignant tumors, FASN, as the hub of lipid metabolism, plays an increasingly prominent role in tumors with lipid-rich phenotypes. In fact, a series of new FASN inhibitors have been designed. Interestingly, an experiment confirmed that the expression of FASN was upregulated in patients with CC and was associated with lymph node metastasis (28). Additionally, the correlation between the expression of FASN and clinicopathological features was evaluated, and FASN was identified as an independent prognostic factor in patients with CC by multivariate Cox proportional hazard analysis. The specific mechanism involves the ability of FASN to regulate cholesterol reprogramming, which leads to disordered lipid raft-related c-Src/PI3K/AKT/FAK signaling and further increases the invasiveness of CC cells (28). This mechanism has also been elucidated in ovarian cancer (68, 69). In addition, FASN induces lymphangiogenesis

through the production of PDGF-AA/IGFBP3. Meanwhile, the FASN inhibitors cerulenin and C75 can significantly inhibit lymph node metastasis of CC (28). Although cerulenin has effects on various types of tumors *in vitro* and *in vivo*, the high activity and off-target activity of cysteine reactive epoxides hinder their clinical development, and the side effects of cerulenin and C75 in mice also include serious weight losses (70, 71). Another FASN inhibitor that has been widely investigated is orlistat, which is an anti-obesity drug approved by the FDA that has been proven to be effective in tumor biology (72, 73). Interestingly, a study demonstrated that the expression of FASN in CC was higher than that in cervical benign lesions and increased with the increase of the disease stage; however, statistical results showed no significant correlation between the expression of FASN and the grade of cervical lesions. However, in cell experiments, orlistat significantly inhibited the growth and proliferation of CC cells, and this effect was more significant in HPV16-positive and HPV18-positive CC cells. The mechanism underlying these effects was not related to necrosis but was related to apoptosis (32). One of the reasons for this result is that the sample size of this study was relatively small, and it may also be possible that FASN plays an important role in early tumor transformation. However, previous studies have shown that the expression of FASN is related to epithelial-mesenchymal transformation (EMT). FASN can promote EMT in breast cancer, while inhibition of FASN can reverse the EMT process (74). These results are compatible with those of other studies showing that the FASN inhibitor orlistat inhibits CC cell proliferation and blocks lymph node metastasis (30, 33). However, oral orlistat can cause significant gastrointestinal dysfunction, such as fat leakage and abdominal distention (75). Considering the important role of FASN inhibitors in cancer, researchers designed new protocols, such as nanoencapsulation, to improve their oral bioavailability and solubility (76).



To overcome the shortcomings of first-generation FASN inhibitors, researchers have focused on designing FASN inhibitors with superior selectivity, reversibility and nonreactivity to improve drug performance. For example, JNJ-54302833, GSK2194069, IPI-9119, and TVB-2640 have been developed, but only TVB-2640 was used in clinical trials (77). Moreover, treatment with TVB-2640 has shown potent effects in all kinds of solid tumors, including breast cancer, KRAS-mutated non-small cell lung cancer, and CC, and the combination of TVB-2640 and paclitaxel has shown effective target binding (78). Moreover, TVB-2640 is well tolerated, and adverse effects can be reversed when the drug is discontinued (79). A clinical trial involving TVB-2640 in combination with paclitaxel and trastuzumab in HER2-positive advanced breast cancer is under evaluation (80).

Certainly, FASN inhibitors are not universal, there are differences in sensitivity to different metabolic inhibitors and in metabolic characteristics of different tumors and different subtypes of the same tumor. Therefore, it is necessary to clearly understand the metabolic susceptibility of different tumors. After metabolite analysis, pancreatic cancer cells can be divided into three subtypes, namely, the low-proliferative subtype, the lipogenic subtype and the glycolytic subtype. Only the lipogenic subtype shows good sensitivity to FASN inhibitors, indicating the plasticity of the metabolic network of cancer cells (81). Therefore, to accurately predict the sensitivity of cancer cells to FASN inhibitors, we first need to understand the interactions between the different metabolic networks of cancer cells.

## 2.2 ATP-citrate lyase (ACLY)

ACLY catalyzes the conversion of citrate to oxaloacetate and acetyl-CoA. A variety of ACLY inhibitors have been used to treat hyperlipidemia (82, 83). ACLY is a key enzyme linking fatty acid synthesis with glycolysis. ACLY has been shown to be highly expressed in a variety of cancers (84), and its inhibitor has a more significant anticancer effect in high-glycolytic cells (85). The PI3K/Akt pathway plays an important role in CC (86). Hyperglycolysis promotes tumor growth by increasing ACLY levels and fatty acid synthesis through the activation of PI3K/Akt signaling (85). Caffeic acid combined with metformin downregulates the expression of the ACLY protein by activating AMPK, which further reduces fatty acid synthesis, resulting in an increase in the apoptosis rate of metastatic cervical HTB-34 cells (87). Mei et al. showed that the level of ACLY was increased in CC cells. Furthermore, miR-22 could mediate the downregulation of ACLY and accelerate the apoptosis of CC cells. It was also found that the tumor weight in mice treated with miR-22 was much lower than that in the control group. The mechanism underlying these effects may be that miR-22 reduced the ability of *de novo* lipid synthesis by inhibiting the expression of ACLY, thus inhibiting the proliferation and invasion of cancer cells (34). The combination of an AMPK activator and an ACLY inhibitor may be another strategy for cancer treatment (88). There are few studies on targeting ACLY in the treatment of CC, but it is undeniable that it may be a powerful potential target for the treatment of CC.

## 2.3 Acetyl-CoA carboxylase (ACC)

ACC is a rate-limiting enzyme that catalyzes the formation of malonyl-CoA from acetyl-CoA. There are two subtypes of mammalian ACC, ACC $\alpha$  (ACC1 or ACACA) and ACC $\beta$  (ACC2 or ACACB) (89). While ACC $\alpha$  is enriched in adipose tissue (90), ACC $\beta$  mainly exists in oxidized tissues (91). These expression patterns determine the difference in its metabolism in different tissues. Gu et al. performed immunohistochemical staining of CD147, a transmembrane glycoprotein, in 85 cases of CC and 24 cases of normal cervical epithelia. CD147 was highly expressed in CC, with a positive rate of 78.7%. *In vitro* experiments showed that CD147 could promote the proliferation and lymph node metastasis of CC cells. The mechanism involves the reprogramming of lipid metabolism by CD147 through FAS and ACC1. After CD147 knockdown, the lipid content of CC cells was markedly reduced, and the migration ability of cancer cells was also greatly reduced (33). Li et al. reported that SIRT3 could accelerate lipid synthesis by upregulating ACC $\alpha$  in CC oncogenic tissues, thereby increasing their invasion. Moreover, in an allograft mouse model, the tumors were significantly larger in the high SIRT3 expression group than in the SIRT3 knockout group (35). Consistent with this finding, studies have shown that the level of ACACA is upregulated in CC cells. Silencing ACACA can accelerate the apoptosis of CC cells (36). Previous studies have shown that berberine can inhibit the proliferation of CC cells by reducing the activity of ACC and the synthesis of intracellular fatty acids, resulting in the decreased production of extracellular vesicles (37). Similarly, metformin can activate AMPK and downregulate ACC $\alpha$  levels in CC cells to inhibit lipid synthesis, thereby inhibiting tumor growth (87). Interestingly, silencing ACC $\alpha$  or ACC $\beta$  can promote NADPH-dependent redox balance, leading to the accelerated growth of lung cancer cells (92). At the same time, ACC levels may be useful for predicting the prognosis of some patients undergoing anticancer treatment. A MITO phase III trial found that the increase in the phosphorylation level of ACC predicted poor outcomes in patients with ovarian cancer treated with paclitaxel/carboplatin (93). The role of ACC in tumors is complex, but these indicate that targeting ACC is a potential therapeutic strategy for CC. However, to date, no ACC inhibitor has reached the stage of clinical trials for gynecological cancers.

## 2.4 Stearoyl-CoA desaturase-1 (SCD1)

The transformation of saturated fatty acids to monounsaturated fatty acids requires the catalysis by SCD1, which can promote the occurrence of a variety of tumors and accelerate their malignant progression. However, cancer progression may result from an imbalance between unsaturated and saturated fatty acids (94, 95). The expression level of SCD1 is highly upregulated in several malignancies, such as ovarian (96, 97), gastric (98), and lung cancer (99), and is associated with poor prognosis. SCD1 targeting or gene knockout can significantly inhibit tumor growth and restore cisplatin resistance (99–101). Wang et al. analyzed the role of SCD1 in CC using the GEPIA database. A total of 306 CC

samples and 13 normal samples were included. It was found that the expression levels of SCD1 in CC tissues were high and were related to the overall survival time and staging of patients. At the same time, the low expression of KLF9 was found in advanced CC and negatively correlated with that of SCD1. The final results showed that the expression of KLF9/SCD1 could regulate the Akt/GSK3- $\beta$  signaling pathway in CC cells and affect the proliferation, invasion and EMT process of CC cells. This phenomenon can be suppressed by knocking out SCD1 (38). Studies have also shown that SCD1 can regulate the level of miR-1908, and its high expression levels can promote the proliferation and invasion of CC cells (59, 102). Interestingly, a study has shown that metformin can downregulate SCD1 expression, thereby inhibiting CC cells (87). Notably, SCD1 protects tumor cells from ferroptosis (103). Therefore, targeting SCD1 provides a new idea for the treatment of CC. To date, however, virtually no SCD1 inhibitors have been clinically tested as cancer therapies in humans.

### 3 Targeting fatty acid uptake

The growth of tumor cells depends on the intake of exogenous fatty acids, which can promote tumor progression and metastasis (104). The intake of exogenic fatty acids mainly depends on FABP, LDLR, and CD36, which is a member of the FATP family (105). CD36 is negatively linked to the prognosis of patients and is an important biomarker of malignant tumors (106). Previous studies have demonstrated that CD36 levels are upregulated in some malignancies, such as ovarian cancer (104), breast cancer (107), gastric cancer (108), oral cancer (109), melanoma (110), and colorectal cancer (111), to maintain cancer cell progression and metastasis. In one experiment, 133 cases of CC and 47 cases of normal cervical tissues were evaluated. In normal cervical tissues, CD36 expression was detected only in 19.15% of tissues (9/47), while in CC cases, CD36 immunoreactivity was detected in 73.68% of tissues (98/133). The evaluation results showed that CD36 was closely associated with CC progression. High CD36 levels are associated with enhanced EMT, tumor differentiation and lymph node metastasis through synergistic interactions with TGF- $\beta$  (39). Another study showed that dietary oleic acid, was linked with an increase in malignant tumors in HeLa cells. Oleic acid induced the activation of Src kinase and the downstream ERK1/2 pathway in a CD36-dependent manner, and the overexpression of CD36 in HeLa cells aggravated tumor growth and invasion in xenograft mice. The CD36 inhibitor sulfonyl-n-succinic acid oleic acid (SSO) can specifically and irreversibly bind to CD36 and reverse the process of malignant transformation by inhibiting the uptake of fatty acids (40). Increasing expression level of miR-1254 could inhibit the invasion of SiHa and CaSki cells. Additionally, the increase in the expression of CD36 significantly enhanced the proliferation of CC cells, and the increase in the expression of CD36 reversed the inhibitory effect of miR-1254 (41). Similarly, An et al. confirmed that the expression of CD36 in CSCC tissues was higher than that in normal cervical tissues, and the change in CD36 expression level was a unique feature associated with HR HPV infection. HR HPV infections could promote the tumorigenesis and progression of CC

and are associated with shorter recurrence-free survival (42). In conclusion, we predict that CD36 is a breakthrough target for the treatment of CC.

### 4 Targeting fatty acid activation

Fatty acids need to be converted into acyl-CoA to be activated before lipid synthesis and oxidation. The enzyme mediating this process is long-chain acyl-CoA synthetase (ACSL), which can activate the most abundant long-chain fatty acids (112, 113). There are 5 subtypes of ACSL in mammals (ACSL1, ACSL3, ACSL4, ACSL5 and ACSL6), each with specific functions. Among them, ACSL4 is the best studied. ACSL4 can promote uncontrolled cell growth and enhance tumor escape from programmed cell death and invasion (112, 114, 115). ACSL4 is highly expressed in ovarian (116), prostate (113), liver (117), breast (118) and other tumors and is associated with poor prognosis. Interestingly, oleic acid (OA), which is naturally present in plant fruits and leaves, enables dramatic inhibition of the mass and volume of CC tumors in mice, and ACSL4 expression remains highly upregulated in CC cells and xenograft models treated with OA. When the level of ACSL4 is inhibited by siRNA, OA no longer has the ability to inhibit cancer cells (48). The mechanism underlying these effects may be that OA promotes ferroptosis by upregulating ACSL4 levels. Circular RNA (circRNA) has been shown to limit the progression of malignant tumors. Circular RNA (CircLMO1) has been demonstrated to promote ferroptosis induced by the high expression of ACSL4 in CC cells and prevent the growth and invasion. Additionally, ACSL4 knockdown abolished the inhibitory effect of CircLMO1 on CC cells (49). Zhao et al. demonstrated that ACSL4-mediated ferroptosis plays an essential role in the effect of the combination of paclitaxel and propofol against cancer (50). More interestingly, Li et al. demonstrated that the expression of ACSL4 was significantly lower in patients with lung adenocarcinoma, and the prognosis was poor compared with that in patients with high expression of ACSL4 (119). By contrast, some studies have also proven that the high expression of ACSL4 promotes the development of lung cancer. Owing to the heterogeneity of tumors, the role of ACSL4 in different cancers is not consistent, and the mechanism of ACSL4 in cancer promotion and inhibition is complex and variable. However, targeting ACSL4 can regulate tumor progression, so ACSL4 is very likely to be a novel target for treatment.

### 5 Targeting fatty acid oxidation

Fatty acid oxidation (FAO) must first occur through the action of carnitine palmitoyl transferase (CPT), which is composed of CPT1 and CPT2 located in the outer and inner membranes of mitochondria. CPT1 has three isoforms, CPT1A, CPT1B and CPT1C (120, 121). Recently, FAO has been suggested to be closely linked to cancer progression, proliferation and drug resistance. ATP is significantly decreased by blocking FAO in cancer cells (121–123). CPT1A is highly expressed in prostate cancer (124), nasopharyngeal carcinoma (125, 126), glioblastoma

(127), etc. Inhibition of CPT1A significantly inhibits tumor growth, improves survival, and increases the sensitivity of nasopharyngeal carcinoma to radiotherapy (125). Almost all CCs are associated with high-risk HPV infections, and HPV16 is responsible for nearly 50% of infections (12, 13). The level of CPT1A in HPV16-positive CC tissues was reported to be markedly higher than that in normal tissues, suggesting that CPT1A could promote cervical cancer progression through lipid metabolism modifications (51). The overexpression of adipose-triglyceride lipase (ATGL) was also found to be dependent on the induction of hypoxia-inducible factor-1 $\alpha$  (HIF1 $\alpha$ ) by reactive oxygen species (ROS), which are mediated by increased mitochondrial FAO to promote CC cell proliferation (52). Xiao et al. demonstrated that SIRT3 can promote the invasion of CC cells by activating the AMPK/PPAR pathway (128). Notably, AMPK activators and PPAR activators can induce CPT1 expression, thereby enhancing FAO (129, 130). In a phase III clinical trial conducted in a resource-scarce environment, eugenol, a CPT1 inhibitor, as one of the ingredients of antiviral AV2, was slightly effective in inducing the regression of cervical precancerous lesions, although there was no statistically significant difference between the treatment and placebo groups. However, this lack of statistical significance may change in a later stage in a high-resource environment and by expanding the sample size (131). Research on the involvement of CPT in cervical cancer seems to have received little attention, but it may bring new insights into the treatment of CC.

## 6 Targeting the intracellular transport of fatty acids

Fatty acid-binding proteins (FABPs) are a series of lipid chaperones and members of the superfamily of intracellular lipid-binding proteins. These proteins are mainly involved in the transport of intracellular fatty acids between organelles and promote fatty acid solubilization and metabolism. Recent studies have found that FABPs play an increasingly prominent role in oncology, and tumor progression and invasion may be linked to an elevated level of an exogenous FABP (132). A study has shown that circulating levels of A-FABP, also known as FABP4, are significantly higher in obese patients with breast cancer than in those without breast cancer, and circulating A-FABP enhances tumor stemness and aggressiveness by activating the IL-6/STAT3/ALDH1 pathway (133). FABPs are found not only in breast cancer but also in ovarian cancer (134, 135), acute myeloid leukemia (136), and liver cancer (137, 138). Interestingly, both FABP4 and FABP5 seem to play a role in CC. Real-time quantitative PCR and western blotting were used to evaluate the expression of FABP5 in 206 CC and 40 normal cervical tissues, and the mRNA and protein expression of the FABP5 was found to be significantly upregulated in CC tissues ( $P < 0.05$ ). *In vitro* experiments with silenced FABP5 showed that cell proliferation and migration were significantly decreased. In an *in vivo* xenograft model and lung metastasis model, the tumor formation ability of mice was significantly reduced ( $P < 0.001$ ), and tumor metastasis in each side

of the lung lobe was also significantly reduced ( $P < 0.001$ ). The mechanism may involve the promotion of the occurrence and metastasis of CC through the upregulation of MMP-2 and MMP-9 (139). Consistent with the results of Liu et al, an experiment found that FABP5 expression was significantly upregulated in CC with lymph node metastasis, and FABP5 was an independent prognostic factor in multivariate Cox proportional risk model analysis. A Kaplan-Meier survival curve and log-rank test showed that patients with high FABP5 expression had significantly lower RFS and OS. In nude mice with lymph node metastasis, FABP5 knockdown resulted in a higher survival. Mechanistically, FABP5 expression promotes the invasion, EMT, and lymphangiogenesis by increasing the levels of intracellular fatty acids in CC to activate NF- $\kappa$ B signaling. Treatment with orlistat suppresses this effect (43). Previous work has suggested that high expression of FABP5 is positively correlated with the existence of lymph node metastasis in CC (44, 45). An experiment found that the long noncoding RNA LNMICC could promote the tumor growth, CC cell proliferation and lymph node metastasis by recruiting NPM1 to the promoter of FABP5 (46). Additionally, Jin et al. found that the FABP4 level in CSCC was strikingly higher than that in normal tissue (47), which is in line with the conclusions of previous investigations (140, 141). Moreover, the elevation of FABP4 has been shown to promote EMT through the activation of the AKT/GSK3 $\beta$ /Snail pathway in CSCC. Li et al. screened 243 genes related to lymph node metastasis in 178 TCGA CC samples and analyzed these genes by univariate and multivariate Cox regression analyses of FABP4 (HR=1.582,  $P < 0.001$ ) FABP4 (HR=1.384,  $P=0.024$ ). It was proven that FABP4 could be used as a prognostic factor to evaluate OS. Cell experiments also showed that FABP4 could promote the occurrence of lymph node metastasis by activating the AKT signaling pathway, thus accelerating the process of EMT (140). FABPs are undoubtedly potential biomarkers or targets in patients with CC.

## 7 Targeting the intracellular lipolytic pathway

It has been reported that intracellular lipolysis may be closely related to the survival and growth of tumor cells. Lipolysis is the process in which triglycerides stored in fat cells are hydrolyzed to produce fatty acids, thereby supplying internal or whole-body energy (142–144). This process occurs through the actions of ATGL, hormone-sensitive lipase (HSL) and monoglyceride lipase (MAGL) in turn. However, the role of lipase in cancer is still unclear. Various exceptional literature reports and reviews have also elaborated the association between lipases and cancer (144–146), among which the relationship between MAGL and cancer has been discussed the most. Castelli et al. showed that the expression of ATGL in CC was extremely high, they verified their results by bioinformatics analysis of a large human cervical cancer sample data set on an Affymetrix-U133-plus2.0 array and found that the expression level of ATGL was positively correlated with the grade of CC. Additionally, ATGL promotes tumor cell proliferation and

invasion through ROS production and HIF1 $\alpha$  induction (52). Meanwhile, HIF1 $\alpha$  is also closely related to radiotherapy resistance and paclitaxel resistance in CC (147, 148). One study demonstrated that 2,4-dienyl-CoA reductase (DEC1) enhanced the expression of HSL to increase lipolysis and thus promote the release of fatty acids, leading to malignant progression of CC (53). Interestingly, a study also showed that the level of MAGL was upregulated in CC cells and tissues. The use of the MAGL inhibitor JZL184 or gene knockout induces apoptosis in CC cells by mediating the downregulation of Bcl-2 and the upregulation of cleaved caspase-3 and Bax (54). Lipase may be a promising target to treat CC and alleviate its drug resistance.

## 8 Targeting transcriptional regulators of fatty acid metabolism

In addition to FASN, another key factor worth noting is sterol regulatory element binding protein 1 (SREBP-1). SREBP-1 activation promotes the expression of FASN, ACC, and SCD1, thereby enhancing lipid synthesis (149). SREBP binds to SREBP cleavage-activating protein (SCAP) in the ER and is negatively regulated by endogenous sterol levels (150). When sterols are abundant, INSIGs bind tightly to SCAP and restrict SREBP to the endoplasmic reticulum. Once sterol levels drop, INSIGs dissociate from the SCAP protein, and the SREBP-SCAP complex enters the Golgi. These proteins are sequentially cleaved at the Golgi by site-1 and site-2 proteases (S1P and S2P). This releases the N-terminus of SREBP, which eventually binds to sterol response elements (SREs) in the nucleus to activate transcription (Figure 2) (150, 151). Several excellent reviews have elucidated the role of SREBP-1 in cancer, and tumor proliferation can be inhibited by knocking down or inhibiting SREBP-1 expression (62, 149, 152). One experiment proved that the level of SREBP-1 was high in CC cells, and quercetin (a naturally occurring polyphenolic flavonoid) could reduce the levels of SREBP-1 and its transcriptional targets by reducing the O-

GlcNAcylation of AMPK. Thus, the growth of CC cells are inhibited and apoptosis is induced (Figure 3) (55). This is compatible with several studies suggesting that AMPK activation leads to the phosphorylation of SREBP-1, which slows cancer progression by inhibiting its nuclear translocation and the transcription of target genes (153, 154). Interestingly, O-GlcNAcylation-mediated inactivation of AMPK also accelerated the growth of colon cancer cells (155). An experiment also showed that O-linked N-acetylglucosamine transferase (OGT) upregulated the expression of O-GlcNAcylated LXRs and increased sCLU (a glycoprotein) levels by inducing SREBP-1 expression to regulate apoptosis, the cell cycle and cisplatin resistance (Figure 3) (56). Interestingly, Yang et al. showed that the levels of human hydroxysteroid dehydrogenase 2 (HSDL2) in CC tissues were significantly higher than those in normal tissues and HSDL2 upregulated the expression of FASN, ACSL and SREBP-1, thus inducing stronger invasiveness of CC. When SREBP-1 was knocked down, the proliferation and migration of CC cells were significantly inhibited (156). As a transcriptional regulator of lipid metabolism, SREBP-1 may become a new therapeutic breakthrough.

## 9 Targeting other lipid metabolic pathways

Lipids are a class of substances that are insoluble in water and include glycerol phosphates, triglycerides, sterols, and sphingolipids (157). A large number of studies have proved that disorders of lipid metabolism are closely related to the occurrence of various cancers. It is worth noting that the relationship between phospholipids and cholesterol levels and cancer has received much less attention in the past. However, research has shown that lysophosphatidic acid (LPA) may be a potential biomarker of gynecological cancer (65). LPA is a glycerophospholipid that stimulates cell migration and tumor cell invasion. Interestingly, Sui et al. showed that the serum LPA level in cervical cancer patients was significantly higher than

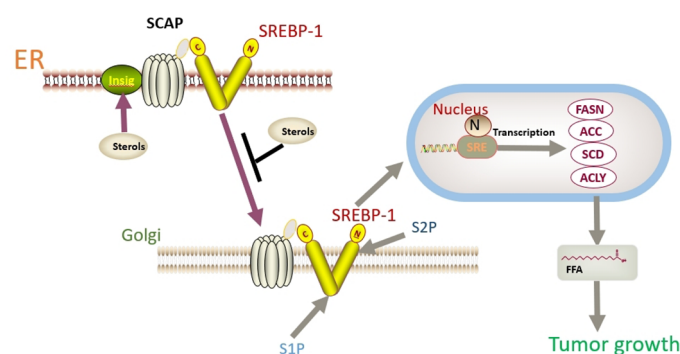


FIGURE 2

SREBP binds to SCAP in the ER and is negatively regulated by endogenous sterol levels. When sterols are abundant, INSIGs bind tightly to SCAP and restrict SREBP to the endoplasmic reticulum. Once sterol levels drop, INSIGs dissociate from the SCAP protein, and the SREBP-SCAP complex enters the Golgi. These proteins are sequentially cleaved at the Golgi by S1P and S2P. This releases the N-terminus of SREBP, which eventually binds to sterol response elements (SREs) in the nucleus to activate transcription.



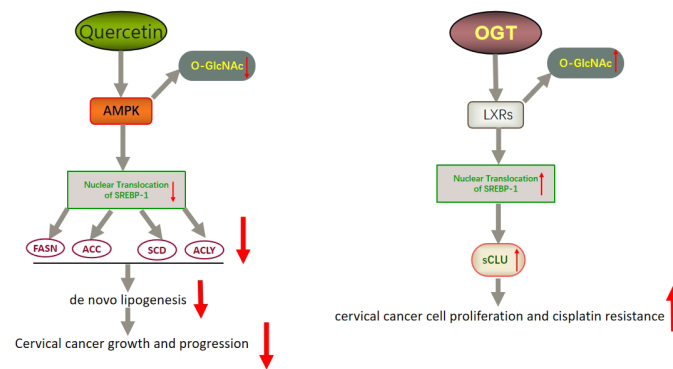


FIGURE 3

Schematic representation of quercetin- and OGT-mediated effects on adipogenesis and cell growth in CC. Quercetin could reduce the expression of SREBP-1 and its transcriptional targets by reducing the O-GlcNAcylation of AMPK. Thus, the growth of CC cells is inhibited and apoptosis is induced. OGT upregulated the expression of O-GlcNAcylated LXRs and increased sCLU levels by inducing SREBP-1 expression. Thus, CC cells become resistant to chemotherapy drugs such as cisplatin. LXRs, liver X receptors; sCLU, secretory clusterin.

that in healthy people, which was consistent with the results of Xu et al. (65), and found that LPA stimulated the progression of CC through the Ras/Raf1/MEK/ERK pathway. Noticeably, LPA could block the alterations in the caspase-3 enzyme activity caused by cisplatin, resulting in the resistance to cisplatin-induced apoptosis (57). An experiment also showed that LPA markedly reduced the expression level of the caspase-3 protein in doxorubicin hydrochloride-induced CC cells and protected CC cells from doxorubicin hydrochloride-induced apoptosis (58). These results provide sufficient experimental basis for the possibility of using LPA as a therapeutic target for CC. Lipogenesis generally includes fatty acid synthesis and the mevalonate pathway, the latter referring to isoprenoid and cholesterol synthesis. It is well known that acetyl-CoA is the raw material for the synthesis of fatty acids and cholesterol (158). Studies have shown that HMG-CoA inhibitors, statins, can not only reduce cholesterol levels but also inhibit cell proliferation and chemical resistance in gynecological cancers, including CC (159). At the same time, an experiment has found an unexpected link between fatty acid metabolism and cholesterol metabolism (160). MiR-1908 is a miRNA located in the intron of fatty acid desaturase 1 gene. It has been found that miR-1908 is highly expressed in CC, ovarian cancer, breast cancer and other tumors and is related to their poor prognosis. It is interesting that the expression of miR-1908 is regulated by free fatty acids, cholesterol, SCD1 and other factors (59). Liu et al. proved that FASN, a key enzyme in fatty acid synthesis, was highly expressed in patients with CC and found that FASN could regulate cholesterol metabolism, increase total cholesterol and free cholesterol when overexpressed, lead to lipid raft reprogramming and actin remodeling, and help enhance the invasion and migration of CC cells. After targeted inhibition of FASN, the total amount of cholesterol and free cholesterol decreased, thus effectively reducing the lymph node metastasis of CC (28). A recent experiment showed that the mechanism of FASN regulation of cholesterol metabolism in liver cancer was similar to this mechanism (161). The interference between these metabolic pathways provides more possibilities for targeted therapy of CC.

## 10 Dietary interventions

In several large studies, obesity and a high body mass index have been found to be positively associated with the development of CC (162, 163). These studies have also proved that the diet influences the occurrence and progression of cancer, and the level of fatty acid intake has been shown to contribute to these effects (164–166). Among fatty acids, omega-3 polyunsaturated fatty acids ( $\omega$ -3 PUFAs), such as  $\alpha$ -linolenic acid ( $\alpha$ -ALA), docosahexaenoic acid (DHA), and eicosapentaenoic acid (EPA), are widely believed to have triglyceride-lowering and anti-inflammatory properties, whereas  $\omega$ -6 PUFAs, including linoleic acid (LA) and arachidonic acid (AA), are thought to be involved in proinflammatory mechanisms (167–169). One study showed that increased consumption of  $\omega$ -3 PUFAs (EPA) in men with prostate cancer reduced tumor vascularization and inhibited the progression of prostate cancer (170). Similarly,  $\omega$ -3 PUFAs inhibit the invasion of gastric cancer through the COX-1/PGE3 signaling axis, and  $\omega$ -6 PUFAs enhance the potential of malignant metastasis through COX-2/PGE2 (171). A randomized controlled study suggested that increasing the intake of  $\omega$ -3 PUFAs was effective in maintaining the nutritional status and skeletal muscle mass in women with CC and alleviating the toxicity of chemoradiotherapy (172).  $\alpha$ -ALA inhibits the growth of CC cells by downregulating the expression of HPV oncoproteins E6 and E7, thereby restoring the expression of Rb and p53 (173). Notably, DHA could induce the apoptosis of CC cells by reducing the levels of the anti-apoptotic proteins Bax, cleaved caspase-3 and Bcl-2 and regulate the levels of VEGF and MMP-9 to control the invasion of CC cells (174). However, excessive intake of  $\omega$ -3 PUFAs may result in immunosuppression and other adverse effects. Since  $\omega$ -3 PUFAs and  $\omega$ -6 PUFAs are both essential fatty acids, it is necessary to reasonably adjust the diet, aiming to control their appropriate levels. Olive oil, a component of the Mediterranean diet, has recently been found to have antitumor effects in breast, prostate and other cancers (175). The main ingredient in olive oil is oleic acid (OA), which has recently been found to promote the progression of CC *in vitro* and



*in vivo* (40, 176). However, Muhammad et al. found that monounsaturated and diunsaturated fatty acids could improve the sensitivity of obese patients with CC to radiotherapy, and the tumor volume was significantly reduced in a mouse xenograft tumor model treated with oleate and radiotherapy compared with that in the radiotherapy alone group. The supplementation of oleate and linoleate during radiotherapy increases the expression of P53, PPAR $\gamma$ , and CD36 to support increased free fatty acid uptake, thereby regulating the cell cycle and inducing apoptosis (177). However, these contradictory results make the effect of dietary olive oil or OA on cancer inconclusive. Complex interactions between environmental factors and genetics may partially explain this phenomenon. At a later stage, much research is still needed to explain the link between dietary olive oil or OA and cancer. Certainly, a diet combined with other treatments may have greater potential for the treatment of CC.

## 11 Conclusion

Lipid reprogramming has been widely confirmed as an important marker of CC that can act on membrane production, energy production and signal transduction to control cell growth, differentiation and motility. This review analyzed in detail the involvement of various pathways of fatty acid metabolism in CC. Targeting or knocking down proteins or enzymes involved in the process of fatty acid metabolism can effectively limit the growth and progression of CC cells, inhibit lymph node metastasis to a certain extent, improve the sensitivity of CC to chemoradiotherapy, and significantly improve the treatment effect and prognosis. Therefore, targeting fatty acid metabolism is extraordinarily attractive for the treatment of CC to achieve precise antitumor effects. However, due to the plasticity of tumor fatty acid metabolism, few preclinical

studies can be effectively applied to the clinical field. A novel combination strategy or strict diet provides promising prospects. Further experiments to investigate the dynamic relationship between fatty acid metabolism reprogramming and CC and to overcome the complexity and plasticity of fatty acid metabolism in cancer are extremely important. Although this road is tortuous, fatty acid metabolism and its related lipid metabolism pathways are expected to become new targets for CC treatment.

## Author contributions

All authors contributed to the review conception and design. The first draft of the manuscript was written by PP and all authors commented on previous versions of the manuscript. All authors contributed to the article and approved the submitted version.

## Conflict of interest

The authors declare that the research was conducted in the absence of any commercial or financial relationships that could be construed as a potential conflict of interest.

## Publisher's note

All claims expressed in this article are solely those of the authors and do not necessarily represent those of their affiliated organizations, or those of the publisher, the editors and the reviewers. Any product that may be evaluated in this article, or claim that may be made by its manufacturer, is not guaranteed or endorsed by the publisher.

## References

- Serrano B, Brotons M, Bosch FX, Bruni L. Epidemiology and burden of hpv-related disease. *Best Pract Res Clin Obstetrics Gynaecol* (2018) 47:14–26. doi: 10.1016/j.bpobgyn.2017.08.006
- Falcaro M, Castañón A, Ndlela B, Checchi M, Soldan K, Lopez-Bernal J, et al. The effects of the national hpv vaccination programme in England, uk, on cervical cancer and grade 3 cervical intraepithelial neoplasia incidence: A register-based observational study. *Lancet (London England)* (2021) 398(10316):2084–92. doi: 10.1016/s0140-6736(21)02178-4
- Siegel RL, Miller KD, Fuchs HE, Jemal A. Cancer statistics, 2022. *CA Cancer J Clin* (2022) 72(1):7–33. doi: 10.3322/caac.21708
- Cohen PA, Jhingran A, Oaknin A, Denny L. Cervical cancer. *Lancet (London England)* (2019) 393(10167):169–82. doi: 10.1016/s0140-6736(18)32470-x
- Watson M, Saraiya M, Benard V, Coughlin SS, Flowers L, Cokkinides V, et al. Burden of cervical cancer in the united states, 1998–2003. *Cancer* (2008) 113(10 Suppl):2855–64. doi: 10.1002/cncr.23756
- Wang W, Zhang F, Hu K, Hou X. Image-guided, intensity-modulated radiation therapy in definitive radiotherapy for 1433 patients with cervical cancer. *Gynecol Oncol* (2018) 151(3):444–8. doi: 10.1016/j.ygyno.2018.09.024
- Hu K, Wang W, Liu X, Meng Q, Zhang F. Comparison of treatment outcomes between squamous cell carcinoma and adenocarcinoma of cervix after definitive radiotherapy or concurrent chemoradiotherapy. *Radiat Oncol (London England)* (2018) 13(1):249. doi: 10.1186/s13014-018-1197-5
- Fu J, Wang W, Wang Y, Liu C, Wang P. The role of squamous cell carcinoma antigen (ScC Ag) in outcome prediction after concurrent chemoradiotherapy and treatment decisions for patients with cervical cancer. *Radiat Oncol (London England)* (2019) 14(1):146. doi: 10.1186/s13014-019-1355-4
- Jeong BK, Choi DH, Huh SJ, Park W, Bae DS, Kim BG. The role of squamous cell carcinoma antigen as a prognostic and predictive factor in carcinoma of uterine cervix. *Radiat Oncol J* (2011) 29(3):191–8. doi: 10.3857/roj.2011.29.3.191
- Xu F, Li Y, Fan L, Ma J, Yu L, Yi H, et al. Preoperative scc-Ag and thrombocytosis as predictive markers for pelvic lymphatic metastasis of squamous cervical cancer in early figo stage. *J Cancer* (2018) 9(9):1660–6. doi: 10.7150/jca.24049
- Lee SW, Hong JH, Yu M, Jeong S, Kim SH, Kim YS, et al. Serum conversion pattern of scc-Ag levels between pre- and post-chemoradiotherapy predicts recurrence and metastasis in cervical cancer: A multi-institutional analysis. *Clin Exp Metastasis* (2021) 38(5):467–74. doi: 10.1007/s10585-021-10115-w
- Quist KM, Solorzano I, Wendel SO, Chintala S, Wu C, Wallace NA, et al. Cervical cancer development: Implications of Hpv16 E6e7-Nfx1-123 regulated genes. *Cancers (Basel)* (2021) 13(24):6182. doi: 10.3390/cancers13246182
- Zeng J, He SL, Li LJ, Wang C. Hsp90 up-regulates pd-L1 to promote hpv-positive cervical cancer Via Her2/Pi3k/Akt pathway. *Mol Med* (2021) 27(1):130. doi: 10.1186/s10020-021-00384-2
- Fernandes A, Viveros-Carreño D, Hoegl J, Ávila M, Pareja R. Human papillomavirus-independent cervical cancer. *Int J Gynecol Cancer* (2022) 32(1):1–7. doi: 10.1136/ijgc-2021-003014
- Lee JE, Chung Y, Rhee S, Kim TH. Untold story of human cervical cancers: Hpv-negative cervical cancer. *BMB Rep* (2022) 55(9):429–38. doi: 10.5483/BMBRep.2022.55.9.042

16. Castle PE, Einstein MH, Sahasrabudhe VV. Cervical cancer prevention and control in women living with human immunodeficiency virus. *CA Cancer J Clin* (2021) 71(6):505–26. doi: 10.3322/caac.21696
17. Olawaiye AB, Baker TP, Washington MK, Mutch DG. The new (Version 9) American joint committee on cancer tumor, node, metastasis staging for cervical cancer. *CA Cancer J Clin* (2021) 71(4):287–98. doi: 10.3322/caac.21663
18. Schmeler KM, Batman SH. Human papillomavirus-independent cervical cancer: What are the implications? *Int J Gynecol Cancer* (2022) 32(1):8. doi: 10.1136/ijgc-2021-003250
19. Koh WJ, Abu-Rustum NR, Bean S, Bradley K, Campos SM, Cho KR, et al. Cervical cancer, version 3.2019, nccn clinical practice guidelines in oncology. *J Natl Compr Cancer Netw JNCCN* (2019) 17(1):64–84. doi: 10.6004/jnccn.2019.0001
20. Rose PG, Bundy BN, Watkins EB, Thigpen JT, Deppe G, Maiman MA, et al. Concurrent cisplatin-based radiotherapy and chemotherapy for locally advanced cervical cancer. *N Engl J Med* (1999) 340(15):1144–53. doi: 10.1056/nejm199904153401502
21. Lee YH, Chong GO, Kim SJ, Hwang JH, Kim JM, Park NJ, et al. Prognostic value of lymph node characteristics in patients with cervical cancer treated with radical hysterectomy. *Cancer Manag Res* (2021) 13:8137–45. doi: 10.2147/cmar.S332612
22. Pinto PJJ, Chen MJ, Santos Neto E, Faloppa CC, De Brot L, Guimaraes APG, et al. Prognostic factors in locally advanced cervical cancer with pelvic lymph node metastasis. *Int J Gynecol Cancer* (2022) 32(3):239–45. doi: 10.1136/ijgc-2021-003140
23. Obrzut B, Semczuk A, Naróg M, Obrzut M, Król P. Prognostic parameters for patients with cervical cancer figo stages Ia2-iiB: A long-term follow-up. *Oncology* (2017) 93(2):106–14. doi: 10.1159/000471766
24. Frenel JS, Le Tourneau C, O'Neill B, Ott PA, Piha-Paul SA, Gomez-Roca C, et al. Safety and efficacy of pembrolizumab in advanced, programmed death ligand 1-positive cervical cancer: Results from the phase Ib keynote-028 trial. *J Clin Oncol* (2017) 35(36):4035–41. doi: 10.1200/jco.2017.74.5471
25. Tewari KS, Sill MW, Penson RT, Huang H, Ramondetta LM, Landrum LM, et al. Bevacizumab for advanced cervical cancer: Final overall survival and adverse event analysis of a randomised, controlled, open-label, phase 3 trial (Gynecologic oncology group 240). *Lancet (London England)* (2017) 390(10103):1654–63. doi: 10.1016/s0140-6736(17)31607-0
26. Warburg O. On the origin of cancer cells. *Science* (1956) 123(3191):309–14. doi: 10.1126/science.123.3191.309
27. Koundouros N, Poulogiannis G. Reprogramming of fatty acid metabolism in cancer. *Br J Cancer* (2020) 122(1):4–22. doi: 10.1038/s41416-019-0650-z
28. Du Q, Liu P, Zhang C, Liu T, Wang W, Shang C, et al. Fasn promotes lymph node metastasis in cervical cancer via cholesterol reprogramming and lymphangiogenesis. *Cell Death Dis* (2022) 13(5):488. doi: 10.1038/s41419-022-04926-2
29. Rios Garcia M, Steinbauer B, Srivastava K, Singhal M, Mattijssen F, Maida A, et al. Acetyl-coa carboxylase 1-dependent protein acetylation controls breast cancer metastasis and recurrence. *Cell Metab* (2017) 26(6):842–55.e5. doi: 10.1016/j.cmet.2017.09.018
30. Shang C, Li Y, He T, Liao Y, Du Q, Wang P, et al. The prognostic mir-532-5p-Correlated cerna-mediated lipid droplet accumulation drives nodal metastasis of cervical cancer. *J Adv Res* (2022) 37:169–84. doi: 10.1016/j.jare.2021.09.009
31. Li B, Sui L. Metabolic reprogramming in cervical cancer and metabolomics perspectives. *Nutr Metab* (2021) 18(1):93. doi: 10.1186/s12986-021-00615-7
32. Nascimento J, Mariot C, Vianna DRB, Kliemann LM, Chaves PS, Loda M, et al. Fatty acid synthase as a potential new therapeutic target for cervical cancer. *Anais Acad Bras Cienc* (2022) 94(2):e20210670. doi: 10.1590/0001-376520220210670
33. Guo W, Abudumijiti H, Xu L, Hasim A. Cd147 promotes cervical cancer migration and invasion by up-regulating fatty acid synthase expression. *Int J Clin Exp Pathol* (2019) 12(12):4280–8.
34. Xin M, Qiao Z, Li J, Liu J, Song S, Zhao X, et al. Mir-22 inhibits tumor growth and metastasis by targeting atp citrate lyase: Evidence in osteosarcoma, prostate cancer, cervical cancer and lung cancer. *Oncotarget* (2016) 7(28):44252–65. doi: 10.18632/oncotarget.10020
35. Xu LX, Hao LJ, Ma JQ, Liu JK, Hasim A. Sirt3 promotes the invasion and metastasis of cervical cancer cells by regulating fatty acid synthase. *Mol Cell Biochem* (2020) 464(1–2):11–20. doi: 10.1007/s11010-019-03644-2
36. Huang D, Li C. Circ-acaca promotes proliferation, invasion, migration and glycolysis of cervical cancer cells by targeting the mir-582-5p/Ero1a signaling axis. *Oncol Lett* (2021) 22(5):795. doi: 10.3892/ol.2021.13056
37. Gu S, Song X, Xie R, Ouyang C, Xie L, Li Q, et al. Berberine inhibits cancer cells growth by suppressing fatty acid synthesis and biogenesis of extracellular vesicles. *Life Sci* (2020) 257:118122. doi: 10.1016/j.lfs.2020.118122
38. Wang L, Ye G, Wang Y, Wang C. Stearoyl-coa desaturase 1 regulates malignant progression of cervical cancer cells. *Bioengineered* (2022) 13(5):12941–54. doi: 10.1080/21655979.2022.2079253
39. Deng M, Cai X, Long L, Xie L, Ma H, Zhou Y, et al. Cd36 promotes the epithelial-mesenchymal transition and metastasis in cervical cancer by interacting with tgfb- $\beta$ . *J Trans Med* (2019) 17(1):352. doi: 10.1186/s12967-019-2098-6
40. Yang P, Su C, Luo X, Zeng H, Zhao L, Wei L, et al. Dietary oleic acid-induced Cd36 promotes cervical cancer cell growth and metastasis via up-regulation Src/Erk pathway. *Cancer Lett* (2018) 438:76–85. doi: 10.1016/j.canlet.2018.09.006
41. Zhang J, Li X, Yang J, Zhang Y. Mir-1254 suppresses the proliferation and invasion of cervical cancer cells by modulating Cd36. *J Trans Med* (2022) 19(Suppl 2):531. doi: 10.1186/s12967-022-03582-6
42. An J, Oh HE, Kim H, Lee JH, Lee ES, Kim YS, et al. Significance of altered fatty acid transporter expressions in uterine cervical cancer and its precursor lesions. *Anticancer Res* (2022) 42(4):2131–7. doi: 10.21873/anticancer.15695
43. Zhang C, Liao Y, Liu P, Du Q, Liang Y, Ooi S, et al. Fapb5 promotes lymph node metastasis in cervical cancer by reprogramming fatty acid metabolism. *Theranostics* (2020) 10(15):6561–80. doi: 10.7150/thno.44868
44. Wang W, Jia HL, Huang JM, Liang YC, Tan H, Geng HZ, et al. Identification of biomarkers for lymph node metastasis in early-stage cervical cancer by tissue-based proteomics. *Br J Cancer* (2014) 110(7):1748–58. doi: 10.1038/bjc.2014.92
45. Wang W, Chu HJ, Liang YC, Huang JM, Shang CL, Tan H, et al. Fapb5 correlates with poor prognosis and promotes tumor cell growth and metastasis in cervical cancer. *Tumour Biol* (2016) 37(11):14873–83. doi: 10.1007/s13277-016-5350-1
46. Shang C, Wang W, Liao Y, Chen Y, Liu T, Du Q, et al. Lnmic promotes nodal metastasis of cervical cancer by reprogramming fatty acid metabolism. *Cancer Res* (2018) 78(4):877–90. doi: 10.1158/0008-5472.Can-17-2356
47. Jin J, Zhang Z, Zhang S, Chen X, Chen Z, Hu P, et al. Fatty acid binding protein 4 promotes epithelial-mesenchymal transition in cervical squamous cell carcinoma through Akt/Gsk3 $\beta$ /Snail signaling pathway. *Mol Cell Endocrinol* (2018) 461:155–64. doi: 10.1016/j.mce.2017.09.005
48. Xiaofei J, Mingqing S, Miao S, Yizhen Y, Shuang Z, Qinhua X, et al. Oleonic acid inhibits cervical cancer hela cell proliferation through modulation of the Acl4 ferroptosis signaling pathway. *Biochem Biophys Res Commun* (2021) 545:81–8. doi: 10.1016/j.bbrc.2021.01.028
49. Ou R, Lu S, Wang L, Wang Y, Lv M, Li T, et al. Circular rna Cirlmo1 suppresses cervical cancer growth and metastasis by triggering mir-4291/Acl4-Mediated ferroptosis. *Front Oncol* (2022) 12:858598. doi: 10.3389/fonc.2022.858598
50. Zhao MY, Liu P, Sun C, Pei LJ, Huang YG. Propofol augments paclitaxel-induced cervical cancer cell ferroptosis in vitro. *Front Pharmacol* (2022) 13:816432. doi: 10.3389/fphar.2022.816432
51. Abudula A, Rouzi N, Xu L, Yang Y, Hasimu A. Tissue-based metabolomics reveals potential biomarkers for cervical carcinoma and hpv infection. *Bosnian J Basic Med Sci* (2020) 20(1):78–87. doi: 10.17305/bjbm.2019.4359
52. Castelli S, Ciccarone F, Taviani D, Ciriolo MR. Ros-dependent Hif1 $\alpha$  activation under forced lipid catabolism entails glycolysis and mitophagy as mediators of higher proliferation rate in cervical cancer cells. *J Exp Clin Cancer Res* (2021) 40(1):94. doi: 10.1186/s13046-021-01887-w
53. Zhou H, Zhang J, Yan Z, Qu M, Zhang G, Han J, et al. Decr1 directly activates hsl to promote lipolysis in cervical cancer cells. *Biochim Biophys Acta Mol Cell Biol Lipids* (2022) 1867(3):159090. doi: 10.1016/j.bbalip.2021.159090
54. Wang C, Li Z, Zhong L, Chen Y. Inhibition of monoacylglycerol lipase restrains proliferation, migration, invasion, tumor growth and induces apoptosis in cervical cancer. *J Obstetrics Gynaecol Res* (2022) 48(2):456–66. doi: 10.1111/jog.15110
55. Ali A, Kim MJ, Kim MY, Lee HJ, Roh GS, Kim HJ, et al. Quercetin induces cell death in cervical cancer by reducing O-glucacylation of adenosine monophosphate-activated protein kinase. *Anat Cell Biol* (2018) 51(4):274–83. doi: 10.5115/acb.2018.51.4.274
56. Kim MJ, Choi MY, Lee DH, Roh GS, Kim HJ, Kang SS, et al. O-Linked n-acetylglucosamine transferase enhances secretory clusterin expression via liver X receptors and sterol response element binding protein regulation in cervical cancer. *Oncotarget* (2018) 9(4):4625–36. doi: 10.18632/oncotarget.23588
57. Sui Y, Yang Y, Wang J, Li Y, Ma H, Cai H, et al. Lysophosphatidic acid inhibits apoptosis induced by cisplatin in cervical cancer cells. *BioMed Res Int* (2015) 2015:598386. doi: 10.1155/2015/598386
58. Wang X, Wang H, Mou X, Xu Y, Han W, Huang A, et al. Lysophosphatidic acid protects cervical cancer hela cells from apoptosis induced by doxorubicin hydrochloride. *Oncol Lett* (2022) 24(2):267. doi: 10.3892/ol.2022.13387
59. Shen J, Wu Y, Ruan W, Zhu F, Duan S. Mir-1908 dysregulation in human cancers. *Front Oncol* (2022) 12:857743. doi: 10.3389/fonc.2022.857743
60. Butler LM, Perone Y, Dehairs J, Lupien LE, de Laat V, Talebi A, et al. Lipids and cancer: Emerging roles in pathogenesis, diagnosis and therapeutic intervention. *Adv Drug Delivery Rev* (2020) 159:245–93. doi: 10.1016/j.addr.2020.07.013
61. Corn KC, Windham MA, Rafat M. Lipids in the tumor microenvironment: From cancer progression to treatment. *Prog Lipid Res* (2020) 80:101055. doi: 10.1016/j.plipres.2020.101055
62. Cheng C, Geng F, Cheng X, Guo D. Lipid metabolism reprogramming and its potential targets in cancer. *Cancer Commun (Lond)* (2018) 38(1):27. doi: 10.1186/s40880-018-0301-4
63. Singh KB, Hahm ER, Kim SH, Wendell SG, Singh SV. A novel metabolic function of myc in regulation of fatty acid synthesis in prostate cancer. *Oncogene* (2021) 40(3):592–602. doi: 10.1038/s41388-020-01553-z
64. Madak-Erdogan Z, Band S, Zhao YC, Smith BP, Kulkoyluoglu-Cotul E, Zuo Q, et al. Free fatty acids rewire cancer metabolism in obesity-associated breast cancer via estrogen receptor and mtor signaling. *Cancer Res* (2019) 79(10):2494–510. doi: 10.1158/0008-5472.Can-18-2849

65. Xu Y, Shen Z, Wiper DW, Wu M, Morton RE, Elson P, et al. Lysophosphatidic acid as a potential biomarker for ovarian and other gynecologic cancers. *Jama* (1998) 280(8):719–23. doi: 10.1001/jama.280.8.719
66. Shen Z, Wu M, Elson P, Kennedy AW, Belinson J, Casey G, et al. Fatty acid composition of lysophosphatidic acid and lysophosphatidylinositol in plasma from patients with ovarian cancer and other gynecological diseases. *Gynecol Oncol* (2001) 83(1):25–30. doi: 10.1006/gyno.2001.6357
67. Koundouros N, Karali E, Tripp A, Valle A, Inglese P, Perry NJS, et al. Metabolic fingerprinting links oncogenic Pik3ca with enhanced arachidonic acid-derived eicosanoids. *Cell* (2020) 181(7):1596–611.e27. doi: 10.1016/j.cell.2020.05.053
68. Grunt TW, Wagner R, Grusch M, Berger W, Singer CF, Marian B, et al. Interaction between fatty acid synthase- and erbb-systems in ovarian cancer cells. *Biochem Biophys Res Commun* (2009) 385(3):454–9. doi: 10.1016/j.bbrc.2009.05.085
69. Tomek K, Wagner R, Varga F, Singer CF, Karlic H, Grunt TW. Blockade of fatty acid synthase induces ubiquitination and degradation of phosphoinositide-3-Kinase signaling proteins in ovarian cancer. *Mol Cancer Res* (2011) 9(12):1767–79. doi: 10.1158/1541-7786.MCR-10-0467
70. Loftus TM, Jaworsky DE, Frehywot GL, Townsend CA, Ronnett GV, Lane MD, et al. Reduced food intake and body weight in mice treated with fatty acid synthase inhibitors. *Science* (2000) 288(5475):2379–81. doi: 10.1126/science.288.5475.2379
71. Angeles TS, Hudkins RL. Recent advances in targeting the fatty acid biosynthetic pathway using fatty acid synthase inhibitors. *Expert Opin Drug Discovery* (2016) 11(12):1187–99. doi: 10.1080/17460441.2016.1245286
72. Zhou X, Chang TL, Chen S, Liu T, Wang H, Liang JF. Polydopamine-decorated orlistat-loaded hollow capsules with an enhanced cytotoxicity against cancer cell lines. *Mol Pharm* (2019) 16(6):2511–21. doi: 10.1021/acs.molpharmaceut.9b00116
73. Zhang C, Sheng L, Yuan M, Hu J, Meng Y, Wu Y, et al. Orlistat delays hepatocarcinogenesis in mice with hepatic Co-activation of akt and c-met. *Toxicol Appl Pharmacol* (2020) 392:114918. doi: 10.1016/j.taap.2020.114918
74. Li J, Dong L, Wei D, Wang X, Zhang S, Li H. Fatty acid synthase mediates the epithelial-mesenchymal transition of breast cancer cells. *Int J Biol Sci* (2014) 10(2):171–80. doi: 10.7150/ijbs.7357
75. Silva R, Zarricueta ML, Moreira DKT, de Moraes TR, Rizzardi KF, Parisotto TM, et al. Structured lipid containing behenic acid versus orlistat for weight loss: An experimental study in mice. *PharmaNutrition* (2020) 14:100213. doi: 10.1016/j.phanu.2020.100213
76. Pohlmann AR, Fonseca FN, Paese K, Detoni CB, Coradini K, Beck RC, et al. Poly (ε-caprolactone) microcapsules and nanocapsules in drug delivery. *Expert Opin Drug Delivery* (2013) 10(5):623–38. doi: 10.1517/17425247.2013.769956
77. Singh S, Karthikeyan C, Moorthy N. Recent advances in the development of fatty acid synthase inhibitors as anticancer agents. *Mini Rev Med Chem* (2020) 20(18):1820–37. doi: 10.2174/1389557520666200811100845
78. Falchook G, Infante J, Arkenau HT, Patel MR, Dean E, Borazanci E, et al. First-in-Human study of the safety, pharmacokinetics, and pharmacodynamics of first-in-Class fatty acid synthase inhibitor tvb-2640 alone and with a taxane in advanced tumors. *EClinicalMedicine* (2021) 34:100797. doi: 10.1016/j.eclinm.2021.100797
79. Loomba R, Mohseni R, Lucas KJ, Gutierrez JA, Perry RG, Trotter JF, et al. Tv-2640 (Fasn inhibitor) for the treatment of nonalcoholic steatohepatitis: Fascinate-1, a randomized, placebo-controlled phase 2a trial. *Gastroenterology* (2021) 161(5):1475–86. doi: 10.1053/j.gastro.2021.07.025
80. Heuer TS, Ventura R, Mordek K, Lai J, Fridlib M, Buckley D, et al. Fasn inhibition and taxane treatment combine to enhance anti-tumor efficacy in diverse xenograft tumor models through disruption of tubulin palmitoylation and microtubule organization and fasn inhibition-mediated effects on oncogenic signaling and gene expression. *EBioMedicine* (2017) 16:51–62. doi: 10.1016/j.ebiom.2016.12.012
81. Daemen A, Peterson D, Sahu N, McCord R, Du X, Liu B, et al. Metabolite profiling stratifies pancreatic ductal adenocarcinomas into subtypes with distinct sensitivities to metabolic inhibitors. *Proc Natl Acad Sci U.S.A.* (2015) 112(32):E4410–7. doi: 10.1073/pnas.1501605112
82. Ray KK, Bays HE, Catapano AL, Lalwani ND, Bloedon LT, Sterling LR, et al. Safety and efficacy of bempedoic acid to reduce ldl cholesterol. *N Engl J Med* (2019) 380(11):1022–32. doi: 10.1056/NEJMoa1803917
83. Morrow MR, Batchuluun B, Wu J, Ahmadi E, Leroux JM, Mohammadi-Shemirani P, et al. Inhibition of atp-citrate lyase improves Nash, liver fibrosis, and dyslipidemia. *Cell Metab* (2022) 34(6):919–36.e8. doi: 10.1016/j.cmet.2022.05.004
84. Icard P, Wu Z, Fournel L, Coquerel A, Lincet H, Alifano M. Atp citrate lyase: A central metabolic enzyme in cancer. *Cancer Lett* (2020) 471:125–34. doi: 10.1016/j.canlet.2019.12.010
85. Hatzivassiliou G, Zhao F, Bauer DE, Andreadis C, Shaw AN, Dhanak D, et al. Atp citrate lyase inhibition can suppress tumor cell growth. *Cancer Cell* (2005) 8(4):311–21. doi: 10.1016/j.ccr.2005.09.008
86. Zhang F, Zhang H. Udp-glucose ceramide glycosyltransferase contributes to the proliferation and glycolysis of cervical cancer cells by regulating the Pi3k/Akt pathway. *Ann Clin Lab Sci* (2021) 51(5):663–9.
87. Tyska-Czochara M, Konieczny P, Majka M. Caffeic acid expands anti-tumor effect of metformin in human metastatic cervical carcinoma htb-34 cells: Implications of ampk activation and impairment of fatty acids *De novo* biosynthesis. *Int J Mol Sci* (2017) 18(2):462. doi: 10.3390/ijms18020462
88. Shah S, Carrière WJ, Li J, Campbell SL, Kopinski PK, Lim HW, et al. Targeting acyl sensitizes castration-resistant prostate cancer cells to an antagonism by impinging on an acyl-Ampk-Ar feedback mechanism. *Oncotarget* (2016) 7(28):43713–30. doi: 10.18632/oncotarget.9666
89. Abu-Elheiga L, Almaraz-Ortega DB, Baldini A, Wakil SJ. Human acetyl-coa carboxylase 2. molecular cloning, characterization, chromosomal mapping, and evidence for two isoforms. *J Biol Chem* (1997) 272(16):10669–77. doi: 10.1074/jbc.272.16.10669
90. Zang Y, Wang T, Xie W, Wang-Fischer YL, Getty L, Han J, et al. Regulation of acetyl coa carboxylase and carnitine palmitoyl transferase-1 in rat adipocytes. *Obes Res* (2005) 13(9):1530–9. doi: 10.1038/oby.2005.188
91. Oh SY, Lee MY, Kim JM, Yoon S, Shin S, Park YN, et al. Alternative usages of multiple promoters of the acetyl-coa carboxylase beta gene are related to differential transcriptional regulation in human and rodent tissues. *J Biol Chem* (2005) 280(7):5909–16. doi: 10.1074/jbc.M409037200
92. Jeon SM, Chandel NS, Hay N. Ampk regulates nadph homeostasis to promote tumour cell survival during energy stress. *Nature* (2012) 485(7400):661–5. doi: 10.1038/nature11066
93. Perrone F, Baldassarre G, Indraco S, Signoriello S, Chiappetta G, Esposito F, et al. Biomarker analysis of the Mito2 phase iii trial of first-line treatment in ovarian cancer: Predictive value of DNA-Pk and phosphorylated acc. *Oncotarget* (2016) 7(45):72654–61. doi: 10.18632/oncotarget.12056
94. Lien EC, Westermarck AM, Zhang Y, Yuan C, Li Z, Lau AN, et al. Low glycaemic diets alter lipid metabolism to influence tumour growth. *Nature* (2021) 599(7884):302–7. doi: 10.1038/s41586-021-04049-2
95. Kubota CS, Espenshade PJ. Targeting stearyl-coa desaturase in solid tumors. *Cancer Res* (2022) 82(9):1682–8. doi: 10.1158/0008-5472.Can-21-4044
96. Tesfay L, Paul BT, Konstorum A, Deng Z, Cox AO, Lee J, et al. Stearyl-coa desaturase 1 protects ovarian cancer cells from ferroptotic cell death. *Cancer Res* (2019) 79(20):5355–66. doi: 10.1158/0008-5472.Can-19-0369
97. Carbone M, Melino G. Stearyl coa desaturase regulates ferroptosis in ovarian cancer offering new therapeutic perspectives. *Cancer Res* (2019) 79(20):5149–50. doi: 10.1158/0008-5472.Can-19-2453
98. Wang C, Shi M, Ji J, Cai Q, Zhao Q, Jiang J, et al. Stearyl-coa desaturase 1 (Scd1) facilitates the growth and anti-ferroptosis of gastric cancer cells and predicts poor prognosis of gastric cancer. *Aging (Albany NY)* (2020) 12(15):15374–91. doi: 10.18632/aging.103598
99. Pisanu ME, Noto A, De Vitis C, Morrone S, Scognamiglio G, Botti G, et al. Blockade of stearyl-CoA-Desaturase 1 activity reverts resistance to cisplatin in lung cancer stem cells. *Cancer Lett* (2017) 406:93–104. doi: 10.1016/j.canlet.2017.07.027
100. Xuan Y, Wang H, Yung MM, Chen F, Chan WS, Chan YS, et al. Scd1/Fads2 fatty acid desaturases equipose lipid metabolic activity and redox-driven ferroptosis in ascites-derived ovarian cancer cells. *Theranostics* (2022) 12(7):3534–52. doi: 10.7150/thno.70194
101. Lucarelli G, Ferro M, Loizzo D, Bianchi C, Terracciano D, Cantello F, et al. Integration of lipidomics and transcriptomics reveals reprogramming of the lipid metabolism and composition in clear cell renal cell carcinoma. *Metabolites* (2020) 10(12):509. doi: 10.3390/metabo10120509
102. Yu DS, Song XL, Yan C. Oncogenic mirna-1908 targets Hdac10 and promotes the aggressive phenotype of cervical cancer cell. *Kaohsiung J Med Sci* (2021) 37(5):402–10. doi: 10.1002/kjm2.12348
103. Luis G, Godfroid A, Nishiumi S, Cimino J, Blacher S, Maquoi E, et al. Tumor resistance to ferroptosis driven by stearyl-coa desaturase-1 (Scd1) in cancer cells and fatty acid binding protein-4 (Fabp4) in tumor microenvironment promote tumor recurrence. *Redox Biol* (2021) 43:102006. doi: 10.1016/j.redox.2021.102006
104. Ladanyi A, Mukherjee A, Kenny HA, Johnson A, Mitra AK, Sundaresan S, et al. Adipocyte-induced Cd36 expression drives ovarian cancer progression and metastasis. *Oncogene* (2018) 37(17):2285–301. doi: 10.1038/s41388-017-0093-z
105. Yang D, Li Y, Xing L, Tan Y, Sun J, Zeng B, et al. Utilization of adipocyte-derived lipids and enhanced intracellular trafficking of fatty acids contribute to breast cancer progression. *Cell Commun Signaling CCS* (2018) 16(1):32. doi: 10.1186/s12964-018-0221-6
106. Luo X, Cheng C, Tan Z, Li N, Tang M, Yang L, et al. Emerging roles of lipid metabolism in cancer metastasis. *Mol Cancer* (2017) 16(1):76. doi: 10.1186/s12943-017-0646-3
107. Gyamfi J, Yeo JH, Kwon D, Min BS, Cha YJ, Koo JS, et al. Interaction between Cd36 and Fabp4 modulates adipocyte-induced fatty acid import and metabolism in breast cancer. *NPJ Breast Cancer* (2021) 7(1):129. doi: 10.1038/s41523-021-00324-7
108. Wang R, Tao B, Fan Q, Wang S, Chen L, Zhang J, et al. Fatty-acid receptor Cd36 functions as a hydrogen sulfide-targeted receptor with its Cys333-Cys272 disulfide bond serving as a specific molecular switch to accelerate gastric cancer metastasis. *EBioMedicine* (2019) 45:108–23. doi: 10.1016/j.ebiom.2019.06.037
109. Pascual G, Avgustinova A, Mejetta S, Martin M, Castellanos A, Attolini CS, et al. Targeting metastasis-initiating cells through the fatty acid receptor Cd36. *Nature* (2017) 541(7635):41–5. doi: 10.1038/nature20791
110. Martini C, DeNichilo M, King DP, Cockshell MP, Ebert B, Dale B, et al. Cd36 promotes vasculogenic mimicry in melanoma by mediating adhesion to the extracellular matrix. *BMC Cancer* (2021) 21(1):765. doi: 10.1186/s12885-021-08482-4



111. Drury J, Rychahou PG, He D, Jafari N, Wang C, Lee EY, et al. Inhibition of fatty acid synthase upregulates expression of Cd36 to sustain proliferation of colorectal cancer cells. *Front Oncol* (2020) 10:1185. doi: 10.3389/fonc.2020.01185
112. Tang Y, Zhou J, Hooi SC, Jiang YM, Lu GD. Fatty acid activation in carcinogenesis and cancer development: Essential roles of long-chain acyl-coa synthetases. *Oncol Lett* (2018) 16(2):1390–6. doi: 10.3892/ol.2018.8843
113. Ma Y, Zhang X, Alsaidan OA, Yang X, Sulejmani E, Zha J, et al. Long-chain acyl-coa synthetase 4-mediated fatty acid metabolism sustains androgen receptor pathway-independent prostate cancer. *Mol Cancer Res* (2021) 19(1):124–35. doi: 10.1158/1541-7786.Mcr-20-0379
114. Quan J, Bode AM, Luo X. AclS family: The regulatory mechanisms and therapeutic implications in cancer. *Eur J Pharmacol* (2021) 909:174397. doi: 10.1016/j.ejphar.2021.174397
115. Kuwata H, Hara S. Role of acyl-coa synthetase AclS4 in arachidonic acid metabolism. *Prostaglandins Other Lipid Mediat* (2019) 144:106363. doi: 10.1016/j.prostaglandins.2019.106363
116. Ma LL, Liang L, Zhou D, Wang SW. Tumor suppressor mir-424-5p abrogates ferroptosis in ovarian cancer through targeting AclS4. *Neoplasia* (2021) 68(1):165–73. doi: 10.4149/neo\_2020\_200707N705
117. Wang J, Wang Z, Yuan J, Wang J, Shen X. The positive feedback between AclS4 expression and O-glcacylation contributes to the growth and survival of hepatocellular carcinoma. *Aging (Albany NY)* (2020) 12(9):7786–800. doi: 10.18632/aging.103092
118. Dattilo MA, Benzo Y, Herrera LM, Prada JG, Castillo AF, Orlando UD, et al. Regulatory mechanisms leading to differential acyl-coa synthetase 4 expression in breast cancer cells. *Sci Rep* (2019) 9(1):10324. doi: 10.1038/s41598-019-46776-7
119. Zhang Y, Li S, Li F, Lv C, Yang QK. High-fat diet impairs ferroptosis and promotes cancer invasiveness Via downregulating tumor suppressor AclS4 in lung adenocarcinoma. *Biol Direct* (2021) 16(1):10. doi: 10.1186/s13062-021-00294-7
120. Wang M, Wang K, Liao X, Hu H, Chen L, Meng L, et al. Carnitine palmitoyltransferase system: A new target for anti-inflammatory and anticancer therapy? *Front Pharmacol* (2021) 12:760581. doi: 10.3389/fphar.2021.760581
121. Wang J, Xiang H, Lu Y, Wu T, Ji G. The role and therapeutic implication of cpts in fatty acid oxidation and cancers progression. *Am J Cancer Res* (2021) 11(6):2477–94.
122. Zhelev Z, Aoki I, Lazarova D, Vlaykova T, Higashi T, Bakalova R. A "Weird" mitochondrial fatty acid oxidation as a metabolic "Secret" of cancer. *Oxid Med Cell Longevity* (2022) 2022:2339584. doi: 10.1155/2022/2339584
123. Lee H, Woo SM, Jang H, Kang M, Kim SY. Cancer depends on fatty acids for atp production: A possible link between cancer and obesity. *Semin Cancer Biol* (2022) 86(Pt 2):347–57. doi: 10.1016/j.semcancer.2022.07.005
124. Rios-Colon L, Kumar P, Kim S, Sharma M, Su Y, Kumar A, et al. Carnitine palmitoyltransferase 1 regulates prostate cancer growth under hypoxia. *Cancers (Basel)* (2021) 13(24):6302. doi: 10.3390/cancers13246302
125. Tan Z, Xiao L, Tang M, Bai F, Li J, Li L, et al. Targeting Cpt1a-mediated fatty acid oxidation sensitizes nasopharyngeal carcinoma to radiation therapy. *Theranostics* (2018) 8(9):2329–47. doi: 10.7150/thno.21451
126. Tang M, Dong X, Xiao L, Tan Z, Luo X, Yang L, et al. Cpt1a-mediated fatty acid oxidation promotes cell proliferation Via nucleoside metabolism in nasopharyngeal carcinoma. *Cell Death Dis* (2022) 13(4):331. doi: 10.1038/s41419-022-04730-y
127. Luo M, Liu YQ, Zhang H, Luo CH, Liu Q, Wang WY, et al. Overexpression of carnitine palmitoyltransferase 1a promotes mitochondrial fusion and differentiation of glioblastoma stem cells. *Lab Invest* (2022) 102(7):722–30. doi: 10.1038/s41374-021-00724-0
128. Xiao JB, Ma JQ, Yakefu K, Tursun M. Effect of the Sirt3-Ampk/Ppar pathway on invasion and migration of cervical cancer cells. *Int J Clin Exp Pathol* (2020) 13(10):2495–501.
129. Wu H, Liu B, Chen Z, Li G, Zhang Z. Msc-induced lncrna Hcp5 drove fatty acid oxidation through mir-3619-5p/Ampk/Pgc1 $\alpha$ /Cebp $\beta$  axis to promote stemness and chemo-resistance of gastric cancer. *Cell Death Dis* (2020) 11(4):233. doi: 10.1038/s41419-020-2426-z
130. Dusabimana T, Park EJ, Je J, Jeong K, Yun SP, Kim HJ, et al. P2y2r deficiency ameliorates hepatic steatosis by reducing lipogenesis and enhancing fatty acid  $\beta$ -oxidation through ampk and pgc-1 $\alpha$  induction in high-fat diet-fed mice. *Int J Mol Sci* (2021) 22(11):5528. doi: 10.3390/ijms22115528
131. Baleka Mutombo A, Tozin R, Kanyiki H, Van Geertruyden JP, Jacquemyn Y. Impact of antiviral Av2 in the topical treatment of hpv-associated lesions of the cervix: Results of a phase iii randomized placebo-controlled trial. *Contemp Clin Trials Commun* (2019) 15:100377. doi: 10.1016/j.conctc.2019.100377
132. Hua TNM, Kim MK, Vo VTA, Choi JW, Choi JH, Kim HW, et al. Inhibition of oncogenic src induces Fabp4-mediated lipolysis Via ppar activation exerting cancer growth suppression. *EBioMedicine* (2019) 41:134–45. doi: 10.1016/j.ebiom.2019.02.015
133. Hao J, Zhang Y, Yan X, Yan F, Sun Y, Zeng J, et al. Circulating adipose fatty acid binding protein is a new link underlying obesity-associated Breast/Mammary tumor development. *Cell Metab* (2018) 28(5):689–705.e5. doi: 10.1016/j.cmet.2018.07.006
134. Gharpure KM, Pradeep S, Sans M, Rupaimoole R, Ivan C, Wu SY, et al. Fabp4 as a key determinant of metastatic potential of ovarian cancer. *Nat Commun* (2018) 9(1):2923. doi: 10.1038/s41467-018-04987-y
135. Yu C, Niu X, Du Y, Chen Y, Liu X, Xu L, et al. Il-17a promotes fatty acid uptake through the il-17a/Il-17ra/P-Stat3/Fabp4 axis to fuel ovarian cancer growth in an adipocyte-rich microenvironment. *Cancer Immunol Immunother* (2020) 69(1):115–26. doi: 10.1007/s00262-019-02445-2
136. Yan F, Shen N, Pang JX, Zhang YW, Rao EY, Bode AM, et al. Fatty acid-binding protein Fabp4 mechanistically links obesity with aggressive aml by enhancing aberrant DNA methylation in aml cells. *Leukemia* (2017) 31(6):1434–42. doi: 10.1038/leu.2016.349
137. Seo J, Jeong DW, Park JW, Lee KW, Fukuda J, Chun YS. Fatty-Acid-Induced Fabp5/Hif-1 reprograms lipid metabolism and enhances the proliferation of liver cancer cells. *Commun Biol* (2020) 3(1):638. doi: 10.1038/s42003-020-01367-5
138. Ohira M, Yokoo H, Ogawa K, Fukai M, Kamiyama T, Sakamoto N, et al. Serum fatty acid-binding protein 5 is a significant factor in hepatocellular carcinoma progression independent of tissue expression level. *Carcinogenesis* (2021) 42(6):794–803. doi: 10.1093/carcin/bgab025
139. Zhan YZ, Liu F, Zhang Y, Mo XY, Cheng WD, Wang W. Fabp5 promotes cell growth, invasion and metastasis in cervical cancer. *Zhonghua Zhong Liu Za Zhi* (2019) 41(3):200–7. doi: 10.3760/cma.j.issn.0253-3766.2019.03.009
140. Li G, Wu Q, Gong L, Xu X, Cai J, Xu L, et al. Fabp4 is an independent risk factor for lymph node metastasis and poor prognosis in patients with cervical cancer. *Cancer Cell Int* (2021) 21(1):568. doi: 10.1186/s12935-021-02273-4
141. Yang P, Ruan Y, Yan Z, Gao Y, Yang H, Wang S. Comprehensive analysis of lymph nodes metastasis associated genes in cervical cancer and its significance in treatment and prognosis. *BMC Cancer* (2021) 21(1):1230. doi: 10.1186/s12885-021-08945-8
142. Kulytė A, Lundbäck V, Arner P, Strawbridge RJ, Dahlman I. Shared genetic loci for body fat storage and adipocyte lipolysis in humans. *Sci Rep* (2022) 12(1):3666. doi: 10.1038/s41598-022-07291-4
143. Kulytė A, Lundbäck V, Lindgren CM, Luan J, Lotta LA, Langenberg C, et al. Genome-wide association study of adipocyte lipolysis in the genetics of adipocyte lipolysis (Genial) cohort. *Mol Metab* (2020) 34:85–96. doi: 10.1016/j.jmolmet.2020.01.009
144. Yang A, Mottillo EP. Adipocyte lipolysis: From molecular mechanisms of regulation to disease and therapeutics. *Biochem J* (2020) 477(5):985–1008. doi: 10.1042/bcj20190468
145. Deng H, Li W. Monoacylglycerol lipase inhibitors: Modulators for lipid metabolism in cancer malignancy, neurological and metabolic disorders. *Acta Pharm Sin B* (2020) 10(4):582–602. doi: 10.1016/j.apsb.2019.10.006
146. Reczens E, Mouiel E, Langin D. Hormone-sensitive lipase: Sixty years later. *Prog Lipid Res* (2021) 82:101084. doi: 10.1016/j.plipres.2020.101084
147. Burri P, Djonov V, Aebersold DM, Lindel K, Studer U, Altmatt HJ, et al. Significant correlation of hypoxia-inducible factor-1 $\alpha$  with treatment outcome in cervical cancer treated with radical radiotherapy. *Int J Radiat Oncol Biol Phys* (2003) 56(2):494–501. doi: 10.1016/s0360-3016(02)04579-0
148. Peng X, Gong F, Chen Y, Jiang Y, Liu J, Yu M, et al. Autophagy promotes paclitaxel resistance of cervical cancer cells: Involvement of warburg effect activated lipoxia-induced factor 1- $\alpha$ -Mediated signaling. *Cell Death Dis* (2014) 5(8):e1367. doi: 10.1038/cddis.2014.297
149. Zhao Q, Lin X, Wang G. Targeting srebp-1-Mediated lipogenesis as potential strategies for cancer. *Front Oncol* (2022) 12:952371. doi: 10.3389/fonc.2022.952371
150. Horton JD, Goldstein JL, Brown MS. Srebps: Activators of the complete program of cholesterol and fatty acid synthesis in the liver. *J Clin Invest* (2002) 109(9):1125–31. doi: 10.1172/jci15593
151. Brown MS, Goldstein JL. The srebp pathway: Regulation of cholesterol metabolism by proteolysis of a membrane-bound transcription factor. *Cell* (1997) 89(3):331–40. doi: 10.1016/s0092-8674(00)80213-5
152. Nickels JT Jr. New links between lipid accumulation and cancer progression. *J Biol Chem* (2018) 293(17):6635–6. doi: 10.1074/jbc.H118.002654
153. Zheng Y, Jin J, Gao Y, Luo C, Wu X, Liu J. Phospholipase  $\alpha$ 2 regulates prostate cancer lipid metabolism and proliferation by targeting amp-activated protein kinase (Ampk)/Sterol regulatory element-binding protein 1 (Srebp-1) signaling pathway. *Med Sci Monitor* (2020) 26:e924328. doi: 10.12659/msm.924328
154. Li Y, Xu S, Mihaylova MM, Zheng B, Hou X, Jiang B, et al. Ampk phosphorylates and inhibits srebp activity to attenuate hepatic steatosis and atherosclerosis in diet-induced insulin-resistant mice. *Cell Metab* (2011) 13(4):376–88. doi: 10.1016/j.cmet.2011.03.009
155. Ishimura E, Nakagawa T, Moriwaki K, Hirano S, Matsumori Y, Asahi M. Augmented O-glcacylation of amp-activated kinase promotes the proliferation of lovo cells, a colon cancer cell line. *Cancer Sci* (2017) 108(12):2373–82. doi: 10.1111/cas.13412
156. Yang Y, Han A, Wang X, Yin X, Cui M, Lin Z. Lipid metabolism regulator human hydroxysteroid dehydrogenase-like 2 (Hsd12) modulates cervical cancer cell proliferation and metastasis. *J Cell Mol Med* (2021) 25(10):4846–59. doi: 10.1111/jcmm.16461

157. Fahy E, Cotter D, Sud M, Subramaniam S. Lipid classification, structures and tools. *Biochim Biophys Acta* (2011) 1811(11):637–47. doi: 10.1016/j.bbali.2011.06.009
158. Kouba S, Ouldamer L, Garcia C, Fontaine D, Chantome A, Vandier C, et al. Lipid metabolism and calcium signaling in epithelial ovarian cancer. *Cell Calcium* (2019) 81:38–50. doi: 10.1016/j.ceca.2019.06.002
159. Wang KH, Liu CH, Ding DC. Statins as repurposed drugs in gynecological cancer: A review. *Int J Mol Sci* (2022) 23(22):13937. doi: 10.3390/ijms232213937
160. Carroll RG, Zaslona Z, Galván-Peña S, Koppe EL, Sévin DC, Angiari S, et al. An unexpected link between fatty acid synthase and cholesterol synthesis in proinflammatory macrophage activation. *J Biol Chem* (2018) 293(15):5509–21. doi: 10.1074/jbc.RA118.001921
161. Che L, Chi W, Qiao Y, Zhang J, Song X, Liu Y, et al. Cholesterol biosynthesis supports the growth of hepatocarcinoma lesions depleted of fatty acid synthase in mice and humans. *Gut* (2020) 69(1):177–86. doi: 10.1136/gutjnl-2018-317581
162. Parr CL, Batty GD, Lam TH, Barzi F, Fang X, Ho SC, et al. Body-mass index and cancer mortality in the Asia-Pacific cohort studies collaboration: Pooled analyses of 424,519 participants. *Lancet Oncol* (2010) 11(8):741–52. doi: 10.1016/S1470-2045(10)70141-8
163. Bhaskaran K, Douglas I, Forbes H, dos-Santos-Silva I, Leon DA, Smeeth L. Body-mass index and risk of 22 specific cancers: A population-based cohort study of 5.24 million uk adults. *Lancet (London England)* (2014) 384(9945):755–65. doi: 10.1016/S0140-6736(14)60892-8
164. Lien EC, Vander Heiden MG. A framework for examining how diet impacts tumour metabolism. *Nat Rev Cancer* (2019) 19(11):651–61. doi: 10.1038/s41568-019-0198-5
165. Shahidi F, Ambigaipalan P. Omega-3 polyunsaturated fatty acids and their health benefits. *Annu Rev Food Sci Technol* (2018) 9:345–81. doi: 10.1146/annurev-food-111317-095850
166. Kanarek N, Petrova B, Sabatini DM. Dietary modifications for enhanced cancer therapy. *Nature* (2020) 579(7800):507–17. doi: 10.1038/s41586-020-2124-0
167. D'Angelo S, Motti ML, Meccariello R.  $\Omega$ -3 and  $\Omega$ -6 polyunsaturated fatty acids, obesity and cancer. *Nutrients* (2020) 12(9):2751. doi: 10.3390/nu12092751
168. Saini RK, Keum YS. Omega-3 and omega-6 polyunsaturated fatty acids: Dietary sources, metabolism, and significance - a review. *Life Sci* (2018) 203:255–67. doi: 10.1016/j.lfs.2018.04.049
169. Bojková B, Winkowski PJ, Wszedybyl-Winkowska M. Dietary fat and cancer - which is good, which is bad, and the body of evidence. *Int J Mol Sci* (2020) 21(11):4114. doi: 10.3390/ijms21114114
170. Gevariya N, Lachance G, Robitaille K, Joly Beuparlant C, Beaudoin L, Fournier É, et al. Omega-3 eicosapentaenoic acid reduces prostate tumor vascularity. *Mol Cancer Res* (2021) 19(3):516–27. doi: 10.1158/1541-7786.Mcr-20-0316
171. Ma J, Zhang C, Liang W, Li L, Du J, Pan C, et al.  $\Omega$ -3 and  $\Omega$ -6 polyunsaturated fatty acids regulate the proliferation, invasion and angiogenesis of gastric cancer through Cox/Pge signaling pathway. *Front Oncol* (2022) 12:802009. doi: 10.3389/fonc.2022.802009
172. Aredes MA, da Camara AO, de Paula NS, Fraga KYD, do Carmo M, Chaves GV. Efficacy of  $\Omega$ -3 supplementation on nutritional status, skeletal muscle, and chemoradiotherapy toxicity in cervical cancer patients: A randomized, triple-blind, clinical trial conducted in a middle-income country. *Nutr (Burbank Los Angeles County Calif)* (2019) 67-68:110528. doi: 10.1016/j.nut.2019.06.009
173. Deshpande R, Mansara P, Kaul-Ghanekar R. Alpha-linolenic acid regulates Cox2/Vegf/Map kinase pathway and decreases the expression of hpv oncoproteins E6/E7 through restoration of P53 and Rb expression in human cervical cancer cell lines. *Tumour Biol* (2016) 37(3):3295–305. doi: 10.1007/s13277-015-4170-z
174. Yang C, Zhang GP, Chen YN, Meng FL, Liu SS, Gong SP. Effects of docosahexaenoic acid on cell apoptosis, invasion and migration of cervical cancer cells in vitro. *Nan Fang Yi Ke Xue Xue Bao J South Med Univ* (2016) 36(6):848–56.
175. Owen RW, Giacosa A, Hull WE, Haubner R, Würtele G, Spiegelhalter B, et al. Olive-oil consumption and health: The possible role of antioxidants. *Lancet Oncol* (2000) 1:107–12. doi: 10.1016/S1470-2045(00)00015-2
176. Zhang X, Yang P, Luo X, Su C, Chen Y, Zhao L, et al. High olive oil diets enhance cervical tumour growth in mice: Transcriptome analysis for potential candidate genes and pathways. *Lipids Health Dis* (2019) 18(1):76. doi: 10.1186/s12944-019-1023-6
177. Muhammad N, Ruiz F, Stanley J, Rashmi R, Cho K, Jayachandran K, et al. Monounsaturated and diunsaturated fatty acids sensitize cervical cancer to radiation therapy. *Cancer Res* (2022) 82(24):4515–27. doi: 10.1158/0008-5472.Can-21-4369





## OPEN ACCESS

## EDITED BY

Anna Sebestyén,  
Semmelweis University, Hungary

## REVIEWED BY

Parul Singh,  
National Institutes of Health (NIH),  
United States  
Bela Ozsvári,  
University of Salford, United Kingdom

## \*CORRESPONDENCE

Zhengkai Liao

✉ zlliao@whu.edu.cn

Ling Yan

✉ lingyan@whu.edu.cn

RECEIVED 14 December 2022

ACCEPTED 17 April 2023

PUBLISHED 02 May 2023

## CITATION

Fang R, Yan L and Liao Z (2023) Abnormal lipid metabolism in cancer-associated cachexia and potential therapy strategy. *Front. Oncol.* 13:1123567. doi: 10.3389/fonc.2023.1123567

## COPYRIGHT

© 2023 Fang, Yan and Liao. This is an open-access article distributed under the terms of the [Creative Commons Attribution License \(CC BY\)](https://creativecommons.org/licenses/by/4.0/). The use, distribution or reproduction in other forums is permitted, provided the original author(s) and the copyright owner(s) are credited and that the original publication in this journal is cited, in accordance with accepted academic practice. No use, distribution or reproduction is permitted which does not comply with these terms.

# Abnormal lipid metabolism in cancer-associated cachexia and potential therapy strategy

Ruoxin Fang<sup>1</sup>, Ling Yan<sup>2\*</sup> and Zhengkai Liao<sup>1\*</sup>

<sup>1</sup>Department of Radiation and Medical Oncology, Zhongnan Hospital of Wuhan University, Hubei Key Laboratory of Tumor Biological Behaviors, Hubei Cancer Clinical Study Center, Wuhan, Hubei, China,

<sup>2</sup>Department of Cardiology, Renmin Hospital of Wuhan University, Hubei Key Laboratory of Metabolic and Chronic Diseases, Wuhan, Hubei, China

Cancer-associated cachexia (CAC) is a major characteristic of advanced cancer, associates with almost all types of cancer. Recent studies have found that lipopenia is an important feature of CAC, and it even occurs earlier than sarcopenia. Different types of adipose tissue are all important in the process of CAC. In CAC patients, the catabolism of white adipose tissue (WAT) is increased, leading to an increase in circulating free fatty acids (FFAs), resulting in "lipotoxic". At the same time, WAT also is induced by a variety of mechanisms, browning into brown adipose tissue (BAT). BAT is activated in CAC and greatly increases energy expenditure in patients. In addition, the production of lipid is reduced in CAC, and the cross-talk between adipose tissue and other systems, such as muscle tissue and immune system, also aggravates the progression of CAC. The treatment of CAC is still a vital clinical problem, and the abnormal lipid metabolism in CAC provides a new way for the treatment of CAC. In this article, we will review the mechanism of metabolic abnormalities of adipose tissue in CAC and its role in treatment.

## KEYWORDS

lipid metabolism, adipose tissue, cancer, cachexia, therapy strategy

## 1 Introduction

Cancer-associated cachexia (CAC) is a "multifactorial syndrome" characterized by increased catabolism, weight loss, and decreased skeletal muscle mass and strength (with or without adipose tissue loss) (1). CAC associates with almost all types of cancer and accounts for a quarter of cancer-related deaths (2). Prevalence of cachexia ranges 50 to 80% in advanced cancer (3). CAC is a continuum with three stages of clinical relevance: precachexia, cachexia, and refractory cachexia. Patients who have more than 5% loss of stable body weight over the past 6 months, or a body-mass index (BMI) less than 20 kg/m<sup>2</sup> and ongoing weight loss of more than 2%, or sarcopenia and ongoing weight loss of more than 2%, but have not entered the refractory stage, are classified as having cachexia (1). Early CAC can also occur in patients with curable cancer and can be reversed by

appropriate treatment (4). However, we often do not diagnose CAC in cancer patients until weight loss has occurred, and there are still few methods for early diagnosis of CAC.

CAC is due to the negative energy balance metabolic changes caused by higher energy demand from the tumor and reduced calorie intake of the host, including inflammation, increased catabolism and excessive energy consumption (5–7). It can lead to multi-organ functional disturbance, which is associated with increased susceptibility to infection, higher incidence of metastasis, decreased response of cancer cells to treatment, decreased quality of life, and poor prognosis (1, 8–11). CAC is affected by endogenous and environmental factors, such as complications, genetic risk factors, gender, age, and anti-tumor treatment (12–14). It has been pointed out that tumor or host derived cytokines can affect the metabolism of CAC (15). Cachexia mainly damages skeletal muscle, adipose tissue, liver, brain, intestine, pancreas, bone, and heart (16). The metabolic disorders can further aggravate this multifactorial syndrome (17).

There are many changes in adipose tissue metabolism in cancer patients. Increasing evidence demonstrates that adipose wasting occurs before muscle loss in the early stage of CAC (18). No matter what the patient's weight is, fat loss is an adverse prognostic factor for terminal cancer (19). Studies have shown that the changes of adipose tissue morphology and function in CAC patients have important clinical significance, preserving adipose mass and correcting abnormal lipid metabolism in CAC represents a promising therapeutic strategy (20).

However, the knowledge about mechanisms of abnormal lipid metabolism in CAC is still limited. In this review, we summarized the classification and characteristics of adipose tissue and the changes of them in patients with CAC. Finally, we described existing therapeutic approaches and discussed potential new strategies that arose by targeting the link between adipose tissue and cachexia, with a view to providing directions for future clinical treatment of CAC.

## 2 Adipose tissue

Adipose tissue is a large, interactive multi-chamber organ with clear histological and anatomical structure (21). Mature adipocytes account for only one-third of adipose tissue, and the remaining two-thirds of adipose tissue are composed of nerves, blood vessels, fibroblasts, and adipocyte precursor cells (22). It was found that adipose tissue not only played multiple and complex roles in mechanical buffering and energy storage, but also had paracrine and endocrine functions as an important secretory organ (23, 24). It can regulate energy balance and homeostasis *in vivo* from many aspects, including appetite, inflammation, insulin sensitivity, and lipid metabolism (25). Nowadays, increasing evidence shows that there are changes in lipid metabolism in patients with CAC.

According to its distribution, adipose tissue can be divided into subcutaneous adipose tissue (SCAT) and visceral adipose tissue (VAT), which have different anatomical, metabolic and endocrine characteristics. SCAT accounts for about 80% of total body fat in healthy adults (26). SCAT can be further divided into superficial

SCAT and deep SCAT (27). VAT is mainly distributed in the abdominal cavity and retroperitoneum. The metabolic functions of VAT and SCAT are quite different. For example, compared with SCAT, visceral adipocytes have more active metabolism and greater lipolysis activity. Adipocytes of VAT have stronger insulin resistance than those of SCAT (28, 29). At the same time, SCAT is the main source of leptin production (26). Excess energy accumulates in adipocytes of SCAT, which acts as a metabolic pool. Visceral fat accumulation occurs only when SCAT capacity is insufficient or damaged.

According to functional characteristics, adipose tissue can be divided into three types: white adipose tissue (WAT), brown adipose tissue (BAT), or beige adipose tissue.

WAT is the most common type. White adipocytes are the main storage space of triglyceride. The main function of white adipocytes is to store fat and regulate free fatty acids (FFAs). It is mainly composed of large spherical adipocytes, in which single lipid droplets occupy the majority of the cell volume and mainly store energy in the form of triglycerides (21). WAT exists in subcutaneous and visceral tissues, and the increase of WAT quality in viscera is associated with increased metabolic risk (27, 30). WAT has important endocrine and paracrine effects (21, 31, 32).

Unlike WAT, brown adipocytes in BAT contain a large number of mitochondria and scattered lipid droplets. The main function of BAT is energy dissipation, which provides non-shivering thermogenesis to the body during energy-demanding conditions such as exercise, fasting or cold stimulus (33). BAT is mainly located in the interscapular region and perirenal regions of rodents and infants (34, 35), but BAT is normal component of several subcutaneous and visceral depots and is not exclusive to these areas (21). The development and gene characteristics of WAT and BAT are different (36–38). Classic brown adipocytes come from myogenic factor 5 (Myf-5) cell lines, while white adipocytes come from non Myf-5 cell lines (39). Thus, brown adipocytes are labeled with Myf-5 (40) and paired box 7 (41), similar to myogenic precursor cells. BAT contains rich vascular tree and dense capillary network (25). BAT consumes energy in the form of heat production (42–44), which is mainly due to the high level expression of uncoupling protein 1 (UCP1) in mitochondria and its proton leakage pathway (45–47), which is vital to lipid oxidation and thermogenesis. BAT, as an endocrine organ, regulates energy homeostasis by consuming fatty acids and glucose, and plays a key role in carbohydrate and lipid metabolism (47, 48).

Thirdly, there is a type of adipocyte, defined as “Brite” (white brown) (49) or “Beige” (50), which is derived from pre-existing white adipocytes (21). Beige adipocytes have plasticity and can be transformed from WAT by a variety of different pathways (21, 51, 52). The function of beige adipocytes is similar to that of brown adipocytes (49). In patients with CAC, beige adipocytes can develop, expand and activate under multiple environmental stimulation, which is the target of endocrine and paracrine stimulation (53, 54). The formation of beige adipocytes can be triggered by inflammatory mediators (such as interleukin-6 [IL-6] (55)) and tumor-derived compounds (such as parathyroid hormone related protein [PTHrP] (56, 57)). In mouse models, the formation

of most beige adipocytes is a strong response to environmental factors, such as long-term low-temperature exposure (35).

The genetic characteristics of brown adipocytes and beige adipocytes partially overlap, except for specific markers, such as zinc finger (Zic1) in cerebellum (58). The common characteristics of brown and beige adipocytes are a large number of lipid droplets and dense accumulation of UCP1 positive mitochondria, although brown adipocytes had higher UCP1 expression level (39). Although brown and beige adipocytes are similar in morphology and biochemistry, they also have some distinct characteristics (35), because they come from different embryonic precursor cells (40). For example, brown adipocytes are mainly located in the interscapular and perirenal regions of rodents, while beige adipocytes exist in various WAT pools, especially in inguinal subcutaneous adipose tissue (59).

All three types of adipose tissue are important in the energy balance disrupted by CAC. WAT and BAT usually have opposite physiological functions. WAT is responsible for energy accumulation of lipid droplets in cells, while BAT is responsible for energy dissipation through heat production. Clinically, browning of WAT and activation of BAT are effective methods to combat obesity and metabolic syndrome, but in CAC we may need to block these mechanisms in order to preserve more adipose tissue. Changes in lipid metabolism under local or systemic stimulation make it a potential cause of CAC. In the case of congenital or acquired lipodystrophy, cachexia or any other severe malnutrition, there is almost total lack of adipose tissue, even severe multiple organ dysfunction results from the lack of leptin and other adipokines.

### 3 Changes of lipid metabolism in patients with CAC

Lipid metabolism and adipose tissue mass are regulated by two pathways: lipolysis and lipogenesis. Lipolysis and lipogenesis balance maintain the dynamic balance of adipocytes and regulate the energy balance of CAC patients. Adipose tissue atrophy in cancer patients is attributed to increased lipolysis and lipid oxidation, decreased lipogenesis, impaired fat deposition and lipogenesis, and browning of WAT (60). Compared with non-cancer patients, the volume of adipocytes in cancer patients was smaller, but the total number of adipocytes did not change. Adipocytes isolated from patients with cachexia showed stronger catecholamine and natriuretic peptide-induced lipolysis (61). Weight loss patients also showed more sensitive characteristics to catecholamine signal (62). In addition, compared with cancer patients without cachexia, the expression of UCP1 in adipose tissue of CAC patients is higher, which may lead to adipose tissue atrophy and more heat production (55).

Patients with CAC often show systemic hypermetabolism with reduced energy intake and increased energy consumption, especially the abnormal increase of resting energy expenditure is

considered to be the main cause of energy consumption. CAC, which is characterized by adipose tissue loss (60), is the terminal manifestation of metabolic changes in adipose tissue. The metabolic changes of adipose tissue have been proved to play an important role in CAC. In the context of CAC, changes in lipid metabolism and energy consumption have been shown to be harmful (16). In patients with terminal cancer, reduced adipose tissue is associated with poor prognosis (18, 19). In cachexia, fat loss is faster and earlier than lean tissue loss, especially in the period before death.

Adipose tissue contributes to weight loss in starvation, while skeletal muscle and adipose tissue mass decrease significantly in CAC patients. Lipolysis of adipocytes is the main cause of adipose tissue loss in cancer patients, and plays an important role in the course of CAC, and it is not related to malnutrition (63). The mechanism of adipose tissue loss in CAC is believed to be due to increased lipolytic activity and lipid utilization (64), while other mechanisms, such as impaired lipogenesis, may also be one of the reasons (Figure 1). In the experimental model of cachexia, the decrease of adipose tissue appeared before the decrease of skeletal muscle mass and food intake (65). Studies have also shown that the decrease in adipose tissue is due to a significant decrease in adipocyte size resulting from a decrease in fat reserve, rather than a decrease in the number of cells (cell death) (64, 66). Some studies have found that lipogenesis and lipoprotein lipase (LPL) expression and activity have not been significantly down regulated in CAC patients (67, 68). A study identified the marker components of “cachectin” including Ataxin-10, which are sufficient to trigger abnormal fatty acid metabolism and cardiac atrophy. The serum level of Ataxin-10 is significantly increased in CAC patients (69).

#### 3.1 Catabolism of WAT

The reduction of WAT in visceral and subcutaneous tissues plays an important role in CAC (60). High lipolysis is an important feature of cachexia in cancer patients and rodents (70, 71). Lipolysis depends on three kinds of lipases: adipose triglyceride lipase (ATGL), hormone-sensitive lipase (HSL) and monoglyceride lipase (MGL). Increased expression and activity of these three enzymes lead to the decrease of adipose tissue and the increase of circulating FFAs and glycerol (68, 72).

In CAC patients, the high levels of circulating FFAs and glycerol is caused by the involvement of ATGL and HSL in the catabolism of triglyceride in WAT (73). Excess free lipid molecules are “lipotoxic”, leading to cellular dysfunction and even death, insulin resistance in animals and humans, and have side effects on many organs (16, 74, 75). Compared with cancer patients with stable weight, the expression of HSL was increased in patients with CAC (61, 76). A large amount of evidence shows that the overexpression of ATGL and HSL in WAT of CAC patients is related to the decrease of BMI (73). Inhibition of HSL or ATGL expression in mice not only retained WAT, but also reduced the loss of skeletal muscle, which indicated that mutual regulation between adipose tissue and muscle

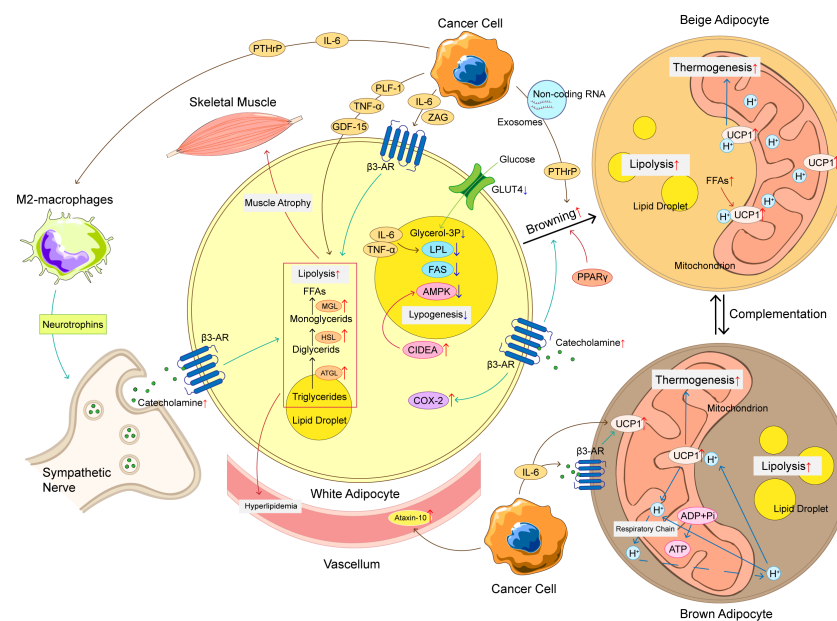


FIGURE 1

The mechanism of adipose tissue loss in CAC. The mechanism of adipose tissue loss in CAC is complicated, and these mechanisms can be roughly divided into increased lipolysis, browning of WAT, increased thermogenesis of BAT, and decreased lipogenesis. Cancer cells produce a variety of cytokines to promote adipose tissue loss, such as IL-6, TNF- $\alpha$ , PTHrP, etc. These cytokines not only promote lipolysis, but also promote WAT browning and upregulation of UCP1 in BAT, ultimately leading to an increase in thermogenesis and energy consumption. At the same time, the crosstalk between adipocyte and immune cells and nervous system also plays an important role in abnormal lipid metabolism of CAC. The loss of adipose tissue has a chain reaction that can produce hyperlipidemia and promote skeletal muscle atrophy, making CAC patients' condition worse. CAC, cancer-associated cachexia; WAT, white adipose tissue; BAT, brown adipose tissue; FFAs, free fat acids; ATGL, adipose triglyceride lipase; HSL, hormone-sensitive lipase; MGL, monoglyceride lipase; LPL, lipoprotein lipase; FAS, fatty acid synthase; UCP1, uncoupling protein 1;  $\beta$ 3-AR, adrenoceptor beta 3; ADP, adenosine diphosphate; ATP, adenosine triphosphate; IL-6, interleukin-6; TNF- $\alpha$ , tumor necrosis factor  $\alpha$ ; PTHrP, parathyroid hormone related protein; ZAG, zinc- $\alpha$  2-glycoprotein; PLF-1, proliferin-1; GDF15, growth differentiation factor 15; CIDEA, DNA fragmentation factor like effector A; AMPK, adenosine 5'-monophosphate (AMP)-dependent protein kinase; COX-2, cyclooxygenase 2; GLUT-4, glucose transporter 4.

play an important role in CAC (71, 73). CGI-58 can bind and activate ATGL (ATGL is the only lipase activated by CGI-58) (77). G0S2 (G0/S2 switch gene 2) is considered to be the main selective inhibitor of ATGL, which can weaken the effect of ATGL *in vitro* and *in vivo*, and regulate triglyceride hydrolysis through this mechanism (78).

In addition, patients with cachexia often have insulin resistance or decreased insulin secretion (79), which may be due to the fact that the body prevents insulin from playing its anti-lipolysis role in CAC. Transcriptome analysis of adipose tissue from patients with gastrointestinal cancer cachexia showed that the expression of related pathways regulating energy conversion was up-regulated (64). Both tumor cells and host immune cells (such as macrophages and lymphocytes) release cytokines or hormones, such as IL-6, tumor necrosis factor  $\alpha$  (TNF- $\alpha$ ), zinc- $\alpha$  2-glycoprotein (ZAG, also known as lipid mobilization factor), proliferin-1, catecholamines, and natriuretic peptide, which can promote lipolysis and reduce insulin sensitivity in CAC patients (6, 73, 80, 81). They are involved in the regulation of proinflammatory state, stress response, anorexia, disease behavior, hypermetabolism and accelerated decomposition of protein, muscle and adipose tissue in CAC patients (82). Systemic inflammation and changes in the human immune system are important determinants of this state (83, 84),

which suggest that inflammatory cytokines may be biomarkers for the diagnosis of CAC (71).

### 3.2 Adipose tissue browning

In mammals, adaptive thermogenesis occurs mainly in brown and beige adipocytes (35). The increase of energy consumption can also be explained by the increased heat production and "browning" of WAT (55, 56). WAT browning refers to the transformation from WAT to BAT, and its name comes from the dark color associated with mitochondria. The gradual transformation of adipose tissue types is an interesting feature of CAC.

This process promotes mitochondrial respiration, leading to thermogenesis rather than ATP synthesis, thus activating lipid mobilization and increasing energy consumption (85). Beige adipocytes, which are phenotypically different from those in WAT and BAT, can appear under severe cold exposure (86), adrenergic stimulation (87) and prostaglandin synthase (cyclooxygenase 2, COX-2) (88). These cells can significantly promote total energy consumption and lead to fat loss (89). Obesity related studies have shown that the central nervous system, especially the hypothalamus, is an important regulatory

organ for browning (87). Klaus Felix et al. found that the level of glucagon-like peptide-1 (GLP-1) was increased in pancreatic cancer cachexia patients (90), GLP-1 appears to trigger satiety and inhibit food intake through molecular regulation in the hypothalamus (91). At the molecular level, transcription factors such as peroxisome proliferator activated receptor gamma (PPAR $\gamma$ ), PPAR $\gamma$  coactivator 1 $\alpha$  (PGC-1 $\alpha$ ), transcription factor PR domain-containing 16 (PDRM16) and CCAAT enhancer binding protein  $\beta$  (C/EBP- $\beta$ ) regulate the transcription events of differentiation into brown adipocytes (92, 93). This is related to upregulation of UCP1 expression, increased heat production (non-shivering), loss of ATP production and increased energy catabolism (73). WAT atrophy and adipose tissue browning occurred in the early stage of CAC (94). The loss of brown adipocytes may lead to browning of WAT, which indicates that there is a compensatory mechanism between mature brown adipocytes and beige adipocytes (95).

In adipose tissue, proinflammatory factors promote the browning of WAT. With the development of CAC, inflammatory microenvironment and metabolic disorder caused by IL-6, TNF- $\alpha$  and parathyroid related peptide secreted by tumors and host immune system will promote browning of WAT (59, 94). IL-6 promotes systemic metabolism to a certain extent by regulating BAT activation and adipose tissue browning (80). In addition, tumor-derived IL-6 and adrenoceptor beta 3 ( $\beta$ 3-AR) activation is associated with CAC mediated adipose tissue browning. Neutralization of IL-6 or  $\beta$ 3-AR can significantly improve cachexia (55). The introduction of IL-6 into the brain by adenovirus vector can significantly increase the expression of UCP1 in sympathetic innervated brown adipocytes, but not in denervated brown adipocytes, indicating that IL-6 might activate BAT through  $\beta$ 3-AR signaling pathway (96). Although PTHrP treatment did not change tumor size in Lewis mouse lung CAC model, it resulted in CAC related weight loss and skeletal muscle atrophy, and activated beige cells to produce heat. On the contrary, blocking PTHrP with neutralizing antibody can prevent adipose tissue and skeletal muscle atrophy. In addition, PTHrP shares the G-protein coupled receptor signaling pathway with  $\beta$ 3-AR agonists, and upregulates the protein expression level of UCP1 in white and brown adipocytes (56). Therefore, tumor cell-derived IL-6 and PTHrP may play an important role in CAC by activating BAT and/or adipose tissue browning.

Two G-protein coupled receptors, called FFA receptor 1 (FFA1) and FFA receptor 4 (FFA4), were identified as molecular targets for  $\omega$ -3 polyunsaturated fatty acids (97, 98). When activated, these receptors can promote a variety of effects, such as increasing insulin sensitivity, inducing adipose tissue browning, promoting analgesia by releasing  $\beta$ -endorphin, controlling energy homeostasis, and reducing food intake (99, 100). Activation of FFA4 results in browning of adipose tissue (99, 101). Lewis lung cancer mouse models lacking the adipose tissue specific PRDM16 showed reduced browning, thermogenesis and lipotrophy (56). By neutralizing browning promoting hormones, such as PTHrP, the improvement of CAC and the reduction of adipose tissue loss were observed in animal models (56). WAT showed heterogeneity in browning efficiency. Some parts such as visceral adipose tissue is resistant to browning. It has been reported that visceral adipose

tissue browning may be a compensatory heat production mechanism (102), but its conversion mechanism is still unclear. Hongmei Yang et al. found that exosomes from Lewis lung carcinoma cells can induce lipolysis *in vitro* and *in vivo* by delivering PTHrP, and inhibition of exosome generation prevented the fat loss of tumor bearing mice (103, 104). Furthermore, there have been many studies in recent years confirming that non-coding RNA plays an important role in the browning of WAT. Wenjuan Di et al. found that miR-146b-5p was enriched in cancer-related exosomes, which plays an essential role in WAT browning. miR-146b-5p can directly repress the downstream gene homeodomain-containing gene C10 (HOXC10), thereby regulating lipolysis (105). Non-coding RNA such as miR-155, miR-425-3p, and miR-182-5p have also been shown to play a role in promoting WAT catabolism and browning in several cancer species (106–108). Further study on the mechanism of systemic metabolic and inflammatory changes leading to the transformation of WAT into BAT can further improve our understanding and treatment of cachexia.

### 3.3 Activation of BAT

There is a lot of evidence that BAT is activated under different conditions of cachexia. The enhanced heat production of BAT is considered to be one of the main reasons for the increase of resting energy expenditure in cancer patients (72). The activity of BAT was also positively correlated with the stage of cancer (109).

BAT is characterized by high mitochondrial content and increased expression of UCP1. UCP1 regulates body temperature through oxidative phosphorylation of uncoupling ATP, resulting in increased energy consumption, increased heat production, and lipolysis, leading to weight loss and progression of CAC (56, 59, 94). The activation of BAT is mediated by  $\beta$ 3-AR, which is activated by the sympathetic nervous system, leading to adipocyte contraction (56).  $\beta$ 3-AR was activated and UCP1 expression was increased, which activated the delipidation in BAT (110). Catecholamine signaling in BAT transduction was enhanced in cachexia mice, but blocking the  $\beta$ 3-AR by propranolol could prevent the increase of body temperature (111). Catecholamine levels are associated with BAT activity and BMI (112). Moreover, FFAs released by lipolysis are direct activators of UCP1 (33), indicating that enhanced WAT catabolism in CAC will promote BAT activation.

Brown adipose precursor cells expressing early B-cell factor 2 and platelet-derived growth factor receptor  $\alpha$  differentiated into mature brown adipocytes (113). The regulation of BAT depends on a variety of cytokines.  $\beta$ 1-adrenergic receptor (ADRB1) mediates norepinephrine induced BAT formation (114). The expression of ADRB1 was correlated with the rate of lipolysis in patients with CAC (76). Prep1 is a adipo-osteogenesis regulatory factor, which is related to the increase of BAT density and osteogenesis reduction (115). IL-6 also plays an important role in mediating BAT activation by increasing the expression of UCP1 and activating fatty acid  $\beta$ -oxidation related gene thermogenesis in gastric cancer and colon cancer patients with cachexia (80). With Lewis lung



cancer model, it has been proved that tumor-derived PTHrP regulates the expression of genes involved in adipose tissue thermogenesis, lipolytic enzymes and muscle atrophy. These studies suggest that blocking BAT activation may be a way to treat cachexia. However, due to the difficulty of BAT localization in human body, the research progress on BAT is very slow at present.

### 3.4 Crosstalk between adipocyte and non-adipocyte

In the context of CAC, there are communications between adipocytes and a variety of non-adipocytes, which is the key to control energy homeostasis and prevent metabolic diseases. DNA fragmentation factor like effector A (CIDEA) is an important metabolic regulator and apoptosis inducing factor. Adipocyte dysfunction leads to the increase of CIDEA, followed by the degradation of adenosine 5'-monophosphate (AMP)-dependent protein kinase (AMPK) in cachexia adipose tissue (116). By hypothalamic AMPK signal, the secretion of leptin, adiponectin and insulin are controlled (117). When the effect of insulin is enhanced, IL-6 secreted by skeletal muscle will increase. IL-6 acts on muscle contraction also by activating AMPK (117). Meanwhile, IL-6 induces Toll-like receptor-4 gene expression via activation of STAT3, leading to insulin resistance in human skeletal muscle, which further accelerates muscle wasting (118). Lipolysis results in increased FFAs in circulation, and FFAs will eventually enter skeletal muscle and cause muscle atrophy (91). Blocking fatty acid oxidation not only rescued human myotubes, but also improved muscle mass and body weight in CAC models *in vivo*, which indicates that there may be interaction between adipose tissue and skeletal muscle (119). Rowena Suriben's study has indicated that growth differentiation factor 15 (GDF15) elicits a lipolytic response in adipose tissue and leads to reduced adipose and muscle mass and function in tumor-bearing mice, inhibiting GDF15-driven lipid mobilization and oxidation can be translated to preservation of skeletal muscle mass (120). GDF15 regulates survival of motor and chipmaker sensory neurons (121), so lipid and skeletal muscle may interact through neurons.

During cachexia, systemic inflammation is one of the main driving forces of fat consumption. Cancer cells secrete a variety of mediators, such as TNF- $\alpha$ , IL-6, IFN- $\gamma$ , ZAG and PTHrP, which can promote browning (55, 56, 122). TNF- $\alpha$  belongs to cachectin (123), which can be released from adipose tissue and mediates CAC by reducing the expression of glucose transporter 4 (GLUT4), which in turn inhibits glucose transport and adipogenesis (124). In addition, adipose tissue is closely related to inflammatory cells, the cross-talk between immune response and adipose tissue biology has been proved. Macrophages can infiltrate WAT and activate immune responses in cachexia mice. A study has shown that macrophages can regulate WAT browning through paracrine heat shock protein A12A (125). Recently, Hao Xie et al. demonstrated that the immune-sympathetic neuron communication axis is essential for WAT browning in CAC. IL-6 and PTHrP can activate immune

cells, including macrophages. Then, the type 2 macrophages will produce neurotrophins and increase polyamine synthesis and secretion. This increases neuronal activity, leading to enhanced local catecholamine synthesis,  $\beta$ -adrenergic stimulation of WAT, and WAT browning (126). Not only that, virus-specific CD8(+) T cells caused morphologic and molecular changes in adipose tissue, which may also lead to cachexia (127). Another study implicates adipocytes as predominantly negative regulators of the surrounding myeloid cells (128). At the same time, studies have shown that the imbalance of the immune system affects the gut microbiota (129), which also plays an important role in CAC. One clinical study has shown that compared with non-cachexic people, *Proteobacteria*, an unknown genus from the *Enterobacteriaceae* family, and *Veillonella* were more abundant among CAC patients (130). Currently, the crosstalk between adipose tissue and other tissues is attracting more and more attention, and the study of these mechanisms may provide us with a more holistic understanding of CAC, so as to develop diagnosis and treatment strategies.

### 3.5 Reduced lipogenesis

The decrease of fat mass in cancer patients depends on the decrease of lipid deposition and lipogenesis. In the process of lipogenesis in adipose tissue, some fatty acids will be re-esterified to triglycerides, forming a futile cycle, which is mediated by AMPK pathway, and the activity of AMPK pathway in cachexia adipose tissue is decreased (116). The activities of fatty acid synthase (FAS) and LPL in adipose tissue of cancer patients were decreased (131). A large number of animal studies have also shown that the activity of LPL is reduced in cancer (132). LPL hydrolyses free circulating triacylglycerol present in chylomicrons very-low-density lipoproteins (VLDLs), whose decreased activity is associated with increased IL-6 (133). Compared with cancer patients with stable weight, patients with CAC have more adipose tissue oxidation (134). Mice-bearing colon adenocarcinoma showed an increase in LPL activity in the heart and adipose tissue increasing weight loss but decreasing with further weight loss. It is suggested that the initial rise in LPL activity provides more oxidation of fatty acids in cachexia state (7, 135). These evidences suggest that the dysfunction of LPL is related to the occurrence and development of CAC, and testing the activity of LPL may be useful for the diagnosis of cachexia. In the experimental model of CAC, the process of lipogenesis was weakened and the expression of lipogenic transcription factors was decreased, which was related to the decrease of adipocyte size and the higher expression of TNF- $\alpha$  (136–138). Besides, non-coding RNA also affects lipogenesis, Diya Sun et al. found that the expression of miR-410-3p was higher in subcutaneous adipose tissues and serum exosomes of CAC patients, which significantly inhibited adipogenesis and lipid accumulation (139). Additionally, due to anorexia associated with CAC or the difficulty of eating due to cancer, the intake of lipids and other nutrients will be reduced, which will also lead to the reduction of lipogenesis.

## 4 Therapy strategy

However, the research progress in the treatment of CAC and the improvement of patients' prognosis is relatively slow, there is also no definite treatment plan for the abnormal lipid metabolism of CAC patients. Studies have shown that CAC is often reversible if intervention is carried out in pre-cachexia or cachexia stage (10, 140). The main treatment strategies used in these stages include exercise and nutritional support, as well as the elimination of any direct cause of cancer (such as reduced food intake or malnutrition due to obstruction or compression) (140, 141). Unfortunately, many cases have been diagnosed as refractory cachexia, when CAC is usually irreversible (1, 140). At present, the main researches focus on the treatment of CAC. Several treatment options have been proposed, but have not been clinically confirmed. The treatment combination mainly involves two pathways: the anabolic pathway and the antimetabolic pathway for muscle and fat catabolism (82). Neutralization of metabolic changes is the first task to overcome cachexia, including the control of skeletal muscle protein decomposition rate, as well as the control of liver, lipid and carbohydrate protein metabolism abnormalities.

A retrospective study by Dingemans et al. included 12 phase II clinical trials involving 11 compounds. These drugs fight CAC through one of the following mechanisms: increase appetite, improve digestion, reduce systemic inflammation, and increase the ratio of muscle synthesis and degradation (142). Many other drugs have entered phase III trials, but it is difficult to achieve multiple clinical endpoints at the same time. Anamorelin, an auxin receptor agonist, has demonstrated its ability to improve lean weight in phase II clinical trials in patients with non-small cell lung cancer and CAC (143). However, the results of this phase II trial and subsequent phase III trial showed that although lean weight was improved, grip strength did not improve (143, 144), which was rejected by the European Drug Administration in 2017. Enobosarm, a selective androgen receptor regulator, showed a significant increase in total lean body weight in the phase II study (145), but it did not produce consistent end-point results in the phase III trial (146, 147). There are many influencing factors in CAC. Current studies cannot fully elucidate the pathophysiological mechanisms of CAC, so as to effectively reduce or reverse all clinical factors of CAC. Therefore, even if the development of many drugs is moving in the right direction, few of them can pass phase II and III studies.

As we mentioned above, lipopenia is an important feature of CAC, and several studies have suggested potential therapeutic strategies for lipid metabolism in CAC, which are summarized in Table 1. Our summary shows that although so many potential strategies have been identified, they are still far from clinical practice. Based on the available evidence, nutritional strategies such as supplementing patients with unsaturated fatty acids and marine phospholipids may be effective (7, 164). Some chemotherapeutic agents, such as cytarabine, promote fat depletion, and we can intervene early in the treatment of patients using these chemotherapeutic agents (165). Exercise training may also reduce inflammation and improve the condition of muscle and

adipose tissue in CAC patients (166). What's more, the application of some new technologies may be helpful to this field. The appearance of 3D bioprinted WAT model is helpful for us to further study and understand the mechanism of adipose tissue metabolism in cachexia (167). Portable biosensors can make it easier for us to monitor lipolysis in patients (168). However, these strategies still need more clinical data to support, the treatment of CAC is still a major challenge for clinicians.

## 5 Conclusions

CAC is a chronic disease involving multiple organs and tissues, which requires multi-mode treatment, including drug treatment, nutritional support and physical exercise, so as to better adapt to the complex mechanisms of body consumption. While enhancing the balance of anabolism/catabolism, it can improve the physical condition and improve the quality of life (169, 170). However, the ideal drugs against CAC are still under development.

Studies have shown that adipose tissue is involved in the formation of CAC, and abnormal lipid metabolism plays an important role in the development of CAC (Figure 2). In adipose tissue, WAT guides the system energy production through the balance between lipogenesis and lipolysis. BAT has been found to have important physiological and pathological functions in adults. Browning stimulates the differentiation and thermogenesis of beige adipocytes. These adipose tissues contribute differently to CAC. In the development of CAC, adipose tissue interacts with other cells or organs, showing therapeutic potential. Since abnormal lipid metabolism occurs at the early stage of CAC, correcting abnormal lipid metabolism and appropriately increasing adipose tissue may delay or even prevent the further deterioration of CAC. Therefore, it is also very important to explore related biomarkers to monitor lipid metabolism in cancer patients. In this field, we need to continue to pay attention to and think about the following questions: (1) At present, there is a lack of clinical monitoring indicators of lipid metabolism, and it is difficult for us to identify abnormal fat loss in cancer patients at an early stage. At the same time, the specific changes of each fat depot during fat loss are still not clear. (2) Some studies have shown that appropriate diet control and exercise can increase muscle strength and promote metabolic health in cancer patients. However, there is still a lack of relevant research conclusions on whether these measures are safe for patients with CAC and whether these interventions should be implemented in patients with CAC. (3) The related side effects of anti-tumor therapy may also promote the development of CAC. The effects of these therapies, including chemotherapy, radiotherapy, immunotherapy and targeted therapy, on lipid metabolism remain unclear. (4) Current animal models of CAC may not adequately simulate the actual physiological changes of CAC, many mechanistic details of abnormal lipid metabolism in CAC need to be further explored, and the interaction between different types of cancers and adipose tissue may also be different.

In this review, we systematically summarize the currently known mechanisms related to abnormal lipid metabolism in

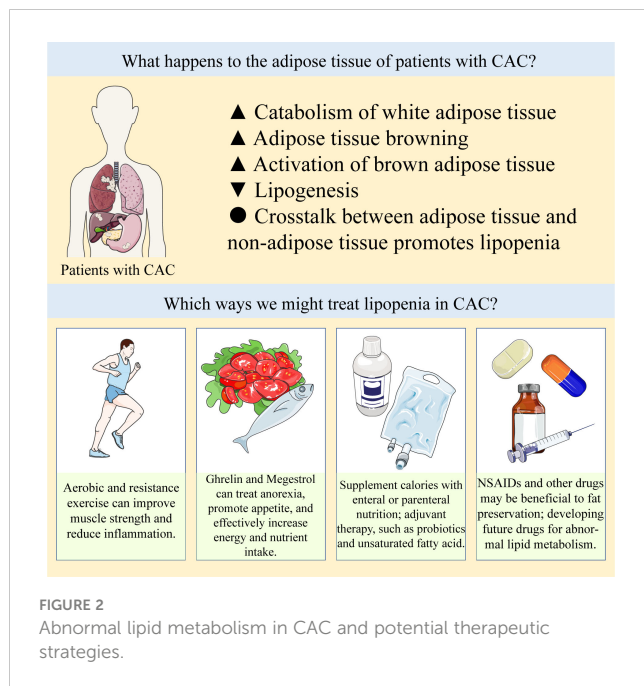
TABLE 1 Potential therapeutic strategies for lipopenia in CAC.

| Therapy strategy                  | Object   | Evidence   | Reference  |
|-----------------------------------|--|--|------------|
| Exercise training                 | Patients with cancer                                 | Aerobic and resistance exercise can improve patients' muscle strength and decrease the levels of TNF- $\alpha$ and CRP.  | (148, 149) |
| NSAIDs                            | Patients with CAC                                    | A pilot study shows patients who received celecoxib experienced statistically significant increases in weight and BMI over controls, NSAIDs may improve weight in CAC patients.  | (150, 151) |
| Unsaturated fatty acid            | Patients with digestive system neoplasm              | The plasma levels of unsaturated fatty acids were decreased in patients with cachexia. Supplementation with omega-3 fatty acids significantly increased skeletal muscle mass and decreased IL-6 and TNF- $\alpha$ in patients.   | (152–154)  |
| Enteral feeding                   | Patients with CAC                                    | Enteral feeding is associated with improvement in decreasing body fat mass and inflammatory markers (CRP) and increasing in lean body mass.  | (155)      |
| Ghrelin                           | Cancer patients with anorexia                        | Ghrelin increases the energy intake of cancer patients with anorexia. It's found to have a predominantly positive effect on growth hormone plasma levels, weight gain, increases in lean mass, and reductions in loss of adipose tissue.                                 | (156, 157) |
| Megestrol                         | Patients with CAC                                    | High dose megestrol can significantly improve the appetite and body weight of some cancer patients with cachexia, especially the body fat mass.  | (158)      |
| Gut microbiome                    | Patients with CAC                                    | There are differences in gut microbiota between CAC patients and non-cachexic people, however, in one prospective study, fecal microbiota transplantation is reported to be negative.  | (130, 155) |
| Anti-diabetic agents              | <i>In vitro</i> model and murine model               | Metformin can deactivate HSL and counteract TNF- $\alpha$ induced lipolysis thereby increasing lipid synthesis and decreasing WAT browning. Rosiglitazone is able to rescue breast cell induced lipid accumulation.  | (159, 160) |
| Lipid lowering agents             | Rat model of CAC                                     | Simvastatin attenuates loss of body weight as well as muscle mass and improves cardiac function.   | (161)      |
| AMPK-stabilizing peptide (ACIP)   | <i>In vitro</i> model and tumor-bearing murine model | ACIP is able to ameliorate WAT wasting <i>in vitro</i> and <i>in vivo</i> by shielding the Cidea-targeted interaction surface on AMPK.   | (116)      |
| Carnosol                          | <i>In vitro</i> model and tumor-bearing murine model | Carnosol and its analogues exhibits anti-cachexia effects mainly by inhibiting TNF- $\alpha$ /NF- $\kappa$ B pathway and decreasing muscle and adipose tissue loss.  | (162)      |
| Piceatannol                       | <i>In vitro</i> model and tumor-bearing murine model | Piceatannol can modulate the stability of lipolytic proteins, protect tumor-bearing mice against weight-loss in early stage in CAC through preserving adipose tissue.  | (20)       |
| Farrerol                          | <i>In vitro</i> model                                | Farrerol attenuates TNF- $\alpha$ -induced lipolysis and increases adipogenic differentiation in 3T3-L1 cells.   | (163)      |
| ESM                               | Murine model   | ESM supplementation ameliorates anorexia, lean fat tissue mass, skeletal muscle wasting, reduced physical function, lipid metabolism and microbial dysbiosis.  | (129)      |
| Anti-PTHrP antibody               | <i>In vitro</i> model and tumor-bearing murine model | Neutralization of PTHrP in tumor-bearing mice blocks adipose tissue browning and also loss of muscle mass and strength. It also prevents the lipolytic effects of extracellular vesicles.  | (56, 104)  |
| Anti-IL-6 receptor antibody       | Murine model   | Anti-IL-6 receptor antibody can inhibit WAT lipolysis and browning in cachectic mice.  | (80)       |
| Selective $\beta$ 3-AR antagonist | Tumor-bearing murine model                           | Treating mice with the selective $\beta$ 3-AR antagonist ameliorates cachexia and decreases UCP1 levels in subcutaneous WAT.   | (55)       |
| Anti-GDF15-GFRAL antibody (3P10)  | Tumor-bearing murine model                           | 3P10 targets GFRAL and inhibits RET signaling by preventing the GDF15-driven interaction of RET with GFRAL on the cell surface. Treatment with 3P10 reverses excessive lipid oxidation in tumor-bearing mice and prevents CAC, even under calorie-restricted conditions. | (120)      |

TNF- $\alpha$ , tumor necrosis factor- $\alpha$ ; NSAIDs, non-steroidal anti-inflammatory drugs; CAC, cancer-associated cachexia; IL-6, interleukin-6; CRP, C-reactive-protein; HSL, hormone-sensitive lipase; WAT, white adipose tissue; AMPK, adenosine 5'-monophosphate (AMP)-dependent protein kinase; NF- $\kappa$ B, nuclear factor kappa-B; ESM, eggshell membrane; PTHrP, parathyroid hormone related protein;  $\beta$ 3-AR, adrenoceptor beta 3; UCP1, uncoupling protein 1; GDF15, growth differentiation factor 15; GFRAL, GDNF family receptor alpha like; RET, ret proto-oncogene.

CAC. Although we have summarized a number of potential treatments for abnormal lipid metabolism in CAC in this review, most of them still require further drug development and clinical validation. CAC is still an unavoidable problem for oncologists.

Through this review of abnormal lipid metabolism in CAC, we hope that drugs targeting abnormal lipid metabolism in CAC can be developed in the future, so as to effectively treat CAC and improve the prognosis of patients with CAC.



Abnormal lipid metabolism in CAC can be summarized as increased catabolism and decreased synthesis of white adipose tissue, increased browning of adipose tissue and abnormal activation of brown adipose tissue, and crosstalk between adipose tissue and non-adipose tissue further promotes adipose loss. There are a number of treatments available to prevent lipopenia, such as exercise, appetite promotion, caloric and nutrient supplementation by oral or parenteral nutrition, and NSAIDs and other drugs that may be beneficial to fat preservation, the specific items are listed in Table 1. In clinical practice, these strategies are often used in combination to prevent the progression of CAC, and drugs

targeting the above abnormal lipid metabolism need to be developed and explored in the future.

## Author contributions

RF: Writing—Original Draft Preparation; LY, ZL: Supervision and writing — Review and Editing. All authors contributed to the article and approved the submitted version.

## Funding

This work was supported by grants from the National Natural Science Foundation of China [grant numbers 81870299], Guiding Fund of Renmin Hospital of Wuhan University [grant numbers RMYD2018M39].

## Conflict of interest

The authors declare that the research was conducted in the absence of any commercial or financial relationships that could be construed as a potential conflict of interest.

## Publisher's note

All claims expressed in this article are solely those of the authors and do not necessarily represent those of their affiliated organizations, or those of the publisher, the editors and the reviewers. Any product that may be evaluated in this article, or claim that may be made by its manufacturer, is not guaranteed or endorsed by the publisher.

## References

1. Fearon K, Strasser F, Anker SD, Bosaeus I, Bruera E, Fainsinger RL, et al. Definition and classification of cancer cachexia: an international consensus. *Lancet Oncol* (2011) 12:489–95. doi: 10.1016/S1470-2045(10)70218-7
2. Laviano A, Meguid MM, Inui A, Muscaritoli M, Rossi-Fanelli F. Therapy insight: cancer anorexia-cachexia syndrome—when all you can eat is yourself. *Nat Clin Pract Oncol* (2005) 2:158–65. doi: 10.1038/ncponc0112
3. von Haehling S, Anker SD. Prevalence, incidence and clinical impact of cachexia: facts and numbers—update 2014. *J Cachexia Sarcopenia Muscle* (2014) 5:261–3. doi: 10.1007/s13539-014-0164-8
4. Arends J, Bachmann P, Baracos V, Barthelemy N, Bertz H, Bozzetti F, et al. ESPEN guidelines on nutrition in cancer patients. *Clin Nutr* (2017) 36:11–48. doi: 10.1016/j.clnu.2016.07.015
5. Baracos VE, Martin L, Korc M, Guttridge DC, Fearon KCH. Cancer-associated cachexia. *Nat Rev Dis Primers* (2018) 4:17105. doi: 10.1038/nrdp.2017.105
6. Petruzzelli M, Wagner EF. Mechanisms of metabolic dysfunction in cancer-associated cachexia. *Genes Dev* (2016) 30:489–501. doi: 10.1101/gad.276733.115
7. Joshi M, Patel BM. The burning furnace: alteration in lipid metabolism in cancer-associated cachexia. *Mol Cell Biochem* (2022) 477:1709–23. doi: 10.1007/s11010-022-04398-0
8. Prado CM, Bekaii-Saab T, Doyle LA, Shrestha S, Ghosh S, Baracos VE, et al. Skeletal muscle anabolism is a side effect of therapy with the MEK inhibitor: selumetinib in patients with cholangiocarcinoma. *Br J Cancer* (2012) 106:1583–6. doi: 10.1038/bjc.2012.144
9. Prado CM, Sawyer MB, Ghosh S, Lieffers JR, Esfandiari N, Antoun S, et al. Central tenet of cancer cachexia therapy: do patients with advanced cancer have exploitable anabolic potential? *Am J Clin Nutr* (2013) 98:1012–9. doi: 10.3945/ajcn.113.060228
10. Fearon K, Arends J, Baracos V. Understanding the mechanisms and treatment options in cancer cachexia. *Nat Rev Clin Oncol* (2013) 10:90–9. doi: 10.1038/nrclinonc.2012.209
11. Bachmann J, Ketterer K, Marsch C, Fechtner K, Krakowski-Roosen H, Buchler MW, et al. Pancreatic cancer related cachexia: influence on metabolism and correlation to weight loss and pulmonary function. *BMC Cancer* (2009) 9:255. doi: 10.1186/1471-2407-9-255
12. Dewys WD, Begg C, Lavin PT, Band PR, Bennett JM, Bertino JR, et al. Prognostic effect of weight loss prior to chemotherapy in cancer patients. Eastern cooperative oncology group. *Am J Med* (1980) 69:491–7. doi: 10.1016/S0149-2918(05)80001-3
13. Hendifar A, Yang D, Lenz F, Lurje G, Pohl A, Lenz C, et al. Gender disparities in metastatic colorectal cancer survival. *Clin Cancer Res* (2009) 15:6391–7. doi: 10.1158/1078-0432.CCR-09-0877
14. Baracos VE, Reiman T, Mourtzakis M, Gioulbasanis I, Antoun S. Body composition in patients with non-small cell lung cancer: a contemporary view of cancer cachexia with the use of computed tomography image analysis. *Am J Clin Nutr* (2010) 91:1133S–7S. doi: 10.3945/ajcn.2010.28608C
15. Tisdale MJ. Molecular pathways leading to cancer cachexia. *Physiol (Bethesda)* (2005) 20:340–8. doi: 10.1152/physiol.00019.2005



16. Argiles JM, Stemmler B, Lopez-Soriano FJ, Busquets S. Inter-tissue communication in cancer cachexia. *Nat Rev Endocrinol* (2018) 15:9–20. doi: 10.1038/s41574-018-0123-0
17. Porporato PE. Understanding cachexia as a cancer metabolism syndrome. *Oncogenesis* (2016) 5:e200. doi: 10.1038/oncsis.2016.3
18. Fouladi M, Korner U, Bosaeus I, Daneryd P, Hyltander A, Lundholm KG. Body composition and time course changes in regional distribution of fat and lean tissue in unselected cancer patients on palliative care—correlations with food intake, metabolism, exercise capacity, and hormones. *Cancer* (2005) 103:2189–98. doi: 10.1002/cncr.21013
19. Murphy RA, Wilke MS, Perrine M, Pawlowicz M, Mourtzakis M, Lieffers JR, et al. Loss of adipose tissue and plasma phospholipids: relationship to survival in advanced cancer patients. *Clin Nutr* (2010) 29:482–7. doi: 10.1016/j.clnu.2009.11.006
20. Kershaw JC, Elzey BD, Guo XX, Kim KH. Piceatannol, a dietary polyphenol, alleviates adipose tissue loss in pre-clinical model of cancer-associated cachexia via lipolysis inhibition. *Nutrients* (2022) 14:2306. doi: 10.3390/nu14112306
21. Cinti S. The adipose organ at a glance. *Dis Model Mech* (2012) 5:588–94. doi: 10.1242/dmm.009662
22. Avram AS, Avram MM, James WD. Subcutaneous fat in normal and diseased states: 2. anatomy and physiology of white and brown adipose tissue. *J Am Acad Dermatol* (2005) 53:671–83. doi: 10.1016/j.jaad.2005.05.015
23. Deng T, Lyon CJ, Bergin S, Caligiuri MA, Hsueh WA. Obesity, inflammation, and cancer. *Annu Rev Pathol* (2016) 11:421–49. doi: 10.1146/annurev-pathol-012615-044359
24. Dahlman I, Elsen M, Tennagels N, Korn M, Brockmann B, Sell H, et al. Functional annotation of the human fat cell secretome. *Arch Physiol Biochem* (2012) 118:84–91. doi: 10.3109/13813455.2012.685745
25. Cinti S. The adipose organ. *Prostaglandins Leukot Essent Fatty Acids* (2005) 73:9–15. doi: 10.1016/j.plefa.2005.04.010
26. Wajchenberg BL. Subcutaneous and visceral adipose tissue: their relation to the metabolic syndrome. *Endocr Rev* (2000) 21:697–738. doi: 10.1210/edrv.21.6.0415
27. Smith SR, Lovejoy JC, Greenway F, Ryan D, deJonge L, de la Bretonne J, et al. Contributions of total body fat, abdominal subcutaneous adipose tissue compartments, and visceral adipose tissue to the metabolic complications of obesity. *Metabolism* (2001) 50:425–35. doi: 10.1053/meta.2001.21693
28. Abate N, Garg A, Peshock RM, Stray-Gundersen J, Grundy SM. Relationships of generalized and regional adiposity to insulin sensitivity in men. *J Clin Invest* (1995) 96:88–98. doi: 10.1172/JCI118083
29. Frayn KN. Visceral fat and insulin resistance—causative or correlative? *Br J Nutr* (2000) 83 Suppl 1:S71–77. doi: 10.1017/S0007114500000982
30. Macotela Y, Emanuelli B, Mori MA, Gesta S, Schulz TJ, Tseng YH, et al. Intrinsic differences in adipocyte precursor cells from different white fat depots. *Diabetes* (2012) 61:1691–9. doi: 10.2337/db11-1753
31. Romacho T, Elsen M, Rohrborn D, Eckel J. Adipose tissue and its role in organ crosstalk. *Acta Physiol (Oxf)* (2014) 210:733–53. doi: 10.1111/apha.12246
32. McGown C, Biredinc A, Younossi ZM. Adipose tissue as an endocrine organ. *Clin Liver Dis* (2014) 18:41–58. doi: 10.1016/j.cld.2013.09.012
33. Li Y, Li Z, Ngandiri DA, Llerins Perez M, Wolf A, Wang Y. The molecular brakes of adipose tissue lipolysis. *Front Physiol* (2022) 13:826314. doi: 10.3389/fphys.2022.826314
34. Rosen ED, Spiegelman BM. What we talk about when we talk about fat. *Cell* (2014) 156:20–44. doi: 10.1016/j.cell.2013.12.012
35. Ikeda K, Maretich P, Kajimura S. The common and distinct features of brown and beige adipocytes. *Trends Endocrinol Metab* (2018) 29:191–200. doi: 10.1016/j.tem.2018.01.001
36. Giral M, Villarroja F. White, brown, beige/brite: different adipose cells for different functions? *Endocrinology* (2013) 154:2992–3000. doi: 10.1210/en.2013-1403
37. Hilton C, Karpe F, Pinnick KE. Role of developmental transcription factors in white, brown and beige adipose tissues. *Biochim Biophys Acta* (2015) 1851:686–96. doi: 10.1016/j.bbalip.2015.02.003
38. Ussar S, Lee KY, Dankel SN, Boucher J, Haering MF, Kleinridders A, et al. ASC-1, PAT2, and P2RX5 are cell surface markers for white, beige, and brown adipocytes. *Sci Transl Med* (2014) 6:247ra103. doi: 10.1126/scitranslmed.3008490
39. Wu J, Bostrom P, Sparks LM, Ye L, Choi JH, Giang AH, et al. Beige adipocytes are a distinct type of thermogenic fat cell in mouse and human. *Cell* (2012) 150:366–76. doi: 10.1016/j.cell.2012.05.016
40. Seale P, Bjork B, Yang W, Kajimura S, Chin S, Kuang S, et al. PRDM16 controls a brown fat/skeletal muscle switch. *Nature* (2008) 454:961–7. doi: 10.1038/nature07182
41. Lepper C, Fan CM. Inducible lineage tracing of Pax7-descendant cells reveals embryonic origin of adult satellite cells. *Genesis* (2010) 48:424–36. doi: 10.1002/dvg.20630
42. Schulz TJ, Tseng YH. Emerging role of bone morphogenetic proteins in adipogenesis and energy metabolism. *Cytokine Growth Factor Rev* (2009) 20:523–31. doi: 10.1016/j.cytogfr.2009.10.019
43. Nicholls DG, Rial E. A history of the first uncoupling protein, UCP1. *J Bioenerg Biomembr* (1999) 31:399–406. doi: 10.1023/A:1005436121005
44. Klingenberg M, Huang SG. Structure and function of the uncoupling protein from brown adipose tissue. *Biochim Biophys Acta* (1999) 1415:271–96. doi: 10.1016/S0005-2736(98)00232-6
45. Nicholls DG. The bioenergetics of brown adipose tissue mitochondria. *FEBS Lett* (1976) 61:103–10. doi: 10.1016/0014-5793(76)81014-9
46. Lean ME. Brown adipose tissue in humans. *Proc Nutr Soc* (1989) 48:243–56. doi: 10.1079/PNS19890036
47. Townsend KL, Tseng YH. Brown fat fuel utilization and thermogenesis. *Trends Endocrinol Metab* (2014) 25:168–77. doi: 10.1016/j.tem.2013.12.004
48. Cypess AM, Lehman S, Williams G, Tal I, Rodman D, Goldfine AB, et al. Identification and importance of brown adipose tissue in adult humans. *N Engl J Med* (2009) 360:1509–17. doi: 10.1056/NEJMoa0810780
49. Petrovic N, Walden TB, Shabalina IG, Timmons JA, Cannon B, Nedergaard J. Chronic peroxisome proliferator-activated receptor gamma (PPARgamma) activation of epididymally derived white adipocyte cultures reveals a population of thermogenically competent, UCP1-containing adipocytes molecularly distinct from classic brown adipocytes. *J Biol Chem* (2010) 285:7153–64. doi: 10.1074/jbc.M109.053942
50. Ishibashi J, Seale P. Medicine. Beige Can be slimming. *Sci* (2010) 328:1113–4. doi: 10.1126/science.1190816
51. Rosen ED, Spiegelman BM. Adipocytes as regulators of energy balance and glucose homeostasis. *Nature* (2006) 444:847–53. doi: 10.1038/nature05483
52. Vitali A, Murano I, Zingaretti MC, Frontini A, Ricquier D, Cinti S. The adipose organ of obesity-prone C57BL/6J mice is composed of mixed white and brown adipocytes. *J Lipid Res* (2012) 53:619–29. doi: 10.1194/jlr.M018846
53. Celi FS, Le TN, Ni B. Physiology and relevance of human adaptive thermogenesis response. *Trends Endocrinol Metab* (2015) 26:238–47. doi: 10.1016/j.tem.2015.03.003
54. Boström P, Wu J, Jedrychowski MP, Korde A, Ye L, Lo JC, et al. A PGC1- $\alpha$ -dependent myokine that drives brown-fat-like development of white fat and thermogenesis. *Nature* (2012) 481:463–8. doi: 10.1038/nature10777
55. Petruzzelli M, Schweiger M, Schreiber R, Campos-Olivas R, Tsoli M, Allen J, et al. A switch from white to brown fat increases energy expenditure in cancer-associated cachexia. *Cell Metab* (2014) 20:433–47. doi: 10.1016/j.cmet.2014.06.011
56. Kir S, White JP, Kleiner S, Kazak L, Cohen P, Baracos VE, et al. Tumour-derived PTH-related protein triggers adipose tissue browning and cancer cachexia. *Nature* (2014) 513:100–4. doi: 10.1038/nature13528
57. Kir S, Komaba H, Garcia AP, Economopoulos KP, Liu W, Lanske B, et al. PTH/PTHrP receptor mediates cachexia in models of kidney failure and cancer. *Cell Metab* (2016) 23:315–23. doi: 10.1016/j.cmet.2015.11.003
58. Walden TB, Hansen IR, Timmons JA, Cannon B, Nedergaard J. Recruited vs. nonrecruited molecular signatures of brown, "brite," and white adipose tissues. *Am J Physiol Endocrinol Metab* (2012) 302:E19–31. doi: 10.1152/ajpendo.00249.2011
59. Kir S, Spiegelman BM. Cachexia & brown fat: a burning issue in cancer. *Trends Cancer* (2016) 2:461–3. doi: 10.1016/j.trecan.2016.07.005
60. Ebadi M, Mazurak VC. Evidence and mechanisms of fat depletion in cancer. *Nutrients* (2014) 6:5280–97. doi: 10.3390/nu6115280
61. Agustsson T, Ryden M, Hoffstedt J, van Harmelen V, Dicker A, Laurencikienė J, et al. Mechanism of increased lipolysis in cancer cachexia. *Cancer Res* (2007) 67:5531–7. doi: 10.1158/0008-5472.CAN-06-4585
62. Drott C, Persson H, Lundholm K. Cardiovascular and metabolic response to adrenalectomy in weight-losing patients with and without cancer. *Clin Physiol* (1989) 9:427–39. doi: 10.1111/j.1475-097X.1989.tb00997.x
63. Ryden M, Agustsson T, Laurencikienė J, Britton T, Sjölin E, Isaksson B, et al. Lipolysis—not inflammation, cell death, or lipogenesis—is involved in adipose tissue loss in cancer cachexia. *Cancer* (2008) 113:1695–704. doi: 10.1002/cncr.23802
64. Dahlman I, Mejhert N, Linder K, Agustsson T, Mutch DM, Kulyte A, et al. Adipose tissue pathways involved in weight loss of cancer cachexia. *Br J Cancer* (2010) 102:1541–8. doi: 10.1038/sj.bjc.6605665
65. Byerley LO, Lee SH, Redmann S, Culbertson C, Clemens M, Lively MO. Evidence for a novel serum factor distinct from zinc  $\alpha$ -2 glycoprotein that promotes body fat loss early in the development of cachexia. *Nutr Cancer* (2010) 62:484–94. doi: 10.1080/0163580903441220
66. Mracek T, Stephens NA, Gao D, Bao Y, Ross JA, Ryden M, et al. Enhanced ZAG production by subcutaneous adipose tissue is linked to weight loss in gastrointestinal cancer patients. *Br J Cancer* (2011) 104:441–7. doi: 10.1038/sj.bjc.6606083
67. Zechner R, Zimmermann R, Eichmann TO, Kohlwein SD, Haemmerle G, Lass A, et al. FAT SIGNALS—lipases and lipolysis in lipid metabolism and signaling. *Cell Metab* (2012) 15:279–91. doi: 10.1016/j.cmet.2011.12.018
68. Arner P, Langin D. Lipolysis in lipid turnover, cancer cachexia, and obesity-induced insulin resistance. *Trends Endocrinol Metab* (2014) 25:255–62. doi: 10.1016/j.tem.2014.03.002
69. Schäfer M, Oeing CU, Rohm M, Baysal-Temel E, Lehmann LH, Bauer R, et al. Ataxin-10 is part of a cachexia cocktail triggering cardiac metabolic dysfunction in cancer cachexia. *Mol Metab* (2016) 5:67–78. doi: 10.1016/j.molmet.2015.11.004
70. Zuidgeest-van Leeuwen SD, van den Berg JW, Wattimena JL, van der Gaast A, Swart GR, Wilson JH, et al. Lipolysis and lipid oxidation in weight-losing cancer



- patients and healthy subjects. *Metabolism* (2000) 49:931–6. doi: 10.1053/meta.2000.6740
71. Das SK, Eder S, Schauer S, Diwoky C, Temmel H, Guertl B, et al. Adipose triglyceride lipase contributes to cancer-associated cachexia. *Science* (2011) 333:233–8. doi: 10.1126/science.1198973
  72. Tisdale MJ. Mechanisms of cancer cachexia. *Physiol Rev* (2009) 89:381–410. doi: 10.1152/physrev.00016.2008
  73. Dalal S. Lipid metabolism in cancer cachexia. *Ann Palliat Med* (2019) 8:13–23. doi: 10.21037/apm.2018.10.01
  74. Unger RH. Lipotoxic diseases. *Annu Rev Med* (2002) 53:319–36. doi: 10.1146/annurev.med.53.082901.104057
  75. Savage DB, Petersen KF, Shulman GI. Disordered lipid metabolism and the pathogenesis of insulin resistance. *Physiol Rev* (2007) 87:507–20. doi: 10.1152/physrev.00024.2006
  76. Cao DX, Wu GH, Yang ZA, Zhang B, Jiang Y, Han YS, et al. Role of beta1-adrenoceptor in increased lipolysis in cancer cachexia. *Cancer Sci* (2010) 101:1639–45. doi: 10.1111/j.1349-7006.2010.01582.x
  77. Schweiger M, Schreiber R, Haemmerle G, Lass A, Fledelius C, Jacobsen P, et al. Adipose triglyceride lipase and hormone-sensitive lipase are the major enzymes in adipose tissue triacylglycerol catabolism. *J Biol Chem* (2006) 281:40236–41. doi: 10.1074/jbc.M608048200
  78. Yang X, Lu X, Lombs M, Rha GB, Chi YI, Guerin TM, et al. The G(0)/G(1) switch gene 2 regulates adipose lipolysis through association with adipose triglyceride lipase. *Cell Metab* (2010) 11:194–205. doi: 10.1016/j.cmet.2010.02.003
  79. Rofe AM, Bourgeois CS, Coyle P, Taylor A, Abdi EA. Altered insulin response to glucose in weight-losing cancer patients. *Anticancer Res* (1994) 14:647–50.
  80. Han J, Meng Q, Shen L, Wu G. Interleukin-6 induces fat loss in cancer cachexia by promoting white adipose tissue lipolysis and browning. *Lipids Health Dis* (2018) 17:14. doi: 10.1186/s12944-018-0657-0
  81. Nguyen TD, Miyatake Y, Yoshida T, Kawahara H, Hanayama R. Tumor-secreted proliferin-1 regulates adipogenesis and lipolysis in cachexia. *Int J Cancer* (2021) 148:1982–92. doi: 10.1002/ijc.33418
  82. Argiles JM, Busquets S, Stemmler B, Lopez-Soriano FJ. Cancer cachexia: understanding the molecular basis. *Nat Rev Cancer* (2014) 14:754–62. doi: 10.1038/nrc3829
  83. Purcell SA, Elliott SA, Baracos VE, Chu QS, Prado CM. Key determinants of energy expenditure in cancer and implications for clinical practice. *Eur J Clin Nutr* (2016) 70:1230–8. doi: 10.1038/ejcn.2016.96
  84. Vazeille C, Jouinot A, Durand JP, Neveux N, Boudou-Rouquette P, Huillard O, et al. Relation between hypermetabolism, cachexia, and survival in cancer patients: a prospective study in 390 cancer patients before initiation of anticancer therapy. *Am J Clin Nutr* (2017) 105:1139–47. doi: 10.3945/ajcn.116.140434
  85. Abdullahi A, Jeschke MG. White adipose tissue browning: a double-edged sword. *Trends Endocrinol Metab* (2016) 27:542–52. doi: 10.1016/j.tem.2016.06.006
  86. Loncar D, Bedrica L, Mayer J, Cannon B, Nedergaard J, Afzelius BA, et al. The effect of intermittent cold treatment on the adipose tissue of the cat. apparent transformation from white to brown adipose tissue. *J Ultrastruct Mol Struct Res* (1986) 97:119–29. doi: 10.1016/S0889-1605(86)80012-X
  87. Cao L, Choi EY, Liu X, Martin A, Wang C, Xu X, et al. White to brown fat phenotypic switch induced by genetic and environmental activation of a hypothalamic-adipocyte axis. *Cell Metab* (2011) 14:324–38. doi: 10.1016/j.cmet.2011.06.020
  88. Vegiopoulos A, Muller-Decker K, Strzoda D, Schmitt I, Chichelnitskiy E, Ostertag A, et al. Cyclooxygenase-2 controls energy homeostasis in mice by *de novo* recruitment of brown adipocytes. *Science* (2010) 328:1158–61. doi: 10.1126/science.1186034
  89. Yoneshiro T, Aita S, Matsushita M, Kayahara T, Kameya T, Kawai Y, et al. Recruited brown adipose tissue as an antiobesity agent in humans. *J Clin Invest* (2013) 123:3404–8. doi: 10.1172/JCI67803
  90. Felix K, Fakelman F, Hartmann D, Giese NA, Gaida MM, Schnölzer M, et al. Identification of serum proteins involved in pancreatic cancer cachexia. *Life Sci* (2011) 88:218–25. doi: 10.1016/j.lfs.2010.11.011
  91. Poulika KA, Sarantis P, Antoniadou D, Kostas E, Papadimitropoulou A, Papavassiliou AG, et al. Pancreatic cancer and cachexia-metabolic mechanisms and novel insights. *Nutrients* (2020) 12:1543. doi: 10.3390/nu12061543
  92. Ohno H, Shinoda K, Spiegelman BM, Kajimura S. PPAR $\gamma$  agonists induce a white-to-brown fat conversion through stabilization of PRDM16 protein. *Cell Metab* (2012) 15:395–404. doi: 10.1016/j.cmet.2012.01.019
  93. Seale P, Kajimura S, Yang W, Chin S, Rohas LM, Uldry M, et al. Transcriptional control of brown fat determination by PRDM16. *Cell Metab* (2007) 6:38–54. doi: 10.1016/j.cmet.2007.06.001
  94. Daas SI, Rizeq BR, Nasrallah GK. Adipose tissue dysfunction in cancer cachexia. *J Cell Physiol* (2018) 234:13–22. doi: 10.1002/jcp.26811
  95. Schulz TJ, Huang P, Huang TL, Xue R, McDougall LE, Townsend KL, et al. Brown-fat paucity due to impaired BMP signalling induces compensatory browning of white fat. *Nature* (2013) 495:379–83. doi: 10.1038/nature11943
  96. Li G, Klein RL, Matheny M, King MA, Meyer EM, Scarpace PJ. Induction of uncoupling protein 1 by central interleukin-6 gene delivery is dependent on sympathetic innervation of brown adipose tissue and underlies one mechanism of body weight reduction in rats. *Neuroscience* (2002) 115:879–89. doi: 10.1016/S0306-4522(02)00447-5
  97. Briscoe CP, Tadavayon M, Andrews JL, Benson WG, Chambers JK, Eilert MM, et al. The orphan G protein-coupled receptor GPR40 is activated by medium and long chain fatty acids. *J Biol Chem* (2003) 278:11303–11. doi: 10.1074/jbc.M211495200
  98. Hirasawa A, Tsumaya K, Awaji T, Katsuma S, Adachi T, Yamada M, et al. Free fatty acids regulate gut incretin glucagon-like peptide-1 secretion through GPR120. *Nat Med* (2005) 11:90–4. doi: 10.1038/nm1168
  99. Quesada-Lopez T, Cereijo R, Turatsinze JV, Planavila A, Cairo M, Gavalda-Navarro A, et al. The lipid sensor GPR120 promotes brown fat activation and FGF21 release from adipocytes. *Nat Commun* (2016) 7:13479. doi: 10.1038/ncomms13479
  100. Oliveira V, Marinho R, Vitorino D, Santos GA, Moraes JC, Dragano N, et al. Diets containing  $\alpha$ -linolenic ( $\omega$ 3) or oleic ( $\omega$ 9) fatty acids rescues obese mice from insulin resistance. *Endocrinology* (2015) 156:4033–46. doi: 10.1210/en.2014-1880
  101. Schilperoord M, van Dam AD, Hoeke G, Shabalina IG, Okolo A, Hanyaloglu AC, et al. The GPR120 agonist TUG-891 promotes metabolic health by stimulating mitochondrial respiration in brown fat. *EMBO Mol Med* (2018) 10:e8047. doi: 10.15252/emmm.201708047
  102. Yang X, Sui W, Zhang M, Dong M, Lim S, Seki T, et al. Switching harmful visceral fat to beneficial energy combustion improves metabolic dysfunctions. *JCI Insight* (2017) 2:e89044. doi: 10.1172/jci.insight.89044
  103. Hu W, Ru Z, Xiao W, Xiong Z, Wang C, Yuan C, et al. Adipose tissue browning in cancer-associated cachexia can be attenuated by inhibition of exosome generation. *Biochem Biophys Res Commun* (2018) 506:122–9. doi: 10.1016/j.bbrc.2018.09.139
  104. Hu W, Xiong H, Ru Z, Zhao Y, Zhou Y, Xie K, et al. Extracellular vesicles-released parathyroid hormone-related protein from Lewis lung carcinoma induces lipolysis and adipose tissue browning in cancer cachexia. *Cell Death Dis* (2021) 12:134. doi: 10.1038/s41419-020-03382-0
  105. Di W, Zhang W, Zhu B, Li X, Tang Q, Zhou Y. Colorectal cancer prompted adipose tissue browning and cancer cachexia through transferring exosomal miR-146b-5p. *J Cell Physiol* (2021) 236:5399–410. doi: 10.1002/jcp.30245
  106. Liu A, Pan W, Zhuang S, Tang Y, Zhang H. Cancer cell-derived exosomal miR-425-3p induces white adipocyte atrophy. *Adipocyte* (2022) 11:487–500. doi: 10.1080/21623945.2022.2108558
  107. Ding Z, Sun D, Han J, Shen L, Yang F, Sah S, et al. Novel noncoding RNA CircPTK2 regulates lipolysis and adipogenesis in cachexia. *Mol Metab* (2021) 53:101310. doi: 10.1016/j.molmet.2021.101310
  108. Liu Y, Wang M, Deng T, Liu R, Ning T, Bai M, et al. Exosomal miR-155 from gastric cancer induces cancer-associated cachexia by suppressing adipogenesis and promoting brown adipose differentiation via C/EBP $\beta$ . *Cancer Biol Med* (2022) 19:1301–14. doi: 10.20892/j.issn.2095-3941.2021.0220
  109. Huang YC, Chen TB, Hsu CC, Li SH, Wang PW, Lee BF, et al. The relationship between brown adipose tissue activity and neoplastic status: an (18)F-FDG PET/CT study in the tropics. *Lipids Health Dis* (2011) 10:238. doi: 10.1186/1476-511X-10-238
  110. Tsoli M, Moore M, Burg D, Painter A, Taylor R, Lockie SH, et al. Activation of thermogenesis in brown adipose tissue and dysregulated lipid metabolism associated with cancer cachexia in mice. *Cancer Res* (2012) 72:4372–82. doi: 10.1158/0008-5472.CAN-11-3536
  111. Brooks SL, Neville AM, Rothwell NJ, Stock MJ, Wilson S. Sympathetic activation of brown-adipose-tissue thermogenesis in cachexia. *Biosci Rep* (1981) 1:509–17. doi: 10.1007/BF01121584
  112. Wang Q, Zhang M, Ning G, Gu W, Su T, Xu M, et al. Brown adipose tissue in humans is activated by elevated plasma catecholamines levels and is inversely related to central obesity. *PLoS One* (2011) 6:e21006. doi: 10.1371/journal.pone.0021006
  113. Wang W, Kissig M, Rajakumari S, Huang L, Lim HW, Won KJ, et al. Ebf2 is a selective marker of brown and beige adipogenic precursor cells. *Proc Natl Acad Sci USA* (2014) 111:14466–71. doi: 10.1073/pnas.1412685111
  114. Lee YH, Petkova AP, Konkar AA, Granneman JG. Cellular origins of cold-induced brown adipocytes in adult mice. *FASEB J* (2015) 29:286–99. doi: 10.1096/fj.14-263038
  115. Maroni G, Panetta D, Luongo R, Krishnan I, La Rosa F, Campani D, et al. The role of Prep1 in the regulation of mesenchymal stromal cells. *Int J Mol Sci* (2019) 20:3639. doi: 10.3390/ijms20153639
  116. Rohm M, Schafer M, Laurent V, Ustunel BE, Niopek K, Algire C, et al. An AMP-activated protein kinase-stabilizing peptide ameliorates adipose tissue wasting in cancer cachexia in mice. *Nat Med* (2016) 22:1120–30. doi: 10.1038/nm.4171
  117. Schnyder S, Handschin C. Skeletal muscle as an endocrine organ: PGC-1 $\alpha$ , myokines exercise. *Bone* (2015) 80:115–25. doi: 10.1016/j.bone.2015.02.008
  118. Cannon TY, Guttridge D, Dahlman J, George JR, Lai V, Shores C, et al. The effect of altered toll-like receptor 4 signaling on cancer cachexia. *Arch Otolaryngol Head Neck Surg* (2007) 133:1263–9. doi: 10.1001/archotol.133.12.1263
  119. Fukawa T, Yan-Jiang BC, Min-Wen JC, Jun-Hao ET, Huang D, Qian CN, et al. Excessive fatty acid oxidation induces muscle atrophy in cancer cachexia. *Nat Med* (2016) 22:666–71. doi: 10.1038/nm.4093
  120. Suriben R, Chen M, Higbee J, Oeffinger J, Ventura R, Li B, et al. Antibody-mediated inhibition of GDF15-GFRAL activity reverses cancer cachexia in mice. *Nat Med* (2020) 26:1264–70. doi: 10.1038/s41591-020-0945-x

121. Strelau J, Strzelczyk A, Rusu P, Bendner G, Wiese S, Diella F, et al. Progressive postnatal motoneuron loss in mice lacking GDF-15. *J Neurosci* (2009) 29:13640–8. doi: 10.1523/JNEUROSCI.1133-09.2009
122. Elattar S, Dimri M, Satyanarayana A. The tumor secretory factor ZAG promotes white adipose tissue browning and energy wasting. *FASEB J* (2018) 32:4272–43. doi: 10.1096/fj.201701465RR
123. Uversky VN, El-Baky NA, El-Fakharany EM, Sabry A, Mattar EH, Uversky AV, et al. Functionality of intrinsic disorder in tumor necrosis factor- $\alpha$  and its receptors. *FEBS J* (2017) 284:3589–618. doi: 10.1111/febs.14182
124. Choe SS, Huh JY, Hwang JJ, Kim JJ, Kim JB. Adipose tissue remodeling: its role in energy metabolism and metabolic disorders. *Front Endocrinol (Lausanne)* (2016) 7:30. doi: 10.3389/fendo.2016.00030
125. Cheng H, Qi T, Zhang X, Kong Q, Min X, Mao Q, et al. Deficiency of heat shock protein A12A promotes browning of white adipose tissues in mice. *Biochim Biophys Acta Mol Basis Dis* (2019) 1865:1451–9. doi: 10.1016/j.bbdis.2019.02.017
126. Xie H, Heier C, Meng X, Bakiri L, Pototschnig I, Tang Z, et al. An immune-sympathetic neuron communication axis guides adipose tissue browning in cancer-associated cachexia. *Proc Natl Acad Sci USA* (2022) 119:e2112840119. doi: 10.1073/pnas.2112840119
127. Baazim H, Schweiger M, Moschinger M, Xu H, Scherer T, Popa A, et al. CD8 (+) T cells induce cachexia during chronic viral infection. *Nat Immunol* (2019) 20:701–10. doi: 10.1038/s41590-019-0397-y
128. Naveiras O, Nardi V, Wenzel PL, Hauschka PV, Fahey F, Daley GQ. Bone-marrow adipocytes as negative regulators of the haematopoietic microenvironment. *Nature* (2009) 460:259–63. doi: 10.1038/nature08099
129. Jia H, Lyu W, Hirota K, Saito E, Miyoshi M, Hohjoh H, et al. Eggshell membrane modulates gut microbiota to prevent murine pre-cachexia through suppression of T helper cell differentiation. *J Cachexia Sarcopenia Muscle* (2022) 13:2088–101. doi: 10.1002/jcsm.13019
130. Ubachs J, Ziemons J, Soons Z, Aarnoutse R, van Dijk DPJ, Penders J, et al. Gut microbiota and short-chain fatty acid alterations in cachectic cancer patients. *J Cachexia Sarcopenia Muscle* (2021) 12:2007–21. doi: 10.1002/jcsm.12804
131. Notarnicola M, Miccolis A, Tutino V, Lorusso D, Caruso MG. Low levels of lipogenic enzymes in peritumoral adipose tissue of colorectal cancer patients. *Lipids* (2012) 47:59–63. doi: 10.1007/s11745-011-3630-5
132. Lopez-Soriano J, Argiles JM, Lopez-Soriano FJ. Lipid metabolism in rats bearing the Yoshida AH-130 ascites hepatoma. *Mol Cell Biochem* (1996) 165:17–23. doi: 10.1007/BF00229741
133. Greenberg AS, Nordan RP, McIntosh J, Calvo JC, Scow RO, Jablons D. Interleukin 6 reduces lipoprotein lipase activity in adipose tissue of mice *in vivo* and in 3T3-L1 adipocytes: a possible role for interleukin 6 in cancer cachexia. *Cancer Res* (1992) 52:4113–6.
134. Catanese S, Beuchel CF, Sawall T, Lordick F, Brauer R, Scholz M, et al. Biomarkers related to fatty acid oxidative capacity are predictive for continued weight loss in cachectic cancer patients. *J Cachexia Sarcopenia Muscle* (2021) 12:2101–10. doi: 10.1002/jcsm.12817
135. Briddon S, Beck SA, Tisdale MJ. Changes in activity of lipoprotein lipase, plasma free fatty acids and triglycerides with weight loss in a cachexia model. *Cancer Lett* (1991) 57:49–53. doi: 10.1016/0304-3835(91)90062-M
136. Bing C, Russell S, Becket E, Pope M, Tisdale MJ, Trayhurn P, et al. Adipose atrophy in cancer cachexia: morphologic and molecular analysis of adipose tissue in tumour-bearing mice. *Br J Cancer* (2006) 95:1028–37. doi: 10.1038/sj.bjc.6603360
137. Batista ML Jr., Neves RX, Peres SB, Yamashita AS, Shida CS, Farmer SR, et al. Heterogeneous time-dependent response of adipose tissue during the development of cancer cachexia. *J Endocrinol* (2012) 215:363–73. doi: 10.1530/JOE-12-0307
138. Tsoli M, Schweiger M, Vanniasinghe AS, Painter A, Zechner R, Clarke S, et al. Depletion of white adipose tissue in cancer cachexia syndrome is associated with inflammatory signaling and disrupted circadian regulation. *PLoS One* (2014) 9:e92966. doi: 10.1371/journal.pone.0092966
139. Sun D, Ding Z, Shen L, Yang F, Han J, Wu G. miR-410-3P inhibits adipocyte differentiation by targeting IRS-1 in cancer-associated cachexia patients. *Lipids Health Dis* (2021) 20:115. doi: 10.1186/s12944-021-01530-9
140. Vignano A, Del Fabbro E, Bruera E, Borod M. The cachexia clinic: from staging to managing nutritional and functional problems in advanced cancer patients. *Crit Rev Oncol* (2012) 17:293–303. doi: 10.1615/CritRevOncol.v17.i3.70
141. Blum D, Stene GB, Solheim TS, Fayes P, Hjermstad MJ, Baracos VE, et al. Validation of the consensus-definition for cancer cachexia and evaluation of a classification model—a study based on data from an international multicentre project (EPCRC-CSA). *Ann Oncol* (2014) 25:1635–42. doi: 10.1093/annonc/mdl0086
142. Dingemans AM, de Vos-Geelen J, Langen R, Schols AM. Phase II drugs that are currently in development for the treatment of cachexia. *Expert Opin Investig Drugs* (2014) 23:1655–69. doi: 10.1517/13543784.2014.942729
143. Takayama K, Katakami N, Yokoyama T, Atagi S, Yoshimori K, Kagamu H, et al. Anamorelin (ONO-7643) in Japanese patients with non-small cell lung cancer and cachexia: results of a randomized phase 2 trial. *Support Care Cancer* (2016) 24:3495–505. doi: 10.1007/s00520-016-3144-z
144. Temel JS, Abernethy AP, Currow DC, Friend J, Duus EM, Yan Y, et al. Anamorelin in patients with non-small-cell lung cancer and cachexia (ROMANA 1 and ROMANA 2): results from two randomised, double-blind phase 3 trials. *Lancet Oncol* (2016) 17:519–31. doi: 10.1016/S1470-2045(15)00558-6
145. Dobs AS, Boccia RV, Croot CC, Gabrail NY, Dalton JT, Hancock ML, et al. Effects of enobosarm on muscle wasting and physical function in patients with cancer: a double-blind, randomised controlled phase 2 trial. *Lancet Oncol* (2013) 14:335–45. doi: 10.1016/S1470-2045(13)70055-X
146. Stewart Coats AJ, Ho GF, Prabhaskar K, von Haehling S, Tilson J, Brown R, et al. Espindolol for the treatment and prevention of cachexia in patients with stage III/IV non-small cell lung cancer or colorectal cancer: a randomized, double-blind, placebo-controlled, international multicentre phase II study (the ACT-ONE trial). *J Cachexia Sarcopenia Muscle* (2016) 7:355–65. doi: 10.1002/jcsm.12126
147. Molino A, Amabile MI, Rossi Fanelli F, Muscaritoli M. Novel therapeutic options for cachexia and sarcopenia. *Expert Opin Biol Ther* (2016) 16:1239–44. doi: 10.1080/14712598.2016.1208168
148. Stene GB, Helbostad JL, Balstad TR, Riphagen II, S. Kaasa LM. Oldervoll, effect of physical exercise on muscle mass and strength in cancer patients during treatment—a systematic review. *Crit Rev Oncol Hematol* (2013) 88:573–93. doi: 10.1016/j.critrevonc.2013.07.001
149. Khosravi N, Stoner L, Farajivafa V, Hanson ED, training E. Circulating cytokine levels and immune function in cancer survivors: a meta-analysis. *Brain Behav Immun* (2019) 81:92–104. doi: 10.1016/j.bbi.2019.08.187
150. Lai V, George J, Richey L, Kim HJ, Cannon T, Shores C, et al. Results of a pilot study of the effects of celecoxib on cancer cachexia in patients with cancer of the head, neck, and gastrointestinal tract. *Head Neck* (2008) 30:67–74. doi: 10.1002/hed.20662
151. Solheim TS, Fearon KC, Blum D, Kaasa S. Non-steroidal anti-inflammatory treatment in cancer cachexia: a systematic literature review. *Acta Oncol* (2013) 52:6–17. doi: 10.3109/0284186X.2012.724536
152. Mocellin MC, Fernandes R, Chagas TR, Trindade E. A meta-analysis of n-3 polyunsaturated fatty acids effects on circulating acute-phase protein and cytokines in gastric cancer. *Clin Nutr* (2018) 37:840–50. doi: 10.1016/j.clnu.2017.05.008
153. Abe K, Uwagawa T, Haruki K, Takano Y, Onda S, Sakamoto T, et al. Effects of  $\omega$ -3 fatty acid supplementation in patients with bile duct or pancreatic cancer undergoing chemotherapy. *Anticancer Res* (2018) 38:2369–75. doi: 10.21873/anticancer.12485
154. Riccardi D, das Neves RX, de Matos-Neto EM, Camargo RG, Lima J, Radloff K, et al. Plasma lipid profile and systemic inflammation in patients with cancer cachexia. *Front Nutr* (2020) 7:4. doi: 10.3389/fnut.2020.00004
155. Hendifar A, Akinsola R, Muranaka H, Osipov A, Thomassian S, Moshayedi N, et al. Gut microbiome and pancreatic cancer cachexia: an evolving relationship. *World J Gastrointest Oncol* (2022) 14:1218–26. doi: 10.4251/wjgo.v14.i7.1218
156. Mansson JV, Alves FD, Biolo A, Souza GC. Use of ghrelin in cachexia syndrome: a systematic review of clinical trials. *Nutr Rev* (2016) 74:659–69. doi: 10.1093/nutrit/nuw029
157. Neary NM, Small CJ, Wren AM, Lee JL, Druce MR, Palmieri C, et al. Ghrelin increases energy intake in cancer patients with impaired appetite: acute, randomized, placebo-controlled trial. *J Clin Endocrinol Metab* (2004) 89:2832–6. doi: 10.1210/jc.2003-031768
158. Maltoni M, Nanni O, Scarpi E, Rossi D, Serra P, Amadori D. High-dose progestins for the treatment of cancer anorexia-cachexia syndrome: a systematic review of randomised clinical trials. *Ann Oncol* (2001) 12:289–300. doi: 10.1023/A:1011156811739
159. Wilson HE, Stanton DA, Rellick S, Geldenhuys W, Pistilli EE. Breast cancer-associated skeletal muscle mitochondrial dysfunction and lipid accumulation is reversed by SPARG. *Am J Physiol Cell Physiol* (2021) 320:C577–c590. doi: 10.1152/ajpcell.00264.2020
160. Auger C, Knuth CM, Abdullahi A, Samadi O, Parousis A, Jeschke MG. Metformin prevents the pathological browning of subcutaneous white adipose tissue. *Mol Metab* (2019) 29:12–23. doi: 10.1016/j.molmet.2019.08.011
161. Palus S, von Haehling S, Flach VC, Tschirner A, Doehner W, Anker SD, et al. Simvastatin reduces wasting and improves cardiac function as well as outcome in experimental cancer cachexia. *Int J Cardiol* (2013) 168:3412–8. doi: 10.1016/j.ijcard.2013.04.150
162. Lu S, Li Y, Shen Q, Zhang W, Gu X, Ma M, et al. Carnosol and its analogues attenuate muscle atrophy and fat lipolysis induced by cancer cachexia. *J Cachexia Sarcopenia Muscle* (2021) 12:779–95. doi: 10.1002/jcsm.12710
163. Chae J, Kim JS, Choi ST, Lee SG, Ojulari OV, Kang YJ, et al. Farrerol induces cancer cell death via ERK activation in SKOV3 cells and attenuates TNF- $\alpha$ -Mediated lipolysis. *Int J Mol Sci* (2021) 22:9400. doi: 10.3390/ijms22179400
164. Yang YH, Hao YM, Liu XF, Gao X, Wang BZ, Takahashi K, et al. Docosahexaenoic acid-enriched phospholipids and eicosapentaenoic acid-enriched phospholipids inhibit tumor necrosis factor- $\alpha$ -induced lipolysis in 3T3-L1 adipocytes by activating sirtuin 1 pathways. *Food Funct* (2021) 12:4783–96. doi: 10.1039/D1FO00157D

165. Brendle C, Stefan N, Stef I, Ripkens S, Soekler M, la Fougère C, et al. Impact of diverse chemotherapeutic agents and external factors on activation of brown adipose tissue in a large patient collective. *Sci Rep* (2019) 9:1901. doi: 10.1038/s41598-018-37924-6
166. Solheim TS, Laird BJA, Balstad TR, Bye A, Stene G, Baracos V, et al. Cancer cachexia: rationale for the MENAC (Multimodal-exercise, nutrition and anti-inflammatory medication for cachexia) trial. *BMJ Support Palliat Care* (2018) 8:258–65. doi: 10.1136/bmjspcare-2017-001440
167. Xue W, Yu SY, Kuss M, Kong Y, Shi W, Chung S, et al. 3D bioprinted white adipose model for *in vitro* study of cancer-associated cachexia induced adipose tissue remodeling. *Biofabrication* (2022) 14:034106. doi: 10.1088/1758-5090/ac6c4b
168. Degrelle SA, Delile S, Moog S, Mouisel E, O'Gorman D, Moro C, et al. DietSee: an on-hand, portable, strip-type biosensor for lipolysis monitoring via real-time amperometric determination of glycerol in blood. *Anal Chim Acta* (2021) 1155:338358. doi: 10.1016/j.aca.2021.338358
169. Ebner N, Anker SD, von Haehling S. Recent developments in the field of cachexia, sarcopenia, and muscle wasting: highlights from the 11th cachexia conference. *J Cachexia Sarcopenia Muscle* (2019) 10:218–25. doi: 10.1002/jcsm.12408
170. Ebner N, Springer J, Kalantar-Zadeh K, Lainscak M, Doehner W, Anker SD, et al. Mechanism and novel therapeutic approaches to wasting in chronic disease. *Maturitas* (2013) 75:199–206. doi: 10.1016/j.maturitas.2013.03.014



## OPEN ACCESS

## EDITED BY

Mo Aljofan,  
Nazarbayev University, Kazakhstan

## REVIEWED BY

Gulam M. Rather,  
Rutgers, The State University of New  
Jersey, United States  
Lan Bai,  
Sichuan Academy of Medical Sciences &  
Sichuan Provincial People's Hospital, China

## \*CORRESPONDENCE

Shanta M. Messerli

✉ Shanta.Messerli@sanfordhealth.org

W. Keith Miskimins

✉ Keith.Miskimins@sanfordhealth.org

RECEIVED 18 May 2023

ACCEPTED 07 July 2023

PUBLISHED 31 July 2023

## CITATION

Zhuang Y, Haugrud AB, Schaefer MA,  
Messerli SM and Miskimins WK (2023)  
Ability of metformin to deplete NAD<sup>+</sup>  
contributes to cancer cell susceptibility to  
metformin cytotoxicity and is dependent  
on NAMPT expression.  
*Front. Oncol.* 13:1225220.  
doi: 10.3389/fonc.2023.1225220

## COPYRIGHT

© 2023 Zhuang, Haugrud, Schaefer, Messerli  
and Miskimins. This is an open-access article  
distributed under the terms of the [Creative  
Commons Attribution License \(CC BY\)](#). The  
use, distribution or reproduction in other  
forums is permitted, provided the original  
author(s) and the copyright owner(s) are  
credited and that the original publication in  
this journal is cited, in accordance with  
accepted academic practice. No use,  
distribution or reproduction is permitted  
which does not comply with these terms.

# Ability of metformin to deplete NAD<sup>+</sup> contributes to cancer cell susceptibility to metformin cytotoxicity and is dependent on NAMPT expression

Yongxian Zhuang<sup>1</sup>, Allison B. Haugrud<sup>1</sup>, Meg A. Schaefer<sup>1,2</sup>,  
Shanta M. Messerli<sup>1\*</sup> and W. Keith Miskimins<sup>1\*</sup>

<sup>1</sup>Cancer Biology and Immunotherapies, Sanford Research, Sioux Falls, SD, United States, <sup>2</sup>Sanford Program for Undergraduate Research (SPUR) Program, Sanford Research, Sioux Falls, SD, United States

**Background:** Nicotinamide adenine dinucleotide (NAD<sup>+</sup>) is vital for not only energy metabolism but also signaling pathways. A major source of NAD<sup>+</sup> depletion is the activation of poly (ADP-ribose) polymerase (PARP) in response to DNA damage. We have previously demonstrated that metformin can cause both caspase-dependent cell death and PARP-dependent cell death in the MCF7 breast cancer cells but not in the MDA-MB-231 (231) breast cancer cells while in high-glucose media. We hypothesize that depletion of NAD<sup>+</sup> in MCF7 cells via activation of PARP contributes to the cell death caused by metformin. Nicotinamide phosphoribosyltransferase (NAMPT), a key rate-limiting step in converting nicotinamide (vitamin B3) into NAD<sup>+</sup>, is essential for regenerating NAD<sup>+</sup> for normal cellular processes. Evidence shows that overexpression of NAMPT is associated with tumorigenesis. We hypothesize that NAMPT expression may determine the extent to which cancer cells are sensitive to metformin.

**Results:** In this study, we found that metformin significantly decreases NAD<sup>+</sup> levels over time, and that this could be delayed by PARP inhibitors. Pretreatment with NAD<sup>+</sup> in MCF7 cells also prevents cell death and the enlargement of mitochondria and protects mitochondria from losing membrane potential caused by metformin. This leads to MCF7 cell resistance to metformin cytotoxicity in a manner similar to 231 cells. By studying the differences in NAD<sup>+</sup> regulation in these two breast cancer cell lines, we demonstrate that NAMPT is expressed at higher levels in 231 cells than in MCF7 cells. When NAMPT is genetically repressed in 231 cells, they become much more sensitive to metformin-induced cell death. Conversely, overexpressing NAMPT in HEK-293 (293) cells causes the cells to be more resistant to metformin's growth inhibitory effects. The addition of a NAMPT activator also decreased the sensitivity of MCF7 cells to metformin, while the NAMPT activator, P7C3, protects against metformin-induced cytotoxicity.



**Conclusions:** Depletion of cellular NAD<sup>+</sup> is a key aspect of sensitivity of cancer cells to the cytotoxic effects of metformin. NAMPT plays a key role in maintaining sufficient levels of NAD<sup>+</sup>, and cells that express elevated levels of NAMPT are resistant to killing by metformin.

#### KEYWORDS

metformin, nicotinamide adenine dinucleotide (NAD<sup>+</sup>), nicotinamide phosphoribosyltransferase (NAMPT), tumorigenesis, breast cancer

## Introduction

Metformin, a commonly prescribed anti-type 2 diabetes drug, has gained attention due to its effects on cancer cell growth and survival (1–10) and possible effects on reducing cancer risk in type 2 diabetes patients who take metformin (11–13). This has been suggested to be related to its effects on inhibition of cell growth (1, 3, 4, 6, 14, 15) and induction of cell death (2, 10, 16–18). Our previous study demonstrates that metformin causes both caspase-dependent and poly (ADP-ribose) polymerase (PARP)-dependent cell death (10). The activation of poly (ADP-ribose) polymerase-1 (PARP-1), a nuclear enzyme that catalyzes the synthesis of long, branching (ADP-ribose) polymers (PAR) from nicotinamide adenine dinucleotide (NAD<sup>+</sup>), can transfer multiple ADP-ribose moieties from NAD<sup>+</sup> to nuclear proteins and to PARP itself (19–23). This process is also expected to deplete the NAD<sup>+</sup> reservoir.

NAD<sup>+</sup> is required for multiple reactions by regulating numerous enzymes including dehydrogenases, poly(ADP-ribose) polymerases, Sir2 family proteins (sirtuins), mono (ADP ribosyl) transferases, and ADP-ribosyl cyclases (24). By regulating the aforementioned enzymes, NAD<sup>+</sup> levels intercede in cell cycle progression, DNA repair, metabolic regulation, and circadian rhythms, which are important in the pathogenesis in various diseases and the functionality of various cells. Several studies have shown that maintaining NAD<sup>+</sup> level in the cell can profoundly decrease cell death (25–27). These studies have fundamentally changed our understanding about NAD<sup>+</sup>, suggesting novel paradigms about the metabolism and biological activities of NAD<sup>+</sup>. Consumption of NAD<sup>+</sup> severely compromises ATP synthesis, whereas synthesis of NAD<sup>+</sup> requires ATP during glycolysis and oxidative phosphorylation (28, 29). Therefore, activation of PARP may lead to an energy deficit and contribute to cell death caused by metformin.

Understanding how cancer cells maintain and replenish NAD<sup>+</sup> levels is essential in understanding if depleting NAD<sup>+</sup> reserves through metformin treatment will work. Nicotinamide phosphoribosyltransferase (NAMPT) is a rate-limiting enzyme in the regeneration of NAD<sup>+</sup> from nicotinamide. Mammalian cells can use other sources such as nicotinic acid or tryptophan to produce NAD<sup>+</sup>, even though using nicotinamide through NAMPT is the most efficient and predominant manner of regenerating NAD<sup>+</sup> (30–

32). Although crucial to normal systemic functionality, NAMPT has recently been associated with tumorigenesis (33), and its increased expression is associated with the pathogenesis or various cancers (34–36). NAMPT may prove to be a key factor in determining the resiliency of cancers to cancer therapies, which induce metabolic stress or DNA damage.

In this study, we explore metformin's effects on NAD<sup>+</sup> levels, if PARP plays a role in NAD<sup>+</sup> depletion, and how NAD<sup>+</sup> levels affect metformin cytotoxicity. Since NAMPT plays an essential role in NAD<sup>+</sup> replenishment, we explore how NAMPT levels can affect cancer susceptibility to metformin. We hypothesize that metformin-induced depletion of NAD augments the cytotoxicity following metformin exposure.

## Materials and methods

### Chemicals and cell culture

Metformin (1, 1-dimethylbiguanide, #D5035, Sigma, St. Louis, USA), PARP inhibitor II (INH2BP, #407850, Calbiochem, USA), MCF7, 293T, and 231-MDA-MB (231) cells were purchased from ATCC (Manassas, USA) and maintained in Dulbecco's modified Eagle's medium (DMEM) with 10% fetal bovine serum supplemented with 100 U/ml penicillin and 100 µg/ml streptomycin in a humidified incubator with 5% CO<sub>2</sub>. Upon receiving the cell lines, cells were immediately cultured and expanded to prepare frozen ampule stocks. Cells were passaged for no more than 2–3 months before establishing new cultures from the early passage frozen ampules. Cell lines were routinely checked for mycoplasma contamination and were verified to be mycoplasma free by IDEXX RADIL Laboratories.

### Trypan blue exclusive assay

For the MCF7 and 293T experiments, cells were plated into 35-mm dishes. For the 231 experiments, cells were plated in a 24-well plate. The following day, cells were treated as indicated. After incubation for the indicated time, cells were trypsinized and stained using 0.2% trypan blue. Trypan blue-positive cells and -negative cells were determined using a hemacytometer.

## Phase microscopy

Cells were treated as indicated and pictures were taken at 200× magnification using a Zeiss Axiovert 35 light microscope equipped with a Nikon digital camera.

## Confocal microscopy

MCF7 cells that stably transfected with pAcGFP-Mito Vector were plated on the cover glass in 35-mm dishes and treated as indicated. Cells were washed in 1× PBS and fixed in 4% paraformaldehyde for 15 min. Finally, slides were washed in 1× PBS three times and mounted using Vectorshield medium containing DAPI. Slides were observed using an Olympus FV1000 confocal microscope. pAcGFP1-Mito Vector was purchased from Clontech, USA.

## Flow cytometry

MCF7 cells were treated as indicated in the figure. Then, cells were incubated with 100 nM TMRE for 10 min, and cells were washed in 1× PBS once and trypsinized. All flow cytometry measurements were done using an Accuri C6 flow cytometer.

## Western blot

Cells were plated on 35-mm dishes. After treatment for the indicated time period, live cells were harvested and lysed by the addition of sodium dodecyl sulfate (SDS) sample buffer [2.5 mM Tris-HCl (pH 6.8), 2.5% SDS, 100 mM dithiothreitol, 10% glycerol, and 0.025% bromophenol blue]. Equal amounts of protein were separated on a 4%–20% Mini-PROTEAN<sup>®</sup> TGX<sup>™</sup> Gel (Bio-Rad Laboratories). Proteins were transferred to Trans-Blot<sup>®</sup> Turbo<sup>™</sup> RTA Mini PVDF with a Bio-Rad Trans-blot apparatus using a transfer buffer [48 mM Tris-HCl, 39 mM glycine]. The membranes were immersed in 5% non-fat dry milk in Tris-buffered saline containing Tween20 (TBS-T) [10 mM Tris-HCl (pH 7.5), 150 mM NaCl, and 0.1% Tween-20] with an NAMPT antibody (Raybiotech cat # RR08-0003) for either 3 h at room temperature or 4°C overnight. After thoroughly washing with TBS-T, an appropriate secondary antibody conjugated to horseradish peroxidase (HRP) was applied. The membrane was again washed, and proteins were then detected using GE Healthcare Amersham<sup>™</sup> ECL<sup>™</sup> Prime Western Blotting Detection Reagent imaged on a BioSpectrum Imaging System (UVP, LLC).

In the NAD<sup>+</sup> assay for the 231 experiments, cells were grown at 75% confluence in 60-mm dishes. For the 293T experiments, 300,000 cells were plated in each well in a six-well plate. The following day, 231 cells were treated with 2.5 mM glucose complete media while 293T cells received 10 mM glucose complete media and appropriate dishes were treated with 8 mM metformin. After 24 h of treatment, cells were trypsinized and counted via a hemacytometer.

Cells were then rinsed with 1× PBS and vortexed in NAD extraction buffer included in the EnzyChrom<sup>™</sup> NAD/NADH Assay Kit (BioAssay Systems) and kit directions were followed from this point. The 231 experiments used 300,000 cells/sample while the 293T experiments used 500,000 cells/sample.

For MCF7 experiments, MCF7 cells were grown to 75% confluence in 60-mm tissue culture dishes, with 500,000 cells plated per dish. After plating for 24 h, the following drugs were added: Metformin (8 mM), P7C3 (5 μM), and Metformin (8 mM) combined with P7C3 (5 μM). NAD was obtained using the EnzyChrom NAD/NADH (E2ND-100) kit as instructed by the vendor BioAssay.

## ATP assay

A total of 150,000 231 cells were plated in each well of a 12-well plate. The following day, 2.5 mM glucose complete media was added along with indicated treatments. After 24 h of treatment, cells were trypsinized and counted via a hemacytometer. A total of 100,000 cells were placed in a tube and rinsed with 1× PBS. ATP Determination Kit (Life Technologies) was used to determine ATP content.

## Cytotoxicity assay

A total of 1,000 MCF7 cells were plated in a 96-well plate, and concentrations of P7C3 (Selleckchem) ranging from 0 to 5 μM in the presence and absence of metformin (10 mM) were added 24 h after plating. After drug administration for 48 h, a cytotoxicity assay was performed using Sytox Green (Invitrogen). After adding Sytox Green for 15 min, 0.6% Triton X was added to determine the total number of cells.

## xCELLigence data

After a background reading was completed on E-plates, 20,000 231 NAMPT knockdown stable cells were plated per well. Cells were allowed to plate at room temperature for 20 min before placing plates in the xCELLigence Real-Time Cell Analyzer (RTCA) (Acea Biosciences, Inc.). The following day, fresh media and treatments were added as indicated. Cell index, which is a dimensionless measurement of electrical impedance from cells that reflects cell number, cell morphology, and adhesion, was measured.

## Construction of stable cell lines

MDA-MB-231 cells were retrovirally transduced using a NAMPT shRNA-mir (clone ID RLGH-GU42575, Transomic Technologies). Puromycin (0.5 μg/ml) was used to select out stables. Once colonies were established, cloning rings were used to isolate colonies. Western blotting was used to determine the level of NAMPT protein expression.

## Overexpression of NAMPT

HEK-293 cells were plated at 300,000 cells/well in a six-well plate in triplicate. The following day, NAMPT mRNA (GeneCopeia Cat # EX-A1275-M02) or empty vector (GeneCopeia Cat # EX-NEG-M02) were transfected using Dreamfect (OZ Biosciences). Forty-eight hours later, the NAD assay was performed as described above.

## Statistical analysis

Comparison of two groups was done using unpaired *t*-test in GraphPad Prism software (La Jolla, CA). *p*-values less than or equal to 0.05 were considered to have significance.

## Results

Our previous data have shown that metformin causes cell death in MCF7 cells via caspase-dependent and PARP-dependent cell death (10). Since NAD<sup>+</sup> is used in PARP activation [19–23], we looked at the NAD<sup>+</sup> level in association with PARP-dependent cell death. In Figure 1A, we evaluated the level of NAD<sup>+</sup> after 1 and 2 days of metformin treatment. After 1 day of treatment, NAD<sup>+</sup> levels significantly decreased and further decreased on day 2. To verify the link between PARP and NAD<sup>+</sup> levels, a PARP inhibitor was utilized. In Figure 1B, MCF7 cells were pretreated with the PARP inhibitor for 1 day and then treated with or without metformin for an additional 2 days. The PARP inhibitor pretreatment prevented the reduction of NAD<sup>+</sup> caused by metformin treatment. This suggests that the depletion of NAD<sup>+</sup> caused by metformin is partially due to the activation of PARP.

Our previous data have shown that PARP inhibition could partially prevent the cell death caused by metformin (10). This correlates with the prevention of the decrease of NAD<sup>+</sup> shown in Figure 1, so we assessed whether the addition of exogenous NAD<sup>+</sup>

to the media could delay the cell death caused by metformin. MCF7 cells were pretreated with NAD<sup>+</sup> for 3 days and then treated with or without metformin for 2 days. As seen in Figure 2, NAD<sup>+</sup> pretreatment increased the number of live cells (Figure 2A) and prevented the cell death (Figure 2B) caused by metformin, which further confirms that the cell death is partially caused by depletion of NAD<sup>+</sup> by metformin.

As shown in our previous study, metformin can cause enlargement of mitochondria, which could be prevented by a PARP inhibitor (10). We next studied whether pretreating with exogenous NAD<sup>+</sup> could prevent mitochondrial enlargement. MCF7 stable cells expressing pAcGFP-Mito Vector were pretreated with NAD<sup>+</sup> for 3 days, then treated with or without metformin for 2 days. Figure 3A displays phase contrast pictures showing an accumulation of large, clear vesicles present in the metformin-treated cells while the pretreatment of NAD<sup>+</sup> with metformin lacks these vesicles. Confocal images shown in Figure 3B confirm that the large vesicles are enlarged mitochondria, which was also demonstrated in our previous paper. The NAD<sup>+</sup> pretreatment prevented the enlargement of mitochondria caused by metformin. Furthermore, membrane potential was investigated since NAD<sup>+</sup> has been documented to be involved in the membrane potential maintenance (37). MCF7 cells were pretreated with NAD<sup>+</sup> for 3 days and were subsequently treated with or without metformin for 2 days. NAD<sup>+</sup> pretreatment could partially reverse metformin's effects on mitochondrial membrane potential as seen in Figure 3C. NAD<sup>+</sup> protects the mitochondrial membrane potential from metformin, allowing the mitochondria to maintain morphology leading to the delay of cell death. This finding further elucidates the mechanism of metformin function in causing cell death in MCF7 breast cancer cells.

Since NAD<sup>+</sup> levels are important in determining the fate of a cancer cell to surviving a therapy, we examined if the protein NAMPT, the rate-limiting enzyme in NAD biosynthesis, played a role in a cancer cell line resistance to metformin treatment. In our previous study, we found that the breast cancer cell line MDA-MB-231 (231) cells were resistant to metformin's apoptotic effects in

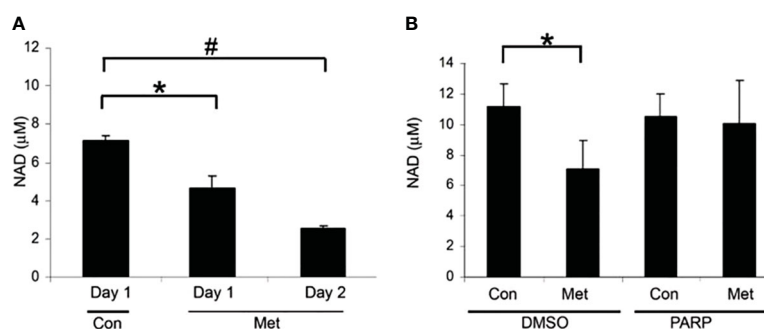


FIGURE 1

Metformin decreased NAD<sup>+</sup> levels after 1 day of treatment and can partially be blocked by PARP inhibitors. (A) NAD<sup>+</sup> levels of MCF7 cells that were treated with 8 mM metformin as indicated. (B) NAD<sup>+</sup> levels of MCF7 cells that were pretreated with a PARP inhibitor (10 μM) for 1 day and treated subsequently with metformin (8 mM) for 1 or 2 additional days in the presence of the PARP inhibitor. The same number of cells was used for each sample in the NAD assay (true for all subsequent NAD<sup>+</sup> assays). (\* and # indicate significant difference between groups with *p* < 0.05.) Lanes labeled Con represent cells not treated with metformin and lanes labeled Met denote those treated with metformin. Lanes labeled PARP indicate cells treated with a PARP inhibitor and DMSO indicates control samples not treated with PARP inhibitor.

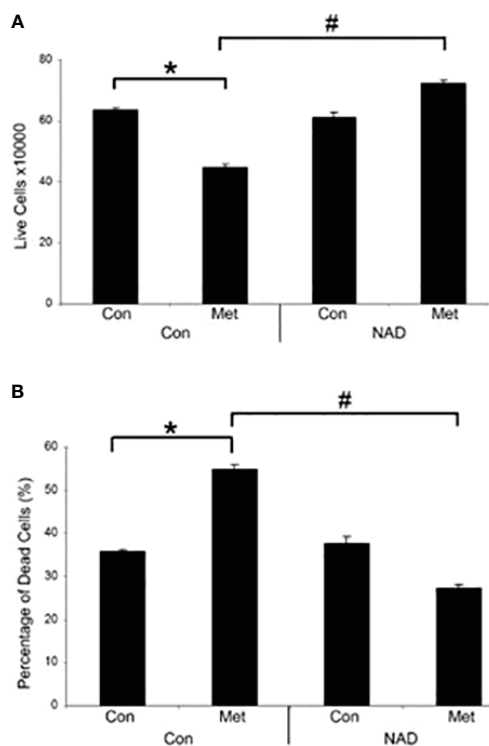


FIGURE 2

Metformin decreases live cells and induces cell death *in vitro*, which can be prevented by the addition of exogenous NAD<sup>+</sup>. MCF7 cells were pretreated with NAD<sup>+</sup> (1 mM) for 3 days and subsequently treated with or without metformin (8 mM) for 2 days. Dead and live cell numbers were obtained using the trypan blue exclusion assay. (\* and # indicate significant difference between groups with  $p < 0.05$ ).

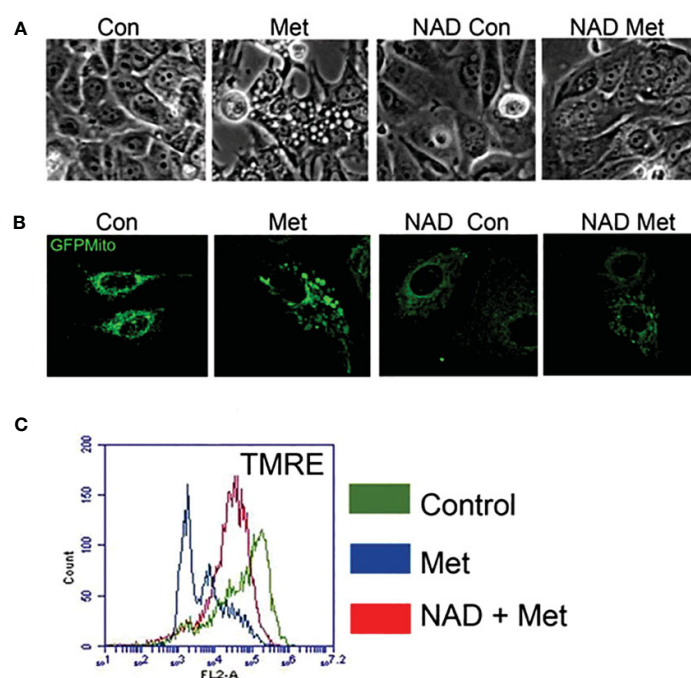


FIGURE 3

Pretreatment of MCF7 cells with NAD<sup>+</sup> prevents the enlargement of mitochondria and protects mitochondria from losing membrane potential caused by metformin. MCF7 cells were pretreated with NAD<sup>+</sup> (1 mM) for 3 days and then treated with or without metformin for 2 days. **(A)** Phase contrast image of MCF7 cells. **(B)** MCF7 stable cells expressing pAcGFP1-Mito Vector were visualized using confocal microscopy to see the morphology of the mitochondria. **(C)** Cells were stained using TMRE. Flow cytometry was used to detect the change of mitochondrial membrane potential.



culture media containing 25 mM glucose. Of note is that in another study of ours, 231 cells were metformin sensitive when incubated in a lower glucose level media (38). In Figure 4A, NAMPT protein levels were examined in MCF7 and 231 cells via Western blot. 231 cells had much higher levels of NAMPT, which may partially account for the metformin resistance in 231 cells in high-glucose media while MCF7 cells are sensitive.

To elucidate the role that NAMPT plays in protecting 231 cells from metformin-induced apoptosis, we created stable knockdowns of NAMPT and confirmed expression of NAMPT by Western blot in Figure 4B. To verify that the NAMPT knockdown causes a decrease in NAD<sup>+</sup>, a NAD<sup>+</sup> assay was performed as shown in Figure 4C. Indeed, there was a significant decrease of NAD<sup>+</sup> levels comparing the SHCONTROL and SHNAMPT cell lines in the control treatment. When treated with metformin, the SHCONTROL line had a significant decrease in NAD<sup>+</sup> compared to control treatment. Interestingly, when the SHNAMPT cells were treated with metformin, they were not able to reach an even lower level of NAD<sup>+</sup>.

Since NAD<sup>+</sup> is not only involved in PARP activation but also a key factor in maintaining metabolism, an ATP assay was performed as shown in Figure 4D. The SHCONTROL cells had a large drop in

ATP levels when treated with metformin. However, an even more striking significant drop in ATP was found between the SHCONTROL metformin-treated cells and the SHNAMPT metformin-treated cells, indicating that maintaining NAD<sup>+</sup> levels is also important for the maintenance of ATP.

We have shown that NAMPT expression is important in maintaining NAD<sup>+</sup> and ATP levels when cells are under metabolic stress, such as following metformin-induced ROS activity [Haugrad, 2014]. We hypothesized that NAMPT overexpression would be involved in determining cancer cell sensitivity to metformin. In Figure 4E, a trypan blue exclusion assay was performed, which displayed the significant increase in cell death in SHNAMPT metformin-treated cells compared to SHCONTROL metformin-treated cells after 1 day. To further confirm this result, an xCELLigence assay was utilized to track the time the cell index reached less than one while cells were treated with metformin in low glucose (2.5 mM glucose). As shown in Figure 4F, the two 231 SHNAMPT stables reached a cell index of less than 1 with an estimated 37 h sooner than the 231 SHCONTROL cells, which confirms that the status of NAMPT may determine the rate at which the 231 cells die from metformin and low-glucose treatment.

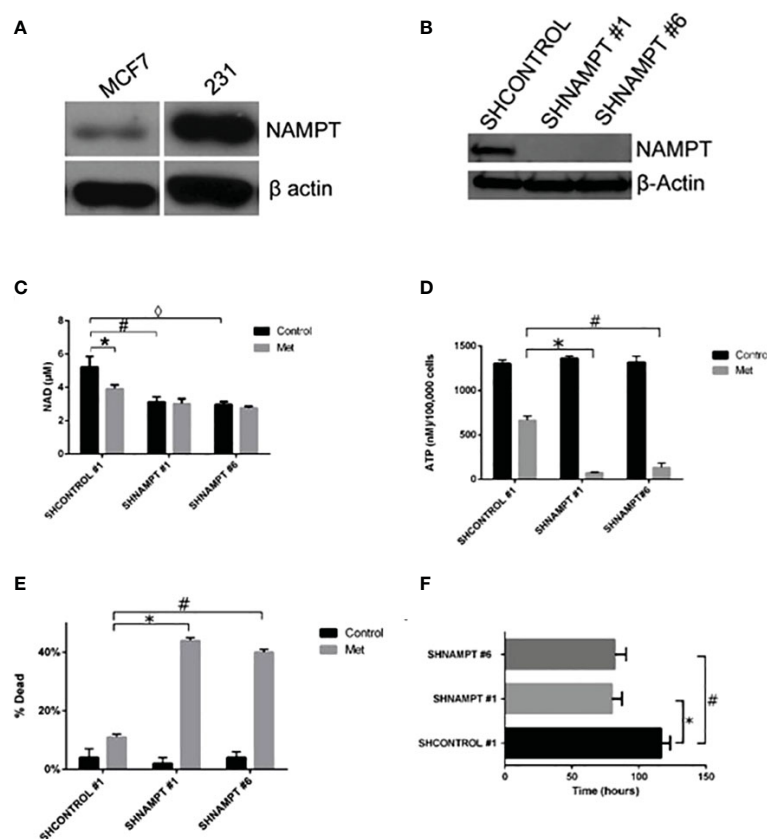


FIGURE 4

231 cells overexpress NAMPT compared to MCF7 cells. When NAMPT is knocked down in 231 cells, NAD<sup>+</sup> and ATP levels are depleted following metformin treatment, inducing metformin sensitivity. (A) Western blot showing that metformin-resistant 231 cells have higher levels of NAMPT compared to metformin-sensitive MCF7 cells. (B) Western blot showing 231 stable cells expressing shNAMPT have low NAMPT expression. (C) NAMPT knockdown leads to lower NAD<sup>+</sup> levels after 1 day of treatment with 8 mM metformin (\* $p = 0.0029$ , # $p = 0.0069$ , <math>p = 0.004). (D) ATP depletion was also seen with the same treatments (\* $p = 0.000029$ , # $p = 0.00018$ ). (E) Enhanced cell death in shNAMPT stables following metformin treatment shown in a Trypan Blue exclusion assay (\* $p = 0.0000024$ , # $p = 0.0000037$ ). (F) Depiction of the time that the cell index reached less than 1 after 8 mM metformin treatment (\* $p = 0.0003$ , # $p = 0.0008$ ).

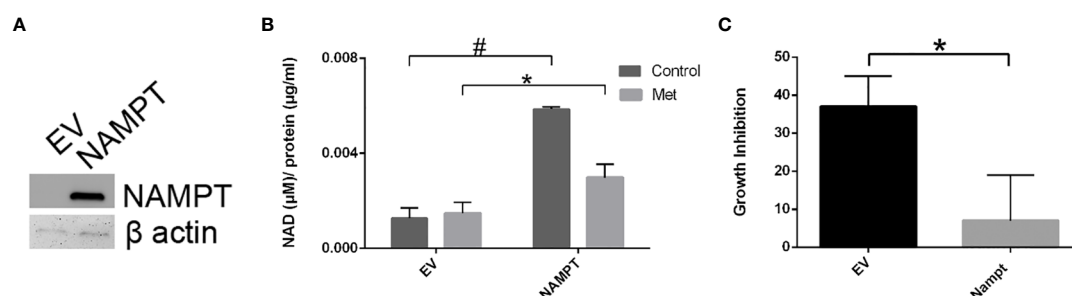


FIGURE 5

293T cell NAMPT overexpression results in higher NAD<sup>+</sup> levels and lower growth inhibition in the presence of metformin. (A) Western blot analysis following transfection of NAMPT mRNA or Empty Vector (EV) in 293T cells. (B) Following NAMPT mRNA transfection, 293T cells were treated for 1 day, counted via trypan exclusion assay (\**p* = 0.023, #*p* = 0.00060). (C) Growth inhibition analysis via Trypan Blue assay of 293T mRNA transfection followed by metformin treatment (\**p* = 0.023).

To further support the importance of NAMPT and NAD levels in cells, we examined how overexpression of NAMPT affected NAD<sup>+</sup> levels and cytotoxicity. We used 293T cells to overexpress NAMPT as shown in Western blot analysis in Figure 5A. Overexpressing NAMPT in 293T cells led to statistically significant higher NAD levels not only in the control-treated cells but also in the metformin-treated cells (Figure 5B). Figure 5C shows that the higher levels of NAMPT significantly prevented growth inhibition when 293T cells were treated with metformin. Similarly, activation of NAMPT with P7C3 in MCF7 cells significantly reduced metformin-induced cytotoxicity at concentrations of 1 and 5 μM P7C3 (Figure 6A). Increased NAD levels were observed when P7C3 was combined with metformin as compared to metformin alone (Figure 6B). The NAMPT activator P7C3 protects against metformin-induced cytotoxicity, suggesting that increased NAD<sup>+</sup> levels may hinder metformin-induced cytotoxicity.

## Discussion

Our present findings support the importance of NAD<sup>+</sup> in sensitivity of cancer cells to metformin cytotoxicity. In our previous study (10), we showed that metformin induces cell death in MCF7 cells in a caspase-dependent and PARP-dependent manner. As supported by other literature (39) and by other studies of ours (38, 40), metformin inhibits complex I of the electron transport chain. This inhibition leads to an accumulation of reactive oxygen species (ROS) causing DNA damage. In response to the DNA damage, PARP is activated and uses NAD<sup>+</sup> to create PAR to start DNA repair. While DNA repair is advantageous to the cancer cell, overactivation of PARP leads to NAD<sup>+</sup> depletion. NAD<sup>+</sup> is not only involved in DNA repair but also necessary for glycolysis and oxidative phosphorylation. Metformin, by inducing PARP overactivation, may cause a “metabolic catastrophe” as supported in the depletion of ATP in Figure 4D in cells with low NAD<sup>+</sup> levels (38).

As demonstrated in our previous work, metformin induced ROS production in mitochondria as measured by flow cytometry using the dye Mitosox in MCF7 cells (40). Our unpublished data illustrate that 231 SHNAMPT stables experienced ROS levels

similar to those of SHCONTROL cells in response to metformin using the same assay. Even though metformin induced similar oxidative stress in 231 SHCONTROL and SHNAMPT stable cell lines, 231 SHNAMPT cells had significant increased sensitivity to metformin cytotoxicity, which is due to their already depleted NAD<sup>+</sup> available to the cells to maintain metabolism while combating DNA damage. Our studies on both MCF7 and 231 cells further highlight the importance of NAMPT in maintaining cellular NAD<sup>+</sup> levels and in the ability of cancer cells to maintain an energy balance to avoid cancer therapy cytotoxicity. Metformin or other therapies inducing DNA damage may cause metabolic catastrophes through NAD<sup>+</sup> shortage in some tumors but may not be as effective in other tumors depending on the levels of NAMPT expression.

Even though intensive studies have been done to understand the mechanisms of metformin on cancer cell growth inhibition and cell death, it has been shown that there is quite a bit of variation in response to metformin in different cancer cells (2, 16). By further understanding the differences between cancer cells, it may shed light on further understanding mechanisms of metformin and provide important information in the application of metformin for cancer prevention and treatment.

The group of Isakovic has shown that metformin caused massive induction of caspase-dependent apoptosis associated with c-Jun N-terminal kinase (JNK) activation, mitochondrial depolarization, and oxidative stress in confluent C6 cultures, and metformin-triggered apoptosis was completely prevented by a mitochondrial permeability transition blocker (cyclosporin A) (2). However, our unpublished data indicate that cyclosporin A could not block the cell death caused by metformin in MCF7 cells. This suggests that even though metformin can cause apoptotic cell death in different cell types, the mechanisms of cell death may not be the same and may depend on the response of mitochondria to metformin treatment in various cell types. As shown in Figure 3A, MCF7 cells respond to metformin with the enlargement of mitochondria when in high-glucose media, which can be prevented with the addition of NAD<sup>+</sup> or a PARP inhibitor (10). This also brings the possible link between the morphological changes of mitochondria and cell death. Furthermore, while metformin-sensitive MCF7 cells have drastic mitochondrial morphology changes, metformin-resistant 231 cells that have

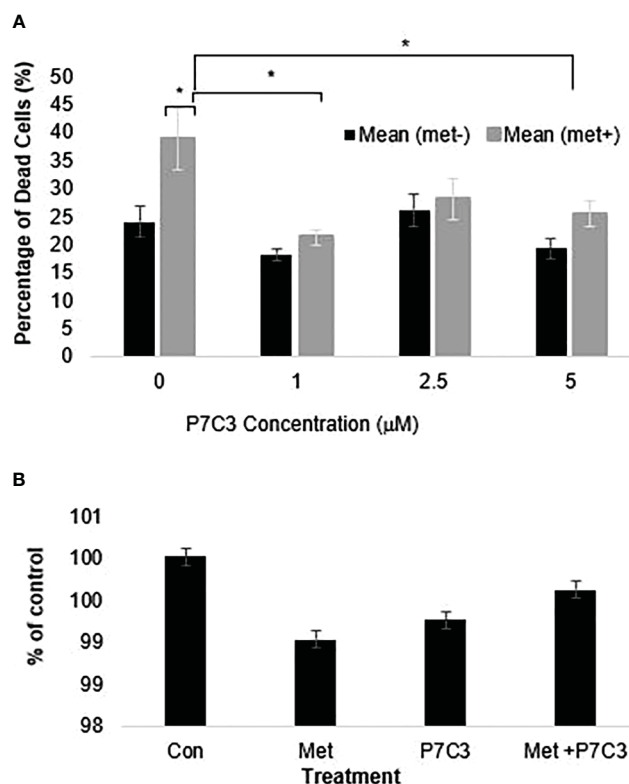


FIGURE 6

(A) P7C3 protects against metformin-induced cytotoxicity and reduces NAD. Sytox Green assays indicate that P7C3 significantly protected against metformin-induced cytotoxicity at 1 and 5 μM P7C3, with error bars denoting standard deviation, according to an unpaired *t*-test with  $p < 0.05$  (\*). (B) NAD assays conducted after 48 h indicate that metformin (8 mM) reduces NAD while 5 mM P7C3 protects against metformin-induced NAD reduction. NAD levels were increased when P7C3 was combined with metformin as compared to metformin alone.

higher NAMPT expression do not, leading us to propose that mitochondrial dynamics and metabolic phenotype are different in these two cell lines while in high-glucose media. However, as mentioned before, we have shown an enhanced sensitivity to metformin in low-glucose media in both MCF7 and 231 cells while MCF10A cells were left unaffected (38), showing promise for the specificity of this treatment to be on tumor cells. Interestingly, mitochondrial changes were not seen in the MCF7 cells in low-glucose/metformin treatment. This is due to an enhanced metabolic catastrophe that does not allow time for mitochondrial morphology changes.

Future studies on mitochondrial dynamics and proteins involved will further aid in understanding why metformin is more effective in some cell lines than others. Such studies will provide essential information concerning the potential use of metformin as an anti-cancer drug and also in understanding the drug mode of action in the treatment of type 2 diabetes.

NAMPT, the critical rate-limiting enzyme of the NAD<sup>+</sup> salvage pathway, has recently become an intriguing protein for a target in creating new drug therapies or for being used as a biomarker. NAMPT levels are often significantly elevated in a number of tumor types (33, 36), are associated with advanced tumor progression (35), and can be induced by hypoxia, which is another marker of poor prognosis (34). Here, we demonstrate that the level of NAMPT expression determines the sensitivity of cells to metformin

treatment, which makes NAMPT an attractive target for drug development. NAMPT inhibitors such as FK866 (also known as APO866) have shown promise in *in vitro* and *in vivo* studies. For example, *in vitro*, FK866 induces cell death in both chemotherapy-sensitive and -resistant small cell lung cancer cell lines (40). In chronic lymphocytic leukemia, FK866 has been identified as a possible targeted therapeutic in high-risk patients, and three clinical trials have been completed showing that FK866 was well tolerated (41). These drugs could be used as cancer sensitizers to treatments that induce NAD<sup>+</sup> depletion such as a low-glucose diet or metformin.

Our overall model is that metformin inhibits Complex I of the electron transport chain (NADH:ubiquinone oxidoreductase), leading to an increase in superoxide and accumulation of ROS. Metformin-mediated increases in cellular ROS causes DNA damage, which promotes an increase in PARP activity. This is supported by studies that show that when PARP is inhibited, there is a decrease in metformin-induced cell death. Since PARP uses NAD<sup>+</sup> as the substrate to synthesize poly(ADP-ribose), metformin-induced PARP activity leads to NAD<sup>+</sup> depletion. Therefore, treating with exogenous NAD<sup>+</sup> or increasing NAMPT activity reduces metformin-induced cell death, while knocking down NAMPT levels enhances metformin-induced cell death.

Overall, this study highlights the role that NAD<sup>+</sup> availability plays in not only metformin treatment, but also other potential

treatments. NAMPT expression may considerably alter how cancer cells may react to different treatments. If further large-scale clinical trials confirm the antitumor effects of metformin, this drug may become an alternative cancer adjuvant therapy in conjunction with standard-of-care chemotherapeutics.

## Data availability statement

The datasets presented in this article are not readily available because There are no datasets which require filing as this paper does not involve any genomic or transcriptomic data. Requests to access the datasets should be directed to [Keith.Miskimins@sanfordhealth.org](mailto:Keith.Miskimins@sanfordhealth.org).

## Author contributions

YZ, AH, and SM wrote the manuscript. YZ, AH, MS, and SMM performed the laboratory experiments. YZ, AH, SMM, and WM edited the manuscript. WM provided conceptualization. WM and SM provided funding for work. All authors contributed to the article and approved the submitted version.

## Funding

This work was supported by a pilot grant entitled “Investigation of the mechanism by which metformin induces cytotoxicity in Triple Negative Breast Cancer (TNBC)” (SM) from the COBRE grant P20 GM103548-06 (PI: WM) from the National Institutes of Health and the R01 CA180033-04 entitled “Molecular mechanisms by which the diabetic drug metformin kills cancer cells” (WM) from the National Cancer Institute (NCI). This project used Sanford Research Histology and Imaging and Flow Cytometry Cores, which are supported by COBRE grant received from the COBRE grant P20

GM103548-06 (WM) from the National Institutes of Health. Additional support was received from Geographical Management of Cancer Health Disparities Program (GMaP) Region 6 Research Scholar award (SM) from the National Cancer Institute of the National Institutes of Health P30CA042014 GMaP Region 6 and the National Institute of General Medical Sciences, U54 GM115458, which funds the Great Plains IDeA-CTR Network. The content is solely the responsibility of the authors and does not necessarily represent the official views of the National Institutes of Health and the National Science Foundation.

## Acknowledgments

The authors would like to thank Claire Evans, Kelly Graber, and Marisela Killian from the Histology, Imaging, and Flow Cytometry core, respectively, at Sanford Research, and the Sanford Program for Undergraduate Research (SPUR) program at Sanford Research, Sioux Falls, SD.

## Conflict of interest

The authors declare that the research was conducted in the absence of any commercial or financial relationships that could be construed as a potential conflict of interest.

## Publisher's note

All claims expressed in this article are solely those of the authors and do not necessarily represent those of their affiliated organizations, or those of the publisher, the editors and the reviewers. Any product that may be evaluated in this article, or claim that may be made by its manufacturer, is not guaranteed or endorsed by the publisher.

## References

- Buzzai M, Jones RG, Amaravadi RK, Lum JJ, DeBerardinis RJ, Zhao F, et al. Systemic treatment with the antidiabetic drug metformin selectively impairs p53-deficient tumor cell growth. *Cancer Res* (2007) 67(14):6745–52. doi: 10.1158/0008-5472.CAN-06-4447
- Isakovic A, Harhaji L, Stevanovic D, Markovic Z, Sumarac-Dumanovic M, Starcevic V, et al. Dual antiglioma action of metformin: cell cycle arrest and mitochondria-dependent apoptosis. *Cell Mol Life Sci* (2007) 64(10):1290–302. doi: 10.1007/s00018-007-7080-4
- Zakikhani M, Dowling R, Fantus IG, Sonenberg N, Pollak M. Metformin is an AMP kinase-dependent growth inhibitor for breast cancer cells. *Cancer Res* (2006) 66(21):10269–73. doi: 10.1158/0008-5472.CAN-06-1500
- Zhuang Y, Miskimins WK. Cell cycle arrest in Metformin treated breast cancer cells involves activation of AMPK, downregulation of cyclin D1, and requires p27Kip1 or p21Cip1. *J Mol Signal* (2008) 3:18. doi: 10.1186/1750-2187-3-18
- Algire C, Amrein L, Zakikhani M, Panasci L, Pollak M. Metformin blocks the stimulative effect of a high-energy diet on colon carcinoma growth in vivo and is associated with reduced expression of fatty acid synthase. *Endocrine-related cancer*. (2010) 17(2):351–60. doi: 10.1677/ERC-09-0252
- Alimova IN, Liu B, Fan Z, Edgerton SM, Dillon T, Lind SE, et al. Metformin inhibits breast cancer cell growth, colony formation and induces cell cycle arrest in vitro. *Cell Cycle* (2009) 8(6):909–15. doi: 10.4161/cc.8.6.7933
- Bao B, Wang Z, Ali S, Ahmad A, Azmi AS, Sarkar SH, et al. Metformin inhibits cell proliferation, migration and invasion by attenuating CSC function mediated by deregulating miRNAs in pancreatic cancer cells. *Cancer Prev Res* (2012) 3:355–64. doi: 10.1158/1940-6207.CAPR-11-0299
- Chen G, Xu S, Renko K, Derwahl M. Metformin inhibits growth of thyroid carcinoma cells, suppresses self-renewal of derived cancer stem cells, and potentiates the effect of chemotherapeutic agents. *J Clin Endocrinol Metab* (2012) 97(4):E510–20. doi: 10.1210/jc.2011-1754
- Taubes G. Cancer research. Cancer prevention with a diabetes pill? *Science* (2012) 335(6064):29. doi: 10.1126/science.335.6064.29
- Zhuang Y, Miskimins WK. Metformin induces both caspase-dependent and poly(ADP-ribose) polymerase-dependent cell death in breast cancer cells. *Mol Cancer Res* (2011) 9(5):603–15. doi: 10.1158/1541-7786.MCR-10-0343
- Evans JM, Donnelly LA, Emslie-Smith AM, Alessi DR, Morris AD. Metformin and reduced risk of cancer in diabetic patients. *Bmj* (2005) 330(7503):1304–5. doi: 10.1136/bmj.38415.708634.F7
- Aldea M, Tomuleasa C, Petrushev B, Susman S, Kacso GI, Irimie A, et al. Antidiabetic pharmacology: a link between metabolic syndrome and neuro-oncology? *J BUON Off J Balkan Union Oncol* (2011) 16(3):409–13.
- Bo S, Ciccone G, Rosato R, Villosio P, Appendino G, Ghigo E, et al. Cancer mortality reduction and metformin: a retrospective cohort study in type 2 diabetic



patients. *Diabetes Obes Metab* (2012) 14(1):23–9. doi: 10.1111/j.1463-1326.2011.01480.x

14. Gallagher EJ, LeRoith D. Diabetes, cancer, and metformin: connections of metabolism and cell proliferation. *Ann New York Acad Sci* (2011) 1243(1):54–68. doi: 10.1111/j.1749-6632.2011.06285.x

15. Liu B, Fan Z, Edgerton SM, Deng XS, Alimova IN, Lind SE, et al. Metformin induces unique biological and molecular responses in triple negative breast cancer cells. *Cell Cycle* (2009) 8(13):2031–40. doi: 10.4161/cc.8.13.8814

16. Wang LW, Li ZS, Zou DW, Jin ZD, Gao J, Xu GM. Metformin induces apoptosis of pancreatic cancer cells. *World J Gastroenterol WJG*. (2008) 14(47):7192–8. doi: 10.3748/wjg.14.7192

17. Malki A, Youssef A. Antidiabetic drug metformin induces apoptosis in human MCF breast cancer via targeting ERK signaling. *Oncol Res* (2011) 19(6):275–85. doi: 10.3727/096504011X13021877989838

18. Wu N, Gu C, Gu H, Hu H, Han Y, Li Q. Metformin induces apoptosis of lung cancer cells through activating JNK/p38 MAPK pathway and GADD153. *Neoplasma* (2011) 58(6):482–90. doi: 10.4149/neo\_2011\_06\_482

19. Abd Elmageed ZY, Naura AS, Errami Y, Zerfaoui M. The poly(ADP-ribose) polymerases (PARPs): new roles in intracellular transport. *Cell signalling*. (2012) 24(1):1–8. doi: 10.1016/j.cellsig.2011.07.019

20. Boulu RG, Mesenge C, Charriaud-Marlangue C, Verrecchia C, Plotkine M. [Neuronal death: potential role of the nuclear enzyme, poly (ADP-ribose) polymerase]. *Bull l'Academie nationale medecine*. (2001) 185(3):555–63. doi: 10.1016/S0001-4079(19)34539-X

21. Burkle A. Poly(ADP-ribose). The most elaborate metabolite of NAD<sup>+</sup>. *FEBS J* (2005) 272(18):4576–89. doi: 10.1111/j.1742-4658.2005.04864.x

22. Burkle A. Physiology and pathophysiology of poly(ADP-ribose)ylation. *BioEssays News Rev molecular Cell Dev Biol* (2001) 23(9):795–806. doi: 10.1002/bies.1115

23. Burkle A. Poly(ADP-ribose)ylation, genomic instability, and longevity. *Ann New York Acad Sci* (2000) 908:126–32. doi: 10.1111/j.1749-6632.2000.tb06641.x

24. Ying W. NAD<sup>+</sup> and NADH in cellular functions and cell death. *Front bioscience J virtual library*. (2006) 11:3129–48. doi: 10.2741/2038

25. Egi Y, Matsuura S, Maruyama T, Fujio M, Yuki S, Akira T. Neuroprotective effects of a novel water-soluble poly(ADP-ribose) polymerase-1 inhibitor, MP-124, in *in vitro* and *in vivo* models of cerebral ischemia. *Brain Res* (2011) 1389:169–76. doi: 10.1016/j.brainres.2011.03.031

26. Kristian T, Balan I, Schuh R, Onken M. Mitochondrial dysfunction and nicotinamide dinucleotide catabolism as mechanisms of cell death and promising targets for neuroprotection. *J Neurosci Res* (2011) 89(12):1946–55. doi: 10.1002/jnr.22626

27. Okamoto H. Recent advances in physiological and pathological significance of tryptophan-NAD<sup>+</sup> metabolites: lessons from insulin-producing pancreatic beta-cells. *Adv Exp Med Biol* (2003) 527:243–52. doi: 10.1007/978-1-4615-0135-0\_28

28. Kim MY, Zhang T, Kraus WL. Poly(ADP-ribosyl)ation by PARP-1: 'PAR-laying' NAD<sup>+</sup> into a nuclear signal. *Genes Dev* (2005) 19(17):1951–67. doi: 10.1101/gad.1331805

29. Kirkland JB. Poly ADP-ribose polymerase-1 and health. *Exp Biol Med* (2010) 235(5):561–8. doi: 10.1258/ebm.2010.009280

30. Preiss J, Handler P. Biosynthesis of diphosphopyridine nucleotide. *J Biol Chem* (1958) 233(2):488–92. doi: 10.1016/S0021-9258(18)64789-1

31. Preiss J, Handler P. Biosynthesis of diphosphopyridine nucleotide II. *ENZYMATIC Aspects J Biol Chem* (1958) 233(2):493–500. doi: 10.1016/S0021-9258(18)64790-8

32. Magni G, Orsomo G, Raffelli N, Ruggieri S. Enzymology of mammalian NAD metabolism in health and disease. *Front Bioscience*. (2008) 13(6):6135–54. doi: 10.2741/3143

33. Bi TQ, Che XM. Nampt/PBEF/visfatin and cancer. *Cancer Biol Ther* (2010) 10(2):119–25. doi: 10.4161/cbt.10.2.12581

34. Bae SK, Kim SR, Kim JG, Kim JY, Koo TH, Jang HO, et al. Hypoxic induction of human visfatin gene is directly mediated by hypoxia-inducible factor-1. *FEBS Letters*. (2006) 580(17):4105–13. doi: 10.1016/j.febslet.2006.06.052

35. Nakajima TE, Yamada Y, Hamano T, Furuta K, Matsuda T, Fujita S, et al. Adipocytokines as new promising markers of colorectal tumors: Adiponectin for colorectal adenoma, and resistin and visfatin for colorectal cancer. *Cancer Science*. (2010) 101(5):1286–91. doi: 10.1111/j.1349-7006.2010.01518.x

36. Wang B, Hasan MK, Alvarado E, Yuan H, Wu H, Chen WY. NAMPT overexpression in prostate cancer and its contribution to tumor cell survival and stress response. *Oncogene* (2011) 30(8):907–21. doi: 10.1038/onc.2010.468

37. Pittelli M, Felici R, Pitozzi V, Giovannelli L, Bigagli E, Cialdai F, et al. Pharmacological effects of exogenous NAD on mitochondrial bioenergetics, DNA repair, and apoptosis. *Mol Pharmacol* (2011) 80(6):1136–46. doi: 10.1124/mol.111.073916

38. Zhuang Y, Chan DK, Haugrud AB, Miskimins WK. Mechanisms by which low glucose enhances the cytotoxicity of metformin to cancer cells both *in vitro* and *in vivo*. *PLoS One* (2014) 9(9):e108444. doi: 10.1371/journal.pone.0108444

39. Owen MR, Doran E, Halestrap AP. Evidence that metformin exerts its anti-diabetic effects through inhibition of complex 1 of the mitochondrial respiratory chain. *Biochem J* (2000) 348 Pt 3:607–14. doi: 10.1042/bj3480607

40. Haugrud AB, Zhuang Y, Coppock JD, Miskimins WK. Dichloroacetate enhances apoptotic cell death via oxidative damage and attenuates lactate production in metformin-treated breast cancer cells. *Breast Cancer Res Treat* (2014) 147(3):539–50. doi: 10.1007/s10549-014-3128-y

41. Gehrke I, Bouchard ED, Beiggi S, Poepl AG, Johnston JB, Gibson SB, et al. On-target effect of FK866, a nicotinamide phosphoribosyl transferase inhibitor, by apoptosis-mediated death in chronic lymphocytic leukemia cells. *Clin Cancer Res* (2014) 20(18):4861–72. doi: 10.1158/1078-0432.CCR-14-0624



## OPEN ACCESS

## EDITED BY

Carlos Pérez-Plasencia,  
National Autonomous University of Mexico,  
Mexico

## REVIEWED BY

Guofang Zhang,  
Duke University, United States  
Jossimar Coronel Hernández,  
National Institute of Cancerology (INCAN),  
Mexico

## \*CORRESPONDENCE

Ketao Jin

✉ jinketao2001@zju.edu.cn

Yefeng Chen

✉ 4158168@qq.com

<sup>†</sup>These authors have contributed equally to  
this work

RECEIVED 10 May 2023

ACCEPTED 24 July 2023

PUBLISHED 10 August 2023

## CITATION

Xu E, Ji B, Jin K and Chen Y (2023)  
Branched-chain amino acids catabolism  
and cancer progression: focus on  
therapeutic interventions.  
*Front. Oncol.* 13:1220638.  
doi: 10.3389/fonc.2023.1220638

## COPYRIGHT

© 2023 Xu, Ji, Jin and Chen. This is an  
open-access article distributed under the  
terms of the [Creative Commons Attribution  
License \(CC BY\)](#). The use, distribution or  
reproduction in other forums is permitted,  
provided the original author(s) and the  
copyright owner(s) are credited and that  
the original publication in this journal is  
cited, in accordance with accepted  
academic practice. No use, distribution or  
reproduction is permitted which does not  
comply with these terms.

# Branched-chain amino acids catabolism and cancer progression: focus on therapeutic interventions

Er Xu<sup>1†</sup>, Bangju Ji<sup>2†</sup>, Ketao Jin<sup>3\*</sup> and Yefeng Chen<sup>4\*</sup>

<sup>1</sup>Department of Hospital Infection Management, Affiliated Hospital of Shaoxing University, Shaoxing, Zhejiang, China, <sup>2</sup>Department of Colorectal Surgery, Shaoxing People's Hospital, Shaoxing, Zhejiang, China, <sup>3</sup>Department of Colorectal Surgery, Affiliated Jinhua Hospital, Zhejiang University School of Medicine, Jinhua, Zhejiang, China, <sup>4</sup>Department of Respiratory Medicine, Shaoxing People's Hospital, Shaoxing, Zhejiang, China

Branched-chain amino acids (BCAAs), including valine, leucine, and isoleucine, are crucial amino acids with significant implications in tumorigenesis across various human malignancies. Studies have demonstrated that altered BCAA metabolism can influence tumor growth and progression. Increased levels of BCAAs have been associated with tumor growth inhibition, indicating their potential as anti-cancer agents. Conversely, a deficiency in BCAAs can promote tumor metastasis to different organs due to the disruptive effects of high BCAA concentrations on tumor cell migration and invasion. This disruption is associated with tumor cell adhesion, angiogenesis, metastasis, and invasion. Furthermore, BCAAs serve as nitrogen donors, contributing to synthesizing macromolecules such as proteins and nucleotides crucial for cancer cell growth. Consequently, BCAAs exhibit a dual role in cancer, and their effects on tumor growth or inhibition are contingent upon various conditions and concentrations. This review discusses these contrasting findings, providing valuable insights into BCAA-related therapeutic interventions and ultimately contributing to a better understanding of their potential role in cancer treatment.

## KEYWORDS

branched-chain amino acids, cancer, metabolism, catabolism, cancer therapy

## 1 Introduction

Cancer is one of the most critical problems related to human health, which affects millions of people worldwide every year and leads to numerous deaths (1). Studies have revealed that the metabolism of tumor and immune cells in the tumor microenvironment (TME) plays a crucial role in cancer development and antitumor immune responses (2). For instance, tumor cells utilize various metabolic pathways to produce biological macromolecules that support their energy and proliferation (3, 4). On the other hand, the concentration of nutrients in the TME affects the selection of the metabolic pathways

and macromolecules by tumor cells to reach the optimum conditions for their growth and survival. Among the macromolecules used by tumor and immune cells, amino acids, glucose, and fatty acids are essential for producing energy and growth (5–7).

Recent studies have suggested that an imbalance in amino acids, including essential and non-essential ones, may contribute to the pathogenesis of various human disorders, including cancer (8). Among these amino acids, branched-chain amino acids (BCAAs), including leucine, isoleucine, and valine, are essential and cannot be synthesized by the human body. Therefore, including BCAA-rich proteins in the diet is necessary to support protein synthesis, increase albumin levels, and prevent proteolysis (9, 10). Interestingly, BCAAs have been found to inhibit tumor cell migration and metastasis by reducing the expression of N-cadherin (11). However, the role of BCAAs in cancer remains controversial, as some studies have indicated that the catabolism of these amino acids can enhance tumor growth and progression in a dose-dependent manner (12). As a result, targeting the enzymes involved in BCAA catabolism or utilizing BCAA-rich diets has emerged as potential therapeutic interventions (13). Nonetheless, due to the dual role of BCAAs in cancer, the implementation of these therapeutic approaches may present challenges and limitations (14).

This review delves into the role of BCAAs in cancer pathogenesis, and therapeutic interventions involving the inhibition of BCAA catabolism and the utilization of BCAA-rich diets for cancer treatment are summarized. Additionally, the achievements and limitations of these approaches are discussed, providing a comprehensive analysis of BCAA-related strategies in cancer treatment.

## 2 BCAA biology

The nine essential amino acids include valine, leucine, isoleucine, histidine, lysine, tryptophan, methionine, phenylalanine, and threonine (15). Among these crucial amino acids, BCAAs (leucine, isoleucine, and valine) have an aliphatic side chain and a branch composed of a central carbon bound to three or more carbon atoms. BCAAs are non-polar aliphatic amino acids consisting of a carboxylic acid group, an amino group, and an isopropyl group on the side chains. Valine ( $\text{HO}_2\text{CCH}(\text{NH}_2)\text{CH}(\text{CH}_3)_2$ ) is an aliphatic and highly hydrophobic amino acid found in the interior of globular proteins. Valine preserves mental strength, promotes muscle growth, aids in tissue repair, and provides energy support as a glycogenic essential amino acid. Soy, fish, cheese, vegetables, and meats are rich sources of valine. L-Valine is one of the twenty proteinogenic amino acids encoded by GUC, GUU, GUA, and GUG codons (16).

Leucine ( $\text{HO}_2\text{CCH}(\text{NH}_2)\text{CH}_2\text{CH}(\text{CH}_3)_2$ ) is a hydrophobic amino acid encoded by UUA, UUG, CUC, CUU, CUG, and CUA codons. It is a critical component of astacin and ferritin subunits. Leucine deficiency is rare because it is available in several foods (17). Another BCAA, isoleucine ( $\text{HO}_2\text{CCH}(\text{NH}_2)\text{CH}(\text{CH}_3)\text{CH}_2\text{CH}_3$ ), is synthesized from pyruvate by bacteria that utilize leucine

biosynthesis enzymes. Isoleucine is encoded by the AUU, AUC, and AUA codons and is found in seeds, nuts, meats, cheese, fish, and eggs (18).

BCAAs belong to the proteinogenic amino acids category (19). They play a role in several physiological and metabolic mechanisms, such as promoting protein synthesis and degradation in skeletal muscles and other tissues, hormone production, detoxification of nitrogenous wastes, wound healing, initiating signaling pathways, regulating gene expression, cell apoptosis and regeneration, insulin resistance, and glucose metabolism (20–22). BCAAs can promote glycogen sparing, and there is a close association between BCAAs, brain levels of tryptophan, and serotonin (23). The oxidation of BCAAs primarily occurs in skeletal muscles by specific enzymes, enhancing fatty acid oxidation and preventing obesity. However, other amino acids are catabolized in the liver (20). BCAAs also participate in immune system processes. It has been revealed that immune cells produce decarboxylase and dehydrogenase enzymes responsible for breaking down BCAAs, thereby improving lymphocyte growth and proliferation, dendritic cell (DC) maturation, and boosting cytotoxic T cell activity (24, 25).

Cells sense the availability of intracellular concentrations of BCAAs, such as leucine, to regulate ribosome biogenesis and protein synthesis. Phosphorylated sestrin2, by binding to gator2, negatively regulates the mammalian target of rapamycin complex 1 (mTORC1) protein kinase, which is involved in cell growth. It has been shown that sestrin is dephosphorylated after binding to leucine, reducing its inhibitory effect on gator2. As a result, the mTORC1 pathway is activated and leads to cell growth (26, 27). Another interesting interaction of leucine with mTORC1 is enhancing the acetylation of Raptor (a partner of mTORC1) by leucine-derived acetyl-CoA, which improves growth signals (28). Therefore, leucine can significantly promote cell growth by activating the mTORC1 pathway (29). Evidence suggests that uncontrolled activation of the mTOR pathway has been reported in several human cancers. Therefore, increasing the concentrations of BCAAs, especially leucine, may enhance the growth of tumor cells (30).

## 3 BCAAs catabolism

As mentioned before, BCAAs can be catabolized by enzymes, which affect the levels of leucine, isoleucine, and valine in an overlapping manner (29). Since leucine is abundant in proteins, the breakdown of exogenous proteins from foods or internal sources such as muscles releases a large amount of this amino acid (31). The final product of the oxidation of BCAAs varies depending on their type because studies have shown that the carbon precursors used for glucose production, which occurs independently of acetyl-CoA, are only produced by the catabolism of valine and isoleucine (29). Moreover, the production of carbon derived from BCAAs during their catabolism can provide the necessary fuel for the tricarboxylic acid (TCA) cycle and oxidative phosphorylation, supplying energy to the cells. Additionally, it has been shown that BCAA catabolism can facilitate the synthesis of other amino acids and

nucleotides through the *de novo* pathway, as well as proteins, by affecting proteinogenic amino acids or enhancing nutritional cell signals. The breakdown of BCAAs produces metabolites that can potentially influence the epigenome. One notable example is the generation of acetyl-CoA from BCAA catabolism (29). Acetyl-CoA serves as a crucial supplier of acetyl groups for histone acetylation, thereby influencing the epigenetic characteristics of cells by affecting acetyl-CoA levels (32–34).

Transamination is an essential phenomenon in the catabolism of free BCAAs, carried out by the enzymes branched-chain amino acid transaminase 1 (BCAT1) and BCAT2. BCAAs can undergo transamination, and the transfer of nitrogen to  $\alpha$ -ketoglutarate ( $\alpha$ -KG) leads to the generation of glutamate and branched-chain keto acids (BCKAs), including ketovaline ( $\alpha$ -ketoisovalerate), ketoleucine ( $\alpha$ -ketoisocaproate), and ketoisoleucine ( $\alpha$ -keto- $\beta$ -methylvalerate). BCAT1 and BCAT2, both highly active reversible enzymes present in the cytosol and mitochondria, act upon all three BCAAs and their corresponding BCKAs. Interestingly, to regenerate  $\alpha$ -KG and BCAA, BCAT1 and BCAT2 transfer nitrogen from glutamate back to a BCKA (29). Therefore, nitrogen can be replaced quickly between BCAAs, glutamate,  $\alpha$ -KG, and BCKAs even in a minimum BCAAs catabolism state. A multimeric enzyme complex called BCKA dehydrogenase (BCKDH), which consists of E1, E2, and E3 subunits, catalyzes the oxidative decarboxylation of BCKAs to generate acyl-CoA derivatives, including isovaleryl-CoA, 2-methylbutyryl-CoA, and isobutyryl-CoA in various cells and tissues. These acyl-CoA derivatives are metabolized through distinct pathways. Specifically, valine catabolism yields propionyl-CoA, leucine

generates acetyl-CoA and acetoacetate, and isoleucine produces acetyl-CoA and propionyl-CoA (35).

In mammals, the activity of BCKDH is irreversible. Additionally, the absence of enzymes synthesizing BCKAs from the *de novo* pathway makes it impossible to produce BCAAs in the body (36).

## 4 BCAA catabolism and cancer

Recent investigations show that several human disorders, such as cancer, can be associated with increased circulatory levels of BCAAs (Figure 1). Furthermore, whole-body protein turnover and dietary intake determine the plasma levels of BCAAs because the gut is responsible for BCAA absorption and their release into the blood circulation (37–39). In the conditions of need, BCAAs are released from proteins and catabolized in the tissues that express BCATs, such as skeletal muscles, leading to the production of BCKA and its release into the bloodstream. Due to the expression of BCKDH in the liver, circulatory BCKAs provide carbon for fatty acid synthesis, ketogenesis, and gluconeogenesis (40).

Systemic glucose metabolism can be affected by BCAAs via the regulation of insulin release and tissue sensitivity to this hormone (41, 42). On the other hand, insulin, through regulating the BCKDH enzyme in the liver, is involved in regulating BCAA catabolism. Therefore, impairment in the normal function of the pancreas, obesity, diabetes, and insulin resistance can affect BCAA breakdown in skeletal muscles, liver BCKA breakdown, and plasma concentrations of BCAAs (43). It has been reported that tumor

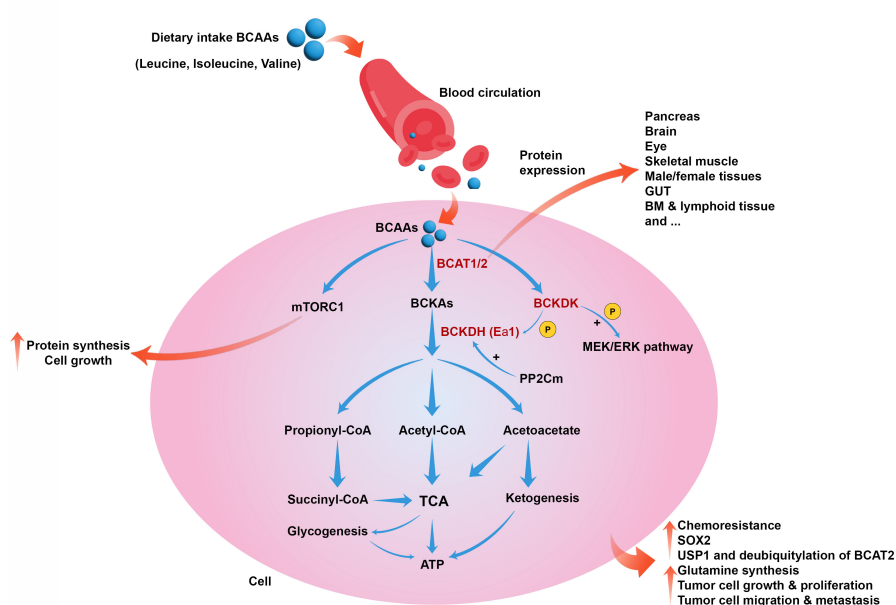


FIGURE 1

Role of BCAAs catabolism in cancer. BCAAs catabolism is induced by BCAT1, BCAT2, BCKDK, and BCKDH to produce metabolic intermediates such as acetyl-CoA, initiating the TCA cycle and producing energy. BCAAs also can induce mTORC1 and cell growth and proliferation. BCAAs catabolism can collectively lead to chemoresistance, upregulation of SOX2, induction of USP1 and deubiquitylation of BCAT2, glutamine synthesis, tumor cell growth, proliferation, migration, and metastasis.



cells may reprogram the systemic metabolism of BCAAs, leading to cancer progression (29, 44). Glutamine is one of the essential amino acids produced from BCAA catabolism and is a basic requirement for numerous tumor cells (35). Tumor cells use BCAAs as fuel, increasing the expression of BCAT1 and catabolizing them to provide glutamine. Studies have reported that the increase in BCAT1 enzyme levels is associated with tumor growth and proliferation in various cancers, and inhibiting it in certain cases, such as glioblastoma, leads to a decrease in tumor development (45–47).

Interestingly, in Hepatocellular carcinoma (HCC), only the levels of BCAT1/2 are upregulated, leading to chemoresistance, while BCKDH and other enzymes involved in BCAA catabolism are decreased (45, 48). In contrast, an investigation revealed that in breast cancer, along with BCAT1, the expression of BCKDHA and BCKDHB was upregulated, thus promoting tumor cell growth (49). BCAT1 also can induce the mTORC1 pathway to amplify mitochondrial biogenesis and generate ATP, providing energy and enhancing tumor cells' growth and colony formation in breast cancer (49). Upregulation of BCAT1 is also reported in other human malignancies, such as ovarian cancer. An investigation on ovarian cancer cells showed that suppressing BCAT1 can downregulate involved genes in tumorigenesis and reduce ATP levels generated by the TCA cycle (50). BCAAs are used as a potential carbon source for the biogenesis of fatty acids to facilitate cell proliferation (12). In pancreatic ductal adenocarcinoma (PDAC), the concentrations of BCAA levels are significantly elevated, which is associated with tumor growth and development because BCAT2 is upregulated in PDAC, and the inhibition of this enzyme is associated with suppressing PDAC progression (51, 52).

Moreover, pancreatic stellate cells (PSCs) in PDAC regulate BCAA metabolism. Assessment of serum and tissue BCAAs in patients with PDAC revealed their levels significantly increased; however, adding BCAA to PDAC cell culture medium in several concentrations cannot affect tumor cell proliferation and migration. This study showed that following coculture of aPSCs with PDAC cells induced the proliferation of tumor cells by affecting the pattern of proteins involved in the BCAA degradation pathway (53).

A significant upregulation of BCKDK was reported in patients with colorectal cancer and was accompanied by an unpromising prognosis. Preclinical studies on colorectal cancer demonstrated that BCKDK activates MEK/ERK pathway, inducing tumorigenesis (54, 55).

Leucine is a ketogenic amino acid that can be imported from the circulation into the brain parenchyma (56). In this way, it can provide the metabolic requirements of cancer cells in brain tumors as an effective substrate and complement of glucose. Evidence shows that brain tumor cells can eliminate leucine from their milieu and augment their media with the metabolite 2-oxoisocaproate. Moreover, enriched media with a high leucine concentration produced 3-hydroxybutyrate and citrate, indicating metabolic reprogramming of tumor cells. In human tumor samples as well as cultured cancer cells, the expression of 3-methylcrotonyl-CoA carboxylase was detected. This enzyme is involved in the irreversible leucine catabolic processes (57). Accordingly, tumor

cells can catabolize leucine and deliver its carbon atoms to the TCA cycle. In addition, leucine contributes to the production of lipids required for citrate to be withdrawn from the TCA cycle (57).

Serum metabolites in patients with non-small-cell lung cancer (NSCLC) and NSCLC cell cultures supernatant were examined, and findings showed that following upregulation of BCKDK, BCAA concentration significantly increased. At the same time, citrate levels were reduced in preoperative NSCLC patients than in healthy subjects. Furthermore, knockout of BCKDK inhibited tumor cell proliferation and induced apoptosis of NSCLC cells *ex vivo*. The oxidative phosphorylation and ROS levels increased, and glycolysis was repressed. These data indicated that BCKDK affects oxidative phosphorylation and glycolysis via regulating BCAA and citrate degradation, inducing NSCLC progression (58).

It has been revealed that liver cancer cells induce BCAA catabolism in the absence of glutamine, increasing carbon and nitrogen to generate nucleotide and enhancing the cell cycle and cell survival. Under glutamine deficiency conditions, O-linked-N-acetylglucosaminylation is increased, stabilizing mitochondrion protein phosphatase 1K (PPM1K) protein, as well as increasing BCKDHA dephosphorylation and BCAAs decomposition. An upregulation of BCKDHA and dephosphorylated BCKDHA induces tumorigenesis and is associated with poor prognosis in patients with HCC (59).

Analysis of genes involved in BCAA catabolism in pancreatic cancer showed that among dihydrolipoamide branched chain transacylase E2 (*DBT*), 4-aminobutyrate aminotransferase (*ABAT*), acetyl-CoA acetyltransferase 1 (*ACAT1*), *BCAT1*, and *BCAT2*, which were correlated to poor prognosis, *ABAT* and *BCAT2* were hub genes with satisfactory prognosis values. Moreover, the upregulation of *BCAT2* was associated with increased infiltration of stromal CD68<sup>+</sup> macrophage in the TME of the high-risk group (60). Studies on breast cancer cell lines, such as BCC and MCF-7, showed that these cells provide their required energy via degrading BCAAs and can generate mevalonate by leucine degradation. Additionally, metabolic flux analysis around the mevalonate node demonstrated that high concentrations of acetoacetate were produced from BCAA-derived carbon, and this metabolite could be a potential source for lipid synthesis (61). These data indicate that the degradation of BCAAs could be a potential carbon/energy source for tumor cell proliferation and a potential therapeutic target for cancer treatment.

Unexpectedly, an investigation found that the increased levels of BCAA, by increasing dietary intake in mice or the genetic model, inhibited tumor growth and breast cancer lung metastasis. According to the survival analysis results, the expression of genes involved in BCAA catabolism, such as PPM1K, is robustly correlated to tumorigenesis in patients with breast cancer. Knockout of *ppm1k* in mice led to the accumulation of BCAAs due to impaired BCAA catabolism, increasing infiltrated NK cells and inhibiting tumor growth in the studied animals without affecting tumor cell proliferation and vasculature (11).

Metabolic diseases, such as type 2 diabetes mellitus and obesity, could be associated with human malignancies, and adipose tissue is actively involved in developing these disorders. Based on available knowledge, white adipose tissue stores excess energy, whereas

brown and beige adipose tissues (thermogenic fats) can convert energy to heat and act as metabolic sinks of glucose, amino acids, and fatty acids (62). In the TME, these activated thermogenic adipocytes induce cancer development by providing fuel sources and leading to chemoresistance (63). Therefore, there seems to be a close relationship between adipose tissue and BCAA catabolism, which can affect tumor metabolism and lead to cancer development (64). Angiopoietin-like-4 (ANGPTL4) regulates lipids and BCAAs metabolism and is involved in tumor metastasis and progression. A study shows that ANGPTL4 is downregulated in osteosarcoma (OS). There is a negative correlation between the ANGPTL4 expression and BCAA catabolism in OS cell lines and human samples. Therefore, *ANGPTL4* knockdown in OS cells leads to accumulating BCAAs, activating the mTOR pathway, and boosting OS cell proliferation and progression. Accordingly, targeting the ANGPTL4/BCAA/mTOR axis could be a potential therapeutic target to reduce OS development (65).

It has been discovered that BCAT1 is overexpressed at the protein level in tumor cells and tissues isolated from patients with metastatic lung cancer. Transcriptomic data analysis in the TCGA database also demonstrated that upregulation of *BCAT1* transcription was associated with poor overall survival. This is because high concentrations of BCAT1 depleted  $\alpha$ -KG and increased SOX2 expression. Since SOX2 is a transcription factor in regulating stemness and metastasis of cancer cells, upregulation of BACT1 can induce tumor development (66).

In human blood malignancies, a study reported that BCAA metabolism affects human leukemia cells to preserve their stemness regardless of lymphoid or myeloid types. Analysis of human primary acute leukemic cells showed that these cells could express BCAA

transporters for BCAA uptake, BCAT1, and had higher levels of cellular BCAA as well as  $\alpha$ -KG than CD34<sup>+</sup> hematopoietic stem progenitor cells (HSPCs) as control (67). In xenograft leukemia models, BCAA deprivation from the daily diet significantly suppressed tumor cells' self-renewal, expansion, and engraftment. Moreover, suppressing BCAA catabolism in primary ALL or AML cells lead to the inactivation of the polycomb repressive complex 2 (PRC2) function. PRC2 regulates stem cell signatures by preventing embryonic ectoderm development (EED) and zeste homolog 2 (EZH2) transcriptions as PRC components (67).

Considering the dual role of BCAAs in inhibiting the growth of tumor cells and tumor development, it appears that targeting different components involved in the catabolic pathways of BCAAs can be a merit in cancer therapy.

## 5 Therapeutic interventions

BCAAs play an essential role in the metabolism and biogenesis of macromolecules, and as discussed, their catabolism can affect the metabolism and behavior of tumor cells through different mechanisms. This section discusses the BCAA-related therapeutic intervention for treating various human malignancies (Table 1).

### 5.1 Targeted therapies

Evidence revealed that modulating the accumulation of BCAAs can regulate tumor cell proliferation, tumor burden, and overall survival. Dietary BCAA intake is also associated with cancer

TABLE 1 BCAA-related therapeutic approaches for the treatment of cancer.

|                           | Approach/drug                          | Type of cancer                                      | Outcomes   | Ref  |
|---------------------------|--|---|--|------|
| <b>Targeted Therapies</b> | BCAT1 knockdown                        | Malignant melanoma<br>Human study                   | • Inhibiting the proliferation and migration of melanoma cells and decreasing oxidative phosphorylation  | (68) |
|                           | BT2                                    | HCC<br><i>In vitro</i>                              | • Increasing the residuals of BCKDH in culture medium<br>• Inhibiting BCKDK  | (55) |
|                           | Silencing of BCKDK + doxorubicin       | TNBC<br><i>In vitro</i>                             | • Downregulating BCKDK expression<br>• Reducing the intracellular concentrations of BCKAs<br>• Reducing the expression of genes involved in mitochondrial metabolism and electron complex protein<br>• Consuming oxygen and ATP generation<br>• Intensifying apoptosis and caspase activity<br>• Inhibiting the proliferation of TNBC cells<br>• Upregulating sestrin 2 and simultaneously decreasing mTORC1 signaling and protein synthesis | (69) |
|                           | BCKDK inhibition by siRNA + paclitaxel | Breast and ovarian cancer cells<br><i>In vitro</i>  | • Decreasing BCAA levels<br>• Inducing the antitumor effects of paclitaxel<br>• Deactivating the mTORC1-Aurora pathway   | (70) |
|                           | BCKDK knockdown with shRNAs            | Ovarian cancer<br><i>In vivo</i> and <i>ex vivo</i> | • Repressing ovarian cancer cell proliferation and migration   | (71) |
|                           | Transfection of anti-BCKDK siRNA       | Non-small cell lung cancer<br><i>In vitro</i>       | • Reducing the expression of BCKDK<br>• Decreasing BCKDE1 $\alpha$ phosphorylation<br>• Inhibiting the proliferation of the mentioned tumor cells  | (72) |

(Continued)

TABLE 1 Continued

|                              | Approach/drug        | Type of cancer   | Outcomes   | Ref  |
|------------------------------|----------------------|--|--|------|
|                              |                      |  | <ul style="list-style-type: none"> <li>• G0/G1 cell cycle arrest</li> <li>• Upregulating P21</li> </ul>  |      |
| <b>Dietary interventions</b> | Rich-BCAA diet       | Pancreatic intraepithelial neoplasia<br><i>LSL-Kras<sup>G12D/+</sup>; Pdx1-Cre</i> (KC) mice | <ul style="list-style-type: none"> <li>• Inducing tumor progression</li> </ul>   | (73) |
|                              | Rich-BCAA diet       | Pancreatic cancer<br>Case-control study  | <ul style="list-style-type: none"> <li>• A positive association between dietary BCAA intake and the risk of pancreatic cancer</li> </ul>   | (74) |
|                              | BCAA supplementation | HCC<br>Human study   | <ul style="list-style-type: none"> <li>• Improving nPRQ</li> <li>• Increasing albumin levels</li> <li>• Improving the quality of life</li> <li>• Reducing the Child-Pugh score</li> <li>• Decreasing the recurrence rate</li> <li>• Prolonging the overall survival</li> </ul> | (8)  |
|                              | High-BCAA diets      | Breast cancer<br><i>In vitro/In vivo</i>   | <ul style="list-style-type: none"> <li>• Suppressing the growth of breast cancer cells and related lung metastases in mice</li> <li>• Impairing tumor cell migration and invasion</li> <li>• Downregulating N-cadherin</li> </ul>  | (11) |
|                              | High-BCAA diets      | Postmenopausal breast cancer<br>Human study  | <ul style="list-style-type: none"> <li>• Decreased risk of Postmenopausal breast cancer</li> </ul>   | (75) |
|                              | High-BCAA diets      | CRC<br>A large case-control study  | <ul style="list-style-type: none"> <li>• An inverse association between BCAA intake and the risk of sigmoid colon cancer risk</li> </ul>   | (76) |
|                              | High-BCAA diets      | CRC<br>Human study   | <ul style="list-style-type: none"> <li>• A positive association between a higher dietary BCAAs intake and the risk of all-cause mortality in CRC patients</li> </ul>   | (77) |

development in some malignancies. Moreover, reducing BCAA catabolism via therapeutic tumor interventions could have functional benefits (48). Based on the available studies, the enzymes involved in the catabolism of BCAAs, such as BCAT1, BCAT2, and BCKDK, could be potential therapeutic targets for cancer treatment (35, 78). However, some studies reported that BCAT1 and BCAT2 are not involved in human cancers such as PDAC because these enzymes can not induce PDAC tumor formation.

Consequently, the origin tissue is a critical factor in how tumors meet their metabolic needs (79). Based on these findings, perhaps the inhibition of these enzymes may not be effective in some cancers. Nonetheless, analysis of samples from patients with malignant melanoma and mouse malignant B16 melanoma cell lines showed that BCAT1 was overexpressed in both sample types. Moreover, BCAT1 knockdown inhibited the proliferation and migration of melanoma cells and decreased oxidative phosphorylation (68). These findings show that BCAT1 can be a suitable therapeutic target in treating human cancers such as malignant melanoma. It has been revealed that the cytosolic BCAT isoform could be associated with human epidermal growth factor receptor 2 (HER2)-positive tumors, while its mitochondrial isoform is highly expressed in estrogen (ER)-positive tumors. Therefore, targeting BCAT enzymes should consider their isoforms in various cancers with different phenotypes (80).

Evidence has shown that targeting BCKDK with small-molecule and allosteric inhibitors could be effective in suppressing tumor cell

development. The mechanism of action of these inhibitors is binding to BCKDK, prompting movements within the N-terminal domain helix, and finally detaching BCKDK from BCKDH and degrading BCKDK (55, 81). (S)- $\alpha$ -chlorophenylpropionate and 3,6-dichloro-1-benzothiophene-2-carboxylic acid (BT2) are BCKDK allosteric inhibitors (82, 83). However, BT2 is more effective than (S)- $\alpha$ -chlorophenylpropionate, and has greater metabolic stability. After treatment with BT2, BCKDH activities increased in the culture medium of primary hepatocytes (55). BCKDK also activates the RAS/RAF/MEK/ERK pathway by phosphorylating MEK, which promotes tumor cell proliferation (54). It has been reported that, like genetic and pharmacological inhibition of BCKDK, treating triple-negative breast cancer (TNBC) cells with doxorubicin downregulated BCKDK expression, reducing the intracellular concentrations of BCKAs. Additionally, silencing of BCKDK in TNBC cells reduced the expression of genes involved in mitochondrial metabolism and complex electron protein, as well as the consumption of oxygen and ATP generation. BCKDK silencing also induced apoptotic pathways. Silencing BCKDK in combination with doxorubicin intensified apoptosis and caspase activity, inhibiting TNBC cell proliferation. Suppressing BCKDK in TNBC cells could also upregulate sestrin 2 while simultaneously decreasing mTORC1 signaling and protein synthesis. Thus, BCAAs flux remodeling by BCKDK inhibition in TNBC could be a potential therapeutic approach to hinder tumor growth and progression (69). Another investigation showed that inhibition of BCKDK by siRNA or chemical inhibitors could reduce BCAA levels and synergistically

induce the antitumor effects of paclitaxel in breast and ovarian cancer cells. However, BCKDK inhibition also deactivated the mTORC1-Aurora pathway, overcoming M phase cell cycle arrest stimulated by paclitaxel (70). In patients with ovarian cancer, a higher level of BCKDK is associated with advanced pathological grades. Moreover, BCKDK overexpression promotes ovarian cancer cell proliferation and migration by inducing the MEK/ERK pathway. Accordingly, BCKDK knockdown with shRNAs repressed ovarian cancer cell proliferation and migration *in vivo* and *ex vivo* (71). Transfection of anti-BCKDK siRNA into non-small cell lung cancer cells, including A549, HCC827, and H1299, reduced the expression of BCKDK, decreased BCKDE1 $\alpha$  phosphorylation, and inhibited the proliferation of tumor cells in these cancers. In addition, G0/G1 cell cycle arrest and an increase in the expression of P21 occurred following the inhibition of BCKDK (72). Ubiquitin-specific protease 1 (USP1), a human deubiquitinase, plays a significant role in regulating the cellular responses to DNA damage and controlling cell differentiation (84). BCAAs promote the expression of USP1 protein, and USP1 can deubiquitylate BCAT2. Furthermore, suppressing USP1 can inhibit tumor cell growth and proliferation as well as clone formation in PDAC mice models. These outcomes indicate that targeting USP1/BCAT2 in the BCAA metabolic pathway could be a therapeutic strategy for treating PDAC (73).

## 5.2 Dietary interventions

The results of studies on different cancers show several contradictions regarding the dietary intake of BCAAs as a therapeutic approach. For instance, an experimental study on *LSL-Kras<sup>G12D/+</sup>; Pdx1-Cre* (KC) mice revealed that a BCAA-rich diet stimulates the progression of pancreatic intraepithelial neoplasia (73). A multicentric Italian case-control study also reported a positive association between dietary intake of BCAAs and the risk of pancreatic cancer (74). Supplementation of BCAAs to 1594 HCC patients undergoing locoregional therapies, including radiofrequency ablation, hepatic artery infusion chemotherapy, or transarterial chemoembolization, could improve the non-protein respiratory quotient (npRQ, which represents the ratio of carbohydrate to fat oxidation), increase albumin levels, and improve quality of life. Furthermore, BCAA supplementation reduced the Child-Pugh score (a score used to evaluate the prognosis of chronic liver disease), decreased the recurrence rate, and prolonged overall survival (8). It is possible that supplement therapy with BCAAs can help reduce the side effects caused by conventional cancer therapies, such as chemotherapy, radiotherapy, or surgery. In this regard, an investigation revealed that administering BCAAs during the oncological surgical period led to satisfactory outcomes in reducing post-operative morbidity from ascites and infections (85). However, it should be noted that the catabolism of this group of amino acids may potentially benefit tumor growth, and further studies in this field are needed to determine the optimal dosage as well as the specific types of cancer.

On the other hand, it has been reported that high-BCAA diets can suppress the growth of breast cancer cells and lung metastases

in mice. A high concentration of BCAAs in the culture medium impaired the ability of breast cancer cells to migrate and invade, likely due to the downregulation of N-cadherin. Additionally, a low BCAA diet increased the colonization of tumor cells in the lung. These data revealed that high BCAA diets effective in treating breast cancer by suppressing tumor cell growth and metastasis (11). Another study also found a significant association between higher dietary intake of BCAAs and a decreased risk of postmenopausal breast cancer (75). However, the evaluation of the association between long-term dietary intakes of BCAAs and invasive breast cancer risk showed no association between dietary intakes of total or individual BCAAs and the risk of breast cancer (86).

A large case-control study on colorectal cancer patients showed an inverse association between BCAA intake and the risk of sigmoid colon cancer risk (76). These data are consistent with findings from several large US cohorts that do not support the hypothesis of a positive association between dietary BCAA intake and colorectal cancer risk (78). Another investigation suggested positive associations between higher dietary intake of BCAAs and the risk of all-cause mortality in CRC patients (77). Considering the contradictions in this area, further studies are needed to confirm these results, identify underlying mechanisms, and caution should be exercised when supplementing BCAAs in individuals with cancer (87).

## 6 Concluding remarks

In conclusion, extensive research has established the undeniable role of BCAAs and the activated biological pathways they engage in cancer. Activation of various enzymes in the catabolism of BCAAs leads to the production of metabolites that indirectly contribute to tumor growth and development. Therefore, targeting these enzymes presents a promising therapeutic approach for cancer treatment. However, the effectiveness of such interventions varies across different cancers due to the presence of diverse isoforms of these enzymes in distinct cancer phenotypes, posing challenges in treatment.

Contrastingly, supplement therapy with BCAAs has demonstrated tumor growth inhibition in certain cancers while showing no impact on others. Consequently, it is essential to consider the contradictory data derived from different studies and acknowledge the presence of numerous confounding factors that influence the results. To obtain reliable and valid outcomes, it is imperative to conduct studies with larger sample sizes and employ rigorous measures to minimize the impact of confounding factors. By doing so, we can comprehensively understand the complex relationship between BCAAs, cancer, and potential therapeutic interventions.

## Author contributions

KJ: Conception, design, and inviting co-authors to participate. EX, BJ and YC: Writing original manuscript draft. KJ and YC: Review and editing of manuscript critically for important intellectual content and provided comments and feedback for the



scientific contents of the manuscript. All authors contributed to the article and approved the submitted version.

## Conflict of interest

The authors declare that the research was conducted in the absence of any commercial or financial relationships that could be construed as a potential conflict of interest.

## References

1. Siegel RL, Miller KD, Wagle NS, Jemal A. Cancer statistics, 2023. *CA: Cancer J Clin* (2023) 73(1):17–48. doi: 10.3322/caac.21763
2. Patel CH, Powell JD. Immune cell metabolism and immuno-oncology. *Annu Rev Cancer Biol* (2023) 7:93–110. doi: 10.1146/annurev-cancerbio-061421-042605
3. Jiang P, Du W, Wu M. Regulation of the pentose phosphate pathway in cancer. *Protein Cell* (2014) 5(8):592–602. doi: 10.1007/s13238-014-0082-8
4. Amelio I, Cutruzzola F, Antonov A, Agostini M, Melino G. Serine and glycine metabolism in cancer. *Trends Biochem Sci* (2014) 39(4):191–8. doi: 10.1016/j.tibs.2014.02.004
5. Altman BJ, Stine ZE, Dang CV. From Krebs to clinic: glutamine metabolism to cancer therapy. *Nat Rev Cancer* (2016) 16(10):619–34. doi: 10.1038/nrc.2016.71
6. Liu Q, Luo Q, Halim A, Song G. Targeting lipid metabolism of cancer cells: A promising therapeutic strategy for cancer. *Cancer Lett* (2017) 401:39–45. doi: 10.1016/j.canlet.2017.05.002
7. Chen Y, Li P. Fatty acid metabolism and cancer development. *Sci Bull* (2016) 61(19):1473–9. doi: 10.1007/s11434-016-1129-4
8. Sideris GA, Tsaramanidis S, Vyllioti AT, Njuguna N. The role of branched-chain amino acid supplementation in combination with locoregional treatments for hepatocellular carcinoma: systematic review and meta-analysis. *Cancers* (2023) 15(3):926. doi: 10.3390/cancers15030926
9. Kawaguchi T, Izumi N, Charlton MR, Sata M. Branched-chain amino acids as pharmacological nutrients in chronic liver disease. *Hepatology* (2011) 54(3):1063–70. doi: 10.1002/hep.24412
10. Bifari F, Nisoli E. Branched-chain amino acids differently modulate catabolic and anabolic states in mammals: a pharmacological point of view. *Br J Pharmacol* (2017) 174(11):1366–77. doi: 10.1111/bph.13624
11. Chi R, Yao C, Chen S, Liu Y, He Y, Zhang J, et al. Elevated BCAA suppresses the development and metastasis of breast cancer. *Front Oncol* (2022) 12. doi: 10.3389/fonc.2022.887257
12. Li J-T, Yin M, Wang D, Wang J, Lei M-Z, Zhang Y, et al. BCAT2-mediated BCAA catabolism is critical for development of pancreatic ductal adenocarcinoma. *Nat Cell Biol* (2020) 22(2):167–74. doi: 10.1038/s41556-019-0455-6
13. Lei M-Z, Li X-X, Zhang Y, Li J-T, Zhang F, Wang Y-P, et al. Acetylation promotes BCAT2 degradation to suppress BCAA catabolism and pancreatic cancer growth. *Signal transduct targeted Ther* (2020) 5(1):70. doi: 10.1038/s41392-020-0168-0
14. Dimou A, Tsimihodimos V, Bairaktari E. The critical role of the branched chain amino acids (BCAAs) catabolism-regulating enzymes, branched-chain aminotransferase (BCAT) and branched-chain  $\alpha$ -keto acid dehydrogenase (BCKD), in human pathophysiology. *Int J Mol Sci* (2022) 23(7):4022. doi: 10.3390/ijms23074022
15. Akiyama T, Oohara I, Yamamoto T. Comparison of essential amino acid requirements with A/E ratio among fish species. *Fish Sci* (1997) 63(6):963–70. doi: 10.2331/fishsci.63.963
16. Valine. (2023). Available at: <https://pubchem.ncbi.nlm.nih.gov/compound/Valine>.
17. Leucine. (2023). Available at: <https://pubchem.ncbi.nlm.nih.gov/compound/Leucine>.
18. Isoleucine. (2023). Available at: <https://pubchem.ncbi.nlm.nih.gov/compound/Isoleucine>.
19. Sowers S. A primer on branched chain amino acids. *Huntington Coll Health Sci* (2009) 5:1–6.
20. Monirujjaman M, Ferdouse A. Metabolic and physiological roles of branched-chain amino acids. *Adv Mol Biol* (2014) 2014:1–6. doi: 10.1155/2014/364976
21. Babchia N, Calipel A, Mouriaux F, Faussat A-M, Mascarelli F. The PI3K/Akt and mTOR/P70S6K signaling pathways in human uveal melanoma cells: interaction with B-Raf/ERK. *Invest Ophthalmol Visual Sci* (2010) 51(1):421–9. doi: 10.1167/iops.09-3974
22. Kuwahata M, Kubota H, Kanouchi H, Ito S, Ogawa A, Kobayashi Y, et al. Supplementation with branched-chain amino acids attenuates hepatic apoptosis in rats

## Publisher's note

All claims expressed in this article are solely those of the authors and do not necessarily represent those of their affiliated organizations, or those of the publisher, the editors and the reviewers. Any product that may be evaluated in this article, or claim that may be made by its manufacturer, is not guaranteed or endorsed by the publisher.

- with chronic liver disease. *Nutr Res* (2012) 32(7):522–9. doi: 10.1016/j.nutres.2012.06.007
23. Fernstrom JD. Branched-chain amino acids and brain function. *J Nutr* (2005) 135(6):1539S–46S. doi: 10.1093/jn/135.6.1539S
24. Nie C, He T, Zhang W, Zhang G, Ma X. Branched chain amino acids: beyond nutrition metabolism. *Int J Mol Sci* (2018) 19(4):954. doi: 10.3390/ijms19040954
25. Tajiri K, Shimizu Y. Branched-chain amino acids in liver diseases. *World J Gastroenterol: WJG* (2013) 19(43):7620. doi: 10.3748/wjg.v19.i43.7620
26. Wolfson RL, Chantranupong L, Saxton RA, Shen K, Scaria SM, Cantor JR, et al. Sestrin2 is a leucine sensor for the mTORC1 pathway. *Science* (2016) 351(6268):43–8. doi: 10.1126/science.aab2674
27. Wolfson RL, Sabatini DM. The dawn of the age of amino acid sensors for the mTORC1 pathway. *Cell Metab* (2017) 26(2):301–9. doi: 10.1016/j.cmet.2017.07.001
28. Son SM, Park SJ, Lee H, Siddiqi F, Lee JE, Menzies FM, et al. Leucine signals to mTORC1 via its metabolite acetyl-coenzyme A. *Cell Metab* (2019) 29(1):192–201. e7. doi: 10.1016/j.cmet.2018.08.013
29. Sivanand S, Vander Heiden MG. Emerging roles for branched-chain amino acid metabolism in cancer. *Cancer Cell* (2020) 37(2):147–56. doi: 10.1016/j.cccell.2019.12.011
30. Sullivan MR, Danai LV, Lewis CA, Chan SH, Gui DY, Kunchok T, et al. Quantification of microenvironmental metabolites in murine cancers reveals determinants of tumor nutrient availability. *Elife* (2019) 8:e44235. doi: 10.7554/eLife.44235
31. Kamphorst JJ, Nofal M, Comisso C, Hackett SR, Lu W, Grabocka E, et al. Human pancreatic cancer tumors are nutrient poor and tumor cells actively scavenge extracellular protein. *Cancer Res* (2015) 75(3):544–53. doi: 10.1158/0008-5472.CAN-14-2211
32. Campbell SL, Wellen KE. Metabolic signaling to the nucleus in cancer. *Mol Cell* (2018) 71(3):398–408. doi: 10.1016/j.molcel.2018.07.015
33. Kaelin WG, McKnight SL. Influence of metabolism on epigenetics and disease. *Cell* (2013) 153(1):56–69. doi: 10.1016/j.cell.2013.03.004
34. Schvartzman JM, Thompson CB, Finley LW. Metabolic regulation of chromatin modifications and gene expression. *J Cell Biol* (2018) 217(7):2247–59. doi: 10.1083/jcb.201803061
35. Mann G, Mora S, Madu G, Adegoke OA. Branched-chain amino acids: catabolism in skeletal muscle and implications for muscle and whole-body metabolism. *Front Physiol* (2021) 12:702826. doi: 10.3389/fphys.2021.702826
36. Shimomura Y, Honda T, Shiraki M, Murakami T, Sato J, Kobayashi H, et al. Branched-chain amino acid catabolism in exercise and liver disease. *J Nutr* (2006) 136(1):250S–3S. doi: 10.1093/jn/136.1.250S
37. Brosnan JT, Brosnan ME. Branched-chain amino acids: enzyme and substrate regulation. *J Nutr* (2006) 136(1):207S–11S. doi: 10.1093/jn/136.1.207S
38. Mayers JR, Wu C, Clish CB, Kraft P, Torrence ME, Fiske BP, et al. Elevation of circulating branched-chain amino acids is an early event in human pancreatic adenocarcinoma development. *Nat Med* (2014) 20(10):1193–8. doi: 10.1038/nm.3686
39. Brosnan JT. Interorgan amino acid transport and its regulation. *J Nutr* (2003) 133(6):2068S–72S. doi: 10.1093/jn/133.6.2068S
40. Neinast M, Murashige D, Arany Z. Branched chain amino acids. *Annu Rev Physiol* (2019) 81:139–64. doi: 10.1146/annurev-physiol-020518-114455
41. Muoio DM. Metabolic inflexibility: when mitochondrial indecision leads to metabolic gridlock. *Cell* (2014) 159(6):1253–62. doi: 10.1016/j.cell.2014.11.034
42. Newgard CB, An J, Bain JR, Muehlbauer MJ, Stevens RD, Lien LF, et al. A branched-chain amino acid-related metabolic signature that differentiates obese and lean humans and contributes to insulin resistance. *Cell Metab* (2009) 9(4):311–26. doi: 10.1016/j.cmet.2009.02.002
43. Shin AC, Fasshauer M, Filatova N, Grundell LA, Zielinski E, Zhou J-Y, et al. Brain insulin lowers circulating BCAA levels by inducing hepatic BCAA catabolism. *Cell Metab* (2014) 20(5):898–909. doi: 10.1016/j.cmet.2014.09.003

44. Peng H, Wang Y, Luo W. Multifaceted role of branched-chain amino acid metabolism in cancer. *Oncogene* (2020) 39(44):6747–56. doi: 10.1038/s41388-020-01480-z
45. Zheng YH, Hu WJ, Chen BC, Grahm THM, Zhao YR, Bao HL, et al. BCAT 1, a key prognostic predictor of hepatocellular carcinoma, promotes cell proliferation and induces chemoresistance to cisplatin. *Liver Int* (2016) 36(12):1836–47. doi: 10.1111/liv.13178
46. Hattori A, Tsunoda M, Konuma T, Kobayashi M, Nagy T, Glushka J, et al. Cancer progression by reprogrammed BCAA metabolism in myeloid leukaemia. *Nature* (2017) 545(7655):500–4. doi: 10.1038/nature22314
47. Tönjes M, Barbus S, Park YJ, Wang W, Schlotter M, Lindroth AM, et al. BCAT1 promotes cell proliferation through amino acid catabolism in gliomas carrying wild-type IDH1. *Nat Med* (2013) 19(7):901–8. doi: 10.1038/nm.3217
48. Ericksen RE, Lim SL, McDonnell E, Shuen WH, Vadiveloo M, White PJ, et al. Loss of BCAA catabolism during carcinogenesis enhances mTORC1 activity and promotes tumor development and progression. *Cell Metab* (2019) 29(5):1151–1165. doi: 10.1016/j.cmet.2018.12.020
49. Zhang L, Han J. Branched-chain amino acid transaminase 1 (BCAT1) promotes the growth of breast cancer cells through improving mTOR-mediated mitochondrial biogenesis and function. *Biochem Biophys Res Commun* (2017) 486(2):224–31. doi: 10.1016/j.bbrc.2017.02.101
50. Wang Z-Q, Faddaoui A, Bachvarova M, Plante M, Gregoire J, Renaud M-C, et al. BCAT1 expression associates with ovarian cancer progression: possible implications in altered disease metabolism. *Oncotarget* (2015) 6(31):31522. doi: 10.18632/oncotarget.5159
51. Lieu EL, Nguyen T, Rhyne S, Kim J. Amino acids in cancer. *Exp Mol Med* (2020) 52(1):15–30. doi: 10.1038/s12276-020-0375-3
52. Lee JH, Cho Y-r, Kim JH, Kim J, Nam HY, Kim SW, et al. Branched-chain amino acids sustain pancreatic cancer growth by regulating lipid metabolism. *Exp Mol Med* (2019) 51(11):1–11. doi: 10.1038/s12276-019-0350-z
53. Jiang W, Qiao L, Han Y, Zhang A, An H, Xiao J, et al. Pancreatic stellate cells regulate branched-chain amino acid metabolism in pancreatic cancer. *Ann Trans Med* (2021) 9(5):1–11. doi: 10.21037/atm-21-761
54. Xue P, Zeng F, Duan Q, Xiao J, Liu L, Yuan P, et al. BCKDK of BCAA catabolism cross-talking with the MAPK pathway promotes tumorigenesis of colorectal cancer. *EBioMedicine* (2017) 20:50–60. doi: 10.1016/j.ebiom.2017.05.001
55. East MP, Laitinen T, Asquith CR. BCKDK: an emerging kinase target for metabolic diseases and cancer. *Nat Rev Drug Discovery* (2021) 20(498):10.1038. doi: 10.1038/d41573-021-00107-6
56. Murin R, Hamprecht B. Metabolic and regulatory roles of leucine in neural cells. *Neurochemical Res* (2008) 33:279–84. doi: 10.1007/s11064-007-9444-4
57. Gondáš E, Králová Trančíková A, Baranovičová E, Šofranko J, Hatok J, Kowtharapu BS, et al. Expression of 3-methylcrotonyl-CoA carboxylase in brain tumors and capability to catabolize leucine by human neural cancer cells. *Cancers* (2022) 14(3):585. doi: 10.3390/cancers14030585
58. Wang Y, Xiao J, Jiang W, Zuo D, Wang X, Jin Y, et al. BCKDK alters the metabolism of non-small cell lung cancer. *Trans Lung Cancer Res* (2021) 10(12):4459. doi: 10.21037/tlcr-21-885
59. Yang D, Liu H, Cai Y, Lu K, Zhong X, Xing S, et al. Branched-chain amino acid catabolism breaks glutamine addiction to sustain hepatocellular carcinoma progression. *Cell Rep* (2022) 41(8):111691. doi: 10.1016/j.celrep.2022.111691
60. Jiang Z, Zheng J, Liu J, Yang X, Chen K. Novel branched-chain amino acid-catabolism related gene signature for overall survival prediction of pancreatic carcinoma. *J Proteome Res* (2021) 21(3):740–6. doi: 10.1021/acs.jproteome.1c00607
61. Mikalayeva V, Pankevičiūtė M, Žvikas V, Skeberdis VA, Bordel S. Contribution of branched chain amino acids to energy production and mevalonate synthesis in cancer cells. *Biochem Biophys Res Commun* (2021) 585:61–7. doi: 10.1016/j.bbrc.2021.11.034
62. Rui L. Brown and beige adipose tissues in health and disease. *Compr Physiol* (2017) 7(4):1281. doi: 10.1002/cphy.c170001
63. Yin X, Chen Y, Ruze R, Xu R, Song J, Wang C, et al. The evolving view of thermogenic fat and its implications in cancer and metabolic diseases. *Signal Transduct Targeted Ther* (2022) 7(1):324. doi: 10.1038/s41392-022-01178-6
64. Blanchard P-G, Moreira RJ, Castro É, Caron A, Côté M, Andrade ML, et al. PPAR $\gamma$  is a major regulator of branched-chain amino acid blood levels and catabolism in white and brown adipose tissues. *Metabolism* (2018) 89:27–38. doi: 10.1016/j.metabol.2018.09.007
65. Lin S, Miao Y, Zheng X, Dong Y, Yang Q, Yang Q, et al. ANGPTL4 negatively regulates the progression of osteosarcoma by remodeling branched-chain amino acid metabolism. *Cell Death Discovery* (2022) 8(1):225. doi: 10.1038/s41420-022-01029-x
66. Mao L, Chen J, Lu X, Yang C, Ding Y, Wang M, et al. Proteomic analysis of lung cancer cells reveals a critical role of BCAT1 in cancer cell metastasis. *Theranostics* (2021) 11(19):9705. doi: 10.7150/thno.61731
67. Kikushige Y, Miyamoto T, Kochi Y, Semba Y, Ohishi M, Irfune H, et al. Human acute leukemia utilizes branched-chain amino acid catabolism to maintain stemness through regulating PRC2 function. *Blood Adv* (2022) 7:3592–603. doi: 10.1182/bloodadvances.2022008242
68. Zhang B, Xu F, Wang K, Liu M, Li J, Zhao Q, et al. BCAT1 knockdown-mediated suppression of melanoma cell proliferation and migration is associated with reduced oxidative phosphorylation. *Am J Cancer Res* (2021) 11(6):2670.
69. Biswas D, Slade L, Duffley L, Mueller N, Dao KT, Mercer A, et al. Inhibiting BCKDK in triple negative breast cancer suppresses protein translation, impairs mitochondrial function, and potentiates doxorubicin cytotoxicity. *Cell Death Discovery* (2021) 7(1):241. doi: 10.1038/s41420-021-00602-0
70. Ibrahim SL, Abed MN, Mohamed G, Price JC, Abdullah MI, Richardson A. Inhibition of branched-chain alpha-keto acid dehydrogenase kinase augments the sensitivity of ovarian and breast cancer cells to paclitaxel. *Br J Cancer* (2022) 128:1–11. doi: 10.1038/s41416-022-02095-9
71. Li H, Yu D, Li L, Xiao J, Zhu Y, Liu Y, et al. BCKDK promotes ovarian cancer proliferation and migration by activating the MEK/ERK signaling pathway. *J Oncol* (2022) 2022:1–14. doi: 10.1155/2022/3691635
72. Bagheri Y, Saeidi M, Yazdani R, Babaha F, Falak R, Azizi G, et al. Evaluation of effective factors on IL-10 signaling in B cells in patients with selective IgA deficiency. *Eur Cytokine Netw* (2021) 33(1):1–12. doi: 10.1684/ecm.2021.0464
73. Li J-T, Li K-Y, Su Y, Shen Y, Lei M-Z, Zhang F, et al. Diet high in branched-chain amino acid promotes PDAC development by USP1-mediated BCAT2 stabilization. *Natl Sci Rev* (2022) 9(5):nwab212. doi: 10.1093/nsr/nwab212
74. Rossi M, Turati F, Strikoudi P, Ferraroni M, Parpinel M, Serraino D, et al. Dietary intake of branched-chain amino acids and pancreatic cancer risk in a case-control study from Italy. *Br J Nutr* (2022) 129:1–19. doi: 10.1017/S0007114522000939
75. Nouri-Majd S, Salari-Moghaddam A, Benisi-Kohansal S, Azadbakht L, Esmailzadeh A. Dietary intake of branched-chain amino acids in relation to the risk of breast cancer. *Breast Cancer* (2022) 29(6):993–1000. doi: 10.1007/s12282-022-01379-5
76. Rossi M, Mascaretti F, Parpinel M, Serraino D, Crispo A, Celentano E, et al. Dietary intake of branched-chain amino acids and colorectal cancer risk. *Br J Nutr* (2021) 126(1):22–7. doi: 10.1017/S0007114520003724
77. Long L, Yang W, Liu L, Tobias DK, Katagiri R, Wu K, et al. Dietary intake of branched-chain amino acids and survival after colorectal cancer diagnosis. *Int J Cancer* (2021) 148(10):2471–80. doi: 10.1002/ijc.33449
78. Katagiri R, Song M, Zhang X, Lee DH, Tabung FK, Fuchs CS, et al. Dietary intake of branched-chain amino acids and risk of colorectal cancer. *Branched-chain amino acid intake and colorectal cancer. Cancer Prev Res* (2020) 13(1):65–72. doi: 10.1158/1940-6207.CAPR-19-0297
79. Mayers JR, Torrence ME, Danaei LV, Papagiannakopoulos T, Davidson SM, Bauer MR, et al. Tissue of origin dictates branched-chain amino acid metabolism in mutant Kras-driven cancers. *Science* (2016) 353(6304):1161–5. doi: 10.1126/science.aaf5171
80. Shafei MA, Flemban A, Daly C, Kendrick P, White P, Dean S, et al. Differential expression of the BCAT isoforms between breast cancer subtypes. *Breast Cancer* (2021) 28:592–607. doi: 10.1007/s12282-020-01197-7
81. Du C, Liu W-J, Yang J, Zhao S-S, Liu H-X. The role of branched-chain amino acids and branched-chain  $\alpha$ -keto acid dehydrogenase kinase in metabolic disorders. *Front Nutr* (2022) 9. doi: 10.3389/fnut.2022.932670
82. Tso S-C, Gui W-J, Wu C-Y, Chuang JL, Qi X, Skvorak KJ, et al. Benzothioephene carboxylate derivatives as novel allosteric inhibitors of branched-chain  $\alpha$ -ketoacid dehydrogenase kinase. *J Biol Chem* (2014) 289(30):20583–93. doi: 10.1074/jbc.M114.569251
83. 3,6-Dichloro-1-benzothioephene-2-carboxylic acid. (2023). Available at: [https://pubchem.ncbi.nlm.nih.gov/compound/3\\_6-Dichloro-1-benzothioephene-2-carboxylic-acid](https://pubchem.ncbi.nlm.nih.gov/compound/3_6-Dichloro-1-benzothioephene-2-carboxylic-acid).
84. Olazabal-Herrero A, García-Santisteban I, Rodríguez JA. Structure-function analysis of USP1: insights into the role of Ser313 phosphorylation site and the effect of cancer-associated mutations on autocleavage. *Mol Cancer* (2015) 14(1):33. doi: 10.1186/s12943-015-0311-7
85. Cogo E, Elsayed M, Liang V, Cooley K, Guerin C, Psihogios A, et al. Are supplemental branched-chain amino acids beneficial during the oncological peri-operative period: a systematic review and meta-analysis. *Integr Cancer therapies* (2021) 20:1534735421997551. doi: 10.1177/1534735421997551
86. Tobias DK, Chai B, Tamimi RM, Manson JE, Hu FB, Willett WC, et al. Dietary intake of branched chain amino acids and breast cancer risk in the NHS and NHS II prospective cohorts. *JNCI Cancer Spectr* (2021) 5(3):pkab032. doi: 10.1093/jncics/pkab032
87. Lee K, Blanton C. The effect of branched-chain amino acid supplementation on cancer treatment. *Nutr Health* (2023) 34:02601060231153428. doi: 10.1177/02601060231153428



## OPEN ACCESS

## EDITED BY

Satyendra Chandra Tripathi,  
All India Institute of Medical Sciences  
Nagpur, India

## REVIEWED BY

Makoto Kobayashi,  
Fukushima Medical University, Japan  
Shibjyoti Debnath,  
Duke University, United States

## \*CORRESPONDENCE

Ichidai Tanaka  
✉ ichidai@med.nagoya-u.ac.jp

RECEIVED 28 June 2023

ACCEPTED 08 August 2023

PUBLISHED 22 August 2023

## CITATION

Tanaka I, Koyama J, Itoigawa H, Hayai S  
and Morise M (2023) Metabolic barriers  
in non-small cell lung cancer with  
*LKB1* and/or *KEAP1* mutations for  
immunotherapeutic strategies.  
*Front. Oncol.* 13:1249237.  
doi: 10.3389/fonc.2023.1249237

## COPYRIGHT

© 2023 Tanaka, Koyama, Itoigawa, Hayai and  
Morise. This is an open-access article  
distributed under the terms of the [Creative  
Commons Attribution License \(CC BY\)](#). The  
use, distribution or reproduction in other  
forums is permitted, provided the original  
author(s) and the copyright owner(s) are  
credited and that the original publication in  
this journal is cited, in accordance with  
accepted academic practice. No use,  
distribution or reproduction is permitted  
which does not comply with these terms.

# Metabolic barriers in non-small cell lung cancer with *LKB1* and/or *KEAP1* mutations for immunotherapeutic strategies

Ichidai Tanaka\*, Junji Koyama, Hideyuki Itoigawa,  
Shunsaku Hayai and Masahiro Morise

Department of Respiratory Medicine, Nagoya University Graduate School of Medicine, Nagoya, Japan

Currently, immune checkpoint inhibitors (ICIs) are widely considered the standard initial treatment for advanced non-small cell lung cancer (NSCLC) when there are no targetable driver oncogenic alternations. NSCLC tumors that have two alterations in tumor suppressor genes, such as liver kinase B1 (LKB1) and/or Kelch-like ECH-associated protein 1 (KEAP1), have been found to exhibit reduced responsiveness to these therapeutic strategies, as revealed by multiomics analyses identifying immunosuppressed phenotypes. Recent advancements in various biological approaches have gradually unveiled the molecular mechanisms underlying intrinsic reprogrammed metabolism in tumor cells, which contribute to the evasion of immune responses by the tumor. Notably, metabolic alterations in glycolysis and glutaminolysis have a significant impact on tumor aggressiveness and the remodeling of the tumor microenvironment. Since glucose and glutamine are essential for the proliferation and activation of effector T cells, heightened consumption of these nutrients by tumor cells results in immunosuppression and resistance to ICI therapies. This review provides a comprehensive summary of the clinical efficacies of current therapeutic strategies against NSCLC harboring *LKB1* and/or *KEAP1* mutations, along with the metabolic alterations in glycolysis and glutaminolysis observed in these cancer cells. Furthermore, ongoing trials targeting these metabolic alterations are discussed as potential approaches to overcome the extremely poor prognosis associated with this type of cancer.

## KEYWORDS

immune checkpoint blockade, NSCLC, LKB1, KEAP1, metabolic barriers, glycolysis, glutaminolysis, PD-1/PD-L1 inhibitors

## 1 Introduction

The advent of immune checkpoint inhibitor (ICI) therapy has revolutionized the treatment approach for various cancers, including advanced non-small cell lung cancer (NSCLC). Currently, the standard first-line therapy for advanced NSCLC without targetable driver oncogenic alternations consists of multiple treatment regimens

involving ICIs, either alone or in combination with platinum-based chemotherapy (1–8). Predictors such as programmed death 1 ligand-1 (PD-L1) tumor proportion scores (TPS) or tumor mutational burden (TMB) are available but insufficient in accurately forecasting the treatment outcome (9–11). In first-line therapies for advanced NSCLC, ICIs as monotherapy, such as pembrolizumab and atezolizumab, have demonstrated clinical benefits primarily in patients with high tumor PD-L1 expression (2, 3). However, several combinations of ICIs and platinum-based chemotherapies have been approved as standard first-line therapies irrespective of TPS, although the effectiveness of these combinations still relies to some extent on the tumor PD-L1 expression status. Nonetheless, even among the subset of patients with high tumor PD-L1 expression, approximately 20–30% initially exhibit resistance to ICIs, either alone or in conjunction with platinum-based chemotherapy (1, 9).

Recent multiomics analyses, including next-generation sequencing-based tests (NGS), have played a crucial role in identifying predictive biomarkers for ICI therapies and uncovering mechanisms of immune evasion in cancer (9, 12–15). Among them, T cell-inflamed gene expression profile and proteogenomic characterization in addition to NGS data analysis have revealed that specific driver mutations in NSCLC exhibit discrete immune phenotypes (16, 17). Notably, two tumor suppressor genes, liver kinase B1 (LKB1) and Kelch-like ECH-associated protein 1 (KEAP1), are associated with inactivating driver mutations that contribute to an immunosuppressed phenotype (18). Somatic mutations in *LKB1*, encoded by *serine/threonine kinase 11* (*STK11*), occur in approximately 20–25% of lung adenocarcinoma (LUAD), while inactivating mutations in *KEAP1* are observed in approximately 10–15% of LUAD (19–21). Several studies using a large number of clinical specimens have also reported a high frequency of co-occurring mutations in *STK11* and *KEAP1* (22–24). NSCLC with *STK11* and/or *KEAP1* mutations represents one of most aggressive types of cancer, characterized by resistance to standard cytotoxic chemotherapy or radiotherapy (20, 25–27). However, these tumors also exhibit reduced efficacy to immunotherapy, independent of PD-L1 expression and high TMB (18, 28, 29). This highlights the urgent need for novel therapeutic strategies to effectively treat NSCLC patients with these specific mutations. T-cell infiltration in tumors is known to be relatively weak, and researchers have investigated various factors that contribute to this, such as the secretion of immunosuppressive molecules and impairment of antigen presentation (17, 18). Among these factors, the metabolic reprogramming of glycolysis and glutaminolysis in tumor cells has emerged as a current area of focus for explaining the limited response to immunotherapy (30, 31). The intrinsic metabolic reprogramming of tumor cells, which is essential for tumor growth, also impacts various cells within the tumor microenvironment (TME), leading to immune evasion by the tumor (30–34).

To understand how the inactivation of the two tumor suppressors leads to metabolic reprogramming of glycolysis and glutaminolysis, researchers have gradually uncovered the molecular mechanisms through various biological approaches. These metabolic alterations play a significant role in promoting tumor aggressiveness and

reconstructing the TME to support tumor growth (31, 35, 36). In this review, we provide a summary of the current therapeutic strategies and their clinical efficacies against NSCLC with LKB1 and/or KEAP1 inactivation. Furthermore, we delve into the metabolic alterations of glycolysis and glutaminolysis in NSCLC with these mutations, which are associated with ICI resistance, and discuss ongoing trials that target metabolic alterations.

## 2 Clinical efficacies of ICI regimen to advanced NSCLC

### 2.1 Heterogeneity of PD-L1 expression and ICIs efficacy in NSCLC

PD-L1 expression on cancer cells is regulated by various mechanisms, including inflammatory cytokines, mechanical signals, and tumor-intrinsic cell signaling. Consequently, there is heterogeneity in the PD-L1 expression levels across tumors (37–40), making them imperfect markers for predicting the response to ICIs. However, during the clinical development of anti-PD-1/PD-L1 antibodies, tumor PD-L1 expression status was used for patient selection based on the observed association between the objective response rate of anti-PD-1 antibody, pembrolizumab, and tumor PD-L1 expression level (41). The KEYNOTE-010 study demonstrated the durable response of pembrolizumab in patients with high tumor PD-L1 expression, leading to subsequent KEYNOTE-024 trial that compared pembrolizumab monotherapy with platinum-based chemotherapy specifically in patients with high tumor PD-L1 expression (2, 42). In these trials, which selected patients based on tumor PD-L1 expression status, the anti-PD-1 antibody showed superior survival outcomes compared to platinum-based chemotherapy, and subsequently, the anti-PD-L1 antibody atezolizumab also demonstrated overall superiority over platinum-based chemotherapy (3, 43) (Figures 1A, B; Supplementary Table 1). Several phase III studies have investigated the clinical efficacy of combining anti-PD-1/PD-L1 antibodies with platinum-based chemotherapy, irrespective of tumor PD-L1 expression, in comparison to platinum-based cytotoxic chemotherapy. These studies, namely, KEYNOTE-189, IMpower150, IMpower130, IMpower132, and KEYNOTE-407, have now become standard first-line options (4, 5, 44–49) (Figures 1A, B; Supplementary Table 1). In addition, the combination of anti-PD-1 antibody and anti-cytotoxic T-lymphocyte-associated protein 4 (CTLA-4) antibody has also demonstrated similar survival superiority. CheckMate 227 and CheckMate 9LA trials showed that the clinical benefits of nivolumab plus ipilimumab and nivolumab plus ipilimumab in combination with platinum-based chemotherapy, respectively, surpassed those of platinum-based chemotherapy alone (7, 50–52). Moreover, in the phase III POSEIDON study, the combination of anti-PD-L1 antibody durvalumab and anti-CTLA-4 antibody tremelimumab, along with platinum-based chemotherapy, recently showed positive results in terms of both progression-free survival (PFS) and overall survival (OS) when compared to platinum-based chemotherapy alone (8) (Figures 1A, B; Supplementary Table 1).



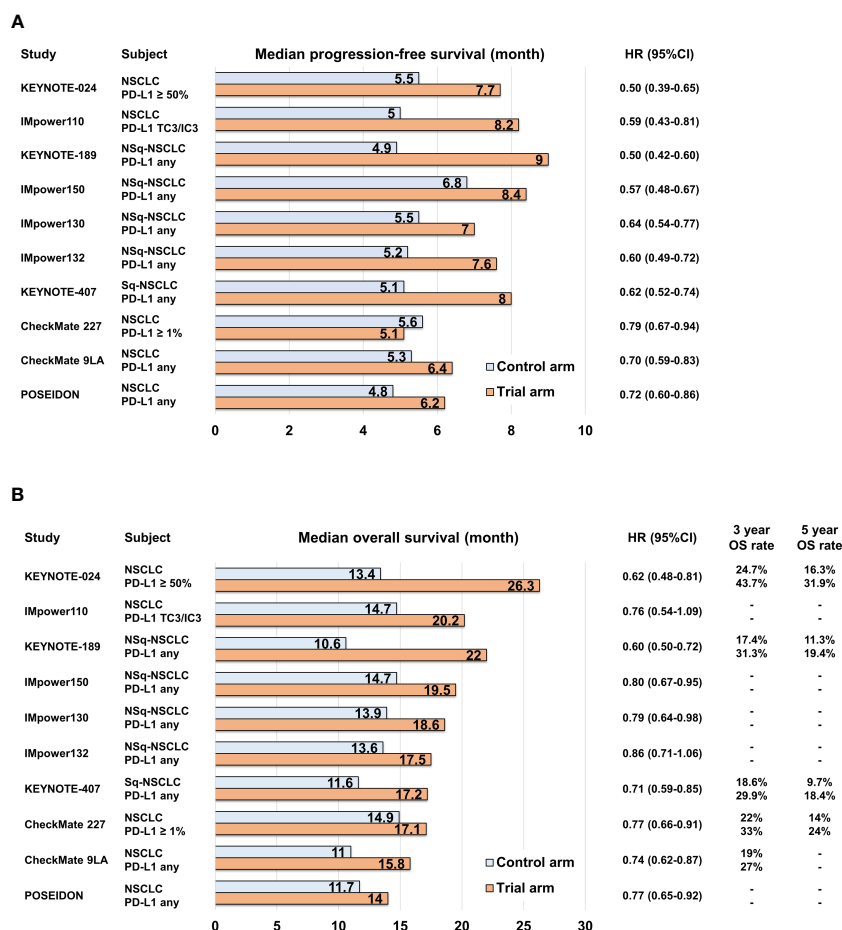


FIGURE 1

Bar graph comparing control and trial arms in pivotal phase III clinical trials in terms of median progression-free survival (A) and median overall survival (B).

These combination regimens involving ICIs have emerged as the leading options for standard first-line therapy in advanced NSCLC cases without targetable drive alterations, regardless of TPS and TMB.

In contrast, most molecular-targeted therapies have become established as the standard first-line treatment for NSCLC cases with *epidermal growth factor receptor* (*EGFR*), *anaplastic lymphoma kinase* (*ALK*), *ROS proto-oncogene 1* (*ROS1*), *B-Raf proto-oncogene* (*BRAF*), and *Ret proto-oncogene* (*RET*) alterations, exhibiting over 50% antitumor response rates and long-term PFS (53). A recent significant advancement in molecular-targeted therapy is the approval of sotorasib for second-line treatment in NSCLC cases with *Kirsten rat sarcoma viral oncogene homolog* (*KRAS*) *G12C* mutation, following immunotherapy-based therapies (54). Interestingly, the presence of oncogenic driver gene mutations has been found to have an impact on the efficacy of ICIs in NSCLC. Specifically, *EGFR* and *KRAS* mutations have been identified as key factors associated with ICI efficacy. NSCLC patients with *KRAS* mutations have shown favorable responses to ICIs with or without platinum-based chemotherapy compared to those without *KRAS* mutations. For instance, in a study involving patients with non-squamous NSCLC treated with pembrolizumab alone or in

combination with chemotherapy, those with *KRAS* mutations had a longer PFS compared to patients with wild-type *KRAS* (median PFS 16.5 months vs. 8.0 months) (55). Another study also reported that *KRAS* mutations were significant favorable prognostic factors in NSCLC patients treated with pembrolizumab in combination with carboplatin plus pemetrexed for non-squamous NSCLC or paclitaxel for squamous NSCLC (56). A subgroup analysis of the IMpower150 trial revealed that the combination of atezolizumab, bevacizumab, carboplatin, and paclitaxel (ABCP) showed a greater PFS benefit in the population with *KRAS* mutations compared to the combination of bevacizumab, carboplatin, and paclitaxel, with hazard ratios (HRs) of 0.42 and 0.65, respectively, in *KRAS* mutation-positive and *KRAS* mutation wild-type populations (57).

Conversely, a meta-analysis of phase III studies comparing ICI monotherapy to docetaxel in the pretreatment setting revealed that ICI monotherapy is less beneficial in NSCLC patients with *EGFR* mutant compared to those of wild-type (58). However, several clinical trials have shown the clinical benefit of combining ICIs with platinum-based chemotherapy and an anti-vascular endothelial growth factor (VEGF) strategy. In a subset analysis of the IMpower150 trial, the combination of atezolizumab, carboplatin, paclitaxel, and bevacizumab demonstrated longer

PFS and OS compared to carboplatin, paclitaxel, and bevacizumab in patients with common *EGFR* mutations (59). VEGF-A has been found to have an immunosuppressive role by promoting the function of regulatory T-cell and driving the growth of *EGFR* mutant NSCLC. Therefore, combining ICIs with VEGF-A inhibitors, such as bevacizumab, has emerged as an appealing treatment strategy for *EGFR* mutant NSCLC after driver-targeted therapy failure (60–62). However, regarding the predictive value of driver oncogenes other than *EGFR* and *KRAS* mutations, conclusive evidence has not been established at this stage. Several small retrospective cohort studies have reported the efficacy of ICI monotherapy in NSCLC patients with other driver oncogenic alterations, with response rates ranging from 0% in NSCLC patients with *ALK* fusion to 24% in NSCLC patients with *BRAF* mutation (40, 63, 64). Nevertheless, these findings are insufficient to draw definitive conclusions regarding the clinical relevance of ICIs for patients with these driver gene alterations other than *EGFR* and *KRAS*. Regarding *RET* alterations, the ongoing phase III trials comparing the *RET* inhibitor selpercatinib to other treatments will provide insights into the clinical efficacy of combination therapy involving ICIs for those patients (65).

## 2.2 Therapeutic efficacies of ICI regimens to advanced NSCLC with *LKB1* and/or *KEAP1* inactivation

Recent large-scale profiling studies using NGS in NSCLC have uncovered multiple non-random patterns of driver gene alterations. These patterns often exhibit co-occurrence or mutual exclusivity and are associated with specific driver alterations. One notable example is the co-occurrence of oncogenic driver alterations, such as *KRAS* and *EGFR* mutations, along with the inactivation of well-known tumor suppressor genes like tumor protein *p53* (*TP53*), *LKB1* (*STK11*), and *KEAP1*. These co-occurring patterns have significant biological implications and can influence tumor evolution and progression (18). Furthermore, these co-occurring patterns also impact the clinical efficacies of various therapies, including ICI and cytotoxic chemotherapy. In patients with *KRAS*-mutant NSCLC who were treated with ICI monotherapies or ICI combination therapies, the response rate was remarkably higher in the group with *TP53* co-mutation compared to the group with *STK11* co-mutation (28). The median PFS and median OS were reported as 3.0 months and 16.0 months, respectively, for patients with *KRAS/TP53* co-mutation (KP group), while it was 1.8 months and 6.4 months for patients with *KRAS/STK11* co-mutation (KL group). The underlying biological mechanism explaining the poor efficacy of ICIs in the KL group may be attributed to the immunosuppressive TME caused by *LKB1* inactivation followed by *STK11* mutation (18). *LKB1* inactivation in cancer cells leads to the production of several immunosuppressive cytokines, such as Interleukin (IL)-6, IL-33, chemokine (C-X-C motif) ligand 7, and granulocyte colony-stimulating factor, which contribute to the mobilization of neutrophils (66). Neutrophils play a role in impeding T-cell movement and function, leading to the development of an “immune desert environment” characterized

by reduced tumor-infiltrating lymphocytes. The limited efficacy of ICI monotherapies and ICI combined with cytotoxic chemotherapies has been observed in NSCLC patients with *STK11* or *KEAP1* mutations. In the subgroup analysis of the IMpower150 trial, the *KRAS*-mutant NSCLC patients and co-occurring *STK11* and/or *KEAP1* mutations exhibited a significantly shorter median PFS of the combination therapy ABCP compared to those with wild type in both *STK11* and *KEAP1* (6.0 months vs. 15.2 months) (57) (Supplementary Table 2). In contrast, NSCLC patients with *KRAS/TP53* co-mutation had a longer median PFS with ABCP compared to those with *KRAS* mutations and wild-type *TP53* (14.3 months vs. 7.3 months) (57). In the subgroup analysis of the KEYNOTE-189 trial, the overall response rate (ORR) of pembrolizumab in combination with platinum plus pemetrexed was 30.6% in NSCLC patients with *STK11* mutation, whereas it was 48.8% in those with *STK11* wild type (67) (Supplementary Table 2). Furthermore, in NSCLC patients with *KEAP1* mutation, the ORR of pembrolizumab in combination with platinum plus pemetrexed was 35.6% (67). The median PFS for patients with *STK11* mutation and those with *KEAP1* mutation were 6.1 and 5.1 months (Figures 2A, C), respectively, indicating that the clinical efficacy of ICIs combined with cytotoxic chemotherapy is also limited in NSCLC patients with both gene mutations. However, since *STK11* and/or *KEAP1* mutations are also associated with poor clinical outcomes to cytotoxic chemotherapy without ICIs, there may still be a benefit in adding PD-1/PD-L1 inhibitors to platinum-based chemotherapy even in this population.

To enhance the clinical outcomes of PD-1/PD-L1 inhibitor-based therapy for “immune desert environment” NSCLC caused by *STK11* and/or *KEAP1* mutations, the addition of CTLA-4 inhibitors to PD-1/PD-L1 inhibitors represents a promising approach. CTLA-4 is expressed on activated T cells upon tumor antigen presentation by dendritic cells. It has a stronger binding affinity to CD80/86 compared to CD28, which is responsible for T-cell activation, thereby suppressing T-cell activation (68). Anti-CTLA-4 antibodies, such as ipilimumab and tremelimumab, block the binding of CTLA-4 to CD80/86, leading to enhanced and sustained T-cell activation (68). The reported clinical benefits of combining PD-1/PD-L1 inhibitors with CTLA-4 inhibitors for NSCLC with *STK11* and/or *KEAP1* mutations are based on exploratory analyses of phase III clinical trials and involve unstratified univariate analysis with a relatively smaller sample size. In the subgroup analysis of CheckMate 227, the PFS-HR of nivolumab plus ipilimumab compared to platinum-based chemotherapy were 1.04 for patients with *STK11* mutation ( $n = 78$ ) and 0.25 for those with *KEAP1* mutation ( $n = 38$ ) (69) (Figures 2A, C; Supplementary Table 2). In the subgroup analysis of CheckMate 9LA, the PFS-HRs of nivolumab plus ipilimumab with platinum-based chemotherapy compared to platinum-based chemotherapy alone were 0.61 (95%CI: 0.37–1.00) for patients with *STK11* mutation and 0.34 (95%CI: 0.14–0.83) for patients with *KEAP1* mutation (52) (Figures 2A, C; Supplementary Table 2). Further, in the subgroup analysis of the POSEIDON trial, the PFS-HRs of durvalumab plus tremelimumab with platinum-based chemotherapy compared to platinum-based chemotherapy alone

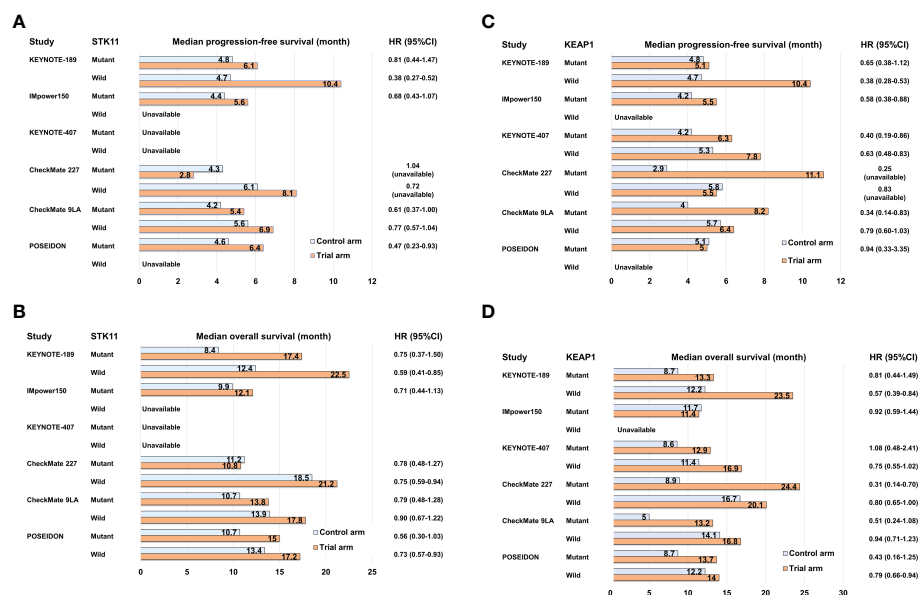


FIGURE 2

Bar graph comparing control and trial arms in subgroup analyses of pivotal clinical trials for NSCLC with *STK11* or *KEAP1* mutation in terms of median progression-free survival (A, C) and median overall survival (B, D).

were 0.47 (95%CI: 0.23–0.93) for patients with *STK11* mutation ( $n = 53$ ) and 0.94 (95%CI: 0.33–3.35) for patients with *KEAP1* mutation ( $n = 28$ ) (70) (Figures 2A, C; Supplementary Table 2). The subgroup analyses of these major clinical trials indicate that certain ICI combination therapies may have some degree of effectiveness in treating NSCLC with *STK11* or *KEAP1* mutations, although their therapeutic benefits are generally limited (Figures 2A–D). Specifically, *KRAS*-mutant NSCLC with *STK11* or *KEAP1* mutations tends to have a poorer prognosis, and comprehensive co-mutation analyses in *KRAS*-mutant NSCLC have not been conducted extensively for other ICI combination therapies except IMpower150 (57). Therefore, for NSCLC cases with these mutations, it is important to continue clinical and molecular analyses and to develop more advanced therapeutic strategies targeting novel therapeutic targets.

### 3 Glycolysis and glutaminolysis in NSCLC with LKB1 and/or KEAP1 inactivation

#### 3.1 Glycolysis in NSCLC with LKB1 inactivation

Cancer cells have possess a distinct metabolic characteristic known as the Warburg effect, wherein they preferentially utilize the glycolytic pathway for energy production, even in the presence of sufficient oxygen (71–73). This unique glycometabolism trait is characterized by increased glucose uptake and enhanced carbohydrate conversion into lactose. By consuming high amounts of glucose, tumor cells can rapidly proliferate and generate ATP, while also obtaining the necessary glycometabolic

intermediates for synthesizing cellular components (73–75). Glucose is not only vital for tumor cell growth but also plays a crucial role in the proliferation and activation of effector T cells. Consequently, intratumoral effector T cells must outcompete tumor cells to acquire glucose (33, 76). Hence, in rapidly growing tumors, high glucose consumption itself may contribute to immunosuppression. In support of this, a study by Zappasodi et al. explored the correlation between tumor immune infiltration and glycolysis of cancer cells in advanced melanoma patients treated with ipilimumab. They discovered that high expression of glucose catabolism genes in melanoma was inversely associated with infiltration of substantial immune cells, suggesting that tumors with low glycolytic activity are more likely to respond to anti-CTLA-4 antibodies (77). Furthermore, lactate dehydrogenase A (LDHA) and monocarboxylate transporter 1 (MCT1), which are key enzymes involved in glycolysis and lactate production, have been found to exhibit an inverse correlation with immune infiltrates even after ipilimumab treatment (77). This suggests that anti-CTLA-4 blockade alone may be insufficient to enhance immune cell infiltration in highly glycolytic tumors.

LKB1 is recognized as a key metabolic regulator that exerts control over glucose metabolism by inducing the expression of critical genes encoding enzymes involved in glycolysis, gluconeogenesis, aerobic oxidation, and the pentose phosphate pathway. It achieves this regulation by acting on several downstream targets, including the central metabolic sensor called AMP-activated protein kinase (AMPK) (78–82). Under conditions of energy stress, LKB1 directly phosphorylates AMPK, which in turn promotes the activation of catabolic pathways such as glycolysis and fatty acid oxidation. Simultaneously, it suppresses anabolic pathways, including gluconeogenic enzymes, to maintain intracellular ATP levels (81, 82). Furthermore, the LKB1-AMPK

axis plays a role in regulating cell growth and division by inhibiting the mammalian target of rapamycin complex 1 (mTORC1), which serves as the central integrator of nutrient and mitogenic signals. Notably, mTORC1 is often activated in cancer cells, contributing to tumor progression (81, 83). When LKB1 function is compromised, these downstream factors become dysregulated, leading to increased glucose uptake and consumption, as well as a metabolic shift toward aerobic glycolysis. Even in benign tumors with LKB1 haploinsufficient, there have been reports of enhanced accumulation of 18F-deoxyglucose on positron emission tomography, indicating that the loss of LKB1 function directly influences glucose metabolic reprogramming (84). Studies using the naturally LKB1-inactivated NSCLC cell line A549 have demonstrated that the activation of hypoxia-inducible factor 1 alpha (HIF-1 $\alpha$ ), induced by LKB1 inactivation, contributes to the enhancement of the aerobic glycolytic system (85). The absence of LKB1 was found to result in increased HIF-1 $\alpha$  expression, which was shown to depend on both mTOR signaling and cellular mitochondrial reactive oxygen species (ROS) levels. Notably, *HIF-1 $\alpha$*  knockdown in LKB1-deficient cell line significantly reduced proliferation under low-glucose conditions, indicating that HIF-1 $\alpha$  promotes the growth of NSCLC with LKB1 inactivation even when nutrients are limited (85). Alongside LKB1 inactivation, *KRAS* mutation, which is the most prevalent oncogenic alteration in tumors with LKB1 inactivation, also leads to heightened glucose uptake and increased glycolytic activity. This is achieved through the upregulation of glucose transporter 1 (GLUT1) and key glycolytic enzymes such as LDHA, hexokinases, and phosphofructokinase 1 (PFK1) (86–88). Mutant *KRAS*, by upregulating GLUT1 and these glycolytic enzymes, further enhances aerobic glycolysis. Therefore, lung cancer cells with simultaneous LKB1 inactivation and *KRAS* mutation are likely to exhibit greater glucose uptake and consumption, contributing to their rapid tumor growth and suppression of intratumor effector T-cell activity (Figure 3A).

Tumor cells that undergo rapid proliferation stimulate the formation of tumor blood vessels by releasing factors that promote angiogenesis. This process is crucial for acquiring nutrients and oxygen. However, the resulting vasculature is often immature and hyperpermeable, leading to the development of hypoxic regions within the tumor. These hypoxic areas create a barrier that hampers the infiltration of immune cells (89). Moreover, the hypoxic tumor microenvironment contributes to the accumulation of immunosuppressive metabolic byproducts. These metabolic alterations negatively impact the function of effector T cells, while they may have little to no effect or even benefit suppressive immune populations like regulatory T cells (Treg) and suppressive myeloid populations (31, 90). The increased glycolytic activity in tumor leads to the production of large amounts of lactate, which in turn acidifies the extracellular spaces. NSCLC with LKB1 inactivation is associated with an elevated extracellular acidification rate (ECAR), which indicates higher lactate levels. Introducing transient expression of LKB1 in an NSCLC cell line with LKB1 inactivation resulted in a 20% decrease in ECAR (85). Despite its ability to lower pH, lactate has diverse effects on immune cell populations. For instance, it promotes a

metabolic shift in Treg to enable their activity in low-glucose environments and induces macrophages to adopt an M2 phenotype, which supports tumor growth (91–93). Notably, the accumulation of lactic acid can suppress the proliferation of CD4+ and CD8+ T cells, as well as inhibit their cytokine production (94). Lactate can deplete intracellular nicotinamide adenine dinucleotide + (NAD+) levels and impair effector T cells because LDH uses lactate to generate NAD+ hydrogen (NADH). Conversely, Treg can continue to function in high lactate environments where conventional T cells are suppressed due to the NAD+ produced by mitochondrial metabolism (91, 93).

Furthermore, it is recognized that circulating lactate is transported into cells via MCT1 and used as an energy source and substrate for lipogenesis in certain cancer types (95). In an analysis that measured the uptake of metabolic intermediates from tumor samples after labeled glucose infusion in NSCLC patients, elevated lactate labeling was observed, indicating the uptake of lactate in tumors compared to glycolytic metabolites (96). In addition, a xenograft model using an NSCLC cell line with LKB1 inactivation showed increased labeled lactate in the tumor, indicating the uptake of extracellular lactate and its incorporation into the tricarboxylic acid (TCA) cycle as a carbon source (96). This study suggests that lactate plays a crucial role as an energy source in LKB1-inactivated NSCLC. Apart from LDHA/B, elevated levels of the lactate transporter MCT1/4 have also been observed in lung cancer cells with LKB1 inactivation (96, 97), suggesting that intracellular lactate is not only incorporated into the TCA cycle but that extracellular lactate released by neighboring cancer cells can be taken up and incorporated into the TCA cycle as an energy source (Figure 3A).

### 3.2 Glutaminolysis in LKB1-inactivated NSCLC

Glutamine (Gln) is a vital amino acid with significant roles in cellular functions, including energy and biomolecule synthesis, as well as ROS scavenging. Upon cellular uptake, Gln is converted into glutamate (Glu) by the enzyme glutaminase (GLS). It is further converted to  $\alpha$ -ketoglutarate, which enters the TCA cycle, generating metabolic intermediates for lipid, nucleic acid, and protein synthesis. In the TME, both tumor cells and infiltrating immune cells have a high demand for Gln, similar to glucose. T-cell activation and proliferation heavily rely on Gln metabolism, and when Gln is insufficient in the TME, the high consumption by tumors can inhibit T-cell activity. Conversely, reduced Gln metabolism in tumors has shown to increase Gln utilization within the TME (34). In a mouse model of colorectal cancer using MC38 tumor-bearing mice, combination therapy of anti-PD-1 monoclonal antibody and a Gln antagonist prodrug, 6-diazo-5-oxo-L-norleucine, resulted in enhanced tumor growth inhibition (98).

Several oncogenes and tumor suppressors play a role in regulating Gln metabolism, and LKB1 inactivation is also implicated in Gln flux regulation. LKB1 ectopic expression in NSCLC cells with LKB1 deficiency led to a decrease in Gln-



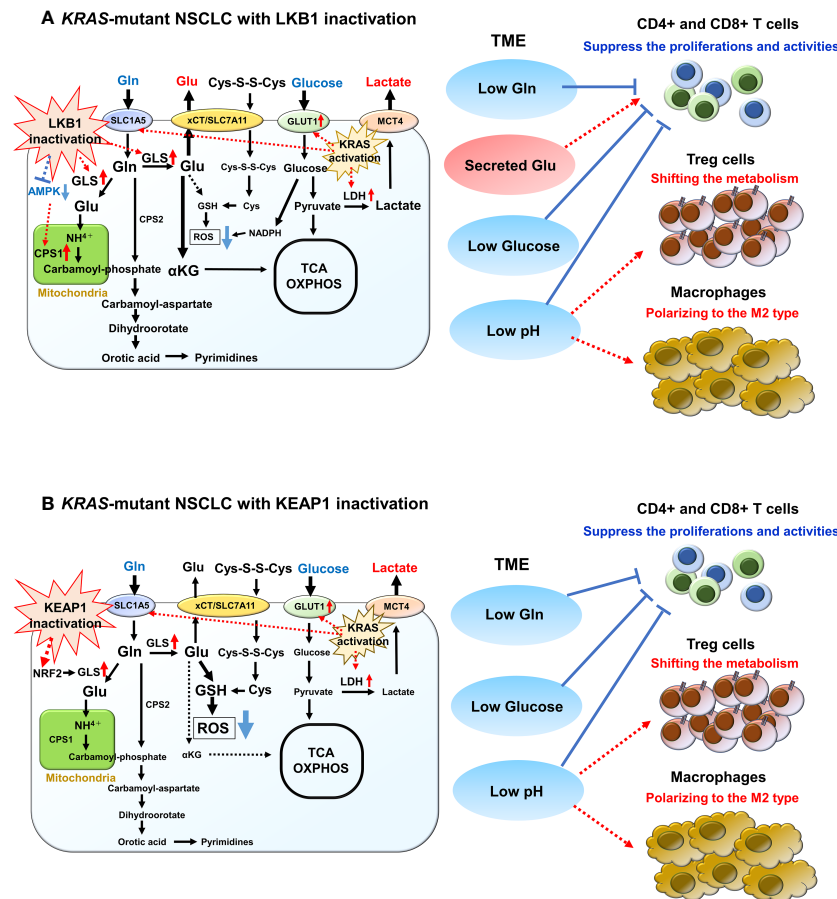


FIGURE 3

Overview of glucose and glutamine (Gln) metabolism in *KRAS*-mutant NSCLC with LKB1 or KEAP1 inactivation. **(A)** Overview of glucose and Gln metabolism in *KRAS*-mutant NSCLC with LKB1 inactivation. Glucose is imported by glucose transporter 1 (GLUT1) and is then metabolized by glycolysis into pyruvate. Pyruvate then either enters the tricarboxylic acid (TCA) cycle for ATP synthesis or is converted to lactate by lactate dehydrogenase (LDH). Mutant-*KRAS* enhances aerobic glycolysis by upregulating GLUT1 and LDH. After exported by monocarboxylate transporter 4 (MCT4), lactate increases extracellular acidification rate of tumor microenvironment (TME) and has diverse effects on various immune cells. Gln is imported by SLC1A5 where it then enters into the mitochondria and is converted to glutamate (Glu) by glutaminase (GLS), which is highly increased in NSCLC with LKB1 inactivation. The released  $\text{NH}_4^+$  during the conversion of Gln to Glu is used for the synthesis of the purine/pyrimidine base. Carbamoyl phosphate synthetase 1 (CPS1), which is the first rate-limiting mitochondrial enzyme in the urea cycle, is overexpressed in NSCLC with LKB1 inactivation. Glu is also used for the precursor of glutathione (GSH), which promotes reactive oxygen species (ROS) detoxification. In addition, the excess synthesized Glu is excreted out via xCT/SLC7A11 and is then required for T-cell activation. **(B)** Overview of glucose and Gln metabolism in *KRAS*-mutant NSCLC with KEAP1 inactivation. Glucose and Gln metabolism are promoted to the anabolic pathway through interaction with the phosphatidylinositol 3'-kinase/protein kinase B signaling. Gln exchanges Glu for cystine via the antiporter xCT (SLC3A2/SLC7A11), which activated NRF2 target. Both cystine and Gln are used to produce GSH, leading to ROS neutralization. Gln is also used in purine base synthesis, and fewer Gln are used for TCA cycle.

derived Glu (85). Furthermore, in the LKB1-deficient NSCLC cell line A549, the majority of Gln-derived carbon entered the TCA cycle compared to glucose-derived carbon, in contrast to the cell line with LKB1 ectopic expression (85). Moreover, LKB1-inactivated NSCLC cells exhibit higher levels of GLS expression and more active conversion of Gln to Glu (99). The released  $\text{NH}_4^+$  during this conversion is used for the synthesis of purine/pyrimidine bases, which are essential for rapid cell proliferation. Notably, studies have demonstrated characteristic overexpression of carbamoyl phosphate synthetase 1 (CPS1), the first rate-limiting mitochondrial enzyme in the urea cycle, in a subset of NSCLC with LKB1 inactivation (100, 101). CPS1 plays a vital role in promoting cell growth by increasing the bioavailability of carbamoyl phosphate, an intermediary metabolite required for *de novo*

pyrimidine synthesis. The CPS1 expression is transcriptionally regulated by LKB1 through AMPK, and cases with high CPS1 expression have been associated with poor prognosis, particularly in NSCLC with LKB1 inactivation (100, 101). Thus, LKB1-inactivated lung cancers effectively utilize excess Gln, and the activation of these metabolic pathways may contribute to their high malignancy. Furthermore, oncogenic *KRAS* has been shown to stimulate Gln catabolism in the mitochondria (87, 88). Since both *KRAS* and LKB1 regulate metabolism, the co-mutation of these two genes could lead to a unique metabolic phenotype not observed with either mutation alone. In fact, CPS1 plays a pivotal role in maintaining the balance between purine and pyrimidine in NSCLC cells with co-mutated *KRAS* and *LKB1*, and the enzyme also provides an alternative pool of carbamoyl phosphate to sustain

pyrimidine availability (101). Hence, apart from glucose metabolism, reprogramming of Gln metabolism in tumors harboring co-mutated *KRAS* and *LKB1* likely contributes to aggressive oncological behavior and impacts TME (Figure 3A). Notably, the clinical response to PD-(L)1 inhibition is significantly poorer in NSCLC patients with co-mutated *KRAS* and *STK11* compared to those with only *STK11* mutation (102).

Cellular metabolism generates ROS, which need to be scavenged to prevent damage to DNA, RNA, and proteins. Gln metabolism also plays an important role in maintaining oxidative homeostasis. Glu, generated from Gln by the catalytic action of GLS, serves as the precursor of glutathione (GSH), which promotes ROS detoxification (103). GSH, along with thioredoxin, plays a major role in neutralizing ROS and is synthesized through an NADPH-dependent mechanism. Loss of *LKB1* activity resulting in metabolic reprogramming leads to elevated ROS levels and metabolic stress, while the conversion of Gln to Glu significantly contributes to ROS neutralization by stimulating the production of GSH (104). Furthermore, due to the increased aerobic glycolysis in cancer cells, metabolites are shunted toward the pentose phosphate pathway (PPP), which aids in ROS scavenging. In *LKB1* mutant cell lines, such as A549 and H460 cells, genes associated with the PPP are upregulated, indicating their dependence on this pathway (105). Meanwhile, A549 cells that re-express *LKB1* exhibit a higher apoptosis rate under ROS stress compared to control cells (104), suggesting that the upregulation of Gln conversion observed in *LKB1*-inactivating mutations may confer increased resistance to ROS.

### 3.3 Glutaminolysis in KEAP1-inactivated NSCLC

The KEAP1-nuclear factor erythroid-derived 2-like 2 (NRF2) pathway plays a crucial role in regulating the cellular response to oxidative stress, and its signaling abnormalities have been observed in various cancer types, including NSCLC (106, 107). In normal conditions, KEAP1 ubiquitinates NRF2, encoded by the *NFE2L2* gene, for degradation through ubiquitination. However, under stress conditions, KEAP1 activity is reduced, leading to increased transcription of NRF2 target genes. This activation of NRF2 signaling enhances antioxidant defense against ROS and regulates drug detoxification and immune response (106, 107). In NSCLC, *KEAP1* deficiency is commonly observed in LUAD, while activating alterations of *NFE2L2* are more prevalent in squamous cell lung carcinoma (~20%), with both alterations being mutually exclusive (108). The constitutive activation of NRF2 signaling in advanced cancer patients diminishes the therapeutic effects of chemotherapy and radiation therapy, as these treatments rely on inducing cell death through DNA replication damage and ROS induction (106, 107). Furthermore, recent studies have revealed that NRF2 activation promotes various metabolic reprogramming processes and is associated with tumor progression in NSCLC, including glutaminolysis (109–111).

Similar to tumors with *LKB1* inactivation, tumors harboring *KEAP1* mutations increased uptake of Gln from TME, leading to

reduced availability of Gln for infiltrating T cells and consequent inhibition of their activation. Activation of NRF2 signaling resulting from KEAP1 inactivation promotes glucose and Gln metabolism toward the anabolic pathway through phosphatidylinositol 3'-kinase/protein kinase B signaling (112). This increased Gln consumption is accompanied by increased expression of the Gln importer SLC1A5 (113). Furthermore, the incorporated Gln exchanges Glu for cystine through the antiporter xCT (SLC3A2/SLC7A11), which is upregulated as a target of NRF2 activation, in a Gln degradation-dependent manner (113, 114). Both cystine and Gln contribute to the production of GSH, thereby enhancing antioxidant activity. In addition, Gln is actively used in purine base synthesis. Therefore, tumors with KEAP1 inactivation may have limited Gln availability for the TCA cycle (Figure 3B). NRF2 knockdown in NSCLC cell lines, such as A549, reduces GSH formation from Gln (104). Furthermore, *KEAP1*-mutant NSCLC cell lines demonstrate sensitivity to GLS inhibition due to their high dependence on Gln uptake in the culture medium (104). Integrating these findings, the combination of GLS inhibition and immunotherapy may offer a promising therapeutic strategy in KEAP1-inactivated NSCLC. By suppressing Gln uptake, this strategy could potentially activate T cells in the TME while attenuating the antioxidant effect of KEAP1-inactivated tumors. Furthermore, Pranavi et al. found that NSCLC with KEAP1 inactivation exhibits increased dependence on glucose under glucose-limiting conditions, as NRF2-dependent SLC7A11 expression is upregulated, resulting in cytotoxicity related to disulfide stress (115). In addition, they demonstrated the high sensitivity of KEAP1-inactivated NSCLC to GLUT inhibitor (115). These findings suggest that targeting Gln and glucose metabolism could be an attractive therapeutic target in NSCLC cases with KEAP1 inactivation or constitutive activation of NRF2.

### 3.4 Glutaminolysis in NSCLC with co-occurring mutations of *STK11* and *KEAP1*

Clinical data analysis reveals that lung cancers characterized by simultaneous mutations in *LKB1* and *KEAP1* exhibit an exceptionally poor prognosis (23). *In vitro* and *in vivo* studies have demonstrated that co-occurring mutations of *STK11* and *KEAP1* in *KRAS*-mutant NSCLC promote tumor growth and confer enhanced resistance to radiotherapy (116). The co-inactivation of *LKB1* and *KEAP1* cooperatively promotes metabolic reprogramming in *KRAS*-mutant tumor, and even in the presence of KEAP1 inactivation, *LKB1* inactivation modulates NRF2 activity through increased ROS levels (104). *LKB1*-mutant cells induce NRF2-dependent Glu cysteine ligase expression, a key enzyme that generates  $\gamma$ -Gly-Gly from Gln and cysteine to increase the GSH pool (104). These results indicate that *KRAS*-mutant NSCLC with co-inactivation of *LKB1* and *KEAP1* enhanced Gln dependence compared to *KRAS*-mutant NSCLC with *LKB1* or *KEAP1* inactivation. Consistently, *KRAS*-mutant NSCLC cell lines with co-inactivation of *LKB1* and *KEAP1* display increased sensitivity to GLS inhibitors compared to other cell lines (104), indicating that targeting glutaminolysis in *KRAS*-mutant NSCLC

with co-inactivation of LKB1 and KEAP1 holds promise as a therapeutic strategy.

In a study conducted by Best et al., distinct metabolic characteristics were observed among KRAS-KEAP1 (KK), KRAS-LKB1 (KL), and KRAS-KEAP1-LKB1 (KKL) mutant LUAD using genetically engineered mouse models (99). In KRAS-mutant LUAD with LKB1 inactivation, the expression of GLS1, an enzyme responsible for metabolizing Gln to Glu, was significantly higher compared to KRAS-mutant NSCLC with co-inactivation of LKB1 and KEAP1. The conversion of Gln to Glu was particularly enhanced in the KL mouse model (Figure 3A). Furthermore, the influx of  $\alpha$ -ketoglutaric acid into the TCA cycle was significantly increased in KL mice compared to KK or KKL mice (99). Tumors from KL mice also exhibited a notable increase in orotic acid, which is synthesized during the Gln to Glu conversion process via carbamoyl phosphate. Orotic acid is a precursor of pyrimidine and its synthesis directly affects pyrimidine production (99). Tumors from KL mice also exhibited a notable increase in orotic acid, which is synthesized during the Gln to Glu conversion process via carbamoyl phosphate. Orotic acid is a precursor of pyrimidine and its synthesis directly affects pyrimidine production (117, 118). Increased orotic acid synthesis is closely linked to enhanced nucleic acid synthesis, as nucleotide synthesis is tightly regulated by pyrimidine. In KRAS-mutant LUAD with LKB1, CPS1, an enzyme responsible for carbamoyl phosphate synthesis in the mitochondria, is highly expressed, and the heightened Gln metabolism contributes to rapid tumor growth through increased nucleic acid synthesis (100, 101). Excess Glu synthesized is also released from cancer cells via xCT/SLC7A11 (119, 120). Best et al. demonstrated that the release of Glu from cancer cells is crucial for T-cell activation and clonal expansion of T-cell receptors (99). Therefore, GLS inhibition attenuates CD8<sup>+</sup> T-cell activation, suggesting that the combining GLS inhibitors with immunotherapy may not enhance the immune response. Particularly in KL mice, the amount of Glu released from cancer cells was higher, and KKL mice exhibited a similar Glu metabolic pattern to KL mice compared to KK mice (99). These findings suggest that GLS inhibitors may be less effective in KRAS-mutant LUAD with LKB1 inactivation and co-occurring mutations of LKB1 and KEAP1 compared to KRAS-mutant LUAD with KEAP1 inactivation.

## 4 Discussion

To date, subgroup analyses of pivotal clinical trials have shown that current ICI combination regimens have some effectiveness in NSCLC patients with LKB1 or KEAP1 inactivation compared to standard platinum doublet chemotherapies (52, 57, 67, 69, 70). However, their efficacy is not sufficient to significantly improve long-term prognosis compared to NSCLC patients without LKB1 and KEAP1 inactivation (52, 57, 67, 69, 70). This indicates that the combination of anti-PD-1/PD-L1 antibodies with cytotoxic chemotherapies and/or anti-CTLA-4 antibodies is unable to fully restore the dysfunctional state of T cells or NK cells in NSCLC with these mutations. Moreover, the clinical efficacy of most regimens

has not yet been analyzed for KRAS-mutant NSCLC with LKB1 or KEAP1 inactivation, which is associated with the poorest prognosis (29, 102). On the other hand, a subgroup analysis of the IMpower150 trial revealed that the trial arm, ABCP regimen, demonstrated superior antitumor effects compared to the control arm in KRAS-mutant NSCLC with *STK11* or *KEAP1* mutations (57). By normalizing abnormal tumor vasculature, the addition of VEGF-A inhibitors to ICIs can increase the infiltration of effector T cells into tumors (121). Furthermore, since VEGF-A receptors are expressed on various tumor-promoting immune cells, such as Tregs and immature dendritic cells, this combination therapy may have additional effects in converting the intrinsically immunosuppressive TME into an immunosupportive one, even in immune cold subtypes (121). However, further analysis is needed to fully understand the significance of VEGF-A inhibition for immune cold tumors from both basic and clinical perspectives. Regarding molecular-targeted agents for KRAS G12C mutations, sotorasib and adagrasib are now indicated as a second-line treatment following ICI regimens and has expanded the therapeutic options for KRAS-mutant NSCLC patients (54). However, its efficacy is limited in cases of NSCLC with co-mutations of *STK11* and *KEAP1* (122). Similarly, in NSCLC with *EGFR* mutations, co-mutations such as *TP53* and *RB transcriptional corepressor 1* can affect the antitumor effect of EGFR-tyrosine kinase inhibitors (123). Therefore, in addition to targeting oncogenic driver alterations, it is increasingly important to identify inactivating mutations in tumor suppressor genes that can impact the efficacy of immunotherapy and of molecularly targeted agents. In fact, some clinical trials of novel molecularly targeted agents targeting KRAS G12C mutation have included *STK11* mutation as a stratification factor (124, 125) (Table 1). These trends underscore the need for novel therapeutic strategies in the treatment of NSCLC with *STK11* and/or *KEAP1* mutations, as the efficacy of ICIs and molecular targeting agents directly affects patient outcomes.

Concurrent with the advancements in immune checkpoint inhibitors (ICIs) and molecularly targeted therapies, recent fundamental research has uncovered that each driver gene alteration has a cancer-specific impact on the TME through metabolic reprogramming. Specifically, the alteration of glucose and glutamine (Gln) metabolism resulting from LKB1 or KEAP1 inactivation appears to play a significant role in diminishing the effectiveness of current immunotherapies by suppressing the activity of effector T cells. Ongoing clinical trials targeting glucose or Gln metabolism, as depicted in Table 1, aim to develop novel therapies for NSCLC with LKB1 or KEAP1 inactivation (126–128).

One therapeutic strategy being explored involves the addition of metformin, a commonly used medication for type 2 diabetes, to cytotoxic chemotherapy. Accumulating evidence supports the antitumor effects of metformin, as it enhances AMPK-mediated cell growth inhibition and cisplatin-induced apoptosis in LKB1-inactivated NSCLC (135, 136). Interestingly, despite initial reports indicating that metformin requires LKB1 for the regulation of gluconeogenesis in the liver, it demonstrates efficacy in LKB1-inactivated NSCLC (137). Clinical trials targeting Gln metabolism have also been initiated, employing Gln antagonists and oral GLS inhibitors, to explore a new therapeutic approach for NSCLC with

TABLE 1 Summary of on-going trials against advanced NSCLC with *STK11* or *KEAP1* mutation.

| Study   | Subject of research   | Treatment setting  | Treatment regimen   | Overcoming mechanism               | Phase              | Primary outcome |
|---|---|--------------------|---|------------------------------------|--------------------|-----------------|
| Ongoing trials where <i>STK11</i> mutation is a stratification factor |   |                    |   |                                    |                    |                 |
| CodeBreak201<br>NCT04933695<br>(124)                                  | <i>KRAS G12C</i> mutant NSCLC with PD-L1 < 1%, stratified by <i>STK11</i> co-mutation       | Treatment naïve    | AMG510 (Sotorasib)  | <i>KRAS G12C</i> inhibitor         | Phase 2            | ORR             |
| KRYSTAL-1<br>NCT03785249<br>(125)                                     | Solid tumor harboring <i>KRAS G12C</i> mutation, stratified by <i>STK11</i> co-mutation     | Previously treated | MRTX849 (Adagrasib)   | <i>KRAS G12C</i> inhibitor         | Phase 1/2          | Safety, ORR     |
| Ongoing trials  |   |                    |   |                                    |                    |                 |
| FAME<br>NCT03709147<br>(126)  | LUAD with LKB1 inactivation   | Treatment naïve    | Platinum+PEM+Pembrolizumab +Metfolmin Platinum+PEM +Pembrolizumab+Metfolmin+FMD | Biguanide and Nutrient Deprivation | Randomized Phase 2 | PFS             |
| BeGIN<br>NCT03872427<br>(127)   | Solid tumor harboring <i>NF1/KEAP1/STK11</i> mutation                                       | Previously treated | CB-839 (Telaglenastat)  | Glutaminase inhibitor              | Phase 2            | ORR             |
| NCT04471415<br>(128)  | NSCLC harboring <i>KEAP1/NFE2L2/STK11</i> alteration  | Previously treated | DRP-104 (Sirpiglenastat)  | Glutamine antagonist               | Phase 1/2a         | Safety, ORR     |
| CAPTUR<br>NCT03297606<br>(129)  | Solid tumor harboring <i>STK11/NF1/NF2</i> /other mutation                                  | Previously treated | Temsirolimus  | mTORC1 inhibitor                   | Phase 2            | ORR             |
| NCT05469178<br>(130)  | NSq-NSCLC harboring <i>STK11</i> mutation   | Treatment naïve    | CBDCA+PEM+Pembrolizumab +Bemcentinib  | AXL inhibitor                      | Phase 1b/2a        | DLT, ORR        |
| NCT05704634<br>(131)  | NSCLC harboring <i>STK11</i> mutation   | Previously treated | Cemiplimab+Sarilumab  | IL6-receptor antibody              | Phase 1b           | Safety, ORR     |
| NCT05275868<br>(132)  | NSCLC harboring <i>NFE2L2/KEAP1/CUL3</i> alteration   | Previously treated | MGY825  | unavailable                        | Phase 1            | Safety          |
| KontRAst-06<br>NCT05445843<br>(133)                                   | <i>KRAS G12C</i> mutant NSCLC harboring co-mutation of <i>STK11</i> and PD-L1 ≥ 1%          | Treatment naïve    | JDQ443 (Opnurasib)  | <i>KRAS G12C</i> inhibitor         | Phase 2            | ORR             |
| NCT05276726<br>(134)  | NSCLC harboring co-mutation of <i>KRAS G12C</i> and <i>STK11</i> and <i>KEAP1</i> wild-type | Any                | JAB-21822   | <i>KRAS G12C</i> inhibitor         | Phase 1b/2         | DLT, ORR        |

NSCLC, Non-small cell lung cancer; NSq-NSCLC, Non-squamous non-small cell lung cancer; LUAD, Lung adenocarcinoma; LKB1, Liver kinase B1; STK11, Serine/threonine kinase 11; KEAP1, Kelch-like ECH-associated protein 1; NFE2L2, Nuclear factor erythroid 2-related factor 2; CUL3, Cullin3; KRAS, Kirsten rat sarcoma virus; mTORC1, Mammalian target of rapamycin complex 1; AXL, AXL receptor tyrosine kinase; IL-6, Interleukin 6; PFS, Progression-free survival; HR, Hazard ratio; DLT, Dose limiting toxicity; ORR, Overall response rate; CBDCA, Carboplatin; PEM, Pemetrexed.

LKB1 inactivation or KEAP1 inactivation/NFE2L2 alteration (127, 128) (Table 1). However, the utilization of glutamate (Glu) released from cancer cells by T cells reveals a complex and interconnected relationship between cancer metabolism and immune cells within the TME (99). Furthermore, NSCLC with concurrent STK11 and KEAP1 mutations exhibit distinct Gln metabolism patterns compared to NSCLC with KEAP1 mutation alone, suggesting that the antitumor effects of targeting Gln metabolism may vary among NSCLC subgroups with different mutation co-occurring patterns (99). Therefore, considering the potential impact of diverse metabolic reprogramming based on specific mutation patterns, it will be crucial to assess the response of each mutated subgroup when treated with Gln metabolism inhibitors, either alone or in combination with a PD-(L)1 inhibitor.

In conclusion, high consumption of glycolysis and glutaminolysis in immune-resistant phenotype tumors, such as NSCLC with LKB1 and/or KEAP1 inactivation, not only contribute to tumor aggressiveness but also impede intratumor T-

cell function. The presence of co-occurring mutations in NSCLC leads to distinct metabolic alterations that impact immune cells within TME. These differences in metabolic reprogramming may affect clinical efficacies of current ICI combination regimens and novel agents targeting metabolic enzymes. To develop new therapeutic strategies that target metabolic alterations in combination with ICI regimens for NSCLC with LKB1 and/or KEAP1 inactivation, further extensive analyses on a larger scale will be necessary.

## Author contributions

IT, JK, HI, SH, and MM were involved in the initial drafting of the manuscript, data collection, and analysis. They also contributed to the conceptualization of the study, reviewed the manuscript, and provided feedback and edits. All authors have read and given their approval for the final version of the manuscript. IT have



demonstrated the dependency of CPS1, a metabolic enzyme, in cell growth, metabolism and prognosis in LKB1-inactivated lung adenocarcinomas. Furthermore, Serglycin secretion, which is a chondroitin sulfate proteoglycan involved in reprogramming to an immunosuppressive TME, is epigenetically induced through nicotinamide N-methyltransferase-induced perturbation of methionine metabolism in TTF-1-negative lung adenocarcinoma. These results were published in *J Natl Cancer Inst* (2017) 109:1-9 and *J Natl Cancer Inst* (2022) 114:290-301.

## Funding

IT received support for this research from the Japan Society for the Promotion of Science through Grant-in-Aid for Scientific Research (B) 23H02920.

## Acknowledgments

The authors would like to thank Enago ([www.enago.jp](http://www.enago.jp)) for providing English language editing services.

## References

- Grant MJ, Herbst RS, Goldberg SB. Selecting the optimal immunotherapy regimen in driver-negative metastatic NSCLC. *Nat Rev Clin Oncol* (2021) 18:625–44. doi: 10.1038/s41571-021-00520-1
- Reck M, Rodriguez-Abreu D, Robinson AG, Hui R, Csozsi T, Fulop A, et al. Pembrolizumab versus chemotherapy for PD-L1-positive non-small-cell lung cancer. *N Engl J Med* (2016) 375:1823–33. doi: 10.1056/NEJMoa1606774
- Herbst RS, Giaccone G, de Marinis F, Reinmuth N, Vergnenegre A, Barrios CH, et al. Atezolizumab for first-line treatment of PD-L1-selected patients with NSCLC. *N Engl J Med* (2020) 383:1328–39. doi: 10.1056/NEJMoa1917346
- Gandhi L, Rodriguez-Abreu D, Gadgeel S, Esteban E, Felip E, De Angelis F, et al. Pembrolizumab plus chemotherapy in metastatic non-small-cell lung cancer. *N Engl J Med* (2018) 378:2078–92. doi: 10.1056/NEJMoa1801005
- Socinski MA, Jotte RM, Cappuzzo F, Orlandi F, Stroyakovskiy D, Nogami N, et al. Atezolizumab for first-line treatment of metastatic nonsquamous NSCLC. *N Engl J Med* (2018) 378:2288–301. doi: 10.1056/NEJMoa1716948
- Reck M, Schenker M, Lee KH, Provencio M, Nishio M, Lesniewski-Kmak K, et al. Nivolumab plus ipilimumab versus chemotherapy as first-line treatment in advanced non-small-cell lung cancer with high tumour mutational burden: patient-reported outcomes results from the randomised, open-label, phase III CheckMate 227 trial. *Eur J Cancer* (2019) 116:137–47. doi: 10.1016/j.ejca.2019.05.008
- Paz-Ares L, Ciuleanu TE, Cobo M, Schenker M, Zurawski B, Menezes J, et al. First-line nivolumab plus ipilimumab combined with two cycles of chemotherapy in patients with non-small-cell lung cancer (CheckMate 9LA): an international, randomised, open-label, phase 3 trial. *Lancet Oncol* (2021) 22:198–211. doi: 10.1016/S1470-2045(20)30641-0
- Johnson ML, Cho BC, Luft A, Alatorre-Alexander J, Geater SL, Laktionov K, et al. Durvalumab with or without tremelimumab in combination with chemotherapy as first-line therapy for metastatic non-small-cell lung cancer: the phase III POSEIDON study. *J Clin Oncol* (2023) 41:1213–27. doi: 10.1200/JCO.22.00975
- Anagnostou V, Niknafs N, Marrone K, Bruhm DC, White JR, Naidoo J, et al. Multimodal genomic features predict outcome of immune checkpoint blockade in non-small-cell lung cancer. *Nat Cancer* (2020) 1:99–111. doi: 10.1038/s43018-019-0008-8
- Gavrielatou N, Shafi S, Gaule P, Rimm DL. PD-L1 expression scoring: noninterchangeable, noninterpretable, neither, or both. *J Natl Cancer Inst* (2021) 113:1613–4. doi: 10.1093/jnci/djab109
- Tanaka I, Furukawa T, Morise M. The current issues and future perspective of artificial intelligence for developing new treatment strategy in non-small cell lung cancer: harmonization of molecular cancer biology and artificial intelligence. *Cancer Cell Int* (2021) 21:454. doi: 10.1186/s12935-021-02165-7
- Faruki H, Mayhew GM, Serody JS, Hayes DN, Perou CM, Lai-Goldman M. Lung adenocarcinoma and squamous cell carcinoma gene expression subtypes demonstrate significant differences in tumor immune landscape. *J Thorac Oncol* (2017) 12:943–53. doi: 10.1016/j.jtho.2017.03.010
- Grenda A, Krawczyk P, Blach J, Chmielewska I, Kubiowski T, Kiesko S, et al. Tissue microRNA expression as a predictor of response to immunotherapy in NSCLC patients. *Front Oncol* (2020) 10:563613. doi: 10.3389/fonc.2020.563613
- Sun J, Zhang Z, Bao S, Yan C, Hou P, Wu N, et al. Identification of tumor immune infiltration-associated lncRNAs for improving prognosis and immunotherapy response of patients with non-small cell lung cancer. *J Immunother Cancer* (2020) 8(1): e000110. doi: 10.1136/jitc-2019-000110
- Zheng Y, Tang L, Liu Z. Multi-omics analysis of an immune-based prognostic predictor in non-small cell lung cancer. *BMC Cancer* (2021) 21:1322. doi: 10.1186/s12885-021-09044-4
- Cristescu R, Mogg R, Ayers M, Albright A, Murphy E, Yearley J, et al. Pan-tumor genomic biomarkers for PD-1 checkpoint blockade-based immunotherapy. *Science* (2018) 362:6411. doi: 10.1126/science.aar3593
- Gillette MA, Satpathy S, Cao S, Dhanasekaran SM, Vasaiak SV, Krug K, et al. Proteogenomic characterization reveals therapeutic vulnerabilities in lung adenocarcinoma. *Cell* (2020) 182:200–25 e35. doi: 10.1016/j.cell.2020.06.013
- Skoulidis F, Heymach JV. Co-occurring genomic alterations in non-small-cell lung cancer biology and therapy. *Nat Rev Cancer* (2019) 19:495–509. doi: 10.1038/s41568-019-0179-8
- Devarakonda S, Morgensztern D, Govindan R. Genomic alterations in lung adenocarcinoma. *Lancet Oncol* (2015) 16:e342–51. doi: 10.1016/S1470-2045(15)00077-7
- Calles A, Sholl LM, Rodig SJ, Pelton AK, Hornick JL, Butaney M, et al. Immunohistochemical loss of LKB1 is a biomarker for more aggressive biology in KRAS-mutant lung adenocarcinoma. *Clin Cancer Res* (2015) 21:2851–60. doi: 10.1158/1078-0432.CCR-14-3112
- Cardnell RJ, Behrens C, Diao L, Fan Y, Tang X, Tong P, et al. An integrated molecular analysis of lung adenocarcinomas identifies potential therapeutic targets among TTF1-negative tumors, including DNA repair proteins and Nrf2. *Clin Cancer Res* (2015) 21:3480–91. doi: 10.1158/1078-0432.CCR-14-3286
- Marinelli D, Mazzotta M, Scalera S, Terrenato I, Sperati F, D'Ambrosio L, et al. KEAP1-driven co-mutations in lung adenocarcinoma unresponsive to immunotherapy despite high tumor mutational burden. *Ann Oncol* (2020) 31:1746–54. doi: 10.1016/j.annonc.2020.08.2105
- Papillon-Cavanagh S, Doshi P, Dobrin R, Szustakowski J, Walsh AM. STK11 and KEAP1 mutations as prognostic biomarkers in an observational real-world lung

## Conflict of interest

The authors declare that the research was conducted in the absence of any commercial or financial relationships that could be construed as a potential conflict of interest.

## Publisher's note

All claims expressed in this article are solely those of the authors and do not necessarily represent those of their affiliated organizations, or those of the publisher, the editors and the reviewers. Any product that may be evaluated in this article, or claim that may be made by its manufacturer, is not guaranteed or endorsed by the publisher.

## Supplementary material

The Supplementary Material for this article can be found online at: <https://www.frontiersin.org/articles/10.3389/fonc.2023.1249237/full#supplementary-material>

- adenocarcinoma cohort. *ESMO Open* (2020) 5(2):e000706. doi: 10.1101/2020.01.23.20017566
24. Singh A, Daemen A, Nickles D, Jeon SM, Foreman O, Sudini K, et al. NRF2 activation promotes aggressive lung cancer and associates with poor clinical outcomes. *Clin Cancer Res* (2021) 27:877–88. doi: 10.1158/1078-0432.CCR-20-1985
25. Binkley MS, Jeon YJ, Nesselbush M, Moding EJ, Nabet BY, Almanza D, et al. KEAP1/NFE2L2 mutations predict lung cancer radiation resistance that can be targeted by glutaminase inhibition. *Cancer Discovery* (2020) 10:1826–41. doi: 10.1158/2159-8290.CD-20-0282
26. Jeong Y, Hellyer JA, Stehr H, Hoang NT, Niu X, Das M, et al. Role of KEAP1/NFE2L2 mutations in the chemotherapeutic response of patients with non-small cell lung cancer. *Clin Cancer Res* (2020) 26:274–81. doi: 10.1158/1078-0432.CCR-19-1237
27. Jeong Y, Hoang NT, Lovejoy A, Stehr H, Newman AM, Gentles AJ, et al. Role of KEAP1/NRF2 and TP53 mutations in lung squamous cell carcinoma development and radiation resistance. *Cancer Discovery* (2017) 7:86–101. doi: 10.1158/2159-8290.CD-16-0127
28. Skoulidis F, Goldberg ME, Greenawalt DM, Hellmann MD, Awad MM, Gainor JF, et al. STK11/LKB1 mutations and PD-1 inhibitor resistance in KRAS-mutant lung adenocarcinoma. *Cancer Discovery* (2018) 8:822–35. doi: 10.1158/2159-8290.CD-18-0099
29. Arbour KC, Jordan E, Kim HR, Dienstag J, Yu HA, Sanchez-Vega F, et al. Effects of co-occurring genomic alterations on outcomes in patients with KRAS-mutant non-small cell lung cancer. *Clin Cancer Res* (2018) 24:334–40. doi: 10.1158/1078-0432.CCR-17-1841
30. Sugiura A, Rathmell JC. Metabolic barriers to T cell function in tumors. *J Immunol* (2018) 200:400–7. doi: 10.4049/jimmunol.1701041
31. DePeaux K, Delgoffe GM. Metabolic barriers to cancer immunotherapy. *Nat Rev Immunol* (2021) 21:785–97. doi: 10.1038/s41577-021-00541-y
32. Nabe S, Yamada T, Suzuki J, Toriyama K, Yasuoka T, Kuwahara M, et al. Reinforce the antitumor activity of CD8(+) T cells via glutamine restriction. *Cancer Sci* (2018) 109:3737–50. doi: 10.1111/cas.13827
33. Cascone T, McKenzie JA, Mbongungu RM, Punt S, Wang Z, Xu C, et al. Increased tumor glycolysis characterizes immune resistance to adoptive T cell therapy. *Cell Metab* (2018) 27:977–87 e4. doi: 10.1016/j.cmet.2018.02.024
34. Leone RD, Zhao L, Englert JM, Sun IM, Oh MH, Sun IH, et al. Glutamine blockade induces divergent metabolic programs to overcome tumor immune evasion. *Science* (2019) 366:1013–21. doi: 10.1126/science.aav2588
35. Choi H, Na KJ. Different glucose metabolic features according to cancer and immune cells in the tumor microenvironment. *Front Oncol* (2021) 11:769393. doi: 10.3389/fonc.2021.769393
36. Arner EN, Rathmell JC. Metabolic programming and immune suppression in the tumor microenvironment. *Cancer Cell* (2023) 41:421–33. doi: 10.1016/j.ccell.2023.01.009
37. Lee SJ, Jang BC, Lee SW, Yang YI, Suh SI, Park YM, et al. Interferon regulatory factor-1 is prerequisite to the constitutive expression and IFN-gamma-induced upregulation of B7-H1 (CD274). *FEBS Lett* (2006) 580:755–62. doi: 10.1016/j.febslet.2005.12.093
38. Miyazawa A, Ito S, Asano S, Tanaka I, Sato M, Kondo M, et al. Regulation of PD-L1 expression by matrix stiffness in lung cancer cells. *Biochem Biophys Res Commun* (2018) 495:2344–9. doi: 10.1016/j.bbrc.2017.12.115
39. Altorki NK, Markowitz GJ, Gao D, Port JL, Saxena A, Stiles B, et al. The lung microenvironment: an important regulator of tumour growth and metastasis. *Nat Rev Cancer* (2019) 19:9–31. doi: 10.1038/s41568-018-0081-9
40. Tanaka I, Morise M. Current immunotherapeutic strategies targeting the PD-1/PD-L1 axis in non-small cell lung cancer with oncogenic driver mutations. *Int J Mol Sci* (2021) 23(1):245. doi: 10.3390/ijms23010245
41. Herbst RS, Baas P, Kim DW, Felip E, Perez-Gracia JL, Han JY, et al. Pembrolizumab versus docetaxel for previously treated, PD-L1-positive, advanced non-small-cell lung cancer (KEYNOTE-010): a randomised controlled trial. *Lancet* (2016) 387:1540–50. doi: 10.1016/S0140-6736(15)01281-7
42. Reck M, Rodriguez-Abreu D, Robinson AG, Hui R, Csoszi T, Fulop A, et al. Five-year outcomes with pembrolizumab versus chemotherapy for metastatic non-small-cell lung cancer with PD-L1 tumor proportion score  $\geq$  50. *J Clin Oncol* (2021) 39:2339–49. doi: 10.1200/JCO.21.00174
43. Jassem J, de Marinis F, Giaccone G, Vergnenegre A, Barrios CH, Morise M, et al. Updated overall survival analysis from IMpower110: atezolizumab versus platinum-based chemotherapy in treatment-naïve programmed death-ligand 1-selected NSCLC. *J Thorac Oncol* (2021) 16:1872–82. doi: 10.1016/j.jtho.2021.06.019
44. Garassino MC, Gadgeel S, Speranza G, Felip E, Esteban E, Domine M, et al. Pembrolizumab plus pemetrexed and platinum in nonsquamous non-small-cell lung cancer: 5-year outcomes from the phase 3 KEYNOTE-189 study. *J Clin Oncol* (2023) 41(11):JCO201989. doi: 10.1200/JCO.22.01989
45. Socinski MA, Nishio M, Jotte RM, Cappuzzo F, Orlandi F, Stroyakovskiy D, et al. IMpower150 final overall survival analyses for atezolizumab plus bevacizumab and chemotherapy in first-line metastatic nonsquamous NSCLC. *J Thorac Oncol* (2021) 16:1909–24. doi: 10.1016/j.jtho.2021.07.009
46. West H, McCleod M, Hussein M, Morabito A, Rittmeyer A, Conter HJ, et al. Atezolizumab in combination with carboplatin plus nab-paclitaxel chemotherapy compared with chemotherapy alone as first-line treatment for metastatic non-squamous non-small-cell lung cancer (IMpower130): a multicentre, randomised, open-label, phase 3 trial. *Lancet Oncol* (2019) 20:924–37. doi: 10.1016/S1470-2045(19)30167-6
47. Nishio M, Barlesi F, West H, Ball S, Bordoni R, Cobo M, et al. Atezolizumab plus chemotherapy for first-line treatment of nonsquamous NSCLC: results from the randomized phase 3 IMpower132 trial. *J Thorac Oncol* (2021) 16:653–64. doi: 10.1016/j.jtho.2020.11.025
48. Paz-Ares L, Luft A, Vicente D, Tafreshi A, Gumus M, Mazieres J, et al. Pembrolizumab plus chemotherapy for squamous non-small-cell lung cancer. *N Engl J Med* (2018) 379:2040–51. doi: 10.1056/NEJMoa1810865
49. Novello S, Kowalski DM, Luft A, Gumus M, Vicente D, Mazieres J, et al. Pembrolizumab plus chemotherapy in squamous non-small-cell lung cancer: 5-year update of the phase III KEYNOTE-407 study. *J Clin Oncol* (2023) 41(11):1999–2006. doi: 10.1200/JCO.22.01990
50. Hellmann MD, Paz-Ares L, Bernabe Caro R, Zurawski B, Kim SW, Carcereny Costa E, et al. Nivolumab plus ipilimumab in advanced non-small-cell lung cancer. *N Engl J Med* (2019) 381:2020–31. doi: 10.1056/NEJMoa1910231
51. Brahmer JR, Lee JS, Ciuleanu TE, Bernabe Caro R, Nishio M, Urban L, et al. Five-year survival outcomes with nivolumab plus ipilimumab versus chemotherapy as first-line treatment for metastatic non-small-cell lung cancer in checkMate 227. *J Clin Oncol* (2023) 41:1200–12. doi: 10.1200/JCO.22.01503
52. Paz-Ares LG, Ciuleanu T-E, Cobo M, Bannouna J, Schenker M, Cheng Y, et al. First-line nivolumab plus ipilimumab with chemotherapy versus chemotherapy alone for metastatic NSCLC in checkMate 9LA: 3-year clinical update and outcomes in patients with brain metastases or select somatic mutations. *J Thorac Oncol* (2023) 18:204–22. doi: 10.1016/j.jtho.2022.10.014
53. Tan AC, Tan DSW. Targeted therapies for lung cancer patients with oncogenic driver molecular alterations. *J Clin Oncol* (2022) 40:611–25. doi: 10.1200/JCO.21.01626
54. Skoulidis F, Li BT, Dy GK, Price TJ, Falchook GS, Wolf J, et al. Sotorasib for lung cancers with KRAS p.G12C mutation. *N Engl J Med* (2021) 384:2371–81. doi: 10.1056/NEJMoa2103695
55. Shen Y, Li J, Qiang H, Lei Y, Chang Q, Zhong R, et al. A retrospective study for prognostic significance of type II diabetes mellitus and hemoglobin A1c levels in non-small cell lung cancer patients treated with pembrolizumab. *Transl Lung Cancer Res* (2022) 11:1619–30. doi: 10.21037/tlcr-22-493
56. Li Q, Zhou Q, Zhao S, Wu P, Shi P, Zeng J, et al. KRAS mutation predict response and outcome in advanced non-small cell lung carcinoma without driver alterations receiving PD-1 blockade immunotherapy combined with platinum-based chemotherapy: a retrospective cohort study from China. *Transl Lung Cancer Res* (2022) 11:2136–47. doi: 10.21037/tlcr-22-655
57. West HJ, McClelland M, Cappuzzo F, Reck M, Mok TS, Jotte RM, et al. Clinical efficacy of atezolizumab plus bevacizumab and chemotherapy in KRAS-mutated non-small cell lung cancer with STK11, KEAP1, or TP53 comutations: subgroup results from the phase III IMpower150 trial. *J Immunother Cancer* (2022) 10(2):e003027. doi: 10.1136/jitc-2021-003027
58. Wu YL, Cheng Y, Zhou X, Lee KH, Nakagawa K, Niho S, et al. Dacomitinib versus gefitinib as first-line treatment for patients with EGFR-mutation-positive non-small-cell lung cancer (ARCHER 1050): a randomised, open-label, phase 3 trial. *Lancet Oncol* (2017) 18:1454–66. doi: 10.1016/S1470-2045(17)30608-3
59. Nogami N, Barlesi F, Socinski MA, Reck M, Thomas CA, Cappuzzo F, et al. IMpower150 final exploratory analyses for atezolizumab plus bevacizumab and chemotherapy in key NSCLC patient subgroups with EGFR mutations or metastases in the liver or brain. *J Thorac Oncol* (2022) 17:309–23. doi: 10.1016/j.jtho.2021.09.014
60. Palazon A, Tyrakis PA, Macias D, Velica P, Rundqvist H, Fitzpatrick S, et al. An HIF-1 $\alpha$ /VEGF-A axis in cytotoxic T cells regulates tumor progression. *Cancer Cell* (2017) 32:669–83 e5. doi: 10.1016/j.ccell.2017.10.003
61. Tanaka I, Morise M, Miyazawa A, Kodama Y, Tamiya Y, Gen S, et al. Potential benefits of bevacizumab combined with platinum-based chemotherapy in advanced non-small-cell lung cancer patients with EGFR mutation. *Clin Lung Cancer* (2020) 21:273–80 e4. doi: 10.1016/j.clcc.2020.01.011
62. Kumagai S, Koyama S, Nishikawa H. Antitumor immunity regulated by aberrant ERBB family signalling. *Nat Rev Cancer* (2021) 21:181–97. doi: 10.1038/s41568-020-00322-0
63. Mazieres J, Drilon A, Lusque A, Mhanna L, Cortot AB, Mezquita L, et al. Immune checkpoint inhibitors for patients with advanced lung cancer and oncogenic driver alterations: results from the IMMUNOTARGET registry. *Ann Oncol* (2019) 30:1321–8. doi: 10.1093/annonc/mdz167
64. Dantoing E, Piton N, Salaun M, Thiberville L, Guisier F. Anti-PD1/PD-L1 immunotherapy for non-small cell lung cancer with actionable oncogenic driver mutations. *Int J Mol Sci* (2021) 22(12):6288. doi: 10.3390/ijms22126288
65. McCoach CE, Rolfo C, Drilon A, Lacouture M, Besse B, Goto K, et al. Hypersensitivity reactions to selpercatinib treatment with or without prior immune checkpoint inhibitor therapy in patients with NSCLC in LIBRETTO-001. *J Thorac Oncol* (2022) 17:768–78. doi: 10.1016/j.jtho.2022.02.004
66. Koyama S, Akbay EA, Li YY, Aref AR, Skoulidis F, Herter-Sprie GS, et al. STK11/LKB1 deficiency promotes neutrophil recruitment and proinflammatory cytokine production to suppress T-cell activity in the lung tumor microenvironment. *Cancer Res* (2016) 76:999–1008. doi: 10.1158/0008-5472.CAN-15-1439
67. Garassino MC, Gadgeel S, Novello S, Halmos B, Felip E, Speranza G, et al. Associations of tissue tumor mutational burden and mutational status with clinical

outcomes with pembrolizumab plus chemotherapy versus chemotherapy for metastatic NSCLC. *JTO Clin Res Rep* (2023) 4:100431. doi: 10.1016/j.jtocr.2022.100431

68. Waldman AD, Fritz JM, Lenardo MJ. A guide to cancer immunotherapy: from T cell basic science to clinical practice. *Nat Rev Immunol* (2020) 20:651–68. doi: 10.1038/s41577-020-0306-5

69. RaMalingam SS, Balli D, Ciuleanu T-E, Pluzanski A, Lee J-S, M. Schenker ea. 4O Nivolumab (NIVO) + ipilimumab (IPI) versus chemotherapy (chemo) as first-line (1L) treatment for advanced NSCLC (aNSCLC) in CheckMate 227 part 1: Efficacy by KRAS, STK11, and KEAP1 mutation status. *Ann Oncol* (2021) 32:S1375–S6. doi: 10.1016/j.jannonc.2021.10.020

70. Peters S, Cho BC, Luft A, Alatorre-Alexander J, Geater SL, Lim S-W, et al. OA15.04 association between KRAS/STK11/KEAP1 mutations and outcomes in POSEIDON: durvalumab ± Tremelimumab + Chemotherapy in mNSCLC. *J Thorac Oncol* (2022) 17:S39–41. doi: 10.1016/j.jtho.2022.07.073

71. Vander Heiden MG, Cantley LC, Thompson CB. Understanding the Warburg effect: the metabolic requirements of cell proliferation. *Science* (2009) 324:1029–33. doi: 10.1126/science.1160809

72. DeBerardinis RJ, Chandel NS. We need to talk about the Warburg effect. *Nat Metab* (2020) 2:127–9. doi: 10.1038/s42255-020-0172-2

73. Bose S, Zhang C, Le A. Glucose metabolism in cancer: the warburg effect and beyond. *Adv Exp Med Biol* (2021) 1311:3–15. doi: 10.1007/978-3-030-65768-0\_1

74. Pavlova NN, Thompson CB. The emerging hallmarks of cancer metabolism. *Cell Metab* (2016) 23:27–47. doi: 10.1016/j.cmet.2015.12.006

75. Bartman CR, Weilandt DR, Shen Y, Lee WD, Han Y, TeSlaa T, et al. Slow TCA flux and ATP production in primary solid tumours but not metastases. *Nature* (2023) 614:349–57. doi: 10.1038/s41586-022-05661-6

76. Cerezo M, Rocchi S. Cancer cell metabolic reprogramming: a keystone for the response to immunotherapy. *Cell Death Dis* (2020) 11:964. doi: 10.1038/s41419-020-03175-5

77. Zappasodi R, Serganova I, Cohen IJ, Maeda M, Shindo M, Senbabaoglu Y, et al. CTLA-4 blockade drives loss of T(reg) stability in glycolysis-low tumours. *Nature* (2021) 591:652–8. doi: 10.1038/s41586-021-03326-4

78. Shackelford DB, Abt E, Gerken L, Vasquez DS, Seki A, Leblanc M, et al. LKB1 inactivation dictates therapeutic response of non-small cell lung cancer to the metabolism drug phenformin. *Cancer Cell* (2013) 23:143–58. doi: 10.1016/j.ccr.2012.12.008

79. Yang R, Li SW, Chen Z, Zhou X, Ni W, Fu DA, et al. Role of INSL4 signaling in sustaining the growth and viability of LKB1-inactivated lung cancer. *J Natl Cancer Inst* (2019) 111:664–74. doi: 10.1093/jnci/djy166

80. Zhang CS, Hawley SA, Zong Y, Li M, Wang Z, Gray A, et al. Fructose-1,6-bisphosphate and aldolase mediate glucose sensing by AMPK. *Nature* (2017) 548:112–6. doi: 10.1038/nature23275

81. Lin SC, Hardie DG. AMPK: sensing glucose as well as cellular energy status. *Cell Metab* (2018) 27:299–313. doi: 10.1016/j.cmet.2017.10.009

82. Jiang S, Wang Y, Luo L, Shi F, Zou J, Lin H, et al. AMP-activated protein kinase regulates cancer cell growth and metabolism via nuclear and mitochondria events. *J Cell Mol Med* (2019) 23:3951–61. doi: 10.1111/jcmm.14279

83. van Veelen W, Korsse SE, van de Laar L, Peppelenbosch MP. The long and winding road to rational treatment of cancer associated with LKB1/AMPK/TSC/mTORC1 signaling. *Oncogene* (2011) 30:2289–303. doi: 10.1038/onc.2010.630

84. Shackelford DB, Vasquez DS, Corbeil J, Wu S, Leblanc M, Wu CL, et al. mTOR and HIF-1 $\alpha$ -mediated tumor metabolism in an LKB1 mouse model of Peutz-Jeghers syndrome. *Proc Natl Acad Sci U S A* (2009) 106:11137–42. doi: 10.1073/pnas.0900465106

85. Faubert B, Vincent EE, Griss T, Samborska B, Izreig S, Svensson RU, et al. Loss of the tumor suppressor LKB1 promotes metabolic reprogramming of cancer cells via HIF-1 $\alpha$ . *Proc Natl Acad Sci U S A* (2014) 111:2554–9. doi: 10.1073/pnas.1312570111

86. Sasaki H, Shitara M, Yokota K, Hikosaka Y, Moriyama S, Yano M, et al. Overexpression of GLUT1 correlates with Kras mutations in lung carcinomas. *Mol Med Rep* (2012) 5:599–602. doi: 10.3892/mmr.2011.736

87. Pupo E, Avanzato D, Middonti E, Bussolino F, Lanzetti L. KRAS-driven metabolic rewiring reveals novel actionable targets in cancer. *Front Oncol* (2019) 9:848. doi: 10.3389/fonc.2019.00848

88. Mukhopadhyay S, Vander Heiden MG, McCormick F. The Metabolic Landscape of RAS-Driven Cancers from biology to therapy. *Nat Cancer* (2021) 2:271–83. doi: 10.1038/s43018-021-00184-x

89. Singleton DC, Macann A, Wilson WR. Therapeutic targeting of the hypoxic tumour microenvironment. *Nat Rev Clin Oncol* (2021) 18:751–72. doi: 10.1038/s41571-021-00539-4

90. Sasidharan Nair V, Saleh R, Toor SM, Cyprian FS, Elkord E. Metabolic reprogramming of T regulatory cells in the hypoxic tumor microenvironment. *Cancer Immunol Immunother* (2021) 70:2103–21. doi: 10.1007/s00262-020-02842-y

91. Angelin A, Gil-de-Gomez L, Dahiya S, Jiao J, Guo L, Levine MH, et al. Foxp3 reprograms T cell metabolism to function in low-glucose, high-lactate environments. *Cell Metab* (2017) 25:1282–93 e7. doi: 10.1016/j.cmet.2016.12.018

92. Haas R, Smith J, Rocher-Ros V, Nadkarni S, Montero-Melendez T, D'Acquisto F, et al. Lactate regulates metabolic and pro-inflammatory circuits in control of T cell migration and effector functions. *PLoS Biol* (2015) 13:e1002202. doi: 10.1371/journal.pbio.1002202

93. Watson MJ, Vignali PDA, Mullett SJ, Overacre-Delgoffe AE, Peralta RM, Grebinoski S, et al. Metabolic support of tumour-infiltrating regulatory T cells by lactic acid. *Nature* (2021) 591:645–51. doi: 10.1038/s41586-020-03045-2

94. Fischer K, Hoffmann P, Voelkl S, Meidenbauer N, Ammer J, Edinger M, et al. Inhibitory effect of tumor cell-derived lactic acid on human T cells. *Blood* (2007) 109:3812–9. doi: 10.1182/blood-2006-07-035972

95. Payen VL, Mina E, Van Hee VF, Porporato PE, Sonveaux P. Monocarboxylate transporters in cancer. *Mol Metab* (2020) 33:48–66. doi: 10.1016/j.molmet.2019.07.006

96. Faubert B, Li KY, Cai L, Hensley CT, Kim J, Zacharias LG, et al. Lactate metabolism in human lung tumors. *Cell* (2017) 171:358–71 e9. doi: 10.1016/j.cell.2017.09.019

97. Bourrouh M, Marignani PA. The tumor suppressor kinase LKB1: metabolic nexus. *Front Cell Dev Biol* (2022) 10:881297. doi: 10.3389/fcell.2022.881297

98. Rais R, Lemberg KM, Tenora L, Arwood ML, Pal A, Alt J, et al. Discovery of DRP-104, a tumor-targeted metabolic inhibitor prodrug. *Sci Adv* (2022) 8:eabq5925. doi: 10.1126/sciadv.abq5925

99. Best SA, Gubser PM, Sethumadhavan S, Kersbergen A, Negron Abril YL, Goldford J, et al. Glutaminase inhibition impairs CD8 T cell activation in STK11-/Lkb1-deficient lung cancer. *Cell Metab* (2022) 34:874–87 e6. doi: 10.1016/j.cmet.2022.04.003

100. Celiktas M, Tanaka I, Tripathi SC, Fahrman JF, Aguilar-Bonavides C, Villalobos P, et al. Role of CPS1 in cell growth, metabolism and prognosis in LKB1-inactivated lung adenocarcinoma. *J Natl Cancer Inst* (2017) 109:1–9. doi: 10.1093/jnci/djw231

101. Kim J, Hu Z, Cai L, Li K, Choi E, Faubert B, et al. CPS1 maintains pyrimidine pools and DNA synthesis in KRAS/LKB1-mutant lung cancer cells. *Nature* (2017) 546:168–72. doi: 10.1038/nature22359

102. Ricciuti B, Arbour KC, Lin JJ, Vajdi A, Vokes N, Hong L, et al. Diminished efficacy of programmed death-(Ligand)1 inhibition in STK11- and KEAP1-mutant lung adenocarcinoma is affected by KRAS mutation status. *J Thorac Oncol* (2022) 17:399–410. doi: 10.1016/j.jtho.2021.10.013

103. Cruzat V, Macedo Rogero M, Noel Keane K, Curi R, Newsholme P. Glutamine: metabolism and immune function, supplementation and clinical translation. *Nutrients* (2018) 10(11):1564. doi: 10.3390/nu10111564

104. Galan-Cobo A, Sitthideatphaiboon P, Qu X, Poteete A, Pisegna MA, Tong P, et al. LKB1 and KEAP1/NRF2 pathways cooperatively promote metabolic reprogramming with enhanced glutamine dependence in KRAS-mutant lung adenocarcinoma. *Cancer Res* (2019) 79:3251–67. doi: 10.1158/0008-5472.CAN-18-3527

105. Martin-Bernabe A, Cortes R, Lehmann SG, Seve M, Cascante M, Bourgoin-Voillard S. Quantitative proteomic approach to understand metabolic adaptation in non-small cell lung cancer. *J Proteome Res* (2014) 13:4695–704. doi: 10.1021/pr500327v

106. Rojo de la Vega M, Chapman E, Zhang DD. NRF2 and the hallmarks of cancer. *Cancer Cell* (2018) 34:21–43. doi: 10.1016/j.ccell.2018.03.022

107. Hayes JD, Dinkova-Kostova AT, Tew KD. Oxidative stress in cancer. *Cancer Cell* (2020) 38:167–97. doi: 10.1016/j.ccell.2020.06.001

108. Cancer Genome Atlas Research N. Comprehensive genomic characterization of squamous cell lung cancers. *Nature* (2012) 489:519–25. doi: 10.1038/nature11404

109. Zhao J, Lin X, Meng D, Zeng L, Zhuang R, Huang S, et al. Nrf2 mediates metabolic reprogramming in non-small cell lung cancer. *Front Oncol* (2020) 10:578315. doi: 10.3389/fonc.2020.578315

110. Tanaka I, Daye D, Tai MC, Mori H, Solis LM, Tripathi SC, et al. SRGN-triggered aggressive and immunosuppressive phenotype in a subset of TTF-1-negative lung adenocarcinomas. *J Natl Cancer Inst* (2022) 114:290–301. doi: 10.1093/jnci/djab183

111. Fahrman JF, Tanaka I, Irajizad E, Mao X, Dennison JB, Murage E, et al. Mutational activation of the NRF2 pathway upregulates kynureninase resulting in tumor immunosuppression and poor outcome in lung adenocarcinoma. *Cancers (Basel)* (2022) 14(10):2543. doi: 10.3390/cancers14102543

112. Mitsuishi Y, Taguchi K, Kawatani Y, Shibata T, Nukiwa T, Aburatani H, et al. Nrf2 redirects glucose and glutamine into anabolic pathways in metabolic reprogramming. *Cancer Cell* (2012) 22:66–79. doi: 10.1016/j.ccr.2012.05.016

113. Romero R, Sayin VI, Davidson SM, Bauer MR, Singh SX, LeBoeuf SE, et al. Keap1 loss promotes Kras-driven lung cancer and results in dependence on glutaminolysis. *Nat Med* (2017) 23:1362–8. doi: 10.1038/nm.4407

114. Hassanein M, Hoeksema MD, Shiota M, Qian J, Harris BK, Chen H, et al. SLC1A5 mediates glutamine transport required for lung cancer cell growth and survival. *Clin Cancer Res* (2013) 19:560–70. doi: 10.1158/1078-0432.CCR-12-2334

115. Koppula P, Olszewski K, Zhang Y, Kondiparthi L, Liu X, Lei G, et al. KEAP1 deficiency drives glucose dependency and sensitizes lung cancer cells and tumors to GLUT inhibition. *iScience* (2021) 24:102649. doi: 10.1016/j.isci.2021.102649

116. Sitthideatphaiboon P, Galan-Cobo A, Negrao MV, Qu X, Poteete A, Zhang F, et al. STK11/LKB1 mutations in NSCLC are associated with KEAP1/NRF2-dependent radiotherapy resistance targetable by glutaminase inhibition. *Clin Cancer Res* (2021) 27:1720–33. doi: 10.1158/1078-0432.CCR-20-2859

117. Brosnan ME, Brosnan JT. Orotic acid excretion and arginine metabolism. *J Nutr* (2007) 137:1656S–61S. doi: 10.1093/jn/137.6.1656S



118. Wang Y, Bai C, Ruan Y, Liu M, Chu Q, Qiu L, et al. Coordinative metabolism of glutamine carbon and nitrogen in proliferating cancer cells under hypoxia. *Nat Commun* (2019) 10:201. doi: 10.1038/s41467-018-08033-9
119. Ji X, Qian J, Rahman SMJ, Siska PJ, Zou Y, Harris BK, et al. xCT (SLC7A11)-mediated metabolic reprogramming promotes non-small cell lung cancer progression. *Oncogene* (2018) 37:5007–19. doi: 10.1038/s41388-018-0307-z
120. Jyotsana N, Ta KT, DelGiorno KE. The role of cystine/glutamate antiporter SLC7A11/xCT in the pathophysiology of cancer. *Front Oncol* (2022) 12:858462. doi: 10.3389/fonc.2022.858462
121. Fukumura D, Kloepper J, Amoozgar Z, Duda DG, Jain RK. Enhancing cancer immunotherapy using antiangiogenics: opportunities and challenges. *Nat Rev Clin Oncol* (2018) 15:325–40. doi: 10.1038/nrclinonc.2018.29
122. Negrao MV, Araujo HA, Lamberti G, Cooper AJ, Akhave NS, Zhou T, et al. Co-mutations and KRAS G12C inhibitor efficacy in advanced NSCLC. *Cancer Discov* (2023) 13(7):1556–71. doi: 10.1158/2159-8290.CD-22-1420
123. Offin M, Chan JM, Tenet M, Rizvi HA, Shen R, Riely GJ, et al. Concurrent RB1 and TP53 Alterations Define a Subset of EGFR-Mutant Lung Cancers at risk for Histologic Transformation and Inferior Clinical Outcomes. *J Thorac Oncol* (2019) 14:1784–93. doi: 10.1016/j.jtho.2019.06.002
124. Amgen. *A Study of Sotorasib (AMG 510) in Participants With Stage IV NSCLC Whose Tumors Harbor a KRAS p.G12C Mutation in Need of First-line Treatment* (2022). Available at: <https://classic.clinicaltrials.gov/show/NCT04933695>.
125. Inc. MT. *Phase 1/2 study of MRTX849 in patients with cancer having a KRAS G12C mutation KRYSTAL-1* (2019). Available at: <https://classic.clinicaltrials.gov/show/NCT03785249>.
126. Garassino MFondazione IRCCS Istituto Nazionale dei Tumori M. *Metformin plus/minus fasting mimicking diet to target the metabolic vulnerabilities of LKB1-inactive lung adenocarcinoma* (2018). Available at: <https://classic.clinicaltrials.gov/show/NCT03709147>.
127. Institute NC. *Testing whether cancers with specific mutations respond better to glutaminase inhibitor, telaglenastat hydrochloride, anti-cancer treatment, beGIN study* (2019). Available at: <https://classic.clinicaltrials.gov/show/NCT03872427>.
128. Dracen Pharmaceuticals I. *Study to investigate DRP-104 in adults with advanced solid tumors* (2020). Available at: <https://classic.clinicaltrials.gov/show/NCT04471415>.
129. ClinicalTrials.gov. *Canadian profiling and targeted agent utilization trial (CAPTUR)*. Available at: <https://www.clinicaltrials.gov/study/NCT03297606> (Accessed June, 2023).
130. ClinicalTrials.gov. *A study to investigate the safety, tolerability, and preliminary anti-tumor activity of bemcentinib in combination with pembrolizumab plus pemetrexed and carboplatin in adult participants with untreated non-squamous non-small cell lung cancer*. Available at: <https://www.clinicaltrials.gov/study/NCT05469178> (Accessed June, 2023).
131. ClinicalTrials.gov. *A Phase Ib Study to Evaluate the Safety and Preliminary Efficacy of IL6-receptor Antibody Sarilumab in Combination With antiPD1 Antibody Cemiplimab for Patients With Non-small Cell Lung Cancer*. Available at: <https://www.clinicaltrials.gov/study/NCT05704634> (Accessed June, 2023).
132. ClinicalTrials.gov. *Study of MGY825 in patients with advanced non-small cell lung cancer*. Available at: <https://www.clinicaltrials.gov/study/NCT05275868> (Accessed June, 2023).
133. ClinicalTrials.gov. *Study of efficacy and safety of JDQ443 single-agent as first-line treatment for patients with locally advanced or metastatic KRAS G12C- mutated non-small cell lung cancer with a PD-L1 expression < 1% or a PD-L1 expression ≥ 1% and an STK11 co-mutation*. Available at: <https://www.clinicaltrials.gov/study/NCT05445843> (Accessed June, 2023).
134. ClinicalTrials.gov. *A Study of JAB-21822 in Advanced or Metastatic NSCLC With KRAS p.G12C and STK11 Co-mutation and Wild-type KEAP1*. Available at: <https://www.clinicaltrials.gov/study/NCT05276726> (Accessed June, 2023).
135. Guo Q, Liu Z, Jiang L, Liu M, Ma J, Yang C, et al. Metformin inhibits growth of human non-small cell lung cancer cells via liver kinase B-1-independent activation of adenosine monophosphate-activated protein kinase. *Mol Med Rep* (2016) 13:2590–6. doi: 10.3892/mmr.2016.4830
136. Moro M, Caiola E, Ganzinelli M, Zulato E, Rulli E, Marabese M, et al. Metformin enhances cisplatin-induced apoptosis and prevents resistance to cisplatin in co-mutated KRAS/LKB1 NSCLC. *J Thorac Oncol* (2018) 13:1692–704. doi: 10.1016/j.jtho.2018.07.102
137. Shaw RJ, Lamia KA, Vasquez D, Koo SH, Bardeesy N, Depinho RA, et al. The kinase LKB1 mediates glucose homeostasis in liver and therapeutic effects of metformin. *Science* (2005) 310:1642–6. doi: 10.1126/science.1120781





## OPEN ACCESS

## EDITED BY

Satyendra Chandra Tripathi,  
All India Institute of Medical Sciences  
Nagpur, India

## REVIEWED BY

Alessandro Carrer,  
Veneto Institute of Molecular Medicine  
(VIMM), Italy  
Tasleem Arif,  
Icahn School of Medicine at Mount Sinai,  
United States

## \*CORRESPONDENCE

Sunjae Lee

✉ leesunjae@gist.ac.kr

Chang-Myung Oh

✉ cmoh@gist.ac.kr

<sup>†</sup>These authors have contributed equally to this work

RECEIVED 08 May 2023

ACCEPTED 09 August 2023

PUBLISHED 24 August 2023

## CITATION

Kim Y, Shin S-Y, Jeung J, Kim Y, Kang Y-W, Lee S and Oh C-M (2023) Integrative analysis of mitochondrial metabolic reprogramming in early-stage colon and liver cancer.

*Front. Oncol.* 13:1218735.

doi: 10.3389/fonc.2023.1218735

## COPYRIGHT

© 2023 Kim, Shin, Jeung, Kim, Kang, Lee and Oh. This is an open-access article distributed under the terms of the [Creative Commons Attribution License \(CC BY\)](#). The use, distribution or reproduction in other forums is permitted, provided the original author(s) and the copyright owner(s) are credited and that the original publication in this journal is cited, in accordance with accepted academic practice. No use, distribution or reproduction is permitted which does not comply with these terms.

# Integrative analysis of mitochondrial metabolic reprogramming in early-stage colon and liver cancer

Yeongmin Kim<sup>1†</sup>, So-Yeon Shin<sup>1†</sup>, Jihun Jeung<sup>2†</sup>, Yumin Kim<sup>1</sup>, Yun-Won Kang<sup>1</sup>, Sunjae Lee<sup>2\*</sup> and Chang-Myung Oh<sup>1\*</sup>

<sup>1</sup>Department of Biomedical Science and Engineering, Gwangju Institute of Science and Technology, Gwangju, Republic of Korea, <sup>2</sup>Department of School of Life Sciences, Gwangju Institute of Science and Technology, Gwangju, Republic of Korea

Gastrointestinal malignancies, including colon adenocarcinoma (COAD) and liver hepatocellular carcinoma (LIHC), remain leading causes of cancer-related deaths worldwide. To better understand the underlying mechanisms of these cancers and identify potential therapeutic targets, we analyzed publicly accessible Cancer Genome Atlas datasets of COAD and LIHC. Our analysis revealed that differentially expressed genes (DEGs) during early tumorigenesis were associated with cell cycle regulation. Additionally, genes related to lipid metabolism were significantly enriched in both COAD and LIHC, suggesting a crucial role for dysregulated lipid metabolism in their development and progression. We also identified a subset of DEGs associated with mitochondrial function and structure, including upregulated genes involved in mitochondrial protein import and respiratory complex assembly. Further, we identified mitochondrial 3-hydroxy-3-methylglutaryl-CoA synthase (*HMGCS2*) as a crucial regulator of cancer cell metabolism. Using a genome-scale metabolic model, we demonstrated that *HMGCS2* suppression increased glycolysis, lipid biosynthesis, and elongation while decreasing fatty acid oxidation in colon cancer cells. Our study highlights the potential contribution of dysregulated lipid metabolism, including ketogenesis, to COAD and LIHC development and progression and identifies potential therapeutic targets for these malignancies.

## KEYWORDS

colon cancer, hepatocellular carcinoma, mitochondria, metabolic reprogramming, 3-hydroxy-3-methylglutaryl-CoA synthase 2 (*HMGCS2*)

## 1 Introduction

Cancer is the leading cause of death worldwide, accounting for 19.3 million new cases and nearly 10.0 million deaths in 2020 (1). The socioeconomic burden of cancer has dramatically increased. In the United States, the economic burden on patients was higher than \$21.09 billion in 2019 (2). Although lung cancer is the major cause of cancer-related deaths (18%),

gastrointestinal (GI) colorectal and liver cancers (9.4% and 8.3%, respectively) are the second most common causes (1). Despite substantial advances in cancer research in recent decades, the survival rate for these cancers remains remarkably low. Colorectal cancer has a 5-year overall survival rate of approximately 60% (14% of patients with distant metastasis) (3), and liver cancer has a 5-year survival rate of approximately 20% (3% of patients with distant metastasis) (4). Although they occur in different organs, these two cancers share common underlying mechanisms such as inflammation, oxidative stress, and alterations in signaling pathways, which promote their development and progression. Therefore, studying the common mechanisms of these two cancers can provide valuable insights into the fundamental processes of cancer biology and have important clinical implications (5).

In 1930, Warburg discovered alterations in cancer cell metabolism, indicating increased aerobic glycolysis with a high rate of lactate production for biomass synthesis and rapid ATP production (6). Reprogramming of cellular metabolism has been identified as a hallmark of cancer (7) and cancer cell metabolism has been recognized as a promising treatment target (8). Intriguingly, epidemiological studies have also revealed that chronic metabolic stress, such as obesity and diabetes mellitus, is associated with the development of these two GI cancers with the highest mortality rate (9–12). However, little is known about the role of metabolic dysregulation in the early stages of tumorigenesis.

Previously, the Warburg effect was considered a compensatory mechanism for mitochondrial dysfunction in cancer cells (13). However, recently, the mitochondria, which are critical players in cellular energy metabolism, were found to play essential roles in promoting cancer cell growth and tumorigenesis (13, 14). Mitochondrial dysregulation can contribute to the development and progression of cancer by altering energy metabolism, promoting oxidative stress and inflammation, and affecting cellular signaling pathways (15).

Therefore, elucidating the complex interplay between mitochondrial function and cancer biology is critical for developing effective therapies. In this study, we performed a comparative analysis of genetic signatures from normal and GI cancer tissues obtained from The Cancer Genome Atlas (TCGA) to gain insight into the pathogenesis of colon adenocarcinoma (COAD) and hepatocellular carcinoma (LIHC) (16). Our analysis revealed that mitochondrial 3-hydroxy-3-methylglutaryl-CoA synthase (HMGCS2), a key enzyme in ketogenesis and member of the HMG-CoA protein family, is a crucial regulator of cancer cell metabolism (17). Specifically, we found that *HMGCS2* expression was downregulated in both COAD and LIHC tissues compared to that in normal tissues. Furthermore, using a genome-scale metabolic model (GSM), we showed that *HMGCS2* suppression increased glycolysis, lipid biosynthesis and elongation, and decreased fatty acid oxidation (FAO). Finally, *in vitro* experiments using cancer cell lines provided further evidence to support the role of *HMGCS2* in cancer cell metabolism. Collectively, our findings suggest that dysregulated lipid metabolism, including decreased ketogenesis due to *HMGCS2* suppression, is a potential therapeutic target for treating GI malignancies.

## 2 Materials and methods

### 2.1 Colon adenocarcinoma and lung adenocarcinoma data

The RNA-seq data for COAD and LIHC were downloaded from TCGA portal (18). The data type derived from TCGA was used only for STAR-Counts. We obtained 437 COAD and 424 LIHC RNA-seq datasets. To identify metabolic alterations during the early stages, stage I cancer data were selected by comparison with the metadata derived from TCGA. Finally, we obtained 39 normal and 62 tumor samples from COAD, and 50 normal and 171 tumor samples from LIHC.

### 2.2 RNA-seq analysis

To ensure data quality, we filtered the STAR counts by removing those with average counts of less than one in all patients. We then applied DESeq2 in Bioconductor (19) to normalize the filtered count data and extract differentially expressed genes (DEGs) from normal and tumor tissues with an adjusted p-value cutoff of 0.01. To visualize the DEGs, we used a cutoff of  $|\log_2\text{foldchange}(\log_2\text{FC})| > 0.58$  and converted any genes with p-adjust value ( $p_{\text{adj}}$ ) or  $\log_2\text{FC}$  as NA to “1” to prevent undetectable error. The DEGs were displayed using Enhanced Volcano in Bioconductor (20), where the gray dots represented “non-DEGs,” red dots represented “ $\log_2\text{FC} > 0.58$  and  $p_{\text{adj}} < 0.01$ ,” and blue dots represented “ $\log_2\text{FC} < -0.58$  and  $p_{\text{adj}} < 0.01$ ”.

### 2.3 Principal component analysis plot generation

Each gene in the normal and tumor tissues in COAD and LIHC contained numerous dimensions. To visualize the genes, dimensionality reduction was performed using principal component analysis (PCA) and the results were visualized using ggplot2 in R (21). The PCA plot visualizes PC1 on the x-axis and PC2 on the y-axis, and the normal and tumor groups are represented by ellipses.

### 2.4 Gene ontology enrichment analysis and gene set enrichment analysis

To comprehensively understand the functions of the DEGs, we conducted a Gene Ontology (GO) enrichment analysis using ClusterProfiler in Bioconductor (22). Specifically, we used a p-adjusted value cutoff of 0.01 for genes with a  $\log_2\text{FC} > 0.58$  and  $\log_2\text{FC} < -0.58$  to indicate upregulated and downregulated genes, respectively. To confirm the metabolic process alterations in the early stages of tumorigenesis, we focused only on biological process (BP) terms that indicate cellular or physiological effects. The results of the GO enrichment analysis are displayed as a heatmap with  $-\log_{10}$  p-values, where the upregulated gene set is depicted in red,

and the downregulated gene set is depicted in blue. After conducting the GO analysis, we visualized the results using a heatmap. A heat map was generated using the pheatmap function in Bioconductor, which showed the expression levels of the identified genes (23).

To further investigate the metabolic processes involved in COAD and LIHC, we utilized the Gene Set Enrichment Analysis (GSEA) tool provided by ClusterProfiler in Bioconductor (24). The analysis was conducted using a p-value cutoff of 0.05, and only BP (biological process) gene set terms were considered to compare metabolic processes in both cancers. The GSEA results are presented using an enrichment plot in Bioconductor (25) and include the normalized enrichment score (NES) and corresponding p-value.

## 2.5 Genome-scale metabolic model analysis

In this study, we performed constraint-based simulations using two genome-scale metabolic models (GSMs) to elucidate the functional role of HMGCS2 in cancer metabolism. Specifically, we utilized the colon cancer model (26) and the iHepatocytes2322 curated liver model (27) and conducted simulations using the COBRA Toolbox v.3.0[28] and the method of minimization of metabolic adjustment (28). We generated *HMGCS2* knock-out colon models by limiting the lower bounds of the *HMGCS2*-related reactions (HMR1437, HMR4604, and HMR1573) to nine, while the *HMGCS2*-overexpressed colon models had upper bounds of 4000 for these three reactions. Similarly, *HMGCS2* knock-out liver models were derived from iHepatocytes2322 by limiting the lower bounds of *HMGCS2*-related five reactions (HMR1437, HMR4604, HMR1573, HMR0027, and HMR0030) to 0, while *HMGCS2*-overexpressed liver models had a lower bound of 2000 and an upper bound of 4000 for these five reactions.

To investigate the functional role of *HMGCS2* in cancer metabolism, we observed changes in reaction flux by genetically altering *HMGCS2*. Specifically, we defined reactions whose flux decreased in *HMGCS2* knock-out models and increased in *HMGCS2* overexpression models as “flux decreasing” reactions, while reactions whose flux increased in *HMGCS2* knock-out models and decreased in *HMGCS2* overexpression models were defined as “flux increasing” reactions. We then counted the number of flux-increasing and decreasing reactions per subsystem and categorized these numbers by the total number of reactions in each subsystem to summarize flux changes.

Next, we analyzed the effects of gene perturbation of *HMGCS2* in glycolysis and lipid metabolism in colon and liver models. Specifically, we calculated flux changes by subtracting the fluxes of the original models from those of the perturbation models and considered flux changes higher than 10% of the original flux with positive and negative signs as “up-regulated” and “down-regulated,” respectively. Reactions whose changes were neither up- nor down-regulated were assigned as “no change,” while reactions that were unidentified in the model were indicated as “unidentified”.

## 2.6 Measurement of oxygen consumption rate and extracellular acidification rate

Colon cancer (Caco-2) cells, derived from human colorectal adenocarcinoma, were procured from ATCC and maintained in Dulbecco's Modified Eagle's Medium supplemented with 10% fetal bovine serum and 1% penicillin-streptomycin-amphotericin B at 37°C with 5% CO<sub>2</sub>. To target *HMGCS2* [NM\_001166107.1 and NM\_005518.3], siRNA sequences were purchased from Bioneer (Korea), and Lipofectamine RNAiMAX (Thermo Fisher Scientific, Inc., MA, USA) was used to transfect the siRNA according to the manufacturer's instructions.

To measure the Oxygen Consumption Rate (OCR) and Extracellular Acidification Rate (ECAR) of Caco-2 monolayers, we employed a Seahorse XFp Extracellular Flux Analyzer (Agilent Technologies, Santa Clara, CA, USA). The Seahorse XFp Sensor Cartridge was pre-hydrated with XFp Callibrant solution one day prior to the test and incubated overnight at 37°C in a CO<sub>2</sub>-free incubator to eliminate CO<sub>2</sub>, which could interfere with pH-sensitive measurements. Subsequently, Caco-2 cells were seeded onto XFp Miniplates at a density of 2×10<sup>4</sup> cells/well and allowed to settle overnight. On the day of the assay, the complete growth medium was replaced with 180 ul/well of XF assay medium, which was maintained at 37°C in a non-CO<sub>2</sub> incubator for 1 h to allow pre-equilibration with the XF assay medium. We then analyzed the mitochondrial function of the cells by sequentially injecting oligomycin (1 μM), carbonyl cyanide-4 (trifluoromethoxy) phenylhydrazone (FCCP, 0.5 μM), and a mix of rotenone and antimycin A. Finally, OCR and ECAR values were normalized using cellular protein content.

## 3 Results

### 3.1 Identifying common and unique transcriptomic signatures of colon cancer and hepatocellular carcinoma

The present study aimed to identify common genetic foundations and related signaling pathways in GI malignancies. We extensively analyzed the publicly accessible TCGA database, focusing on the COAD and LIHC datasets comprising 437 and 424 samples, respectively. To investigate the metabolic changes in early tumorigenesis, we used only Stage I cancer data for further analysis, resulting in 39 normal samples and 62 tumor samples for COAD, and 50 normal samples and 171 tumor samples for LIHC.

As is demonstrated in [Supplementary Figure 1A](#), the PCA plot clearly displays distinct elliptical clusters that effectively separated the normal and tumor samples. This supports the notion that the expression profiles of GI systems change substantially due to tumorigenesis. Using a list of DEGs, we generated volcano plots ([Figure 1A](#)) to identify significant differences in gene expression profiles between normal and cancer tissues. We found 7837 and 8767 up-regulated genes and 7232 and 3642 down-regulated genes in the colon and liver tissues, respectively. [Tables 1, 2](#) show the top

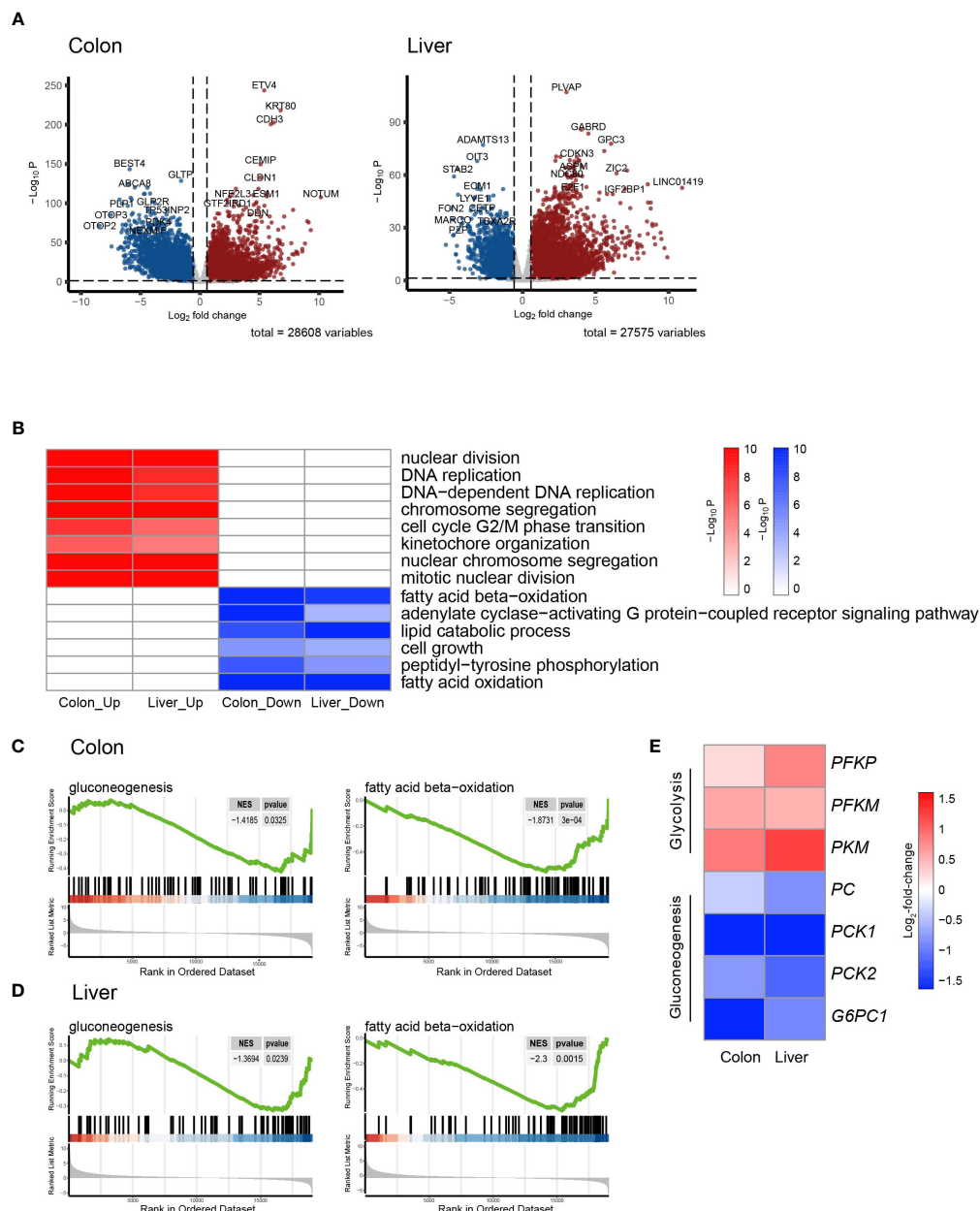


FIGURE 1

Transcriptomic signatures of colon cancer and hepatocellular carcinoma. (A) Volcano plot showing the differentially expressed genes (DEGs) in colon adenocarcinoma (COAD) and hepatocellular carcinoma (LIHC) compared to normal tissue. (B) Heatmap of GSEA enriched pathways from the common DEGs of COAD and LIHC. (C) Enrichment plots related to glycolysis and lipid metabolism in COAD. (D) Enrichment plots related to glycolysis and lipid metabolism in LIHC. (E) Heatmap of gene sets related glycolysis and gluconeogenesis in COAD and LIHC. DEG, differentially expressed gene; COAD, colon adenocarcinoma; LIHC, liver hepatocellular carcinoma; GSEA, gene set enrichment analysis.

ten upregulated and downregulated DEGs in both COAD and LIHC tissues based on p-values. In COAD, ETS variant transcription factor 4 (*ETV4*), keratin 80 (*KRT80*), and forkhead box Q1 (*FOXQ1*) were the top three upregulated genes, whereas estrophin 4 (*BEST4*), glycolipid transfer protein (*GLTP*), and carbonic anhydrase 7 (*CA7*) were the top three downregulated genes. Similarly, in LIHC, plasmalemma vesicle-associated protein (*PLVAP*), collagen type XV alpha 1 chain (*COL15A1*), and gamma-aminobutyric acid type A receptor subunit delta (*GABRD*) were the top three upregulated genes, whereas ADAM metalloproteinase with

thrombospondin type 1 motif 13 (*ADAMTS13*), oncoprotein induced transcript 3 (*OIT3*), and stabilin 2 (*STAB2*) were the top three downregulated genes.

To gain further insight into the metabolic pathways that were enriched during the early stages of tumorigenesis, we conducted a pathway enrichment analysis using GSEA. As shown in Figure 1B and Supplemental Figure 1B, the heatmap displays the enriched pathways in cancer and normal tissues. The analysis revealed that the genes differentially expressed during early tumorigenesis are associated with various aspects of cell cycle regulation. Notably,



TABLE 1 List of top ten up- and down-regulated differentially expressed genes between colon cancer and normal tissue.

|      | Gene     | p-Value   | p-Adj     | Log2FC   | Description                                   |
|------|----------|-----------|-----------|----------|---|
| Up   | ETV4     | 6.69E-249 | 1.92E-244 | 5.388356 | ETS variant transcription factor 4            |
|      | KRT80    | 4.39E-223 | 6.29E-219 | 6.767    | keratin 80                                    |
|      | FOXQ1    | 2.57E-207 | 2.46E-203 | 6.185771 | forkhead box Q1                               |
|      | CDH3     | 3.61E-205 | 2.59E-201 | 5.942379 | cadherin 3                                    |
|      | CEMIP    | 5.39E-154 | 3.09E-150 | 5.079765 | cell migration inducing hyaluronidase 1       |
|      | CLDN1    | 4.40E-137 | 1.80E-133 | 5.050994 | claudin 1                                     |
|      | AJUBA    | 1.66E-122 | 3.97E-119 | 3.008937 | ajuba LIM protein                             |
|      | CASC19   | 1.92E-122 | 4.23E-119 | 4.896743 | prostate cancer associated transcript 2       |
|      | ESM1     | 2.16E-116 | 4.29E-113 | 5.556778 | endothelial cell specific molecule 1          |
|      | NFE2L3   | 2.24E-116 | 4.29E-113 | 2.753282 | NFE2 like bZIP transcription factor 3         |
| Down | BEST4    | 9.91E-148 | 4.73E-144 | -5.91417 | bestrophin 4                                  |
|      | GLTP     | 8.82E-133 | 3.16E-129 | -1.59429 | glycolipid transfer protein                   |
|      | CA7      | 9.20E-129 | 2.93E-125 | -5.9989  | carbonic anhydrase 7                          |
|      | ABCA8    | 2.90E-124 | 8.33E-121 | -5.48495 | ATP binding cassette subfamily A member 8     |
|      | TMEM100  | 7.48E-124 | 1.95E-120 | -4.4167  | transmembrane protein 100                     |
|      | SLC25A34 | 2.61E-116 | 4.68E-113 | -4.19548 | solute carrier family 25 member 34            |
|      | FAM135B  | 7.26E-116 | 1.22E-112 | -4.71194 | family with sequence similarity 135 member B  |
|      | MAMDC2   | 1.54E-108 | 1.84E-105 | -5.73998 | MAM domain containing 2                       |
|      | PCSK2    | 2.00E-108 | 2.29E-105 | -6.76073 | proprotein convertase subtilisin/kexin type 2 |
|      | GLP2R    | 4.44E-106 | 4.72E-103 | -3.9582  | glucagon like peptide 2 receptor              |

genes involved in “DNA replication,” “mitotic nuclear division,” and “cell cycle G2/M phase transition” were found to be positively enriched in both COAD and LIHC. Furthermore, the results indicate that genes related to lipid metabolism were significantly enriched in COAD and LIHC. Specifically, “fatty acid beta-oxidation (FAO)” and “cellular lipid catabolic process” were found to be negatively associated with early tumorigenesis in both cancer types (Figures 1B–D). These findings suggested that dysregulated lipid metabolism is crucial in the development and progression of COAD and LIHC.

To assess glucose metabolism in both COAD and LIHC groups, we compared the gene expression of key irreversible enzymes involved in regulating glycolysis and gluconeogenesis (Figure 1E). The major rate-limiting enzymes in glycolysis, including phosphofructokinase homologs (*PFKP* and *PFKM*) and pyruvate kinase (*PKM*), which were significantly increased in both COAD and LIHC. Conversely, the levels of key enzymes related to gluconeogenesis, such as pyruvate kinase (*PC*), phosphoenolpyruvate carboxykinase (*PCK1* and *PCK2*), and glucose-6-phosphatase (*G6PC1* and *G6PC2*), were significantly decreased. These findings were consistent with the expected alterations in glucose metabolism in COAD and LIHC, commonly known as the Warburg effect (29), suggesting a shift towards increased glucose uptake and utilization through glycolysis in these malignancies.

### 3.2 Comparison of transcriptomic signatures for mitochondrial energy metabolism in colon cancer and hepatocellular carcinoma

Mitochondria are key organelles in cellular energy metabolism, as they serve as the primary sites for oxidative phosphorylation (OXPHOS) and FAO, and for ATP production (30). When analyzing the DEGs in COAD and LIHC, we identified a specific subset of 426 and 325 genes, respectively, that were significantly linked to mitochondrial function and structure (31) (Figure 2A). Notably, among the mitochondrial genes identified, 164 were common DEGs between the two cancers (Figure 2B).

As shown in Figure 2C and Supplementary Figure 2, our results demonstrate the enrichment of mitochondrial genes based on the DEGs identified between cancer and normal tissue samples. Interestingly, we observed an upregulation in genes involved in “mitochondrial protein import” and “mitochondrial respiratory complex assembly,” which are critical components of mitochondrial biogenesis and energy generation (32, 33), in both COAD and LIHC. Conversely, we noted a downregulation of genes related to “FAO” and “lipid catabolic process.” Our findings suggest a potential shift in the metabolic profile of GI cancers towards an

TABLE 2 List of top ten up- and down-regulated differentially expressed genes in colon cancer and normal tissue.

|      | Gene     | p-Value   | p-Adj     | Log2FC   | Description  |
|------|----------|-----------|-----------|----------|--|
| Up   | PLVAP    | 2.52E-111 | 6.97E-107 | 3.002353 | plasmalemma vesicle associated protein                     |
|      | COL15A1  | 1.26E-90  | 1.74E-86  | 4.023823 | collagen type XV alpha 1 chain                             |
|      | GABRD    | 3.05E-88  | 2.81E-84  | 4.507174 | gamma-aminobutyric acid type A receptor subunit delta      |
|      | GPC3     | 2.33E-82  | 1.61E-78  | 6.061433 | glypican 3   |
|      | THBS4    | 4.98E-78  | 2.29E-74  | 5.593584 | thrombospondin 4   |
|      | DIPK2B   | 7.57E-75  | 2.99E-71  | 2.301232 | divergent protein kinase domain 2B                         |
|      | SLC26A6  | 1.27E-74  | 4.39E-71  | 2.598325 | solute carrier family 26 member 6                          |
|      | CDKN3    | 2.48E-74  | 7.62E-71  | 3.725304 | cyclin dependent kinase inhibitor 3                        |
|      | FOXM1    | 1.17E-72  | 3.23E-69  | 3.231552 | forkhead box M1  |
|      | NUF2     | 2.19E-72  | 5.50E-69  | 3.854367 | NUF2 component of NDC80 kinetochore complex                |
| Down | ADAMTS13 | 1.38E-81  | 7.63E-78  | -2.70486 | ADAM metalloproteinase with thrombospondin type 1 motif 13 |
|      | OIT3     | 6.41E-72  | 1.26E-68  | -3.10719 | oncoprotein induced transcript 3                           |
|      | STAB2    | 4.16E-67  | 4.79E-64  | -4.43614 | stabilin 2   |
|      | ECM1     | 1.75E-57  | 1.10E-54  | -3.08879 | extracellular matrix protein 1                             |
|      | MAP2K1   | 2.27E-55  | 1.08E-52  | -1.33004 | mitogen-activated protein kinase kinase 1                  |
|      | CCL23    | 4.26E-55  | 1.96E-52  | -2.87074 | C-C motif chemokine ligand 23                              |
|      | BMPER    | 4.82E-52  | 1.73E-49  | -4.41371 | BMP binding endothelial regulator                          |
|      | TRIB1    | 1.33E-51  | 4.61E-49  | -1.99208 | tribbles pseudokinase 1                                    |
|      | PTH1R    | 1.68E-50  | 5.00E-48  | -3.26794 | parathyroid hormone 1 receptor                             |
|      | LYVE1    | 5.70E-50  | 1.56E-47  | -3.28161 | lymphatic vessel endothelial hyaluronan receptor 1         |

increased reliance on mitochondrial biogenesis and a decreased dependence on lipid metabolism.

The heat map displayed in Figure 2D shows the common DEGs involved in mitochondria-related metabolism in both COAD and LIHC. Our analysis revealed a significant increase in the expression of genes associated with fatty acid synthesis, whereas most genes related to FAO were downregulated. Furthermore, we observed a decrease in several genes involved in tryptophan metabolism, including kynurenine 3-monooxygenase (KMO) (34) and monoamine oxidase A (MAOA) (35). Additionally, we noted a decrease in the expression of the succinate dehydrogenase complex subunit D (SDHD) gene, which encodes a subunit of the mitochondrial enzyme responsible for succinate oxidation and is a well-known tumor suppressor (36). These results provide important insights into the altered metabolic pathways in GI cancers, which may contribute to their development and progression.

### 3.3 HMGCS2: a possible key determinant of energy metabolism in GI malignancies

To identify crucial candidates that regulate energy metabolism in GI malignancies, we conducted a correlation network analysis using the GeneBridge toolkit (37). This newly developed bioinformatics tool allows the imputation of gene functions and biological connectivity

using large-scale multispecies expression datasets (37). The analysis revealed that 285 genes in COAD and 2399 genes, including 3-Hydroxy-3-Methylglutaryl-CoA Synthase 2 (*HMGCS2*), were associated with “fatty acid oxidation” (GO:0006635) (Figure 3A). Among these genes, 25 genes including 3-Hydroxy-3-Methylglutaryl-CoA Synthase 2 (*HMGCS2*) are common mitochondrial genes between COAD and LIHC. To identify crucial mitochondrial genes associated with GI malignancies, we calculated the hazard ratio (HR) for each gene’s related all-cause mortality in COAD and LIHC. Figure 3B displays the HR of common mitochondrial genes, with *HMGCS2* being one of the most highly expressed HR genes in both cancers. Patients with low *HMGCS2* expression had higher HR than those with high *HMGCS2* expression in both malignancies.

Then, we performed survival analyses of cancer patients based on the expressions of DEGs that are commonly observed in COAD and LIHC using the GEPIA tool (38). By analyzing common DEGs, we identified a set of 25 genes that were particularly linked to FAO. Moreover, our investigation revealed 6 genes that have a noteworthy impact on the survival of patients with cancer. Of these 6 genes, *HMGCS2* was the only gene that displayed a statistically significant difference in the overall survival rates of patients with both COAD and LIHC (Figure 3C; Supplementary Figure 3). Notably, the expression of *HMGCS2* was found to be considerably reduced in lung cancer and rectosigmoid junction cancer, and in COAD and LIHC, compared to

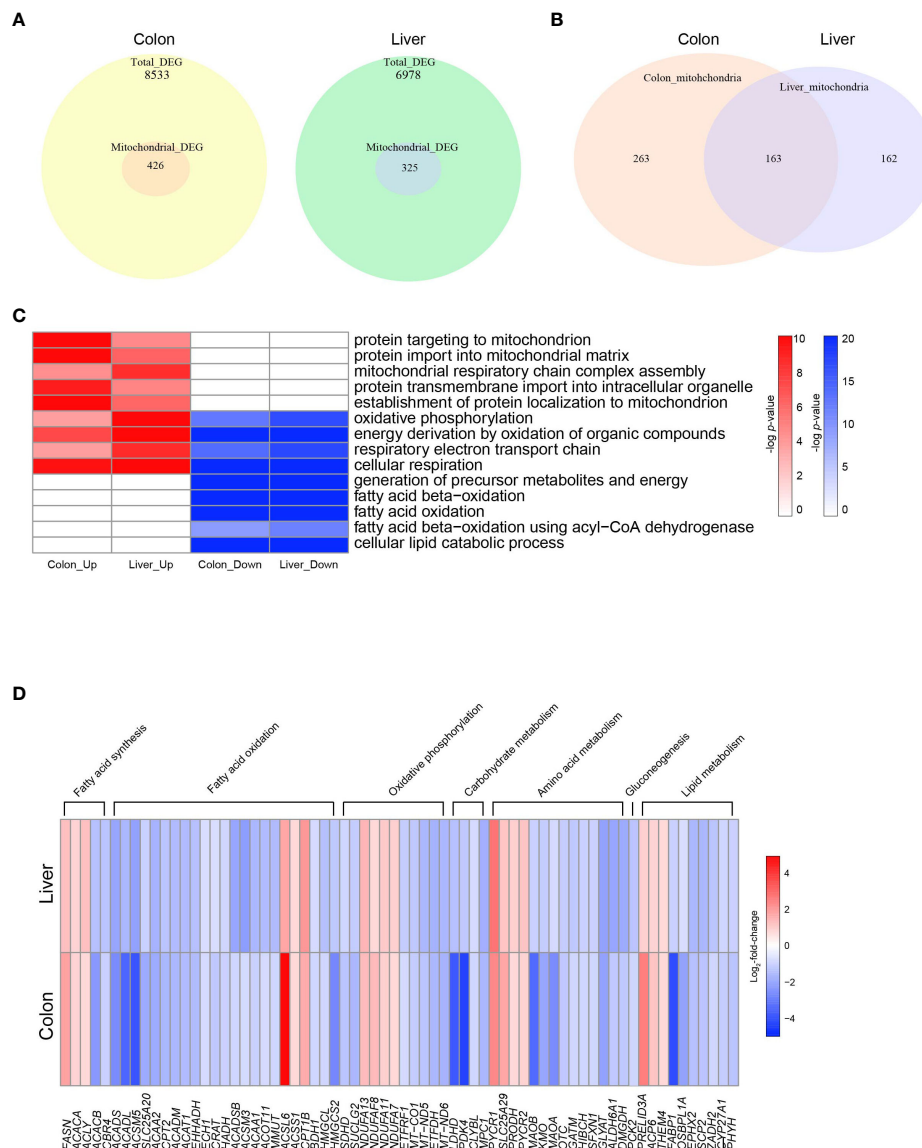


FIGURE 2

Altered mitochondrial energy metabolism in colon cancer and hepatocellular carcinoma. **(A)** Venn diagrams indicating the numbers of total DEGs and mitochondrial DEGs in COAD and LIHC. **(B)** Venn diagrams indicating overlapping genes between mitochondrial DEGs of COAD and LIHC. **(C)** Heatmap of GSEA enriched pathways from the common mitochondrial DEGs of COAD and LIHC. **(D)** Heatmap of DEGs related glucose and lipid metabolism. DEG, differentially expressed gene; COAD, colon adenocarcinoma; LIHC, liver hepatocellular carcinoma.

normal tissues (Figure 3D). In addition, HMGCS2 expression was also found to be significantly lower in colon and liver cancer, as shown in Supplementary Figure 4, where we analyzed public cancer datasets for colon and liver cancer. These results indicated that HMGCS2 may play a critical role in the pathogenesis of GI malignancies.

### 3.4 Predictive modeling of HMGCS2-driven metabolic flux in GI malignancies

To gain further insight into the metabolic functions of HMGCS2 in GI malignancies, we conducted genome-scale metabolic simulations using the COAD and LIHC models. In the COAD model, the suppression of *HMGCS2* led to a significant increase in

the fluxes of over half of the reactions in the fatty acid synthesis subsystems (i.e., fatty acid biosynthesis and elongation), whereas the fluxes in the fatty acid degradation subsystems (i.e., fatty acid destruction, beta-oxidation, and mitochondrial carnitine shuttle) were significantly reduced (Figures 4A, B; Supplementary Figure 2). Furthermore, HMGCS2 inhibition resulted in a notable upregulation in the flux of glycolysis subsystems and downregulation in the flux of oxidative phosphorylation. Remarkably, the suppression of *HMGCS2* resulted in similar changes in metabolic flux in a normal liver tissue model (Supplementary Figure 5). However, in the LIHC model, suppression of HMGCS2 did not cause significant changes in metabolic flux prediction.

To further investigate the role of HMGCS2 in energy metabolism in cancer cells, we measured oxidative phosphorylation and

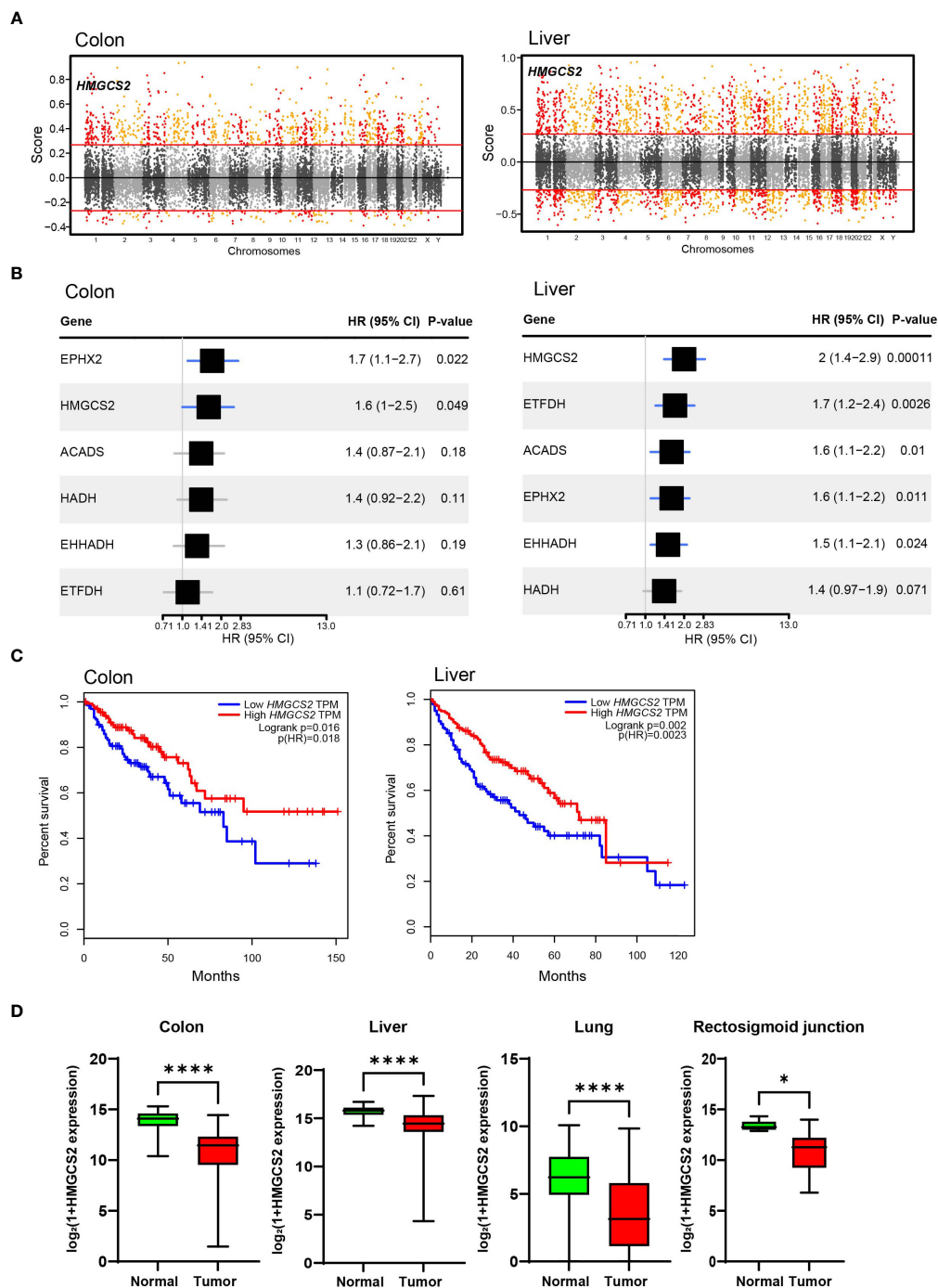


FIGURE 3

Significance of HMGCS2 as a Prognostic Marker for GI Malignancies. (A) Manhattan plot for module: fatty acid oxidation in colon and liver. (B) Overall survival according to *HMGCS2* expression in COAD and LIHC. (C) *HMGCS2* expression in colon, liver, lung, and rectosigmoid junction cancer. COAD, colon adenocarcinoma; LIHC, liver hepatocellular carcinoma. \* $p < 0.05$ ; \*\*\*\* $p < 0.0001$ .

glycolysis using a Seahorse extracellular flux analyzer (39). Our investigation focused on human Caco-2 cells and aimed to explore the effects of HMGCS2 inhibition on these metabolic pathways. *HMGCS2* knockdown resulted in a discernible decrease in the OCR of Caco-2 cells, suggesting decreased oxidative phosphorylation (Figure 4C). We also noticed a corresponding increase in the ECAR in these cells, indicating enhanced glycolysis (Figure 4D; Supplementary Figure 6). These results support the notion that the

inhibitory effects of HMGCS2 alter the metabolic flux, which is in line with the predictions made by our model.

## 4 Discussion

In this study, we aimed to identify common genetic profiles and related signaling pathways in gastrointestinal malignancies,



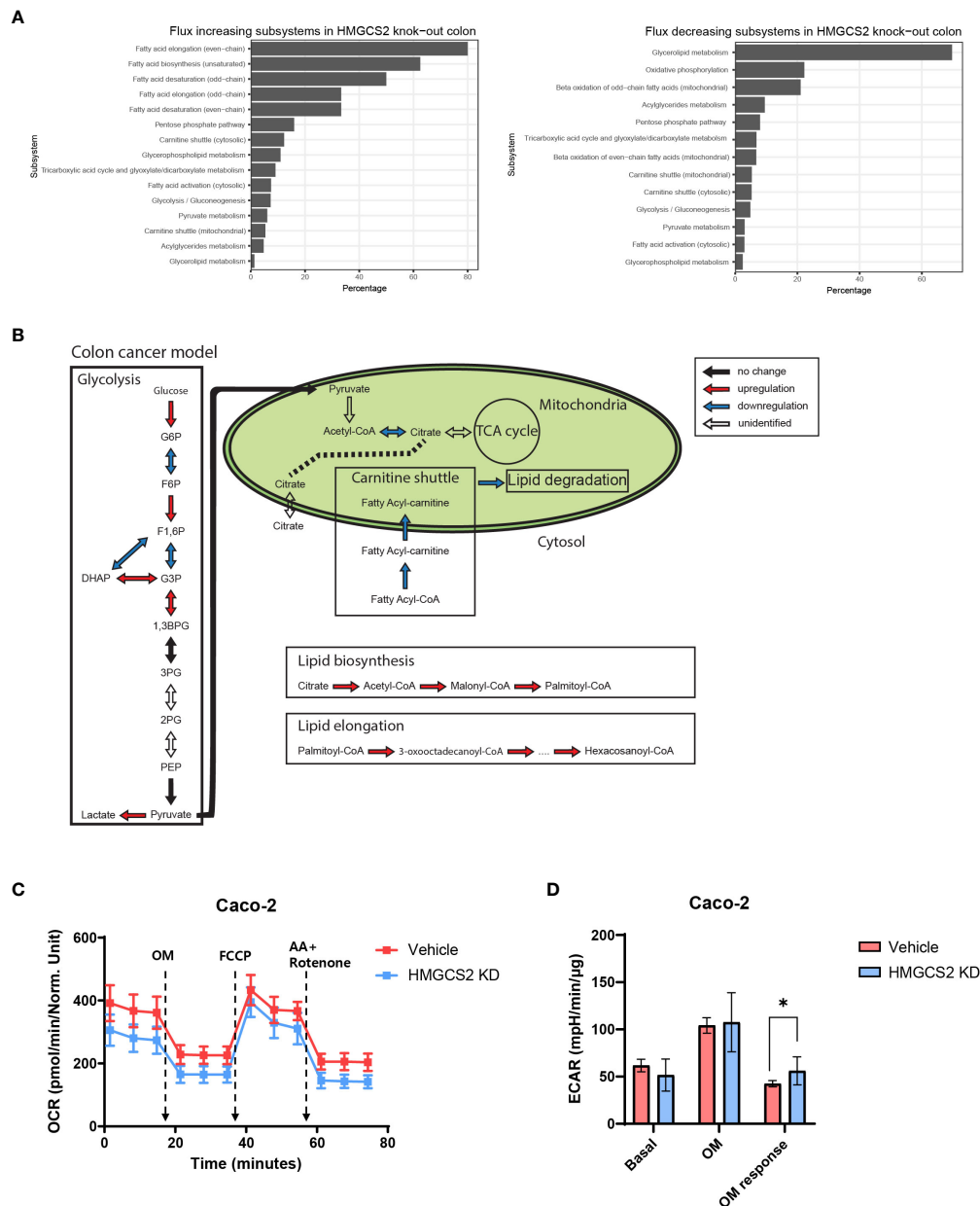


FIGURE 4

Prediction of HMGCS2-driven metabolic flux. (A) Bar plots of predicted increasing and decreasing subsystems according to *HMGCS2* knock-out in colon cancer using genome-scale metabolic model. (B) Schematic overview of the metabolic flux according to *HMGCS2* knock-out in colon cancer in the genome-scale metabolic model. (C) Real-time assessment of oxygen-consumption rate in control (Vehicle) and *HMGCS2* knockdown (KD) Caco-2 Cells: basal and mitochondrial stress conditions with oligomycin, FCCP, and rotenone plus antimycin. (D) Normalized extracellular acidification rate in Vehicle and *HMGCS2* KD cells. OM, oligomycin. \*p<0.05.

specifically COAD and LIHC. Transcriptomic analysis using TCGA database revealed that the expression profiles of GI systems resulting from tumorigenesis effectively separated normal and cancer tissues, as was evidenced by distinct elliptical clusters in the PCA plot. From DEG analysis, we identified significant changes in gene expression between normal and cancerous tissues. In COAD, *ETV4* was the most highly upregulated gene compared to normal tissues. Recently, this transcription factor was shown to be

critical for cancer growth and was positively correlated with poor prognosis in cancer patients (40, 41). In terms of metabolism, *ETV4* activates PPAR $\gamma$  signaling (42), which directly regulated glycolysis and fatty acid metabolism in cancer cells (43, 44). Similarly, cadherin 3 (*CDH3*) is another highly expressed gene in COAD that encodes P-cadherin and has been linked to poor prognosis in cancer patients and increased glycolysis in cancer cells (45). In LIHC, *PLVAP* was most significantly upregulated compared to

normal tissues. This gene has also been found to critically influence cancer development, including facilitating vascular growth (46, 47). Regarding carbohydrate metabolism, we observed an increase in gene sets associated with glycolysis and a decrease in those associated with gluconeogenesis in both COAD and LIHC. These changes in gene expression may indicate a shift towards glycolytic metabolism in these types of cancers. This is consistent with the Warburg effect, a phenomenon in cancer cells in which glycolysis is preferentially used instead of oxidative phosphorylation to generate energy, even in the presence of oxygen.

We investigated the DEGs related to mitochondrial function in COAD and LIHC. Our results showed that genes associated with mitochondrial protein import were significantly upregulated in both COAD and LIHC. Mitochondrial protein import is a crucial component of various physiological processes such as mitochondrial biogenesis, energy metabolism, and maintenance of mitochondrial morphology (48). Recently, the upregulation of mitochondrial protein import-related genes was observed in different cancers (49). Although the exact mechanisms underlying this increase remain unclear, one possible explanation is that the overexpression of these genes may contribute to an increase in mitochondrial biomass (49). Cancer cells rely on glycolysis, which produces less ATP than oxidative phosphorylation, for ATP generation. Therefore, in cancer cells, an increase in mitochondrial biomass may compensate for the reduced ATP generation via glycolysis (50, 51).

Moreover, the present study revealed that in both COAD and LIHC, FAO-associated DEGs were significantly downregulated, whereas the DEGs related to fatty acid synthesis were upregulated. Increased *de novo* lipogenesis (DNL) is a metabolic reprogramming phenomenon in cancer cells. DNL provides a diverse cellular pool of lipid species with various functions, such as membrane structure, ATP synthesis substrate, energy storage, and pro-tumorigenic signaling molecules (52, 53). An increase in DNL is also linked to the activation of oncogenic signaling pathways, such as the PI3K/Akt/mTOR pathway, which is frequently dysregulated in cancer (52). Therefore, further investigation into the role of lipid metabolism in cancer cells is essential for developing new therapeutic strategies targeting cancer-specific metabolic vulnerabilities.

Our results revealed an alteration in the mitochondrial gene *HMGCS2*, which encodes mitochondrial 3-hydroxy-3-methylglutaryl CoA synthase (HMC-CoA synthase), a rate-limiting enzyme for ketogenesis (54). *HMGCS2*-mediated conversion of Acetoacetyl-CoA to HMG-CoA leads to the production of acetoacetate, which is subsequently converted to  $\beta$ -hydroxybutyric acid, a specific type of ketone body (55). Genome-scale metabolic model analysis showed that *HMGCS2* perturbation upregulated the committed steps in the glycolysis pathway and lipid biosynthesis, whereas the committed step in lipid degradation was downregulated. These results suggested that *HMGCS2* is important for the metabolic reprogramming of cancer cells.

*HMGCS2* is a pivotal enzyme in ketogenesis, a process that is essential for providing alternative energy sources to cells under certain metabolic conditions. Decreased *HMGCS2* expression may

lead to reduced ketone body production, which may be a critical factor in the development and progression of GI cancers. The importance of ketogenesis in cancer metabolism is well established, as it contributes to the enhanced energy demands of rapidly proliferating cancer cells. Disruption of ketogenesis can result in the accumulation of reactive oxygen species (ROS) and inflammation, both of which have been linked to tumorigenesis (56). Conversely, ketone supplementation has been shown to exert anti-cancer effects on various types of malignancies. Recently, Ruozheng et al. demonstrated that a ketogenic diet decreased tumor growth and enhanced the anti-cancer effects of immune checkpoint inhibitors in colon cancer (57). Increased ketogenesis due to *HMGCS2* overexpression led to similar results. This study revealed that increased ketogenesis suppressed KLF-5 dependent CXCL12 signaling, which is implicated in the growth and metastasis of cancer cells (57). These findings suggest that modulating *HMGCS2* activity could be a promising therapeutic strategy for treating colon cancer.

This study had several limitations. First, we assessed metabolic changes based on transcriptome analysis of COAD and LIHC. Further studies using independent datasets and functional experiments are necessary to confirm and extend the findings of the present study. Secondly, this study focused only on early-stage colon and liver cancer samples, and the results may not be applicable to late-stage or other cancer types.

## 5 Conclusions

In conclusion, we identified common and unique transcriptomic signatures associated with COAD and LIHC. These findings suggested that dysregulated lipid metabolism and mitochondrial function play critical roles in the development and progression of these malignancies. Decreased *HMGCS2* activity and the related decrease in ketogenesis in GI cancer cells may play crucial roles in the altered energy metabolism observed in these cells. Further investigation into the role of *HMGCS2* in GI cancer development and progression could help identify novel therapeutic targets for treating these malignancies.

## Data availability statement

The original contributions presented in the study are included in the article/Supplementary Material. Further inquiries can be directed to the corresponding authors.

## Ethics statement

Ethical approval was not required for the study involving humans in accordance with the local legislation and institutional requirements. Written informed consent to participate in this study was not required from the participants or the participants' legal

guardians/next of kin in accordance with the national legislation and the institutional requirements.

## Author contributions

SL, and C-MO contributed to the conceptual design of the project and the experiments described in the manuscript. The experiments were performed by YeMK, YuMK and S-YS. The data were analyzed by YeMK and JJ. The manuscript was written by SL, YeMK, and C-MO. Then, the manuscript was edited and critically evaluated by SL and C-MO. All authors read and approved the final version of the manuscript.

## Funding

This research was supported by the Basic Science Research Program through the National Research Foundation of Korea (NRF) funded by the Ministry of Education (2020R1C1C1004999) and “GIST Research Institute IIBR” grants funded by the GIST in 2022.

## References

- Sung H, Ferlay J, Siegel RL, Laversanne M, Soerjomataram I, Jemal A, et al. Global cancer statistics 2020: GLOBOCAN estimates of incidence and mortality worldwide for 36 cancers in 185 countries. *CA: a cancer journal for clinicians* (2021) 71(3):209–49. doi: 10.3322/caac.21660
- Tabuchi T. Cancer and socioeconomic status. In: *Social Determinants of Health in Non-communicable Diseases*. Singapore: Springer (2020). p. 31–40.
- Moghimidehkordi B, Safaei AJ. An overview of colorectal cancer survival rates and prognosis in Asia. *Wjgo* (2012) 4(4):71. doi: 10.4251/wjgo.v4.i4.71
- Hawkes N. Cancer survival data emphasise importance of early diagnosis. *Br Med J Publishing Group* (2019). doi: 10.1136/bmj.l408
- Sun B, Karin M. Obesity, inflammation, and liver cancer. *Jhep* (2012) 56(3):704–13. doi: 10.1016/j.jhep.2011.09.020
- Vaupel P, Schmidberger H, Mayer A. The Warburg effect: essential part of metabolic reprogramming and central contributor to cancer progression. *Int J Cancer* (2019) 95(7):912–9. doi: 10.1080/09553002.2019.1589653
- Hanahan D. Hallmarks of cancer: new dimensions. *J Cell Biol* (2022) 12(1):31–46. doi: 10.1158/2159-8290.CD-21-1059
- Lemberg KM, Gori SS, Tsukamoto T, Rais R, Slusher BS. Clinical development of metabolic inhibitors for oncology. *JTOCI* (2022) 132(1). doi: 10.1172/JCI148550
- Giovannucci E, Harlan DM, Archer MC, Bergenstal RM, Gapstur SM, Habel LA, et al. Diabetes and cancer: a consensus report. *Diabetes Care* (2010) 33(7):1674–85. doi: 10.3322/caac.20078
- Bardou M, Barkun AN, Martel MJG. Obesity and colorectal cancer. *Gut* (2013) 62(6):933–47. doi: 10.1136/gutjnl-2013-304701
- Ma Y, Yang W, Song M, Smith-Warner SA, Yang J, Li Y, et al. Type 2 diabetes and risk of colorectal cancer in two large US prospective cohorts. *Br J Cancer* (2018) 119(11):1436–42. doi: 10.1038/s41416-018-0314-4
- Jun BG, Kim M, Shin HS, Yi J-J, Yi S-W. Impact of overweight and obesity on the risk of hepatocellular carcinoma: a prospective cohort study in 14.3 million Koreans. *JBIC* (2022) 127, 1–7. doi: 10.1038/s41416-022-01771-0
- Wallace DC. Mitochondria and cancer. *JNRC* (2012) 12(10):685–98. doi: 10.1038/nrc3365
- Boland ML, Chourasia AH, Macleod KF. Mitochondrial dysfunction in cancer. *JFio* (2013) 292. doi: 10.3389/fonc.2013.00292
- Kuo C-L, Ponneri Babuharisankar A, Lin Y-C, Lien H-W, Lo YK, Chou H-Y, et al. Mitochondrial oxidative stress in the tumor microenvironment and cancer immunoescape: foe or friend? *J Biomed Sci* (2022) 29(1):74. doi: 10.1186/s12929-022-00859-2
- Tomczak K, Czerwińska P, Wiznerowicz M. Review The Cancer Genome Atlas (TCGA): an immeasurable source of knowledge. *JCO* (2015) 2015(1):68–77. doi: 10.5114/wo.2014.47136
- Asif S, Kim RY, Fatica T, Sim J, Zhao X, Oh Y, et al. Hmgs2-mediated ketogenesis modulates high-fat diet-induced hepatosteatosis. *Mol Metab* (2022) 61:101494. doi: 10.1016/j.molmet.2022.101494
- Chandran UR, Medvedeva OP, Barnada MM, Blood PD, Chakka A, Luthra S, et al. TCGA expedition: a data acquisition and management system for TCGA data. *PLoS ONE* (2016) 11(10). doi: 10.1371/journal.pone.0165395
- Love MI, Huber W, Anders S. Moderated estimation of fold change and dispersion for RNA-seq data with DESeq2. *JGB* (2014) 15(12):1–21. doi: 10.1186/s13059-014-0550-8
- Blighe K, Rana S, Lewis M. EnhancedVolcano: Publication-ready volcano plots with enhanced colouring and labeling. *JRpv* (2019) 1(0).
- Villanueva RAM, Chen ZJ. *ggplot2: elegant graphics for data analysis*. UK: Taylor & Francis (2019).
- Wu T, Hu E, Xu S, Chen M, Guo P, Dai Z, et al. clusterProfiler 4.0: A universal enrichment tool for interpreting omics data. *Innovation (Camb)* (2021) 2(3):100141. doi: 10.1016/j.xinn.2021.100141
- Kolde R. Pheatmap: pretty heatmaps. (2012) 1(2):726.
- Yu G, Wang L-G, Han Y, He Q-Y. clusterProfiler: an R package for comparing biological themes among gene clusters. *JOaoib* (2012) 16(5):284–7. doi: 10.1089/omi.2011.0118
- Subramanian A, Tamayo P, Mootha VK, Mukherjee S, Ebert BL, Gillette MA, et al. Gene set enrichment analysis: a knowledge-based approach for interpreting genome-wide expression profiles. *Proc Natl Acad Sci* (2005) 102(43):15545–50. doi: 10.1073/pnas.0506580102
- Uhlén M, Fagerberg L, Hallström BM, Lindskog C, Oksvold P, Mardinoglu A, et al. Tissue-based map of the human proteome. *Science* (2015) 347(6220):1260419. doi: 10.1126/science.1260419
- Mardinoglu A, Agren R, Kampf C, Asplund A, Uhlén M, Nielsen J. Genome-scale metabolic modelling of hepatocytes reveals serine deficiency in patients with non-alcoholic fatty liver disease. *Nat Commun* (2014) 5(1):3083. doi: 10.1038/ncomms4083
- Segrè D, Vitkup D, Church GM. Analysis of optiMality in natural and perturbed metabolic networks. *Proc Natl Acad Sci* (2002) 99(23):15112–7. doi: 10.1073/pnas.232349399
- Vaupel P, Multhoff G. Revisiting the Warburg effect: Historical dogma versus current understanding. *JTOP* (2021) 599(6):1745–57. doi: 10.1113/JP278810

## Conflict of interest

The authors declare that the research was conducted in the absence of any commercial or financial relationships that could be construed as a potential conflict of interest.

## Publisher's note

All claims expressed in this article are solely those of the authors and do not necessarily represent those of their affiliated organizations, or those of the publisher, the editors and the reviewers. Any product that may be evaluated in this article, or claim that may be made by its manufacturer, is not guaranteed or endorsed by the publisher.

## Supplementary material

The Supplementary Material for this article can be found online at: <https://www.frontiersin.org/articles/10.3389/fonc.2023.1218735/full#supplementary-material>

30. Martínez-Reyes I, Chandel NS. Mitochondrial TCA cycle metabolites control physiology and disease. *JNc* (2020) 11(1):102. doi: 10.1038/s41467-019-13668-3
31. Rath S, Sharma R, Gupta R, Ast T, Chan C, Durham TJ, et al. MitoCarta3.0: an updated mitochondrial proteome now with sub-organelle localization and pathway annotations. *Nucleic Acids Res* (2021) 49(D1):D1541–D7. doi: 10.1093/nar/gkaa1011
32. Priesnitz C, Becker T. Pathways to balance mitochondrial translation and protein import. *JG Dev* (2018) 32(19–20):1285–96. doi: 10.1101/gad.316547.118
33. Needs HI, Protasoni M, Henley JM, Prudent J, Collinson I, Pereira GC. Interplay between mitochondrial protein import and respiratory complexes assembly in neuronal health and degeneration. *JL* (2021) 11(5):432. doi: 10.3390/life11050432
34. Platten M, Nollen EA, Röhrig UF, Fallarino F, Opitz CA. Tryptophan metabolism as a common therapeutic target in cancer, neurodegeneration and beyond. *JNrd* (2019) 18(5):379–401. doi: 10.1038/s41573-019-0016-5
35. Badawy AA-B. Tryptophan metabolism and disposition in cancer biology and immunotherapy. *JBR* (2022) 42(11):BSR20221682. doi: 10.1042/BSR20221682
36. Hensen EF, Bayley J-P. Recent advances in the genetics of SDH-related paraganglioma and pheochromocytoma. *JFc* (2011) 10:355–63. doi: 10.1007/s10689-010-9402-1
37. Li H, Rukina D, David FP, Li TY, Oh C-M, Gao AW, et al. Identifying gene function and module connections by the integration of multispecies expression compendia. *Genome Res* (2019) 29(12):2034–45. doi: 10.1101/gr.251983.119
38. Tang Z, Li C, Kang B, Gao G, Li C, Zhang Z. GEPIA: a web server for cancer and normal gene expression profiling and interactive analyses. *JNar* (2017) 45(W1):W98–W102. doi: 10.1093/nar/gkx247
39. Zhang J, Zhang Q. Using seahorse machine to measure OCR and ECAR in cancer cells. *JCMM Protoc* (2019), 353–63. doi: 10.1007/978-1-4939-9027-6\_18
40. Jiang W, Xu Y, Chen X, Pan S, Zhu X. E26 transformation-specific variant 4 as a tumor promoter in human cancers through specific molecular mechanisms. *JMT-O* (2021) 22:518–27. doi: 10.1016/j.omto.2021.07.012
41. Fonseca AS, Ramão A, Bürger MC, de Souza JES, Zanette DL, de Molfetta GA, et al. ETV4 plays a role on the primary events during the adenoma-adenocarcinoma progression in colorectal cancer. *BMC Cancer* (2021) 21(1):1–14. doi: 10.1186/s12885-021-07857-x
42. Park KW, Waki H, Choi S-P, Park K-M, Tontonoz P. The small molecule phenamil is a modulator of adipocyte differentiation and PPAR $\gamma$  expression. *Jlollr* (2010) 51(9):2775–84. doi: 10.1194/jlr.M008490
43. Shu Y, Lu Y, Pang X, Zheng W, Huang Y, Li J, et al. Phosphorylation of PPAR $\gamma$  at Ser84 promotes glycolysis and cell proliferation in hepatocellular carcinoma by targeting PFKFB4. *Oncotarget* (2016) 7(47):76984. doi: 10.18632/oncotarget.12764
44. Hernandez-Quiles M, Broekema MF, Kalkhoven E. PPAR $\gamma$  in metabolism, immunity, and cancer: unified and diverse mechanisms of action. *JFie* (2021) 12:624112. doi: 10.3389/fendo.2021.624112
45. Sousa B, Pereira J, Paredes J. The crosstalk between cell adhesion and cancer metabolism. *IJjoms* (2019) 20(8):1933. doi: 10.3390/ijms20081933
46. Guo L, Zhang H, Hou Y, Wei T, Liu J. Plasmalemma vesicle-associated protein: A crucial component of vascular homeostasis. *JE Med t* (2016) 12(3):1639–44. doi: 10.3892/etm.2016.3557
47. Wang Y-H, Cheng T-Y, Chen T-Y, Chang K-M, Chuang VP, Kao K-J. Plasmalemmal Vesicle Associated Protein (PLVAP) as a therapeutic target for treatment of hepatocellular carcinoma. *JBc* (2014) 14(1):1–12. doi: 10.1186/1471-2407-14-815
48. Dudek J, Rehling P, van der Laan M. Mitochondrial protein import: common principles and physiological networks. *JBeBA-MCR* (2013) 1833(2):274–85. doi: 10.1016/j.bbamcr.2012.05.028
49. Palmer CS, Anderson AJ, Stojanovski D. Mitochondrial protein import dysfunction: Mitochondrial disease, neurodegenerative disease and cancer. *JFI* (2021) 595(8):1107–31. doi: 10.1002/1873-3468.14022
50. Vyas S, Zaganjor E, Haigis MC. Mitochondria and cancer. *JC* (2016) 166(3):555–66. doi: 10.1016/j.cell.2016.07.002
51. Zheng J. Energy metabolism of cancer: Glycolysis versus oxidative phosphorylation. *Jol* (2012) 4(6):1151–7. doi: 10.3892/ol.2012.928
52. Koundouros N, Poulogiannis G. Reprogramming of fatty acid metabolism in cancer. *JBjoc* (2020) 122(1):4–22. doi: 10.1038/s41416-019-0650-z
53. Hoxha M, Zappacosta B. A review on the role of fatty acids in colorectal cancer progression. *JFiP* (2022) 5277. doi: 10.3389/fphar.2022.1032806
54. Newman JC, Verdin E. Ketone bodies as signaling metabolites. *Trends Endocrinol Metab* (2014) 25(1):42–52. doi: 10.1016/j.tem.2013.09.002
55. Yurista SR, Chong C-R, Badimon JJ, Kelly DP, de Boer RA, Westenbrink BD. Therapeutic potential of ketone bodies for patients with cardiovascular disease: JACC state-of-the-art review. *J Am Coll Cardiol* (2021) 77(13):1660–9. doi: 10.1016/j.jacc.2020.12.065
56. Hwang CY, Choe W, Yoon K-S, Ha J, Kim SS, Yeo E-J, et al. Molecular mechanisms for ketone body metabolism, signaling functions, and therapeutic potential in cancer. *Nutrients* (2022) 14(22):4932. doi: 10.3390/nu14224932
57. Wei R, Zhou Y, Li C, Rychahou P, Zhang S, Titlow WB, et al. Ketogenesis attenuates KLF5-dependent production of CXCL12 to overcome the immunosuppressive tumor microenvironment in colorectal cancer. *Cancer Res.* (2022) 82(8):1575–88. doi: 10.1158/0008-5472.CAN-21-2778



Glossary

|          |   |
|----------|---|
| ADAMTS13 | ADAM metallopeptidase with thrombospondin type 1 motif 13 |
| ATCC     | American type culture collection                          |
| ATP      | Adenosine triphosphate                                    |
| BEST4    | Bestrophin 4  |
| BP       | Biological process  |
| CA7      | carbonic anhydrase 7                                      |
| COAD     | colon adenocarcinoma                                      |
| COL15A1  | collagen type XV alpha 1                                  |
| DEGs     | Differentially expressed genes                            |
| DMEM     | Dulbecco's Modified Eagle Medium                          |
| DNL      | <i>de novo</i> lipogenesis                                |
| ECAR     | Extracellular acidification Rate                          |
| ETV4     | ETS variant transcription factor 4                        |
| FAO      | fatty acid beta-oxidation                                 |
| FCCP     | Carbonyl cyanide-p-trifluoromethoxyphenylhydrazine        |
| FOXQ1    | Forkhead box Q1   |
| G6PC1    | Glucose-6-phosphatase 1                                   |
| G6PC2    | Glucose-6-phosphatase                                     |
| GABRD    | gamma-aminobutyric acid type A receptor subunit delta     |
| GI       | Gastrointestinal  |
| GLTP     | glycolipid transfer protein                               |
| GO       | Gene ontology   |
| GSEA     | Gene set Enrichment Analysis                              |
| GSM      | Genome-scale metabolic model                              |
| HMG-CoA  | 3-hydroxy-3-methyl-glutaryl-coenzyme                      |
| HMGCS2   | 3-hydroxy-3-methylglutaryl-CoA synthase 2                 |
| HR       | Hazard ratio  |
| KMO      | kynurenine 3-monooxygenase                                |
| KRT80    | keratin 80  |
| LIHC     | liver hepatocellular carcinoma                            |
| log2FC   | log2foldchange  |
| MAOA     | monoamine oxidase A                                       |
| mTOR     | mammalian target of rapamycin                             |
| NES      | Normalized enrichment score                               |
| OCR      | Oxygen Consumption Rate                                   |
| OIT3     | oncoprotein induced transcript 3                          |
| OXPHOS   | Oxidative phosphorylation                                 |
| padj     | adjusted p-value  |

(Continued)

Continued

|       |   |
|-------|---|
| PC    | Pyruvate kinase                           |
| PCA   | Principal Component Analysis              |
| PCK1  | phosphoenolpyruvate carboxykinase 1       |
| PCK2  | phosphoenolpyruvate carboxykinase 2       |
| PFKM  | Phosphofructokinase                       |
| PFKP  | Phosphofructokinase                       |
| PI3K  | Phosphoinositide 3-kinases                |
| PKM   | Pyruvate kinase                           |
| PLVAP | plasmalemma vesicle associated protein    |
| ROS   | Reactive oxygen species                   |
| SDHD  | succinate dehydrogenase complex subunit D |
| siRNA | Small interfering RNA                     |
| STAB2 | stabilin 2                                |
| TCGA  | The Cancer Genome Atlas                   |



## OPEN ACCESS

## EDITED BY

Satyendra Chandra Tripathi,  
All India Institute of Medical Sciences  
Nagpur, India

## REVIEWED BY

Amila Suraweera,  
Queensland University of Technology,  
Australia  
Praveen Neeli,  
Baylor College of Medicine, United States

## \*CORRESPONDENCE

Chandler Bray  
✉ c.bray21@imperial.ac.uk

RECEIVED 21 July 2023

ACCEPTED 04 September 2023

PUBLISHED 19 September 2023

## CITATION

Bray C, Balcells C, McNeish IA and  
Keun HC (2023) The potential and  
challenges of targeting *MTAP*-negative  
cancers beyond synthetic lethality.  
*Front. Oncol.* 13:1264785.  
doi: 10.3389/fonc.2023.1264785

## COPYRIGHT

© 2023 Bray, Balcells, McNeish and Keun.  
This is an open-access article distributed  
under the terms of the [Creative Commons  
Attribution License \(CC BY\)](#). The use,  
distribution or reproduction in other  
forums is permitted, provided the original  
author(s) and the copyright owner(s) are  
credited and that the original publication in  
this journal is cited, in accordance with  
accepted academic practice. No use,  
distribution or reproduction is permitted  
which does not comply with these terms.

# The potential and challenges of targeting *MTAP*-negative cancers beyond synthetic lethality

Chandler Bray<sup>1\*</sup>, Cristina Balcells<sup>1</sup>, Iain A. McNeish<sup>2</sup>  
and Hector C. Keun<sup>1</sup>

<sup>1</sup>Cancer Metabolism & Systems Toxicology Group, Division of Cancer, Department of Surgery  
& Cancer, Imperial College London, London, United Kingdom, <sup>2</sup>Ovarian Cancer Action Research  
Centre, Department of Surgery and Cancer, Imperial College London, London, United Kingdom

Approximately 15% of cancers exhibit loss of the chromosomal locus 9p21.3 – the genomic location of the tumour suppressor gene *CDKN2A* and the methionine salvage gene *methylthioadenosine phosphorylase (MTAP)*. A loss of MTAP increases the pool of its substrate methylthioadenosine (MTA), which binds to and inhibits activity of protein arginine methyltransferase 5 (PRMT5). PRMT5 utilises the universal methyl donor S-adenosylmethionine (SAM) to methylate arginine residues of protein substrates and regulate their activity, notably histones to regulate transcription. Recently, targeting PRMT5, or MAT2A that impacts PRMT5 activity by producing SAM, has shown promise as a therapeutic strategy in oncology, generating synthetic lethality in *MTAP*-negative cancers. However, clinical development of PRMT5 and MAT2A inhibitors has been challenging and highlights the need for further understanding of the downstream mediators of drug effects. Here, we discuss the rationale and methods for targeting the MAT2A/PRMT5 axis for cancer therapy. We evaluate the current limitations in our understanding of the mechanism of MAT2A/PRMT5 inhibitors and identify the challenges that must be addressed to maximise the potential of these drugs. In addition, we review the current literature defining downstream effectors of PRMT5 activity that could determine sensitivity to MAT2A/PRMT5 inhibition and therefore present a rationale for novel combination therapies that may not rely on synthetic lethality with *MTAP* loss.

## KEYWORDS

MTAP, MAT2A, PRMT5, methionine, metabolism, synthetic lethality

## 1 Introduction

### 1.1 MTAP deletion creates therapeutic vulnerabilities in tumours

Gain-of-function or activating genetic alterations that occur in many cancers have proven useful as precision therapy targets. However, loss-of-function alterations must be targeted indirectly. To utilise these alterations for therapy, there must be a thorough understanding of the altered processes associated with the loss of gene products and any cancer-specific susceptibilities that may arise. Large genomic deletions that occur in cancers can lead to a growth or survival advantage by loss of tumour suppressor function. However, co-deletion of other genetic material in close physical proximity (“passenger deletions”) may create new “synthetically lethal” or “collateral” vulnerabilities to therapy (1, 2). The chromosome 9p21.3 region is deleted in approximately 15% of cancers (3, 4) and contains the tumour suppressor gene *cyclin-dependent kinase inhibitor 2A* (*CDKN2A*). This gene encodes for the p14 (5) and p16 (6) proteins that stabilise p53 and block G1 progression respectively. Only 100 kb away from the *CDKN2A* locus resides a key gene in the methionine metabolism cycle, 5'-deoxy-5'-methylthioadenosine phosphorylase (*MTAP*) (7). *MTAP* is co-deleted with homozygous loss of *CDKN2A* in approximately 80–90% of cases of 9p21.3 homozygous deletion (8) and its loss is associated with poor prognosis (9–11). The co-occurrence of *CDKN2A/MTAP* deletion may explain early literature that observed *MTAP* loss in leukaemia (12, 13) and breast cancer (14).

*MTAP* metabolises methylthioadenosine (MTA) in the methionine salvage cycle, regenerating methionine for further cycling (Figure 1) (15). Methionine is an essential amino acid and loss of *MTAP* increases cellular dependence upon exogenous methionine (16), with implications for nucleotide synthesis, folate metabolism, glutathione synthesis and the urea cycle. MTA is a

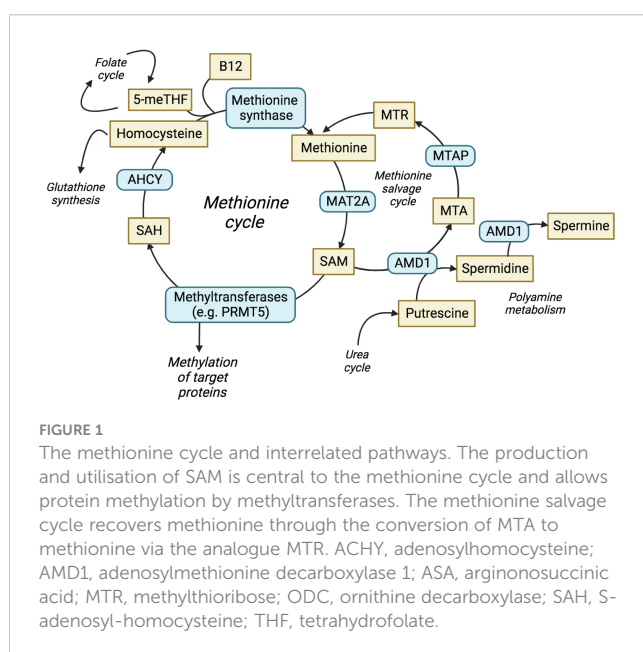
product of the synthesis of the universal methyl donor, S-adenosylmethionine (SAM), and the polyamine synthesis pathway. MTA was shown to be secreted into culture medium by *MTAP*-negative leukaemia cells *in vitro* (17), whilst elevated levels of MTA and MTA secretion have frequently been observed in multiple cell lines derived from solid tumours with homozygous deletion of *MTAP* (18–20). *MTAP* is the only enzyme known to metabolise MTA, which highlights a lack of redundancy in this process and suggests that targeting methionine metabolism may be an effective therapy against *MTAP*-negative malignancies. Furthermore, loss of 9p21.3 has been shown to be a driver, or trunk event, that occurs early in cancer evolution (21). This suggests that *MTAP* deletion is present before additional branch mutations have occurred, i.e. before other adaptive processes can take place.

Multiple studies in 2016 undertook short hairpin RNA (shRNA) screens to identify genes that cause synthetic lethality with both endogenous and genetically engineered loss of *MTAP* (18–20). All provided evidence of a conditional dependence on protein arginine methyl transferase 5 (PRMT5), RIOK1, WDR77 (MEP50) and methionine adenosyltransferase II alpha (MAT2A). These proteins are involved in the methionine cycle or subsequent methylation reactions: MAT2A catalyses the direct production of SAM (22, 23); PRMT5 and its associated binding partners RIOK1 (24) and MEP50 (25, 26) utilise SAM as methyl donor to methylate specific protein targets.

In this review, we examine the current understanding of therapeutic vulnerabilities intrinsic to *MTAP*-negative tumours, focusing on MAT2A and PRMT5, which are receiving increasing attention in clinical development. We discuss the function of MAT2A and PRMT5, including binding partners, current methods of inhibition, downstream signalling and effect on metabolic pathways. We review the interplay between these proteins, and how therapeutic inhibition impacts growth, cell cycle, apoptosis or DNA damage response. Finally, we highlight the challenges that face the therapeutic targeting of the MAT2A/PRMT5 axis, the need for additional predictive biomarkers other than *MTAP* status, and how these biomarkers could predict rational combination therapies.

## 2 The structure and function of PRMT5

PRMT5 is a member of the family of protein arginine methyltransferases responsible for methylating specific arginine residues of a wide range of proteins and thus regulate protein activity. This includes histones that regulate chromatin structure and epigenetic regulation of gene expression (27). The nine members of the PRMT family can be split into four distinct types that distinguish their activity. Type I, II and III PRMTs catalyse the formation of monomethylarginine intermediates at the terminal guanidino nitrogen atom of arginine, which can be subsequently modified to produce asymmetric dimethylarginines (ADMA) by the type I PRMTs (e.g. PRMT1) or symmetric dimethylarginines (SDMA) by the type II PRMTs (e.g. PRMT5). Type IV PRMTs



can also monomethylate arginine, but they do this at the internal guanidine nitrogen atom of arginine (28, 29).

PRMT5 is the principal type II PRMT and functions mainly as a negative regulator of transcription (30). PRMT5 contains two distinct domains: a C-terminal catalytic domain that interacts with the methyl donor SAM and a N-terminal TIM barrel domain that allows interaction with binding partners such as MEP50 (26). PRMT5 binds to MEP50 to produce PRMT5-MEP50 heterodimers, which in turn form a tetramer complex; these interactions are essential for stimulating the activity of PRMT5. SAM is then utilised by the complex as a methyl donor to allow the addition of the methyl group to the target arginine. PRMT5 binds to substrate adaptor proteins (SAPs) that are required for PRMT5 targeting and subsequent methylation. All SAPs share the peptide sequence GQF[D/E]DA[D/E] known as the PRMT5 binding motif (PBM), which facilitates PRMT5 binding (31), and the specific SAP that binds to PRMT5 can localise its activity to different substrates (Figure 2). The PRMT5 complex has been shown to preferentially bind an arginine- and glycine-rich (GRG) domain in the target substrate proteins as the site of arginine methylation (32). More than 100 substrates have been identified that are methylated by PRMT5 to regulate their functions, including proteins that promote survival and tumorigenesis (32, 33).

### 3 PRMT5 activity and cancer

Many studies have identified that increased activity and upregulation of PRMT5 is a key regulator of cancer progression and marker for poor prognosis in multiple malignancies, including breast (34), gastric (35), glioblastoma (36), leukaemia (37), lung (38), lymphoma (39), ovarian (40), pancreatic (41) and prostate cancer (42). PRMT5 can act to promote tumorigenesis by methylating histone and non-histone proteins to regulate

transcriptional and post-translational cell growth pathways, respectively (Table 1).

#### 3.1 Epigenetic control of tumour regulating genes by PRMT5

Overexpression of PRMT5 has important consequences for the epigenetic landscape of cancer across different cancer types. An early study identified PRMT5 as a binding partner of hSWI/SNF complexes that cooperatively target tumour suppressor genes *ST7* and *NM23* to inhibit their transcription (51). Transcriptome profiling of PRMT5/MEP50 shRNA knockdown lung cancer models identified differential expression of components of the TGF $\beta$  pathway, suggesting that PRMT5 may be important for the TGF $\beta$  response and subsequent cancer metastasis (46). Knockdown of PRMT5 and MEP50 showed a reduction of activating epigenetic methylation markers (H3R2me1 and H3R4me3) at the promoters of *SNAIL1* and *VIM*, both key epithelial-mesenchymal transition (EMT) and metastasis activator genes. In the same conditions, a reduction of repressive marks (H4R3me2) at the tumour suppressor genes *SPDEF* and *CDH1* was observed (46). Co-operator of PRMT5 (COPR5), a SAP, is essential for PRMT5 binding and H4R3 methylation at transcription start sites of genes such as *CCNE1* (44). In prostate cancer cells, the *androgen receptor* (*AR*) promoter was shown to be an epigenetic target of PRMT5, and knockdown of PRMT5 caused a reduction in H4R3me2 marks at the *AR* promoter and a subsequent reduction in *AR* expression (42). In breast cancer stem cells, it was shown that PRMT5 functions to methylate H3R2, allowing SET1 binding and H3K4 trimethylation at the *FOXP1* promoter to activate *FOXP1* transcription both *in vitro* and *in vivo*. The expressed *FOXP1* protein promoted breast cancer cell proliferation by activating oestrogen receptor (ER) signalling (34). PRMT5 was reported to deposit H4R3me2 marks at the c-Myc-binding E-box element (CANNTG), and that, in addition to c-Myc, PRMT5 binding results in the silencing of downstream genes. The genes affected include negative regulators of cell cycle, such as *PTEN*, *CDKN2C*, *CDKN1A*, *CDKN1C* and *p63* (35). PRMT5 has also been shown to epigenetically silence the promoter region (via an increase of H4R3me2 and H3K9me3 marks) of the c-Myc regulator gene *FBW7* (41). A reduction in PRMT5 activity also has a negative regulatory effect on the DNA damage repair Fanconi Anaemia (FA) family genes via reduced H3R2 monomethylation markers at FA gene promoters (48). PRMT5 was also suggested to regulate MHC II expression by histone methylation at the promoters of *CD74* and *CIITA*, therefore affecting how tumours present to the immune system (45). Hence, PRMT5 has shown specific epigenetic control of a range of cancer-relevant genes and promotes growth and progression.

#### 3.2 Transcription factor regulation by PRMT5

p53 is a widely studied tumour suppressor protein that responds to DNA damage by arresting growth and inducing an apoptotic

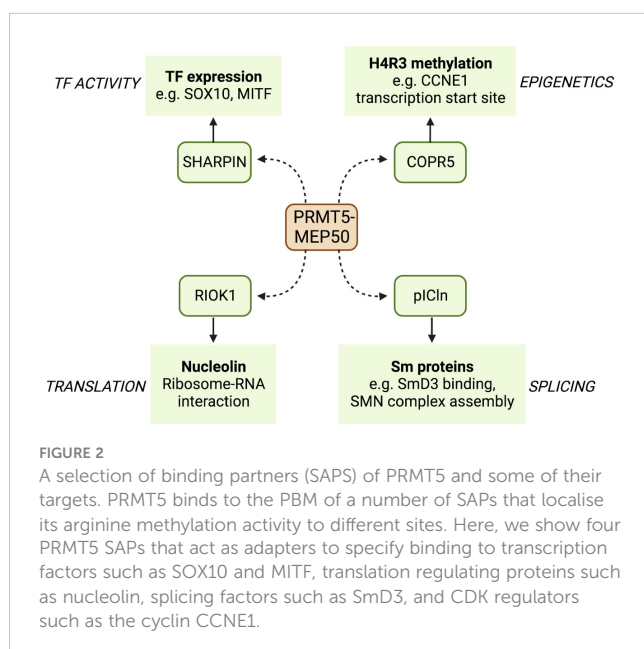




TABLE 1 PRMT5 targets.

| PRMT5 target   | Function  | PRMT5 action on target   | Cell line/cancer type  | Citation |
|----------------|---|--|--|----------|
| ALYREF         | Pre-mRNA transport and splicing   | Methylation of protein   | THP-1 (AML)  | (37)     |
| AR             | Tumour promoting gene   | Increased expression via epigenetic regulation                   | LNCaP, C4-2 (Prostate cancer)                                      | (42)     |
| C-Myc          | Regulate NF- $\kappa$ B pathway   | Increased expression and stabilise protein                       | T24, 5637 (Bladder cancer), MUA PaCa-2, SW1990 (Pancreatic cancer) | (41, 43) |
| CANNTG         | C-Myc-binding E-box element   | Reduced expression of downstream genes via epigenetic regulation | BGC823 and SGC7901 (Gastric cancer)                                | (35)     |
| CCNE1          | G1/S transition via CDK2 regulation   | Reduced expression via epigenetic regulation                     | U2OS   | (44)     |
| CCT4           | Component of TRiC complex   | Methylation of protein   | THP-1 (AML)  | (37)     |
| CCT7           | Component of TRiC complex   | Methylation of protein   | THP-1 (AML)  | (37)     |
| CD74           | Component of MHC II molecule  | Reduced expression via epigenetic regulation                     | Liver cancer   | (45)     |
| CDH1           | Tumour suppressor gene  | Reduced expression via epigenetic regulation                     | A549 (Lung cancer)   | (46)     |
| CIITA          | Component of MHC II molecule  | Reduced expression via epigenetic regulation                     | Liver cancer   | (45)     |
| CPSF6          | 3' RNA cleavage and polyadenylation   | Methylation of protein   | THP-1 (AML)  | (37)     |
| E2F1           | Transcription factor that can regulate apoptosis                                  | Methylation and destabilisation of protein                       | U2OS   | (47)     |
| FA genes       | Inter-strand crosslink (CIL)-induced DNA damage repair                            | Increased expression via epigenetic regulation                   | U251MG, T98G, U118MG (Glioblastoma)                                | (48)     |
| FBW7           | C-Myc regulator gene  | Reduced expression via epigenetic regulation                     | PaCa-2, SW1990 (Pancreatic cancer)                                 | (41)     |
| FOXP1          | Activates oestrogen receptor (ER)   | Increased expression via epigenetic regulation                   | MCF7 (Breast cancer)   | (34)     |
| IFI16 (IFI204) | Regulator of STING/cGAS signalling pathway  | Methylation of protein to control function                       | A375, WM115, B16 (Melanoma)  | (49)     |
| Mxi1           | C-Myc agonist   | Methylation of protein leading to degradation                    | H1299, A549, H460, H522, H358 (NSCLC)                              | (50)     |
| NLRC5          | Regulator of MHC I gene expression  | Decreased expression of gene                                     | B16, CCLE melanoma cell lines (Melanoma)                           | (49)     |
| NM23           | Tumour suppressor gene  | Reduced expression via epigenetic regulation                     | NIH/3T3  | (51)     |
| p53            | Promotes cell cycle arrest to allow DNA repair, regulates apoptosis               | Methylation of protein to inactivate pro-apoptotic function      | U2OS, HSPCs  | (52, 53) |
| PNN            | Part of exon junction complex (EJC)   | Methylation of protein   | THP-1 (AML)  | (37)     |
| RPS10          | Component of the 40S ribosomal subunit  | Methylation of protein   | THP-1 (AML)  | (37)     |
| RUVBL1         | Component of TIP60 complex for directing DNA damage repair towards the HR pathway | Methylation of protein to allow complex formation                | HeLa (Cervical cancer)   | (54)     |
| SFPQ           | Early splicing factor   | Methylation of protein   | THP-1 (AML)  | (37)     |
| Sm proteins    | Formation of the spliceosome  | Methylation required for smRNP biogenesis                        | HeLa (Cervical cancer)   | (55)     |
| SNAIL1         | Epithelial-mesenchymal transition (EMT) and metastatic activator factor           | Increased expression via epigenetic regulation                   | A549 (Lung cancer)   | (46)     |
| SNRNPB         | Component of SMN-Sm complex   | Methylation of protein   | THP-1 (AML)  | (37)     |

(Continued)

TABLE 1 Continued

| PRMT5 target | Function  | PRMT5 action on target                         | Cell line/cancer type      | Citation |
|--------------|---|--|----------------------------|----------|
| SPDEF        | Tumour suppressor gene  | Reduced expression via epigenetic regulation   | A549 (Lung cancer)         | (46)     |
| SRSF1        | Prevents exon skipping  | Methylation of protein                         | THP-1 (AML)                | (37)     |
| ST7          | Tumour suppressor gene  | Reduced expression via epigenetic regulation   | NIH/3T3                    | (51)     |
| SUPT5H       | mRNA processing, transcription and elongation of RNAP II                | Methylation of protein                         | THP-1 (AML)                | (37)     |
| VIM          | Epithelial-mesenchymal transition (EMT) and metastatic activator factor | Increased expression via epigenetic regulation | A549 (Lung cancer)         | (46)     |
| WDR33        | mRNA polyadenylation  | Methylation of protein                         | THP-1 (AML)                | (37)     |
| ZNF326       | Subunit of DBIRD complex that regulates alternative splicing            | Methylation requires for accurate splicing     | MDA-MB-231 (Breast cancer) | (56)     |

response (57). PRMT5 has been shown to associate with STRAP (DNA damage cofactor) and p53, leading to the subsequent methylation of p53, whilst low expression of PRMT5 led to p53-induced apoptosis (52). The presence and methyltransferase activity of PRMT5 was later shown to be sufficient to inactivate p53 in haematopoietic stem progenitor cells (HSPCs), inhibit apoptosis and increase self-renewal *in vitro* and *in vivo* (53). Thus, an increase in PRMT5 expression will positively impact cancer proliferation.

As with p53, the transcription factor E2F1 can promote apoptosis by activating pro-apoptotic genes. PRMT5 has been found to methylate and destabilise E2F1 (47) and short interfering RNA (siRNA) knockdown of PRMT5 caused an increase in E2F1 mRNA and protein levels in ovarian cancer cells, resulting in decreased growth rate and induction of apoptosis (40). E2F1 can act in a mutually exclusive pro- or anti-proliferative manner, the former when marked with the symmetric methylation of R111/R113 by PRMT5. Conversely, asymmetric methylation of R109 by PRMT1 induces apoptosis. PRMT5 methylation of E2F1 and PRMT1 knockdown were both linked to a decrease in mRNA levels of apoptosis associated proteins (APAF1, p73 and E2F-1). Moreover, symmetric arginine methylation of E2F1 via PRMT5 was read by proliferation-promoting protein p100-TSN, which increased the binding of p100-TSN to promoters of proliferation-inducing genes (cyclin E, Cdc6 and DHFR) (58). Knockdown or inhibition of E2F1 and PRMT5 in HCT116 cells was later shown to lead to reduced expression of cell migration and invasion genes (e.g. *cortactin/CTTN*) and consequently defects in these processes. Further, *PRMT5/E2F1* expression and *cortactin/CTTN* expression showed positive correlations across different types of cancer in the Cancer Genome Atlas datasets (TCGA) (59), suggesting that E2F1 and PRMT5 regulate the process of cell migration and invasion.

PRMT5 has been reported to promote c-Myc expression and consequently up-regulate the NF- $\kappa$ B pathway (43). Furthermore, PRMT5 has been shown to stabilise c-Myc in pancreatic cancer cells (41). PRMT5 also methylates the c-Myc agonist Mxi1 to promote  $\beta$ -Trcp ligase-directed degradation of Mxi1. Consequently, inhibition of PRMT5 achieved radiosensitivity in non-small cell lung cancer

(NSCLC) (50). These results highlight an important and widespread role of PRMT5 in promoting the oncogenic mechanisms of cancer. Reduction or inhibition of PRMT5 could therefore be an approach for treating cancer.

### 3.3 The role of PRMT5 in splicing and DNA damage repair

Seven small nuclear ribonucleoproteins (snRNPs) formed of Sm proteins and small nuclear RNA assemble to form the spliceosome (60). The spliceosome requires the snRNP assembly factor SMN to accurately assemble and bind at sites that require splicing (61). SMN binds the dimethylated arginine/glycine (GRG) domains of Sm proteins to allow for accurate recognition (62). Sm dimethylation is attributed to the 20S methyltransferase complex, or methylosome, comprising PRMT5, MEP50 and the SAP pICln (63). The methylosome (specifically PRMT5) acts to add SDMA modifications to Sm proteins that are required for snRNP biogenesis and the resulting process of splicing *in vivo* (55). Post-translational dimethylation of the splicing-associated protein ZNF326 was reduced upon PRMT5 inhibition by causing inclusion of AT rich introns in target genes, which phenocopied the loss of ZNF326 protein (56, 64). Deletion of *PRMT5* has been shown to cause perturbed splicing leading to reduced canonical, and increased alternative, splicing specifically in pre-mRNAs with a weak 5' donor site (65). This study highlighted alternatively spliced *Mdm4* mRNA as a recurrent product of *PRMT5* deletion. *Mdm4* encodes for a key activator of p53 and alternative splicing leads to increased activation of the p53 transcription process and indicates a response to PRMT5 inhibitors (66).

RNA sequencing of cells in which PRMT5 has been pharmacologically inhibited, demonstrated that a reduction in activity of PRMT5 caused an increase in detained introns (67). A detained intron (DI) describes the presence of a post-transcriptional intron in pre-mRNA that results in the transcript being detained within the nucleus (68). DI-containing transcripts are then either processed further by post-transcriptional splicing or degraded –

leading to an overall reduction in the translated protein product (69). These types of alternative splicing upon PRMT5 downregulation in breast cancer cell line MDA-MB-231 were found to be enriched for transcription products associated with RNA processing such as splicing genes- *HNRNPC*, *HNRNPH1*, *RBM5*, *RBM23*, *RBM39* and *U2AF1* (56). In glioblastoma, PRMT5 inhibition globally increased abnormal splicing events, while mis-spliced transcripts were enriched in cell cycle progression pathways (70). Profiling the PRMT5 methylome identified 11 proteins that are essential in the proliferation of acute myeloid leukaemia (AML) cells (37). Nine of these PRMT5 substrates are regulators of RNA metabolism and splicing (Figure 3). AML cells were also shown to have increased DI-containing transcripts encoding the transcription factor ATF4 when PRMT5 was inhibited, decreasing levels of ATF4 and increasing oxidative stress and senescence (71). AML cells with genetic abnormalities in splicing gene *Srsf2* were preferentially killed over *Srsf2* WT cells when treated with PRMT5 inhibitors (72).

PRMT5 methylation has been identified as an important regulating process for the DNA damage repair pathways. Under normal conditions, the TIP60 (KAT5) complex acetylates H4K16, displaces the non-homologous end joining (NHEJ)-promoting 53BP1 protein and directs DNA damage repair towards the homologous recombination (HR) pathway (54, 73). By contrast, PRMT5 deficiency leads to alternative splicing of TIP60, impairing

acetyltransferase activity (73). In addition, PRMT5 directly methylates the TIP60 complex cofactor protein RUVBL1 that is essential for accurate complex function (54). In a PRMT5-deficient environment, the TIP60 complex cannot function to promote HR and consequently error-prone NHEJ is favoured – a potential explanation for upregulation of p53 seen previously (65). When MAT2A or PRMT5 were inhibited pharmacologically, Kalev et al. observed an increase in R-loop nuclear signals, micronuclei and the DNA damage marker  $\gamma$ H2AX (74). The formation of R-loops and consequent DNA damage (and vice-versa) was attributed to irregular splicing arising from lack of PRMT5 activity. Furthermore, this study showed an increase in DIs located in the key DNA damage repair regulator *ATM*, and FA pathway transcripts *FANCL*, *FANCA* and *FANCD2*, and an associated reduction in protein levels. FA pathway proteins and ATM facilitate HR upon DNA damage (75).

## 4 The function of MAT2A

MAT2A was identified as a top synthetically-lethal hit in three independent shRNA screens in *MTAP*-negative cell lines (18–20). The methionine adenosyltransferase (MAT) enzymes are a family of three proteins that are involved in the synthesis of the molecule

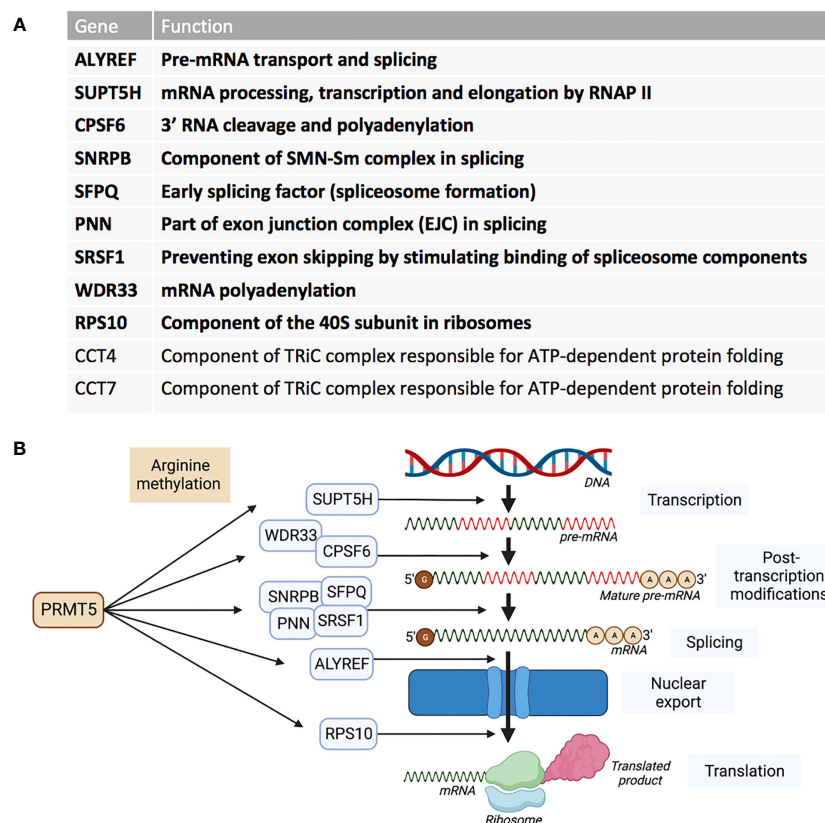


FIGURE 3

PRMT5 substrates associated with AML proliferation outlined by Radziszewska et al., 2019. (A) The eleven PRMT5 substrate genes identified as responsible for proliferation in AML and their functions. The genes in bold represent the nine genes that are involved in RNA metabolism and splicing. (B) The nine RNA metabolism and splicing proteins that are methylated by PRMT5 and whereabouts they act in the process of RNA metabolism and splicing.

SAM (76). The MAT2A substrates methionine and ATP are processed to produce SAM via an adenosine intermediate (77). SAM can then be utilised by methyltransferases, such as PRMT5, for downstream methylation processes. The enhanced expression and activity of MAT2A results in an elevated production of SAM and has been associated with tumour progression in liver cancer (78), hepatocellular carcinoma (HCC) (79, 80) and colorectal cancer (81, 82). Therefore, targeting MAT2A as a possible strategy for treating cancers (especially in *MTAP*-negative cancers) may reduce tumour growth.

## 5 Pharmacological PRMT5/MAT2A inhibition and selectivity for *MTAP*-deficient cells

A limiting factor to targeting PRMT5 directly is its important role in normal tissue function, but a synthetically lethal interaction with an *MTAP*-negative background should, in principle, provide a suitable therapeutic window. However, since MTA and SAM bind competitively to the substrate binding pocket of PRMT5 (19), MTA accumulation downstream of *MTAP* loss is a 'double-edged sword' in the context of PRMT5 inhibition. A SAM-uncompetitive pharmacological inhibitor of PRMT5 (EPZ015666/GSK3326595) was shown to be an effective anti-proliferative agent in mantle cell lymphoma (MCL) models with overexpression of PRMT5 (83). However, EPZ015666 showed no substantial antiproliferative effect in endogenous and engineered *MTAP*-negative cell lines (18) due to increased levels of MTA outcompeting SAM binding; PRMT5 has a lower affinity for SAM than MTA (19, 25, 84). Additional compounds found to bind in a SAM/MTA-competitive manner, including LLY-283 (85) and JNJ-64619178 (86, 87), are also less effective in conditions of elevated MTA levels. Subsequently compounds have recently been produced that interact with PRMT5 when bound to MTA, and which selectively target *MTAP*-negative cancer cells to varying degrees or elicit a synergistic effect in a *MTAP*-negative background (88, 89). Also, interaction between PRMT5 and SAPs can be targeted by BRD0639 and blocking this interaction reduced PRMT5 function and perturbed cellular growth in *MTAP*-negative cell lines *in vitro* (90). Several PRMT5 inhibitors are now in early-stage clinical trials for different types of cancers (Table 2).

Inhibiting MAT2A and reducing SAM levels has been proposed to cause PRMT5 inhibition both by removing its substrate and, in the case of *MTAP*-negative tumours, by providing a greater opportunity for MTA binding. Inhibiting MAT2A will therefore act to reduce protein methylation via PRMT5 (Figure 4), in addition to broader metabolism (nucleotide synthesis, glutathione synthesis, etc). Targeting MAT2A rather than PRMT5 directly has shown a greater selectivity for cells with an *MTAP*-negative background (19). As the MAT2A paralog MAT1A is the primary SAM producer in hepatic tissues there is also a lower risk of liver toxicity with selective inhibition of MAT2A (76). The first inhibitors of MAT2A (Table 3) were substrate-competitive molecules adapted from the structure of methionine - cycloleucine (91) and aminobicyclohexanecarboxylic

acid (92). However, these analogues did not possess the potency and binding specificity for an effective and accurate therapy. The development of small molecules called FIDAS (fluorinated N,N-dialkylaminostilbene) agents showed an improved potency down to low nanomolar concentrations (93, 94). However, the compounds did not show high selectivity for MAT2A at higher drug dosages *in vitro* (94). A non-substrate competitive inhibitor, PF-9366, showed promise with a higher potency for MAT2A; this molecule competitively binds to an allosteric site which mediates interactions with the binding partner MAT2B (95). MAT2B has been suggested to regulate MAT2A in low methionine or high methionine conditions by respectively activating or inhibiting MAT2A activity (95). Other data have suggested that the presence of MAT2B does not affect MAT2A activity but does improve MAT2A stability and longevity in low substrate concentrations (98). Therefore, these data suggest that the capacity of MAT2A inhibition via PF-9366 may be dependent on MAT2B levels or methionine/ATP availability. Extended PF-9366 and cycloleucine treatment led to adaptation in cultured cell lines resulting in an upregulation of MAT2A expression, indicating possible resistance mechanisms (95).

A series of further non-substrate competitive inhibitors was developed, including an orally bioavailable *in vivo* candidate molecule AGI-25696 (96). AGI-25696 was a poor candidate for human treatment due to high plasma protein binding and consequent low tissue uptake. By masking polarity internally and reducing the hydrogen donors of the molecule, the absorption was improved, and potency maintained (96). The final compound produced, AG-270, has been shown to be effective in reducing proliferation both within *in vitro* cell lines and *in vivo* xenograft models (74). AG-270 is being investigated in a *MTAP*-negative solid tumour and lymphoma phase 1 clinical trial (NCT03435250) and a phase 1/2 clinical trial in advanced and metastatic oesophageal squamous cell carcinoma (ESCC) (NCT05312372). A similar study used a fragment approach to design new MAT2A inhibitors that show a high potency and functionality *in vivo* (97). The study resulted in a drug called compound 28, showed comparable features to AG-270 in that both are orally bioavailable and bind to the MAT2B allosteric region of MAT2A. Both AG-270 (74) and compound 28 (97) showed high potency *in vitro*; reducing proliferation and SDMA markers in a HCT116 *MTAP*-negative background. In a xenograft study of HCT116 *MTAP*-negative tumours AG-270 resulted in 75% growth inhibition (96), while treatment with compound 28 led to complete tumour stasis (97). Another small molecule MAT2A inhibitor by IDEAYA (IDE397) is also in phase 1 clinical trials for *MTAP*-negative solid-tumours (NCT04794699).

PRMT5 clinical trials for PRT543 (NCT03886831) and GSK3326595 (NCT04676516) have been completed and have reported disappointing clinical responses to the monotherapy (99, 100). Just one of the baseline 49 patients achieved complete remission after treatment with PRT543 (101) and GSK has discontinued the trial with GSK3326595 (100). Even though these studies have not reported results selectively in an *MTAP*-negative tumour background, other clinical evidence is emerging that *MTAP*-negativity does not predict intra tumoral MTA accumulation as seen in model systems (102). This suggests that



TABLE 2 Protein arginine methyltransferase 5 inhibitors.

| Drug Name                | Structure     | Clinical trial identifier (if applicable) | Clinical trial stage (if applicable) | Cancer type in trial (if applicable)   | Citation        |
|--------------------------|---------------|---|--------------------------------------|--|-----------------|
| EPZ015666/<br>GSK3326595 |               | NCT04676516                               | Phase 2                              | Early-stage breast cancer  | (83)            |
| LLY-283                  |               |   |                                      |  | (85)            |
| JNJ-<br>64619178         |               | NCT03573310                               | Phase 1                              | Neoplasms, Solid tumour (adult), Non-Hodgkin Lymphoma, Myelodysplastic Syndromes   | (86, 87)        |
| BRD0639                  |               |   |                                      |  | (90)            |
| AMG193                   | Not published | NCT05094336                               | Phase 1/2                            | MTAP-null solid tumours  | No publications |
| TNG908                   | Not published | NCT05275478                               | Phase 1/2                            | MTAP-null solid tumours  | No publications |
| SCR-6920                 | Not published | NCT05528055                               | Phase 1                              | Solid tumour, Non-Hodgkin Lymphoma   | No publications |
| PRT543                   | Not published | NCT03886831                               | Phase 1                              | Solid tumours/ lymphomas, Haematological malignancies  | No publications |
| PRT811                   | Not published | NCT04089449                               | Phase 1                              | Advanced solid tumour, Recurrent Glioma  | No publications |
| MRTX1719                 |               | NCT05245500                               | Phase 1/2                            | Mesothelioma, Non-small cell lung cancer, Malignant peripheral nerve sheath tumour, Solid tumours, Pancreatic adenocarcinoma | (89)            |

despite substantive pre-clinical evidence, this genomic biomarker may not sufficiently predict response to MAT2A/PRMT5 inhibition sensitivity in the clinic.

## 6 Determinants of response to MAT2A/PRMT5 targeting beyond MTAP status as a route to effective treatment

The selective sensitivity of *MTAP*-negative cancer to MAT2A or PRMT5 inhibition is argued to result from abnormally high levels of MTA. While high MTA levels have been demonstrated extensively

in *MTAP*-negative cancer cells *in vitro* (18–20), lower than expected levels of MTA have been observed *in vivo* (102). Barekatin et al. conducted metabolomic analysis of 17 primary glioblastoma multiforme (GBM) tumours, xenograft tumours derived from a series of GBM lines and a 50 GBM tumour metabolomic dataset, which overall showed no significant difference in MTA levels between *MTAP*-negative and *MTAP*-positive primary tumours (102). Consequently, there was not the expected PRMT5 inhibition in primary *MTAP*-negative tumours (shown by a lack of significant reduction in SDMA markers). Barekatin et al. showed evidence that MTA produced from the *MTAP*-negative tumour is being processed by the intratumour, *MTAP*-positive stromal cells. A noticeable finding highlighted that *in vivo* xenografts may not accurately model endogenous tumour

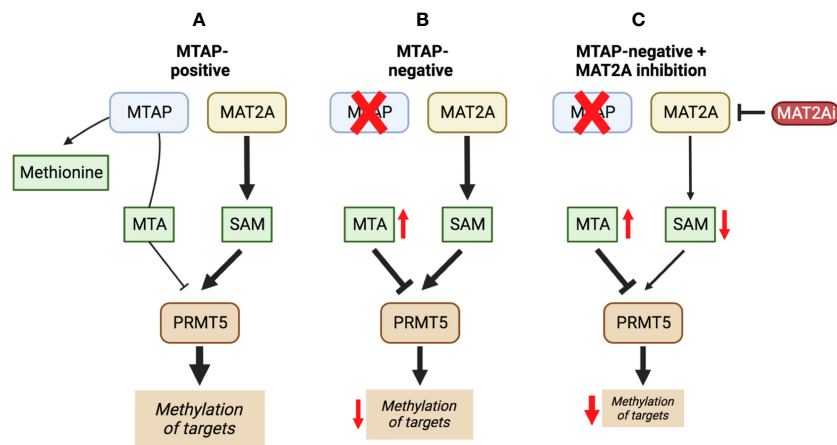


FIGURE 4

The inhibition of MAT2A exacerbates the reduction in PRMT5 activity present in a MTAP-negative background. Here, we show the changes in PRMT5 activity over different genetic backgrounds [MTAP-positive (A) and MTAP-negative (B)] and in an MAT2A inhibited state within an MTAP-negative background (C). The outcome of these differences is a change in levels of methylation of PRMT5 targets.

response, as xenografts are less populated by stromal cells when comparing their histology to primary GBM tumour tissue (102). These challenges emphasise the importance of reproducible model systems that result in more “patient-like” models. Overall, this study suggests caution in the use of *MTAP* status as the sole predictive biomarker for identifying patients to receive MAT2A/PRMT5 inhibitor therapy.

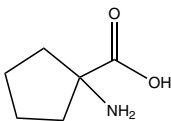
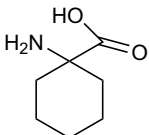
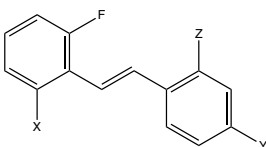
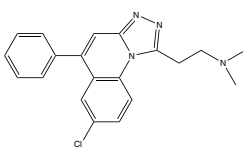
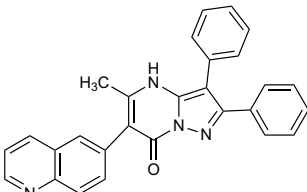
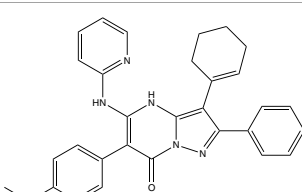
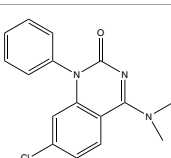
In general, metabolite levels are likely to differ between cultured cells *in vitro* and patient tumours *in vivo*, not least because the composition of common culture media and levels of oxygenation do not recapitulate the physiological environment where tumours form in the body (103). Furthermore, tissue lineage can also influence the metabolic phenotype of a tumour, even when they share the same oncogenic driver mutations (104). For example, it has been shown that the accumulation of MTA resulting from a homozygous *MTAP* deletion was only reproducible between cell lines when grown in a complete nutrient culture medium, and not when cultured in methionine- or cysteine-depleted media (105). Each cell line in this study demonstrated distinct metabolic profiles upon amino acid restriction, which were clustered more by tissue type than *MTAP* status. These observations also imply that nutrient supply, including dietary methionine or cysteine, could add to patient-to-patient variability in response to therapy targeting the MAT2A/PRMT5/MTAP axis and that combining MAT2A/PRMT5 inhibition with nutrient depletion could result in enhanced responses. Reducing the level of methionine in the body, either enzymatically (106) or through dietary restriction (107), has been shown to reduce tumour volume or increase life span in mice, respectively. Methionine depletion has also been shown to be tolerable with no clinical toxicity in patients (108). When polyamine synthesis is increased in *MTAP*-deleted cells, it can cause reactive oxygen species (ROS) to form and lead to cell death by ferroptosis through lipid oxidation. This effect is amplified by a reduction in cysteine, which impairs the transsulfuration pathway that normally helps to resolve lipid oxidation and reduces the production of glutathione (109).

Given the fundamental importance of SAM levels or arginine methylation in normal tissue function and the systemic impact of MAT2A/PRMT5 inhibitors to lower these, it is important to consider how the combination of such agents with standard-of-care therapies can be rationally designed to benefit from synergy, reduce dosage and alleviate on-target toxicity. In particular, difficult-to-treat cancers could benefit from combination approaches with MAT2A/PRMT5 inhibitors alongside compounds that target the DNA damage response (110).

As described above, PRMT5 activity results in alternative splicing of the transcripts of key DNA damage repair proteins, such as ATM and FA family members, which facilitate repair of double strand DNA breaks, e.g. induced by inter-strand crosslinking. The combination of PRMT5 inhibitors and interstrand crosslinking agents induced an increase in unrepaired inter-strand crosslinks and lead to greater genomic instability (48), implying that MAT2A or PRMT5 inhibitors create a deficiency in the HR DNA repair pathway. Tumours with a defective HR pathway, such as *BRCA2*-negative breast and ovarian cancer, become dependent on PARP1-mediated repair pathways (111). This finding suggests that MAT2A/PRMT5 inhibition may act synergistically in combination with PARP inhibitors, as has been reported in one study of AML (73). PARP inhibitors have also shown significant synergy with type I PRMT inhibitors in NSCLC and in ovarian cancer, where type I PRMT inhibition re-sensitised resistant PEO4 ovarian cancer cells to PARP inhibitor treatment *in vitro* (112). Combination therapy using well characterised chemotherapies alongside PRMT5 inhibitors has shown promising results by targeting both PRMT5 inhibitor sensitive and resistant cells simultaneously. In one study, PRMT5 inhibition resistance was found to be associated with the upregulation of the microtubule regulator, stathmin 2 (*STMN2*) (113). Upregulation of *STMN2* was found to be essential for resistance, and was also responsible for sensitivity to taxanes, such as paclitaxel (113). A combination of MAT2A inhibitors and taxanes was also shown to produce synergy when treating engineered (HCT116) and intrinsically (KP4) *MTAP*-negative cell lines (74).

Pharmacological inhibition of PRMT5 has been suggested to combine effectively with anti-PD1 immune checkpoint therapy

TABLE 3 Methionine adenosyltransferase II alpha inhibitors.

| Drug Name   | Structure   | Clinical trial identifier (if applicable) | Clinical trial stage (if applicable) | Cancer type in trial (if applicable)  | Citation        |
|---|---|---|--------------------------------------|---|-----------------|
| Cycloleucine  |    |   |                                      |   | (91)            |
| Aminobicyclo-hexane-carboxylic acid                               |    |   |                                      |   | (92)            |
| FIDAS agents (generic structure) - X, Y and Z are variable groups |    |   |                                      |   | (93, 94)        |
| PF-9366   |    |   |                                      |   | (95)            |
| AGI-25696   |   |   |                                      |   | (96)            |
| AG-270 (S095033)  |  | NCT03435250,<br>NCT05312372               | Phase 1,<br>Phase 1/2                | Advanced solid tumours,<br>Lymphoma, Oesophageal<br>squamous cell carcinoma | (74)            |
| Compound 28   |  |   |                                      |   | (97)            |
| IDE397  | Not published   | NCT04794699                               | Phase 1                              | Solid tumour  | No publications |

(ICT) drugs in different types of cancers. In murine melanoma cell lines, PRMT5 was shown to methylate IFN- $\gamma$ -inducible protein 204 (IFI16/IFI204) and negatively regulate *NLR5* transcription (49). Pharmacological inhibition or shRNA knockdown of PRMT5 increased production of type-I interferons by inhibiting IFI16 (IFI204) and increased *NLR5*-promotion of major histocompatibility complex (MHC) I antigen presentation genes (49). PRMT5 inhibition was later reported to induce lymphocyte infiltration and MHC II expression in mouse liver HCC tumours, which was demonstrated by an increase in CD45.1, CD4 and CD8 staining in fixed liver tumours and up-regulation of H2-Ab1, Cd74

and MHC II transactivator Ciita at the mRNA level (45). The combination of a PRMT5 inhibitor and anti-PD1 therapy produced a significant reduction in tumour volume and an increase in CD4+ and CD8+ T cell infiltration compared to either therapy alone *in vivo* (45). In contrast, PRMT5 inhibition has also been reported to promote PD-L1 expression in lung cancer and ultimately disrupt antitumour immunity by increasing the marker for immune inhibition (114). While combining PRMT5 inhibition with PD-L1 therapy has potential benefits, it has been reported that the MTA-rich environment in *MTAP*-negative cancer cells stimulate the immunosuppressive (M2) state in macrophages through

activation of the adenosine A<sub>2B</sub> receptor (115), thus inhibiting immune invasion. SAM and MTA secreted by tumours can reduce global chromatin accessibility in T cells, leading to dysfunction that may contribute to a poor anti-tumour immune response (116). As such, investigating the impact of MAT2A inhibitors on the function of tumour-associated T cells may provide additional insight into how the efficacy of immune-checkpoint inhibitors could be improved.

## 7 Conclusions

Deletion of *MTAP* is frequently observed in a wide variety of cancers due to its proximity to the key tumour suppressor gene *CDKN2A*. The codeletion of *MTAP* provides a selectable marker for the identification of cancer patients who might benefit from targeting of methionine metabolism and/or protein methylation due to accumulation of the metabolite MTA. Here we have reviewed current pharmacological methods of targeting SAM production via MAT2A inhibition and direct PRMT5 inhibition (both of which reduce PRMT5-specific methylation reactions) and reported evidence for and against the selectivity of these treatments for *MTAP*-negative tumours. Future generations of drugs that target PRMT5 activity in an *MTAP*-negative background must focus on maximising their selectivity for inhibiting PRMT5 specifically within the cancer cell (i.e. when PRMT5 is bound to MTA). Moving forward, to best understand the population of patients that will benefit from therapeutic treatment with MAT2A/PRMT5 inhibitors we require a greater understanding of the molecular rewiring after inhibition. Our current understanding of the downstream effects of PRMT5 inhibition include the impairment of pre-mRNA splicing and DNA damage repair, co-treatment of cancers with agents that target these pathways such as PARP inhibitors and chemotherapy, is potentially synergistic. Such a strategy provides an alternative rationale for the use of MAT2A/PRMT5 inhibitors beyond synthetic lethality with *MTAP* loss and presents additional predictive biomarkers for future clinical development of combination treatments.

## References

1. Muller FL, Aquilanti EA, DePinho RA. Collateral lethality: A new therapeutic strategy in oncology. *Trends Cancer* (2015) 1(3):161–73. doi: 10.1016/j.trecan.2015.10.002
2. Muller FL, Colla S, Aquilanti E, Manzo VE, Genovese G, Lee J, et al. Passenger deletions generate therapeutic vulnerabilities in cancer. *Nature* (2012) 488:7411. doi: 10.1038/nature14609
3. Beroukhi R, Mermel CH, Porter D, Wei G, Raychaudhuri S, Donovan J, et al. The landscape of somatic copy-number alteration across human cancers. *Nature* (2010) 463:7283. doi: 10.1038/nature08822
4. Campbell PJ, Getz G, Korbel JO, Stuart JM, Jennings JL, Stein LD, et al. Pan-cancer analysis of whole genomes. *Nature* (2020) 578:7793. doi: 10.1038/s41586-020-1969-6
5. Pomerantz J, Schreiber-Agus N, Liégeois NJ, Silverman A, Alland L, Chin L, et al. The Ink4a Tumor Suppressor Gene Product, p19Arf, Interacts with MDM2 and Neutralizes MDM2's Inhibition of p53. *Cell* (1998) 92(6):713–23. doi: 10.1016/s0092-8674(00)81400-2
6. Sherr C. Cancer cell cycles. *Science* (1996) 274(5293):1672–4. doi: 10.1126/science.274.5293.1672
7. Carrera CJ, Eddy RL, Shows TB, Carson DA. Assignment of the gene for methylthioadenosine phosphorylase to human chromosome 9 by mouse-human somatic cell hybridization. *Proc Natl Acad Sci USA* (1984) 81(9):2665. doi: 10.1073/pnas.81.9.2665
8. Zhang H, Chen ZH, Savarese TM. Codeletion of the genes for p16INK4, methylthioadenosine phosphorylase, interferon- $\alpha$ 1, interferon- $\beta$ 1, and other 9p21 markers in human Malignant cell lines. *Cancer Genet Cytogenetics* (1996) 86(1):22–8. doi: 10.1016/0165-4608(95)00157-3
9. Hansen LJ, Sun R, Yang R, Singh SX, Chen LH, Pirozzi CJ, et al. MTAP loss promotes stemness in glioblastoma and confers unique susceptibility to purine starvation. *Cancer Res* (2019) 79(13):3383–94. doi: 10.1158/0008-5472.CAN-18-1010
10. Alhalabi O, Zhu Y, Hamza A, Qiao W, Lin Y, Wang RM, et al. Integrative clinical and genomic characterization of MTAP-deficient metastatic urothelial cancer. *Eur Urol Oncol* (2021) 6(2):228–32. doi: 10.1016/j.euo.2021.10.006
11. Su CY, Chang YC, Chan YC, Lin TC, Huang MS, Yang CJ, et al. MTAP is an independent prognosis marker and the concordant loss of MTAP and p16 expression predicts short survival in non-small cell lung cancer patients. *Eur J Surg Oncol* (2014) 40(9):1143–50. doi: 10.1016/j.ejso.2014.04.017
12. Fitch JH, Riscoe MK, Dana BW, Lawrence HJ, Ferro AJ. Methylthioadenosine phosphorylase deficiency in human leukemias and solid tumors. *Cancer Res* (1986) 46(10):5409–12.
13. Traweek ST, Riscoe MK, Ferro AJ, Brazier RM, Magenis RE, Fitch JH. Methylthioadenosine phosphorylase deficiency in acute leukemia: pathologic,

## Author contributions

CB: Writing – original draft. CB: Writing – review & editing. IM: Writing – review & editing. HK: Writing – review & editing.

## Funding

The author declare financial support was received for the research, authorship, and/or publication of this article. CB is supported by the Medical Research Council in collaboration with AstraZeneca (MR/R015732/1).

## Acknowledgments

We would like to thank Muireann Coen, Valentina Fogal and Anke Nijhuis for evaluating this review article and the entire Cancer Metabolism & Systems Toxicology Group for their support. Schematic images were created with BioRender.com.

## Conflict of interest

The authors declare that the research was conducted in the absence of any commercial or financial relationships that could be construed as a potential conflict of interest.

## Publisher's note

All claims expressed in this article are solely those of the authors and do not necessarily represent those of their affiliated organizations, or those of the publisher, the editors and the reviewers. Any product that may be evaluated in this article, or claim that may be made by its manufacturer, is not guaranteed or endorsed by the publisher.



cytogenetic, and clinical features. *Blood* (1988) 71(6):1568–73. doi: 10.1182/blood.V71.6.1568.1568

14. Smaaland R, Schanche JS, Kvinnsland S, Høstmark J, Ueland PM. Methylthioadenosine phosphorylase in human breast cancer. *Breast Cancer Res Treat* (1987) 9(1):53–9. doi: 10.1007/BF01806694

15. Pegg AE, Williams-Ashman HG. Phosphate-stimulated breakdown of 5'-methylthioadenosine by rat ventral prostate. *Biochem J* (1969) 115(2):241–7. doi: 10.1042/bj1150241

16. Toohey JJ. Methylthioadenosine nucleoside phosphorylase deficiency in methylthio-dependent cancer cells. *Biochem Biophys Res Commun* (1978) 83(1):27–35. doi: 10.1016/0006-291X(78)90393-5

17. Kamatani N, Carson DA. Abnormal regulation of methylthioadenosine and polyamine metabolism in methylthioadenosine phosphorylase-deficient human leukemic cell lines. *Cancer Res* (1980) 40(11):4178–82.

18. Mavrakis KJ, McDonald ER, Schlabach MR, Billy E, Hoffman GR, deWeck A, et al. Disordered methionine metabolism in MTAP/CDKN2A-deleted cancers leads to dependence on PRMT5. *Science* (1979) 351(6278):1208–13. doi: 10.1126/science.aad5944

19. Marjon K, Cameron MJ, Quang P, Clasquin MF, Mandley E, Kunii K, et al. MTAP deletions in cancer create vulnerability to targeting of the MAT2A/PRMT5/RIOK1 axis. *Cell Rep* (2016) 15(3):574–87. doi: 10.1016/j.celrep.2016.03.043

20. Kryukov G, Wilson FH, Ruth JR, Paulk J, Tsherniak A, Marlow SE, et al. MTAP deletion confers enhanced dependency on the PRMT5 arginine methyltransferase in cancer cells. *Science* (2016) 351(6278):1214–8. doi: 10.1126/science.aad5214

21. Gerstung M, Jolly C, Leshchiner I, Dentre SC, Gonzalez S, Rosebrock D, et al. The evolutionary history of 2,658 cancers. *Nature* (2020) 578(7793):122–8. doi: 10.1038/s41586-019-1907-7

22. Sakata SF, Shelly LL, Ruppert S, Schutz G, Chou JY. Cloning and expression of murine S-adenosylmethionine synthetase. *J Biol Chem* (1993) 268(19):13978–86. doi: 10.1016/S0021-9258(19)85198-0

23. Fujimoto S, Okumura S, Matsuda K, Horikawa Y, Maeda M, Kawasaki K, et al. Effect of fasting on methionine adenosyltransferase expression and the methionine cycle in the mouse liver. *J Nutr Sci Vitaminol* (2005) 51:118–23. doi: 10.3177/JNSV.51.118

24. Guderian G, Peter C, Wiesner J, Sickmann A, Schulze-Osthoff K, Fischer U, et al. RioK1, a new interactor of protein arginine methyltransferase 5 (PRMT5), competes with pICln for binding and modulates PRMT5 complex composition and substrate specificity. *J Biol Chem* (2011) 286(3):1976–86. doi: 10.1074/jbc.M110.148486

25. Sun L, Wang M, Lv Z, Yang N, Liu Y, Bao S, et al. Structural insights into protein arginine symmetric dimethylation by PRMT5. *Proc Natl Acad Sci* (2011) 108(51):20538–43. doi: 10.1073/pnas.1106946108

26. Ho MC, Wilczek C, Bonanno JB, Xing L, Seznec J, Matsui T, et al. Structure of the arginine methyltransferase PRMT5-MEP50 reveals a mechanism for substrate specificity. *PLoS One* (2013) 8(2):e57008. doi: 10.1371/journal.pone.0057008

27. Blanc RS, Richard S. Arginine methylation: the coming of age. *Mol Cell* (2017) 65(1):8–24. doi: 10.1016/j.molcel.2016.11.003

28. Bedford MT, Clarke SG. Protein arginine methylation in mammals: who, what, and why. *Mol Cell* (2009) 33(1):1–13. doi: 10.1016/j.molcel.2008.12.013

29. Lorenzo A, Bedford MT. Histone arginine methylation. *FEBS Lett* (2011) 585(13):2024–31. doi: 10.1016/j.febslet.2010.11.010

30. Fabbriozzi E, Messaoudi S, Polanowska J, Paul C, Cook JR, Lee JH, et al. Negative regulation of transcription by the type II arginine methyltransferase PRMT5. *EMBO Rep* (2002) 3(7):641–5. doi: 10.1093/embo-reports/kvf136

31. Mulvaney KM, Blomquist C, Acharya N, Li R, Ranaghan MJ, O'Keefe M, et al. Molecular basis for substrate recruitment to the PRMT5 methyltransferase. *Mol Cell* (2021) 81(17):3481–3495.e7. doi: 10.1016/j.molcel.2021.07.019

32. Musiani D, Bok J, Massignani E, Wu L, Tabaglio T, Ippolito MR, et al. Proteomics profiling of arginine methylation defines PRMT5 substrate specificity. *Sci Signaling* (2019) 12(575):8388. doi: 10.1126/scisignal.aat8388

33. Stopa N, Krebs JE, Shechter D. The PRMT5 arginine methyltransferase: many roles in development, cancer and beyond. *Cell Mol Life Sci* (2015) 72(11):2041–59. doi: 10.1007/s00018-015-1847-9

34. Chiang K, Zielinska AE, Shaaban AM, Sanchez-Bailon MP, Jarrold J, Clarke TL, et al. PRMT5 is a critical regulator of breast cancer stem cell function via histone methylation and FOXPI expression. *Cell Rep* (2017) 21(12):3498–513. doi: 10.1016/j.celrep.2017.11.096

35. Liu M, Yao B, Gui T, Guo C, Wu X, Li J, et al. PRMT5-dependent transcriptional repression of c-Myc target genes promotes gastric cancer progression. *Theranostics* (2020) 10(10):4437–52. doi: 10.7150/thno.42047

36. Yan F, Alinari L, Lustberg ME, Martin LK, Cordero-Nieves HM, Banasavadi-Siddegowda Y, et al. Genetic validation of the protein arginine methyltransferase PRMT5 as a candidate therapeutic target in glioblastoma. *Cancer Res* (2014) 74(6):1752–65. doi: 10.1158/0008-5472.CAN-13-0884

37. Radzishewska A, v. SP, Grinev V, Lorenzini E, Kovalchuk S, Shlyueva D, et al. PRMT5 methylome profiling uncovers a direct link to splicing regulation in acute myeloid leukemia. *Nat Struct Mol Biol* (2019) 26(11):999–1012. doi: 10.1038/s41594-019-0313-z

38. Gu Z, Gao S, Zhang F, Wang Z, Ma W, Davis RE, et al. Protein arginine methyltransferase 5 is essential for growth of lung cancer cells. *Biochem J* (2012) 446(2):235–41. doi: 10.1042/BJ20120768

39. Koh CM, Bezzi M, Low DHP, Ang WX, Teo SX, Gay FPH, et al. MYC regulates the core pre-mRNA splicing machinery as an essential step in lymphomagenesis. *Nature* (2015) 523(7558):96–100. doi: 10.1038/nature14351

40. Bao X, Zhao S, Lius T, Liu Y, Liu Y, Yang X. Overexpression of PRMT5 promotes tumor cell growth and is associated with poor disease prognosis in epithelial ovarian cancer. *J Histochem Cytochem* (2013) 61(3):206–17. doi: 10.1369/0022155413475452

41. Qin Y, Hu Q, Xu J, Ji S, Dai W, Liu W, et al. PRMT5 enhances tumorigenicity and glycolysis in pancreatic cancer via the FBW7/cMyc axis. *Cell Communication Signaling* (2019) 17(1):1–15. doi: 10.1186/s12964-019-0344-4

42. Deng X, Shao G, Zhang HT, Li C, Zhang D, Cheng L, et al. Protein arginine methyltransferase 5 functions as an epigenetic activator of the androgen receptor to promote prostate cancer cell growth. *Oncogene* (2016) 36(9):1223–31. doi: 10.1038/ncr.2016.287

43. Zhang L, Shao G, Shao J, Zhao J. PRMT5-activated c-Myc promote bladder cancer proliferation and invasion through up-regulating NF-κB pathway. *Tissue Cell* (2022) 76:101788. doi: 10.1016/j.tice.2022.101788

44. Lacroix M, el Messaoudi S, Rodier G, le Cam A, Sardet C, Fabbriozzi E. The histone-binding protein COPR5 is required for nuclear functions of the protein arginine methyltransferase PRMT5. *EMBO Rep* (2008) 9(5):452–8. doi: 10.1038/embor.2008.45

45. Luo Y, Gao Y, Liu W, Yang Y, Jiang J, Wang Y, et al. Myelocytomatosis-protein arginine N-methyltransferase 5 axis defines the tumorigenesis and immune response in hepatocellular carcinoma. *Hepatology* (2021) 74(4):1932–51. doi: 10.1002/hep.31864

46. Chen H, Lorton B, Gupta V, Shechter D. A TGFβ-PRMT5-MEP50 axis regulates cancer cell invasion through histone H3 and H4 arginine methylation coupled transcriptional activation and repression. *Oncogene* (2017) 36(3):373–86. doi: 10.1038/ncr.2016.205

47. Cho EC, Zheng S, Munro S, Liu G, Carr SM, Moehlenbrink J, et al. Arginine methylation controls growth regulation by E2F-1. *EMBO J* (2012) 31(7):1785–97. doi: 10.1038/emboj.2012.17

48. Du C, Li SW, Singh SX, Roso K, Sun MA, Pirozzi CJ, et al. Epigenetic regulation of fanconi anemia genes implicates PRMT5 blockage as a strategy for tumor chemosensitization. *Mol Cancer Res* (2021) 19(12):2046–56. doi: 10.1158/1541-7786.MCR-21-0093

49. Kim H, Kim H, Feng Y, Li Y, Tamiya H, Tocci S, et al. PRMT5 control of cGAS/STING and NLRP3 pathways defines melanoma response to antitumor immunity. *Sci Trans Med* (2020) 12(551):5683. doi: 10.1126/scitranslmed.aaz5683

50. Yang X, Zeng Z, Jie X, Wang Y, Han J, Zheng Z, et al. Arginine methyltransferase PRMT5 methylates and destabilizes Mxi1 to confer radioresistance in non-small cell lung cancer. *Cancer Lett* (2022) 532:215594. doi: 10.1016/j.canlet.2022.215594

51. Pal S, Vishwanath SN, Erdjument-Bromage H, Tempst P, Sif S. Human SWI/SNF-associated PRMT5 methylates histone H3 arginine 8 and negatively regulates expression of S17 and NM23 tumor suppressor genes. *Mol Cell Biol* (2004) 24(21):9630. doi: 10.1128/MCB.24.21.9630-9645.2004

52. Jansson M, Durant ST, Cho EC, Sheahan S, Edelmann M, Kessler B, et al. Arginine methylation regulates the p53 response. *Nat Cell Biol* (2008) 10(12):1431–9. doi: 10.1038/ncb1802

53. Li Y, Chitnis N, Nakagawa H, Kita Y, Natsugoe S, Yang Y, et al. PRMT5 is required for lymphomagenesis triggered by multiple oncogenic drivers. *Cancer Discovery* (2015) 5(3):288–303. doi: 10.1158/2159-8290.CD-14-0625

54. Clarke TL, Sanchez-Bailon MP, Chiang K, Reynolds JJ, Herrero-Ruiz J, Bandejas TM, et al. PRMT5-dependent methylation of the TIP60 coactivator RUVBL1 is a key regulator of homologous recombination. *Mol Cell* (2017) 65(5):900–916.e7. doi: 10.1016/j.molcel.2017.01.019

55. Gonsalves GB, Tian L, Ospina JK, Boisvert FM, Lamond AI, Matera AG. Two distinct arginine methyltransferases are required for biogenesis of Sm-class ribonucleoproteins. *J Cell Biol* (2007) 178(5):733. doi: 10.1083/jcb.200702147

56. Rengasamy M, Zhang F, Vashisht A, Song WM, Aguilo F, Sun Y, et al. The PRMT5/WDR77 complex regulates alternative splicing through ZNF326 in breast cancer. *Nucleic Acids Res* (2017) 45(19):11106–20. doi: 10.1093/nar/gkx727

57. Vousden KH, Lu X. Live or let die: the cell's response to p53. *Nat Rev Cancer* (2002) 2(8):594–604. doi: 10.1038/nrc864

58. Zheng S, Moehlenbrink J, Lu YC, Zalmas LP, Sagum CA, Carr S, et al. Arginine methylation-dependent reader-writer interplay governs growth control by E2F-1. *Mol Cell* (2013) 52(1):37–51. doi: 10.1016/j.molcel.2013.08.039

59. Barczak W, Jin L, Carr SM, Munro S, Ward S, Kanapin A, et al. PRMT5 promotes cancer cell migration and invasion through the E2F pathway. *Cell Death Dis* (2020) 11(7):1–13. doi: 10.1038/s41419-020-02771-9

60. Will CL, Lüthmann R. Spliceosomal UsnRNP biogenesis, structure and function. *Curr Opin Cell Biol* (2001) 13(3):290–301. doi: 10.1016/s0955-0674(00)00211-8

61. Seng CO, Magee C, Young PJ, Lorson CL, Allen JP. The SMN structure reveals its crucial role in snRNP assembly. *Hum Mol Genet* (2015) 24(8):2138–46. doi: 10.1093/hmg/ddu734

62. Friesen WJ, Massenet S, Pauskhin S, Wyce A, Dreyfuss G. SMN, the product of the spinal muscular atrophy gene, binds preferentially to dimethylarginine-containing protein targets. *Mol Cell* (2001) 7(5):1111–7. doi: 10.1016/s1097-2765(01)00244-1

63. Friesen WJ, Pauskhin S, Wyce A, Massenet S, Pesiridis GS, van Duyn G, et al. The methylome, a 20S complex containing JBP1 and pICln, produces dimethylarginine-modified sm proteins. *Mol Cell Biol* (2001) 21(24):8289–300. doi: 10.1128/MCB.21.24.8289-8300.2001

64. Close P, East P, Dirac-Svejstrup AB, Hartmann H, Heron M, Maslen S, et al. DBIRD complex integrates alternative mRNA splicing with RNA polymerase II transcript elongation. *Nature* (2012) 484(7394):386–9. doi: 10.1038/nature10925
65. Bezzi M, Teo SX, Muller J, Mok WC, Sahu SK, Vardy LA, et al. Regulation of constitutive and alternative splicing by PRMT5 reveals a role for Mdm4 pre-mRNA in sensing defects in the spliceosomal machinery. *Genes Dev* (2013) 27(17):1903–16. doi: 10.1101/gad.219899.113
66. Gerhart SV, Kellner WA, Thompson C, Pappalardi MB, Zhang XP, Montes De Oca R, et al. Activation of the p53-MDM4 regulatory axis defines the anti-tumour response to PRMT5 inhibition through its role in regulating cellular splicing. *Sci Rep* (2018) 8(1):1–15. doi: 10.1038/s41598-018-28002-y
67. Braun CJ, Stanciu M, Boutz PL, Patterson JC, Calligaris D, Higuchi F, et al. Coordinated splicing of regulatory detained introns within oncogenic transcripts creates an exploitable vulnerability in Malignant glioma. *Cancer Cell* (2017) 32(4):411–426.e11. doi: 10.1016/j.ccell.2017.08.018
68. Boutz PL, Bhutkar A, Sharp PA. Detained introns are a novel, widespread class of post-transcriptionally spliced introns. *Genes Dev* (2015) 29(1):63–80. doi: 10.1101/gad.247361.114
69. Bresson SM, Hunter OV, Hunter AC, Conrad NK. Canonical poly(A) polymerase activity promotes the decay of a wide variety of mammalian nuclear RNAs. *PLoS Genet* (2015) 11(10):e1005610. doi: 10.1371/journal.pgen.1005610
70. Sachamit P, Ho JC, Ciamponi FE, Ba-Alawi W, Coutinho FJ, Guilhamon P, et al. PRMT5 inhibition disrupts splicing and stemness in glioblastoma. *Nat Commun* (2021) 12(1):1–17. doi: 10.1038/s41467-021-21204-5
71. Szczyk MM, Luciani GM, Vu V, Murison A, Dilworth D, Barghout SH, et al. PRMT5 regulates ATF4 transcript splicing and oxidative stress response. *Redox Biol* (2022) 51:102282. doi: 10.1016/j.redox.2022.102282
72. Fong JY, Pignata L, Goy PA, Kawabata KC, Lee SCW, Koh CM, et al. Therapeutic targeting of RNA splicing catalysis through inhibition of protein arginine methylation. *Cancer Cell* (2019) 36(2):194–209.e9. doi: 10.1016/j.ccell.2019.07.003
73. Hamard PJ, Santiago GE, Liu F, Karl DL, Martinez C, Man N, et al. PRMT5 regulates DNA repair by controlling the alternative splicing of histone-modifying enzymes. *Cell Rep* (2018) 24(10):2643–57. doi: 10.1016/j.celrep.2018.08.002
74. Kalev P, Hyer ML, Gross S, Konteatis Z, Chen CC, Fletcher M, et al. MAT2A inhibition blocks the growth of MTAP-deleted cancer cells by reducing PRMT5-dependent mRNA splicing and inducing DNA damage. *Cancer Cell* (2021) 39(2):209–224.e11. doi: 10.1016/j.ccell.2020.12.010
75. Cai MY, Dunn CE, Chen W, Kochupurakkal BS, Nguyen H, Moreau LA, et al. Cooperation of the ATM and fanconi anemia/BRCA pathways in double-strand break end resection. *Cell Rep* (2020) 30(7):2402–2415.e5. doi: 10.1016/j.celrep.2020.01.052
76. Lu SC, Mato JM. S-adenosylmethionine in liver health, injury, and cancer. *Physiol Rev* (2012) 92(4):1515–42. doi: 10.1152/physrev.00047.2011
77. Murray B, Antonyuk SV, Marina A, Lu SC, Mato JM, Samar Hasnain S, et al. Crystallography captures catalytic steps in human methionine adenosyltransferase enzymes. *Proc Natl Acad Sci U.S.A.* (2016) 113(8):2104–9. doi: 10.1073/pnas.1510959113
78. Liu Q, Chen J, Liu L, Zhang J, Wang D, Ma L, et al. The X protein of hepatitis B virus inhibits apoptosis in hepatoma cells through enhancing the methionine adenosyltransferase 2A gene expression and reducing S-adenosylmethionine production. *J Biol Chem* (2011) 286(19):17168–80. doi: 10.1074/jbc.M110.167783
79. Yang H, Huang ZZ, Wang J, Lu SC. The role of c-Myb and Sp1 in the up-regulation of methionine adenosyltransferase 2A gene expression in human hepatocellular carcinoma. *FASEB J* (2001) 15(9):1507–16. doi: 10.1096/fj.01-0040com
80. Yang H, Sada MR, Yu V, Zeng Y, Lee TD, Ou X, et al. Induction of human methionine adenosyltransferase 2A expression by tumor necrosis factor  $\alpha$ . *J Biol Chem* (2003) 278(51):50887–96. doi: 10.1074/jbc.M307600200
81. Ito K, Ikeda S, Kojima N, Miura M, Shimizu-Saito K, Yamaguchi I, et al. Correlation between the expression of methionine adenosyltransferase and the stages of human colorectal carcinoma. *Surg Today* (2000) 30(8):706–10. doi: 10.1007/s005950070081
82. Chen H, Xia M, Lin M, Yang H, Kuhlenskamp J, Li T, et al. Role of methionine adenosyltransferase 2A and S-adenosylmethionine in mitogen-induced growth of human colon cancer cells. *Gastroenterology* (2007) 133(1):207–18. doi: 10.1053/j.gastro.2007.03.114
83. Chan-Penebre E, Kuplast KG, Majer CR, Boriack-Sjodin PA, Wigle TJ, Johnston LD, et al. A selective inhibitor of PRMT5 with *in vivo* and *in vitro* potency in MCL models. *Nat Chem Biol* (2015) 11(6):432–7. doi: 10.1038/nchembio.1810
84. Antonyamy S, Bonday Z, Campbell RM, Doyle B, Druzina Z, Gheyi T, et al. Crystal structure of the human PRMT5:MEP50 complex. *Proc Natl Acad Sci* (2012) 109(44):17960–5. doi: 10.1073/pnas.1209814109
85. Bonday ZQ, Cortez GS, Grogan MJ, Antonyamy S, Weichert K, Bocchinfuso WP, et al. LLY-283, a potent and selective inhibitor of arginine methyltransferase 5, PRMT5, with antitumor activity. *ACS Medicinal Chem Lett* (2018) 9(7):612–7. doi: 10.1021/acsmedchemlett.8b00014
86. Wu T, Millar H, Gaffney D, Beke L, Mannens G, Vinken P, et al. Abstract 4859: JNJ-64619178, a selective and pseudo-irreversible PRMT5 inhibitor with potent *in vitro* and *in vivo* activity, demonstrated in several lung cancer models. *Cancer Res* (2018) 78(13 Supplement):4859–9. doi: 10.1158/1538-7445.AM2018-4859
87. Brehmer D, Beke L, Wu T, Millar HJ, Moy C, Sun W, et al. Discovery and pharmacological characterization of JNJ-64619178, a novel small molecule inhibitor of PRMT5 with potent anti-tumor activity. *Mol Cancer Ther* (2021) 20(12):2317–28. doi: 10.1158/1535-7163.MCT-21-0367
88. Malik R, Park PK, Barbieri CM, Blat Y, Sheriff S, Weigelt CA, et al. Abstract 1140: A novel MTA non-competitive PRMT5 inhibitor. *Cancer Res* (2021) 81(13 Supplement):1140–0. doi: 10.1158/1538-7445.AM2021-1140
89. Smith CR, Aranda R, Bobinski TP, Briere DM, Burns AC, Christensen JG, et al. Fragment-based discovery of MRTX1719, a synthetic lethal inhibitor of the PRMT5•MTA complex for the treatment of MTAP-deleted cancers. *J Medicinal Chem* (2022) 65(3):1749–66. doi: 10.1021/acs.jmedchem.1c01900
90. McKinney DC, McMillan BJ, Ranaghan MJ, Moroco JA, Brousseau M, Mullin-Bernstein Z, et al. Discovery of a first-in-class inhibitor of the PRMT5–substrate adaptor interaction. *J Medicinal Chem* (2021) 64(15):11148–68. doi: 10.1021/acs.jmedchem.1c00507
91. Lombardini JB, Coulter AW, Talalay P. Analogues of methionine as substrates and inhibitors of the methionine adenosyltransferase reaction. *Mol Pharmacol* (1970) 6(5):481–99.
92. Lombardini JB, Sufrin JR. Chemotherapeutic potential of methionine analogue inhibitors of tumor-derived methionine adenosyltransferases. *Biochem Pharmacol* (1983) 32(3):489–95. doi: 10.1016/0006-2952(83)90528-2
93. Zhang W, Sviripa V, Chen X, Shi J, Yu T, Hamza A, et al. N-dialkylaminostilbenes repress colon cancer by targeting methionine S-adenosyltransferase 2A. *ACS Chem Biol* (2013) 8(4):796–803. doi: 10.1021/cb3005353
94. Sviripa VM, Zhang W, Balia AG, Tsodikov OV, Nickell JR, Gizard F, et al. 2',6'-dihalostrylanilines, pyridines, and pyrimidines for the inhibition of the catalytic subunit of methionine S-adenosyltransferase-2. *J Medicinal Chem* (2014) 57(14):6083–91. doi: 10.1021/jm5004864
95. Quinlan CL, Kaiser SE, Bolaños B, Nowlin D, Grantner R, Karlicek-Bryant S, et al. Targeting S-adenosylmethionine biosynthesis with a novel allosteric inhibitor of MAT2A. *Nat Chem Biol* (2017) 13(7):785–92. doi: 10.1038/nchembio.2384
96. Konteatis Z, Travins J, Gross S, Marjon K, Barnett A, Mandley E, et al. Discovery of AG-270, a first-in-class oral MAT2A inhibitor for the treatment of tumors with homozygous MTAP deletion. *J Medicinal Chem* (2021) 64(8):4430–49. doi: 10.1021/acs.jmedchem.0c01895
97. de Fusco C, Schimpl M, Börjesson U, Cheung T, Collie I, Evans L, et al. Fragment-based design of a potent MAT2a inhibitor and *in vivo* evaluation in an MTAP null xenograft model. *J Med Chem* (2021) 64:6826. doi: 10.1021/acs.jmedchem.1c00067
98. Bailey J, Douglas H, Masino L, Carvalho LPS, Argyrou A. Human mat2A uses an ordered kinetic mechanism and is stabilized but not regulated by mat2B. *Biochemistry* (2021) 60(47):3621–32. doi: 10.1021/acs.biochem.1c00672
99. GSK. Press Release. Full Year and Fourth Quarter 2021 (2021). Available at: <https://www.gsk.com/media/7377/fy-2021-results-announcement.pdf> (Accessed April 28, 2023).
100. Evaluate Vantage. GSK Raises More Questions About Synthetic Lethality (2022). Available at: <https://www.evaluate.com/vantage/articles/news/deals/gsk-raises-more-questions-about-synthetic-lethality> (Accessed April 28, 2023).
101. McKean M, Patel MR, Wesolowski R, Ferrarotto R, Stein EM, Shoushtari AN, et al. Abstract P039: A phase 1 dose escalation study of protein arginine methyltransferase 5 (PRMT5) inhibitor PRT543 in patients with advanced solid tumors and lymphoma. *Mol Cancer Ther* (2021) 20(12 Supplement):P039–9. doi: 10.1158/1535-7163.TARG-21-P039
102. Berekaitay Y, Ackroyd JJ, Yan VC, Khadka S, Wang L, Chen KC, et al. Homozygous MTAP deletion in primary human glioblastoma is not associated with elevation of methylthioadenosine. *Nat Commun* (2021) 12(1):1–13. doi: 10.1038/s41467-021-24240-3
103. Ackermann T, Tardito S. Cell culture medium formulation and its implications in cancer metabolism. *Trends Cancer* (2019) 5(6):329–32. doi: 10.1016/j.trecan.2019.05.004
104. Mayers JR, Torrence ME, Danai LV, Papagiannakopoulos T, Davidson SM, Bauer MR, et al. Tissue of origin dictates branched-chain amino acid metabolism in mutant Kras-driven cancers. *Science* (2016) 353(6304):1161–5. doi: 10.1126/science.aaf5171
105. Sanderson SM, Mikhael PG, Ramesh V, Dai Z, Locasale JW. Nutrient availability shapes methionine metabolism in p16/MTAP-deleted cells. *Sci Adv* (2019) 5(6):eaav7769. doi: 10.1126/sciadv.aav7769
106. Kawaguchi K, Han Q, Li S, Tan Y, Igarashi K, Murakami T, et al. Efficacy of recombinant methioninase (rMETase) on recalcitrant cancer patient-derived orthotopic xenograft (PDOX) mouse models: A review. *Cells* (2019) 8(5):410. doi: 10.3390/cells8050410
107. Bárcena C, Quirós PM, Durand S, Mayoral P, Rodríguez F, Caravia XM, et al. Methionine restriction extends lifespan in progeroid mice and alters lipid and bile acid metabolism. *Cell Rep* (2018) 24(9):2392–403. doi: 10.1016/j.celrep.2018.07.089
108. Hoffman RM, Tan Y, Li S, Han Q, Zavala J, Zavala J. Pilot phase I clinical trial of methioninase on high-stage cancer patients: rapid depletion of circulating methionine. *Methods Mol Biol* (2019) 1866:231–42. doi: 10.1007/978-1-4939-8796-2\_17
109. Zhang T, Bauer C, Newman AC, Uribe AH, Athineos D, Blyth K, et al. Polyamine pathway activity promotes cysteine essentiality in cancer cells. *Nat Metab* (2020) 2(10):1062. doi: 10.1038/s42255-020-0253-2

110. Lisio MA, Fu L, Goyeneche A, Gao ZH, Telleria C. High-grade serous ovarian cancer: basic sciences, clinical and therapeutic standpoints. *Int J Med Sci* (2019) 20 (4):952. doi: 10.3390/ijms20040952
111. Bryant HE, Schultz N, Thomas HD, Parker KM, Flower D, Lopez E, et al. Specific killing of BRCA2-deficient tumours with inhibitors of poly(ADP-ribose) polymerase. *Nature* (2005) 434(7035):913–7. doi: 10.1038/nature03443
112. Dominici C, Sgarioni N, Yu Z, Sesma-Sanz L, Masson JY, Richard S, et al. Synergistic effects of type I PRMT and PARP inhibitors against non-small cell lung cancer cells. *Clin Epigenet* (2021) 13(1):54. doi: 10.1186/s13148-021-01037-1
113. Mueller HS, Fowler CE, Dalin S, Moiso E, Udomlumleart T, Garg S, et al. Acquired resistance to PRMT5 inhibition induces concomitant collateral sensitivity to paclitaxel. *Proc Natl Acad Sci* (2021) 118(34):e2024055118. doi: 10.1073/pnas.2024055118
114. Hu R, Zhou B, Chen Z, Chen S, Chen N, Shen L, et al. PRMT5 inhibition promotes PD-L1 expression and immuno-resistance in lung cancer. *Front Immunol* (2022) 0:722188. doi: 10.3389/fimmu.2021.722188
115. Hansen LJ, Yang R, Roso K, Wang W, Chen L, Yang Q, et al. MTAP loss correlates with an immunosuppressive profile in GBM and its substrate MTA stimulates alternative macrophage polarization. *Sci Rep* (2022) 12:1. doi: 10.1038/s41598-022-07697-0
116. Hung MH, Lee JS, Ma C, Diggs LP, Heinrich S, Chang CW, et al. Tumor methionine metabolism drives T-cell exhaustion in hepatocellular carcinoma. *Nat Commun* (2021) 12(1):1–15. doi: 10.1038/s41467-021-21804-1



## OPEN ACCESS

## EDITED BY

Satyendra Chandra Tripathi,  
All India Institute of Medical Sciences  
Nagpur, India

## REVIEWED BY

Xingyu Chen,  
Cedars Sinai Medical Center, United States  
Dengxiang Li,  
Sichuan University, China

## \*CORRESPONDENCE

Ke Peng  
✉ pengke620@163.com

RECEIVED 06 July 2023

ACCEPTED 01 September 2023

PUBLISHED 19 September 2023

## CITATION

Li X, Du G, Li L and Peng K (2023) Cellular specificity of lactate metabolism and a novel lactate-related gene pair index for frontline treatment in clear cell renal cell carcinoma.  
*Front. Oncol.* 13:1253783.  
doi: 10.3389/fonc.2023.1253783

## COPYRIGHT

© 2023 Li, Du, Li and Peng. This is an open-access article distributed under the terms of the [Creative Commons Attribution License \(CC BY\)](https://creativecommons.org/licenses/by/4.0/). The use, distribution or reproduction in other forums is permitted, provided the original author(s) and the copyright owner(s) are credited and that the original publication in this journal is cited, in accordance with accepted academic practice. No use, distribution or reproduction is permitted which does not comply with these terms.

# Cellular specificity of lactate metabolism and a novel lactate-related gene pair index for frontline treatment in clear cell renal cell carcinoma

Xiangsheng Li, Guangsheng Du, Liqi Li and Ke Peng\*

Department of General Surgery, Xinqiao Hospital, Army Medical University, Chongqing, China

**Background:** Although lactate metabolism-related genes (LMRGs) have attracted attention for their effects on cancer immunity, little is known about their function in clear cell renal cell carcinoma (ccRCC). The aim of this study was to examine the cellular specificity of lactate metabolism and how it affected the first-line treatment outcomes in ccRCC.

**Methods:** GSE159115 was used to examine the features of lactate metabolism at the single-cell level. Utilizing the transcriptome, methylation profile, and genomic data from TCGA-KIRC, a multi-omics study of LMRG expression characteristics was performed. A prognostic index based on a gene-pair algorithm was created to assess how LMRGs affected patients' clinical outcomes. To simulate the relationship between the prognostic index and the frontline treatment, pRRophetic and Subclass Mapping were used. E-MTAB-1980, E-MTAB-3267, Checkmate, and Javelin-101 were used for external validation.

**Results:** The variable expression of some LMRGs in ccRCC can be linked to variations in DNA copy number or promoter methylation levels. Lactate metabolism was active in tumor cells and vSMCs, and LDHA, MCT1, and MCT4 were substantially expressed in tumor cells, according to single-cell analysis. The high-risk patients would benefit from immune checkpoint blockade monotherapy (ICB) and ICB plus tyrosine kinase inhibitors (TKI) therapy, whereas the low-risk individuals responded to mTOR-targeted therapy.

**Conclusions:** At the single-cell level, our investigation demonstrated the cellular specificity of lactate metabolism in ccRCC. We proposed that the lactate-related gene pair index might be utilized to identify frontline therapy responders in ccRCC patients as well as predict prognosis.

## KEYWORDS

lactate metabolism, single cell analysis, gene pair algorithm, mTOR-targeted therapy, immune checkpoint blockade



## Introduction

Metabolic disorders are widely involved in the occurrence and development of various diseases (1, 2), and recent evidence has accumulated that metabolic disorders in cancer cells are not only a hallmark of cancer, but may also be the fundamental cause of tumors. In 1923, Otto Warburg observed that tumor cells tend to take up large amounts of glucose and produce excess lactic acid through anaerobic glycolysis. This property will not change in the presence of sufficient oxygen, a phenomenon known as the Warburg effect (3). Lactate has long been considered a metabolic waste product, but recent studies have identified lactate as one of the most significant metabolites in the tumor microenvironment that contributes to microenvironmental acidosis and immunosuppression. Malignant cell-produced lactic acid causes acidification of the tumor microenvironment (TME), promotes proliferation and accumulation of myeloid-derived suppressive cells (MDSCs), and inhibits the cytolytic function of effector cells (4). Lactic acid inhibits the differentiation and maturation of monocytes into dendritic cells, and several studies have confirmed the ability of lactic acid to induce polarization into M2-type macrophages (5–7). Lactic acid inhibits antigen presentation function by activating GPR81 in DC cells and inhibiting the production of cAMP, IL-6, IL-12, MHC-II, and other immunoreactive factors (8). A recent study reported that lactate inhibits RIG-I-like signaling and suppresses type I interferon production by inhibiting MAVS protein polymerization (9). Lactate signaling also promotes Treg differentiation and its mediated inhibition, promotes inflammatory Th17 cell differentiation, and inhibits the killing effect of CD8<sup>+</sup> T cells and NK cells (10, 11). Moreover, lactate serves as an important carbon source for tumor cells as well as immune cells, and it is taken up by cells to mediate various intracellular signaling and function changes. Zhao et al. reported for the first time that lactate can also act as a modifying substrate to mediate lysine lactylation modification of histones under the action of histone acetyltransferase p300, which regulates the expression of genes related to macrophage polarization during immune activation (12, 13). Subsequently, HDAC1-3 was identified as the most potent lysine lactylation modification “eraser” (14).

The modern lifestyle has greatly changed the disease spectrum of cancer. In developed countries or urban areas, the incidence rate of cancer related to obesity and westernized lifestyle raised very high, including colorectal cancer, prostate cancer, kidney cancer and bladder cancer {Chen:fh}. Clear cell renal cell carcinoma (ccRCC) is a typical metabolic disorder tumor with robust lipid and glycogen accumulation, and recent studies have increasingly focused on the role of lactate-related metabolic factors in renal carcinogenesis. Lactate dehydrogenase, which catalyzes the production of lactate from pyruvate and is deeply involved in the regulation of the Warburg effect, was the first widely studied regulator in RCC. Hala et al. reported for the first time the correlation between LDHA upregulation and poor prognosis in RCC patients through tissue immunohistochemical studies (15). Zhao et al. discovered that LDHA was highly expressed in RCC tissues and that it mediated tumor metastasis by promoting epithelial-mesenchymal transition (EMT) (16, 17). Further research revealed that the promoting effect of lactate on EMT may be partially

dependent on Sirtuin-1 activity inhibition (18). LDH reflects tumor tissue hypoxia and neovascularization levels and is widely used as a tumor load-related marker. A retrospective clinical trial reported that serum baseline LDH levels were an independent risk factor for postoperative PFS in patients with metastatic ccRCC treated with Nivolumab and were associated with poorer PFS in patients in the IMDC staging favorable group (19). Systematic reviews and meta-analyses announced that a high baseline serum LDH to lymphocyte ratio was independently correlated to the prognosis of metastatic RCC patients treated with tyrosine kinase inhibitors (TKI) (20, 21). Zhang et al. conducted a meta-analysis of lactate dehydrogenase's prognostic role in metastatic RCC and found that high preoperative serum LDH levels were significantly correlated with poor postoperative overall survival (OS) and progression-free survival (PFS) (22). In addition, MCTs, which mediate the intercellular lactate shuttle, have also received extensive attention. By analyzing microarray data constructed from a large number of surgical specimens and performing immunohistochemical staining, Paul et al. demonstrated that MCT1 was an independent predictor of cancer-specific survival (CSS) in ccRCC (23). Overexpression of MCT1 and its partner CD147 have also been used to predict ccRCC progression (24). These findings suggest that lactate-related metabolism factors profoundly influence RCC progression and hold predictive value for frontline adjuvant therapy.

The value of lactate metabolism-related genes (LMRGs) in the prognosis of ccRCC has been recently investigated, but there are several shortcomings (25, 26). First, the lactate metabolism regulators discussed in prior publications were not comprehensive; second, their conclusions have not been validated in real-world patient cohorts treated with targeted therapy or immune checkpoint blockade (ICB); and, in addition, there is a lack of single-cell level investigation to elucidate the cell type specificity of lactate metabolism. In the present study, we explain the alteration of lactate metabolism-related processes and regulators with respect to different immune cell types. We proposed a novel prognostic index by constructing lactate-related gene pairs, which has exhibited robust stability and predictive power in previously published datasets because it does not depend on absolute gene expression level. Most importantly, validation in cohorts treated with TKI or ICB directly demonstrated the value of the lactate-related gene pair index (LRGPI) in guiding the selection of frontline adjuvant strategies.

## Materials and methods

### Data acquisition and pre-processing

In this study, we integrated several independent datasets for comprehensive analysis. We obtained transcriptomic and 450K methylation sequencing profiles and the Masked Copy Number segment file for the TCGA-KIRC cohort from the Xena portal as a development dataset. FPKM values were transformed into TPM values to maintain comparability with MicroArray platform-derived data. Gene expression and clinical profiles of E-MTAB-1980 and E-MTAB-3267 were obtained from the ArrayExpress

portal (<https://www.ebi.ac.uk/arrayexpress/>) as the test set. In addition, several datasets were obtained from the GEO portal (<https://www.ncbi.nlm.nih.gov/gds/?term=>) for external validation. Specifically, six datasets based on the GPL570 platform (GSE36895, GSE53757, GSE66272, GSE73731, GSE46699, and GSE22541) were combined into the external validation set GPL570, and three datasets based on GPL10588 (GSE40435, GSE105261, and GSE65615) were merged into GPL10588. The “sva” function of the “Combat” package was used to merge data generated from the same platform to remove batch effects. The Checkmate cohort consisted of 181 cases of metastatic ccRCC treated with Nivolumab and 130 cases treated with Everolimus, with TPM transcriptome data and corresponding clinical information obtained from the report of Brau et al. (27). In addition, the phase III clinical trial Javelin-101 enrolled 726 cases of advanced RCC and compared the efficacy of Sunitinib and Avelumab plus Axitinib. The TPM transcriptome data and clinical outcome of Javelin-101 were obtained from Motzer et al. (28). The log ratio transformed proteomic expression data and their biospecimen information were downloaded from the CPTAC portal (<https://proteomics.cancer.gov/programs/cptac>) for protein level validation. Briefly, there were 83 normal samples and 111 ccRCC tumor samples in the CPTAC-ccRCC cohort. Representative normal kidney tissue and renal cancer pathology IHC slides were downloaded from the HPA portal (<https://www.proteinatlas.org>).

## Curation of genes involved in the lactate metabolism process

Six GO processes involved in lactate metabolism were archived and collected from MSigDB, including GO\_LACTATION, GO\_LACTATE\_METABOLIC\_PROCESS, GO\_LACTATE\_TRANSMEMBRANE\_TRANSPORT, GO\_LACTATE\_TRANSMEMBRANE\_TRANSPORTER\_ACTIVITY, GO\_LACTATE\_DEHYDROGENASE\_ACTIVITY, GO\_L\_LACTATE\_DEHYDROGENASE\_ACTIVITY. In total, these gene sets contain 74 hub genes related to lactate metabolism.

## Differentially expressed genes analysis and genomic heterogeneity analysis

The “limma” package was used to perform DEG analysis on high throughput sequencing/Microarray-derived data. Nonsynonymous mutations of a single gene were extracted from the Mutect file and defined with reference to Brau et al (27). The methylation data were preprocessed with reference to the published report (29). The gene promoter region was defined as TSS1500, TSS200, 5'-UTR, and 1stExon. The median value of the promoter region probe was used to represent the promoter region methylation level of a single gene. The copy number variation (CNV) file and reference markers file were submitted to the GISTIC 2.0 modules in the GenePattern platform (<https://cloud.genepattern.org/gp/pages/index.jsf>) to perform CNV

analysis. The Human Hg38 reference genome was set as a reference, the amplifications and deletions threshold were set at 0.3 (q value<0.05), and the confidence level was set at 0.99.

## Single-cell RNA sequencing data analysis

sc-RNA seq data for seven ccRCC tumors and six normal samples, along with cell type annotations, were stored as GSE159115 in the GEO database. The “Seurat” package was used to create single-cell objects for each sample, retaining cells with mitochondrial genes 25% of the time and nFeature\_RNA > 300. The data of each sample was normalized, and 2000 genes with the highest variance were chosen based on variance stabilization transformation. Anchors were identified using the FindIntegrationAnchors function, and all samples were integrated into one Seurat object using the IntegrateData function to remove batch effects. The Seurat objects were then downscaled using the umap method, and visualization was done using the “scRNAtoolVis” package. Gene set enrichment assessment at the single-cell level was performed using the “AUCell” and “SCpubr” packages, respectively. Cell-specific molecular markers were identified by the FindAllMarkers function (logFCfilter=0.25, adjusted p-value <0.05, min.pct=0.25). CytoTRACE can assess the differentiation status of individual cells while also generating a numeric vector of each gene’s Pearson correlation with CytoTRACE (30). The degree of dedifferentiation of individual tumor tissues was assessed using a curated stem gene set of 109 genes with proliferation and immune-related genes removed as proposed by Miranda et al. (31).

## Western blotting

The human normal renal epithelial cell line HK2 and the tumor cell lines ACHN, 786-O, and OS-RC-2 were used for western blotting analysis in according to the standard procedure. The antibodies were purchased from the ABclonal Technology company (LDHA, #A0861, LDHB, #A7625).

## Lactate metabolism-related gene pairs construction

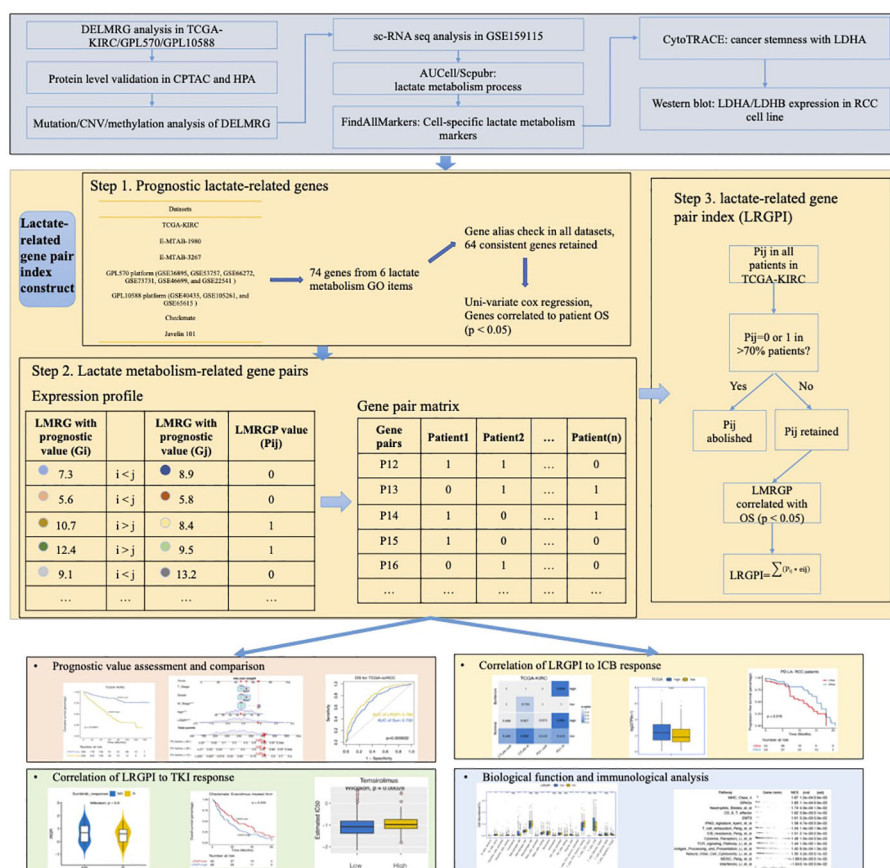
Gene alias in different datasets was manually checked to keep consistent with the current gene symbols in Genecard (<https://www.genecards.org/>), and we retained 64 lactate metabolism genes detected in all datasets to construct lactate-related gene pairs. The gene pair construction procedure was based on that previously reported in the literature, with some modifications to the details (32). The main steps include the following: 1) identification of genes significantly associated with OS using uni-variate Cox regression ( $p < 0.05$ ); 2) pairwise comparison of the prognostic gene  $G_i$  with all LMRGs  $G_j$ , and for each gene pair ( $P_{ij}$ ) starting with  $G_i$ ,  $\text{Score}_{ij} = 1$  if  $G_i > G_j$  and 0 otherwise; 3) if  $\text{Score}_{ij}$  is consistent (i.e.  $\text{Score}_{ij} = 0$  or 1) in more than 70% of the samples, then this gene pair was abolished. This method calculates scores based on the relative

corresponding coefficients. The scheme of LRGPI construction and workflow of this study is illustrated in Figure 1.

## Deconvolution of the immune infiltration and gene set activity evaluation

We used the “IOBR” package to analyze the TME components. IOBR integrated nine mostly used deconvolution methods, including CIBERSORT, EPIC, MCPcounter, xCELL, ESTIMATE, TIMER, quanTIseq, and IPS, and numeric published gene sets related to tumor metabolism, cancer hallmarks, TME, etc. (33). CIBERSORT was selected for deconvolution assessment of the level of infiltrating immune cells. The “ssgsva” algorithm built into this package was used for gene set enrichment to assess the activity of the tumor metabolism activity. Enrichment analysis of cancer hallmarks and TME was performed using the “fgsea” package.

The “pRRophetic” package was used to estimate the drug sensitivity of individual samples, as reported by Zhou et al. (34).



Specifically, the transcriptomic data of urological cell lines and experimentally determined IC50 values for the target drugs were designated as standard data, and the package used the transcriptomic data of the samples to be tested to construct a ridge regression model, thereby deriving the estimated IC50 values of the samples to be tested. A gene expression pattern similarity comparison was performed using the Subclass Mapping module of the GenePattern portal. Specifically, 47 melanoma patients treated with CTLA4/PD-1 blockade and their drug response labels were designated as standards. Their transcriptome data and tags were submitted to the portal module together with the samples to be tested and grouping labels to obtain gene expression similarity test p-values (35).

## Statistical analysis

Visual image plotting and statistical analysis of this study were completed using R 4.1.1. The classic Kaplan-Meier curve was used to visualize patient survival status, while the log-rank test was used to differentiate survival differences between groups. The prognostic value of numerical or categorical factors was assessed using univariate or multivariate Cox regression models, and forest plots were drawn using the “forestplot” package. The nomogram under the univariate model was plotted using the “rms” package, and the predictive efficacy of the model was assessed using ROC curves and calibration curves. The heat map in the paper is drawn using the “ComplexHeatmap” package. We used the Wilcoxon test or the Kruskal-Wallis test for two-group or multi-group continuous variables, and a two-sided test with a p-value < 0.05 was considered a statistically significant difference. The Bonferroni correction was used to reduce the likelihood of Type I error in multiple replicate tests.

## Results

### Multi-omics analysis of differentially expressed lactate metabolism-related genes in ccRCC

DEG analysis of the three cohorts (TCGA-KIRC, GPL570, and GPL10588) identified 30 DELMRGs (Figures S1A–C). The mutation landscape did not find high-frequency mutations in DELMRGs (Figure 2A, frequency > 5%), but CNV analysis revealed frequent gene copy number amplification and deletion (Figure 2B). Further, we examined the promoter methylation levels of DELMRGs and found that several genes (such as OAS2, KALRN, SLC16A7, PER2) had significantly lower methylation levels in tumor samples, while several genes (SLC6A3, CDO1, and SERPINC1) were significantly higher methylated (Figure 2C). Proteomic data verified that LDHA, HK2, NCOR2, CAV1, CCND1, OAS2, VEGFA, MED1, and PAM were significantly higher expressed, while PFKFB2, LDHB, PNKD, LDHD, HAGH, SLC16A7, SLC5A12, GOT2, and SLC25A12 were lower expressed in tumor samples (Figure S1D; Supplementary Table 1). In addition,

the DELMRGs were further validated in protein expression level by their representative normal and tumor tissue staining slides in HPA portal (Figure S2). We then described the correlation and prognostic value of the DELMRGs using an integrated network (Figure 2D). Most DELMRGs interacted positively, and many genes, including MED1, ZBTB7B, SOCS2, SLC6A3, SLC5A12, SLC25A12, PRLR, PER2, PAM, NCOA1, LDHD, LDHA, KALRN, HAGH, GOT2, CCND1, and APLN played protective roles in patients' overall survival (OS).

### Disordered lactate metabolism processes in different cell types

Sc-RNA seq data can provide complementary information on cell-level variation beyond bulk-tissue sequencing data. According to the original literature (36), tumor tissue-derived cells were annotated into 13 cell types (Figure 3A). Each single cell was scored for six lactate metabolism-related biological process activities by the AUCell algorithm, and activities of these processes of the tumor tissue-derived cells were all significantly higher than those of the normal tissue-derived cells (Figure 3B). Further comparison across all tumor tissue cell types revealed that tumor cells, pericytes, endothelial cells, and vSMC cells hold the highest lactate metabolism activity than other cell types, while lactate transport across membranes was most active in tumor cells. The lactate dehydrogenase and L-lactate dehydrogenase activities of tumor cells, CD8<sup>+</sup> T cells, vSMC cells, and MKI67<sup>+</sup> macrophages were also higher than other cell types (Figures S3A–F). In addition, the enrichment results produced by “SCpubr” package highlighted the prominent lactate dehydrogenase and L-lactate dehydrogenase activities in tumor cells (Figure 3C).

We explored the expression levels of four major lactate dehydrogenase (LDHA, LDHB, LDHC, and LDHD) and found that LDHA was significantly higher expressed in tumor tissue-derived cells and LDHB was higher expressed in normal tissue-derived cells (Figure 4A). Further, cell line experiments showed a significant increase in LDHA expression and a significant decrease in LDHB expression in the tumor cell lines ACHN, 786-O, and OS-RC-2 relative to the human normal renal epithelial cell line HK2 (Figure 4B). Cell-specific molecular markers were then extracted (Supplementary Table 2). We observed the expression level of LMRGs in different cell types, and we found that LDHA was mainly expressed in tumor cells and ACKR1<sup>+</sup> endothelial, while LDHB was highly expressed in vSMC, tumor cells, mast cells, and CD8<sup>+</sup> T cells (Figure S4). Cells absorb glucose via GLUT1 (SLC2A1), hypoxic cells release lactate through MCT4 (SLC16A4), while tumor cells and endothelial cells absorb lactate through MCT1 (SLC16A1). We explored the expression levels of transporter proteins in different cell types and found that GLUT1 and MCT1/4 were most highly expressed in ccRCC tumor cells (Figure 4C). These results suggest the idea that that lactate in the TME is mainly produced by vSMC and consumed and utilized by ccRCC tumor cells. Moreover, pericytes, endothelial cells, MKI67<sup>+</sup> macrophages, and CD8<sup>+</sup> T cells also hold a certain lactate uptake ability, suggesting the potential impact of lactate on their biological



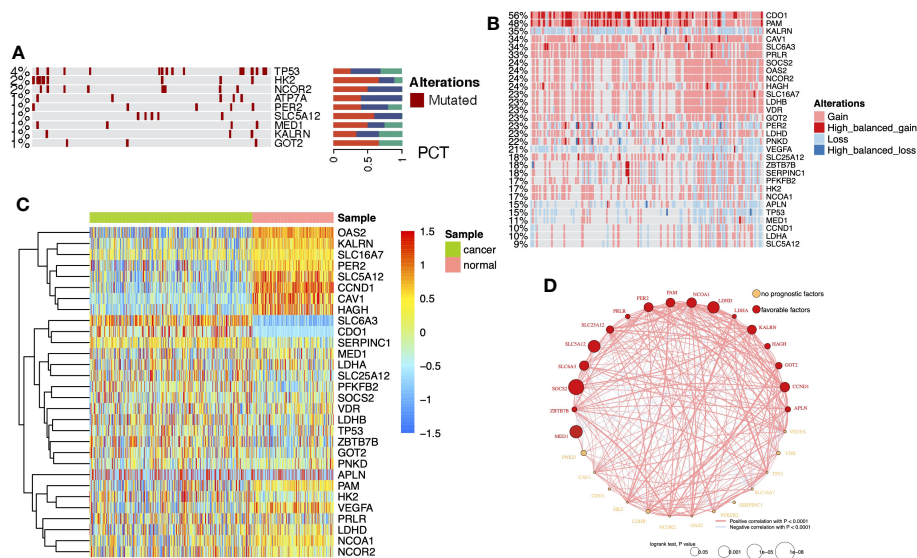


FIGURE 2

(A) Heatmap with bar plots displayed the mutation rates of DELMRGs. (B) Heatmap displayed the amplification and deletion landscape of 30 DELMRGs. (C) Heatmap showed the promoter methylation level of 30 DELMRGs. (D) Integrated network of correlation and prognostic value of the DELMRGs.

functions. In addition, the results of CytoTRACE showed that LDHA is highly correlated with inferred cancer stemness at the single-cell level (Figure 4D), and we verified the correlation at the bulk-tissue level using the TCGA cohort (Figure 4E).

## Establishment of a LRGPI to predict patients' prognosis

Here, we wonder whether the lactate metabolism-related prognostic index could be used to assess the clinical outcome of ccRCC patients. To minimize the impact caused by different sequencing platforms and standardization methods, we converted the lactate metabolism-related gene expression matrix into a gene pair matrix with values of 0 or 1. The univariate Cox regression identified 29 prognosis-related lactate metabolism genes. A total of 129 gene pairs were generated, and 96 gene pairs were significantly correlated to patients' OS. Adaptive lasso regression yielded the best combination of 18 gene pairs (Figures 5A, B, Supplementary Table S3). LRGPI was calculated as the method described. Patients were divided into high- and low-LRGPI groups based on the median LRGPI value, and the survival curves showed that patients in the high- LRGPI group had significantly lower overall survival (OS) and disease-free survival (DFS) rates than those in the low-LRGPI group (Figures 5C, D). The predictive efficiency of LRGPI for 1-year, 3-year, and 5-year prognosis reached 0.778, 0.755, and 0.803 for OS and 0.678, 0.720, and 0.723 for DFS, respectively (Figures 5E, F). LRGPI was proved to be an independent risk factor for patients' prognosis by adjusting clinical parameters in the multivariate Cox model (Figure 5G). To further improve the accuracy of clinical application, we integrated tumor T-stage, histologic grade, metastatic status, patient age, and LRGPI to construct a

nomogram to predict patients' OS (Figure 5H). The ROC curve was used to assess the predictive capacity of the nomogram, and the area under the curve (AUC) reached 0.89, 0.85, and 0.86 for overall survival at 1, 3, and 5 years, respectively (Figure 5I). The predictive accuracy of the nomogram was further evaluated using the calibration curve, and the predicted OS status at 1, 3, and 5 years was found to be very close to the actual observation, indicating a robust predictive capability of the nomogram (Figure 5J).

The GSEA results suggest activation of metabolic activities such as glycolysis, lipogenesis, fatty acid metabolism, and hypoxia in the high-LRGPI group samples, indicating high proliferation and energy demand in these samples. Meanwhile, immune response signals such as IFN responses, TGF $\beta$  signaling, IL2/STAT5 signaling, and KRAS signaling were also significantly upregulated (Figure S5A). To elucidate the association between LRGPI and cancer metabolism, enrichment scores for 103 tumor metabolism signals were calculated, and 75 signals were differentially distributed between the two groups (Figure 6A). We found that aerobic energy production pathways such as glycogen degradation, sugar degradation, the tricarboxylic acid cycle, pyruvate metabolism, and lactate degradation were significantly inhibited in patients with high LRGPI scores. At the same time, LRGPI was also negatively correlated to fatty acid degradation and long-chain fatty acid synthesis (Figure 6B), suggesting that fatty acids accumulated in the samples of the high-LRGPI subgroup.

## External validation and efficacy comparison of LRGPI

LRGPI were then generated for each tumor sample in E-MTAB1980 and E-MTAB3267 for external validation. Similar to

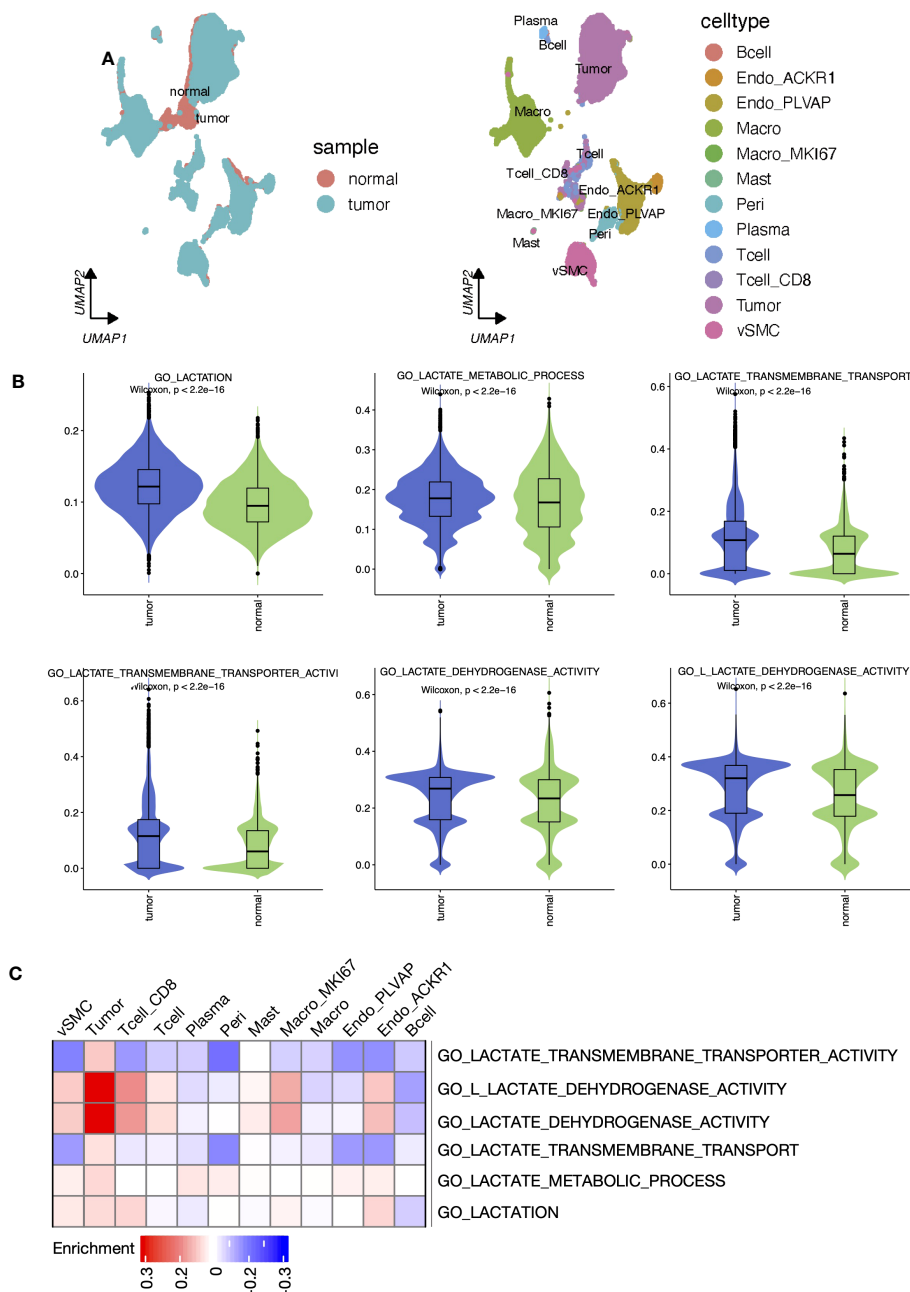


FIGURE 3

Lactate metabolism was activated in ccRCC tumor samples and different cell types. **(A)** UMAP reduction plots of cells grouped by sample and cell types. **(B)** The boxplots presented the "AUCell" scores that evaluated lactate metabolism processes at the single-cell level between tumor and normal samples. **(C)** Heatmap presented the enrichment scores produced by 'Scpubr' package in tumor sample-derived single cells.

the TCGA-KIRC, patients in the high-LRGPI subgroup identically showed significantly lower OS or PFS rates than patients in the low-LRGPI subgroup (Figures 6C, D). The predictive efficacy of LRGPI for 1-year, 3-year, and 5-year OS in E-MTAB-1980 was 0.753, 0.780, and 0.722, respectively (Figure 6E). For metastatic ccRCC patients treated by Sunitinib, the predictive power for PFS at 1, 2, and 3 years was 0.657, 0.725, and 0.768, respectively (Figure 6F). LRGPI remained an independent risk factor after adjusting clinical factors in E-MTAB1980 (Figure S5B). In addition, we applied the nomogram established in TCGA-KIRC to E-MTAB1980 (Figure S5C), and the calibration curve still observed a high degree of

agreement between predicted and actual survival status (Figure S5D). The clinical nomogram achieved impressive predictive powers of 0.89, 0.92, and 0.87 for 1-year, 3-year, and 5-year OS, respectively (Figure S5E).

Sun et al. used 3 lactate metabolism genes (FBP1, HADH, and TYMP) to establish a prognostic signature to predict the ccRCC prognosis (26). We compared the predictive efficacy of Sun with LRGPI (Figures 6G–J). LRGPI achieved comparable or higher predictive power with Sun in all cohorts, but only in the TCGA-KIRC did the difference in the AUC value reach a statistically significant level.

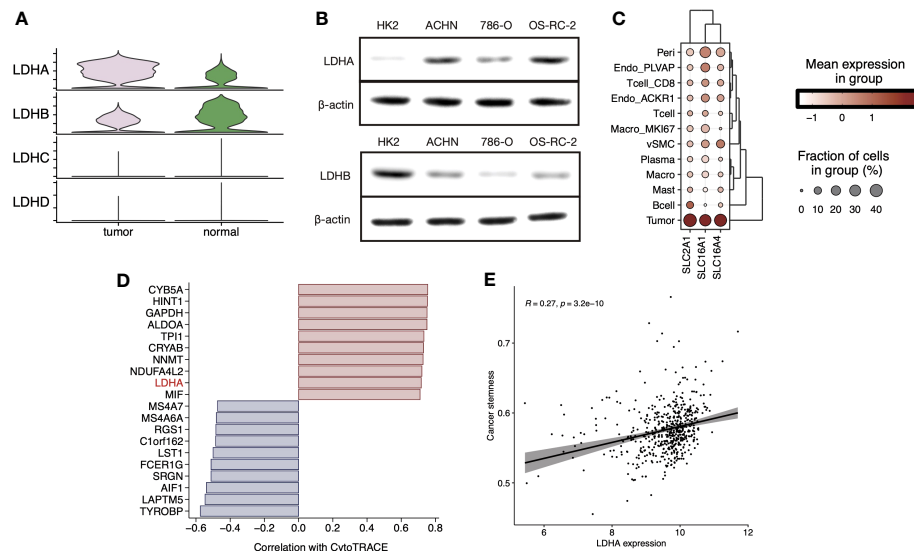


FIGURE 4

(A) Stacked violin plot displayed the expression level of LDHA, LDHB, LDHC, and LDHD in tumor and normal sample cells in sc-RNA Seq data (GSE159115). (B) LDHA and LDHB expression level were validated in RCC cell lines by Western blot. (C) Clustered dot plots of SLC2A1, SLC16A1, and SLC16A4 in tumor sample cells. (D) Bar plot showed the Pearson's correlation of the top20 genes with dedifferentiation status calculated by CytoTRACE. (E) Scatter plot with a linear regression correlation of LDHA expression and cancer stemness evaluated by PNAS stem gene set in TCGA-KIRC.

## Correlation of LRGPI and targeted therapy for ccRCC patients

E-MTAB-3267 included 53 patients with metastatic ccRCC treated with sunitinib and responsive labels. For Sun's lactate score, no significant difference in PFS between the high- and low-score groups was observed (Figure 7A). Patients were grouped according to Sunitinib responsiveness, and no significant differences in IRGPI or Sun's lactate score were observed between the two groups (Figures 7B, C). The Checkmate trial documented clinical data from patients who failed initial treatment with sunitinib, and among 130 advanced ccRCC patients with complete records, we found that while no significant difference in PFS between the high- and low-IRGPI groups was observed, patients in the low-IRGPI subgroup showed extended OS time (Figures 7D, E). To further validate our findings, ridge regression was run to calculate the estimated IC50 values for each tumor sample in the 4 cohorts (TCGA, E-MTAB1980, GPL570, and GPL10558) using drug sensitivity data (IC50 values) provided by GDSC for urological tumor cell lines. Simulation results for the four cohorts consistently showed significantly lower IC50 values for Sunitinib and Temsirolimus in the low-IRGPI subgroup samples than in the high-IRGPI subgroup samples (Figures 7F–I). Validation results from drug-sensitivity simulation extrapolation and real-world cohorts exhibited a high degree of consistency in terms of mechanistic target of rapamycin (mTOR)-targeted agents, suggesting that patients in the low-IRGPI subgroup could benefit from mTOR-targeted therapy.

## Correlation of LRGPI and immunotherapy benefit for ccRCC patients

According to the immunophenotype, inflammatory and lymphocyte-depleted ccRCC scored the lowest, and the wound-healing subtype scored the highest (Figure S5F). Using CIBERSORT to deconvolute the immune components, we found that the low-IRGPI subgroup harbored a significantly higher abundance of antigen-presenting cells (DCs, macrophages), monocytes, mast cells, and memory CD4<sup>+</sup> T cell infiltrates, whereas the high-IRGPI subgroup had a higher abundance of Treg (Figure 8A). We then performed GSEA analysis of 119 TME-related signals and found significant activation of important immune activation markers such as angiogenic genes (GPAGs), effector CD8<sup>+</sup> T, TCR signaling, antigen presentation signaling, MHC-II class signaling, natural killer cytotoxicity, and Merck18 signaling, as well as activation of ICB resistance signaling in the high-IRGPI subgroup (Figure 8B).

To clarify whether the immunoreactivity difference ultimately affects immunotherapy outcomes, we divided all patients in the Checkmate cohort into high- and low- LRGPI subgroups and found that patients in the low- IRGPI subgroup who received Nivolumab treatment showed no significant survival benefit beyond those who received Everolimus in terms of either PFS or OS (Figures S6A, B). However, patients in the high-IRGPI subgroup who received Nivolumab showed significantly longer OS time in comparison to those treated with Everolimus (Figures S6C, D). There are two possible explanations: either the high-IRGPI subgroup patients

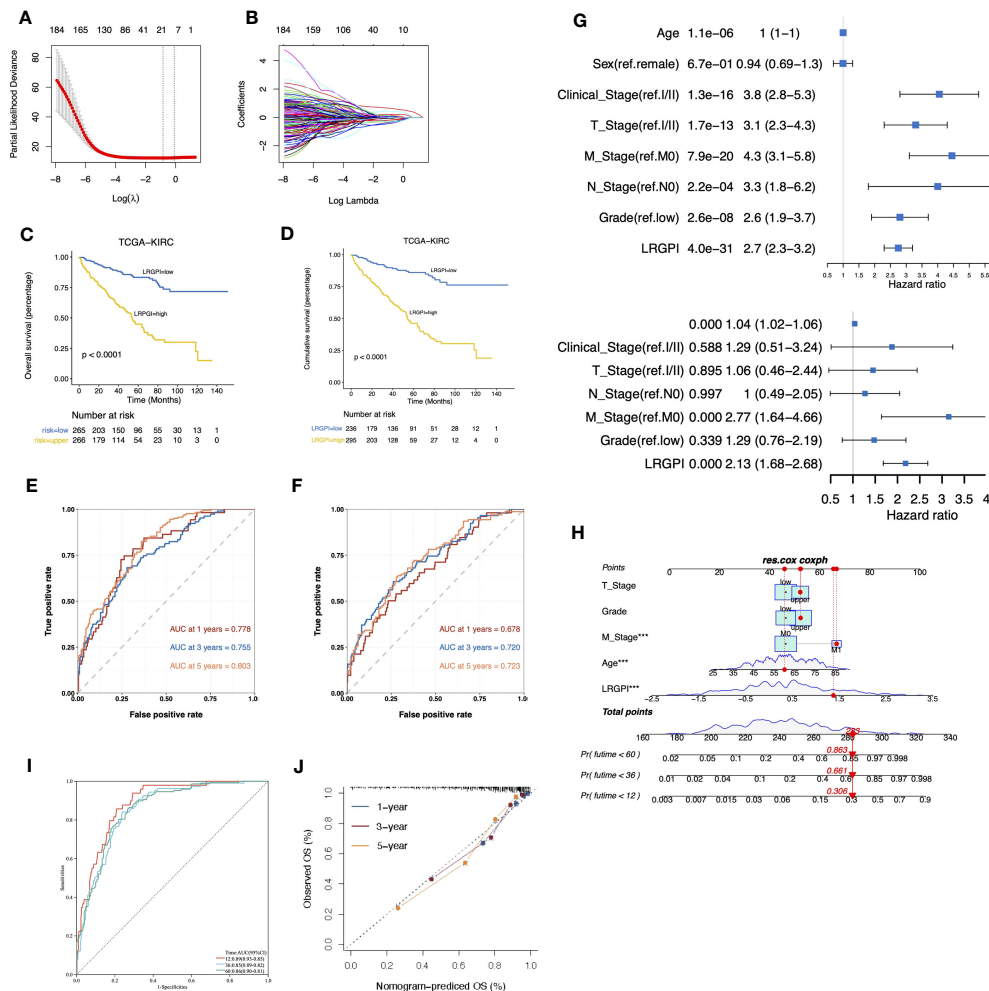


FIGURE 5

(A, B) The best combination of LMRG pairs was selected by adaptive-Lasso regression. (C, D) Survival analysis showed a different survival portion between the high- and low- LRGPI subgroups in TCGA-KIRC for OS (C) and DFS (D). (E, F) Time-dependent ROC curves evaluated the prediction capacity of LRGPI for OS (E) and DFS (F) in TCGA-KIRC cohort. (G) Forest plots of uni- and multivariate Cox regression models demonstrated that LRGPI is an independent risk factor for patients' prognosis. (H) Nomogram to predict patients' OS in TCGA-KIRC. The model incorporated the AJCC T stage, ISUP grade, metastatic status, patients' age, and LRGPI. (I) Time-dependent ROC curves to evaluate the prediction capacity of the nomogram for patients' OS. (J) Calibration curves evaluated the prediction accuracy of the nomogram for patients' OS. \*\*\* $p < 0.001$ .

were not the best population to benefit from Everolimus, or the high-IRGPI subgroup patients had a significant response to Nivolumab. To test the above conjecture, we performed a gene expression profile comparison using melanoma samples treated with CTLA4/PD-1 blockade. The results showed that the gene expression profiles of the high-IRGPI samples showed significant concordance with PD-1-responsive melanoma samples in the four cohorts (Figures 8C–F, Bonferroni adjusted  $p$ -value  $< 0.05$ ), demonstrating that the high-IRGPI samples were likely to respond to PD-1 blockade. High-IRGPI samples showed significantly higher levels of PD-1 expression in the four cohorts (Figures 8G–J).

The strategy of ICB plus TKI adjuvant therapy has pushed the adjuvant treatment of RCC into a new era, and the combination strategy is believed to be beneficial in reducing the multiple adverse effects of monotherapy and improving patient response rates (37). We then ask whether LRGPI has predictive value for the

combination treatment outcomes. The Javelin-101 trial enrolled 354 RCC patients treated with Avelumab plus Axitinib. Patients' survival differences were not observed when grouping patients based on median LRGPI values (Figure 8K). When PD-L1 staining positive or negative subgroups were compared (Figures 8L, M), we were ecstatic to discover that the high-IRGPI subgroup had significantly longer PFS among PD-L1 patients. This is an interesting finding, and more prospective clinical trial cohorts are needed to further validate our findings in the future.

## Discussion

It has been well known that the lactate content of tumor tissue is higher than that of normal tissue, and lactate is necessary for cancer development. Lactate-related coding genes, or lncRNA, have been identified and shown to have predictive value in cancers such as



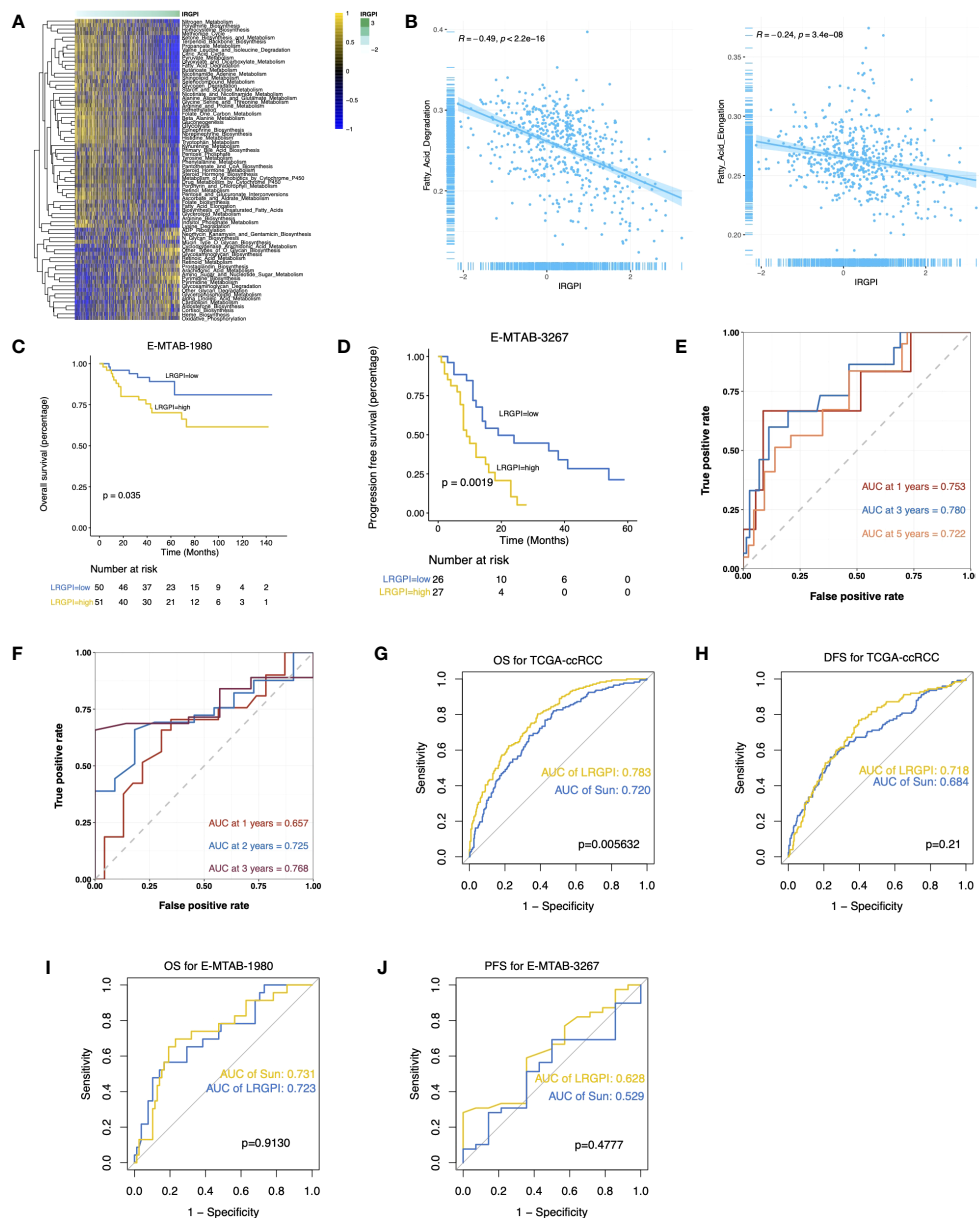


FIGURE 6

(A) Heatmap displays the differentially distributed cancer metabolism gene sets between high- and low-LRGPI subgroups in TCGA-KIRC cohort. The samples are ordered by LRGPI from lowest to highest. (B) Scatter plots with a linear regression correlation of LRGPI and fatty acid degradation and fatty acid elongation activity. (C, D) Survival analysis showed a different survival portion between the high- and low- LRGPI subgroups in E-MTAB-1980 for OS (C) and in E-MTAB-3267 for PFS (D). (E, F) Time-dependent ROC curves evaluated the prediction capacity of LRGPI for OS in E-MTAB-1980 (E) and for PFS in E-MTAB-3267 (F). (G–J) ROC curves displayed the prognosis prediction power of LRGPI and Sun's lactate score for patients' clinical outcomes in several cohorts.

colon cancer and lung cancer in thorough studies of tumor bulk tissue sequencing data (38, 39). The prognostic value of LMRGs in ccRCC was first discussed and reported by Sun et al. including 267 LMRGs involved in the lactate metabolic process, HP increased serum lactate, HP lactic acidosis, and HP lactic aciduria (26). Almost at the same time, Guo et al. focused on 27 genes involved in lactate metabolism and transport in ccRCC. In this presented report, we included 64 LMRGs from lactate metabolism, transporter proteins, and lactate dehydrogenase activity, which is a difference from previous reports (25). Here we constructed a novel prognostic

index, the IRGPI, and demonstrated the advantage of the LRGPI in distinguishing the prognosis of ccRCC patients. Compared to the previously developed lactate-related scoring system, re-assigning gene pairs by comparing the relative expression levels of genes within each gene pair to construct a scoring system has stability across detection platforms, which means that individual tumor scores can be easily reproduced through quantitative RT-PCR in clinical practice (40).

The combined multi-omics analysis revealed that the different expression levels of these LMRGs can be partially attributed to

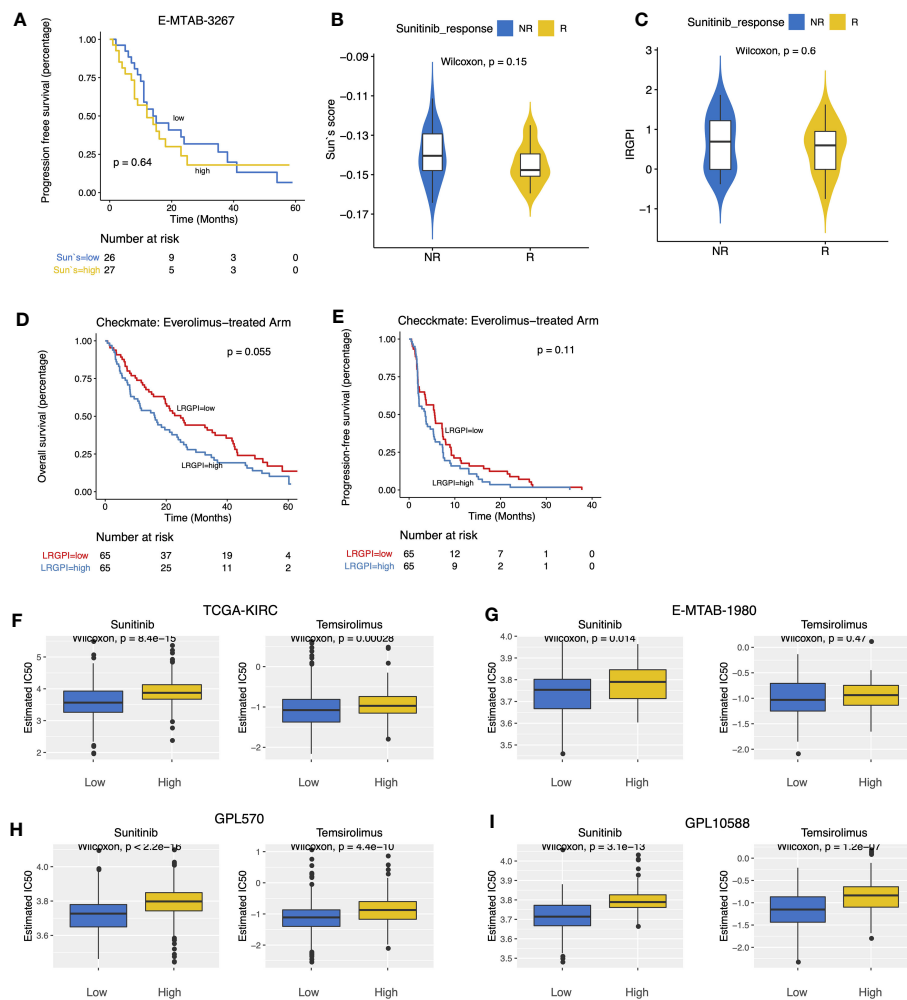
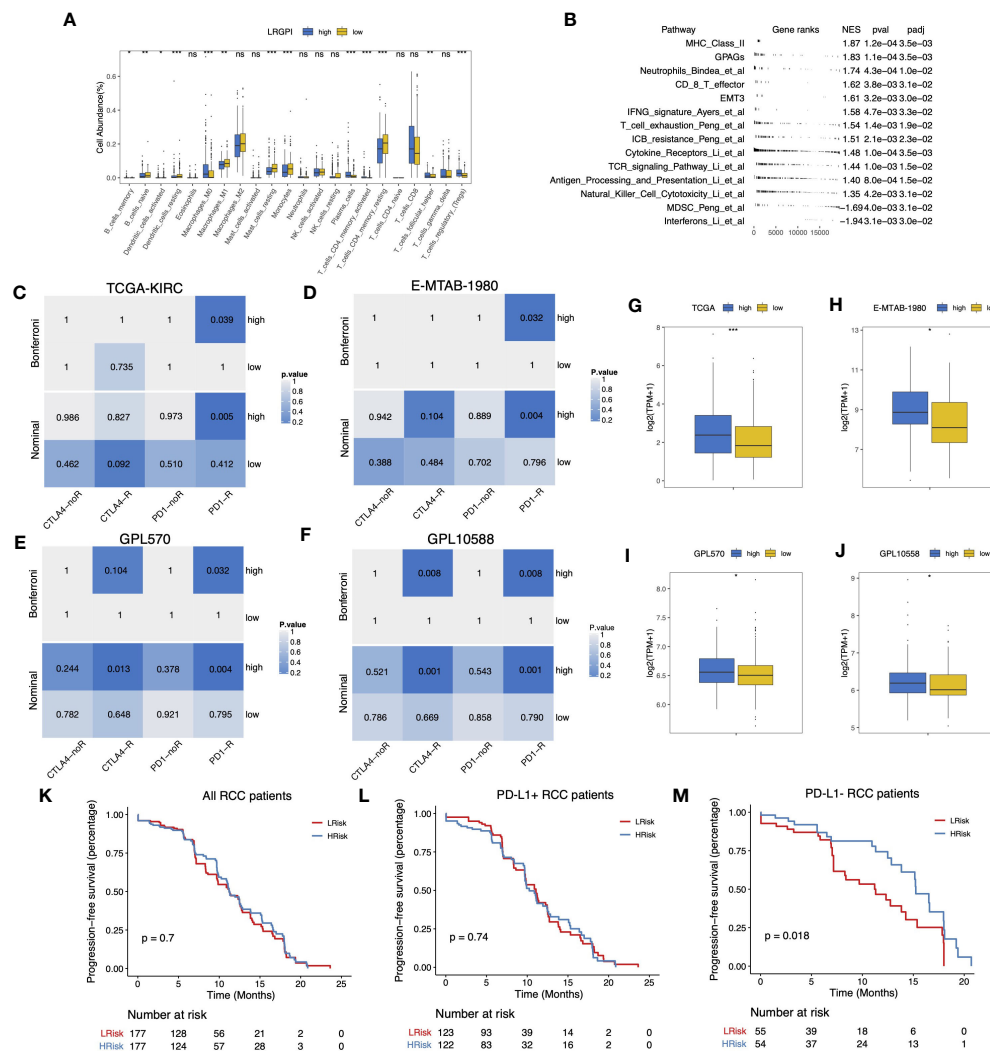


FIGURE 7

(A) Survival curves showed no significant difference in PFS between high- and low- Sun's lactate score subgroups. (B, C) Boxplots displayed the comparison of Sun's lactate score and LRGPi between the Sunitinib response and non-response samples. (D, E) Survival curves demonstrated that LRGPi was able to distinguish the OS (D) but not the PFS (E) in Everolimus-treated patients. (F–I) The predicted IC50 values of ccRCC samples for Sunitinib and Temsirolimus between high- and low- LRGPi groups in the TCGA-KIRC (F), E-MTAB-1980 (G), GPL570 (H), GPL10588 (I) cohorts.

changes in promoter methylation levels or to single-gene DNA copy number variation. We provide the first single-cell level evidence to confirm the disordered regulation of lactate metabolism, lactate transport processes, and lactate dehydrogenase activity in ccRCC tumor samples. We identified lactate metabolism markers for ccRCC cell types and found high expression levels of LDHA in tumor cells and CD8<sup>+</sup> T cells. Besides tumor cells, MCT1 was also expressed on Pericytes and endothelial cells, while MCT4 was expressed on vSMC. Meanwhile, we observed highly active lactate dehydrogenase in tumor cells, ACKR1<sup>+</sup> endothelial cells, MKI67<sup>+</sup> macrophages, CD8<sup>+</sup> T cells, and vSMC cells. Mild lactate metabolic activity was also observed in endothelial cells such as vSMC, Plasmacytes, Pericytes, and endothelial cells, but lactate transport was invariably inhibited in these cell types (Figure 3C). These findings suggest that vSMC cells act as the “producers” of lactic acid, while tumor cells and peripheral cells are the “consumers” under certain conditions. The phenomenon of tumor cells and vascular endothelial cells being able to survive, proliferate, and migrate in hypoxic environments has long been observed. The new

vascular system can withstand the challenging environment of fluctuating oxygen tension because to the choice of respiratory-independent metabolism in endothelial cells. In addition, the accumulation of lactic acid in tumors is achieved by inhibiting PHD2 and activating HIF1- $\alpha$  and NF- $\kappa$ B, and to a large extent, it contributes to the angiogenesis phenotype (41). The driving force of lactic acid promoting angiogenesis provides new therapeutic options without the drawbacks of traditional anti-angiogenic drugs for ccRCC (42, 43). Interestingly, despite such high lactate dehydrogenase activity in T cells and MKI67<sup>+</sup> macrophages, there is an apparent lack of lactate metabolic processes. Although this is consistent with the previously observed near absence of glycolytic activity in tumor-infiltrating T cells, no plausible mechanistic elaboration can be provided for this purpose (8, 44). Ubaldo et al. (45) first reported that lactic acid promotes stemness-related genes expression in breast cancer. Vineet et al. found that the LDHA product L-2 hydroxyglutamic acid (L-2HG) acts as an epigenetic modifier leading to H3 hypermethylation, thereby regulating stemness-related gene transcription in pancreatic tumors (46). To



**FIGURE 8**  
**(A)** Boxplot displayed the percentage of infiltrated immune cell types deconvoluted by CIBERSORT in TCGA-KIRC cohort. Wilcoxon test, ns,  $p > 0.05$ , \* $p < 0.05$ , \*\* $p < 0.01$ ; \*\*\* $p < 0.001$ . **(B)** GSEA table of significantly altered TME-related gene sets between high- and low-LRGPI subgroups in TCGA-KIRC cohort. **(C–F)** Heatmaps displayed the nominal and Bonferroni-corrected p-values of Subclass mapping results in the TI-KIRC **(C)**, E-MTAB-1980 **(D)**, GPL570 **(E)**, GPL10588 **(F)** cohorts. **(G–J)** Boxplots showed that PD-1 was higher expressed in the high-LRGPI groups in the TCGA-KIRC **(G)**, E-MTAB-1980 **(H)**, GPL570 **(I)**, GPL10588 **(J)** cohorts. **(K–M)** Survival curves showed that LRGPI was able to distinguish the PFS in PD-L1+ patients under Avelumab plus Axitinib treatment. ns,  $p < 0.05$ .

our knowledge, this is the first report to propose the correlation between LDHA and ccRCC stemness, and future elaborate experiments *in vivo* and *in vitro* are warranted to reveal the underlying mechanism.

Of note, Sun et al. reported that the low score samples were sensitive to Sunitinib and Temsirolimus, but did not validate their inference in a real-world cohort. We replicated the Sun's lactate score and validated it in E-MTAB-3267, but unfortunately failed to find the efficacy of the Sun's score in distinguishing sunitinib responsiveness or patients' prognosis. IRGPI was sufficient to distinguish the prognosis of Sunitinib-treated patients, but the difference between responders and non-responders in the real-world cohort also did not reach statistical significance. One possible reason is that the number of cases included in E-MTAB-

3267 was too small, and further validation in a larger cohort is desired. Our drug sensitivity simulation inference and real-world cohort validation confirmed the responsiveness of the low-LRGPI samples to Temsirolimus. The PI3K-Akt-mTOR-HIF axis drives cellular glycolysis and the Warburg effect, and its dysregulation is common in carcinogenesis (47). Thus, the intrinsic link between LRGPI and the responsiveness of mTOR-targeted therapy is not difficult to understand.

Proliferating tumor cells and activated immune cells exhibit enhanced metabolic activity, taking up large amounts of glucose to generate lactic acid via the Warburg effect and transporting the products for uptake by surrounding cells as energy-consuming substances or anabolic substrates. The idea that harmful lactate accumulation in the TME is one of the main causes of

immunosuppression has been widely recognized (47, 48). Lactate accumulation inhibits the viability and cytotoxic products of antitumor effector cells, such as CD8<sup>+</sup> T cells and NK cells, and promotes the differentiation and expansion of immunosuppressive cell populations, such as Treg, TAM, and MDSC (47). We investigated the relationship between LRGPI and the TME of ccRCC and found decreased antigen-presenting cells (DC, M1) and increased Treg/Tfh infiltration, as well as activation of CD8<sup>+</sup> T effector signaling, TCR signaling, IFN signaling, antigen-presenting signaling, and NK cytotoxicity in high-LRGPI samples. We also observed elevated PD-1 expression in high-IRGPI samples and similar gene expression patterns to PD-1-blockade responders. The inference and external validation demonstrate that high-LRGPI ccRCC samples would benefit from PD-1 blockade therapy. Recently, Kumagai et al. reported that lactate upregulates PD-1 expression on Treg through massive uptake by MCT1 but inhibits PD-1 expression in CD8<sup>+</sup> T cells. PD-1 blockade leading to Treg activation but not CD8<sup>+</sup> T cells is the main mechanism of lactate-induced ICB failure (49). In addition, it has been demonstrated that ICB plus lactate blockade/lactate dehydrogenase inhibitors synergistically reduce Treg function, resulting in a more potent anti-tumor capacity than ICB monotherapy (11). The use of the LDH inhibitor oxamate to reduce lactate production in combination with pembrolizumab significantly increased CD8<sup>+</sup> T cell infiltration in a humanized mouse model of non-small cell lung cancer and enhanced the effect of pembrolizumab monotherapy (50). We are aware that there are still no animal studies or clinical trials to test the lactate-targeted regimen in RCC. Based on these pan-cancer study facts, it is interesting to introduce the lactate-targeted strategy to RCC. Notably, lactate and its products have significant cell type-specific effects (51, 52). More detailed preclinical experiments are urgently needed to explore the biological response of immune cells to lactic acid changes before designing intervention strategies to precisely manipulate anti-tumor immunity. We have examined the guiding utility of LRGPI for patients undergoing combination therapy with ICB + TKI for the first time, in contrast to earlier studies on the establishment of prognostic markers for ccRCC. Interestingly, the findings showed that LRGPI is a significant factor in determining how patients with PD-L1-RCC would fare. Patients with greater oxygen transport and lipid metabolism activity in the arm receiving the combination of avelumab and Axitinib had longer PFS, according to the original study by Mozter et al (28). In an era where personalized treatment is increasingly emphasized, patient subgroup analysis reveals that the patient population for which the scoring system is applicable has more positive clinical significance.

This study has the inherent shortcomings of retrospective bioinformatics studies; using real-world tumor samples for PCR quantification of the LGRPI proposed in this study and validation of its prognostic guiding value in ccRCC, or even RCC of different pathological types, in different therapeutic contexts, will be the focus of the next research efforts. In immune cells, the lactate signaling pathway may be the link between metabolism and immunity. For example, how are key lactate metabolism and transport molecules

such as LDGA, GLUT1, MCT1, and MCT4 expressed in renal cancer cells, vSMC, endothelial cells, macrophages, CD8<sup>+</sup> T cells, and what are the effects on lactate uptake and utilization in cells? How does lactate in the microenvironment affect the aggregation and functional activation of immune cell populations dominated by macrophages and CD8<sup>+</sup> T cells? Due to article length constraints, exploration of the specific mechanisms by which lactate promotes kidney cancer progression and modulates the immune microenvironment will also be the focus of the next study.

## Conclusion

Altogether, this study illustrates the cellular specificity of lactate metabolism in ccRCC at the single-cell level. We proposed that LRGPI could be used to not only predict prognosis but also effectively distinguish frontline therapy responders in ccRCC patients.

## Data availability statement

The datasets presented in this study can be found in online repositories. The names of the repository/repositories and accession number(s) can be found in the article/[Supplementary Material](#).

## Author contributions

XL: Conceptualization, Formal Analysis, Investigation, Supervision, Writing – review & editing. GD: Data curation, Formal Analysis, Investigation, Methodology, Writing – original draft. LL: Validation, Visualization, Writing – review & editing. KP: Conceptualization, Data curation, Formal Analysis, Supervision, Writing – original draft.

## Funding

The authors declare that no financial support was received for the research, authorship, and/or publication of this article.

## Conflict of interest

The authors declare that the research was conducted in the absence of any commercial or financial relationships that could be construed as a potential conflict of interest.

## Publisher's note

All claims expressed in this article are solely those of the authors and do not necessarily represent those of their affiliated organizations, or those of the publisher, the editors and the



reviewers. Any product that may be evaluated in this article, or claim that may be made by its manufacturer, is not guaranteed or endorsed by the publisher.

## Supplementary material

The Supplementary Material for this article can be found online at: <https://www.frontiersin.org/articles/10.3389/fonc.2023.1253783/full#supplementary-material>

### SUPPLEMENTARY FIGURE 1

(A–D) Volcano plots of DELMRGs identified in the TCGA-KIRC, GPL570, GPL10588, and CPTAC-KIRC datasets. For CPTAC-KIRC cohort (D), protein expression level of PER2, SLC6A3, CDO1, SOCS2, TP53, APLN, and PRLR were not detected. Up-/down-regulated and not significantly altered LMRGs were labeled in red, blue, and yellow, respectively.

### SUPPLEMENTARY FIGURE 2

Representative normal and tumor tissue slides in HPA portal demonstrated the overall staining level of LDHA, HK2, NCOR2, CAV1, CCND1, OAS2, VEGFA, MED1, and PAM were significantly higher, while PFKFB2, LDHB, PNKD, LDHD, HAGH, SLC16A7, SLC5A12, GOT2, and SLC25A12 were lower in tumor renal cancer samples than normal samples.

### SUPPLEMENTARY FIGURE 3

(A–F) Violin plots of the AUCell-evaluated gene set enrichment scores in cell types of tumor samples.

### SUPPLEMENTARY FIGURE 4

Cell-specific molecular markers were identified by the FindAllMarkers function. Stacked violin plot displayed the expression level of key lactate metabolism-related genes in different cell types.

### SUPPLEMENTARY FIGURE 5

(A) GSEA table of significantly altered cancer hallmarks between high- and low-LRGPI subgroups in TCGA-KIRC cohort. (B) Forest plots of uni- and multi-variate Cox regression models demonstrated that LRGPI is an independent risk factor for patients' OS in E-MTAB-1980. (C) Nomogram to predict patients' OS in E-MTAB-1980. The model incorporated the AJCC T stage, ISUP grade, metastatic status, patients' age, and LRGPI. (D) Calibration curves evaluated the prediction accuracy of the nomogram for patients' OS in E-MTAB-1980. (E) Time-dependent ROC curves evaluated the prediction capacity of the nomogram for patients' OS in E-MTAB-1980. (F) Boxplot displayed the LRGPI of predefined immune subtypes of ccRCC.

### SUPPLEMENTARY FIGURE 6

(A, B) No significant survival difference was observed between Nivolumab- and Everolimus-treated groups in low-LRGPI subgroup patients. (C, D) Nivolumab showed significant overall survival benefit over Everolimus in high-LRGPI subgroup patients.

### SUPPLEMENTARY TABLE 1

The differentially expressed proteins identified in CPTAC-KIRC cohort.

### SUPPLEMENTARY TABLE 2

Cell markers of different cell types identified in sc-RNA seq GSE159115.

### SUPPLEMENTARY TABLE 3

The gene pairs and coefficients to replicate the LRGPI.

## References

- Xu D, Liao S, Li P, Zhang Q, Lv Y, Fu X, et al. Metabolomics coupled with transcriptomics approach deciphering age relevance in sepsis. *Aging Dis* (2019) 10:854–70. doi: 10.14336/AD.2018.1027
- García-Serrano AM, Mohr AA, Philippe J, Skoug C, Spégl P, Duarte JMN. Cognitive impairment and metabolite profile alterations in the hippocampus and cortex of male and female mice exposed to a fat and sugar-rich diet are normalized by diet reversal. *Aging Dis* (2022) 13:267–83. doi: 10.14336/AD.2021.0720
- Hanahan D, Weinberg RA. Hallmarks of cancer: the next generation. *Cell* (2011) 144:646–74. doi: 10.1016/j.cell.2011.02.013
- Husain Z, Seth P, Sukhatme VP. Tumor-derived lactate and myeloid-derived suppressor cells: Linking metabolism to cancer immunology. *Oncoimmunology* (2013) 2:e26383. doi: 10.4161/onci.26383
- Mu X, Shi W, Xu Y, Xu C, Zhao T, Geng B, et al. Tumor-derived lactate induces M2 macrophage polarization via the activation of the ERK/STAT3 signaling pathway in breast cancer. *Cell Cycle* (2018) 17:428–38. doi: 10.1080/15384101.2018.1444305
- Zhang J, Muri J, Fitzgerald G, Gorski T, Gianni-Barrera R, Masschelein E, et al. Endothelial lactate controls muscle regeneration from ischemia by inducing M2-like macrophage polarization. *Cell Metab* (2020) 31:1136–1153.e7. doi: 10.1016/j.cmet.2020.05.004
- Noe JT, Rendon BE, Geller AE, Conroy LR, Morrissey SM, Young LEA, et al. Lactate supports a metabolic-epigenetic link in macrophage polarization. *Sci Adv* (2021) 7:eabi8602. doi: 10.1126/sciadv.abi8602
- Reinfeld BI, Madden MZ, Wolf MM, Chytil A, Bader JE, Patterson AR, et al. Cell-programmed nutrient partitioning in the tumour microenvironment. *Nature* (2021) 593:282–8. doi: 10.1038/s41586-021-03442-1
- Zhang W, Wang G, Xu ZG, Tu H, Hu F, Dai J, et al. Lactate is a natural suppressor of RLR signaling by targeting MAVS. *Cell* (2019) 178:176–189.e15. doi: 10.1016/j.cell.2019.05.003
- Hermans D, Gautam S, García-Cañaveras JC, Gromer D, Mitra S, Spolski R, et al. Lactate dehydrogenase inhibition synergizes with IL-21 to promote CD8+ T cell stemness and antitumor immunity. *Proc Natl Acad Sci USA* (2020) 117:6047–55. doi: 10.1073/pnas.1920413117
- Gu J, Zhou J, Chen Q, Xu X, Gao J, Li X, et al. Tumor metabolite lactate promotes tumorigenesis by modulating MOESIN lactylation and enhancing TGF- $\beta$  signaling in regulatory T cells. *Cell Rep* (2022) 40:111122. doi: 10.1016/j.celrep.2022.111122
- Zhang D, Tang Z, Huang H, Zhou G, Cui C, Weng Y, et al. Metabolic regulation of gene expression by histone lactylation. *Nature* (2019) 574:575–80. doi: 10.1038/s41586-019-1678-1
- Varner EL, Trefely S, Bartee D, von Krusenstiern E, Izzo L, Bekeova C, et al. Quantification of lactoyl-CoA (lactyl-CoA) by liquid chromatography mass spectrometry in mammalian cells and tissues. *Open Biol* (2020) 10:200187. doi: 10.1098/rsob.200187
- Moreno-Yruela C, Zhang D, Wei W, Bæk M, Liu W, Gao J, et al. Class I histone deacetylases (HDAC1–3) are histone lysine deacetylases. *Sci Adv* (2022) 8. doi: 10.1126/sciadv.abi6696
- Girgis H, Masui O, White NM, Scorilas A, Rotondo F, Seivwright A, et al. Lactate dehydrogenase A is a potential prognostic marker in clear cell renal cell carcinoma. *Mol Cancer* (2014) 13:101–10. doi: 10.1186/1476-4598-13-101
- Zhao J, Huang X, Xu Z, Dai J, He H, Zhu Y, et al. LDHA promotes tumor metastasis by facilitating epithelial–mesenchymal transition in renal cell carcinoma. *Mol Med Rep* (2017) 16:8335–44. doi: 10.3892/mmr.2017.7637
- Wang X, Xu L, Wu Q, Liu M, Tang F, Cai Y, et al. Inhibition of LDHA deliver potential anticancer performance in renal cell carcinoma. *UIN* (2017) 99:237–44. doi: 10.1159/000445125
- Miranda-Gonçalves V, Lameirinhas A, Macedo-Silva C, Lobo J, C Dias P, Ferreira V, et al. Lactate increases renal cell carcinoma aggressiveness through sirtuin 1-dependent epithelial mesenchymal transition axis regulation. *Cells* (2020) 9:1053. doi: 10.3390/cells9041053
- Shirotake S, Takamatsu K, Mizuno R, Kaneko G, Nishimoto K, Oya M, et al. Serum lactate dehydrogenase before nivolumab treatment could be a therapeutic prognostic biomarker for patients with metastatic clear cell renal cell carcinoma. *Anticancer Res* (2019) 39:4371–7. doi: 10.21873/anticancer.13606
- Shen J, Chen Z, Zhuang Q, Fan M, Ding T, Lu H, et al. Prognostic value of serum lactate dehydrogenase in renal cell carcinoma: A systematic review and meta-analysis. *PLoS One* (2016) 11:e0166482. doi: 10.1371/journal.pone.0166482
- Li T, Li H, Xie S, Tan Y, Xie Z-P, Li W-Y, et al. Lactate dehydrogenase-to-lymphocyte ratio represents a powerful prognostic tool of metastatic renal cell carcinoma patients treated with tyrosine kinase inhibitors. *Pathol Oncol Res* (2020) 26:1319–24. doi: 10.1007/s12253-019-00707-z
- Zhang N, Zhang H, Zhu D, JiRiGaLa, Yu D, Wang C, et al. Prognostic role of pretreatment lactate dehydrogenase in patients with metastatic renal cell carcinoma: A systematic review and meta-analysis. *Int J Surg* (2020) 79:66–73. doi: 10.1016/j.jisu.2020.05.019
- de Carvalho PA, Bonatelli M, Cordeiro MD, Coelho RF, Reis S, Srougi M, et al. MCT1 expression is independently related to shorter cancer-specific survival in clear cell renal cell carcinoma. *Carcinogenesis* (2021) 42:1420–7. doi: 10.1093/carcin/bgab100

24. Kim Y, Choi J-W, Lee J-H, Kim Y-S. Expression of lactate/H<sup>+</sup> symporters MCT1 and MCT4 and their chaperone CD147 predicts tumor progression in clear cell renal cell carcinoma: immunohistochemical and The Cancer Genome Atlas data analyses. *Hum Pathol* (2015) 46:104–12. doi: 10.1016/j.humpath.2014.09.013
25. Guo T, Zhang J, Wang T, Yuan Z, Tang H, Zhang D, et al. Lactic acid metabolism and transporter related three genes predict the prognosis of patients with clear cell renal cell carcinoma. *Genes (Basel)* (2022) 13:620. doi: 10.3390/genes13040620
26. Sun Z, Tao W, Guo X, Jing C, Zhang M, Wang Z, et al. Construction of a lactate-related prognostic signature for predicting prognosis, tumor microenvironment, and immune response in kidney renal clear cell carcinoma. *Front Immunol* (2022) 13. doi: 10.3389/fimmu.2022.818984
27. Braun DA, Hou Y, Bakouny Z, Ficial M, Sant' Angelo M, Forman J, et al. Interplay of somatic alterations and immune infiltration modulates response to PD-1 blockade in advanced clear cell renal cell carcinoma. *Nat Med* (2020) 26:909–18. doi: 10.1038/s41591-020-0839-y
28. Motzer RJ, Robbins PB, Powles T, Albiges L, Haanen JB, Larkin J, et al. Avelumab plus axitinib versus sunitinib in advanced renal cell carcinoma: biomarker analysis of the phase 3 JAVELIN Renal 101 trial. *Nat Med* (2020) 26:1733–41. doi: 10.1038/s41591-020-1044-8
29. Zhou P, Hu H, Lu Y, Xiao J, Wang Y, Xun Y, et al. Cancer stem/progenitor signatures refine the classification of clear cell renal cell carcinoma with stratified prognosis and decreased immunotherapy efficacy. *Mol Therapy: Oncolytics* (2022) 27:167–81. doi: 10.1016/j.omto.2022.10.005
30. Gulati GS, Sikandar SS, Wesche DJ, Manjunath A, Bharadwaj A, Berger MJ, et al. Single-cell transcriptional diversity is a hallmark of developmental potential. *Science* (2020) 367:405–11. doi: 10.1126/science.aax0249
31. Miranda A, Hamilton PT, Zhang AW, Pattnaik S, Becht E, Mezheyeuski A, et al. Cancer stemness, intratumoral heterogeneity, and immune response across cancers. *Proc Natl Acad Sci USA* (2019) 116:9020–9. doi: 10.1073/pnas.1818210116
32. Lu X, Meng J, Zhu J, Zhou Y, Jiang L, Wang Y, et al. Prognosis stratification and personalized treatment in bladder cancer through a robust immune gene pair-based signature. *Clin Transl Med* (2021) 11. doi: 10.1002/ctm2.453
33. Zeng D, Ye Z, Shen R, Yu G, Wu J, Xiong Y, et al. IOBR: multi-omics immunology biological research to decode tumor microenvironment and signatures. *Front Immunol* (2021) 12:687975. doi: 10.3389/fimmu.2021.687975
34. Zhou P, Liu Z, Hu H, Lu Y, Xiao J, Wang Y, et al. Comprehensive analysis of senescence characteristics defines a novel prognostic signature to guide personalized treatment for clear cell renal cell carcinoma. *Front Immunol* (2022) 13:901671. doi: 10.3389/fimmu.2022.901671
35. Roh W, Chen P-L, Reuben A, Spencer CN, Prieto PA, Miller JP, et al. Integrated molecular analysis of tumor biopsies on sequential CTLA-4 and PD-1 blockade reveals markers of response and resistance. *Sci Transl Med* (2017) 9:eaa3560. doi: 10.1126/scitranslmed.aah3560
36. Zhang Y, Narayanan SP, Mannan R, Raskind G, Wang X, Vats P, et al. Single-cell analyses of renal cell cancers reveal insights into tumor microenvironment, cell of origin, and therapy response. *Proc Natl Acad Sci USA* (2021) 118:e2103240118. doi: 10.1073/pnas.2103240118
37. Massari F, Rizzo A, Mollica V, Rosellini M, Marchetti A, Ardizzoni A, et al. Immune-based combinations for the treatment of metastatic renal cell carcinoma: a meta-analysis of randomised clinical trials. *Eur J Cancer* (2021) 154:120–7. doi: 10.1016/j.ejca.2021.06.015
38. Mai S, Liang L, Mai G, Liu X, Diao D, Cai R, et al. Development and validation of lactate metabolism-related lncRNA signature as a prognostic model for lung adenocarcinoma. *Front Endocrinol (Lausanne)* (2022) 13:829175. doi: 10.3389/fendo.2022.829175
39. Zhu D, Jiang Y, Cao H, Yang J, Shu Y, Feng H, et al. Lactate: A regulator of immune microenvironment and a clinical prognosis indicator in colorectal cancer. *Front Immunol* (2022) 13:876195. doi: 10.3389/fimmu.2022.876195
40. Li B, Cui Y, Diehn M, Li R. Development and validation of an individualized immune prognostic signature in early-stage nonsquamous non-small cell lung cancer. *JAMA Oncol* (2017) 3:1529–37. doi: 10.1001/jamaoncol.2017.1609
41. Polet F, Feron O. Endothelial cell metabolism and tumour angiogenesis: glucose and glutamine as essential fuels and lactate as the driving force. *J Intern Med* (2013) 273:156–65. doi: 10.1111/joim.12016
42. Li D-X, Feng D-C, Shi X, Wu R-C, Chen K, Han P. Identification of endothelial-related molecular subtypes for bladder cancer patients. *Front Oncol* (2023) 13:1101055. doi: 10.3389/fonc.2023.1101055
43. Li D-X, Yu Q-X, Zeng C-X, Ye L-X, Guo Y-Q, Liu J-F, et al. A novel endothelial-related prognostic index by integrating single-cell and bulk RNA sequencing data for patients with kidney renal clear cell carcinoma. *Front Genet* (2023) 14:1096491. doi: 10.3389/fgene.2023.1096491
44. Chang C-H, Qiu J, O'Sullivan D, Buck MD, Noguchi T, Curtis JD, et al. Metabolic competition in the tumor microenvironment is a driver of cancer progression. *Cell* (2015) 162:1229–41. doi: 10.1016/j.cell.2015.08.016
45. Martinez-Outschoorn UE, Prisco M, Ertel A, Tsigirgos A, Lin Z, Pavlides S, et al. Ketones and lactate increase cancer cell “stemness,” driving recurrence, metastasis and poor clinical outcome in breast cancer: achieving personalized medicine via Metabolo-Genomics. *Cell Cycle* (2011) 10:1271–86. doi: 10.4161/cc.10.8.15330
46. Gupta VK, Sharma NS, Durden B, Garrido VT, Kesh K, Edwards D, et al. Hypoxia-driven oncometabolite L-2HG maintains stemness-differentiation balance and facilitates immune evasion in pancreatic cancer. *Cancer Res* (2021) 81:4001–13. doi: 10.1158/0008-5472.CAN-20-2562
47. Heuser C, Renner K, Kreutz M, Gattinoni L. Targeting lactate metabolism for cancer immunotherapy - a matter of precision. *Semin Cancer Biol* (2022) 88:32–45. doi: 10.1016/j.semcancer.2022.12.001
48. Apostolova P, Pearce EL. Lactic acid and lactate: revisiting the physiological roles in the tumor microenvironment. *Trends Immunol* (2022) 43:969–77. doi: 10.1016/j.it.2022.10.005
49. Kumagai S, Koyama S, Itahashi K, Tanegashima T, Lin YT, Togashi Y, et al. Lactic acid promotes PD-1 expression in regulatory T cells in highly glycolytic tumor microenvironments. *Cancer Cell* (2022) 40:201–218.e9. doi: 10.1016/j.ccell.2022.01.001
50. Qiao T, Xiong Y, Feng Y, Guo W, Zhou Y, Zhao J, et al. Inhibition of LDH-A by oxamate enhances the efficacy of anti-PD-1 treatment in an NSCLC humanized mouse model. *Front Oncol* (2021) 11:632364. doi: 10.3389/fonc.2021.632364
51. Elia I, Haigis MC. Metabolites and the tumour microenvironment: from cellular mechanisms to systemic metabolism. *Nat Metab* (2021) 3:21–32. doi: 10.1038/s42255-020-00317-z
52. Kaymak I, Luda KM, Duimstra LR, Ma EH, Longo J, Dahabieh MS, et al. Carbon source availability drives nutrient utilization in CD8<sup>+</sup> T cells. *Cell Metab* (2022) 34:1298–1311.e6. doi: 10.1016/j.cmet.2022.07.012

## Glossary

|        |  |
|--------|--|
| CPTAC  | Clinical Proteomic Tumor Analysis Consortium             |
| HPA    | the Human Protein Atlas                                  |
| MDSC   | myeloid-derived suppressive cell                         |
| TAM    | tumor-associated macrophage                              |
| TME    | tumor microenvironment                                   |
| EMT    | epithelial-mesenchymal transition                        |
| ccRCC  | Clear cell renal cell carcinoma                          |
| OS     | overall survival   |
| PFS    | progression free survival                                |
| CSS    | cancer-specific survival                                 |
| DFS    | disease-free survival                                    |
| LMRG   | lactate metabolism-related genes                         |
| ICB    | Immune checkpoint blockade                               |
| LMRGP  | lactate metabolism-related gene pair                     |
| LRGPI  | Lactate-related gene pair index                          |
| Sc-RNA | seg Single-cell RNA sequencing                           |
| FPKM   | fragments Per Kilobase Million                           |
| TPM    | transcripts Per Kilobase Million                         |
| CNV    | copy number variation                                    |
| DEG    | differentially expressed gene                            |
| DELMRG | differentially expressed lactate metabolism-related gene |
| AUC    | area under curve   |
| ROC    | receptor operative curve                                 |
| ssGSEA | Single sample gene set enrichment analysis               |
| TKI    | Tyrosine kinase inhibitors                               |
| mTOR   | Mechanistic target of rapamycin                          |



## OPEN ACCESS

## EDITED BY

Juan Carlos Gallardo-Pérez,  
National Institute of Cardiology Ignacio  
Chavez, Mexico

## REVIEWED BY

Claudia Volpi,  
University of Perugia, Italy  
Dyah Laksmi Dewi,  
Gadjah Mada University, Indonesia

## \*CORRESPONDENCE

Johannes F. Fahrman  
✉ jffahrman@mdanderson.org

<sup>†</sup>These authors have contributed equally to  
this work

RECEIVED 11 July 2023

ACCEPTED 22 September 2023

PUBLISHED 09 October 2023

## CITATION

León-Letelier RA, Dou R, Vykoukal J,  
Sater AHA, Ostrin E, Hanash S and  
Fahrman JF (2023) The kynurenine  
pathway presents multi-faceted  
metabolic vulnerabilities in cancer.  
*Front. Oncol.* 13:1256769.  
doi: 10.3389/fonc.2023.1256769

## COPYRIGHT

© 2023 León-Letelier, Dou, Vykoukal, Sater,  
Ostrin, Hanash and Fahrman. This is an  
open-access article distributed under the  
terms of the [Creative Commons Attribution  
License \(CC BY\)](#). The use, distribution or  
reproduction in other forums is permitted,  
provided the original author(s) and the  
copyright owner(s) are credited and that  
the original publication in this journal is  
cited, in accordance with accepted  
academic practice. No use, distribution or  
reproduction is permitted which does not  
comply with these terms.

# The kynurenine pathway presents multi-faceted metabolic vulnerabilities in cancer

Ricardo A. León-Letelier<sup>1†</sup>, Rongzhang Dou<sup>1†</sup>, Jody Vykoukal<sup>1</sup>,  
Ali Hussein Abdel Sater<sup>1</sup>, Edwin Ostrin<sup>2</sup>, Samir Hanash<sup>1</sup>  
and Johannes F. Fahrman<sup>1\*</sup>

<sup>1</sup>Department of Clinical Cancer Prevention, The University of Texas MD Anderson Cancer Center,  
Houston, TX, United States, <sup>2</sup>Department of General Internal Medicine, The University of Texas MD  
Anderson Cancer Center, Houston, TX, United States

The kynurenine pathway (KP) and associated catabolites play key roles in promoting tumor progression and modulating the host anti-tumor immune response. To date, considerable focus has been on the role of indoleamine 2,3-dioxygenase 1 (IDO1) and its catabolite, kynurenine (Kyn). However, increasing evidence has demonstrated that downstream KP enzymes and their associated metabolite products can also elicit tumor-microenvironment immune suppression. These advancements in our understanding of the tumor promotive role of the KP have led to the conception of novel therapeutic strategies to target the KP pathway for anti-cancer effects and reversal of immune escape. This review aims to 1) highlight the known biological functions of key enzymes in the KP, and 2) provide a comprehensive overview of existing and emerging therapies aimed at targeting discrete enzymes in the KP for anti-cancer treatment.

## KEYWORDS

kynurenine pathway (KP), cancer, metabolism, therapeutics, immune evasion

## 1 Introduction

The kynurenine pathway (KP) has been recognized as a key mediator of tumor immune escape (1–3). Three enzymes, indoleamine 2,3-dioxygenase 1 and 2 (IDO1, IDO2) and tryptophan 2,3-dioxygenase (TDO) initiate the first steps in the KP, converting tryptophan (Trp) to N-formyl-kynurenine, which can be further metabolized by arylformamidase (AFMID) yielding the immunosuppressive catabolite kynurenine (Kyn). Whereas TDO is predominately expressed in the liver and accounts for the majority of Trp metabolism, IDO-mediated metabolism predominately occurs secondary to inflammation (4, 5). Upregulation of IDO in tumor cells or antigen-presenting cells leads to Trp depletion and accumulation of its downstream catabolite Kyn in the local tumor



microenvironment (TME), resulting in immunosuppression by inducing T cell anergy and apoptosis and suppressing T cell differentiation (1–3, 6–9). Building upon this underlying biological mechanism, substantial efforts have been dedicated to the development of small molecule inhibitors and agonists targeting the KP as anti-cancer agents to circumvent tumor immune suppression. Among the most investigated IDO inhibitors are epacadostat, navoximod, and indoximod, each of which have been explored as a monotherapy and in combination with immune check-point inhibitors (ICI) and/or chemotherapy (10–21). Despite early success in Phase I/II clinical trials, ECHO-202/KEYNOTE-037 failed to demonstrate additional benefit of epacadostat in combination with pembrolizumab (10) and similar findings have since been reported for navoximod with atezolizumab (19), raising uncertainty about the benefits of targeting IDO1 for anti-cancer treatment.

Yet, it is increasingly recognized that, beyond the well covered Trp-IDO-Kyn axis, other enzymes in the KP along with their associated catabolites can modulate the TME to evade immune surveillance and enable tumor progression (22–26). Moreover, emerging data suggests that KP-related enzymes, such as IDO1, can promote tumor progression through functions that are independent of enzymatic activity (27). The purpose of this review is to 1) highlight the known tumor promotive functions of key enzymes in the KP and 2) provide a comprehensive overview of

existing and emerging therapies aimed at targeting discrete enzymes in the KP for anti-cancer treatment.

## 2 Role of the kynurenine pathway in cancer development and immune suppression

### 2.1 Indoleamine 2,3-dioxygenase 1

Indoleamine 2,3-dioxygenase 1 (IDO1) is a rate-limiting enzyme in the metabolism of the essential amino acid Trp into downstream kynurenines (Figure 1) (7). Under physiological conditions, the IDO1 functions to generate cellular nicotinamide adenine dinucleotide (NAD<sup>+</sup>). However, IDO1 is overexpressed in several cancer types (28, 29) and is prognostic for poor disease-free survival and overall survival (30, 31).

Seminal studies by Munn and colleagues demonstrated that reduced bioavailability of Trp due to IDO overactivation in dendritic cells (DCs) leads to accumulation of uncharged Trp-tRNAs in T cells and that the accumulation of Trp-tRNAs induces integrated stress response kinase (GCN2)-mediated suppression of the translation initiation factor 2a (eIF2a) resulting in subsequent cell growth arrest (6). Tryptophan starvation-mediated activation of GCN2 has also been shown to down-regulate the T cell receptor

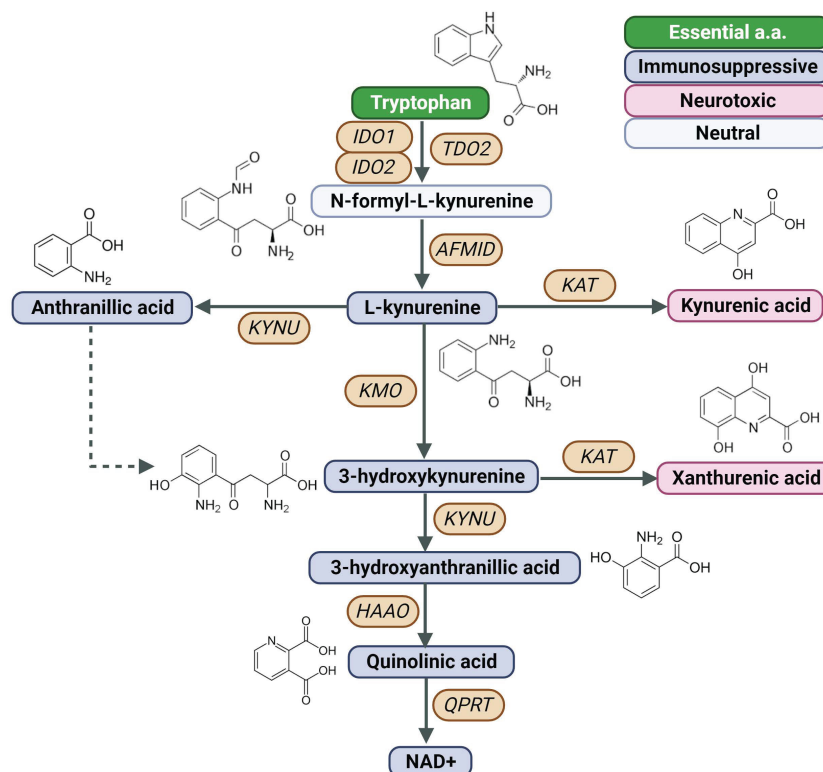


FIGURE 1

Created with BioRender.com. Schematic of the KP, Kynurenine Pathway; AFMID, arylformamidase; HAAO, 3-hydroxyanthranilate 3,4-dioxygenase; IDO1, indoleamine 2,3-dioxygenase 1; IDO2, indoleamine 2,3-dioxygenase 2; KAT, kynurenine aminotransferase; KMO, kynurenine 3-monooxygenase; KYNU, kynureninase; NAD<sup>+</sup>, nicotinamide adenine dinucleotide; TDO2, tryptophan 2,3-dioxygenase; QPRT, quinolinic acid phosphoribosyl transferase.

(TCR) zeta-chain in naïve T cells, resulting in diminished T cell function (32). Another study demonstrated a GCN2-independent mechanism whereby IDO-mediated catabolism of Trp inhibits immunoregulatory kinases mTOR and PKC resulting in induction of autophagy and immunosuppression (18). Subsequent studies demonstrated that IDO-mediated catabolism of Trp results in the accumulation of Kyn (7) that stimulates ligand-activated transcription factor aryl hydrocarbon receptor (AhR) signaling and promotes the generation of immune-tolerant DCs and regulator T cells (Tregs) (1, 7, 8). To this end, Liu and colleagues demonstrated that interferon-gamma (IFN $\gamma$ ) produced by cytotoxic CD8+ T cells stimulates Kyn release by tumor-repopulating cells (TRCs) and that TRC-derived Kyn is subsequently taken up by CD8+ T cells through TCR-mediated upregulation of solute carrier family 7 member 8 (SLC7A8) and Solute Carrier Family 36 Member 4 (SLC36A4, also known as PAT4), resulting in Kyn-AhR-mediated upregulation of programmed cell death protein 1 (PD-1) (33). Inhibition of IDO1 in CD8+ T cells promoted Trp accumulation and downregulation of PD-1 (34). Another study found that IFN $\gamma$  secreted by acute myeloid leukemia (AML) cells upregulated IFN $\gamma$ -dependent genes related to Treg induction, including IDO1, in mesenchymal stromal cells (MSCs). Genetic ablation of IFN $\gamma$  production by AML cells reduced MSC IDO1 expression and Treg infiltration, thereby attenuating AML engraftment (35).

The IDO1-Kyn-AhR axis has also been shown to impair natural killer (NK) cell and macrophage function. Specifically, Kyn inhibits expression of the natural cytotoxicity triggering receptor 1 (NCR1, also known as NKp46) and killer cell lectin like receptor K1 (KLRK1, also referred to as NKG2D) on NK cells resulting in impaired tumor-killing functions (36, 37). Recently, Fang and colleagues demonstrated that IDO1 regulates expression of ADAM metallopeptidase domain 10 (ADAM10) via IDO1-Kyn-AhR pathway in non-small cell lung cancer (NSCLC) cells and that the induction of ADAM10 downregulates the NKG2D Ligand (NKG2DL). Targeting of IDO1 via RY103, a novel IDO1 inhibitor, improved NK cell-mediate anti-tumor activity in xenograft mouse models of lung cancer (38). Takenaka and colleagues reported that increased IDO-mediated release of Kyn by glioblastoma cells promotes AhR activation in tumor-associated macrophages (TAMs); activation of AhR signaling in TAMs increased expression of the ectonucleotidase CD39 and accumulation of adenosine in the tumor microenvironment (TME) leading to suppression of CD8+ T cell function (39). Interestingly, studies by Campesato and colleagues reported that IDO-Kyn-AhR-mediated immunosuppression depends on the interplay between Tregs and TAMs (40). Using a preclinical mouse model of B16-F10 melanoma overexpressing IDO1 (B16<sup>IDO</sup>), authors demonstrated that IDO-expressing tumors have marked increases in Treg frequency and upregulated expression of FoxP3 in tumor infiltrating CD4+ T cells compared to B16<sup>WT</sup>-tumor bearing mice. Concomitant to Tregs was an increased abundance of TAMs (CD11b+F4/80highLy6G<sup>-</sup>) that accumulated during tumor progression. Gene expression analyses of B16<sup>IDO</sup>-derived Tregs and TAMs revealed prominent upregulation of AhR and AhR-responsive genes. Depletion of macrophages with  $\alpha$ CSF1-R or clodronate liposomes delayed the progression of IDO-

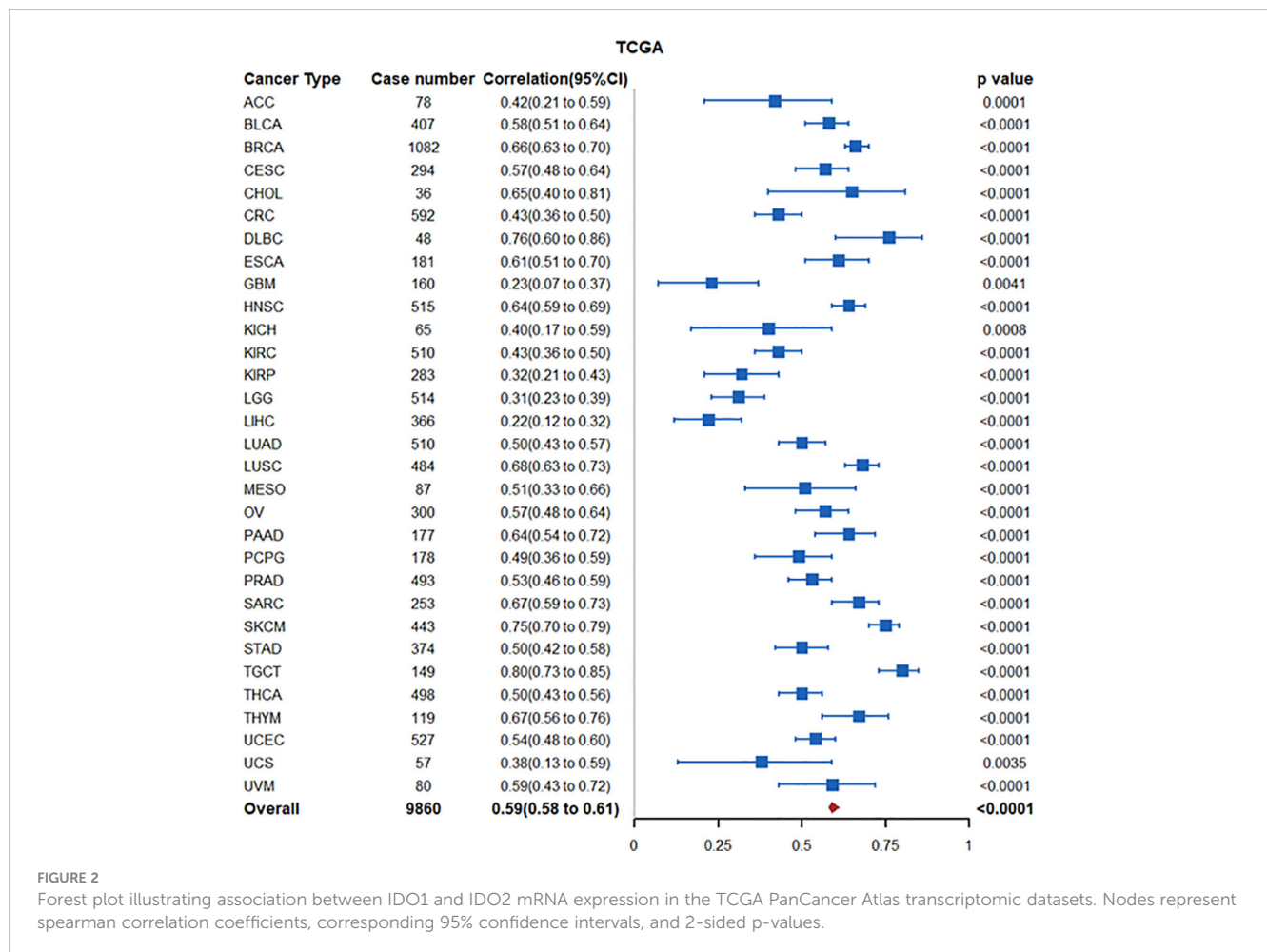
expressing tumors but not wild-type tumors, an effect that could be reversed upon CD8+ T cell depletion. Similarly, specific depletion of Tregs using Foxp3DTR mice significantly abrogated the myeloid-enriched phenotype found in B16<sup>IDO</sup> tumors, with reduced infiltration of CD11b+ cells and M2-like TAMs after treatment with DT. Co-culture experiments further demonstrated that Treg inhibitor function and expansion of M2-like macrophages was dependent on Kyn-AhR signaling (40).

Whereas IDO1 has largely been studied in the context of Trp-IDO1-Kyn-AhR signaling, IDO1 may also promote tumor progression through non-enzymatic functions (27). To this end, IDO1 can act as a signal-transducing molecule via two immunoreceptor Tyrosine-based inhibitory motifs (ITIMs) in the non-enzymatic domain of the enzyme. Phosphorylation of the ITIMs promotes interaction with SHP family tyrosine phosphatases (41, 42). Moreover, IDO1 can directly bind class IA PI3K regulatory subunits, resulting in IDO1 anchoring to early endosomes and activation of ITIM-mediated signaling (43).

In the context of cancer, using B16-F10 mouse melanoma cells transfected with either the wild-type *Ido1* gene (*Ido1*<sup>WT</sup>) or a mutated variant lacking the catalytic, but not signaling activity (*Ido1*<sup>H350A</sup>), Orecchini and colleagues demonstrated that IDO1 promote tumor growth by increasing SHP-2-mediated activation of Ras and Erk signaling *in vitro* and *in vivo*. Furthermore, B16<sup>H350A</sup> tumor bearing mice exhibited markedly enhanced tumor growth, and worse overall survival compared to B16<sup>wt</sup> or B16<sup>mock</sup> control mice. Immunophenotyping of tumors indicated that B16<sup>H350A</sup> tumors had lower IFN $\gamma$ -producing CD4+ and CD8+ T lymphocytes and a significantly higher percentage of CD4<sup>+</sup>Fox3p<sup>+</sup> Tregs compared to respective controls (27). Zhai and colleagues established IDO-deficient glioblastoma (GBM) cell lines reconstituted with IDO wild-type or IDO enzyme-null cDNA to assess tumor promotive roles of IDO1 independent of its catalytic activity. They found that nonenzymatic tumor cell IDO1 activity increased expression of complement factor H (CFH) and its isoform, factor H like protein (FHL-1) in human GBM, resulting in increased intratumoral Tregs and myeloid-derived suppressor cells, accelerated tumor growth and poor survival (44). These findings highlight an increasingly appreciated role of IDO1 in signal transduction, and, importantly, underscore an alternative mechanism of IDO1-mediated immune suppression that may not be impeded by small molecule IDO inhibitors.

## 2.2 Indoleamine 2,3-dioxygenase 2

The IDO1 paralogue IDO2 is another enzyme involved in the catabolism of tryptophan to downstream kynurenines. *INDOL1*, the encoding gene for IDO2, is located on chromosome 8p12 near *INDO* (located on chromosome 8p11), the encoding gene for IDO1 (45). In The Cancer Genome Atlas (TCGA)-PanCancer Atlas transcriptomic datasets, increased tumoral IDO2 is highly correlated with IDO1 expression (Spearman  $\rho$  coefficient: 0.59 (95% CI: 0.58-0.61)) (Figure 2), suggesting potential co-regulation (46). In this regard, studies by Kado and colleagues demonstrated that 2,3,7,8-tetrachlorodibenzo-p-dioxin (TCDD)-mediated



activation of AhR signaling increased IDO2 expression in wildtype MCF7 breast cancer cells but not in CRISPR-cas9 AhR-knockout MCF-7 cells. Promoter analyses identified short-tandem repeat containing four core sequences of a xenobiotic response element (XRE) upstream of the start site of the human *ido2* gene, reinforcing AhR as an upstream regulator (47). TCDD-mediated AhR activation in DC cells also induced expression of IDO1 and IDO2 (48). Interestingly, Li and colleagues demonstrated that tolerogenic phenotype of IFN- $\gamma$ -induced IDO2 expression in DCs is maintained via autocrine IDO-Kyn/AhR-IDO loop (49). Thus, in tumors with high IDO1/IDO2 expression, increased IDO2 expression may be driven through the IDO1-Kyn/AhR signaling axis.

With respect to cancer cell functions, small interfering RNA (siRNA)-mediated knockdown of IDO2 inhibited cancer cell proliferation, induced cell cycle arrest in G1 and apoptosis, and reduced cell migration of B16-BL6 melanoma cells *in vitro*. Mechanistically, IDO2 knockdown increased generation of reactive oxygen species (ROS), and decreased generation of NAD<sup>+</sup> (50).

In the context of the tumor immunophenotype, a pan-cancer analysis of IDO2 in the TCGA transcriptomic datasets revealed IDO2 mRNA expression to be strongly associated with high infiltration of immune cells in the tumor microenvironment, as well as tumor mutational load (TMB), microsatellite instability

(MSI), mismatch repair (MMR), and immune checkpoint related genes (51).

IDO2 may promote tumor immune suppression through the Trp-Kyn-AhR axis. Studies by Yamasuge and colleagues demonstrated that *Ido2* knockout (KO) tumors had higher intratumor Trp and reduced Kyn levels compared to wild-type *Ido2* tumors in a Lewis lung carcinoma mouse model, indicating *Ido2* Trp catalytic activity (52). Moreover, *Ido2* KO tumors had significantly higher CD3<sup>+</sup> and CD8<sup>+</sup> TILs compared to wild-type *Ido2* tumors (52).

Yet, it is unlikely that the biological function(s) of IDO2 are completely redundant with that of IDO1. This is reinforced by the fact that the  $K_m$  of IDO2 for Trp is markedly lower than IDO1 ( $K_m$  500- to 1000-fold lower), despite both enzymes containing residues necessary for Trp catalytic activity (53, 54). Indeed, studies in autoimmune disease have identified several functions of IDO2 that are independent of IDO1 and Trp catalytic activity. For instance, Metz and colleagues found that IDO1-dependent T regulatory cell generation is defective in *Ido2*<sup>-/-</sup> mice. Mechanistically, *Ido2* deficient mice, but not wild-type *Ido2* mice, exhibited lower expression of immune regulatory cytokines, including IFN- $\gamma$ , TNF- $\alpha$ , IL-6, and MCP-1/CCL2 (55). Merlo and colleagues reported that IDO1 mediates T cell suppressive effects whereas IDO2 mediates autoreactive B cell responses to promote

inflammation (56). Using a catalytically inactive IDO2 knock-in mouse model, authors demonstrated that IDO2, but not IDO1, can directly interact with GAPDH, Runx1, RANbp10, and Mgea5 to potentiate an inflammatory response in autoimmune arthritis (57).

The above studies lend to an intriguing question as to whether a concomitant upregulation of tumoral IDO1 and IDO2 may synergize to suppress an anti-cancer immune response, which may lead to additional opportunities for cancer interception (see Section 2 below).

## 2.3 Tryptophan 2,3-dioxygenase

Liver-associated tryptophan 2,3-dioxygenase (TDO2) is another heme-containing enzyme that is involved in the catabolism of Trp to downstream kynurenines (Figure 1) and that has been reported to be frequently overexpressed in various malignancies (58). Elevated tumoral TDO2 expression is associated with poor prognosis in several cancer types including kidney renal papillary cell carcinoma, glioma, testicular germ cell tumors, and uveal melanoma (58) as well as liver (59), colorectal (CRC) (60), and breast cancer (61). Moreover, high TDO2 expression level positively correlated with higher immune infiltration, especially DCs, as well as immune checkpoint-related gene markers, such as LAIR1, CD276, NRP1, CD80, and CD86 (58). Regulation of TDO2 expression has been linked to IL-1 $\beta$ -C/EBP $\beta$ -MAPK signaling activities (62).

Like IDO1, TDO2-mediated Kyn promotes tumor immune suppression through AhR-signaling in various cancer types (63, 64). To this end, single-cell RNA sequencing (scRNA-seq) of 13 cancerous tissues identified a subset of myofibroblasts that exclusively expressed TDO2 and that clustered with CD4+ and CD8+ T cells distal to tumor nests. Functional experiments demonstrated that TDO2+ myofibroblasts induce transformation of CD4+ T cells into Tregs and caused CD8+ T cell dysfunction. In a murine model of oral squamous cell carcinoma (OSCC), small molecule inhibition of TDO2 via LM10 attenuated the inhibitory states of T cells, restored the T cell antitumor response, and prevented malignant transformation (65). Interestingly, Schramme and colleagues demonstrated that C57BL/6 TDO-KO mice (66) engrafted with MC38 CRC cells were more sensitive to anti-CTLA4 or anti-PD1 treatment compared to MC38-tumor bearing wild-type C57BL/6 mice. Enhanced efficacy of ICI in C57BL/6 TDO-KO tumor bearing mice was attributed to higher systemic Trp levels, which could be reversed through a Trp-low diet (67). These studies implicate host metabolism Trp independent of cancer TDO2 status as being a determinant of response to ICI.

In addition to its role in immune suppression, TDO2 has also been demonstrated to promote migration and invasion of liver cancer cells via Wnt5a signaling activities (59). Another study demonstrated that TDO2-Kyn-AhR activation in liver cancer cells induces autocrine interleukin 6 (IL-6)-mediated Signal transducer and activator of transcription 3 (STAT3) and Nuclear factor kappa beta (NF $\kappa$ B)/T Cell Immunoglobulin And Mucin Domain Containing 4 (TIM4) signaling to promote tumor progression (68). Inhibition of AhR signaling by PDM2 attenuated tumor

growth in a xenograft model of liver cancer (68). In the context of CRC, deficiency in adenomatous polyposis coli (APC) results in TCF4/ $\beta$ -catenin-mediated upregulation of the TDO2-Kyn-AhR axis to increase glycolysis and drive anabolic cancer cell growth (69). Knockdown of TDO2 in LoVo and HCT116 CRC cells attenuated cell growth, and reduced migration, invasion and colony formation potential through inactivation of TDO2-kynureninase (KYNU)-AhR signaling (60).

## 2.4 Arylformamidase

Arylformamidase (AFMID) is another downstream KP enzyme that is frequently overexpressed in various malignancies (70), and that catalyzes the hydrolysis of N-formyl-Kynurenine into Kyn and formate (Figure 1) (71). Although the functional role of AFMID upregulation in cancer remains poorly understood, Venkateswaran and colleagues demonstrated that oncogenic MYC increases expression of the Trp importers SLC1A5 and SLC7A5 as well as AFMID in colon cancer. Increased uptake and catabolism of Trp results in the accumulation of Kyn that enables cancer cell proliferation in part through AhR-signaling (72).

Splicing changes in *AFMID* have also been associated with survival and relapse in patients with hepatocellular carcinoma (HCC) (73). Specifically, the switch of AFMID isoforms was found to be an early event in HCC development and was associated with driver mutations in *TP53* and AT-rich interactive domain-containing protein 1A (*ARID1A*). Authors further found that overexpression of the full-length AFMID isoform leads to higher NAD+ levels, lower DNA-damage response, and slower cell growth in HepG2 cells (73). To this end, Tummala and colleagues found that loss of AFMID expression in SNU-449 HCC cells resulted depletion of NAD+, indicating that Trp catabolism in HCC cells supports *de novo* NAD+ synthesis (74). Additional studies are warranted to better elucidate the functional relevance of AFMID in tumorigenesis and progression; however, one may surmise that the elevation of AFMID underlies increased accumulation and secretion of Kyn.

## 2.5 Kynureninase

Kynureninase (KYNU) is a pyridoxal phosphate (PLP)-dependent hydrolase that catalyzes the cleavage of Kyn as well as 3-hydroxykynurenine (3HK) into anthranilic acid (AA) and 3-hydroxyanthranilic acid (3HA), respectively (Figure 1) (75). KYNU has been strongly implicated in the inflammation and immune modulation; however, the exact underlying mechanism (s) remain incomplete (76–81).

Recently, our group demonstrated selective enrichment of KYNU, but not other downstream KP enzymes, in lung adenocarcinomas (LUAD) harboring a loss-of-function *KEAP1* mutation (22). Metabolomic analyses confirmed that KYNU was enzymatically functional, as evidenced by the accumulation of AA in conditioned medium of LUAD cell lines. Activation of the Nuclear factor erythroid 2-related factor 2 (NRF2) pathway



through siRNA-mediated knockdown of *KEAP1* or chemical induction with the NRF2-activator CDDO-Me upregulated KYNU at both the mRNA and protein levels with concomitant increases in AA production. Moreover, elevated tumoral KYNU expression was found to be associated with a tumor suppressive immunophenotype and was prognostic for poor overall survival in a tissue microarray (TMA) of LUAD as well as multiple independent LUAD transcriptomic datasets (22). A pan-cancer analyses further revealed upregulation of KYNU to be a prominent feature of NRF2-activated cancers and is associated with tumor immunosuppression and poor prognosis (23). Interestingly, a recent study by Liu and colleagues demonstrated that KYN<sub>Y</sub>-derived 3HA has anti-oxidant properties and that elevations in cancer cell intracellular 3HA pools infer resistance to ferroptosis (82).

Studies by Heng and colleagues similarly found that KYNU was highly upregulated in HER2-enriched and triple-negative (TN) breast cancers (BrCa), leading to increased production of AA and 3HA (81). Interestingly, stimulation of TNBC cell lines with IFN $\gamma$  resulted in a pronounced 286-fold increase in 3HA and higher serum levels of 3HA was able to distinguish TNBC from the other BrCa molecular subtypes (81). These findings are notable given that 3HA has been shown to enhance the percentage of Tregs, inhibit T-helper (Th)-1 and Th17 cells (24) and suppress antigen-independent proliferation of CD8<sup>+</sup> T cells (83). To this end, a large-scale transcriptomic analysis of 2,994 BrCa tumors found a strong correlation between tumoral KYNU with inflammatory and immune responses; elevated KYNU was also linked to BrCa grade and poorer clinical outcomes (78).

In addition to cancer cell-associated upregulation of KYNU, a recent study by Itoh and colleagues found that KYNU is also elevated in cancer-associated fibroblast (CAF)-educated fibroblasts (CEFs). Specifically, authors demonstrated that CAFs induce CEF generation from normal fibroblasts (NFs) via reactive oxygen species (ROS)-induced activation of NF $\kappa$ B signaling, resulting in induction of a pro-inflammatory loop and secretion of asporin (ASP), a small leucine-rich proteoglycan. ASP in turn promoted upregulation of IDO1 and KYNU in CEFs, which induced cytotoxic effects against CD8<sup>+</sup> T-cells and promoted tumor spreading (79).

## 2.6 Kynurenine 3-monooxygenase

Kynurenine 3-monooxygenase (KMO) is a flavin adenine dinucleotide (FAD)-dependent monooxygenase and is located in the outer mitochondrial membrane that catalyzes the hydroxylation of Kyn into 3-hydroxykynurenine (3HK) (Figure 1) (84). Upregulation of KMO has been reported in several cancer types, including TNBC (85), CRC (86), HCC (87), and astrocytoma (88).

In the context of TNBC, elevated tumoral KMO is associated with worse overall survival and invasive breast cancers have among the highest rates of KMO copy number amplification (81, 89). *In vitro* ectopic overexpression of KMO in TNBC cell lines promoted increased cell growth, colony and mammosphere formation, migration and invasion, as well as increased expression of mesenchymal markers (85). In xenograft models, mice harboring

CRISPR KMO-KD MDA-MB-231 TNBC cells had reduced tumor growth, attenuated capacity for lung metastases, and prolonged overall survival compared to respective control mice. Mechanistically, KMO prevented degradation of  $\beta$ -catenin, thereby enhancing the transcription of pluripotent genes, including CD44, Nanog, Oct4, and SOX2 (85). In support of the aforementioned finding, knockdown of KMO in CRC cells was also reported to decrease expression of cancer stem cell markers CD44 and Nanog, and reduce sphere formation as well as migration and invasion (86). Inhibition of KMO enzymatic activity, using the small molecule inhibitor UPF648, similarly attenuated sphere formation and cell motility of CRC cell lines (86). Interestingly, using immunohistochemistry, flow cytometry, immunofluorescence assay, and transmission electron microscopy, Lai and colleagues demonstrated that KMO is highly expressed on the cell membranes of breast cancer tissues and the cancer cell surfaceome of cell lines (90). Treatment of MDA-MB-231 TNBC cell lines with anti-KMO antibodies reduced the cell viability and inhibited the migration and invasion of the triple-negative (90). Collectively, these findings demonstrate a cancer cell intrinsic function of KMO that promotes tumor aggressiveness and pluripotency.

Notably, induction of KMO in immune cell subtypes has also been linked to dysfunctional anti-tumor activity. Using melanoma-derived cell lines and primary CD4<sup>+</sup> CD25<sup>-</sup> T cell co-cultures, Rad Pour and colleagues demonstrated that activation of CD4<sup>+</sup> T cells results in increased production of IFN $\gamma$  with concomitant increases in Kyn and kynurenic acid that is attributed to reduced KMO expression in CD4<sup>+</sup> T cells (25). Accumulation of Kyn and kynurenic acid suppresses CD4<sup>+</sup> T cell expansion and viability (25). In the context of multiple myeloma (MM), Ray and colleagues demonstrated that KMO is upregulated in plasmacytoid dendritic cells (pDCs), resulting in immune suppression (26). Specifically, using co-culture models of patient autologous pDC-T-NK-MM cells, authors showed that pharmacological blockade of KMO activates pDCs and triggers both MM-specific cytotoxic T-cell lymphocytes (CTL) and NK cells' cytolytic activity against tumor cells. Combination treatment with R0-61-8048, a potent competitive inhibitor of KMO, and anti-PD-L1 antibody yielded superior anti-cancer efficacy compared to either treatment alone (26).

## 2.7 Kynurenine aminotransferase

Kynurenine aminotransferase family members (KATI-KATIV) catalyze the transamination of Kyn and 3HK into kynurenic acid (KA) (91) and xanthurenic acid (XANA), respectively (Figure 1) (4). Although limited information exists regarding the functional role of KAT in tumorigenesis, KAT-derived KA is readily detectable in tumor tissues, as well as in blood and urine of cancer patients (92).

Early studies demonstrated that KAT-derived KA exerts anti-proliferative effects by modulating key pathways associated with proliferation, survival, apoptosis, and migration (93–96). Yet, KA is documented to exert immunosuppressive effects via the G-protein-



coupled receptor 35 (GPR35) (97), which may potentiate tumor progression (98). Moreover, KA has also been reported to be a potent agonist of the AhR that synergistically induces IL-6 (99) with potential pro-tumoral effects (100). To this end, a recent pan-tissue study revealed that interleukin-4-induced-1 (IL4I1) more frequently associates with AhR activity than does IDO1 or TDO2. Mechanistically IL4I1-mediated generation of indole metabolites and KAT-derived KA that activated AhR signaling to promote cancer cell motility and suppression of adoptive immunity (101). The above findings underscore the enigmatic role of KAT and KA in tumor progression. Further investigations are needed.

## 2.8 3-hydroxyanthranilate 3,4-dioxygenase

3-hydroxyanthranilate 3,4-dioxygenase (HAAO) is involved in the synthesis of quinolinic acid (QA) (Figure 1). Expression patterns of HAAO are variable among different cancer types (5, 22, 23); however, studies of endometrial carcinomas revealed promotor hypermethylation of HAAO is prominent and to be associated with microsatellite instability and poor clinical outcomes (102). Hypermethylation of HAAO has also been reported to be higher in prostate cancer tissues compared to adjacent control tissue, and it is associated with a more aggressive phenotype (103).

## 2.9 Quinolinic acid phosphoribosyl transferase

Quinolinic acid phosphoribosyl transferase (QPRT) is a rate-limiting enzyme in *de novo* NAD<sup>+</sup> biosynthesis and catalyzes the conversion of QA to nicotinate ribonucleotide (Figure 1). The cancer cell intrinsic effects of QPRT upregulation have been studied in a variety of cancer types (104–109). For instance, neoplastic transformation in astrocytes is associated with a QPRT-mediated switch in NAD<sup>+</sup> metabolism by exploiting microglia-derived quinolinic acid as an alternative source of replenishing intracellular NAD<sup>+</sup> pools. Mechanistically, the

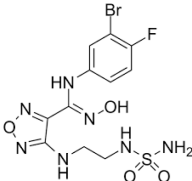
increase in QPRT expression increases resistance to oxidative stress, enabling disease progression (104). Increased expression of QPRT in invasive breast cancer promotes cell migration and invasion through purinergic signaling (105). Another study found down syndrome cell adhesion molecule antisense RNA 1 (DSCAM-AS1) increases QPRT expression in breast cancer cells via competitively binding miRNA-150-5p and miRNA-2467-3p, resulting in increased cell growth, migration, and invasion of estrogen-receptor breast cancer cells (106). Upregulation of QPRT has also been shown to confer resistance to chemotherapy in leukemic cells and ovarian cancer (107, 108). In this regard, Thongon and colleagues evaluated the mechanisms of cancer cell resistance to nicotinamide phosphoribosyltransferase (NAMPT), the rate-limiting enzyme in NAD<sup>+</sup> biosynthesis from nicotinamide. In their study, FK866-resistant CCRF-CEM (T cell acute lymphoblastic leukemia) cells were found to have exceptionally high QPRT activity and exhibited an addiction to exogenous Trp to maintain NAD<sup>+</sup> pools under stress conditions (109).

Despite the above studies, QPRT has also been shown to be inversely associated with other KP pathway enzymes, suggesting reduced expression in some cancer types (5, 22, 23). For example, studies in renal cell carcinoma revealed QPRT to be downregulated in tumors and loss of QPRT expression led to anchorage-independent growth of RCC cells (110). Thus, the relevance of QPRT in promoting tumor progression is likely to be context dependent.

## 3 Targeting the kynurenine pathway for anti-cancer treatment

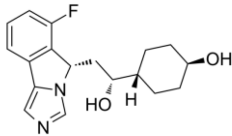
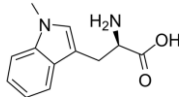
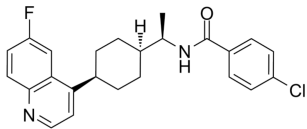
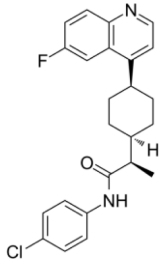
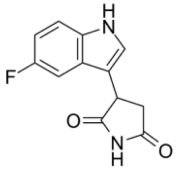
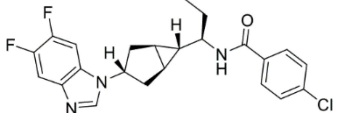
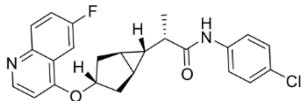
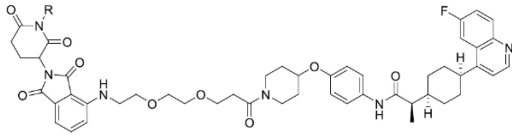
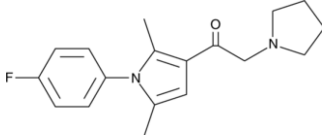
Based on intrinsic malignant properties as well as tumor immune suppression, targeting of the kynurenine pathway has garnered considerable attention, with several small molecule inhibitors being explored for the treatment of solid malignancies as monotherapies or in combination with immunotherapy (Table 1). The below sections highlight existing small molecule inhibitors as well as emergent therapies that target the KP pathway for anti-cancer treatment.

TABLE 1 Existing and emerging therapies that target the Kynurenine Pathway.

| Compound                       | Structure   | Cancer types                           | Phase              |
|--------------------------------|---|--|--------------------|
| IDO1, IDO2 and TDO2 inhibitors |   |  |                    |
| Epacadostat                    |  | SKCM, RCC, NSCLC, BLCA, SARC, CRC, OVC | Clinical/Phase III |

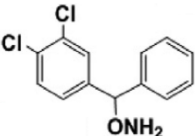
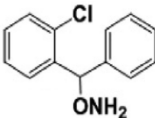
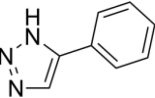
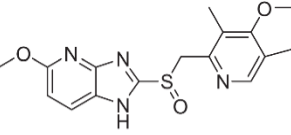
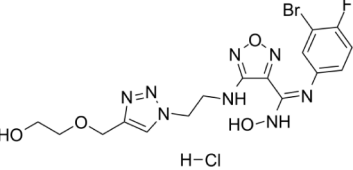
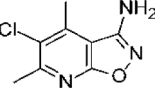
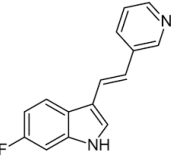
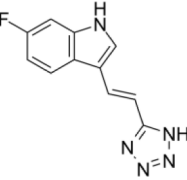
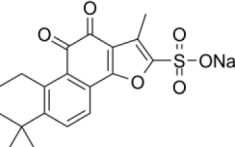
(Continued)

TABLE 1 Continued

| Compound    | Structure   | Cancer types                   | Phase                 |
|-------------|---|--------------------------------|-----------------------|
| Navoximod   |    | Solid tumors                   | Clinical/Phase I      |
| Indoximod   |    | SKCM                           | Clinical/Phase II/III |
| BMS-9862424 |    | OVC                            | PD                    |
| Linrodostat |    | BLCA,                          | Clinical/Phase III    |
| YH29407     | No information available  | CRC                            | Preclinical           |
| PF-06840003 |  | MG                             | Clinical/Phase I      |
| KHK2455     | No information available  | Solid tumors                   | Clinical/Phase I      |
| LY3381916   | No information available  | Solid tumors, NSCLC, RCC, TNBC | Clinical/Phase I      |
| MK-7162     | No information available  | Solid tumors                   | Clinical/Phase I      |
| IACS-9779   |  | None                           | <i>in vitro</i> PD    |
| IACS-70465  |  | None                           | <i>in vitro</i> PD    |
| IDO1-PROTAC |  | GBM                            | Preclinical PD        |
| IU1         |  | CRC                            | Preclinical           |

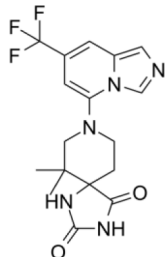
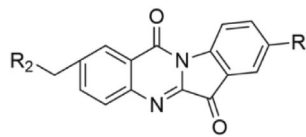
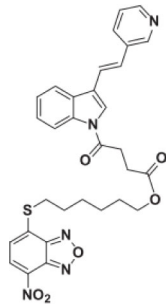
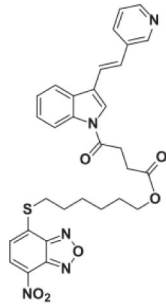
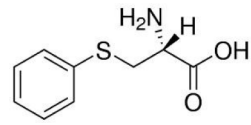
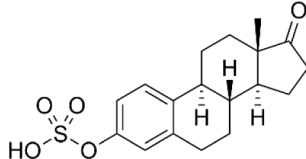
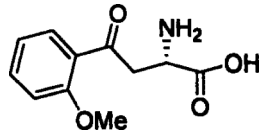
(Continued)

TABLE 1 Continued

| Compound                                    | Structure   | Cancer types       | Phase              |
|---|---|--------------------|--------------------|
| 3,4-dichloro aryl ring diaryl hydroxylamine |    | None               | Preclinical PD     |
| 2-chloro aryl ring diaryl hydroxylamine     |    | None               | Preclinical PD     |
| 4-aryl-1,2,3-triazole                       |    | None               | <i>in vitro</i> PD |
| Tenatoprazole                               |    | None               | <i>in vitro</i>    |
| Compound 4t (He X.)                         |   | CRC                | <i>in vivo</i>     |
| W-0019482                                   |  | GBM, LLC           | Preclinical        |
| 680C91                                      |  | SKCM, CRC, LM, HCC | <i>in vitro</i>    |
| LM10  |  | HCC                | <i>in vitro</i>    |
| Sodium Tanshinone IIA Sulfonate             |  | CRC                | Preclinical        |
| RG70099                                     | No information available  | GBM                | Preclinical        |
| M4112                                       | No information available  | Healthy subjects   | Clinical/Phase I   |
| HTI-1090                                    | No information available  | Solid tumors       | Clinical/Phase I   |
| DN1406131                                   | No information available  | Healthy subjects   | Clinical/Phase I   |

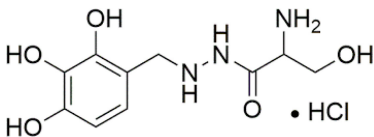
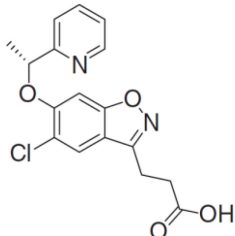
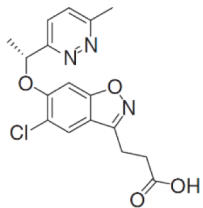
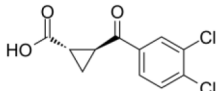
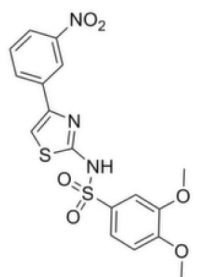
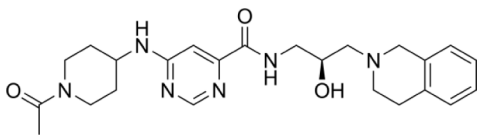
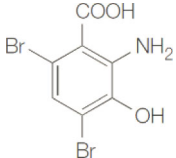
(Continued)

TABLE 1 Continued

| Compound                      | Structure   | Cancer types | Phase           |
|-------------------------------|---|--------------|-----------------|
| IACS-8968                     |    | GBM          | Preclinical     |
| EPL-1410                      | No information available  | SKCM, CRC    | Preclinical     |
| RY103                         |    | GBM, PC      | Preclinical     |
| Compound 4<br>(Hua S.)        |   | HCC          | <i>in vitro</i> |
| Compound 5<br>(Hua S.)        |  | HCC          | <i>in vitro</i> |
| KYNUs inducers                |   |              |                 |
| S-phenyl-L-cysteine sulfoxide |  | NA           | <i>in vitro</i> |
| Oestrone sulphate             |  | NA           | <i>in vitro</i> |
| O-methoxybenzoylalanine       |  | NA           | <i>in vitro</i> |

(Continued)

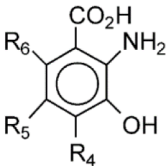
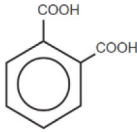
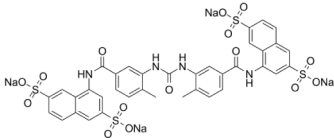
TABLE 1 Continued

| Compound                  | Structure   | Cancer types    | Phase            |
|---------------------------|---|-----------------|------------------|
| Bensarazide hydrochloride |    | NA              | <i>in vitro</i>  |
| PEGylated-KYNU            | NA  | SKCM, TNBC, CRC | Preclinical      |
| KMO inhibitors            |   |                 |                  |
| GSK065                    |    | NA              | <i>in vitro</i>  |
| GSK366                    |   | NA              | <i>in vitro</i>  |
| UPF-648                   |  | CRC             | <i>in vitro</i>  |
| Ro 61-8048                |  | CRC             | <i>in vitro</i>  |
| GSK3335065                |  | NA              | Clinical/Phase I |
| HAAO inhibitors           |   |                 |                  |
| NCR-631                   |  | NA              | Preclinical      |

(Continued)



TABLE 1 Continued

| Compound                              | Structure   | Cancer types | Phase           |
|---------------------------------------|---|--------------|-----------------|
| 3-hydroxyanthranilic acid derivatives |  | NA           | Preclinical     |
| QPRT inhibitors                       |   |              |                 |
| Phthalic acid                         |  | BRCA         | <i>in vitro</i> |
| NF340                                 |  | BRCA         | <i>in vitro</i> |

BLCA, bladder urothelial carcinoma; BRCA, breast cancer; CRC, colorectal cancer; GBM, glioblastoma; HCC, hepatocellular carcinoma; LALM, acute myeloid leukemia; LLC, Lewis lung carcinoma; LM, leiomyoma; MG, malignant glioma; NSCLC, non-small cell lung cancer; OVC, ovarian cancer; PD, pharmacodynamic; RCC, renal cell carcinoma; SARC, sarcoma; SKCM, skin cutaneous melanoma; TNBC, triple negative breast cancer.

### 3.1 Indoleamine 2,3-dioxygenase 1

#### 3.1.1 Epacadostat

Epacadostat (INCB024360) is a selective competitive inhibitor of IDO1 that has been explored for the treatment of solid malignancies as both a standalone agent and in combination with immune check-point inhibitor (ICI) therapies (11–16).

Pharmacokinetic and pharmacodynamic studies have demonstrated that, as a monotherapy, epacadostat is generally well tolerated, with a maximal inhibition of IDO1 activity (based on reductions in circulating kynurenine levels) achieved at doses ≥ 100mg BID. Adverse events (AEs) associated with such treatment included fatigue, nausea, decreased appetite, vomiting, constipation, abdominal pain, diarrhea, dyspnea, back pain, and cough (11). In a Phase I clinical study evaluating efficacy of epacadostat in patients with advanced solid malignancies, 18 out of 52 patients achieved stable disease, with 7 patients (13.5%) having stable disease lasting ≥16 weeks (11).

A seminal study, ECHO-202/KEYNOTE-037, evaluated the efficacy of epacadostat in combination with the PD-1 inhibitor pembrolizumab in advanced melanoma, with reported objective response rates (ORR) of 56% and a disease control rates (DCR; complete response (CR) + partial response (PR) + stable disease (SD)) of 78% (111). Despite early success in Phase I and II clinical trials, a Phase III clinical trial (ECHO-301/KEYNOTE-252) did not demonstrate additional benefit of epacadostat + pembrolizumab compared to placebo + pembrolizumab alone in patients with unresectable or metastatic melanoma (10).

ECHO-202/KEYNOTE-037 also reported results from Phase I/II studies evaluating combination treatment of epacadostat + pembrolizumab in sixty-two patients with various advanced solid tumors (13). Antitumor activity was observed in several cancer types, with ORR being observed in 25 (40.3%) of 62 patients.

Epacadostat 100 mg twice a day plus pembrolizumab 200 mg every 3 weeks was recommended for Phase II evaluation. In the Phase II study, an objective response (OR) occurred in 55% (12 of 22) patients with melanoma and in those with non–small-cell lung cancer, renal cell carcinoma, endometrial adenocarcinoma, urothelial carcinoma, and head and neck squamous cell carcinoma (13). For NSCLC, combination treatment of epacadostat + pembrolizumab resulted in a ORR (CR + PR) of 35% (14 out of 40 patients) and a DCR (CR+PR+SD) of 60% (24 out of 40 patients) (112). Similar results were reported for renal cell carcinoma (15) and urothelial carcinomas (16). ECHO-207/KEYNOTE-723, a Phase I/II study of epacadostat plus pembrolizumab and chemotherapy for advanced solid tumors, also demonstrated ORRs of 31.4% across all treatment groups (113). However, a Phase II study evaluating epacadostat + pembrolizumab in 30 patients with selective sarcoma subtypes failed to achieve meaningful antitumor activity, with ORRs of <5% (114).

Epacadostat has also been explored in combination with other ICIs, including ipilimuab, an anti-cytotoxic T-lymphocyte-associated protein 4 (CTLA4) antibody, and nivolumab, an anti-PD-1 antibody (14, 115). To this end, Gibney and colleagues reported the results of a Phase I/II study of epacadostat in combination with ipilimuab in patients with unresectable or metastatic melanoma (14). In this study, immunotherapy-naïve patients (n= 39) achieved an ORR of 26% according to the immune-related response criteria and 23% by the Response Evaluation Criteria in Solid Tumors (RECIST 1.1); no ORR was observed in patients who received prior immunotherapy (14). Combination treatment of epacadostat plus nivolumab in advanced solid tumors achieved respective DCR (CR+PR+SD) of 24%, 28%, and 100% for colorectal cancer, ovarian cancer, and melanoma (115).

### 3.1.2 Navoximod

Navoximod is an orally available non-competitive inhibitor of IDO1 (17). An open-label Phase Ia study by Nayak-Kapoor and colleagues assessed the safety, pharmacokinetics, pharmacodynamics, and preliminary anti-tumor activity of navoximod as a monotherapy in 22 patients with recurrent/advanced solid tumors (116). Trial-associated adverse events, regardless of causality, included fatigue (59%), cough, decreased appetite, and pruritus (41% each), nausea (36%), and vomiting (27%). Grade  $\geq 3$  AEs occurred in 14 of the 22 patients; however, only 2 were related to navoximod. Navoximod was found to be rapidly absorbed ( $T_{max} \sim 1$  h) with a half-life of approximately 11 hours, and transiently decrease plasma kynurenine levels. No objective responses were met based on RECIST v1.1 criteria; however, stable disease was observed in 36% of efficacy-evaluable patients (116).

Combination of navoximod plus the anti-PD-L1 inhibitor atezolizumab has also been explored for anti-cancer treatment of solid malignancies (19–21). Results from an open-label Phase Ib trial of 52 patients treated with navoximod plus atezolizumab demonstrated acceptable toxicity profiles; efficacy data available for 45 patients included 4 (9%) patients with a partial response and 11 (24%) patients with stable disease (21). Another Phase I study of navoximod plus atezolizumab in 20 Japanese patients with advanced solid tumors achieved stable disease in 65% (13 out of 20) patients. No dose-limiting toxicities were observed. The recommended dose of navoximod monotherapy was determined as 1000 mg orally BID, and 1000 mg orally BID could be considered in combination with atezolizumab (20). Despite these findings, a larger Phase I study of navoximod plus atezolizumab in 157 patients with advanced solid tumors failed to show benefit of adding navoximod to atezolizumab (19).

### 3.1.3 Indoximod

Indoximod, also known as 1-methyl tryptophan (1-MT), is an indirect inhibitor of IDO1/IDO2 and is reported to serve as a high-potency Trp mimetic that reverses mTORC1 inhibition and the accompanying autophagy that is induced by Trp depletion in cells (17, 18). Indoximod has been explored for anti-cancer treatment in several Phase I/II clinical trials, both as a monotherapy as well as in combination with chemotherapy (117–120).

Recently, Zakharia and colleagues reported results from a single-arm Phase II clinical trial evaluating the addition of indoximod to standard of care ICI (pembrolizumab, nivolumab, or ipilimumab) approved for melanoma (121). Indoximod was administered continuously (1200 mg orally two times per day), with concurrent ICI dosed per US Food and Drug Administration (FDA)-approved label. A total of 131 patients were enrolled; pembrolizumab was the most frequently used ICI (114 out of 131; 87%). Efficacy was evaluable in 89 patients from the Phase II cohort with non-ocular melanoma who received indoximod combined with pembrolizumab. The ORR for the evaluable population was 51%, with confirm CR of 20% and DCR of 70%. ORR were highest among PD-L1 positive patients (70% compared to 46% for PD-L1 negative patients). Median progression-free survival was 12.4 months (95% CI 6.4 to 24.9) (121). Another recently completed Phase I/II trial (NCT01042535) evaluated an adenovirus-p53 transduced DC vaccine together with

indoximod for treatment of metastatic breast cancer. A total of 44 patients were recruited, of which 36 completed the study. The results of this trial are pending.

### 3.1.4 Others IDO inhibitors

To date, several additional IDO inhibitors have been developed including BMS-986242 (122), linrodostat (BMS-986205) (123, 124), YH29407 (125), PF-06840003 (126–128), KHK2455 (129), LY3381916 (130), and MK-7162. To this end, a Phase I study of PF-06840003 in 17 patients with recurrent malignant glioma demonstrated acceptable toxicity profiles, and with a reported dose-limiting toxicity (DLT) rate of 500 mg BID (131). Disease control occurred in eight patients (47%). Mean duration of stable disease was 32.1 (12.1–72.3) weeks (131). ENERGIZE, a Phase III study of neoadjuvant chemotherapy alone or with nivolumab with or without linrodostat mesylate for muscle-invasive bladder cancer is currently recruiting (128). Phase I clinical trials for KHK2455, (NCT02867007) LY3381916, (NCT03343613- recently terminated) and MK-7162 (NCT03364049) are on-going.

In addition to the above inhibitors, structural elucidation studies have also led to the discovery of imidazopyridines as potent IDO1 inhibitors (132) and substituted oxalamides as novel heme-displacing IDO1 inhibitors (133), as well as the development of first in class IACS-9779 and IACS-70465 inhibitors that bind the IDO1 apoenzyme (134). Anti-cancer efficacy of the mentioned above agents has been demonstrated in preclinical models; however, they have not been explored yet in clinical trials.

Another alternative approach has been to degrade intratumor IDO1. Bollu and colleagues reported the results of a novel IDO1 degrader using proteolysis targeting chimera (PROTAC) technology, which utilizes an E3 ligase complex to ubiquitinate targets for proteasome-mediated degradation. The IDO1-PROTAC resulted in potent cereblon-mediated proteasomal degradation of IDO1, and prolonged survival in mice with established brain tumors (135). Interestingly, studies by Shi and colleagues suggest that IDO1 expression may be regulated post-transcriptionally. Specifically, authors found that overexpression of USP14, a proteasome-associated deubiquitinating enzyme, in CRC cells deubiquitinates the IDO1 at the K48 residue, thus preventing proteasomal degradation (136). Knockdown or pharmacological targeting of USP14 decreased IDO1 expression, independent of AhR signaling, and improved anti-tumor immunity in a MC38 orthotopic syngeneic mouse model of CRC. Combination treatment of IU1, a selective small molecule inhibitor of USP14, and anti-PD-1 resulted in improved anti-killing effects compared to either treatment alone (136). Targeting IDO1 protein stability, rather than enzymatic activity, may thus provide an alternative approach to circumvent IDO1-mediated anti-cancer immunity.

## 3.2 Indoleamine 2,3-dioxygenase 2 inhibitors

Although the exact crystal structure of IDO2 remains incomplete, its high homology with IDO1 has enabled development of IDO2 inhibitors, including several diaryl

hydroxylamines and 1,2,3-triazoles. For example, diaryl hydroxylamine compounds with a 3,4-dichloro aryl ring substitution exerted potent pan (IDO1/IDO2/TDO) inhibitory function whereas a 2-chloro aryl ring substitution inhibited IDO1 and IDO2 activity with respective  $IC_{50}$  values of 18 and 25  $\mu$ M (137). In cellular assays, 4-Aryl-1,2,3-triazole derivatives were also found to inhibit IDO2 function, with the best compound having an  $IC_{50}$  value of 50  $\mu$ M for mouse IDO2, and a twofold higher selectivity over human IDO1. Functionally, the 4-Aryl-1,2,3-triazole compounds were found to occupy both the A and B pockets of the IDO active site, which inhibited IDO2 more strongly than IDO1. Notably, the  $\mu$ M activity of the 4-Aryl-1,2,3-triazole compounds were similar to L-1MT (138). Another screening study identified the proton pump inhibitor, tenatoprazole, to exhibit an  $IC_{50}$  value of 1.8  $\mu$ M for IDO2 with no observed inhibition of IDO1 or TDO. Similar findings were found with other proton pump inhibitors. Proton pump inhibitors, such as tenatoprazole, were predicted to have one heteroatom coordinating to the heme iron in the active site of IDO2 (139).

A more recent study by He and colleagues reported *in vitro* and *in vivo* findings of their novel dual IDO1/IDO2 inhibitor, 4t. Structurally, 4t is an 1,2,3-triazole with a hydroxyethyl ether substitution with excellent inhibitory activity ( $IC_{50}$  values of 28 nM and 144 nM for IDO1 and IDO2, respectively). Functionally, the hydroxyethyl ether chain of 4t formed two hydrogen bonding interactions with Tyr244 and Lys366 of IDO2, contributing to improved activity against IDO2. Pharmacokinetic experiments demonstrated favorable profiles, with adequate membrane permeability, high plasma protein binding, and safety. Moreover, 4t exhibited potent anti-tumor activity in a CT26 colorectal xenograft mouse model (140). Although promising, it remains to be determined whether the above mentioned IDO2 inhibitors will yield satisfactory anti-tumor activity in the clinical setting.

### 3.3 Tryptophan 2,3-dioxygenase inhibitors

There has been a considerable interest in the development of small molecule inhibitors of TDO2 given recent evidence that TDO2 is upregulated in several cancer types and, like IDO, mediates the catabolism of Trp and promote tumor immune suppression (7). To-date, small molecule inhibitors with high affinity to TDO2 are limited (141, 142).

Recently, W-0019482 was identified to be a potent inhibitor of IDO1, resulting in pronounced reductions in plasma and intratumoral ratios of Kyn-to-Trp and delayed growth of subcutaneous GL261-hIDO1 tumors in mice. Synthetic modification of W-0019482 yielded several analogues with either dual or TDO2-selective profiles. Four analogues, SN36458, SN36896, SN36499, and SN36704, were found to be TDO2 selective, exhibiting  $IC_{50}$  values 5.8 to 8.1-fold lower than that measured against IDO1 (143). The utility of these newer generation TDO2 inhibitors for anti-cancer treatment remains to be determined. Studies using HepG2 liver cancer cells demonstrated that TDO2-inhibitors 680C91 or LM10 significantly reduced Trp degradation and that TDO2, but not IDO1, was the primary source

of Kyn production in these cells (144). 680C91 has also been explored in other cancer types including melanoma (145–147), colon (147), leiomyomas (148), and gliomas (149).

Interestingly, Zhang and colleagues reported that sodium tanshinone IIA sulfonate (STS), a sulfonate derived from tanshinone IIA (TSN), reduced the enzymatic activities of IDO1 and TDO2 with a half inhibitory concentration ( $IC_{50}$ ) of less than 10  $\mu$ M using enzymatic assays (150). STS markedly decreased Kyn synthesis in IDO1- or TDO2-overexpressing cell lines and reduced the percentage of Forkhead Box P3 (FOXP3) T cells. *In vivo*, STS delayed tumor growth and combination treatment of STS with anti-PD-1 yielded superior anti-cancer efficacy compared to either treatment alone (150).

With regards to dual IDO/TDO2 targeting therapies, preclinical studies demonstrated that RG70099, potent dual small molecule inhibitor ( $IC_{50}$  <100 nM) (151), efficiently reduced Kyn levels in plasma by ~90%, and >95% in tumors and draining lymph nodes. Notably, compared to conventional IDO inhibitors, RG70099 was able to reduce tumor Kyn levels by >90% in a TDO+ tumor xenograft, reinforcing that RG70099 exerting TDO2 inhibitory activity (151). EPL-1410, a fused heterocycle-based analogue, showed IDO1/TDO2 inhibitor activity in biochemical assays and demonstrated a significant dose dependent pharmacological efficacy in reducing the tumor volume in the syngeneic cancer models of CT-26 colon carcinoma and B16F10 melanoma (152). Recently, a Phase I clinical trial of M4112, an oral small molecule dual inhibitor of IDO/TDO2, in 15 patients with advanced solid tumors reported tolerable toxicity profiles (153). Treatment-emergent adverse events included fatigue, nausea, and vomiting. Dose-limiting toxicities (DLTs) were observed in one patient (grade 3 allergic dermatitis), and one grade 2 QT prolongation that resulted in a dose reduction. Neither the maximum tolerated dose (MTD) nor recommended Phase II dose was achieved (153).

### 3.4 Kynurenine aminotransferase inhibitors

To date, there exist several selective inhibitors of KAT, however, their applications in the context of anti-cancer treatment has not been readily explored (154–156). Despite this, several cancer types overexpress KAT (5), and, as mentioned in the above sections, KAT-derived KYNA may serve as a ligand for AhR signaling, resulting in tumor immune suppression (101). Evaluation of KAT inhibitors for anti-cancer treatment and potential reversal of immune suppression warrants further exploration.

### 3.5 Kynureninase inhibitors and pegylated-Kynureninase

Considering recent findings by our group as well as others (22, 23, 78, 79, 81, 83, 157), targeting of KYNU for anti-cancer treatment and reversal of immune suppression warrants investigation. To date, a few kynurenine analogues have been developed that selectively inhibit KYNU enzymatic activity (158). Additional molecules reported to inhibit KYNU include S-phenyl-L-cysteine sulfoxide

(159, 160), oestrone sulphate (161), O-methoxybenzoylalanine (162), and benserazide hydrochloride (163).

However, targeting of KYNU should be met with caution. KYNU mediates the catabolism of Kyn to AA, which is thought to be immunologically inert. Administration of PEGylated-KYNU in immune-competent preclinical models of melanoma, breast, and colon cancer resulted in drastic reductions in tumor KYN levels with concomitant elevations in KYNU-derived AA, resulting in increases in tumor-infiltrating CD8+ T cells and subsequent tumor reduction (8). Moreover, anti-cancer efficacy was further enhanced when combining PEG-KYNase with ICIs (8). Overexpression (OE) of KYNU in modified Chimeric Antigen Receptor (CAR)-T cells yields superior anti-cancer efficacy in a NALM6 acute lymphoblastic leukemia mouse model (164). Compared to KYNU-knockout (KO) CAR T cells, KYNU-OE CAR T cells had higher glucose uptake, increased proliferation in carboxyfluorescein diacetate succinimidyl ester (CFSE) assays, and exhibited a higher percentage of effector memory cell and effector CAR T-cells. In cell killing assays, KYNU-OE CAR T cells had higher lytic granules of granzyme B and enhanced cytokine production of IFN $\gamma$ , compared to KYNU-KO CAR T cells. Importantly, KYNU-OE CAR T cells retained anti-cancer efficacy in the presence of high KYN levels (164). In another study, an organic polymer nanoenzyme (SPNK) conjugated with kynureninase (KYNase) via PEGylated singlet oxygen ( $^1O_2$ ) cleavable linker with near-infrared (NIR) photoactivatable immunotherapeutic effects was developed for photodynamic immunometabolic therapy (165). Upon NIR photoirradiation, SPNK generates  $^1O_2$  to induce the immunogenic cell death of cancer and released KYNase to degrade KYN in the TME. *In vivo*, SPNK treatment elicited effector T cell tumor infiltration and expansion, enhanced systemic antitumor T cell activity, and prolonged survival of tumor-bearing mice (165).

The potential of KYNU as a direct target of therapy or as the therapy itself (i.e. pegylated-KYNU) remains an active area of exploration.

### 3.6 Kynurenine 3-Monooxygenase inhibitors

To date, several inhibitors of KMO have been developed, the majority of which share a common pharmacophore containing both an acidic moiety and a mono or 1,2-dichloro substitution of the core phenyl ring (84, 166–169). More recent inhibitors, GSK065 and GSK366, trap the catalytic flavin in a previously unobserved tilting conformation, resulting in picomolar affinities, increased residence times, and an absence of the peroxide production observed with prior inhibitors (166).

Evaluation of KMO inhibitors for anti-cancer treatment remains limited; however, studies by Ray and colleagues demonstrated that Ro 61-8048, a potent, selective inhibitor of KMO (170), activates pDCs and enhances pDC-triggered T cell proliferation and enhanced anti-cancer activity (26). Specifically, in co-culture models of patient pDCs, T cells, or NK cells with autologous multiple myeloma (MM) cells, blockade of KMO via

Ro 61-8048 resulted in a robust MM-specific CD8+ CTL activity as well as significantly increased NK cell cytolytic activity (26). Treatment of CRC cell lines with Ro 61-8048 or UPF 648, another KMO inhibitor, resulted in reduced viability, decreased sphere formation and attenuated cell migration and invasion (86).

The therapeutic potential of KMO inhibitors remains to be determined; however, a prior clinical trial of the KMO inhibitor GSK3335065 was conducted among healthy volunteers. While GSK3335065 rapidly increases kynurenine levels suggesting partial inhibition of KMO activity, the trial was terminated after a serious adverse event (SAE) occurred on the study and a relationship with the study drug could not be excluded (171).

### 3.7 3-hydroxyanthranilic acid 3,4-dioxygenase and Quinolinic acid phosphoribosyl transferase inhibitors

Presently, there are very few inhibitors available that selectively target HAAO. Existing HAAO inhibitors include NCR-631 (AstraZeneca, Sweden) (172) as well as 4,5-, 4,6-disubstituted and 4,5,6-trisubstituted 3-hydroxyanthranilic acid derivatives, which have been shown to reduce the production of the excitotoxin QA (173, 174). To the best of our knowledge, none of these inhibitors have been evaluated to anti-cancer treatment.

Regarding QPRT, existing small molecule inhibitors include phthalic acid (PA) as well as the P2Y<sub>11</sub> antagonist (NF340) (105, 175, 176). To this end, phthalic acid and NF340 were able to attenuate QPRT-enhanced invasiveness pCMV6-QPRT-transfected MDA-MB-231 TNBC cell lines (105). Given that NAD is essential for metabolic and immune homeostasis, QPRT inhibitors for cancer therapy warrants investigation, although should be met with some caution due to potential off target toxicities (177–179).

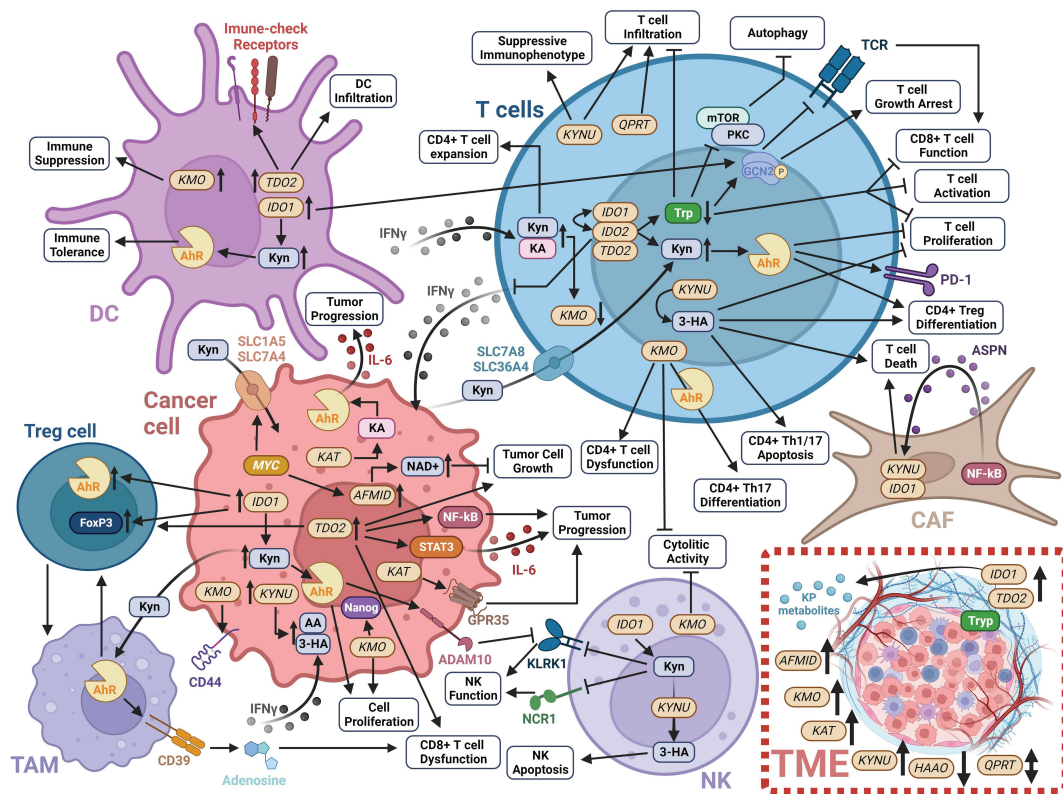
## 4 Perspectives

Over the past few decades, there has been considerable advancement in our understanding of the cancer cell intrinsic and complex extrinsic functions of the KP in tumor development and progression (Figure 3). This progress has led to the development of several small molecule inhibitors that exploit multiple facets of the KP to achieve anti-tumor effects and the reversal of tumor-derived immune suppression (Figure 3; Table 1).

Despite these advances, clinical benefit resulting from targeting the KP pathway has been less than anticipated. Limited clinical success is likely to be multifactorial. For instance, advanced stage tumors have already undergone immunoediting to enable immune escape. Benefit of IDO inhibitors, or other KP inhibitors, may be most efficacious during early stages of disease when the immune system iteratively selects and/or promotes the generation of tumor cell variants with increasing capacities to survive immune attack, also referred to as the equilibrium phase (180).

Lack of clinical benefit may also be attributed to patient selection. Tumors that co-express IDO2 and TDO2 may be less responsive to selective IDO1 inhibitors. Consequently, molecular





Schematic of the impact of KP enzymes and derived metabolites on modulating the tumor immune microenvironment. Detailed information is provided in Section 1 of this review. Created with [BioRender.com](https://BioRender.com). 3-HA, 3-hydroxyanthranilic acid; AA, anthranilic acid; ADAM10, ADAM metalloproteinase domain 10; Ahr, Aryl hydrocarbon receptor; AFMID, arylformamidase; ASPN, asporin; CAF, cancer-associated fibroblast; DC, dendritic cell; FoxP3, forkhead box P3; GCN2, general control non-derepressible 2; GPR35, G-protein-coupled receptor 35; HAAO, 3-hydroxyanthranilate 3,4-dioxygenase; IDO1, indoleamine 2,3-dioxygenase 1; IDO2, indoleamine 2,3-dioxygenase 2; IFN $\gamma$ , interferon-gamma; IL-6, interleukin 6; KA, kynurenic acid; KAT, kynurenine aminotransferase; KLKR1, killer cell lectin like receptor K1; KMO, kynurenine 3-monooxygenase; KP, kynurenine pathway; KYNU, kynureninase; mTOR, mammalian target of rapamycin; NAD $^{+}$ , nicotinamide adenine dinucleotide; NCR1, natural cytotoxicity triggering receptor 1; NF- $\kappa$ B, nuclear factor kappa beta; NK, natural killer cell; PD-1, programmed cell death protein 1; PKC, protein kinase C; SLC1A5, solute carrier family 1 member 5; SLC36A4, solute carrier family 36 member 4; SLC7A5, solute carrier family 7 member 5; SLC7A8, solute carrier family 7 member 8; STAT3, signal transducer and activator of transcription 3; TAM, tumor-associated macrophages; TDO2, tryptophan 2,3-dioxygenase; TME, tumor microenvironment; Trp, tryptophan; QPTR, quinolinic acid phosphoribosyl transferase.

Exposure to other environmental toxicants can also activate AhR signaling (182), which may upregulate IDO expression resulting in immune suppression (48).

The relevance of other downstream KP enzymes also warrants considerations. This is exemplified by our own findings that tumoral KYNU, but not IDO1, is selectively and frequently upregulated in NRF2 activated tumors and that elevated tumoral KYNU is associated with high immune cell infiltration across several cancer types (22, 23). One may infer that elevated tumoral KYNU promotes tumor immune cell infiltration by reducing levels of Kyn and increasing levels of immune inert anthranilic acid in the TME, as evidenced by studies using PEGylated-KYNU (8). Yet, elevated tumoral KYNU coincides with NRF2 activation, which can promote immune suppression by upregulating PD-L1 (183, 184). Crosstalk between cancer cells and TAMs in the TME can also activate NRF2 in TAMs to reshape the tumor immune microenvironment via multiple mechanisms including suppression of pro-inflammatory cytokines, increasing expression



of PD-L1, macrophage colony-stimulating factor (M-CSF) and KYNU, and accelerating catabolism of cytotoxic-labile heme (185). Upregulation of tumoral KYNU, coupled with NRF2 activation may thus synergize to yield a TME that is highly immune suppressed. Whether therapeutic targeting of KYNU alone or in combination with ICI in NRF2-activated KYNU-high tumors reverses tumor immune suppression remains an area of ongoing inquiry.

In summary, the KP remains an active area of investigation, and insights gained from this study are expected reveal additional promising points actionable metabolic vulnerability within the pathway that can be targeted for anti-cancer treatment.

## Author contributions

RL-L: Visualization, Writing – original draft, Conceptualization. RD: Conceptualization, Writing – original draft. JV: Writing – review & editing. AS: Writing – review & editing. EO: Writing – review & editing. SH: Writing – review & editing. JF: Conceptualization, Investigation, Resources, Supervision, Writing – original draft.

## References

- Munn DH, Mellor AL. Indoleamine 2,3 dioxygenase and metabolic control of immune responses. *Trends Immunol* (2013) 34(3):137–43. doi: 10.1016/j.it.2012.10.001
- Solvay M, Holfelder P, Klaessens S, Pilote L, Stroobant V, Lamy J, et al. Tryptophan depletion sensitizes the AHR pathway by increasing AHR expression and GCN2/LAT1-mediated kynurenine uptake, and potentiates induction of regulatory T lymphocytes. *J Immunother Cancer* (2023) 11(6):e006728. doi: 10.1136/jitc-2023-006728
- Minhas PS, Liu L, Moon PK, Joshi AU, Dove C, Mhatre S, et al. Macrophage de novo NAD(+) synthesis specifies immune function in aging and inflammation. *Nat Immunol* (2019) 20(1):50–63. doi: 10.1038/s41590-018-0255-3
- Badawy AA. Kynurenine pathway of tryptophan metabolism: regulatory and functional aspects. *Int J Tryptophan Res* (2017) 10. doi: 10.1177/1178646917691938
- Badawy AA. Tryptophan metabolism and disposition in cancer biology and immunotherapy. *Biosci Rep* (2022) 42(11):1–27. doi: 10.1042/BSR20221682
- Munn DH, Sharma MD, Baban B, Harding HP, Zhang Y, Ron D, et al. GCN2 kinase in T cells mediates proliferative arrest and anergy induction in response to indoleamine 2,3-dioxygenase. *Immunity* (2005) 22(5):633–42. doi: 10.1016/j.immuni.2005.03.013
- Cheong JE, Sun L. Targeting the IDO1/TDO2-KYN-ahR pathway for cancer immunotherapy - challenges and opportunities. *Trends Pharmacol Sci* (2018) 39(3):307–25. doi: 10.1016/j.tips.2017.11.007
- Triplet TA, Garrison KC, Marshall N, Donkor M, Blazek J, Lamb C, et al. Reversal of indoleamine 2,3-dioxygenase-mediated cancer immune suppression by systemic kynurenine depletion with a therapeutic enzyme. *Nat Biotechnol* (2018) 36(8):758–64. doi: 10.1038/nbt.4180
- Platten M, Wick W, Van den Eynde BJ. Tryptophan catabolism in cancer: beyond IDO and tryptophan depletion. *Cancer Res* (2012) 72(21):5435–40. doi: 10.1158/0008-5472.CAN-12-0569
- Long GV, Dummer R, Hamid O, Gajewski TF, Caglevic C, Dalle S, et al. Epacadostat plus pembrolizumab versus placebo plus pembrolizumab in patients with unresectable or metastatic melanoma (ECHO-301/KEYNOTE-252): a phase 3, randomised, double-blind study. *Lancet Oncol* (2019) 20(8):1083–97. doi: 10.1016/S1470-2045(19)30274-8
- Beatty GL, O'Dwyer PJ, Clark J, Shi JG, Bowman KJ, Scherle PA, et al. First-in-human phase I study of the oral inhibitor of indoleamine 2,3-dioxygenase-1 epacadostat (INCB024360) in patients with advanced solid Malignancies. *Clin Cancer Res* (2017) 23(13):3269–76. doi: 10.1158/1078-0432.CCR-16-2272
- Yue EW, Sparks R, Polam P, Modi D, Douth B, Wayland B, et al. INCB24360 (Epacadostat), a highly potent and selective indoleamine 2,3-dioxygenase 1 (IDO1) inhibitor for immuno-oncology. *ACS Med Chem Lett* (2017) 8(5):486–91. doi: 10.1021/acsmchemlett.6b00391
- Mitchell TC, Hamid O, Smith DC, Bauer TM, Wasser JS, Olszanski AJ, et al. Epacadostat plus pembrolizumab in patients with advanced solid tumors: phase I

## Funding

The author(s) declare financial support was received for the research, authorship, and/or publication of this article. Work was supported by the generous philanthropic contributions to The University of Texas MD Anderson Cancer Center Moon Shots Program™.

## Conflict of interest

The authors declare that the research was conducted in the absence of any commercial or financial relationships that could be construed as a potential conflict of interest.

## Publisher's note

All claims expressed in this article are solely those of the authors and do not necessarily represent those of their affiliated organizations, or those of the publisher, the editors and the reviewers. Any product that may be evaluated in this article, or claim that may be made by its manufacturer, is not guaranteed or endorsed by the publisher.

- results from a multicenter, open-label phase I/II trial (ECHO-202/KEYNOTE-037). *J Clin Oncol* (2018) 36(32):3223–30. doi: 10.1200/JCO.2018.78.9602
- Gibney GT, Hamid O, Lutzky J, Olszanski AJ, Mitchell TC, Gajewski TF, et al. Phase 1/2 study of epacadostat in combination with ipilimumab in patients with unresectable or metastatic melanoma. *J Immunother Cancer* (2019) 7(1):80. doi: 10.1186/s40425-019-0562-8
- Lara P, Bauer T, Hamid O, Smith D, Gajewski T, Gangadhar T, et al. Epacadostat plus pembrolizumab in patients with advanced RCC: Preliminary phase I/II results from ECHO-202/KEYNOTE-037. *J Clin Oncol* (2017) 35:4515. doi: 10.1200/JCO.2017.35.15\_suppl.4515
- Smith D, Gajewski T, Hamid O, Wasser J, Olszanski A, Patel S, et al. Epacadostat plus pembrolizumab in patients with advanced urothelial carcinoma: Preliminary phase I/II results of ECHO-202/KEYNOTE-037. *J Clin Oncol* (2017) 35:4503. doi: 10.1200/JCO.2017.35.15\_suppl.4503
- Prendergast GC, Malachowski WP, DuHadaway JB, Muller AJ. Discovery of IDO1 inhibitors: from bench to bedside. *Cancer Res* (2017) 77(24):6795–811. doi: 10.1016/bs.ircmb.2017.07.004
- Metz R, Rust S, DuHadaway JB, Mautino MR, Munn DH, Vahanian NN, et al. IDO inhibits a tryptophan sufficiency signal that stimulates mTOR: A novel IDO effector pathway targeted by D-1-methyl-tryptophan. *Oncimmunology* (2012) 1(9):1460–8. doi: 10.4161/onci.21716
- Jung KH, LoRusso P, Burris H, Gordon M, Bang YJ, Hellmann MD, et al. Phase I study of the indoleamine 2,3-dioxygenase 1 (IDO1) inhibitor navoximod (GDC-0919) administered with PD-L1 inhibitor (Atezolizumab) in advanced solid tumors. *Clin Cancer Res* (2019) 25(11):3220–8. doi: 10.1158/1078-0432.CCR-18-2740
- Ebata T, Shimizu T, Fujiwara Y, Tamura K, Kondo S, Iwasa S, et al. Phase I study of the indoleamine 2,3-dioxygenase 1 inhibitor navoximod (GDC-0919) as monotherapy and in combination with the PD-L1 inhibitor atezolizumab in Japanese patients with advanced solid tumours. *Invest New Drugs* (2020) 38(2):468–77. doi: 10.1007/s10637-019-00787-3
- Burris H, Gordon M, Hellmann M, Lorusso P, Emens L, Hodi F, et al. A phase Ib dose escalation study of combined inhibition of IDO1 (GDC-0919) and PD-L1 (atezolizumab) in patients (pts) with locally advanced or metastatic solid tumors. *J Clin Oncol* (2017) 35:105. doi: 10.1200/JCO.2017.35.15\_suppl.105
- Fahrmann JF, Tanaka I, Irajizad E, Mao X, Dennison JB, Murage E, et al. Mutational activation of the NRF2 pathway upregulates kynureninase resulting in tumor immunosuppression and poor outcome in lung adenocarcinoma. *Cancers (Basel)* (2022) 14(10):1–29. doi: 10.3390/cancers14102543
- Leon-Letelier RA, Abdel Sater AH, Chen Y, Park S, Wu R, Irajizad E, et al. Kynureninase upregulation is a prominent feature of NRF2-activated cancers and is associated with tumor immunosuppression and poor prognosis. *Cancers (Basel)* (2023) 15(3):1–14. doi: 10.3390/cancers15030834

24. Yan Y, Zhang GX, Gran B, Fallarino F, Yu S, Li H, et al. IDO upregulates regulatory T cells via tryptophan catabolite and suppresses encephalitogenic T cell responses in experimental autoimmune encephalomyelitis. *J Immunol* (2010) 185 (10):5953–61. doi: 10.4049/jimmunol.1001628
25. Rad Pour S, Morikawa H, Kiani NA, Yang M, Azimi A, Shafi G, et al. Exhaustion of CD4+ T-cells mediated by the kynurenine pathway in melanoma. *Sci Rep* (2019) 9 (1):12150. doi: 10.1038/s41598-019-48635-x
26. Ray A, Song Y, Du T, Tai YT, Chauhan D, Anderson KC. Targeting tryptophan catabolic kynurenine pathway enhances antitumor immunity and cytotoxicity in multiple myeloma. *Leukemia* (2020) 34(2):567–77. doi: 10.1038/s41375-019-0558-x
27. Orecchini E, Belladonna ML, Pallotta MT, Volpi C, Zizi L, Panfili E, et al. The signaling function of IDO1 incites the Malignant progression of mouse B16 melanoma. *Oncimmunology* (2023) 12(1):2170095. doi: 10.1080/2162402X.2023.2170095
28. Zhai L, Ladomersky E, Lenzen A, Nguyen B, Patel R, Lauing KL, et al. IDO1 in cancer: a Gemini of immune checkpoints. *Cell Mol Immunol* (2018) 15(5):447–57. doi: 10.1038/cmi.2017.143
29. Rohatgi N, Ghoshdastider U, Baruah P, Kulshrestha T, Skanderup AJ. A pan-cancer metabolic atlas of the tumor microenvironment. *Cell Rep* (2022) 39(6):110800. doi: 10.1016/j.celrep.2022.110800
30. Yu CP, Fu SF, Chen X, Ye J, Ye Y, Kong LD, et al. The clinicopathological and prognostic significance of IDO1 expression in human solid tumors: evidence from a systematic review and meta-analysis. *Cell Physiol Biochem* (2018) 49(1):134–43. doi: 10.1159/000492849
31. Brandacher G, Perathoner A, Ladurner R, Schneeberger S, Obrist P, Winkler C, et al. Prognostic value of indoleamine 2,3-dioxygenase expression in colorectal cancer: effect on tumor-infiltrating T cells. *Clin Cancer Res* (2006) 12(4):1144–51. doi: 10.1158/1078-0432.CCR-05-1966
32. Fallarino F, Grohmann U, You S, McGrath BC, Cavener DR, Vacca C, et al. The combined effects of tryptophan starvation and tryptophan catabolites down-regulate T cell receptor zeta-chain and induce a regulatory phenotype in naive T cells. *J Immunol* (2006) 176(11):6752–61. doi: 10.4049/jimmunol.176.11.6752
33. Liu Y, Liang X, Dong W, Fang Y, Lv J, Zhang T, et al. Tumor-repopulating cells induce PD-1 expression in CD8+ T cells by transferring kynurenine and aHR activation. *Cancer Cell* (2018) 33(3):480–94.e7. doi: 10.1016/j.ccell.2018.02.005
34. Qin R, Zhao C, Wang CJ, Xu W, Zhao JY, Lin Y, et al. Tryptophan potentiates CD8 (+) T cells against cancer cells by TRIP12 tryptophanylation and surface PD-1 downregulation. *J Immunother Cancer* (2021) 9(7):e002840. doi: 10.1136/jitc-2021-002840
35. Corradi G, Bassani B, Simonetti G, Sangaletti S, Vadakekolathu J, Fontana MC, et al. Release of IFN $\gamma$  by acute myeloid leukemia cells remodels bone marrow immune microenvironment by inducing regulatory T cells. *Clin Cancer Res* (2022) 28 (14):3141–55. doi: 10.1158/1078-0432.CCR-21-3594
36. Park A, Yang Y, Lee Y, Kim MS, Park YJ, Jung H, et al. Indoleamine-2,3-dioxygenase in thyroid cancer cells suppresses natural killer cell function by inhibiting NKG2D and NKp46 expression via STAT signaling pathways. *J Clin Med* (2019) 8 (6):842. doi: 10.3390/jcm8060842
37. Chiesa MD, Carlomagno S, Frumento G, Balsamo M, Cantoni C, Conte R, et al. The tryptophan catabolite l-kynurenine inhibits the surface expression of NKp46- and NKG2D-activating receptors and regulates NK-cell function. *Blood* (2006) 108 (13):4118–25. doi: 10.1182/blood-2006-03-006700
38. Fang X, Guo L, Xing S, Shi L, Liang H, Li A, et al. IDO1 can impair NK cells function against non-small cell lung cancer by downregulation of NKG2D Ligand via ADAM10. *Pharmacol Res* (2022) 177:106132. doi: 10.1016/j.phrs.2022.106132
39. Takenaka MC, Gabriely G, Rothhammer V, Mascanfroni ID, Wheeler MA, Chao CC, et al. Control of tumor-associated macrophages and T cells in glioblastoma via AHR and CD39. *Nat Neurosci* (2019) 22(5):729–40. doi: 10.1038/s41593-019-0370-y
40. Campesato LF, Budhu S, Tchaicha J, Weng C-H, Gigoux M, Cohen JJ, et al. Blockade of the AHR restricts a Treg-macrophage suppressive axis induced by L-Kynurenine. *Nat Commun* (2020) 11(1):4011. doi: 10.1038/s41467-020-17750-z
41. Pallotta MT, Orabona C, Volpi C, Vacca C, Belladonna ML, Bianchi R, et al. Indoleamine 2,3-dioxygenase is a signaling protein in long-term tolerance by dendritic cells. *Nat Immunol* (2011) 12(9):870–8. doi: 10.1038/ni.2077
42. Pallotta MT, Rossini S, Suvieri C, Coletti A, Orabona C, Macchiarulo A, et al. Indoleamine 2,3-dioxygenase 1 (IDO1): an up-to-date overview of an eclectic immunoregulatory enzyme. *FEBS J* (2022) 289(20):6099–118. doi: 10.1111/febs.16086
43. Iacono A, Pompa A, De Marchis F, Panfili E, Greco FA, Coletti A, et al. Class IA PI3Ks regulate subcellular and functional dynamics of IDO1. *EMBO Rep* (2020) 21(12):e49756. doi: 10.15252/embr.201949756
44. Zhai L, Bell A, Ladomersky E, Lauing KL, Bollu L, Nguyen B, et al. Tumor cell IDO enhances immune suppression and decreases survival independent of tryptophan metabolism in glioblastoma. *Clin Cancer Res* (2021) 27(23):6514–28. doi: 10.1158/1078-0432.CCR-21-1392
45. Metz R, DuHadaway JB, Kamasani U, Laury-Kleintop L, Muller AJ, Prendergast GC. Novel tryptophan catabolic enzyme IDO2 is the preferred biochemical target of the antitumor indoleamine 2,3-dioxygenase inhibitory compound D-1-methyl-tryptophan. *Cancer Res* (2007) 67(15):7082–7. doi: 10.1158/0008-5472.CAN-07-1872
46. Ball HJ, Sanchez-Perez A, Weiser S, Austin CJ, Astelbauer F, Miu J, et al. Characterization of an indoleamine 2,3-dioxygenase-like protein found in humans and mice. *Gene* (2007) 396(1):203–13. doi: 10.1016/j.gene.2007.04.010
47. Kado SY, Bein K, Castaneda AR, Pouraryan AA, Garrity N, Ishihara Y, et al. Regulation of IDO2 by the aryl hydrocarbon receptor (AhR) in breast cancer. *Cells* (2023) 12(10):1403. doi: 10.3390/cells12101433
48. Vogel CF, Goth SR, Dong B, Pessah IN, Matsumura F. Aryl hydrocarbon receptor signaling mediates expression of indoleamine 2,3-dioxygenase. *Biochem Biophys Res Commun* (2008) 375(3):331–5. doi: 10.1016/j.bbrc.2008.07.156
49. Li Q, Harden JL, Anderson CD, Egilmez NK. Tolerogenic phenotype of IFN- $\gamma$ -induced IDO+ Dendritic cells is maintained via an autocrine IDO-kynurenine/AhR-IDO loop. *J Immunol* (2016) 197(3):962–70. doi: 10.4049/jimmunol.1502615
50. Liu Y, Zhang Y, Zheng X, Zhang X, Wang H, Li Q, et al. Gene silencing of indoleamine 2,3-dioxygenase 2 in melanoma cells induces apoptosis through the suppression of NAD+ and inhibits *in vivo* tumor growth. *Oncotarget* (2016) 7 (22):32329–40. doi: 10.18632/oncotarget.8617
51. Mo B, Zhao X, Wang Y, Jiang X, Liu D, Cai H. Pan-cancer analysis, providing a reliable basis for IDO2 as a prognostic biomarker and target for immunotherapy. *Oncologie* (2023) 25(1):17–35. doi: 10.1515/oncologie-2022-1026
52. Yamasuge W, Yamamoto Y, Fujigaki H, Hoshi M, Nakamoto K, Kunisawa K, et al. Indoleamine 2,3-dioxygenase 2 depletion suppresses tumor growth in a mouse model of Lewis lung carcinoma. *Cancer Sci* (2019) 110(10):3061–7. doi: 10.1111/cas.14179
53. Abd El-Fattah EE. IDO/kynurenine pathway in cancer: possible therapeutic approaches. *J Transl Med* (2022) 20(1):347. doi: 10.1186/s12967-022-03554-w
54. Yuasa HJ, Ball HJ, Ho YF, Austin CJD, Whittington CM, Belov K, et al. Characterization and evolution of vertebrate indoleamine 2, 3-dioxygenases: IDOs from monotremes and marsupials. *Comp Biochem Physiol Part B: Biochem Mol Biol* (2009) 153(2):137–44. doi: 10.1016/j.cbpb.2009.02.002
55. Metz R, Smith C, DuHadaway JB, Chandler P, Baban B, Merlo LM, et al. IDO2 is critical for IDO1-mediated T-cell regulation and exerts a non-redundant function in inflammation. *Int Immunol* (2014) 26(7):357–67. doi: 10.1093/intimm/dxt073
56. Merlo LMF, DuHadaway JB, Montgomery JD, Peng WD, Murray PJ, Prendergast GC, et al. Differential roles of IDO1 and IDO2 in T and B cell inflammatory immune responses. *Front Immunol* (2020) 11:1861. doi: 10.3389/fimmu.2020.01861
57. Merlo LMF, Peng W, DuHadaway JB, Montgomery JD, Prendergast GC, Muller AJ, et al. The immunomodulatory enzyme IDO2 mediates autoimmune arthritis through a nonenzymatic mechanism. *J Immunol* (2022) 208(3):571–81. doi: 10.4049/jimmunol.2100705
58. Cui J, Tian Y, Liu T, Lin X, Li L, Li Z, et al. Pan-cancer analysis of revealed TDO2 as a biomarker of prognosis and immunotherapy. *Dis Markers* (2022) 2022:5447017. doi: 10.1155/2022/5447017
59. Liu H, Xiang Y, Zong QB, Dai ZT, Wu H, Zhang HM, et al. TDO2 modulates liver cancer cell migration and invasion via the Wnt5a pathway. *Int J Oncol* (2022) 60 (6):72. doi: 10.3892/ijo.2022.5362
60. Zhao L, Wang B, Yang C, Lin Y, Zhang Z, Wang S, et al. TDO2 knockdown inhibits colorectal cancer progression via TDO2-KYNU-AhR pathway. *Gene* (2021) 792:145736. doi: 10.1016/j.gene.2021.145736
61. Liu Q, Zhai J, Kong X, Wang X, Wang Z, Fang Y, et al. Comprehensive analysis of the expression and prognosis for TDO2 in breast cancer. *Mol Ther Oncolytics* (2020) 17:153–68. doi: 10.1016/j.omto.2020.03.013
62. Kudo T, Prentzell MT, Mohapatra SR, Sahm F, Zhao Z, Grummt I, et al. Constitutive expression of the immunosuppressive tryptophan dioxygenase TDO2 in glioblastoma is driven by the transcription factor C/EBP $\beta$ . *Front Immunol* (2020) 11:657. doi: 10.3389/fimmu.2020.00657
63. Miyazaki T, Chung S, Sakai H, Ohata H, Obata Y, Shikawa D, et al. Stemness and immune evasion conferred by the TDO2-AHR pathway are associated with liver metastasis of colon cancer. *Cancer Sci* (2022) 113(1):170–81. doi: 10.1111/cas.15182
64. Gutiérrez-Vázquez C, Quintana FJ. Regulation of the immune response by the aryl hydrocarbon receptor. *Immunity* (2018) 48(1):19–33. doi: 10.1016/j.immuni.2017.12.012
65. Hu S, Lu H, Xie W, Wang D, Shan Z, Xing X, et al. TDO2+ myofibroblasts mediate immune suppression in Malignant transformation of squamous cell carcinoma. *J Clin Invest* (2022) 132(19):e157649. doi: 10.1172/JCI157649
66. Kanai M, Funakoshi H, Takahashi H, Hayakawa T, Mizuno S, Matsumoto K, et al. Tryptophan 2,3-dioxygenase is a key modulator of physiological neurogenesis and anxiety-related behavior in mice. *Mol Brain* (2009) 2:8. doi: 10.1186/1756-6606-2-8
67. Schramme F, Crosignani S, Frederix K, Hoffmann D, Pilotte L, Stroobant V, et al. Inhibition of tryptophan-dioxygenase activity increases the antitumor efficacy of immune checkpoint inhibitors. *Cancer Immunol Res* (2020) 8(1):32–45. doi: 10.1158/2326-6066.CIR-19-0041
68. Wu Z, Yan L, Lin J, Ke K, Yang W. Constitutive TDO2 expression promotes liver cancer progression by an autocrine IL-6 signaling pathway. *Cancer Cell Int* (2021) 21 (1):538. doi: 10.1186/s12935-021-02228-9
69. Lee R, Li J, Li J, Wu CJ, Jiang S, Hsu WH, et al. Synthetic essentiality of tryptophan 2,3-dioxygenase 2 in APC-mutated colorectal cancer. *Cancer Discovery* (2022) 12(7):1702–17. doi: 10.1158/2159-8290.CD-21-0680
70. Perez-Castro L, Garcia R, Venkateswaran N, Barnes S, Conacci-Sorrell M. Tryptophan and its metabolites in normal physiology and cancer etiology. *FEBS J* (2023) 290(1):7–27. doi: 10.1111/febs.16245

71. Venkateswaran N, Conacci-Sorrell M. Kynurenine: an oncometabolite in colon cancer. *Cell Stress* (2020) 4(1):24–6. doi: 10.15698/cst2020.01.210
72. Venkateswaran N, Lafita-Navarro MC, Hao YH, Kilgore JA, Perez-Castro L, Braverman J, et al. MYC promotes tryptophan uptake and metabolism by the kynurenine pathway in colon cancer. *Genes Dev* (2019) 33(17–18):1236–51. doi: 10.1101/gad.327056.119
73. Lin KT, Ma WK, Scharner J, Liu YR, Krainer AR. A human-specific switch of alternatively spliced AFMID isoforms contributes to TP53 mutations and tumor recurrence in hepatocellular carcinoma. *Genome Res* (2018) 28(3):275–84. doi: 10.1101/gr.227181.117
74. Tummala KS, Gomes AL, Yilmaz M, Graña O, Bakiri L, Ruppen I, et al. Inhibition of *de novo* NAD(+) synthesis by oncogenic URI causes liver tumorigenesis through DNA damage. *Cancer Cell* (2014) 26(6):826–39. doi: 10.1016/j.ccell.2014.10.002
75. Tripathi SC, Fahrman JF, Vykoukal JV, Dennison JB, Hanash SM. Targeting metabolic vulnerabilities of cancer: Small molecule inhibitors in clinic. *Cancer Rep (Hoboken)* (2019) 2(1):e1131. doi: 10.1073/pnas.1521812113
76. Wang M, Wang Y, Zhang M, Duan Q, Chen C, Sun Q, et al. Kynureninase contributes to the pathogenesis of psoriasis through pro-inflammatory effect. *J Cell Physiol* (2022) 237(1):1044–56. doi: 10.1002/jcp.30587
77. Mohapatra SR, Sadik A, Tykocinski LO, Dietze J, Poschet G, Heiland I, et al. Hypoxia inducible factor 1alpha inhibits the expression of immunosuppressive tryptophan-2,3-dioxygenase in glioblastoma. *Front Immunol* (2019) 10:2762. doi: 10.3389/fimmu.2019.02762
78. Li Y, Wang M, Zhao L, Liang C, Li W. KYNU-related transcriptome profile and clinical outcome from 2994 breast tumors. *Heliyon* (2023) 9(6):e17216. doi: 10.1016/j.heliyon.2023.e17216
79. Itoh G, Takagane K, Fukushima Y, Kuriyama S, Umakoshi M, Goto A, et al. Cancer-associated fibroblasts educate normal fibroblasts to facilitate cancer cell spreading and T-cell suppression. *Mol Oncol* (2022) 16(1):166–87. doi: 10.1002/1878-0261.13077
80. Kesarwani P, Kant S, Zhao Y, Prabhu A, Buelow KL, Miller CR, et al. Quinolate promotes macrophage-induced immune tolerance in glioblastoma through the NMDAR/PPARgamma signaling axis. *Nat Commun* (2023) 14(1):1459. doi: 10.1038/s41467-023-37170-z
81. Heng B, Bilgin AA, Lovejoy DB, Tan VX, Milioli HH, Gluch L, et al. Differential kynurenine pathway metabolism in highly metastatic aggressive breast cancer subtypes: beyond IDO1-induced immunosuppression. *Breast Cancer Res* (2020) 22(1):113. doi: 10.1186/s13058-020-01351-1
82. Liu D, Liang CH, Huang B, Zhuang X, Cui W, Yang L, et al. Tryptophan metabolism acts as a new anti-ferroptotic pathway to mediate tumor growth. *Adv Sci (Weinheim)* (2023) 10(6):e2204006. doi: 10.1002/adv.202204006
83. Weber WP, Feder-Mengus C, Chiarugi A, Rosenthal R, Reschner A, Schumacher R, et al. Differential effects of the tryptophan metabolite 3-hydroxyanthranilic acid on the proliferation of human CD8+ T cells induced by TCR triggering or homeostatic cytokines. *Eur J Immunol* (2006) 36(2):296–304. doi: 10.1002/eji.200535616
84. Amaral M, Levy C, Heyes DJ, Lafite P, Outeiro TF, Giorgini F, et al. Structural basis of kynurenine 3-monooxygenase inhibition. *Nature* (2013) 496(7445):382–5. doi: 10.1038/nature12039
85. Huang TT, Tseng LM, Chen JL, Chu PY, Lee CH, Huang CT, et al. Kynurenine 3-monooxygenase upregulates pluripotent genes through beta-catenin and promotes triple-negative breast cancer progression. *EBioMedicine* (2020) 54:102717. doi: 10.1016/j.ebiom.2020.102717
86. Liu CY, Huang TT, Chen JL, Chu PY, Lee CH, Lee HC, et al. Significance of kynurenine 3-monooxygenase expression in colorectal cancer. *Front Oncol* (2021) 11:620361. doi: 10.3389/fonc.2021.620361
87. Shi Z, Gan G, Gao X, Chen F, Mi J. Kynurenine catabolic enzyme KMO regulates HCC growth. *Clin Transl Med* (2022) 12(2):e697. doi: 10.1002/ctm.2.697
88. Vazquez Cervantes GI, Pineda B, Ramirez Ortega D, Salazar A, Gonzalez Esquivel DF, Rembao D, et al. Kynurenine monooxygenase expression and activity in human astrocytomas. *Cells* (2021) 10(8):2028. doi: 10.3390/cells10082028
89. Tsang YW, Liao CH, Ke CH, Tu CW, Lin CS. Integrated molecular characterization to reveal the association between kynurenine 3-monooxygenase expression and tumorigenesis in human breast cancers. *J Pers Med* (2021) 11(10):948. doi: 10.3390/jpm11100948
90. Lai MH, Liao CH, Tsai NM, Chang KF, Liu CC, Chiu YH, et al. Surface expression of kynurenine 3-monooxygenase promotes proliferation and metastasis in triple-negative breast cancers. *Cancer Control* (2021) 28. doi: 10.1177/10732748211009245
91. Yu P, Li Z, Zhang L, Tagle DA, Cai T. Characterization of kynurenine aminotransferase III, a novel member of a phylogenetically conserved KAT family. *Gene* (2006) 365:111–8. doi: 10.1016/j.gene.2005.09.034
92. Walczak K, Wnorowski A, Turski WA, Plech T. Kynurenine acid and cancer: facts and controversies. *Cell Mol Life Sci* (2020) 77(8):1531–50. doi: 10.1007/s00018-019-03332-w
93. Goldsmith ZG, Dhanasekaran DN. G protein regulation of MAPK networks. *Oncogene* (2007) 26(22):3122–42. doi: 10.1038/sj.onc.1210407
94. Walczak K, Turski WA, Rajtar G. Kynurenine acid inhibits colon cancer proliferation *in vitro*: effects on signaling pathways. *Amino Acids* (2014) 46(10):2393–401. doi: 10.1007/s00726-014-1790-3
95. Walczak K, Turski WA, Rzeski W. Kynurenine acid enhances expression of p21 Waf1/Cip1 in colon cancer HT-29 cells. *Pharmacol Rep* (2012) 64(3):745–50. doi: 10.1016/S1734-1140(12)70870-8
96. Walczak K, Zurawska M, Kis J, Starownik R, Zgrajka W, Bar K, et al. Kynurenine acid in human renal cell carcinoma: its antiproliferative and antimigratory action on Caki-2 cells. *Amino Acids* (2012) 43(4):1663–70. doi: 10.1007/s00726-012-1247-5
97. Moroni F, Cozzi A, Sili M, Mannaioni G. Kynurenine acid: a metabolite with multiple actions and multiple targets in brain and periphery. *J Neural Transm* (2012) 119(2):133–9. doi: 10.1007/s00702-011-0763-x
98. Pagano E, Elias JE, Schneditz G, Saveljeva S, Holland LM, Borrelli F, et al. Activation of the GPR35 pathway drives angiogenesis in the tumour microenvironment. *Gut* (2022) 71(3):509–20. doi: 10.1136/gutjnl-2020-323363
99. DiNatale BC, Murray IA, Schroeder JC, Flaveny CA, Lahoti TS, Laurenzana EM, et al. Kynurenine acid is a potent endogenous aryl hydrocarbon receptor ligand that synergistically induces interleukin-6 in the presence of inflammatory signaling. *Toxicol Sci* (2010) 115(1):89–97. doi: 10.1093/toxsci/kfq024
100. Fisher DT, Appenheimer MM, Evans SS. The two faces of IL-6 in the tumor microenvironment. *Semin Immunol* (2014) 26(1):38–47. doi: 10.1016/j.smim.2014.01.008
101. Sadik A, Somarriba Patterson LF, Ozturk S, Mohapatra SR, Panitz V, Secker PF, et al. IL411 is a metabolic immune checkpoint that activates the AHR and promotes tumor progression. *Cell* (2020) 182(5):1252–70.e34. doi: 10.1016/j.cell.2020.07.038
102. Huang YW, Luo J, Weng YI, Mutch DG, Goodfellow PJ, Miller DS, et al. Promoter hypermethylation of CIDEA, HAAO and RXFP3 associated with microsatellite instability in endometrial carcinomas. *Gynecol Oncol* (2010) 117(2):239–47. doi: 10.1016/j.ygyno.2010.02.006
103. Li Y, Meng L, Shi T, Ren J, Deng Q. Diagnosis and prognosis potential of four gene promoter hypermethylation in prostate cancer. *Cell Biol Int* (2021) 45(1):117–26. doi: 10.1002/cbin.11474
104. Sahm F, Oezen I, Opitz CA, Radlwimmer B, von Deimling A, Ahrendt T, et al. The endogenous tryptophan metabolite and NAD+ precursor quinolinic acid confers resistance of gliomas to oxidative stress. *Cancer Res* (2013) 73(11):3225–34. doi: 10.1158/0008-5472.CAN-12-3831
105. Liu CL, Cheng SP, Chen MJ, Lin CH, Chen SN, Kuo YH, et al. Quinolate phosphoribosyltransferase promotes invasiveness of breast cancer through myosin light chain phosphorylation. *Front Endocrinol (Lausanne)* (2020) 11:621944. doi: 10.3389/fendo.2020.621944
106. Yue Z, Shusheng J, Hongtao S, Shu Z, Lan H, Qingyuan Z, et al. Silencing DSCAM-AS1 suppresses the growth and invasion of ER-positive breast cancer cells by downregulating both DCTPP1 and QPRT. *Aging (Albany NY)* (2020) 12(14):14754–74. doi: 10.18632/aging.103538
107. Ullmark T, Montano G, Jarvstrat L, Jernmark Nilsson H, Hakansson E, Drott K, et al. Anti-apoptotic quinolinic phosphoribosyltransferase (QPRT) is a target gene of Wilms' tumor gene 1 (WT1) protein in leukemic cells. *Biochem Biophys Res Commun* (2017) 482(4):802–7. doi: 10.1016/j.bbrc.2016.11.114
108. Niu YC, Tong J, Shi XF, Zhang T. MicroRNA-654-3p enhances cisplatin sensitivity by targeting QPRT and inhibiting the PI3K/AKT signaling pathway in ovarian cancer cells. *Exp Ther Med* (2020) 20(2):1467–79. doi: 10.3892/etm.2020.8878
109. Thongon N, Zucal C, D'Agostino VG, Tebaldi T, Ravera S, Zamporlini F, et al. Cancer cell metabolic plasticity allows resistance to NAMPT inhibition but invariably induces dependence on LDHA. *Cancer Metab* (2018) 6:1. doi: 10.1186/s40170-018-0174-7
110. Hornigold N, Dunn KR, Craven RA, Zougman A, Trainor S, Shreeve R, et al. Dysregulation at multiple points of the kynurenine pathway is a ubiquitous feature of renal cancer: implications for tumour immune evasion. *Br J Cancer* (2020) 123(1):137–47. doi: 10.1038/s41416-020-0874-y
111. Hamid O, Gajewski TF, Frankel AE, Bauer TM, Olszanski AJ, Luke JJ, et al. 1214O - Epcadostad plus pembrolizumab in patients with advanced melanoma: Phase 1 and 2 efficacy and safety results from ECHO-202/KEYNOTE-037. *Ann Oncol* (2017) 28:v428–v9. doi: 10.1093/annonc/mdx377.001
112. Gangadhar T, Schneider B, Bauer T, Wasser J, Spira A, Patel S, et al. Efficacy and safety of epcadostad plus pembrolizumab treatment of NSCLC: Preliminary phase I/II results of ECHO-202/KEYNOTE-037. *J Clin Oncol* (2017) 35:9014–. doi: 10.1200/JCO.2017.35.15\_suppl.9014
113. Powderly JD, Klempner SJ, Naing A, Bendell J, Garrido-Laguna I, Catenacci DVT, et al. Epcadostad plus pembrolizumab and chemotherapy for advanced solid tumors: results from the phase I/II ECHO-207/KEYNOTE-723 study. *Oncologist* (2022) 27(11):905–e848. doi: 10.1093/oncolo/oyac174
114. Kelly CM, Qin LX, Whiting KA, Richards AL, Avutu V, Chan JE, et al. A phase 2 study of epcadostad and pembrolizumab in patients with advanced sarcoma. *Clin Cancer Res* (2023) 29(11):2043–51. doi: 10.1158/1078-0432.ccr604903.v2
115. Perez R, Riese M, Lewis K, Saleh M, Daud A, Berlin J, et al. Epcadostad plus nivolumab in patients with advanced solid tumors: Preliminary phase I/II results of ECHO-204. *J Clin Oncol* (2017) 35:3003. doi: 10.1200/JCO.2017.35.15\_suppl.3003
116. Nayak-Kapoor A, Hao Z, Sadek R, Dobbins R, Marshall L, Vahanian NN, et al. Phase Ia study of the indoleamine 2,3-dioxygenase 1 (IDO1) inhibitor navoximod (GDC-0919) in patients with recurrent advanced solid tumors. *J Immunother Cancer* (2018) 6(1):61. doi: 10.1186/s40425-018-0351-9



117. Zakharia Y, Johnson TS, Colman H, Vahanian NN, Link CJ, Kennedy E, et al. A phase I/II study of the combination of indoximod and temozolomide for adult patients with temozolomide-refractory primary Malignant brain tumors. *J Clin Oncol* (2014) 32 (15\_suppl):TPS2107–TPS. doi: 10.1200/jco.2014.32.15\_suppl.tps2107
118. Soliman HH, Minton SE, Han HS, Ismail-Khan R, Neuger A, Khambati F, et al. A phase I study of indoximod in patients with advanced Malignancies. *Oncotarget* (2016) 7(16):22928–38. doi: 10.18632/oncotarget.8216
119. Soliman HH, Jackson E, Neuger T, Dees EC, Harvey RD, Han H, et al. A first in man phase I trial of the oral immunomodulator, indoximod, combined with docetaxel in patients with metastatic solid tumors. *Oncotarget* (2014) 5(18):8136–46. doi: 10.18632/oncotarget.2357
120. Jha GG, Gupta S, Tagawa ST, Koopmeiners JS, Vivek S, Dudek AZ, et al. A phase II randomized, double-blind study of sipuleucel-T followed by IDO pathway inhibitor, indoximod, or placebo in the treatment of patients with metastatic castration resistant prostate cancer (mCRPC). *J Clin Oncol* (2017) 35(15\_suppl):3066. doi: 10.1200/JCO.2017.35.15\_suppl.3066
121. Zakharia Y, McWilliams RR, Rixe O, Drabick J, Shaheen MF, Grossmann KF, et al. Phase II trial of the IDO pathway inhibitor indoximod plus pembrolizumab for the treatment of patients with advanced melanoma. *J Immunother Cancer* (2021) 9 (6):1–9. doi: 10.1136/jitc.2020-002057
122. Cherney EC, Zhang L, Nara S, Zhu X, Gullo-Brown J, Maley D, et al. Discovery and preclinical evaluation of BMS-986242, a potent, selective inhibitor of indoleamine-2,3-dioxygenase 1. *ACS Med Chem Lett* (2021) 12(2):288–94. doi: 10.1021/acsmchemlett.0c00668
123. Li P, Wu R, Li K, Yuan W, Zeng C, Zhang Y, et al. IDO inhibition facilitates antitumor immunity of Vγ9Vδ2 T cells in triple-negative breast cancer. *Front Oncol* (2021) 11:679517. doi: 10.3389/fonc.2021.679517
124. Pham KN, Yeh SR. Mapping the binding trajectory of a suicide inhibitor in human indoleamine 2,3-dioxygenase 1. *J Am Chem Soc* (2018) 140(44):14538–41. doi: 10.1021/jacs.8b07994
125. Kim DK, Synn CB, Yang SM, Kang S, Baek S, Oh SW, et al. YH29407 with anti-PD-1 ameliorates anti-tumor effects via increased T cell functionality and antigen presenting machinery in the tumor microenvironment. *Front Chem* (2022) 10:998013. doi: 10.3389/fchem.2022.998013
126. Crosignani S, Bingham P, Botteman P, Cannelle H, Cauwenberghs S, Cordonnier M, et al. Discovery of a novel and selective indoleamine 2,3-dioxygenase (IDO-1) inhibitor 3-(5-fluoro-1H-indol-3-yl)pyrrolidine-2,5-dione (EOS200271/PF-06840003) and its characterization as a potential clinical candidate. *J Med Chem* (2017) 60(23):9617–29. doi: 10.1021/acs.jmedchem.7b00974
127. Gomes B, Driessens G, Bartlett D, Cai D, Cauwenberghs S, Crosignani S, et al. Characterization of the selective indoleamine 2,3-dioxygenase-1 (IDO1) catalytic inhibitor EOS200271/PF-06840003 supports IDO1 as a critical resistance mechanism to PD-(L)1 blockade therapy. *Mol Cancer Ther* (2018) 17(12):2530–42. doi: 10.1158/1535-7163.MCT-17-1104
128. Sonpavde G, Necchi A, Gupta S, Steinberg GD, Gschwend JE, van der Heijden MS, et al. ENERGIIZE: A Phase III study of neoadjuvant chemotherapy alone or with nivolumab with/without linrodostat mesylate for muscle-invasive bladder cancer. *Future Oncol* (2020) 16(2):4359–68. doi: 10.2217/fon-2019-0611
129. Yap TA, Sahebjam S, Hong DS, Chiu VK, Yilmaz E, Efuni S, et al. First-in-human study of KHK2455, a long-acting, potent and selective indoleamine 2,3-dioxygenase 1 (IDO-1) inhibitor, in combination with mogamulizumab (Moga), an anti-CCR4 monoclonal antibody, in patients (pts) with advanced solid tumors. *J Clin Oncol* (2018) 36(15\_suppl):3040. doi: 10.1200/JCO.2018.36.15\_suppl.3040
130. Kotecki N, Vuagnat P, O'Neil BH, Jalal S, Rottey S, Prenen H, et al. A phase I study of an IDO-1 inhibitor (LY3381916) as monotherapy and in combination with an anti-PD-L1 antibody (LY3300054) in patients with advanced cancer. *J Immunother* (2021) 44(7):264–75. doi: 10.1097/CJI.0000000000000368
131. Reardon DA, Desjardins A, Rixe O, Cloughesy T, Alekar S, Williams JH, et al. A phase I study of PF-06840003, an oral indoleamine 2,3-dioxygenase 1 (IDO1) inhibitor in patients with recurrent Malignant glioma. *Invest New Drugs* (2020) 38(6):1784–95. doi: 10.1007/s10637-020-00950-1
132. Zhang L, Cherney EC, Zhu X, Lin TA, Gullo-Brown J, Maley D, et al. Discovery of imidazopyridines as potent inhibitors of indoleamine 2,3-dioxygenase 1 for cancer immunotherapy. *ACS Med Chem Lett* (2021) 12(3):494–501. doi: 10.1021/acsmchemlett.1c00014
133. Steeneck C, Kinzel O, Anderhub S, Hornberger M, Pinto S, Morschhauser B, et al. Discovery and optimization of substituted oxalamides as novel heme-displacing IDO1 inhibitors. *Bioorg Med Chem Lett* (2021) 33:127744. doi: 10.1016/j.bmcl.2020.127744
134. Hamilton MM, Mseeh F, McAfoos TJ, Leonard PG, Reyna NJ, Harris AL, et al. Discovery of IACS-9779 and IACS-70465 as potent inhibitors targeting indoleamine 2,3-dioxygenase 1 (IDO1) apoenzyme. *J Med Chem* (2021) 64(15):11302–29. doi: 10.1021/acs.jmedchem.1c00679
135. Bollu LR, Bommi PV, Monsen PJ, Zhai L, Lauing KL, Bell A, et al. Identification and characterization of a novel indoleamine 2,3-dioxygenase 1 protein degrader for glioblastoma. *J Med Chem* (2022) 65(23):15642–62. doi: 10.1021/acs.jmedchem.2c00771
136. Shi D, Wu X, Jian Y, Wang J, Huang C, Mo S, et al. USP14 promotes tryptophan metabolism and immune suppression by stabilizing IDO1 in colorectal cancer. *Nat Commun* (2022) 13(1):5644. doi: 10.1038/s41467-022-33285-x
137. Winters M, DuHadaway JB, Pham KN, Lewis-Ballester A, Badir S, Wai J, et al. Diaryl hydroxylamines as pan or dual inhibitors of indoleamine 2,3-dioxygenase-1, indoleamine 2,3-dioxygenase-2 and tryptophan dioxygenase. *Eur J Med Chem* (2019) 162:455–64. doi: 10.1016/j.ejmech.2018.11.010
138. Rohrig UF, Majjigapu SR, Caldeleri D, Dilek N, Reichenbach P, Ascencio K, et al. 1,2,3-Triazoles as inhibitors of indoleamine 2,3-dioxygenase 2 (IDO2). *Bioorg Med Chem Lett* (2016) 26(17):4330–3. doi: 10.1016/j.bmcl.2016.07.031
139. Bakmiwewa SM, Fatokun AA, Tran A, Payne RJ, Hunt NH, Ball HJ. Identification of selective inhibitors of indoleamine 2,3-dioxygenase 2. *Bioorg Med Chem Lett* (2012) 22(24):7641–6. doi: 10.1016/j.bmcl.2012.10.010
140. He X, He G, Chu Z, Wu H, Wang J, Ge Y, et al. Discovery of the first potent IDO1/IDO2 dual inhibitors: A promising strategy for cancer immunotherapy. *J Med Chem* (2021) 64(24):17950–68. doi: 10.1021/acs.jmedchem.1c01305
141. Kozlova A, Frederick R. Current state on tryptophan 2,3-dioxygenase inhibitors: a patent review. *Expert Opin Ther Pat* (2019) 29(1):11–23. doi: 10.1080/13543776.2019.1556638
142. Pham KN, Lewis-Ballester A, Yeh SR. Structural basis of inhibitor selectivity in human indoleamine 2,3-dioxygenase 1 and tryptophan dioxygenase. *J Am Chem Soc* (2019) 141(47):18771–9. doi: 10.1021/jacs.9b08871
143. Tijono SM, Palmer BD, Tomek P, Flanagan JU, Henare K, Gamage S, et al. Evaluation of novel inhibitors of tryptophan dioxygenases for enzyme and species selectivity using engineered tumour cell lines expressing either murine or human IDO1 or TDO2. *Pharm (Basel)* (2022) 15(9):1–19. doi: 10.3390/ph15091090
144. Oweira H, Lahdou I, Mehrle S, Khajeh E, Nikbaksh R, Ghamarnejad O, et al. Kynurenine is the main metabolite of tryptophan degradation by tryptophan 2,3-dioxygenase in hepG2 tumor cells. *J Clin Med* (2022) 11(16):1–11. doi: 10.3390/jcm11164794
145. Cecchi M, Mannini A, Lapucci A, Silvano A, Lulli M, Luceri C, et al. Dexamethasone promotes a stem-like phenotype in human melanoma cells via tryptophan 2,3 dioxygenase. *Front Pharmacol* (2022) 13:911019. doi: 10.3389/fphar.2022.911019
146. Cecchi M, Paccosi S, Silvano A, Eid AH, Parenti A. Dexamethasone induces the expression and function of tryptophan-2,3-dioxygenase in SK-MEL-28 melanoma cells. *Pharm (Basel)* (2021) 14(3):1–16. doi: 10.3390/ph14030211
147. Paccosi S, Cecchi M, Silvano A, Parenti A. Different effects of tryptophan 2,3-dioxygenase inhibition on SK-Mel-28 and HCT-8 cancer cell lines. *J Cancer Res Clin Oncol* (2020) 146(12):3155–63. doi: 10.1007/s00432-020-03351-2
148. Chuang TD, Quintanilla D, Boos D, Khorram O. Tryptophan catabolism is dysregulated in leiomyomas. *Fertil Steril* (2021) 116(4):1160–71. doi: 10.1016/j.fertnstert.2021.05.081
149. Bostian AC, Maddukuri L, Reed MR, Savenka T, Hartman JH, Davis L, et al. Kynurenine signaling increases DNA polymerase kappa expression and promotes genomic instability in glioblastoma cells. *Chem Res Toxicol* (2016) 29(1):101–8. doi: 10.1021/acs.chemrestox.5b00452
150. Zhang R, Wang Y, Liu D, Luo Q, Du P, Zhang H, et al. Sodium tanshinone IIA sulfonate as a potent IDO1/TDO2 dual inhibitor enhances anti-PD1 therapy for colorectal cancer in mice. *Front Pharmacol* (2022) 13:870848. doi: 10.3389/fphar.2022.870848
151. Gyulveszi G, Fischer C, Mirolo M, Stern M, Green L, Ceppi M, et al. Abstract LB-085: RG70099: A novel, highly potent dual IDO1/TDO inhibitor to reverse metabolic suppression of immune cells in the tumor micro-environment. *Cancer Res* (2016) 76:LB-085. doi: 10.1158/1538-7445.AM2016-LB-085
152. Gullapalli S, Roychowdhury A, Khaladkar T, Sawargave S, Janrao R, Kalhapure V, et al. Abstract 1701: EPL-1410, a novel fused heterocycle based orally active dual inhibitor of IDO1/TDO2, as a potential immune-oncology therapeutic. *Cancer Res* (2018) 78:1701. doi: 10.1158/1538-7445.AM2018-1701
153. Naing A, Eder JP, Piha-Paul SA, Gimmi C, Hussey E, Zhang S, et al. Preclinical investigations and a first-in-human phase I trial of M4112, the first dual inhibitor of indoleamine 2,3-dioxygenase 1 and tryptophan 2,3-dioxygenase 2, in patients with advanced solid tumors. *J Immunother Cancer* (2020) 8(2):1–10. doi: 10.1136/jitc-2020-000870
154. Han Q, Robinson H, Cai T, Tagle DA, Li J. Structural insight into the inhibition of human kynurenine aminotransferase I/glutamine transaminase K. *J Med Chem* (2009) 52(9):2786–93. doi: 10.1021/jm9000874
155. Jacobs KR, Castellano-Gonzalez G, Guillemin GJ, Lovejoy DB. Major developments in the design of inhibitors along the kynurenine pathway. *Curr Med Chem* (2017) 24(23):2471–95. doi: 10.2174/0929867324666170502123114
156. Lemos H, Mohamed E, Ou R, McCardle C, Zheng X, McGuire K, et al. Co-treatments to boost IDO activity and inhibit production of downstream catabolites induce durable suppression of experimental autoimmune encephalomyelitis. *Front Immunol* (2020) 11:1256. doi: 10.3389/fimmu.2020.01256
157. Pérez de la Cruz G, Pérez de la Cruz V, Navarro Cossio J, Vázquez Cervantes GI, Salazar A, Orozco Morales M, et al. Kynureninase promotes immunosuppression and predicts survival in glioma patients: in silico data analyses of the chinese glioma genome atlas (CGGA) and of the cancer genome atlas (TCGA). *Pharm (Basel)* (2023) 16(3):369. doi: 10.3390/ph16030369
158. Phillips RS. Structure, mechanism, and substrate specificity of kynureninase. *Biochim Biophys Acta* (2011) 1814(11):1481–8. doi: 10.1016/j.bbapap.2010.12.003

159. Kasper SH, Bonocora RP, Wade JT, Musah RA, Cady NC. Chemical inhibition of kynureninase reduces pseudomonas aeruginosa quorum sensing and virulence factor expression. *ACS Chem Biol* (2016) 11(4):1106–17. doi: 10.1021/acschembio.5b01082
160. Drysdale MJ, Reinhard JF. S-aryl cysteine S,S-dioxides as inhibitors of mammalian kynureninase. *Bioorg Med Chem Lett* (1998) 8(2):133–8. doi: 10.1016/S0960-894X(97)10209-8
161. Bender DA, Wynick D. Inhibition of kynureninase (L-kynurenine hydrolase, EC 3.7.1.3) by oestrone sulphate: an alternative explanation for abnormal results of tryptophan load tests in women receiving oestrogenic steroids. *Br J Nutr* (1981) 45(2):269–75. doi: 10.1079/bjn19810103
162. Chiarugi A, Carpenedo R, Molina MT, Mattoli L, Pellicciari R, Moroni F. Comparison of the neurochemical and behavioral effects resulting from the inhibition of kynurenine hydroxylase and/or kynureninase. *J Neurochem* (1995) 65(3):1176–83. doi: 10.1046/j.1471-4159.1995.65031176.x
163. Zhang Y, Wang L, Ren W. Blast-related traumatic brain injury is mediated by the kynurenine pathway. *Neuroreport* (2022) 33(13):569–76. doi: 10.1097/WNR.0000000000001817
164. Yang Q, Hao J, Chi M, Wang Y, Xin B, Huang J, et al. Superior antitumor immunotherapy efficacy of kynureninase modified CAR-T cells through targeting kynurenine metabolism. *Oncoimmunology* (2022) 11(1):2055703. doi: 10.1080/2162402X.2022.2055703
165. Zeng Z, Zhang C, Li J, Cui D, Jiang Y, Pu K. Activatable polymer nanoenzymes for photodynamic immunometabolic cancer therapy. *Advanced Materials* (2021) 33(4):2007247. doi: 10.1002/adma.202007247
166. Hutchinson JP, Rowland P, Taylor MRD, Christodoulou EM, Haslam C, Hobbs CI, et al. Structural and mechanistic basis of differentiated inhibitors of the acute pancreatitis target kynurenine-3-monooxygenase. *Nat Commun* (2017) 8:15827. doi: 10.1038/ncomms15827
167. Beaumont V, Mrzljak L, Dijkman U, Freije R, Heins M, Rassoulpour A, et al. The novel KMO inhibitor CHDI-340246 leads to a restoration of electrophysiological alterations in mouse models of Huntington's disease. *Exp Neurol* (2016) 282:99–118. doi: 10.1016/j.expneurol.2016.05.005
168. Smith JR, Jamie JF, Guillemin GJ. Kynurenine-3-monooxygenase: a review of structure, mechanism, and inhibitors. *Drug Discovery Today* (2016) 21(2):315–24. doi: 10.1016/j.drudis.2015.11.001
169. Mole DJ, Webster SP, Uings I, Zheng X, Binnie M, Wilson K, et al. Kynurenine-3-monooxygenase inhibition prevents multiple organ failure in rodent models of acute pancreatitis. *Nat Med* (2016) 22(2):202–9. doi: 10.1038/nm.4020
170. Gao J, Yao L, Xia T, Liao X, Zhu D, Xiang Y. Biochemistry and structural studies of kynurenine 3-monooxygenase reveal allosteric inhibition by Ro 61-8048. *FASEB J* (2018) 32(4):2036–45. doi: 10.1096/fj.201700397RR
171. Fernando D, Dimelow R, Gorey C, Zhu X, Muya C, Parker C, et al. Assessment of the safety, pharmacokinetics and pharmacodynamics of GSK3335065, an inhibitor of kynurenine monooxygenase, in a randomised placebo-controlled first-in-human study in healthy volunteers. *Br J Clin Pharmacol* (2022) 88(2):865–70. doi: 10.1111/bcp.15010
172. Berg M, Polyzos KA, Agardh H, Baumgartner R, Forteza MJ, Kareinen I, et al. 3-Hydroxyanthranilic acid metabolism controls the hepatic SREBP/lipoprotein axis, inhibits inflammasome activation in macrophages, and decreases atherosclerosis in Ldlr<sup>-/-</sup> mice. *Cardiovasc Res* (2020) 116(12):1948–57. doi: 10.1093/cvr/cvz258
173. Agrawal VK, Sohga R, Khadikar PV. QSAR study on inhibition of brain 3-hydroxy-anthranilic acid dioxygenase (3-HAO): a molecular connectivity approach. *Bioorg Med Chem* (2001) 9(12):3295–9. doi: 10.1016/S0968-0896(01)00242-5
174. Linderberg M, Hellberg S, Björk S, Gotthammar B, Höglberg T, Persson K, et al. Synthesis and QSAR of substituted 3-hydroxyanthranilic acid derivatives as inhibitors of 3-hydroxyanthranilic acid dioxygenase (3-HAO). *Eur J Medicinal Chem* (1999) 34(9):729–44. doi: 10.1016/S0223-5234(99)00220-2
175. Braidly N, Guillemin GJ, Grant R. Effects of kynurenine pathway inhibition on NAD metabolism and cell viability in human primary astrocytes and neurons. *Int J Tryptophan Res* (2011) 4:29–37. doi: 10.4137/IJTR.S7052
176. Modoux M, Rolhion N, Mani S, Sokol H. Tryptophan metabolism as a pharmacological target. *Trends Pharmacol Sci* (2021) 42(1):60–73. doi: 10.1016/j.tips.2020.11.006
177. Ahern TP, Spector LG, Damkier P, Öztürk Esen B, Ulrichsen SP, Eriksen K, et al. Medication-associated phthalate exposure and childhood cancer incidence. *J Natl Cancer Inst* (2022) 114(6):885–94. doi: 10.1093/jnci/djac045
178. Guo T, Meng X, Liu X, Wang J, Yan S, Zhang X, et al. Associations of phthalates with prostate cancer among the US population. *Reprod Toxicol* (2023) 116:108337. doi: 10.1016/j.reprotox.2023.108337
179. Kluwe WM. Carcinogenic potential of phthalic acid esters and related compounds: structure-activity relationships. *Environ Health Perspect* (1986) 65:271–8. doi: 10.1289/ehp.8665271
180. Dunn GP, Bruce AT, Ikeda H, Old LJ, Schreiber RD. Cancer immunoediting: from immunosurveillance to tumor escape. *Nat Immunol* (2002) 3(11):991–8. doi: 10.1038/ni1102-991
181. Liang F, Wang GZ, Wang Y, Yang YN, Wen ZS, Chen DN, et al. Tobacco carcinogen induces tryptophan metabolism and immune suppression via induction of indoleamine 2,3-dioxygenase 1. *Signal Transduct Target Ther* (2022) 7(1):311. doi: 10.1038/s41392-022-01127-3
182. Sweeney C, Lazennec G, Vogel CFA. Environmental exposure and the role of AhR in the tumor microenvironment of breast cancer. *Front Pharmacol* (2022) 13:1095289. doi: 10.3389/fphar.2022.1095289
183. Shen X, Zhao Y, Liu G, Zhou HL, Fan J, Zhang L, et al. Upregulation of programmed death ligand 1 by liver kinase B1 and its implication in programmed death 1 blockade therapy in non-small cell lung cancer. *Life Sci* (2020) 256:117923. doi: 10.1016/j.lfs.2020.117923
184. Zhu B, Tang L, Chen S, Yin C, Peng S, Li X, et al. Targeting the upstream transcriptional activator of PD-L1 as an alternative strategy in melanoma therapy. *Oncogene* (2018) 37(36):4941–54. doi: 10.1038/s41388-018-0314-0
185. Feng J, Read OJ, Dinkova-Kostova AT. Nrf2 in TIME: the emerging role of nuclear factor erythroid 2-related factor 2 in the tumor immune microenvironment. *Mol Cells* (2023) 46(3):142–52. doi: 10.14348/molcells.2023.2183





## OPEN ACCESS

## EDITED BY

Johannes Fahrman,  
University of Texas MD Anderson Cancer  
Center, United States

## REVIEWED BY

Ehsan Irajizad,  
University of Texas MD Anderson Cancer  
Center, United States  
Ana Kenney,  
University of California, Irvine, United States  
James Long,  
University of Texas MD Anderson Cancer  
Center, United States

## \*CORRESPONDENCE

Huawei Zhang

✉ slyyzhw@163.com;

✉ zhanghuawei@sdfmu.edu.cn

Jia Qu

✉ qujia19880106@163.com

RECEIVED 05 September 2023

ACCEPTED 11 December 2023

PUBLISHED 04 January 2024

## CITATION

Zhang T, Liu J, Wang M, Liu X, Qu J and  
Zhang H (2024) Prognosis stratification and  
response to treatment in breast cancer based  
on one-carbon metabolism-related signature.  
*Front. Oncol.* 13:1288909.  
doi: 10.3389/fonc.2023.1288909

## COPYRIGHT

© 2024 Zhang, Liu, Wang, Liu, Qu and Zhang.  
This is an open-access article distributed under  
the terms of the [Creative Commons Attribution  
License \(CC BY\)](https://creativecommons.org/licenses/by/4.0/). The use, distribution or  
reproduction in other forums is permitted,  
provided the original author(s) and the  
copyright owner(s) are credited and that the  
original publication in this journal is cited, in  
accordance with accepted academic  
practice. No use, distribution or reproduction  
is permitted which does not comply with  
these terms.

# Prognosis stratification and response to treatment in breast cancer based on one-carbon metabolism-related signature

Tongxin Zhang, Jingyu Liu, Meihuan Wang, Xiao Liu,  
Jia Qu\* and Huawei Zhang\*

Department of Ultrasound, Shandong Provincial Hospital Affiliated to Shandong First Medical University, Jinan, Shandong, China

**Introduction:** Breast cancer (BC) is the most common malignant tumor in the female population. Despite staging and treatment consensus guidelines, significant heterogeneity exists in BC patients' prognosis and treatment efficacy. Alterations in one-carbon (1C) metabolism are critical for tumor growth, but the value of the role of 1C metabolism in BC has not been fully investigated.

**Methods:** To investigate the prognostic value of 1C metabolism-related genes in BC, 72 1C metabolism-related genes from GSE20685 dataset were used to construct a risk-score model via univariate Cox regression analysis and the least absolute shrinkage and selection operator (LASSO) regression algorithm, which was validated on three external datasets. Based on the risk score, all BC patients were categorized into high-risk and low-risk groups. The predictive ability of the model in the four datasets was verified by plotting Kaplan-Meier curve and receiver operating characteristic (ROC) curve. The candidate genes were then analyzed in relation to gene mutations, gene enrichment pathways, immune infiltration, immunotherapy, and drug sensitivity.

**Results:** We identified a 7-gene 1C metabolism-related signature for prognosis and structured a prognostic model. ROC analysis demonstrated that the model accurately predicted the 2-, 3-, and 5-year overall survival rate of BC patients in the four cohorts. Kaplan-Meier analysis revealed that survival time of high-risk patients was markedly shorter than that of low-risk patients ( $p < 0.05$ ). Meanwhile, high-risk patients had a higher tumor mutational burden (TMB), enrichment of tumor-associated pathways such as the IL-17 signaling pathway, lower levels of T follicular helper (Tfh) and B cells naive infiltration, and poorer response to immunotherapy. Furthermore, a strong correlation was found between MAT2B and CHKB and immune checkpoints.

**Discussion:** These findings offer new insights into the effect of 1C metabolism in the onset, progression, and therapy of BC and can be used to assess BC patients' prognosis, study immune infiltration, and develop potentially more effective clinical treatment options.

#### KEYWORDS

one-carbon metabolism, breast cancer, prognosis, immune cell infiltration, immunotherapy, drug sensitivity

## 1 Introduction

As recently reported, the incidence of breast cancer (BC) continues to rise, accounting for 31% of all new cancer cases among the female population in the U.S. in 2023 (1). Currently, BC treatment mainly includes chemotherapy, radiotherapy, targeted therapy, immunotherapy, and preoperative and postoperative endocrine therapy, according to international consensus guidelines (2). However, due to tumor heterogeneity, metastatic heterogeneity, and drug resistance, many BC patients still do not benefit from chemotherapy, endocrine therapy, and other routine treatments and have poor prognoses (3, 4). After diagnosis and routine treatment of the primary tumor, 20%-30% of BC patients may develop metastases (4), and metastatic BC has been reported to have a 5-year survival rate of only 28% (5). Thus, the search for new tumor biomarkers and therapeutic targets is crucial for identifying BC patients with poor prognoses and guiding the treatment of BC.

One-carbon (1C) metabolism involves a range of interrelated metabolic pathways such as the methionine cycle, the folate cycle, and the transsulfuration pathway, which are essential for cellular function and facilitate the distribution of 1C units to different cellular processes through a range of chemical reactions (6). These processes include cellular biosynthesis (DNA, amino acids, polyamines, phospholipids, and creatine, etc.), amino acid homeostasis (serine, glycine, and methionine), redox state maintenance, epigenetics regulation, and genome maintenance via regulation of nucleotide pools (7, 8). Importantly, in addition to the synthesis of nucleotides and certain amino acids, folate-mediated 1C metabolism controls the production of glutathione and S-adenosylmethionine, as well as other critical cellular processes associated with the rapid progression of malignancies (9). In addition, 1C metabolizing enzymes have been demonstrated to be up-regulated in expression in a variety of cancers (10). For example, SHMT2 has been determined to be overexpressed in BC, glioblastoma, and colorectal cancer (11–13). Elevated expression levels of SHMT2 in triple-negative breast cancer (TNBC) patients correlate with their poorer prognosis (14). Expression of DNMT3B in thyroid and hepatocellular carcinoma is closely related to their poor prognosis (15, 16). Today, certain drugs that target 1C

metabolizing enzymes have been developed and applied in the clinic, including methotrexate and pemetrexed (8). These drugs have far-reaching implications in the treatment of many cancers, including BC (17–19).

Immune cells include cancer cells, non-tumor host cells (innate and adaptive immune cells, etc.), and their noncellular components, which are crucial players in the tumor microenvironment (TME) (20). Studies have shown that 1C metabolism affects immune cell function, especially T-cell activation (8). Tumor progression, invasion, metastasis, and drug resistance are emergent characteristics of tumor cell-TME interactions (21). Targeting the TME in combination with multiple therapeutic modalities, such as chemotherapy, radiation, immunotherapy, surgery, and nanotherapy, can synergistically and effectively target key pathways associated with disease pathogenesis (22). However, the specific effect of 1C metabolism on TME needs further study.

In this study, a 1C metabolism-related genes risk score model was constructed. Then the prognostic value of the seven candidate genes was confirmed by extensive analysis. Finally, the correlation of candidate genes with immune checkpoints, related immunotherapy, and sensitivity to common chemotherapeutic drugs was investigated to contribute to guiding the treatment of BC patients.

## 2 Materials and methods

### 2.1 Data source and processing

Gene expression profiles of 327 BC samples in the GSE20685 were obtained from Gene Expression Omnibus (GEO) database (<https://www.ncbi.nlm.nih.gov/geo/>) as a training dataset, together with their clinical data such as age, TNM stage, and survival status. Three additional GEO datasets were also obtained from GEO database as test datasets, including GSE88770, GSE58812, and GSE61304. The samples in dataset GSE58812 were all TNBC. After processing the datasets according to the same filtering criteria such as removing samples with incomplete data, expression profiles and clinical data were used to conduct subsequent analysis. Gene mutation data were acquired from The Cancer Genome Atlas

(TCGA) database (<https://portal.gdc.cancer.gov/>). In addition, 72 1C metabolism-related genes were retrieved from the Molecular Signature Database (MSigDB, <https://www.gsea-msigdb.org/gsea/msigdb>) with the keyword “one-carbon metabolism” (Supplementary Table 1). These genes were used as the basis for our further studies.

## 2.2 Construction of the risk score model

We structured a risk signature assessment system based on the expression of 1C metabolism-related genes to analyze the correlation between these genes' expression and BC prognosis. For this purpose, genes were binarized into high or low according to expression, and then raw expression was used for signature generation. Firstly, 1C metabolism-related genes with prognostic value in BC were extracted by univariate Cox regression analysis, and the genes with  $p < 0.05$  were identified to be overall survival (OS)-related genes. Genes with non-significant differences in survival between high- and low-expression groups were removed by log-rank test. The least absolute shrinkage and selection operator (LASSO) regression (with R packages “glmnet”) was then used to determine non-zero coefficients, to achieve the purpose of eliminating potential predictors and selecting the optimal OS-related genes while preventing model overfitting. The LASSO regression tuned the model with 10-fold cross-validation. Additionally, we conducted multivariate Cox regression analysis to further determine model genes and risk coefficients. Finally, seven genes affecting prognosis were screened, including MAT2B, DNMT3B, AHCYL1, CHDH, SHMT2, CHKB, and CHPT1. For every patient, the product of coefficients and prognostic gene expression level was risk score. Furthermore, BC samples were categorized into two subgroups based on median risk scores, including high- and low-risk groups.

## 2.3 Prognostic model validation

For assessing the feasibility of the 1C metabolism-related genes risk score model, Kaplan-Meier survival analyses of OS were implemented between the high- and low-risk groups in the training set GSE20685, as well as the validation sets GSE88770 and GSE58812, respectively. Meanwhile, we used the outcome events and time in GSE61304 to validate the disease-free survival (DFS) of BC. In addition, the R package “timeROC” was used to plot receiver operating characteristic (ROC) curves of 2-, 3-, and 5-year survival. The area under the ROC curve (AUC) was also calculated to further analyze and validate the accuracy of the model.

## 2.4 Independent prognostic analysis and nomogram construction

Univariate and multivariate Cox regression analyses for age, TNM stage, and risk score were performed from the training

dataset GSE20685 clinical information to assess independent prognostic factors for BC. Then, according to independent prognostic analyses, a nomogram combining the 1C metabolism-related risk score with other clinical characteristics in the training dataset was developed with the “rms” R package. In addition, we plotted calibration curves to visualize the consistency of the nomogram at 2, 3, and 5 years as evidence of its clinical predictive value. Additionally, we constructed a multivariate Cox model containing clinical characteristic information and risk scores on the training dataset, and then performed validation evaluations on the test datasets.

## 2.5 Functional enrichment analysis

To investigate potential biological functions and signaling pathways of the two groups, we employed the R package “Limma” for screening differentially expressed genes (DEGs) among both groups with the criteria of  $|\log FC| > 1$  and  $p\text{-value}_t < 0.05$ , and then analyzed them with Gene Ontology (GO) and Kyoto Encyclopedia of Genes and Genomes (KEGG) analyses. Gene set enrichment analysis (GSEA) was performed on the training set using the R package “ClusterProfiler” to further identify the different biological processes involved in the two risk groups. The annotated gene set was extracted from the R package “org.Hs.eg.db” and used in our analysis.

## 2.6 Somatic mutations and immune infiltration analysis

We retrieved somatic mutation profiles of BC patients from TCGA database to analyze somatic mutations among both groups. The somatic mutation data were further analyzed with the R package “maftools”. Correlations between the expression of seven candidate genes and the tumor mutational burden (TMB) were analyzed, and the results were plotted by selecting those with significant correlations. Moreover, cell type identification by estimating relative subsets of RNA transcripts (CIBERSORT) was utilized to calculate the abundance of 22 tumor immuno-infiltrative cells within TME of BC samples from the GSE20685 cohort. Subsequently, differences in immune cell infiltration were analyzed for the two risk groups, with  $p\text{-value} < 0.05$  considered statistically significant. The results were revealed by box plots.

## 2.7 Immune checkpoints analysis and immunotherapy response assessment

We analyzed the correlation of seven candidate genes with immunological checkpoint genes (ICGs). A list of 79 common ICGs can be obtained from a previous article (Supplementary Table 2) (23), and 71 of them were included in our expression matrix. Five ICGs significantly related to 1C metabolism-related

genes (CD27, HLA-DPB1, HLA-E, CD40, and HLA-DMB) were screened to plot the correlation heat map. Furthermore, immunophenotype score (IPS) were obtained from The Cancer Immunome Atlas (TCIA, <https://tcia.at/>) database, which is helpful in screening patients who are sensitive to immune checkpoint inhibitors (ICIs). To match the sample in the IPS data, we used the TCGA-BRCA dataset for analysis. Hence, IPS differences between high and low expression of seven candidate genes were analyzed, and the results with statistically significant differences were selected to draw violin plots.

## 2.8 Drug sensitivity analysis

Response to chemotherapy in BC patients was assessed with the Genomics of Drug Sensitivity in Cancer database (GDSC, <https://www.cancerrxgene.org>) via the R package “oncoPredict”. Correlations between the two risk groups and the sensitivity to common chemotherapeutic drugs were calculated separately.

## 2.9 Statistical analysis

Statistical analyses were accomplished via R (version 4.2.2). Survival analyses were presented by Kaplan-Meier approach, and differences between groups were assessed with log-rank test. Pearson’s correlation test was used for correlation analysis. Univariate and multivariate analyses were performed with Cox regression models to determine independent risk factors. The *p*-value < 0.05 was regarded as statistically significant.

# 3 Results

## 3.1 Prognostic characteristics and value of 1C metabolism-related genes

The study’s flow is illustrated in Figure 1A. We ultimately constructed a 7-gene 1C metabolism-related prognostic model, including MAT2B, DNMT3B, AHCYL1, CHDH, SHMT2, CHKB, and CHPT1. The process of LASSO regression was shown in Figures 1B, C. Kaplan-Meier analysis revealed seven genes correlated with OS. Among them, five genes, MAT2B, AHCYL1, CHDH, CHKB, and CHPT1, were regarded as protective factors, whereas two other genes, DNMT3B and SHMT2, were considered as risk factors (*p* < 0.05) (Figure 1D). Meanwhile, the following risk score formula was obtained after multivariate Cox regression: risk score =  $(-1.166 \times \text{MAT2B}) + (-0.040 \times \text{DNMT3B}) + (-0.581 \times \text{AHCYL1}) + (-0.067 \times \text{CHDH}) + (0.168 \times \text{SHMT2}) + (-0.609 \times \text{CHKB}) + (-0.346 \times \text{CHPT1})$ . Grouped according to the median risk score, the expression differences of the seven candidate genes in the two risk groups were presented in Figure 1E. The forest plot showed the results of stepwise multivariate Cox proportional hazards regression analysis (Supplementary Figure 1).

## 3.2 Validation of the 1C metabolism-related genes model prediction effect

To demonstrate the credibility of the prediction of the seven 1C metabolism-related genes, we conducted survival analyses and plotted ROC curves on the training and test cohorts, respectively. The AUCs for 2-, 3- and 5-year survival in the GSE20685 training set were 0.79, 0.76, and 0.78, respectively (Figure 2A), while in GSE88770, GSE58812, and GSE61304 the AUCs for 2-, 3- and 5- year were 0.84, 0.71 and 0.76; 0.62, 0.71 and 0.71; 0.70, 0.74 and 0.64, respectively (Figures 2B, 3A, B). In addition, Kaplan-Meier analysis revealed that survival time was markedly shorter in the high-risk group than the other one (GSE20685: *p* < 0.0001; GSE88770: *p* = 0.0031; GSE58812: *p* = 0.037; GSE61304: *p* = 0.043) (Figures 2C, D, 3C, D). Furthermore, risk curves and scatter plots showed that mortality increases with risk scores in all four datasets (Figures 2E, F, 3E, F). The heat maps also showed remarkable expression differences in seven prognostic genes between both groups (Figures 2E, F, 3E, F).

## 3.3 Independent prognostic analysis and nomogram development

For the training dataset GSE20685, in the univariate Cox analysis, TNM stage and risk score were closely linked to OS in BC patients (*p* < 0.001), whereas in multivariate Cox analysis, only N-stage and risk score were independent prognostic predictors (*p* < 0.001) (Figures 4A, B). Therefore, a nomogram was built to quantitatively predict individual OS at 2-, 3-, and 5-year based on independent prognostic markers (N-stage and risk score) (Figure 4C). Then, to verify its predictive effectiveness, calibration curves were plotted to confirm the consistency, which showed the desired predictive accuracy (Figure 4D). In summary, the nomogram can predict short- and long-term OS in BC patients, thus contributing to clinical management. Furthermore, the performance of the multivariate Cox model containing clinical characteristic information and risk score on the training and test datasets was shown in Supplementary Figures 2A-H. In addition, the N-stage was positively linked to risk score (Figure 4E), with a statistically significant difference (*p* < 0.05).

## 3.4 Mutation landscape analysis

To further investigate discrepancies in the genetic landscape between both groups, somatic mutation data from TCGA database of BC patients were used for analysis. In the high-risk group, TP53 had the highest mutation frequency at 48%, followed by PIK3CA, TTN, GATA3, MUC16, and CDH1 (Figure 5A). Correspondingly, in the low-risk group, the top six genes in terms of mutation frequency were PIK3CA, CDH1, TP53, TTN, GATA3, and MAP3K1 (Figure 5B). Meanwhile, the mutation frequency of the same gene differed considerably between groups (Figure 5C). TMB was higher in the high-risk group compared to the other group (Figure 5D). In addition, the expression of SHMT2 and DNMT3B was positively correlated with TMB, while the expression of CHDH

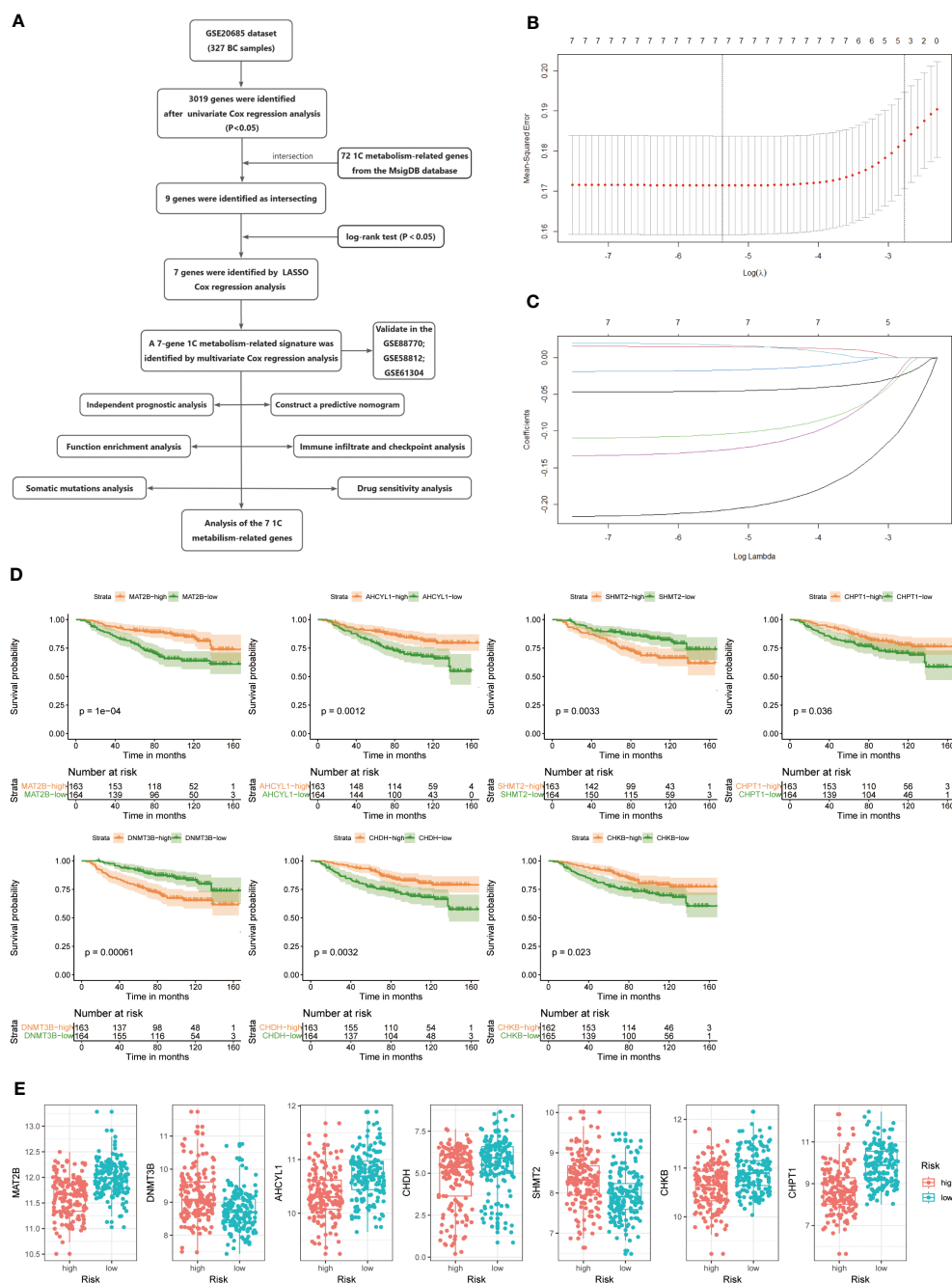


FIGURE 1

(A) Flow chart of the study. (B, C) LASSO Cox regression analysis to develop the prognostic model. (D) Kaplan-Meier survival curves of seven genes associated with OS. (E) Expression of seven genes in the high- and low-risk groups.

was negatively correlated with TMB ( $P < 0.05$ ) (Figure 5E), suggesting that these genes play a role in immunotherapy.

### 3.5 Gene set enrichment analysis

We screened 98 differentially expressed genes (DEGs) by the “limma” variance approach, with 17 up-regulated as well as 81 down-regulated genes (Figure 6A). GO terms in biological process

(BP), cellular component (CC), and molecular function (MF) that were significantly associated with these DEGs were represented in the bubble diagram (Figure 6B), suggesting that these DEGs were mainly related to urogenital system development, female sex differentiation, and collagen-containing extracellular matrix. Furthermore, we found that the IL-17 signaling pathway, relaxin signaling pathway, cellular senescence, lipid and atherosclerosis, phototransduction, and bladder cancer are up-regulated, while breast cancer, hedgehog signaling pathway, neuroactive ligand-



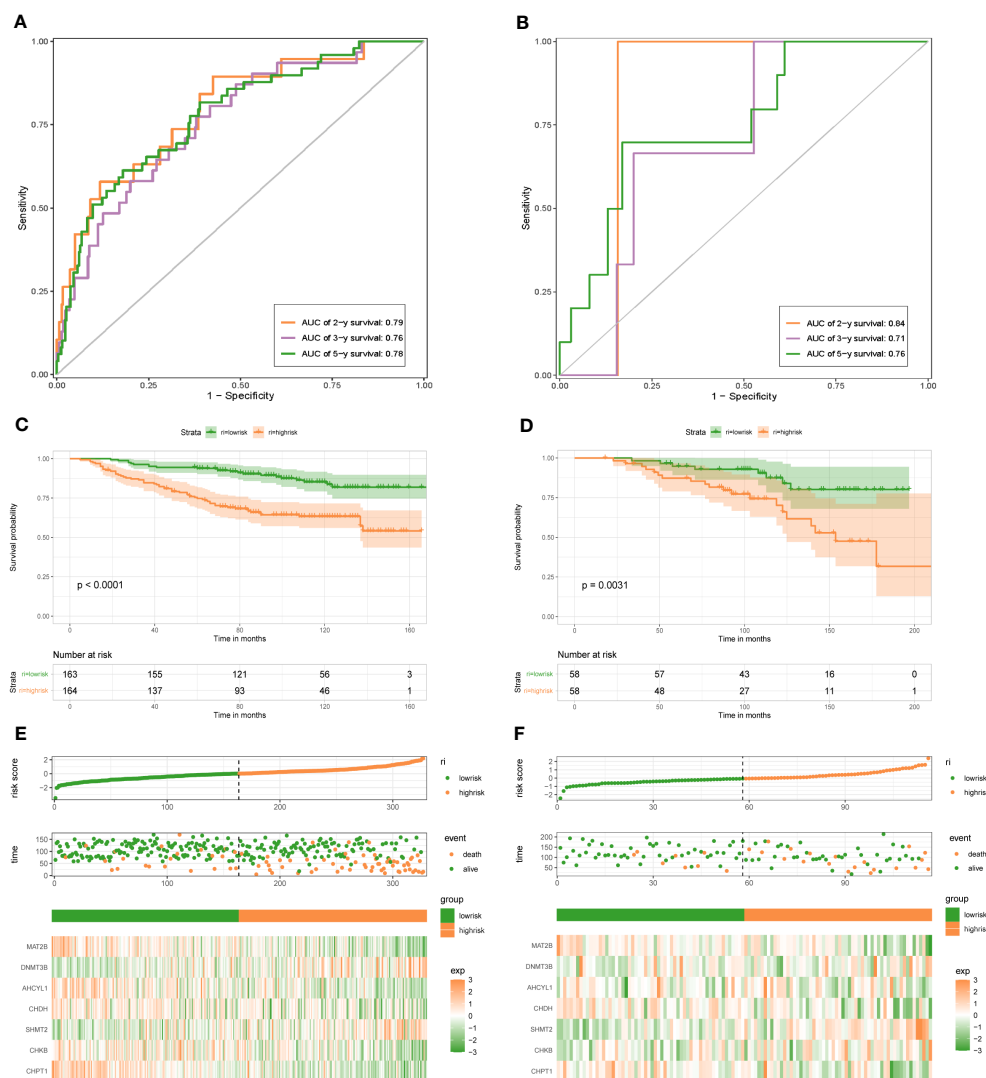


FIGURE 2

1C metabolism-related genes signature associated with the OS of BC patients. (A) The predictive value for the 2-y, 3-y, and 5-y OS in GSE20685 dataset. (B) The predictive value for the 2-y, 3-y, and 5-y OS in GSE88770 dataset. (C) The OS between the high- and low-risk groups in GSE20685 dataset. (D) The OS between the high- and low-risk groups in GSE88770 dataset. (E) The risk plot of the 1C metabolism-related genes signature in GSE20685 dataset. (F) The risk plot of the 1C metabolism-related genes signature in GSE88770 dataset.

receptor interaction, complement and coagulation cascades, and estrogen signaling pathway are down-regulated (Figure 6C). In addition, to identify the underlying biological signaling pathways for molecular discrepancies between both risk groups, we performed GSEA analyses (Figures 6D, E). The results indicated that in the high-risk group, pathways such as alcoholism, cell cycle, cellular senescence, IL-17 signaling pathway, and bladder cancer were significantly enriched, while pathways significantly enriched in the low-risk group included regulation of lipolysis in adipocytes, chemical carcinogenesis-DNA adducts, chemical carcinogenesis-receptor activation, the complement and coagulation cascades, herpes simplex virus 1 infection, and peroxisome.

### 3.6 Immuno-infiltration analysis

We compared the levels of immune infiltration in the two risk groups, and the distribution of immune cells in both was reflected in Figures 7A, B. In addition, the overall immune infiltration in all BC samples in the training set was illustrated in Figure 7C. Further combined with the difference and correlation analysis, some immune cell subpopulations showed statistically significant differences between both groups. In particular, the infiltration levels of T follicular helper (Tfh) and B cells naive were lower in the high-risk group, whereas Neutrophils infiltration abundance was higher in the high-risk group (Figure 7D).

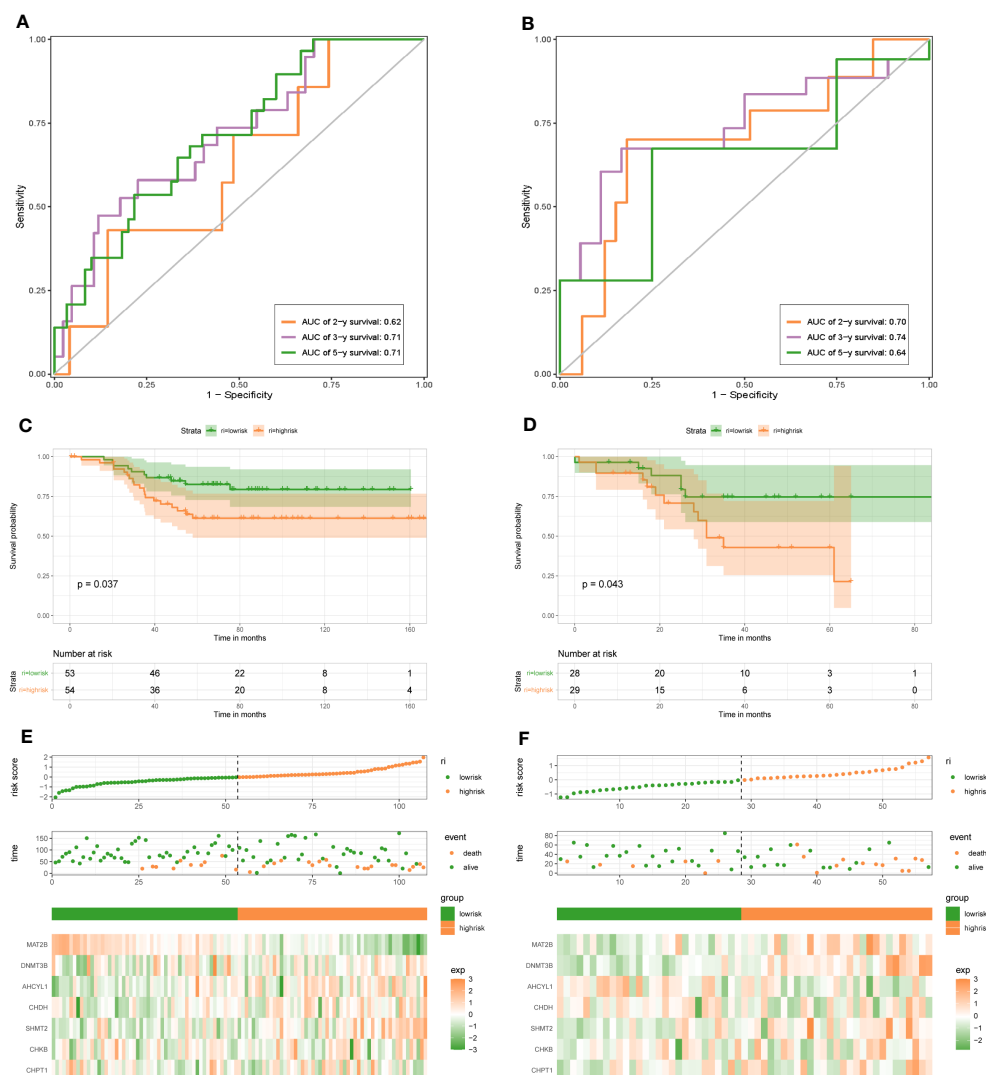


FIGURE 3

1C metabolism-related gene signature associated with the OS and DFS of BC patients. (A) The predictive value for the 2-y, 3-y, and 5-y OS in GSE58812 dataset. (B) The predictive value for the 2-y, 3-y, and 5-y DFS in GSE61304 dataset. (C) The OS between the high- and low-risk groups in GSE58812 dataset. (D) The DFS between the high- and low-risk groups in GSE61304 dataset. (E) The risk plot of the 1C metabolism-related genes signature in GSE58812 dataset. (F) The risk plot of the 1C metabolism-related genes signature in GSE61304 dataset.

### 3.7 Immune checkpoints and immunotherapy research

The heat map of the association between 7 1C metabolism-related genes and 71 ICGs was displayed in [Supplementary Figure 3](#). Among them, the 5 ICGs that were significantly correlated with the 1C metabolism-related genes were selected for redrawing the heat map ([Figure 8A](#)). In addition, MAT2B and CHKB are closely associated with immune checkpoints as shown in [Figures 8B, C](#). Furthermore, BC patients with low expressions of DNMT3B and AHCYL1 had higher IPS, indicating that these patients had higher relative probabilities of responding to ICIs, whereas BC patients with high expressions of MAT2B, CHKB, and SHMT2 had higher relative probabilities of responding to ICIs ([Figure 8D](#)).

### 3.8 Drug sensitivity analysis

To improve the clinical utility of survival models in the management of BC, we calculated and compared IC50 values in two groups of patients, because IC50 values are inversely related to drug sensitivity. The results revealed that low-risk patients were more sensitive to Mitoxantrone, Oxaliplatin, Dabrafenib, Dactinomycin, Leflunomide, Ruxolitinib, Nilotinib, Sorafenib, Irinotecan, and Zoledronate. Meanwhile, high-risk patients were more sensitive to Lapatinib, Afatinib, Osimertinib, and Ibrutinib ( $P < 0.05$ ) ([Figure 9A](#)). In addition, there are drugs targeting 7 1C metabolism-related genes available for the treatment of BC. We discovered a positive association between SHMT2 expression and sensitivity to Paclitaxel, Vinorelbine, Vorinostat, Entinostat,

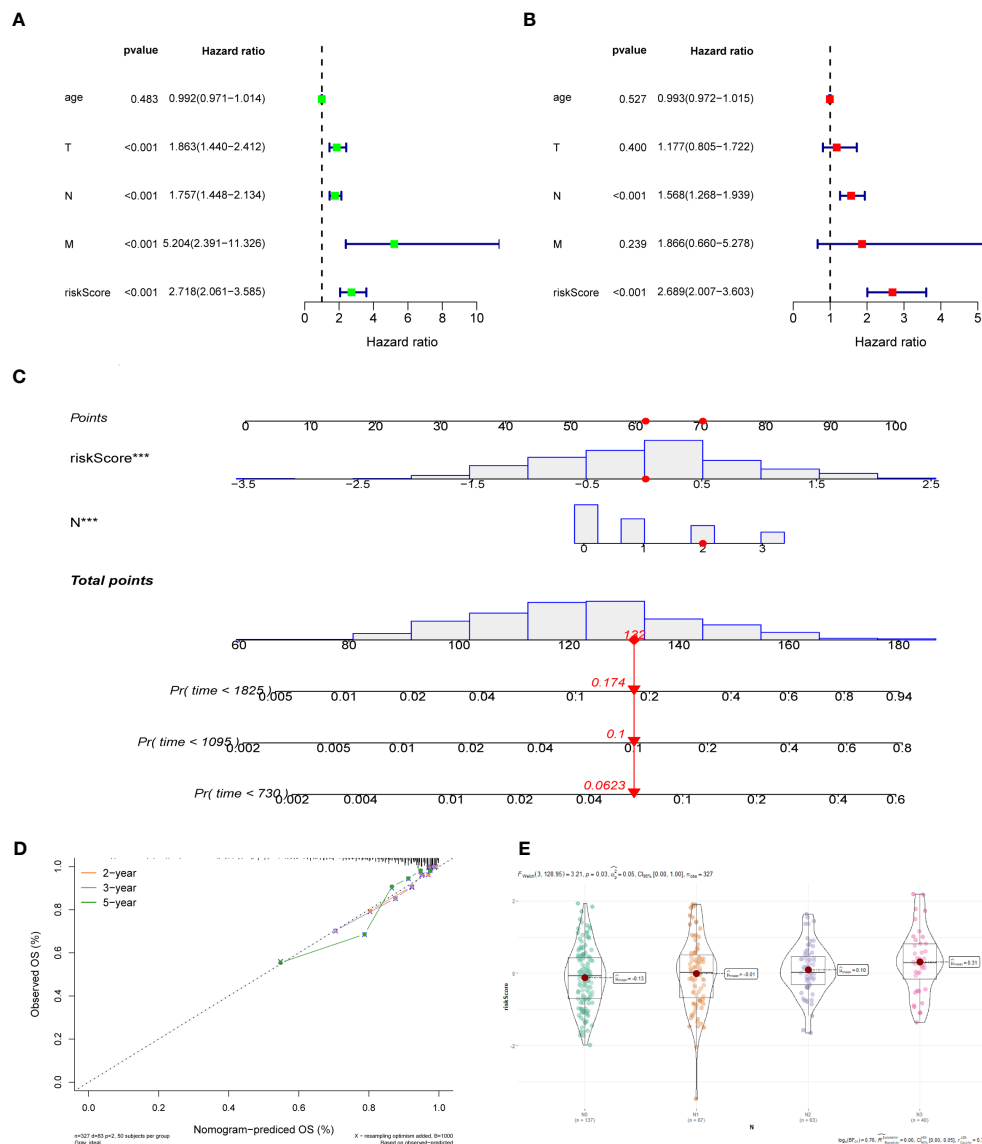


FIGURE 4

(A) Univariate Cox regression analysis of the risk score and clinical parameters. (B) Multivariate Cox regression analysis of the risk score and clinical parameters. (C) The construction of 2-, 3-, and 5-year OS predictive nomogram for patients of the GSE20685. (D) Calibration curves for the nomogram. (E) Distribution of risk scores in different N-stage in GSE20685 dataset.

Docetaxel, Alpelisib, Bortezomib, Crizotinib, Gefitinib, and Erlotinib. The expression of AHCYL1 was negatively associated with Talazoparib, Cisplatin, Dasatinib, Crizotinib, and Bortezomib. The expression of MAT2B was positively related to Ribociclib. The sensitivity to Ribociclib was negatively linked to CHPT1 expression. CHKB expression was positively connected to Niraparib and Selumetinib (Figure 9B). With the above findings, the risk score can be used as a guide for medication administration in BC patients.

## 4 Discussion

BC has surpassed lung cancer as the most prevalent cancer in women (24). Despite improvements in its multidisciplinary

treatment, BC remains the leading cause of death in female cancer patients (24, 25). Alterations in the metabolism of cancer cells are critical for tumor growth, and one of the most remarkable aspects of this metabolic reprogramming is the 1C metabolism (26). However, there is still a lack of studies on the 1C metabolism in BC patients. Therefore, our research aims to make an essential step in that direction.

We constructed a survival risk signature by 1C metabolism-related genes in this study, which performed well in both training and validation set cohorts. Furthermore, Kaplan-Meier analysis showed that two genes can be regarded as risk factors, including SHMT2 and DNMT3B, and five genes were identified as protective factors, including MAT2B, AHCYL1, CHDH, CHKB, and CHPT1. Moreover, the expression values of these genes were also measured

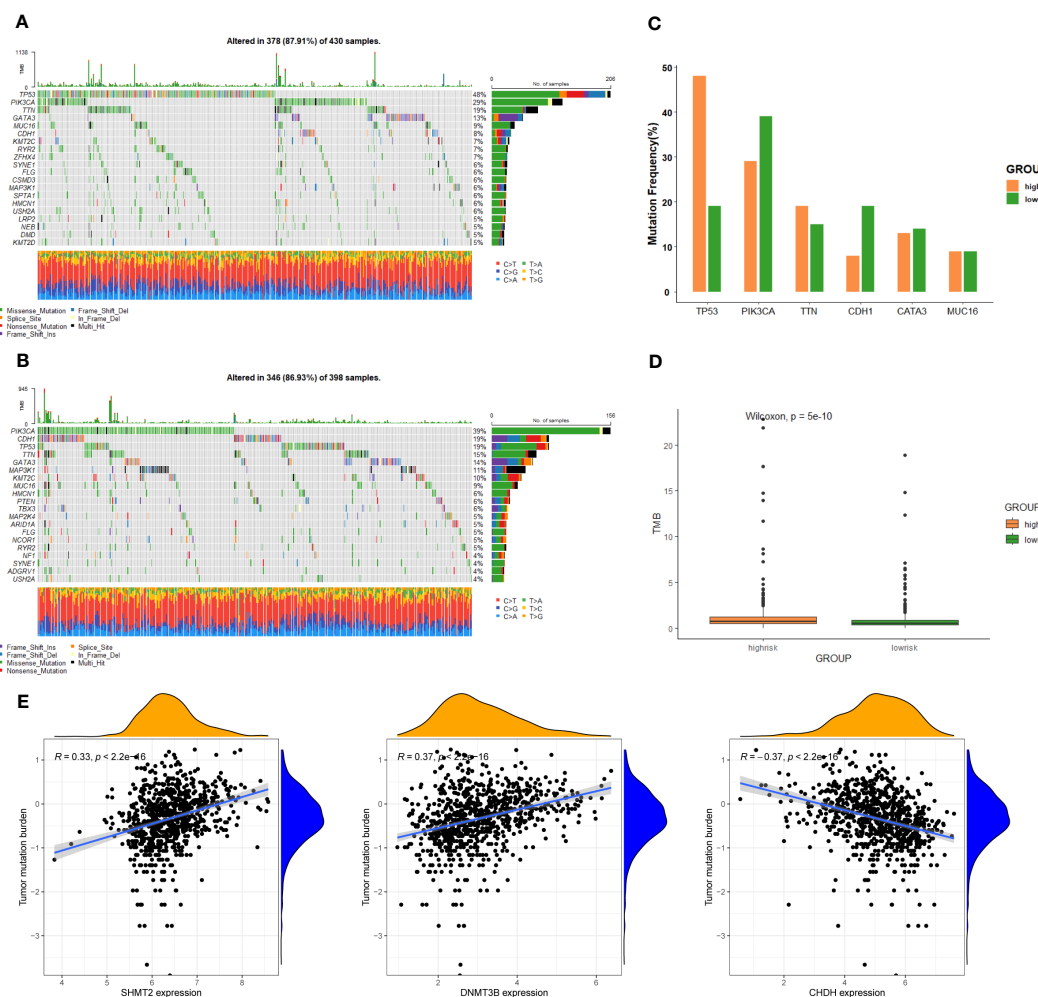


FIGURE 5

Genomic alterations between the high-risk group and low-risk group. (A) The landscape of mutation profiles in the high-risk group. (B) The landscape of mutation profiles in the low-risk group. (C) The six genes with the greatest variation in mutation frequency in the high-risk group and low-risk group. (D) The difference in tumor mutation burden between the high-risk group and low-risk group. (E) Correlation between the expression levels of target genes and tumor mutation burden.

in both groups. Two genes were up-regulated in high-risk patients, consisting of SHMT2 and DNMT3B, while the down-regulated genes included MAT2B, AHCYL1, CHDH, CHKB, and CHPT1, which was consistent with Kaplan-Meier analysis. Among them, SHMT2 is considered to be an important factor in the metabolism of serine and glycine of several cancer cell types (including BC) (27), which is crucial in the development of cancer cells, and high SHMT2 expression is linked to poor prognosis in BC (28). DNMT3B acts as a key player in breast tumorigenesis and development, and targeting DNMT3B may be a potential treatment for BC (29). Conversely, CHDH is an estrogen-regulated gene that is overexpressed in BC patients with good prognosis (30). As an enzyme related to methionine metabolism, MAT2B can act as a cancer suppressor gene in BC development (31). In addition, CHPT1, AHCYL1, and CHKB have been demonstrated to be associated with roles that lead to other cancers and affect patient outcomes, although relevant studies are scarce in BC (32–34).

Tumor-infiltrating immune cells are reported to be an essential component of TME and can be used to predict cancer prognosis (35). Hence, immune cells have been identified as a new cancer treatment target (36). Differences in TME between the two groups were examined using CIBERSORT. The results illustrated higher levels of infiltration of Tfh cells and naive B cells, and lower levels of infiltration of neutrophils in low-risk patients. Tfh cells are reported to be a subset of CD4<sup>+</sup> helper T cells involved in the humoral response (37), whose role is to trigger B cells in the germinal center to differentiate into plasma cells secreting antibodies and memory B cells, which is the key to enhancing the immune response (38, 39). In addition, naive B cells are activated, proliferate, and differentiate into plasma cells and memory B cells, which are involved in antitumor immunity (40). Accordingly, we presume that low-risk patients might benefit more from immunotherapy. Moreover, neutrophils can produce immunosuppressive factors, such as transforming growth factor beta (TGF- $\beta$ ) and arginase1, effectively suppressing adaptive immunity (41), and release growth factors such as hepatocyte growth

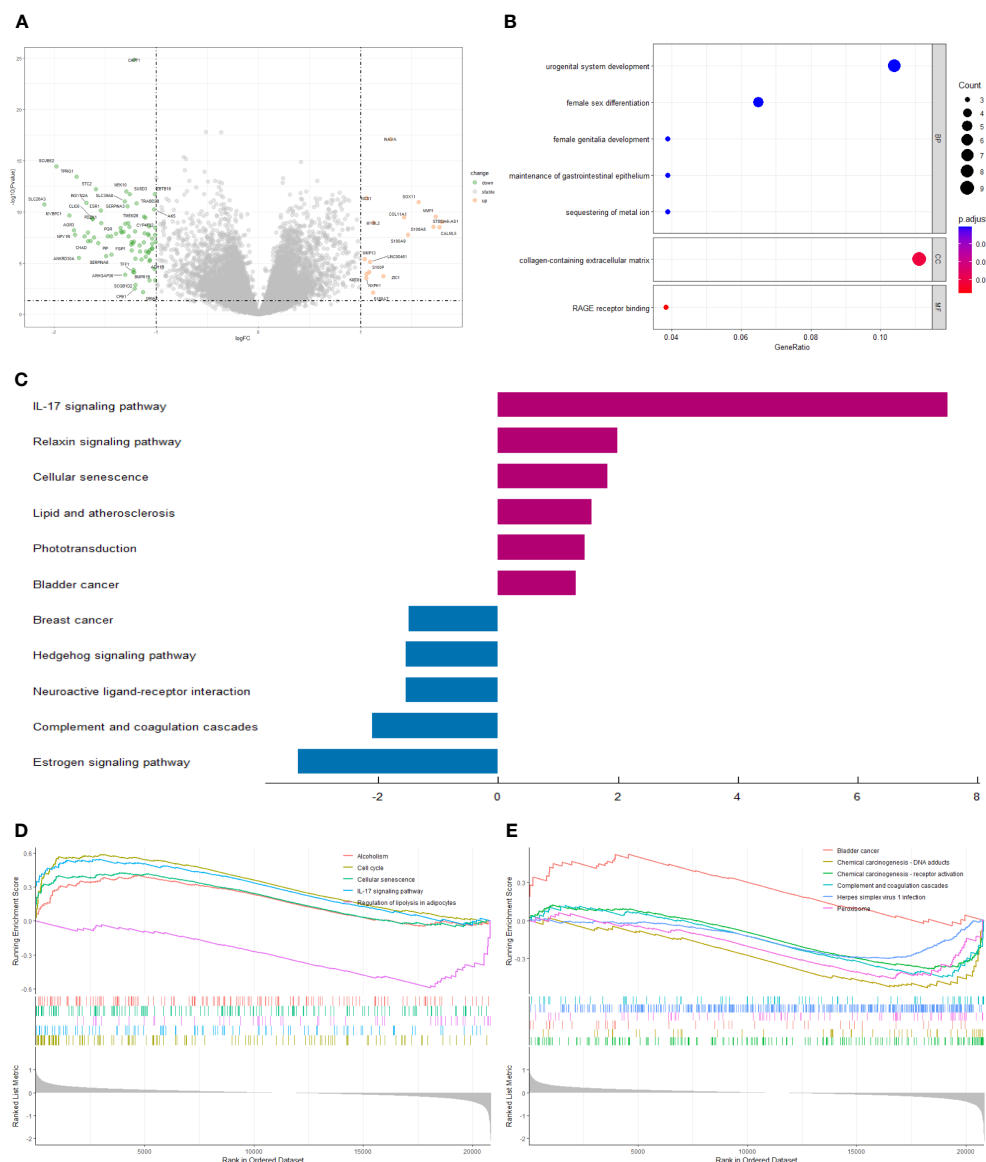


FIGURE 6

(A) The volcano plot of differential gene expression in high- and low-risk groups ( $|\log_2 FC| > 1$  and  $p\text{-value}_t < 0.05$ ). (B) Bubble plot for GO enrichment analysis. (C) Two-way bar chart for KEGG enrichment analysis. (D, E) Results of GSEA in GSE20685 cohort.

factor (42), which promote tumor progression. It has also been shown that a high neutrophil/lymphocyte in the circulation is a poor prognostic factor in breast, liver, colon, and many other types of cancer (41, 43), which is consistent with our findings. However, the results did not demonstrate an effect of 1C metabolism on T cell activation. It has been reported that 1C metabolism contributes to purine and thymidine synthesis, allowing T cell proliferation and survival, whereas genetic inhibition of the metabolic enzyme SHMT2 impaired T cell survival and antigen-specific T cell abundance in culture and *in vivo*, respectively (44). The interaction of these factors may have led to the generation of such inconsistent results. It may also be due to differences in study design and clinical characteristics of the subjects.

In our study, the IL-17 signaling pathway was significantly enriched in KEGG and GSEA. The IL-17 family comprises six

members (IL-17A to IL-17F) with distinct functions and sequence homologies (45). Their aberrant expression is closely linked to chronic inflammatory diseases and acts as an essential player in cancer immunity (46). A number of recent findings have elucidated the effect of the IL-17B/IL-17RB pathway in tumorigenesis. For example, in mice, IL-17B signaling via IL-17RB facilitates cancer cell survival, invasion, proliferation, and metastasis (47–50), whereas in humans, high expression of IL-17B and IL-17RB is linked to a poorer prognostic outcome in BC sufferers (48). In addition, the peroxisome and herpes simplex virus-1 infection were found to be enriched in the low-risk group. Peroxisomes are organelles that affect the growth and survival of cancer cells, and some cancer cells rely on lipolysis by peroxisomes for their energy needs (51). Oncolytic herpes simplex virus-1 infection increases anticancer activity by inducing apoptosis in adjacent cancer cells



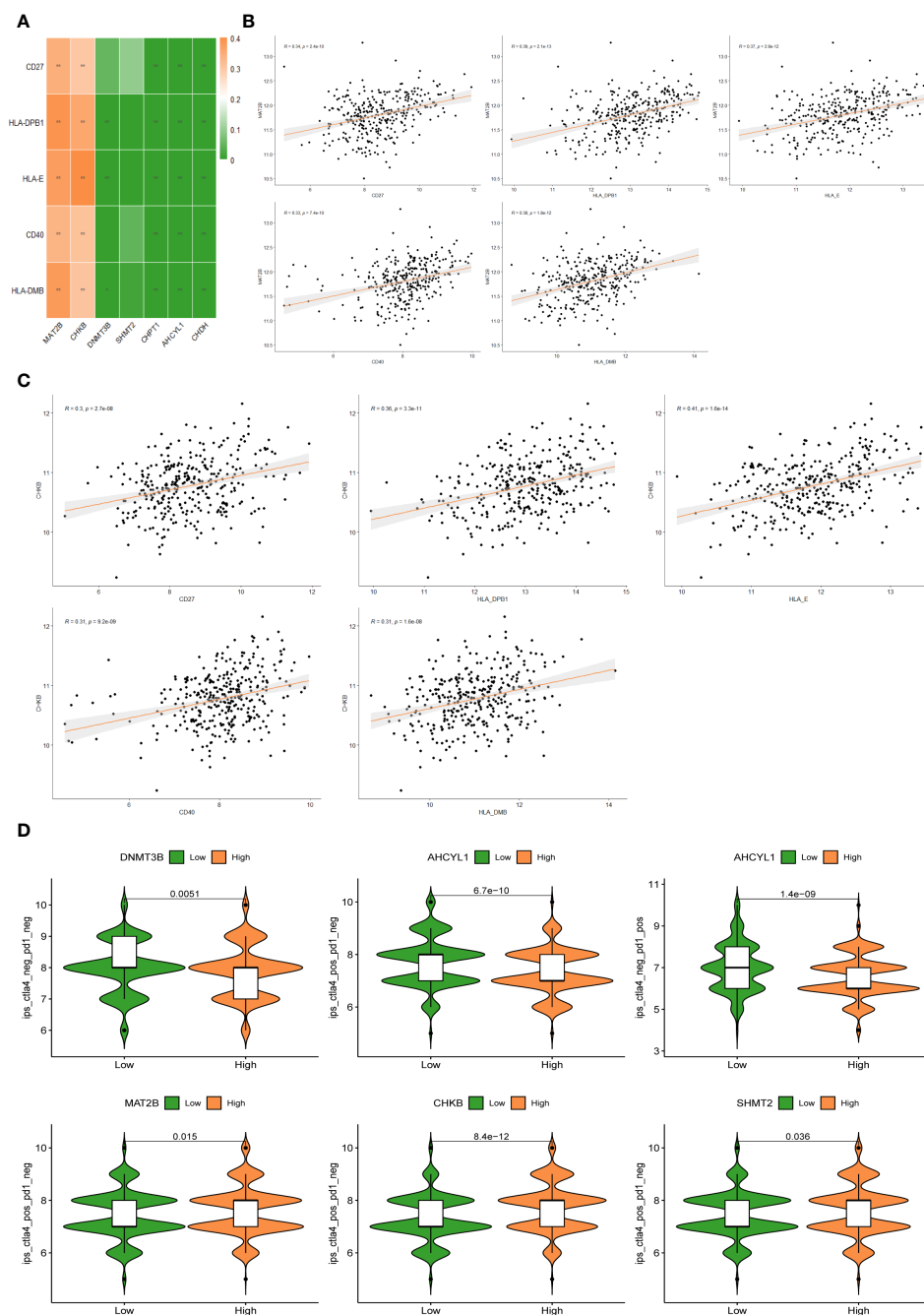


FIGURE 8

(A) Correlation heat map between 5 immune checkpoints and 7 1C metabolism-related genes. (B) Correlation between MAT2B expression levels and 5 immune checkpoints. (C) Correlation between CHKB expression levels and 5 immune checkpoints. (D) Differences in IPS reactivity between high and low expression levels of target genes.

(52). The enrichment of these pathways is consistent with the finding that low-risk patients survived longer.

ICIs rebuild the anti-tumor immune response by blocking co-inhibitory signaling pathways, thereby promoting immune-mediated elimination of tumor cells (53). Although ICIs, particularly anti-CTLA4 and anti-PD-1 antibodies, have radically improved the prognosis of many cancers, especially advanced melanoma (54), they have been less effective in BC patients (55). This approach can be used to identify and screen

patients who respond to treatment. Based on the research results, BC patients with high expression of MAT2B and CHKB may benefit from targeted therapy against immune checkpoints with increased expression, such as CD27, CD40, HLA-DPB1, HLA-E, and HLA-DMB. The results of immunotherapy analysis further proved the potential of these seven candidate genes as novel prognostic indicators and intervention targets for signature development. Therefore, for BC patients, using our 1C metabolism-related genes model to



FIGURE 7

TME immune cell infiltration of BC samples from the GSE20685 cohort. (A) Heat map of the differences in immune cell distribution for each BC patient in high-risk group. (B) Heat map of the differences in immune cell distribution for each BC patient in low-risk group. (C) Histogram of the distribution of immune cells in all BC patients. (D) Differences in the distribution of immune cells in high- and low-risk groups.

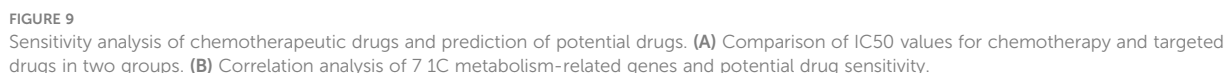
predict their response to ICIs can guide clinical treatment more concretely and effectively.

Although some positive results have been obtained, several limitations of our study remain. Since this is a retrospective study, data omissions and selection bias are inevitable. Secondly, our study is based on data from existing publicly accessible databases, so the results need to be further validated in large cohorts. Further, people in GSE61304 dataset have been followed for only 80 months while in other datasets individuals have been followed up for more than 150

months. This discrepancy in follow-up time can create a problem in the validation. Finally, in-depth characterization of the mechanism through *in vivo* or *in vitro* experiments is required.

## 5 Conclusion

In summary, seven 1C metabolism-related genes were identified, resulting in a risk score model that can accurately



## Author contributions

## Funding

## Data availability statement

Frontiers in Oncology

## Conflict of interest

The authors declare that the research was conducted in the absence of any commercial or financial relationships that could be construed as a potential conflict of interest.

## Publisher's note

All claims expressed in this article are solely those of the authors and do not necessarily represent those of their affiliated

organizations, or those of the publisher, the editors and the reviewers. Any product that may be evaluated in this article, or claim that may be made by its manufacturer, is not guaranteed or endorsed by the publisher.

## Supplementary material

The Supplementary Material for this article can be found online at: <https://www.frontiersin.org/articles/10.3389/fonc.2023.1288909/full#supplementary-material>

## References

1. Siegel RL, Miller KD, Wagle NS, Jemal A. Cancer statistics, 2023. *CA Cancer J Clin* (2023) 73(1):17–48. doi: 10.3322/caac.21763
2. Cardoso F, Paluch-Shimon S, Senkus E, Curigliano G, Aapro MS, André F, et al. 5th ESO-ESMO international consensus guidelines for advanced breast cancer (ABC 5). *Ann Oncol* (2020) 31(12):1623–49. doi: 10.1016/j.annonc.2020.09.010
3. Wang X, Wang C, Guan J, Chen B, Xu L, Chen C. Progress of Breast Cancer basic research in China. *Int J Biol Sci* (2021) 17(8):2069–79. doi: 10.7150/ijbs.60631
4. Liang Y, Zhang H, Song X, Yang Q. Metastatic heterogeneity of breast cancer: Molecular mechanism and potential therapeutic targets. *Semin Cancer Biol* (2020) 60:14–27. doi: 10.1016/j.semcancer.2019.08.012
5. Scherer SD, Riggio AI, Haroun F, DeRose YS, Ekiz HA, Fujita M, et al. An immune-humanized patient-derived xenograft model of estrogen-independent, hormone receptor positive metastatic breast cancer. *Breast Cancer Res* (2021) 23(1):100. doi: 10.1186/s13058-021-01476-x
6. Clare CE, Brassington AH, Kwong WY, Sinclair KD. One-carbon metabolism: linking nutritional biochemistry to epigenetic programming of long-term development. *Annu Rev Anim Biosci* (2019) 7:263–87. doi: 10.1146/annurev-animal-020518-115206
7. Locasale JW. Serine, glycine and one-carbon units: cancer metabolism in full circle. *Nat Rev Cancer* (2013) 13(8):572–83. doi: 10.1038/nrc3557
8. Ducker GS, Rabinowitz JD. One-carbon metabolism in health and disease. *Cell Metab* (2017) 25(1):27–42. doi: 10.1016/j.cmet.2016.08.009
9. Tibbetts AS, Appling DR. Compartmentalization of Mammalian folate-mediated one-carbon metabolism. *Annu Rev Nutr* (2010) 30:57–81. doi: 10.1146/annurev.nutr.012809.104810
10. Mehrmohamadi M, Liu X, Shestov AA, Locasale JW. Characterization of the usage of the serine metabolic network in human cancer. *Cell Rep* (2014) 9(4):1507–19. doi: 10.1016/j.celrep.2014.10.026
11. Li AM, Ducker GS, Li Y, Seoane JA, Xiao Y, Melemenidis S, et al. Metabolic profiling reveals a dependency of human metastatic breast cancer on mitochondrial serine and one-carbon unit metabolism. *Mol Cancer Res* (2020) 18(4):599–611. doi: 10.1158/1541-7786.MCR-19-0606
12. Engel AL, Lorenz NI, Klann K, Münch C, Depner C, Steinbach JP, et al. Serine-dependent redox homeostasis regulates glioblastoma cell survival. *Br J Cancer* (2020) 122(9):1391–8. doi: 10.1038/s41416-020-0794-x
13. Miyo M, Konno M, Colvin H, Nishida N, Koseki J, Kawamoto K, et al. The importance of mitochondrial folate enzymes in human colorectal cancer. *Oncol Rep* (2017) 37(1):417–25. doi: 10.3892/or.2016.5264
14. Aslan M, Hsu EC, Garcia-Marques FJ, Bermudez A, Liu S, Shen M, et al. Oncogene-mediated metabolic gene signature predicts breast cancer outcome. *NPJ Breast Cancer* (2021) 7:141. doi: 10.1038/s41523-021-00341-6
15. Zhu X, Xue C, Kang X, Jia X, Wang L, Younis MH, et al. DNMT3B-mediated FAM111B methylation promotes papillary thyroid tumor glycolysis, growth and metastasis. *Int J Biol Sci* (2022) 18(11):4372–87. doi: 10.7150/ijbs.72397
16. Lai SC, Su YT, Chi CC, Kuo YC, Lee KF, Wu YC, et al. DNMT3b/OCT4 expression confers sorafenib resistance and poor prognosis of hepatocellular carcinoma through IL-6/STAT3 regulation. *J Exp Clin Cancer Res* (2019) 38(1):474. doi: 10.1186/s13046-019-1442-2
17. Robinson AD, Eich ML, Varambally S. Dysregulation of *de novo* nucleotide biosynthetic pathway enzymes in cancer and targeting opportunities. *Cancer Lett* (2020) 470:134–40. doi: 10.1016/j.canlet.2019.11.013
18. Martin M, Spielmann M, Namer M, duBois A, Unger C, Dodwell D, et al. Phase II study of pemetrexed in breast cancer patients pretreated with anthracyclines. *Ann Oncol* (2003) 14(8):1246–52. doi: 10.1093/annonc/mdg339
19. Shakeran Z, Keyhanfar M, Varshosaz J, Sutherland DS. Biodegradable nanocarriers based on chitosan-modified mesoporous silica nanoparticles for delivery of methotrexate for application in breast cancer treatment. *Materials Sci Engineering: C* (2021) 118:111526. doi: 10.1016/j.msec.2020.111526
20. Xiao Y, Yu D. Tumor microenvironment as a therapeutic target in cancer. *Pharmacol Ther* (2021) 221:107753. doi: 10.1016/j.pharmthera.2020.107753
21. Meurette O, Mehlen P. Notch signaling in the tumor microenvironment. *Cancer Cell* (2018) 34(4):536–48. doi: 10.1016/j.ccell.2018.07.009
22. Kumari S, Advani D, Sharma S, Ambasta RK, Kumar P. Combinatorial therapy in tumor microenvironment: Where do we stand? *Biochim Biophys Acta Rev Cancer* (2021) 1876(2):188585. doi: 10.1016/j.bbcan.2021.188585
23. Hu FF, Liu CJ, Liu LL, Zhang Q, Guo AY. Expression profile of immune checkpoint genes and their roles in predicting immunotherapy response. *Brief Bioinform* (2021) 22(3):bbaa176. doi: 10.1093/bib/bbaa176
24. Sung H, Ferlay J, Siegel RL, Laversanne M, Soerjomataram I, Jemal A, et al. Global cancer statistics 2020: GLOBOCAN estimates of incidence and mortality worldwide for 36 cancers in 185 countries. *CA Cancer J Clin* (2021) 71(3):209–49. doi: 10.3322/caac.21660
25. Waks AG, Winer EP. Breast cancer treatment: A review. *JAMA* (2019) 321(3):288–300. doi: 10.1001/jama.2018.19323
26. Rosenzweig A, Blenis J, Gomes AP. Beyond the warburg effect: how do cancer cells regulate one-carbon metabolism? *Front Cell Dev Biol* (2018) 6:90. doi: 10.3389/fcell.2018.00090
27. Jain M, Nilsson R, Sharma S, Madhusudhan N, Kitami T, Souza AL, et al. Metabolite profiling identifies a key role for glycine in rapid cancer cell proliferation. *Science* (2012) 336(6084):1040–4. doi: 10.1126/science.1218595
28. Bernhardt S, Bayerlová M, Vetter M, Wachter A, Mitra D, Hanf V, et al. Proteomic profiling of breast cancer metabolism identifies SHMT2 and ASCT2 as prognostic factors. *Breast Cancer Res* (2017) 19:112. doi: 10.1186/s13058-017-0905-7
29. Man X, Li Q, Wang B, Zhang H, Zhang S, Li Z. DNMT3A and DNMT3B in breast tumorigenesis and potential therapy. *Front Cell Dev Biol* (2022) 10:916725. doi: 10.3389/fcell.2022.916725
30. Wang Z, Dahiya S, Provencher H, Muir B, Carney E, Coser K, et al. The prognostic biomarkers HOXB13, IL17BR, and CHDH are regulated by estrogen in breast cancer. *Clin Cancer Res* (2007) 13(21):6327–34. doi: 10.1158/1078-0432.CCR-07-0310
31. Wang CY, Chiao CC, Phan NN, Li CY, Sun ZD, Jiang JZ, et al. Gene signatures and potential therapeutic targets of amino acid metabolism in estrogen receptor-positive breast cancer. *Am J Cancer Res* (2020) 10(1):95–113.
32. Wen S, He Y, Wang L, Zhang J, Quan C, Niu Y, et al. Aberrant activation of super enhancer and choline metabolism drive antiandrogen therapy resistance in prostate cancer. *Oncogene* (2020) 39(42):6556–71. doi: 10.1038/s41388-020-01456-z
33. Li X, Zhang M, Yu X, Xue M, Li X, Ma C, et al. AHCYL1 is a novel biomarker for predicting prognosis and immunotherapy response in colorectal cancer. *J Oncol* (2022) 2022:5054324. doi: 10.1155/2022/5054324
34. Liu C, Liu D, Wang F, Liu Y, Xie J, Xie J, et al. Construction of a novel choline metabolism-related signature to predict prognosis, immune landscape, and chemotherapy response in colon adenocarcinoma. *Front Immunol* (2022) 13:1038927. doi: 10.3389/fimmu.2022.1038927
35. Bense RD, Sotiriou C, Piccart-Gebhart MJ, Haanen JBAG, van Vugt MATM, de Vries EGE, et al. Relevance of tumor-infiltrating immune cell composition and functionality for disease outcome in breast cancer. *J Natl Cancer Inst* (2017) 109(1):djjw192. doi: 10.1093/jnci/djjw192
36. Lazăr DC, Avram MF, Romoșan I, Cornianu M, Tăban S, Goldiș A. Prognostic significance of tumor immune microenvironment and immunotherapy: Novel insights and future perspectives in gastric cancer. *World J Gastroenterol* (2018) 24(23):3583–616. doi: 10.3748/wjg.v24.i23.3583

37. Crotty S. T follicular helper cell differentiation, function, and roles in disease. *Immunity*. (2014) 41(4):529–42. doi: 10.1016/j.immuni.2014.10.004
38. Johnston RJ, Poholek AC, DiToro D, Yusuf I, Eto D, Barnett B, et al. Bcl6 and blimp-1 are reciprocal and antagonistic regulators of T follicular helper cell differentiation. *Science*. (2009) 325(5943):1006–10. doi: 10.1126/science.1175870
39. Crotty S. Follicular helper CD4 T cells (TFH). *Annu Rev Immunol* (2011) 29(1):621–63. doi: 10.1146/annurev-immunol-031210-101400
40. Downs-Canner SM, Meier J, Vincent BG, Serody JS. B cell function in the tumor microenvironment. *Annu Rev Immunol* (2022) 40:169–93. doi: 10.1146/annurev-immunol-101220-015603
41. Grecian R, Whyte MKB, Walmsley SR. The role of neutrophils in cancer. *Br Med Bull* (2018) 128(1):5–14. doi: 10.1093/bmb/ldy029
42. Wislez M, Rabbe N, Marchal J, Milleron B, Crestani B, Mayaud C, et al. Hepatocyte growth factor production by neutrophils infiltrating bronchioloalveolar subtype pulmonary adenocarcinoma: role in tumor progression and death. *Cancer Res* (2003) 63(6):1405–12.
43. Shaul ME, Fridlender ZG. Tumour-associated neutrophils in patients with cancer. *Nat Rev Clin Oncol* (2019) 16(10):601–20. doi: 10.1038/s41571-019-0222-4
44. Ron-Harel N, Santos D, Ghergurovich JM, Sage PT, Reddy A, Lovitch SB, et al. Mitochondrial biogenesis and proteome remodeling promotes one carbon metabolism for T cell activation. *Cell Metab* (2016) 24(1):104–17. doi: 10.1016/j.cmet.2016.06.007
45. McGeachy MJ, Cua DJ, Gaffen SL. The IL-17 family of cytokines in health and disease. *Immunity*. (2019) 50(4):892–906. doi: 10.1016/j.immuni.2019.03.021
46. Amatya N, Garg AV, Gaffen SL. IL-17 signaling: the yin and the yang. *Trends Immunol* (2017) 38(5):310–22. doi: 10.1016/j.it.2017.01.006
47. Bie Q, Zhang B, Sun C, Ji X, Barnie PA, Qi C, et al. IL-17B activated mesenchymal stem cells enhance proliferation and migration of gastric cancer cells. *Oncotarget*. (2017) 8(12):18914–23. doi: 10.18632/oncotarget.14835
48. Laprevotte E, Cochaud S, du Manoir S, Lapierre M, Dejou C, Philippe M, et al. The IL-17B-IL-17 receptor B pathway promotes resistance to paclitaxel in breast tumors through activation of the ERK1/2 pathway. *Oncotarget*. (2017) 8(69):113360–72. doi: 10.18632/oncotarget.23008
49. Yang YF, Lee YC, Lo S, Chung YN, Hsieh YC, Chiu WC, et al. A positive feedback loop of IL-17B-IL-17RB activates ERK/β-catenin to promote lung cancer metastasis. *Cancer Lett* (2018) 422:44–55. doi: 10.1016/j.canlet.2018.02.037
50. Wu HH, Hwang-Verslues WW, Lee WH, Huang CK, Wei PC, Chen CL, et al. Targeting IL-17B-IL-17RB signaling with an anti-IL-17RB antibody blocks pancreatic cancer metastasis by silencing multiple chemokines. *J Exp Med* (2015) 212(3):333–49. doi: 10.1084/jem.20141702
51. Kim JA. Peroxisome metabolism in cancer. *Cells*. (2020) 9(7):1692. doi: 10.3390/cells9071692
52. Stanziale SF, Petrowsky H, Adusumilli PS, Ben-Porat L, Gonen M, Fong Y. Infection with oncolytic herpes simplex virus-1 induces apoptosis in neighboring human cancer cells: a potential target to increase anticancer activity. *Clin Cancer Res* (2004) 10(9):3225–32. doi: 10.1158/1078-0432.CCR-1083-3
53. Darvin P, Toor SM, Sasidharan Nair V, Elkord E. Immune checkpoint inhibitors: recent progress and potential biomarkers. *Exp Mol Med* (2018) 50(12):1–11. doi: 10.1038/s12276-018-0191-1
54. Carlino MS, Larkin J, Long GV. Immune checkpoint inhibitors in melanoma. *Lancet* (2021) 398(10304):1002–14. doi: 10.1016/S0140-6736(21)01206-X
55. Keenan TE, Tolaney SM. Role of immunotherapy in triple-negative breast cancer. *J Natl Compr Canc Netw* (2020) 18(4):479–89. doi: 10.6004/jnccn.2020.7554





## OPEN ACCESS

## EDITED BY

Satyendra Chandra Tripathi,  
All India Institute of Medical Sciences Nagpur,  
India

## REVIEWED BY

Balkrishna Chaube,  
Yale University, United States  
Rodney Infante,  
University of Texas Southwestern Medical  
Center, United States

## \*CORRESPONDENCE

Axel Stang  
✉ a.stang@asklepios.com

RECEIVED 31 August 2023

ACCEPTED 05 February 2024

PUBLISHED 20 February 2024

## CITATION

More TH, Hiller K, Seifert M, Illig T,  
Schmidt R, Gronauer R, von Hahn T,  
Weilert H and Stang A (2024) Metabolomics  
analysis reveals novel serum metabolite  
alterations in cancer cachexia.  
*Front. Oncol.* 14:1286896.  
doi: 10.3389/fonc.2024.1286896

## COPYRIGHT

© 2024 More, Hiller, Seifert, Illig, Schmidt,  
Gronauer, von Hahn, Weilert and Stang. This is  
an open-access article distributed under the  
terms of the [Creative Commons Attribution  
License \(CC BY\)](#). The use, distribution or  
reproduction in other forums is permitted,  
provided the original author(s) and the  
copyright owner(s) are credited and that the  
original publication in this journal is cited, in  
accordance with accepted academic  
practice. No use, distribution or reproduction  
is permitted which does not comply with  
these terms.

# Metabolomics analysis reveals novel serum metabolite alterations in cancer cachexia

Tushar H. More<sup>1</sup>, Karsten Hiller<sup>1</sup>, Martin Seifert<sup>2,3</sup>,  
Thomas Illig<sup>4,5</sup>, Rudi Schmidt<sup>2,6</sup>, Raphael Gronauer<sup>2,3</sup>,  
Thomas von Hahn<sup>7,8,9</sup>, Hauke Weilert<sup>8,9,10</sup> and Axel Stang<sup>8,9,10\*</sup>

<sup>1</sup>Department of Bioinformatics and Biochemistry, Braunschweig Integrated Centre of Systems Biology (BRICS), Technische Universität Braunschweig, Braunschweig, Germany, <sup>2</sup>Asklepios Precision Medicine, Asklepios Hospitals GmbH & Co KGaA, Königstein (Taunus), Germany, <sup>3</sup>Connexome GmbH, Fischen, Germany, <sup>4</sup>Department of Human Genetics, Hannover Medical School, Hannover, Germany, <sup>5</sup>Hannover Unified Biobank (HUB), Hannover, Germany, <sup>6</sup>Immunettrue, Cologne, Germany, <sup>7</sup>Asklepios Hospital Barmbek, Department of Gastroenterology, Hepatology and Endoscopy, Hamburg, Germany, <sup>8</sup>Asklepios Tumorzentrum Hamburg, Hamburg, Germany, <sup>9</sup>Semmelweis University, Asklepios Campus Hamburg, Budapest, Hungary, <sup>10</sup>Asklepios Hospital Barmbek, Department of Hematology, Oncology and Palliative Care Medicine, Hamburg, Germany

**Background:** Cachexia is a body wasting syndrome that significantly affects well-being and prognosis of cancer patients, without effective treatment. Serum metabolites take part in pathophysiological processes of cancer cachexia, but apart from altered levels of select serum metabolites, little is known on the global changes of the overall serum metabolome, which represents a functional readout of the whole-body metabolic state. Here, we aimed to comprehensively characterize serum metabolite alterations and analyze associated pathways in cachectic cancer patients to gain new insights that could help instruct strategies for novel interventions of greater clinical benefit.

**Methods:** Serum was sampled from 120 metastatic cancer patients (stage UICC IV). Patients were grouped as cachectic or non-cachectic according to the criteria for cancer cachexia agreed upon international consensus (main criterium: weight loss adjusted to body mass index). Samples were pooled by cachexia phenotype and assayed using non-targeted gas chromatography-mass spectrometry (GC-MS). Normalized metabolite levels were compared using *t*-test ( $p < 0.05$ , adjusted for false discovery rate) and partial least squares discriminant analysis (PLS-DA). Machine-learning models were applied to identify metabolite signatures for separating cachexia states. Significant metabolites underwent MetaboAnalyst 5.0 pathway analysis.

**Results:** Comparative analyses included 78 cachectic and 42 non-cachectic patients. Cachectic patients exhibited 19 annotable, significantly elevated (including glucose and fructose) or decreased (mostly amino acids) metabolites associating with aminoacyl-tRNA, glutathione and amino acid metabolism pathways. PLS-DA showed distinct clusters (accuracy: 85.6%), and machine-learning models identified metabolic signatures for separating cachectic states (accuracy: 83.2%; area under ROC: 88.0%). We newly identified altered blood levels of erythronic acid and glucuronic acid in human cancer cachexia, potentially linked to pentose-phosphate and detoxification pathways.

**Conclusion:** We found both known and yet unknown serum metabolite and metabolic pathway alterations in cachectic cancer patients that collectively support a whole-body metabolic state with impaired detoxification capability, altered glucose and fructose metabolism, and substrate supply for increased and/or distinct metabolic needs of cachexia-associated tumors. These findings together imply vulnerabilities, dependencies and targets for novel interventions that have potential to make a significant impact on future research in an important field of cancer patient care.

#### KEYWORDS

cancer cachexia, GC-MS metabolomics, erythronic acid, glucuronic acid, serum metabolites, metabolic pathways, body metabolism

## Introduction

Cancer cachexia is a common adverse effect of cancer with negative impact on patient's physical function, quality of life, and survival (1). Involuntary weight loss (WL), adjusted to the body mass index (BMI), represents the validated cardinal criterium of the international consensus-definition for cancer cachexia, which distinguishes between cachectic and non-cachectic patients with regards to all other cachexia domains proposed (e.g., C-reactive protein [CRP], food intake, appetite loss, performance status [PS]) (1–3). Cachexia is estimated to affect 50–80% of cancer patients, which worsens the susceptibility to toxic side effects of anti-cancer drugs, and to account for up to 20% of cancer deaths (4, 5). Despite its clinical relevance, this cancer-associated body wasting syndrome remains without effective treatment. Current concepts outline a tumor-orchestrated takeover of the whole-body metabolism to promote tumor anabolism and growth at the expense of host tissue catabolism (6, 7). Serum metabolites take part in pathophysiological processes of CC, but apart from altered levels of select metabolites, there is relative paucity of data on the global alterations of the serum metabolome, which integrates the functional readout of the whole-body metabolic state (8–10). Determining variations of the serum metabolome may reveal yet unknown metabolite alterations, broaden the scope of dysregulated metabolic pathways, and drive the translation of chemical metabolome data into biological knowledge (11–13). These results, in turn, may instruct strategies for novel therapeutic interventions of greater clinical benefit.

Metabolomics, or comprehensive metabolite profiling, uses analytical chemistry platforms, such as mass spectroscopy coupled with gas chromatography (GC-MS), to provide an integrated status of the metabolome to metabolic disease research (10, 14). Serum metabolomics, in non-targeted mode, has proven utility for discovering unanticipated metabolites and new metabolic pathways that change between clinical states, and hence for the design of novel intervention strategies aimed at modulating metabolic diseases (10, 13–15). Since metabolites interact and the

structures of metabolomics data are complex, significant metabolites are not necessarily good predictors (15, 16). Therefore, consistent results from both statistical (direct metabolite-level testing between sample groups) and machine learning (ML) methods (train models to label groups of samples) lend strengths to metabolomics study findings, as these complementary methods differentially process the data and validate each other (16–18).

Here, we comprehensively characterize the serum metabolite profiles of 78 cachectic and 42 non-cachectic cancer patients using a non-targeted metabolomics approach followed by pathway analysis. Our objectives were to assess statistically differential cachexia-related serum metabolite alterations and metabolome clusters, to examine top differential metabolite features for associated pathways to help understand what these metabolite changes represent, and to apply an ML strategy to evaluate whether significance-based and prediction-oriented results are distinct or overlapping. Altogether, we aimed to provide a resource for future research that can help define testable hypotheses about mechanisms of action and/or design approaches for novel therapeutic strategies in an important field of cancer patient care.

## Materials and methods

### Study population

For this cross-sectional case-control study, adult patients with newly diagnosed, metastatic cancer (stage UICC IV) were recruited via the cancer care in- and out-patient units and oncology wards of the Asklepios Hospital Barmbek between January 2019 and December 2021. Patients were included at the time of diagnosis before start of any anticancer treatment. Primary cancer types included gastric, colorectal, pancreatic, liver and ovarian cancer. Eligible patients met the following inclusion criteria:  $\geq 18$  years of age, and histologically proven metastatic cancer diagnosis, and either antibiotics treatment within  $\leq 2$  weeks or non-exposure of

≥3 months before inclusion. Exclusion criteria were as follows: acute or chronic diarrhea, acute gastrointestinal illness including ileus, inflammatory bowel disease, acute infection, autoimmune diseases, immunosuppressive therapy including corticosteroids, acquired immunodeficiency syndrome, kidney or liver failure, and need for emergency surgery. and. The study was approved by the Ärztekammer Hamburg, Protocol number: V5649, Date: 23.10.2017 and was conducted according to the Declaration of Helsinki and its revisions. All patients gave written informed consent.

## Clinical assessments

Demographic information (age, gender, cancer type, medication, CRP values) was collected from medical records by the study coordinators at the time of study inclusion. Patient-reported data on height, body weight, WL history, appetite, food intake, and vegetarian diet were collected by means of a structured questionnaire. A research assistant was available and provided help in a face-to-face interview as necessary. Information about actual height and weight, WL at last 6 months, and food intake past month (unchanged or reduced) was provided by the patients using questions from the Scored Patient-Generated Subjective Global Assessment (PG-SGA) (19). Assessment of appetite was performed using a numerical rating scale provided by the Edmonton Symptom Assessment System, scoring 0 (normal appetite) to 10 (no appetite) (20). Diet-based vegetarianism was determined from the intake of animal products (red meat, poultry, fish, dairy products, and eggs). Vegetarians were defined by a plant-based dietary pattern that excludes red meat, and, to different extents, other animal products (subtypes included lacto-/ovo-/pesco-/lacto-ovo-/and pesco-lacto-ovo-vegetarians and vegans depending on the inclusion and exclusion of poultry, fish, dairy products and/or eggs). Smoking was defined as current daily smoking. We used self-reported average absolute alcohol consumption (grams per week) during the last 12 months. Medication use was defined as a drug purchase during the 3 months preceding the study inclusion. Prevalent diabetes was defined as self-reported diabetes, a diabetes diagnosis code indicating diabetes in medical records, and/or use of diabetes medications. Patients were classified into two groups (cachexia versus non-cachexia) based on the agreed and validated diagnostic criteria from the international consensus (1–3). The criterion for cachexia was: WL ≥5% the past 6 months or WL ≥2% the last 6 months and BMI ≤20 kg/m<sup>2</sup> (1). Patients above or below these cut-offs were grouped as cachexia or non-cachexia. BMI is reported as current weight (kg)/height (m)<sup>2</sup>.

## Sample collection

Morning overnight fasting (≥6 hours) venous blood (5–10 mL) was collected in serum tubes. The blood samples were kept at 4°C for 20 minutes for clotting. Clotted samples were centrifuged at 1300 × g for 10 minutes at 4°C. The removed supernatant serum samples were immediately stored at -80°C within ≤30–40 minutes

after blood collection. Samples remained stored on average for 1.2 ± 0.6 years until further processing. Finally, the samples were transported to the Department of Bioinformatics and Biochemistry, Braunschweig Integrated Centre of Systems Biology (BRICS), University of Braunschweig, on dry ice for metabolomics analysis.

## Metabolite extraction

Metabolite extraction was performed as per our previous publication (21). Prior to extraction, the serum samples were thawed on ice for 30 minutes. Then, 11 µL of serum was mixed with 100 µL of an extraction solvent consisting of methanol and water (at a ratio of 8:1) at -20°C. This solvent also contained internal standards, specifically 2 µg/mL of D6-glutaric acid and U13C-ribitol. The mixture was vortexed for 10 minutes at 1400 rpm and 4°C, followed by centrifugation at 13,000 g and 4°C for 10 minutes to precipitate proteins. The resulting supernatants (90 µL) were transferred to glass vials and evaporated using speed-vac at 4°C. The metabolic extracts in the glass vials were sealed with a crimped aluminium cap featuring a septum to prevent oxidation. Typically, the samples were extracted and analyzed immediately after extraction. If storage was necessary, the dried samples were stored at -20°C until GC-MS measurement. The storage time until analysis did not exceed 48 hours. Serum samples were individually extracted in technical triplicates. A fraction (10 µL) from each sample is used to create a pooled quality control (QC) sample, which is then extracted and acquired after every 8th measurement. These QC samples served as a means to normalize untargeted metabolomics data by dividing the sample metabolite intensity by the average intensity of the nearest pool sample, ensuring measurement quality (22).

## Metabolic analysis

Metabolomics measurements were performed using gas chromatography coupled with mass spectrometry (GC-MS). To render the identification of polar metabolites, two-step derivatization was performed prior to analysis. Metabolite extracts were derivatized using a multipurpose sampler (Gerstel MPS). The first derivatization was performed by adding 15 µL of (20 mg/mL) methoxyamine hydrochloride in pyridine (Sigma-Aldrich), shaken for 90 min at 40°C. The second derivatization was performed by adding an equal volume of N-methyl-N-trimethylsilyl-trifluoroacetamide (MSTFA) (Macherey-Nagel) under continuous shaking for 30 min at 40°C. The sample (1 µL) was injected into an SSL injector at 270°C in splitless mode.

GC-MS measurements were performed on Agilent 7890A GC equipped with a 30 m DB-35MS + 5m Duraguard capillary column (0.25 mm inner diameter, 0.25 µm film thickness), which was connected to an Agilent 5977B MSD. Helium was used as the carrier gas at a flow rate of 1.0 mL/min. The GC oven temperature was held at 80°C for 6 min, subsequently increased to 300°C at 6°C/min, and held at that temperature for 10 min. The temperature was

increased to 325°C at 10°C/min and held for an additional 4 min, resulting in a total run time of 60 min per sample. The transfer line temperature was set to 280°C, and the MSD was operating under electron ionization at 70 eV. The MS source was held at 230°C and the quadrupole at 150°C. Full scan mass spectra were acquired from  $m/z$  70 to  $m/z$  800 at a scan rate of 5.2 scans/s. Pooled samples were measured after every eighth GC-MS measurement for quality control and data correction.

## Data processing

All GC-MS chromatograms were processed using our in-house software (23). The software package supports the deconvolution of mass spectra, peak picking, integration, and retention index calibration. Compounds were identified using an in-house mass spectral library by spectral and retention index similarity. The following deconvolution settings were applied to scan data: peak threshold: 5; minimum peak height: 5; bins per scan: 10; deconvolution width: 7; no baseline adjustment; minimum 15 peaks per spectrum; no minimum required base peak intensity. Retention index calibration was based on a C10–C40 even n-alkane mixture (68281, Sigma-Aldrich, Munich, Germany). Relative quantification was done using the batch quantification function of our in-house software (23). Data were normalized to quality control pool measurement and intensity of the internal standard (D6-Glutaric acid).

## Statistical analysis

Group-wise comparisons of cachectic versus non-cachectic cancer patients with regards to items representing cachexia domains and a range of clinical data were performed. Continuous variables with normal distribution are presented as mean (standard deviation) and Welch's two sample t-test was used to examine differences between groups. Continuous variables outside the normal distribution are presented as medians (quartile 1, quartile 3) and Wilcoxon rank sum test was applied to examine differences between groups. Categorical variables were summarized as counts (percentages) and Pearson's Chi-squared test was applied to test for differences between groups. Different statistical approaches were utilized to identify significant metabolic differences between the cachexia and non-cachexia groups. At first, metabolomics data were cube root transformed and range scaled to obtain Gaussian distribution using Metaboanalyst 5.0 (24). Principal component analysis (PCA) was applied to detect intrinsic clustering, while partial least squares discriminant analysis (PLS-DA) was used for supervised clustering. Cross-validation was performed to avoid over-fitting, and  $R^2$  and  $Q^2$  values were employed to evaluate the model's goodness of fit and predictive ability. The variable importance in projection (VIP) score was utilized to extract variables that significantly influenced group discrimination, with a VIP score greater than 1 considered important. Additionally, significant metabolic differences were confirmed within the cachexia and non-cachexia groups using a t-test ( $p < 0.05$ ) that

was adjusted for multiple hypothesis testing using false discovery rate (FDR) correction. The collective analysis was used to determine significant metabolic differences in the cachexia versus the non-cachexia group. In addition, the volcano plot was used to visualize the alterations in metabolites between cachectic and non-cachectic cancer patients. Box-and-whisker plots were generated using SPSS (V27), and heat maps of altered metabolites were created using MetaboAnalyst 5.0. The pathway analysis tool (MetPA) in MetaboAnalyst 5.0 was utilized for the pathway analysis of significant metabolites (24).

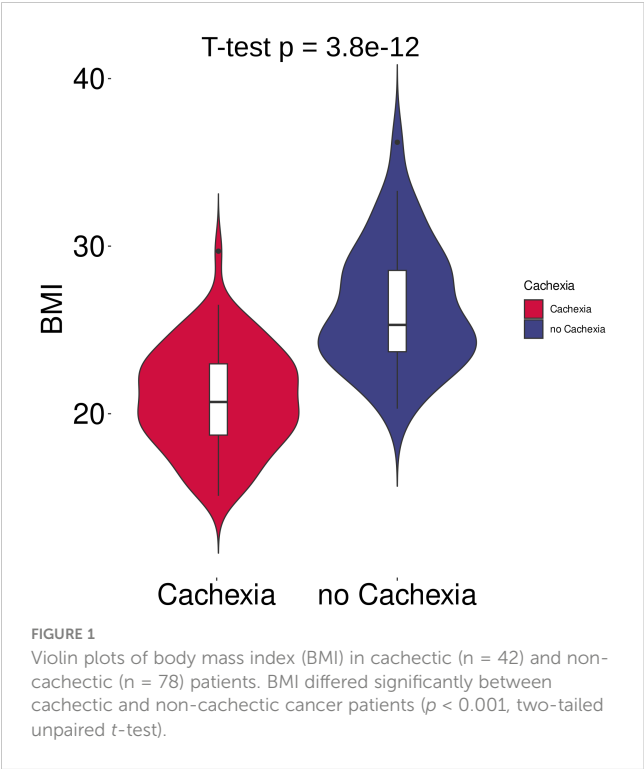
## Machine learning classification

For all ML-based approaches, we used the Waikato Environment for Knowledge Analysis (Weka) (<https://www.cs.waikato.ac.nz/ml/weka/>) (25). For developing a predictive ML model for binominal classification between cachectic and non-cachectic patients to predict the cachexia state, we applied simple logistic regression analyses, because they are typically applied and useful to investigate biomedical regression and classification issues. Simple Logistics in Weka fits a multinomial logistic regression model using the LogitBoost algorithm (26). The number of LogitBoost iterations was manually selected based on an optimization of cross-validation results. We applied a meta classifier approach with reweighted training instances to make base predictors cost-sensitive for balancing positive and negative predictive values, predominantly to avoid false positive prediction and to improve overall true predictive accuracy. Further, we applied a 10-fold cross-validation, with each fold containing a balanced proportion of compared groups to handle dataset imbalances and to avoid overfitting. After applying the trained Simple Logistics model to classify the left-out test set, model's classification performance was estimated by receiver operating characteristic (ROC) methods and by coefficient analysis to determine the predictor composition and predictors contributing to ML models predictive performance.

## Results

### Clinical characteristics of the study population

In total, 120 cancer patients with metastatic disease (UICC stage IV) participated in the study. 41 patients were diagnosed with colorectal cancer, 32 patients with pancreatic cancer, 30 with gastric cancer, 12 with liver cancer, and 5 with ovarian cancer. Among these, 78 patients were classified as cachectic, while 42 patients were non-cachectic (Supplementary Table 1). The cachectic patients had a mean BMI of 20.9 kg/m<sup>2</sup> and a mean WL of 6.5 kg (mean %WL: -9.7%), while the non-cachectic patients had a mean BMI of 26.4 kg/m<sup>2</sup> without WL (Figure 1, Supplementary Table 1,  $p < 0.001$ , respectively). When comparing cachectic versus non-cachectic patients on items representative of key cachexia domains, higher levels of CRP (median 37 versus 14 mg/dl,  $p < 0.001$ ) and appetite loss (median score 4.0 versus 2.0,  $p < 0.001$ ) and reduced food intake (76% versus 26%,  $p < 0.001$ ) was observed for cachectic patients.



The ECOG-PS was significantly lower in cachectic patients compared to non-cachectic patients (ECOG  $\geq 2$ : 44% versus 12%,  $p < 0.001$ ). There were no significant differences in the distribution of cancer types between the two groups analyzed (Table 1,  $p > 0.05$ , respectively). Moreover, the two groups matched in clinical factors (e.g., sex, age, alcohol intake, smoking, diabetes, medication) that could potentially affect the serum metabolite profile (Table 1,  $p > 0.05$ ). Overall, these data underline the legitimacy of using BMI-adjusted WL as diagnostic criterium for cancer cachexia and that there was almost equal distribution of covariables without significant difference between the cachectic and non-cachectic patient group.

### Metabolic profiling reveals distinctive patterns between patients with and without cachexia

Distinct patterns emerged in cancer patients, distinguishing those with and without cachexia following exploratory statistical analysis. Within the metabolic profiling of serum samples, 159 prevalent metabolites were identified, and leveraging an in-house metabolic reference library facilitated the annotation of 60 metabolites. The normalization process employed pooled quality controls and D6-Glutaric acid peak areas as internal standards. Furthermore, the data matrix underwent log transformation and Pareto scaling to achieve a Gaussian distribution. Principal component analysis discerned inherent clusters and outliers within the metabolic dataset (Supplementary Figure S1). Further, distinct clusters between cachexia and non-cachexia groups were evident following partial least square discriminant analysis (PLS-

**TABLE 1** Demographic, clinical and cachexia domain characteristics of the study population (n = 120 cancer patients with metastatic disease, stage UICC IV).

| Cohort  | Cachexia       | No Cachexia     | P-value |
|---|----------------|-----------------|---------|
| Sample size (n)                                 | 78             | 42              |         |
| Patient data                                    |                |                 |         |
| Age, <sup>1</sup> year                          | 68 (10)        | 65 (12)         | 0.074   |
| Male <sup>3</sup>                               | 46 (59)        | 17 (40)         | 0.053   |
| ECOG-PS, <sup>3</sup> score $\leq 1$            | 44 (56)        | 37 (88)         | <0.001  |
| Body mass index (BMI)                           |                |                 |         |
| Height, <sup>1</sup> cm                         | 172 (10)       | 172 (10)        | 0.880   |
| Weight, <sup>1</sup> kg                         | 62 (12)        | 78 (13)         | <0.001  |
| BMI, <sup>1</sup> kg/m <sup>2</sup>             | 20.9 (3.0)     | 26.4 (3.6)      | <0.001  |
| Weight loss (WL)                                |                |                 |         |
| WL, <sup>1</sup> kg                             | -6.5 (1.8)     | -0.2 (1.6)      | <0.001  |
| WL, <sup>1%</sup>                               | -9.7 (3.6)     | -0.3 (2.0)      | <0.001  |
| Food intake                                     |                |                 |         |
| Reduced, <sup>1</sup> (vs. unchanged)           | 59 (76)        | 11 (26)         | <0.001  |
| Appetite loss                                   |                |                 |         |
| ESAS Score, <sup>2</sup> score 0-10             | 4.0 (3.0, 5.0) | 2.0 (0.25, 2.0) | <0.001  |
| C-reactive protein (CRP)                        |                |                 |         |
| CRP values <sup>2</sup> (mg/dl)                 | 37 (9, 61)     | 14 (7, 30)      | <0.001  |
| Clinical data                                   |                |                 |         |
| Smoking <sup>3</sup>                            | 23 (29)        | 10 (24)         | 0.682   |
| Alcohol <sup>3</sup>                            | 26 (33)        | 17 (40)         | 0.713   |
| Vegetarian <sup>3</sup>                         | 5 (6.4)        | 2 (4.7)         | 1.0     |
| Diabetes  | 17 (21)        | 7 (17)          | 0.644   |
| Cancer type                                     |                |                 |         |
| Colon Cancer <sup>3</sup>                       | 25 (32)        | 16 (38.1)       | 0.707   |
| Pancreatic Cancer <sup>3</sup>                  | 23 (29)        | 9 (21)          | 0.532   |
| Gastric Cancer <sup>3</sup>                     | 20 (26)        | 10 (24)         | 1.0     |
| Liver Cancer <sup>3</sup>                       | 7 (9)          | 5 (12)          | 0.754   |
| Ovarian Cancer <sup>3</sup>                     | 3 (3.8)        | 2 (4.8)         | 1.0     |
| Cancer stage                                    |                |                 |         |
| Metastatic Disease (stage UICC IV) <sup>3</sup> | 78 (100)       | 42 (100)        | 1.0     |
| Medication                                      |                |                 |         |
| Morphine <sup>3</sup>                           | 20 (25)        | 7 (17)          | 0.499   |
| Novaminsulfon <sup>3</sup>                      | 23 (29)        | 9 (21)          | 0.523   |
| Non-steroidal Analgetics <sup>3</sup>           | 14 (18)        | 10 (24)         | 0.642   |
| Pantozol <sup>3</sup>                           | 8 (10)         | 7 (16)          | 0.403   |

(Continued)



TABLE 1 Continued

| Cohort   | Cachexia | No Cachexia | P-value |
|--|----------|-------------|---------|
| Medication                                     |          |             |         |
| Diuretics <sup>3</sup>                         | 7 (9)    | 5 (12)      | 0.754   |
| Antibiotics (within ≤2 weeks) <sup>3</sup>     | 20 (25)  | 10 (24)     | 1.0     |
| No Antibiotics (within ≥3 months) <sup>3</sup> | 58 (75)  | 32 (76)     | 1.0     |

<sup>1</sup>Mean (standard deviation) [normal data distribution]; Welch two sample t-test applied to compare groups.  
<sup>2</sup>Median (quartile 1, quartile 3) [outside normal distribution]; Wilcoxon rank sum test applied to compare groups.  
<sup>3</sup>Count (percentage); Pearson’s Chi-squared test applied to compare groups.

DA). Model validation, executed through 100 randomly permuted models in cross-validation analysis (Figure 2A), demonstrated cumulative R2 and Q2 values of 0.69 and 0.48, respectively, emphasizing the robust predictive ability of the original model (Figure 2B).

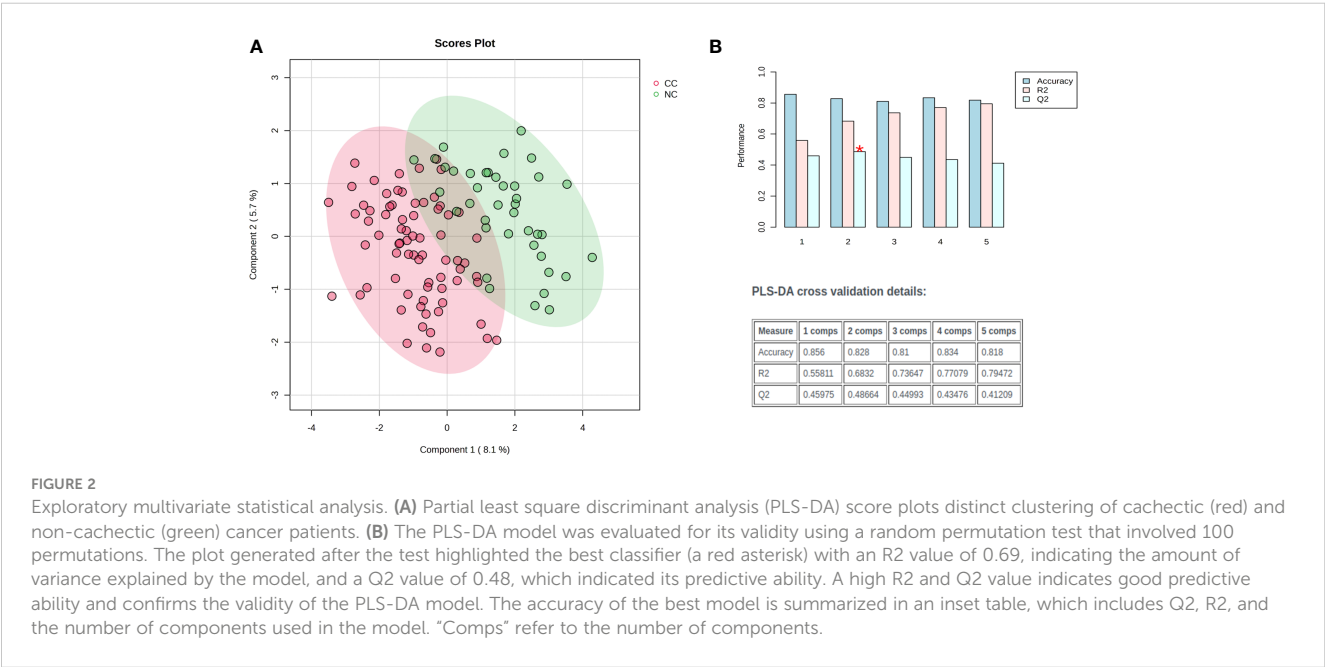
Significant metabolite differences unveiled between cachectic and non-cachectic patients

Significant metabolic differences were revealed through a rigorous analysis of cachexia and non-cachexia groups using various statistical methods. Initially, a *t*-test revealed significant metabolic alterations (FDR-adjusted *p* < 0.05) in both groups. Subsequently, the PLS-DA model’s VIP score identified key variables influencing group discrimination. This comprehensive examination revealed distinctive metabolic differences in 38 metabolites between the cachectic and non-cachectic patients (Supplementary Table S1). Among these, 19 metabolites were confidently annotated in the in-

house library using their spectral data and retention indices. Unidentified metabolites lacking matches in the in-house library were annotated based on their retention indices. Identified metabolites spanned various metabolic classes, such as amino acids, fatty acids, amino sugar derivatives, and organic acids. Significantly higher levels of glucuronic acid, glucose, and fructose were observed in cachectic patients compared to non-cachectic patients. Conversely, lower levels of erythronic acid, lysine, methionine, ornithine, homocysteine, threonine, alanine, proline, valine, leucine, tyrosine, 1,5-anhydro-d-glucitol, isoleucine, maltose, glutamine, and serine were noted in cachectic relative to non-cachectic patients (Figure 3). The metabolite heatmaps depicted distinct metabolic patterns between the cachectic and non-cachectic patients (Figure 4). Additionally, the volcano plot, visualizing statistical significance (*p*-value) versus magnitude of change (fold change), highlighted the altered metabolites within and between the cachectic and non-cachectic patients, with red denoting the up-regulated and blue indicating the down-regulated metabolites (Figure 5). Overall, these results provide robust evidence for a distinct metabolite profile associated with the clinical manifestation of cancer cachexia. Among significant metabolite alterations, the most noticeable ones are yet unknown altered serum levels of erythronic acid and glucuronic acid in human cancer cachexia (Figures 3-5). Moreover, the volcano scatterplot outlines that erythronic acid showed the highest magnitude of down-regulation and glucuronic acid the highest magnitude of up-regulation among the significantly changed metabolites between cachectic and non-cachectic patients (Figure 5).

Pathway analysis highlights global metabolic changes in cancer cachexia

Noteworthy metabolic responses were observed when subjecting these significant metabolites to the pathway analysis



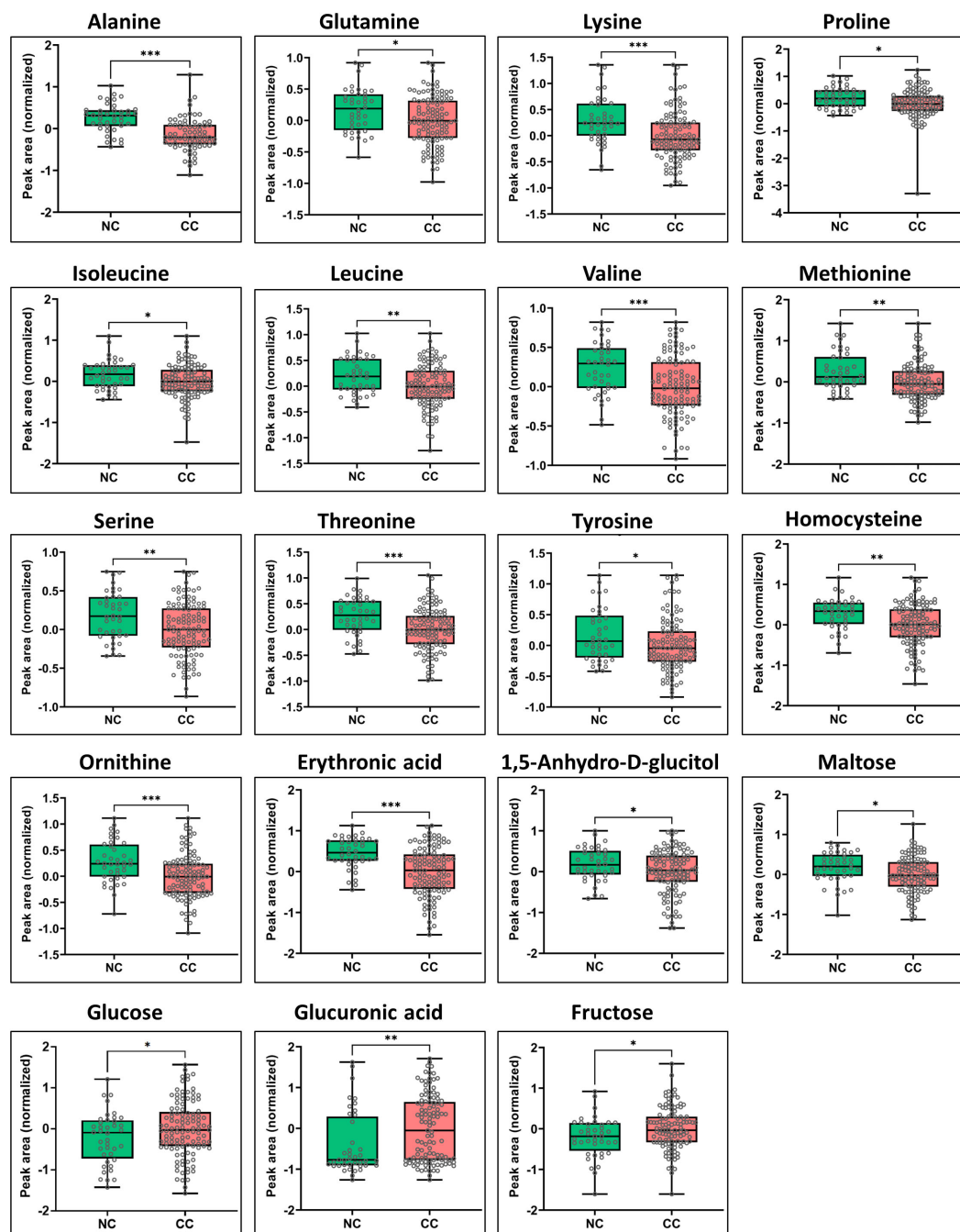
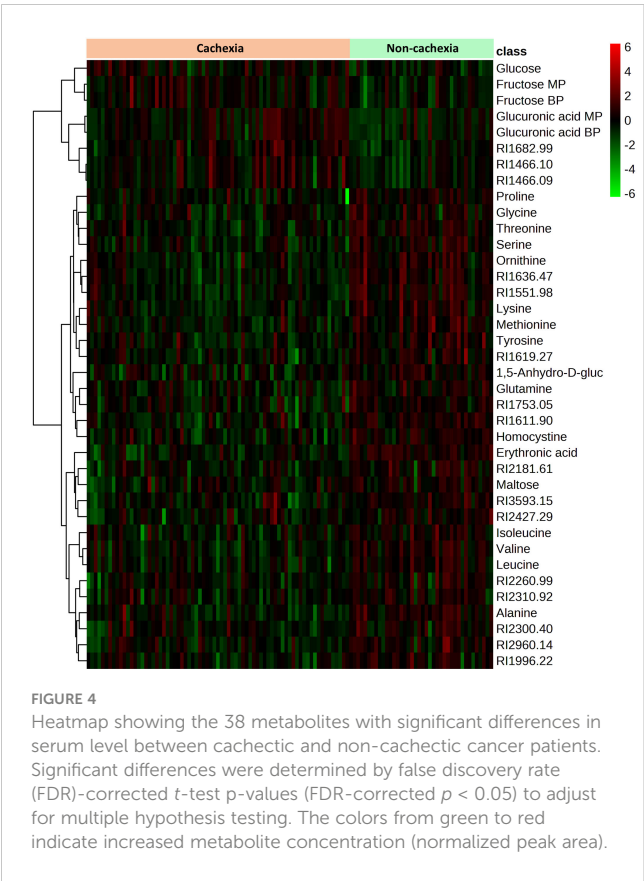


FIGURE 3

Box-and-whisker and dot plots showing significant differences in serum levels of specific metabolites between cachectic and non-cachectic cancer patients. Specific significant metabolite differences were obtained after Tukey's HSD and illustrated as normalized peak area differences. \* $P \leq 0.05$ ; \*\* $P \leq 0.01$ ; \*\*\* $P \leq 0.0001$  and all lower values.

tool (MetPA), revealing compelling insights into metabolic alterations within cachexia groups. Notably, the predominant pathways implicated in these responses included aminoacyl tRNA biosynthesis, valine, leucine, and isoleucine metabolism, glutathione metabolism, valine, leucine, and isoleucine degradation, arginine biosynthesis, alanine, aspartate, and glutamate metabolism, phenylalanine, tyrosine, and tryptophan metabolism, glyoxylate and dicarboxylate metabolism, glycine, serine, and threonine metabolism, and arginine and proline metabolism. A detailed

topology map illustrating the impact of metabolites on these altered metabolic pathways is presented in Figure 6. This pathway map delineates the matched pathways based on their p-values from the pathway enrichment analysis and the pathway impact values from the pathway topology analysis. Overall, the integrative pathway analysis of the metabolite profile differences supports global metabolic changes associated with the manifestation of cachexia in cancer patients, predominantly affecting the amino acid (AA), protein, and glutathione metabolism.



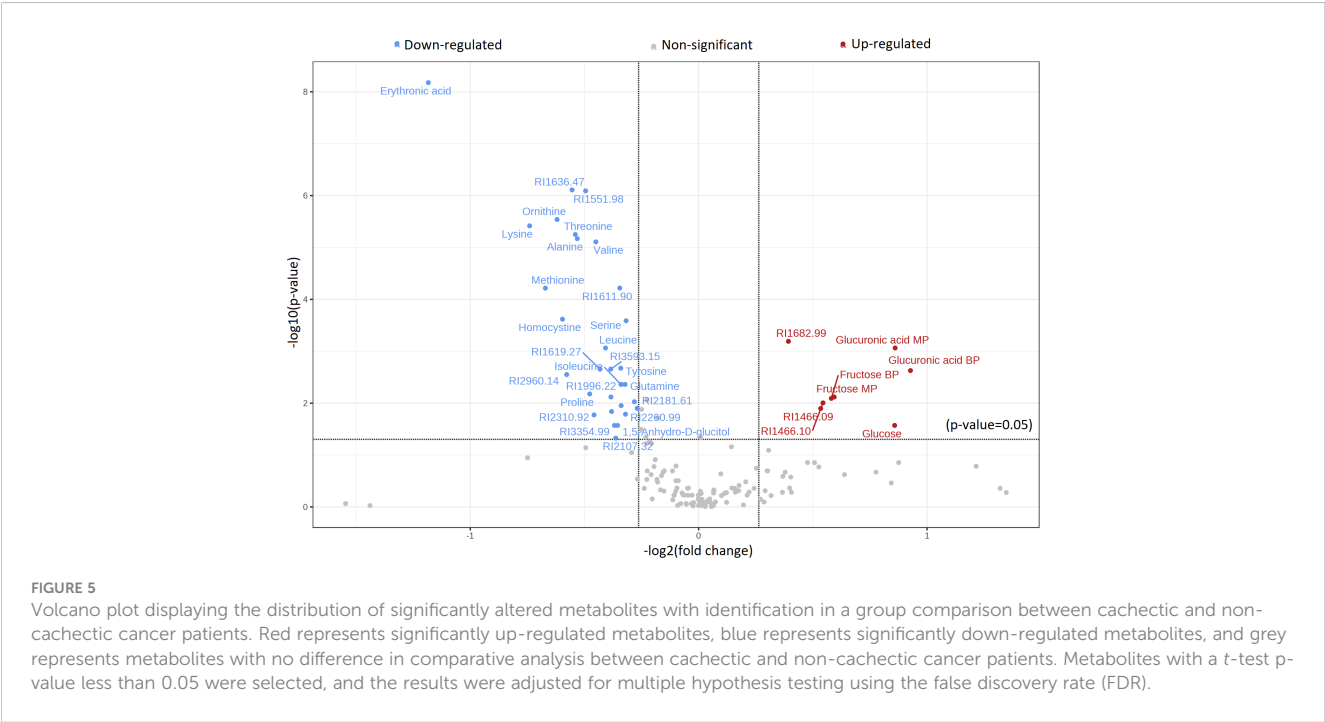
## Robust logistic regression model predicts cancer cachexia with high accuracy

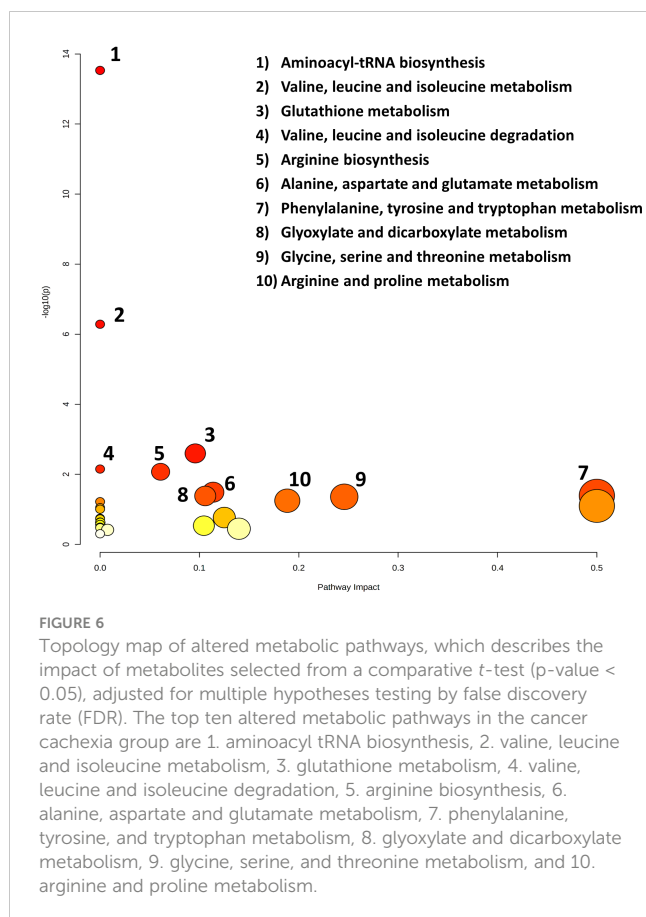
To account for potential combinatorial effects and interrelations among metabolites in our dataset, we implemented a purely

prediction-oriented simple logistic ML-based model for binominal discrimination of cachexia states. Following the training of the simple logistic ML model using a 10-fold cross-validation strategy together with a meta classifier approach to make base predictors cost-sensitive, the predictive ML-based models achieved accuracy of 83.2% and an area under ROC value of 88.0% for the correct binominal discrimination of the samples according to patients cachexia state (Figure 7). Influencing predictors contributing to the correct binominal discrimination comprised 10 non-annotable and 5 annotable metabolites; the identifiable metabolites were erythronic acid, lactic acid, maltose, methionine, and ornithine (Supplementary Table 2). Despite of a small dataset and operations on subsamples through data splits (training/test data), the purely data-driven ML model yielded high predictive performance and identified erythronic acid as influencing predictor variable. This supports ML-based technologies as valuable tool for biomarker discovery, and indicates a benefit from taken account for combinatorial effects and interrelationships among metabolite alterations.

## Discussion

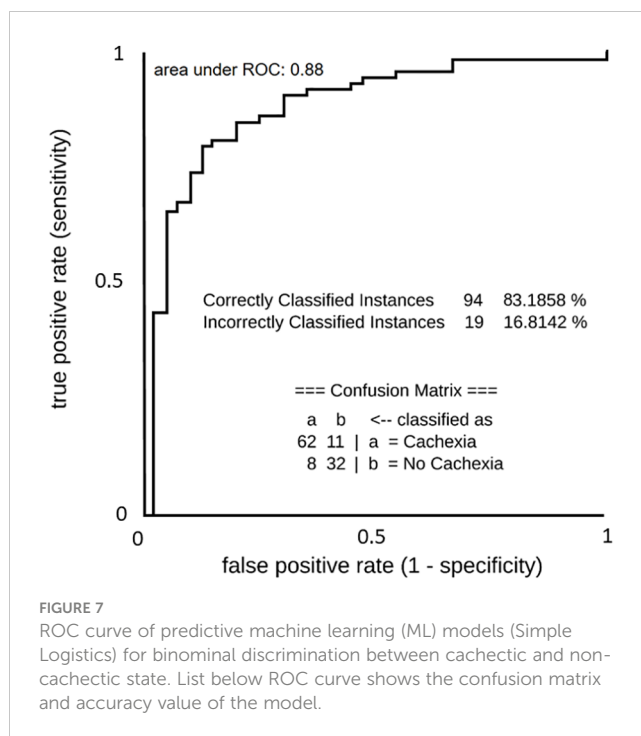
Cachexia alters the cancer patient's metabolism with deleterious consequences, but the ability to understand and effectively treat cachexia remains an unmet need in cancer medicine (1–6). We pursued this by untargeted GC-MS-based metabolomics of overnight-fasting serum samples from previously untreated metastatic cancer patients presenting with and without cachexia according to validated diagnostic criteria agreed upon by international consensus (1–3). The cachectic patient group displayed considerable variations in 38 metabolites, of which 19 annotable metabolites belonged to metabolic classes such as amino





acids, sugars, fatty acids, organic acids, and amino sugar derivatives. The significant differential 19 metabolites, mainly encompassing sugars and amino acids, distinguished accurately the cachectic state in both statistical and ML-based models. Pathway analysis found several pathways to which the metabolites contribute in several ways. To our best knowledge, this study is the first to report decreased erythronic acid and increased glucuronic acid levels in blood in human cancer cachexia. As discussed further, our work broadens the metabolic cancer cachexia landscape and may provide a resource for future study directions.

Elevated serum levels of glucose and fructose are the first noticeable metabolic feature of our cachectic cancer patients. Insulin resistance (IR) induced by the tumor upon the host is commonly present in human cancer cachexia (27, 28). Fasting hyperglycemia, as seen in our cachectic patients, also defines type 2 diabetes mellitus (T2DM) and is largely secondary to inadequate action of the major glucose-lowering hormone insulin (28). IR displays tissue-specific functional alterations in muscle, liver, and adipose tissue, which are unable to mount a coordinated glucose-lowering response, involving cellular uptake of glucose, suppression of gluconeogenesis and lipolysis, and glycogen synthesis (29). In cachectic cancer patients, the disturbed insulin-stimulated anabolic fluxes may shunt substrates to support the tumor anabolism. Tumors benefit from hyperglycemia, as they consume 200x more glucose than normal tissues to generate energy (30). This process termed anaerobic glycolysis (Warburg effect) produces large quantities of lactate, which can be converted back to glucose via



gluconeogenesis in the tumor itself (31) and/or in the liver via the Cori cycle (32). These mechanisms, which maintain glucose supply but avoid lactate acidosis, may be present in our cachectic cancer patients, as they exhibited increased glucose but normal lactate serum levels. Notably, IR is sustained by low-grade inflammation in obesity (33), T2DM (34), and cancer cachexia (35), leading to some overlap in metabolic programming (36). However, clinical outcomes from testing the anti-T2DM drug metformin in anti-cancer therapy have been disappointing (37). Moreover, IR-related defects in obesity and T2DM are readily reversal by weight loss and hypocaloric nutrition, whereas weight loss persists in cancer cachexia despite hypercaloric nutrition. Therefore, future research might focus on investigating tumor-induced mechanisms that specifically sustain IR, glycemia, and fructose circulation in cancer cachexia. Notably, fructose has emerged as an important driver of both IR (38) and the Warburg effect in cancer cells (39). The increased serum fructose signal found in this study supports the inhibition of fructose-induced metabolic alterations as a reasonable approach to reverse cancer cachexia (40).

The second noticeable serum profile alteration in cachectic patients is the decrease of 13 circulating amino acids (AAs). As cancer cachexia refers to a state with increased muscle protein degradation and AA release into the blood circulation (41), this uniform trend likely reflects a disproportional high AA consumption. Tumors have high demands for AAs for energy production and nucleotide, lipid, and protein synthesis needed for tumor growth (42, 43). Especially glycine, serine, homocysteine, and methionine needed for one-carbon metabolism and glutamine needed for glutaminolysis are essential AAs to support tumor metabolism (44–46). The decline of these 5 AAs in our cachectic patients may point to increased one-carbon metabolism and glutaminolysis in cachexia-associated tumors. The three

branched-chain AAs (BCAAs: isoleucine, leucine and valine) are carbon and nitrogen suppliers for energy demands and protein synthesis and sustain the TCA cycle and lipogenesis by providing acetyl-CoA, which is essential for histone acetylation and epigenetic modification (47, 48). BCAA serum levels are increased in IR and T2DM but decreased in several critical illnesses suggesting that the lower cachexia-associated BCAA levels may reflect increased supply to both tumoral and non-tumoral sites (e.g., immune cells sustaining inflammation, hepatic gluconeogenesis) (49, 50). The biological roles of the decreased AAs ornithine, proline, tyrosine, lysine, and alanine are multifaceted. Ornithine helps convert toxic ammonia to urea by the urea cycle and is a key substrate for excess polyamine production in many cancers (51, 52). Proline is involved in collagen and polyamine synthesis, tissue repair, and redox reactions (53, 54). Tyrosine is a precursor of neurotransmitters and a receiver of phosphate groups by way of protein kinases in signal transduction and regulation of enzymatic activity (55). Lysine plays roles in protein synthesis and structure, cross-linking of collagen polypeptides, histone modification, immune response, and tissue repair (56–58). Alanine, released into the bloodstream from muscle proteolysis, serves as major AA for protein resynthesis but also drives the glucose-alanine cycle (Cahill cycle), which regenerates glucose from alanine via hepatic gluconeogenesis (59, 60). Notably, we found lower serum signals in 11 of the 20 proteinogenic AAs (non-proteinogenic: homocysteine, ornithine), of whom 10 (all but lysine) could also act as substrates for gluconeogenesis. Despite the differences in the metabolism of individual AAs, the simultaneous decrease of AAs likely reflects alterations in tumor-associated cachexia-causing pathways that simultaneously affect all of them.

Altogether, cachectic patients exhibited 3 significantly elevated (including glucose and fructose) and 16 decreased (mostly AAs) circulating metabolites. The significance of the distinct metabolite profile for distinguishing cachexia states is shown by the PLS-DA model, which yielded distinct clusters with 85.6% accuracy, and supported by ML-based models, which identified a metabolic signature achieving 83.2% accuracy and an area under the ROC value of 88.0%. Pathway analysis of the observed metabolite variations indicated 10 metabolic pathways to be most significantly involved in cancer cachexia. Among these, the significance of aminoacyl-tRNA biosynthesis supports the crucial role of protein biosynthesis (61, 62), whereas the affected glutathione metabolism outlines the importance of detoxifying and antioxidant processes (63, 64). Collectively, the 7 AA-related metabolic pathways suggest that cachexia-associated tumors display a dependency on AA metabolism. In line with the AA shortage, one may consider AA deprivation to limit tumor anabolism or AA supplementation to limit body catabolism. However, in the tumor-bearing cachectic state, tumor anabolism overrides host catabolism, and AA deprivation may rather exacerbate cachexia and AA supplementation promote tumor growth (65). Instead, targeting the metabolic rewiring behind distinct metabolite dependencies of cachexia-associated tumors, but not normal tissues, may counteract both cancer and cachexia. Metabolic reprogramming, a key distinguishing cancer hallmark, includes unique demands for glucose, fructose and AAs to fuel critical pathways needed for

energy, biosynthetic, methylation, acetylation and reductive metabolism to support tumor growth (28, 39, 66, 67). Commonly affected components of metabolic reprogramming include the one-carbon metabolism encompassing the folate and methionine cycles (43, 44), glutaminolysis (45), anaerobic glycolysis (30), glutathione metabolism (63, 64), the pentose phosphate pathway (68), polyamine synthesis (69), extracellular matrix (ECM) modelling (70), and protein glycolisation (71). Despite the influence of the gut microbiome, diet, and genetics on the human blood metabolome (72), many of the serum metabolite changes seen in our cancer cachexia cohort hint towards a biochemical foundation in overactivated cancer metabolism pathways in cachexia-associated tumors. Understanding cancer cachexia as a cancer metabolism syndrome would imply several novel means for pharmaceutical intervention against cancer, and, by reducing the catabolic drive, against cachexia (28, 39, 46, 62–74).

To our best knowledge, this study is the first to demonstrate a link between decreased erythronic acid levels in blood and cancer cachexia. The consistency of our FDR-corrected statistical tests (highest downregulated metabolite) and ML-based analyses (highest classifier importance) support the biological relevance of this unanticipated finding. However, the factors influencing circulating levels of erythronic acid are poorly characterized. Elevated serum levels of erythronic acid have been found in patients with transaldolase deficiency, which represents a defect in the non-oxidative branch of the reductive pentose-phosphate pathway (PPP) (75). Conversely, reduced erythronic serum levels may reflect increased PPP activity in cancer cells to generate 5-carbon sugars used in nucleotide, DNA and RNA synthesis and to supply reductive NADPH to counteract oxidative damage and support lipogenesis (68). The reduced levels of erythronic acid may be also a result of scavenging reactions against hydroxyl radicals in cachectic patients (76). Notably, erythronic acid is a by-product of the degradation of N-acetylglucosamine (GlcNAc) caused by reactive oxygen species (ROS) (77). Protein GlcNAcylation is the most common posttranslational modification of proteins by sugars, which affects numerous cellular functions, including metabolic enzyme activities (78). Serum erythronic acid levels may reflect alterations of the synthesis and/or degradation of GlcNAc and/or protein GlcNAcylation, which impacts metabolic programming in cancer, including the direction of glucose into the PPP to support tumor growth (79). However, further studies are required to assess whether these hypothetical or other mechanisms influence circulating levels of erythronic acid. Isotope-assisted metabolomics approaches may be a starting point to explore the currently unknown metabolism and turnover of erythronic acid in cancer cachexia.

In the context of cachexia, to our knowledge, this study is also the first to report increased levels of glucuronic acid in the blood. Notably, population-based studies outline glucuronic acid as a biomarker of all-cause mortality and healthspan-related outcomes (80). Several mechanisms may contribute to circulating levels of the glucose metabolite glucuronic acid, which participates in detoxification processes and ECM modelling (81, 82). Firstly, decreased glycosyltransferase activities, as seen in hepatic



dysfunction, lead to decreased toxin-conjugation and, hence, increased glucuronic acid and toxin levels in the bloodstream (83). Secondly, cleavage of glucuronide toxin-conjugates by gut microbial  $\beta$ -glucuronidases can counteract glucuronidation and hepatic-enteric detoxification and make deconjugated glucuronic acid and toxins available for reabsorption into the bloodstream (enteric-hepatic recycling) (84). Thirdly, human  $\beta$ -glucuronidase, which localizes primarily in lysosomes, leads to hydrolytic liberation of glucuronic acid during the remodeling of the ECM (85). Low-grade inflammation, a typical feature accompanying cancer cachexia, can amplify the release of human  $\beta$ -glucuronidase into the bloodstream, where it cleaves glucuronidated conjugates and contributes to circulating glucuronic acid and toxin levels (80, 82, 86). In most clinical scenarios, elevated glucuronic acid levels are likely the result of increased  $\beta$ -glucuronidase activity, ECM remodeling, inflammation and/or cell death by concurrent disease (80–86). Recent drug developments emphasize ECM normalization and  $\beta$ -glucuronidase inhibition as novel strategies in anti-cancer treatment (70, 87), which could also favorably affect the body's glucuronic acid, toxin-conjugation, and detoxification metabolism. To bring the potential anti-cachexia effects of these anti-cancer drugs into perspective, clinical trial designs may expand patient-centered efficacy endpoints toward clinical benefits on symptoms and quality of life to cancer patients suffering from cachexia (88).

For opening up new diagnostic and therapeutic options for cancer cachexia, global metabolic changes and combinatorial effects within metabolomics data are of particular interest. Pathway analysis revealed protein and glutathione metabolism to be involved in cancer cachexia. This correlates with previous work supporting sarcopenia as important feature of cancer cachexia, including a deranged protein metabolism, likely caused by mitochondrial dysfunction in cachectic skeletal muscle tissue (1, 4, 65, 89). Disturbance in glutathione metabolism, the most important detoxifying antioxidant system in human tissues, has been shown to be implicated in increased resistance and toxicity to anti-cancer therapy in cachectic cancer patients (1, 4, 63, 64). Remarkably, purely data-driven ML models, taking into account the combinatorial effects of altered metabolites, yielded high performance for prediction of the cachexia state. The metabolites contributing to ML-based prediction, namely erythronic acid, lactic acid, maltose, methionine and ornithine, reveal intriguing metabolic adaptations. Erythronic acid's levels may be linked to detoxification mechanisms involving GlcNAc and protein GlcAcylation (76–78) and PPP activity (79). Lactic acid correlates well with long-recognized resting energy expenditure in cancer cachexia, which has been related to futile metabolic cycling including an overactivation of the Cori cycle (7, 31, 32). Ornithine and methionine contribute to the urea cycle, glutathione synthesis with interconnection to one-carbon metabolism, and polyamine production (44–46, 69, 90). Research on the relationship between maltose and cancer cachexia is limited, necessitating further investigation to establish potential connections. Overall, contrasted to previous work in cancer cachexia research, we found well-known (glucose, AAs), less-recognized, but potentially important (fructose, maltose) and yet unknown (erythronic acid, glucuronic acid) metabolite alterations. The metabolite profile as a whole points to

global metabolic changes related to cancer cachexia, which are in part long-recognized (e.g. altered glucose, protein, and glutathione metabolism, IR-like state, activated Cori cycle), less-recognized but potentially important (e.g., fructose and polyamine metabolism), or yet unknown (e.g. PPP activation, GlcNAcAcylation, reduced glucuronidation-based detoxification). The robust predictive performance of ML-based models may impact on future research directions and research methodologies. These findings point to a stronger focus on combinatorial effects of metabolic changes that collectively contribute to the development of cancer cachexia. Further, they support ML technologies as valuable tool for biomarker discovery. The validation of a common serum metabolite biomarker panel for early detection of cancer cachexia would provide tremendous advance in the design of clinical trials for new preventive and/or therapeutic interventions (91).

Our study has limitations. First, we used BMI-adjusted WL as the agreed and validated main diagnostic criterium of the internal consensus-definition for cancer cachexia (1–3). The legitimacy of applying this diagnostic criterium in our study cohort is supported by several items representing other cachexia domains that are easily applicable in clinical practice. However, future studies may benefit from additional muscle mass measurements to better assess the role of sarcopenia. Second, the case-control design using cancer patients without cachexia as control isolates results to cachexia as opposed to other phenomena associated with cancer. However, future research may benefit from the inclusion of healthy controls to examine how cancer affects early stages in the cachexia trajectory, which could guide clinical trial designs focusing on prevention, rather than treatment, of cachexia. Third, the serum metabolite profile was assessed only once. This does not represent intra- and inter-day variation of metabolites, which can confound signal detection in metabolomics research. Fourth, covariables, such as diet, medication, diabetes, patient-related factors and cancer type, may affect levels of serum metabolites. There was almost equal distribution of covariables without significant difference between the two patient groups analyzed. Further, pooling samples minimized inter-individual variation, making substantive findings easier to find (92). However, covariables were not assessed in this cross-sectional single-center study by downstream analysis to account for confounding effects. The overall small sample size, the small subgroup sizes but high numbers of metabolite features per sample, and the design-based constraints to measure effect sizes of intra- and interindividual variation in our dataset limited us to produce meaningful data in this respect. Further larger-scale, multi-centric, and longitudinal designed studies in independent patient populations, that include substantially increased numbers for different cancer types and pay attention to intra- and inter-day variation of serum metabolites, are needed to explore confounding factors, variability of metabolite levels, trends of metabolite level changes related to cancer cachexia progression over time, and to verify the extent to which the findings presented here are generalizable. Fifth, metabolome analyses of body fluids are challenging. To obtain high-quality samples and reproducible results, we applied a strict work-up according to recently published guidelines (22) for sample collection, metabolite extraction, quality control, GC-MS measurement, and data acquisition. Further, we applied strict statistical and ML-based (e.g., 10-fold cross-validation,

cost-sensitive base classifier) methods to control overfitting, false discovery, and data misinterpretation. The consistent results obtained by significance-based and prediction-oriented ML-based analyses lend strengths to our findings. Finally, untargeted metabolomics is limited by the ability to identify unknown metabolites. However, no metabolomics approach can be completely comprehensive, and our identified metabolite cluster has biological plausibility. However, despite the aforementioned study limitations, we believe that our dataset and especially our new findings may contribute to the literature, may provide a resource for comparisons across patient cohorts with cancer cachexia and/or other metabolic diseases, and could stimulate future investigations in the field.

## Conclusions

In conclusion, we newly describe altered serum levels of erythronic acid and glucuronic acid as a characteristic feature of cancer cachexia, potentially linked to intra-tumoral PPP activation and impaired body detoxification. Further, we found a distinct serum metabolite profile of cancer cachexia, with glucose, fructose and AAs being the most disturbed metabolites. Some serum metabolite alterations could reflect the supply of overactive metabolic pathways in cachexia-associated tumors needed for energy, biosynthetic, epigenetic and reductive metabolism. Additional studies connecting measurements from both tumor and body metabolism may be an interesting direction to identify actionable targets for distinct metabolic needs of cachexia-associated tumors, but not normal tissues. Altogether, our findings broaden the scope of metabolic vulnerabilities, dependencies and targets in cancer-associated cachexia that can help define testable hypotheses about mechanisms of action and/or design novel therapy approaches to improve patient outcomes in an important field of cancer patient care.

## Data availability statement

The raw data supporting the conclusions of this article will be made available by the authors, without undue reservation.

## Ethics statement

The studies involving humans were approved by Aerztekkammer Hamburg, Protocol number: V5649, Date: 23.10.2017. The studies were conducted in accordance with the local legislation and institutional requirements. The participants provided their written informed consent to participate in this study.

## Author contributions

TM: Data curation, Formal Analysis, Investigation, Supervision, Writing – original draft, Methodology, Software, Validation, Visualization. KH: Formal Analysis, Methodology, Data curation, Funding acquisition, Investigation, Supervision, Validation, Writing – review & editing. MS: Conceptualization, Data

curation, Formal Analysis, Methodology, Software, Supervision, Visualization, Writing – review & editing. TI: Data curation, Formal Analysis, Supervision, Validation, Writing – review & editing. RS: Conceptualization, Data curation, Investigation, Supervision, Validation, Writing – review & editing. RG: Data curation, Formal Analysis, Methodology, Software, Visualization, Writing – review & editing. TV: Data curation, Formal Analysis, Supervision, Validation, Writing – review & editing. HW: Data curation, Formal Analysis, Investigation, Supervision, Validation, Writing – original draft. AS: Conceptualization, Data curation, Formal Analysis, Funding acquisition, Investigation, Project administration, Supervision, Writing – original draft.

## Funding

The author(s) declare financial support was received for the research, authorship, and/or publication of this article. The study was supported by a research grant (#3465) awarded to AS by Asklepios Proresearch, Asklepios Hospitals Hamburg GmbH, Hamburg, Germany, and supported by the Asklepios Campus Hamburg of the Semmelweis University, Budapest, Hungary. In addition, this work was supported by Volkswagen Foundation, Germany (Grant no. 11-76251-19-4/19 (ZN3429)), provided to KH.

## Acknowledgments

The authors thank Nadine Emmerich and Sabine Drießelmann for excellent technical assistance.

## Conflict of interest

The authors declare that the research was conducted in the absence of any commercial or financial relationships that could be construed as a potential conflict of interest.

## Publisher's note

All claims expressed in this article are solely those of the authors and do not necessarily represent those of their affiliated organizations, or those of the publisher, the editors and the reviewers. Any product that may be evaluated in this article, or claim that may be made by its manufacturer, is not guaranteed or endorsed by the publisher.

## Supplementary material

The Supplementary Material for this article can be found online at: <https://www.frontiersin.org/articles/10.3389/fonc.2024.1286896/full#supplementary-material>

### SUPPLEMENTARY FIGURE 1

Principal component analysis score plot depicting clustering of cachectic (red) versus non-cachectic (green) cancer patients.

## References

1. Fearon K, Strasser F, Anker SD, Bosaeus I, Bruera E, Fainsinger RL, et al. Definition and classification of cancer cachexia: an international consensus. *Lancet Oncol* (2011) 12:489–95. doi: 10.1016/S1470-2045(10)70218-7
2. Blum D, Stene GB, Solheim TS, Fayers P, Hjermstad MJ, Baracos VE, et al. Validation of the consensus-definition for cancer cachexia and evaluation of a classification model – a study based on data from an international multicentre project (EPCRC-CSA). *Ann Oncol* (2014) 25:1635–42. doi: 10.1093/annonc/mdl086
3. Martin L, Senesse P, Gioulbasanis I, Antoun S, Bozetti F, Deans C, et al. Diagnostic criteria for classification of cancer-associated weight loss. *J Clin Oncol* (2015) 33:90–9. doi: 10.1200/JCO.2014.56.1894
4. Baracos VE, Martin L, Korc M, Guttridge DC, Fearon KCH. Cancer-associated cachexia. *Nat Rev Dis Primers* (2018) 4:17105. doi: 10.1038/nrdp.2017.105
5. Vazelle C, Jouinot A, Durand JP, Neveux N, Boudou-Rouquette P, Huillard O, et al. Relation between hypermetabolism, cachexia, and survival in cancer patients: a prospective study in 390 cancer patients before initiation of anticancer therapy. *Am J Clin Nutr* (2017) 105:1139–47. doi: 10.3945/ajcn.116.140434
6. Pavlova NN, Zhu J, Thompson CB. The hallmarks of cancer metabolism: still emerging. *Cell Metab* (2022) 34:355–77. doi: 10.1016/j.cmet.2022.01.007
7. Rohm M, Zeigerer A, MaChado J, Herzig S. Energy metabolism in cachexia. *EMBO Rep* (2019) 20:e47258. doi: 10.15252/embr.201847258
8. Yang QJ, Zhao JR, Hao J, Li B, Huo Y, Han YL, et al. Serum and urine metabolomics study reveals a distinct diagnostic model for cancer cachexia. *J Cachexia Sarcopenia Muscle* (2018) 9:71–85. doi: 10.1002/jcsm.12246
9. Cala MP, Agulló-Ortuño MT, Prieto-García E, González-Riano C, Parrilla-Rubio L, Barbas C, et al. Multiplatform plasma fingerprinting in cancer cachexia: a pilot observational and translational study. *J Cachexia Sarcopenia Muscle* (2018) 9:348–57. doi: 10.1002/jcsm.12270
10. Wishart DS. Metabolomics for investigating physiological and pathophysiological processes. *Physiol Rev* (2019) 99:819–1875. doi: 10.1152/physrev.00035.2018
11. Johnson CH, Ivanisevic J, Siuzdak G. Metabolomics: beyond biomarkers and towards mechanisms. *Nat Rev Mol Cell Biol* (2016) 17:451–9. doi: 10.1038/nrm.2016.25
12. Schmidt DR, Patel R, Kirsch DG, Lewis CA, van der Heiden MG, Locasale JW. Metabolomics in cancer research and emerging applications in clinical oncology. *CA Cancer J Clin* (2021) 71:333–58. doi: 10.3322/caac.21670
13. Tebani A, Afonso C, Bekri S. Advances in metabolome information retrieval: turning chemistry into biology. Part II: biological information recovery. *J Inherit Metab Dis* (2018) 41:393–406. doi: 10.1007/s10545-017-0080-0
14. Newgard CB. Metabolomics and metabolic disease: where do we stand? *Cell Metab* (2017) 25:43–56. doi: 10.1016/j.cmet.2016.09.018
15. Schrimpe-Rutledge AC, Codreanu SG, Sherrod SD, McLean JA. Untargeted metabolomics strategies – challenges and emerging directions. *J Am Soc Mass Spectrom* (2016) 26:1897–905. doi: 10.1007/s13361-016-1469-y
16. Lo A, Chernoff H, Zheng T, Lo SH. Why significant variables aren't automatically good predictors. *Proc Natl Acad Sci USA* (2015) 112:13892–7. doi: 10.1073/pnas.1518285112
17. Mendez KM, Reinke SN, Broadhurst DI. A comparative evaluation of generalized predictive ability of eight machine learning algorithms across ten clinical metabolomics data sets for binary classification. *Metabolomics* (2019) 15:150. doi: 10.1007/s11306-019-1612-4
18. Liebal UW, Phan ANT, Sudhakar M, Raman K, Blank LM. Machine learning applications for mass-spectrometry-based metabolomics. *Metabolites* (2020) 10:243. doi: 10.3390/metabo10060243
19. Chen X, Liu X, Ji W, Zhao Y, He Y, Liu Y, et al. The PG-SGA outperforms the NRS 2002 for nutritional risk screening in cancer patients: a retrospective study from China. *Front Nutr* (2023) 10:1272420. doi: 10.3389/fnut.2023.1272420
20. Hui D, Bruera E. The Edmonton Symptom Assessment System 25 years later: past, present, and future developments. *J Pain Symptom Manage* (2017) 53:630–43. doi: 10.1016/j.jpainsymman.2016.10.370
21. More TH, Mozafari B, Märten A, Herr C, Lepper PM, Danziger G, et al. Plasma metabolome alterations discriminate between COVID-19 and non-COVID-19 pneumonia. *Metabolites* (2022) 12:1058. doi: 10.3390/metabo12111058
22. Trezzi JP, Jäger C, Galozzi S, Barkovits K, Marcus K, Mollenhauer B, et al. Metabolic profiling of body fluids and multivariate data analysis. *MethodsX* (2017) 4:95–103. doi: 10.1016/j.mex.2017.02.004
23. Hiller K, Hangebrauk J, Jäger C, Spura J, Schreiber K, Schomburg DK. Metabolite detector: Comprehensive analysis tool for targeted and nontargeted GC/MS based metabolome analysis. *Anal Chem* (2009) 81:3429–39. doi: 10.1021/ac802689c
24. Pang Z, Chong J, Zhou G, de Lima Morais DA, Chang L, Barrette M, et al. MetaboAnalyst 5.0: narrowing the gap between raw spectra and functional insights. *Nucleic Acids Res* (2021) 49:W388–96. doi: 10.1093/nar/gkab382
25. Frank E, Hall M, Trigg L, Holmes G, Witten IH. Data mining in bioinformatics using Weka. *Bioinformatics* (2004) 20:2479–81. doi: 10.1093/bioinformatics/bth261
26. Sumner M, Frank E, Hall M. Speeding up logistic model tree induction. In: Jorge AM, Torgo L, Brazdil P, Camacho R, Gama J, editors. *Knowledge Discovery in Databases: PKDD 2005*, vol. 3721. Springer, Berlin, Heidelberg (2005). p. 675–83. doi: 10.1007/11564126\_72
27. Dev R, Bruera E, Dalal S. Insulin resistance and body composition in cancer patients. *Ann Oncol* (2018) 29:ii18–26. doi: 10.1093/annonc/mdx815
28. Masi T, Patel BM. Altered glucose metabolism and insulin resistance in cancer-induced cachexia: a sweet poison. *Pharmacol Rep* (2021) 73:17–30. doi: 10.1007/s43440-020-00179-y
29. Petersen MC, Shulman GI. Mechanisms of insulin action and insulin resistance. *Physiol Rev* (2018) 98:2133–223. doi: 10.1152/physrev.00063.2017
30. Reinfeld BI, Madden MZ, Wolf MM, Chytil A, Bader JE, Patterson AR, et al. Cell programmed nutrient partitioning in the tumor microenvironment. *Nature* (2021) 593:282–8. doi: 10.1038/s41586-021-03442-1
31. Grasmann G, Smolle E, Olschewski H, Leithner K. Gluconeogenesis in cancer cells – repurposing of a starvation-induced metabolic pathway? *Biochim Biophys Acta Rev Cancer* (2019) 1872:24–36. doi: 10.1016/j.bbcan.2019.05.006
32. Wei L, Wang R, Wazir J, Lin K, Song S, Li L, et al. D-Deoxy-D-glucose alleviates cancer cachexia-induced muscle wasting by enhancing ketone metabolism and inhibiting Cori cycle. *Cells* (2022) 11:2987. doi: 10.3390/cells11192987
33. Theurich S, Tsaousidou E, Hanssen R, Lempradl AM, Mauer J, Timper K, et al. IL-6/Stat3-dependent induction of a distinct, obesity-associated NK cell subpopulation deteriorates energy and glucose homeostasis. *Cell Metab* (2017) 26:171–84. doi: 10.1016/j.cmet.2017.05.018
34. Wang Y, Li M, Chen L, Bian H, Chen X, Zheng H, et al. Natural killer cell-derived exosomal miR-1249-3p attenuates insulin resistance and inflammation in mouse models of type 2 diabetes. *Signal Transduct Target Ther* (2021) 6:409. doi: 10.1038/s41392-021-00805-y
35. McGovern J, Dolan RD, Skipworth RJ, Laird BJ, McMillan DC. Cancer cachexia: a nutritional or a systemic inflammatory syndrome? *Br J Cancer* (2022) 127:379–82. doi: 10.1038/s41416-022-01826-2
36. Maccio A, Sanna E, Neri M, Oppi S, Madeddu CA. Cachexia as evidence of the mechanisms of resistance and tolerance during the evolution of cancer disease. *Int J Mol Sci* (2021) 22:2890. doi: 10.3390/ijms22062890
37. Lord SR, Harris AL. Is it still worth pursuing the repurposing of metformin as a cancer therapeutic? *Br J Cancer* (2023) 128:958–66. doi: 10.1038/s41416-023-02204-2
38. Herman MA, Birnbaum MJ. Molecular aspects of fructose metabolism and metabolic disease. *Cell Metab* (2021) 33:2329–54. doi: 10.1016/j.cmet.2021.09.010
39. Nakagawa T, Lanasa MA, Millan IS, Fini M, Rivard CJ, Sanchez-Lozada LG, et al. Fructose contributes to the Warburg effect for cancer growth. *Cancer Metab* (2020) 18:6. doi: 10.1186/s40170-020-00222-9
40. Gutierrez JA, Liu W, Perez S, Xing G, Sonnenberg G, Kou K, et al. Pharmacologic inhibition of ketohexokinase prevents fructose-induced metabolic dysfunction. *Mol Metabol* (2021) 48:101196. doi: 10.1016/j.molmet.2021.101196
41. Rausch V, Sala V, Penna F, Porporato PE, Ghigo A. Understanding the common mechanisms of heart and skeletal muscle wasting in cancer cachexia. *Oncogenesis* (2021) 10:1. doi: 10.1038/s41389-020-00288-6
42. Vettore L, Westbrook RL, Tennant DA. New aspects of amino acid metabolism in cancer. *Br J Cancer* (2020) 122:150–6. doi: 10.1038/s41416-019-0620-5
43. Lieu EL, Nguyen T, Rhyne S, Kim J. Amino acids in cancer. *Exp Mol Med* (2020) 52:15–30. doi: 10.1038/s12276-020-0375-3
44. Newman AC, Maddocks ODK. One-carbon metabolism in cancer. *Br J Cancer* (2017) 116:1499–504. doi: 10.1038/bjc.2017.118
45. Dekhne AS, Hou Z, Gangjee A, Matherly LH. Therapeutic targeting of mitochondrial one-carbon metabolism in cancer. *Mol Cancer Ther* (2020) 19:2245–55. doi: 10.1158/1535-7163.MCT-20-0423
46. Yang L, Venneti S, Nagrath DL. Glutaminolysis: a hallmark of cancer metabolism. *Annu Rev BioMed Eng* (2017) 19:163–94. doi: 10.1146/annurev-bioeng-071516-044546
47. Sivanand S, van der Heiden MG. Emerging roles for branched-chain amino acid metabolism in cancer. *Cancer Cell* (2020) 37:147–56. doi: 10.1016/j.ccell.2019.12.011
48. Peng H, Wang Y, Luo W. Multifaceted role of branched-chain amino acid metabolism in cancer. *Oncogene* (2020) 39:6747–56. doi: 10.1038/s41388-020-01480-z
49. White PJ, McGarrah RW, Herman MA, Bain JR, Shah SH, Newgard CB. Insulin action, type 2 diabetes, and branched-chain amino acids: a two-way street. *Mol Metabol* (2021) 52:101261. doi: 10.1016/j.molmet.2021.101261
50. Neimast M, Murashige D, Arany Z. Branched chain amino acids. *Annu Rev Physiol* (2019) 81:139–64. doi: 10.1146/annurev-physiol-020518-114455
51. Muthukumaran S, Jaidev J, Umashankar V, Sulochana KN. Ornithine and its role in metabolic diseases: an appraisal. *BioMed Pharmacother* (2017) 86:185–94. doi: 10.1016/j.biopha.2016.12.024
52. Lee MS, Dennis C, Naqvi I, Dailey L, Lorzadeh A, Ye G, et al. Ornithine aminotransferase supports polyamine synthesis in pancreatic cancer. *Nature* (2023) 616:339–47. doi: 10.1038/s41586-023-05891-2

53. Geng P, Qin W, Xu G. Proline metabolism in cancer. *Amino Acids* (2021) 52:1769–77. doi: 10.1007/s00726-021-03060-1
54. Vettore LA, Westbrook RL, Tennant DA. Proline metabolism and redox; maintaining a balance in health and disease. *Amino Acids* (2021) 53:1779–88. doi: 10.1007/s00726-021-03051-2
55. Taddei ML, Pardella E, Pranzini E, Rauegi G, Paoli P. Role of tyrosine phosphorylation in modulation cancer cell metabolism. *Biochim Biophys Acta Rev Cancer* (2020) 1874:1188442. doi: 10.1016/j.bbcan.2020.188442
56. Azevedo C, Saiardi A. Why always lysine? The ongoing tale of one of the most modified amino acids. *Adv Biol Regul* (2016) 60:144–50. doi: 10.1016/j.jbior.2015.09.008
57. Cuesta A, Taunton J. Lysin-targeted inhibitors and chemoproteomic probes. *Annu Rev Biochem* (2019) 88:365–81. doi: 10.1146/annurev-biochem-061516-044805
58. Abbasov ME, Kavanagh ME, Ichu TA, Lazear MR, Tao Y, Crowley VM, et al. A proteome-wide atlas of lysin-reactive chemistry. *Nat Chem* (2021) 13:1081–92. doi: 10.1038/s41557-021-00765-4
59. Kubyshevskiy V, Budisa N. The alanine world model for development of the amino acid repertoire in protein biosynthesis. *Int J Mol Sci* (2019) 20:5507. doi: 10.3390/ijms20215507
60. Sarabhai T, Roden M. Hungry for your alanine: when liver depends on muscle proteolysis. *J Clin Invest* (2019) 129:4563–6. doi: 10.1172/JCI131931
61. Rubio Gomez MA, Ibba M. Aminoacyl-tRNA synthetases. *RNA* (2020) 26:910–36. doi: 10.1261/rna.017120.119
62. Ho JM, Bakkalbasi E, Söll D, Miller CA. Drugging tRNA aminoacylation. *RNA Biol* (2018) 15:667–77. doi: 10.1080/15476286.2018.1429879
63. Bansal A, Simon MC. Glutathione metabolism in cancer progression and treatment resistance. *J Cell Biol* (2018) 217:2291–8. doi: 10.1083/jcb.201804161
64. Kennedy L, Sandhu JK, Harper ME, Cuperlovic-Culf M. Role of glutathione in cancer: from mechanisms to therapies. *Biomolecules* (2020) 10:1429. doi: 10.3390/biom10101429
65. Ragni M, Fornelli C, Nisoli E, Penna F. Amino acids in cancer and cachexia: an integrated view. *Cancers* (2022) 14:5691. doi: 10.3390/cancers14225691
66. Pavlova NN, Zhu J, Thompson CB. The hallmarks of cancer metabolism: still emerging. *Cell Metab* (2022) 34:355–77. doi: 10.1016/j.cmet.2022.01.007
67. Läsche M, Emons G, Gründker C. Shedding new light on cancer metabolism: a metabolic tightrope between life and death. *Front Oncol* (2020) 10:409. doi: 10.3389/fonc.2020.00409
68. Ghanem N, El-Baba C, Araj K, El-Khoury R, Usta J, Darwiche N. The pentose phosphate pathway in cancer: regulation and therapeutic opportunities. *Chemotherapy* (2021) 66:179–91. doi: 10.1159/000519784
69. Casero RA Jr, Murray Stewart T, Pegg AE. Polyamine metabolism and cancer: treatments, challenges and opportunities. *Nat Rev Cancer* (2018) 18:681–95. doi: 10.1038/s41568-018-0050-3
70. Yuan Z, Li Y, Zhang S, Wang X, Dou H, Yu X, et al. Extracellular matrix modelling in tumor progression and immune escape: from mechanisms to treatment. *Mol Cancer* (2023) 22:48. doi: 10.1186/s12943-023-01744-8
71. Thomas D, Rathinavel AK, Radhakrishnan P. Altered glycolysis in cancer: a promising target for biomarkers and therapeutics. *Biochim Biophys Acta Rev Cancer* (2021) 1875:188464. doi: 10.1016/j.bbcan.2020.188464
72. Bar N, Korem T, Weissbrod O, Zeevi D, Rothschild D, Leviatan S, et al. A reference map of potential determinants for the human serum metabolome. *Nature* (2020) 588:135–40. doi: 10.1038/s41586-020-2896-2
73. Islam A, Shaikat Z, Hussain R, Gregory SL. One-carbon and polyamine metabolism as cancer therapy targets. *Biomolecules* (2022) 12:1902. doi: 10.3390/biom12121902
74. Holbert CE, Cullen MT, Casero RA Jr, Stewart TM. Polyamines in cancer: integrating organismal metabolism and antitumor immunity. *Nat Rev Cancer* (2022) 22:467–80. doi: 10.1038/s41568-022-00473-2
75. Engelke UF, Zijlstra FS, Mochel F, Valayannopoulos V, Rabier D, Kluijtmans LA, et al. Mitochondrial involvement and erythronic acid as a novel biomarker in transaldolase deficiency. *Biochim Biophys Acta* (2010) 1802:1028–35. doi: 10.1016/j.bbdis.2010.06.007
76. den Hartog GJ, Boots AW, Adam-Perrot A, Brouns F, Verkooijen IW, Weseler AR, et al. Erythritol is a sweet antioxidant. *Nutrition* (2010) 26:449–58. doi: 10.1016/j.nut.2009.05.004
77. Jahn M, Baynes JW, Spiteller G. The reaction of hyaluronic acid and its monomers, glucuronic acid and N-acetylglucosamine, with reactive oxygen species. *Carbohydr Res* (1999) 321:228–34. doi: 10.1016/s0008-6215(99)00186-x
78. Chatham JC, Zhang J, Wende AR. Role of O-linked N-acetylglucosamine protein modification in cellular (patho) physiology. *Physiol Rev* (2021) 101:427–93. doi: 10.1152/physrev.00043.2019
79. Rao X, Duan X, Mao W, Li X, Li Z, Li Q, et al. O-GlcNAcylation of G6PD promotes the pentose phosphate pathway and tumor growth. *Nat Commun* (2015) 6:8468. doi: 10.1038/ncomms9468
80. Ho A, Sinick J, Esko T, Fischer K, Menni C, Zierer J, et al. Circulating glucuronic acid predicts healthspan and longevity in humans and mice. *Aging (Albany NY)* (2019) 11:7694–706. doi: 10.18632/aging.102281
81. Fujiwara R, Yoda E, Tukey RH. Species differences in drug glucuronidation: humanized UDP-glucuronyltransferase I mice and their application for predicting drug glucuronidation and drug-induced toxicity in humans. *Drug Metab Pharmacokinet* (2018) 33:9–16. doi: 10.1016/j.dmpk.2017.10.002
82. Liu Y, Li L, Wang L, Lu L, Li Y, Huang G, et al. Two faces of hyaluronan, a dynamic barometer of disease progression in tumor microenvironment. *Discovery Oncol* (2023) 14:11. doi: 10.1007/s12672-023-00618-1
83. Meech R, Hu DG, McKinnon RA, Mubarakah SN, Haines AZ, Nair PC, et al. The UDP-glycosyltransferase (UGT) superfamily: new members, new functions, and novel paradigms. *Physiol Rev* (2019) 99:1153–222. doi: 10.1152/physrev.00058.2017
84. Gao S, Sun R, Singh R, So SY, Chan CTY, Savidge T, et al. The role of gut microbial beta-glucuronidase (gmGUS) in drug disposition and development. *Drug Discovery Today* (2022) 27:103316. doi: 10.1016/j.drudis.2022.07.001
85. Naz H, Islam A, Waheed A, Sly WS, Ahmad F, Hassan I. Human  $\beta$ -glucuronidase: structure, function, and application in enzyme replacement therapy. *Rejuvenation Res* (2013) 16:352–63. doi: 10.1089/rej.2013.1407
86. Kavčič N, Pegan K, Turk B. Lysosomes in programmed cell death pathways: from initiators to amplifiers. *Biol Chem* (2017) 398:289–301. doi: 10.1515/hsz-2016-0252
87. Awolade P, Cele N, Kerru N, Gummidu L, Oluwakemi E, Singh P. Therapeutic significance of  $\beta$ -glucuronidase activity and its inhibitors: a review. *Eur J Med Chem* (2020) 187:111921. doi: 10.1016/j.ejmech.2019.111921
88. Gyawali B, Hwang TJ, Vokinger KN, Booth CM, Amir E, Tibau A. Patient-centred cancer drug development: clinical trials, regulatory approval, and value assessment. *Am Soc Clin Oncol Educ Book* (2019) 39:374–87. doi: 10.1200/EDBK\_242229
89. Kunzke T, Buck A, Prade VM, Feuchtinger A, Prokopchuk O, Martignoni ME, et al. Derangements of amino acids in cachectic skeletal muscle are caused by mitochondrial dysfunction. *J Cachexia Sarcopenia Muscle* (2020) 11:226–40. doi: 10.1002/jcsm.12498
90. Xuan M, Gu X, Li J, Huang D, Xue C, He Y. Polyamines: their significance for maintaining health and contributing to diseases. *Cell Commun Signal* (2023) 21:348. doi: 10.1186/s12964-023-01373-0
91. O'Connell TM, Golzarri-Arroyo L, Pin F, Barreto R, SL D, Couch ME, et al. Metabolic biomarkers for the early detection of cancer cachexia. *Front Cell Dev Biol* (2021) 9:720096. doi: 10.3389/fcell.2021.720096
92. Kendzierski C, Irizarry RA, Chen KS, Haag JD, Gould MN. On the utility of pooling biological samples in microarray experiments. *Proc Natl Acad Sci USA* (2005) 102:4252–7. doi: 10.1073/pnas.0500607102



# Frontiers in Oncology

Advances knowledge of carcinogenesis and tumor progression for better treatment and management

The third most-cited oncology journal, which highlights research in carcinogenesis and tumor progression, bridging the gap between basic research and applications to improve diagnosis, therapeutics and management strategies.

## Discover the latest Research Topics

[See more →](#)

### Frontiers

Avenue du Tribunal-Fédéral 34  
1005 Lausanne, Switzerland  
[frontiersin.org](https://frontiersin.org)

### Contact us

+41 (0)21 510 17 00  
[frontiersin.org/about/contact](https://frontiersin.org/about/contact)

